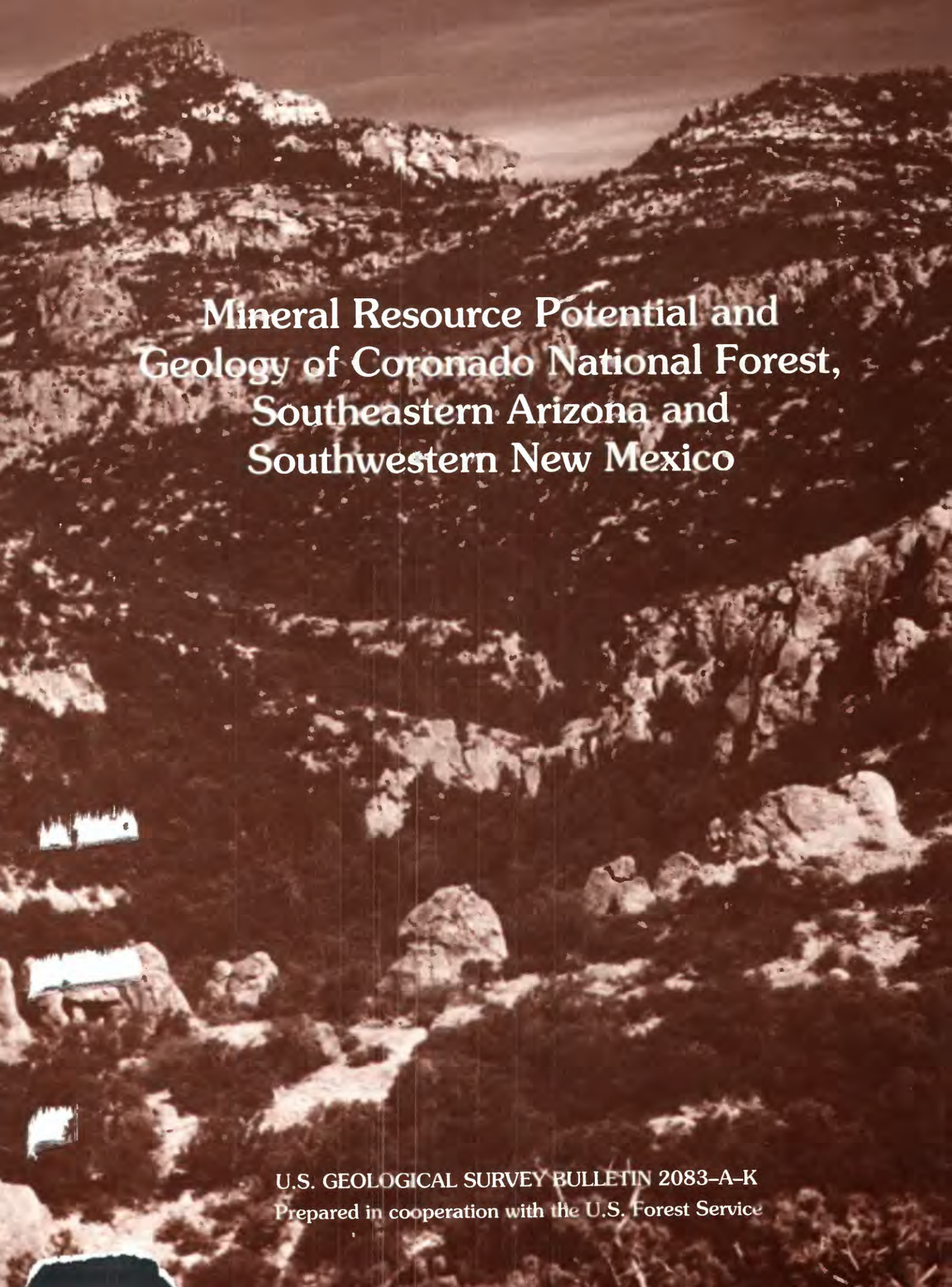

Mineral Resource Potential and Geology of Coronado National Forest, Southeastern Arizona and Southwestern New Mexico

U.S. GEOLOGICAL SURVEY BULLETIN 2083–A–K
Prepared in cooperation with the U.S. Forest Service

AVAILABILITY OF BOOKS AND MAPS OF THE U.S. GEOLOGICAL SURVEY

Instructions on ordering publications of the U.S. Geological Survey, along with prices of the last offerings, are given in the current-year issues of the monthly catalog "New Publications of the U.S. Geological Survey." Prices of available U.S. Geological Survey publications released prior to the current year are listed in the most recent annual "Price and Availability List." Publications that may be listed in various U.S. Geological Survey catalogs (**see back inside cover**) but not listed in the most recent annual "Price and Availability List" may no longer be available.

Reports released through the NTIS may be obtained by writing to the National Technical Information Service, U.S. Department of Commerce, Springfield, VA 22161; please include NTIS report number with inquiry.

Order U.S. Geological Survey publications **by mail** or **over the counter** from the offices listed below.

BY MAIL

Books

Professional Papers, Bulletins, Water-Supply Papers, Techniques of Water-Resources Investigations, Circulars, publications of general interest (such as leaflets, pamphlets, booklets), single copies of Earthquakes & Volcanoes, Preliminary Determination of Epicenters, and some miscellaneous reports, including some of the foregoing series that have gone out of print at the Superintendent of Documents, are obtainable by mail from

U.S. Geological Survey, Information Services
Box 25286, Federal Center
Denver, CO 80225

Subscriptions to periodicals (Earthquakes & Volcanoes and Preliminary Determination of Epicenters) can be obtained ONLY from the

Superintendent of Documents
Government Printing Office
Washington, DC 20402

(Check or money order must be payable to Superintendent of Documents.)

Maps

For maps, address mail orders to

U.S. Geological Survey, Information Services
Box 25286, Federal Center
Denver, CO 80225

Residents of Alaska may order maps from

U.S. Geological Survey, Earth Science Information Center
101 Twelfth Ave., Box 12
Fairbanks, AK 99701

OVER THE COUNTER

Books and Maps

Books and maps of the U.S. Geological Survey are available over the counter at the following U.S. Geological Survey offices, all of which are authorized agents of the Superintendent of Documents.

- **ANCHORAGE, Alaska**–Rm. 101, 4230 University Dr.
- **LAKEWOOD, Colorado**–Federal Center, Bldg. 810
- **MENLO PARK, California**–Bldg. 3, Rm. 3128, 345 Middlefield Rd.
- **RESTON, Virginia**–USGS National Center, Rm. 1C402, 12201 Sunrise Valley Dr.
- **SALT LAKE CITY, Utah**–Federal Bldg., Rm. 8105, 125 South State St.
- **SPOKANE, Washington**–U.S. Post Office Bldg., Rm. 135, West 904 Riverside Ave.
- **WASHINGTON, D.C.**–Main Interior Bldg., Rm. 2650, 18th and C Sts., NW.

Maps Only

Maps may be purchased over the counter at the following U.S. Geological Survey offices:

- **FAIRBANKS, Alaska**–New Federal Bldg, 101 Twelfth Ave.
- **ROLLA, Missouri**–1400 Independence Rd.
- **STENNIS SPACE CENTER, Mississippi**–Bldg. 3101

Mineral Resource Potential and Geology of Coronado National Forest, Southeastern Arizona and Southwestern New Mexico

Edited by Edward A. du Bray

U.S. GEOLOGICAL SURVEY BULLETIN 2083–A–K

Prepared in cooperation with the U.S. Forest Service

UNITED STATES GOVERNMENT PRINTING OFFICE, WASHINGTON : 1996

U.S. DEPARTMENT OF THE INTERIOR
BRUCE BABBITT, Secretary

U.S. GEOLOGICAL SURVEY
Gordon P. Eaton, Director

For sale by U.S. Geological Survey, Information Services
Box 25286, Federal Center
Denver, CO 80225

Library of Congress Cataloging-in-Publication Data

Mineral resource potential and geology of Coronado National Forest, southeastern Arizona and southwestern New Mexico / edited by Edward A. du Bray.
p. cm.—(U.S. Geological Survey bulletin ; 2083–A–K)
Includes bibliographical reference
Supt. of Docs. no. : I 19.3:2083–A–K
1. Mines and mineral resources—Coronado National Forest (Ariz. and N.M.) 2. Geology—Coronado National Forest (Ariz. and N.M.)
I. du Bray, E. A. II. Series.
QE75.B9 no. 2083–A–K
[TN24.A6]
557.3 s—dc20
[553′.097915] 94–2417
CIP

CONTENTS

PLATES

[Plates are in pocket. As shown on plates 2–4 and 6–32, the northern part of Coronado National Forest includes the Santa Catalina–Rincon, Santa Teresa, Galiuro, Winchester, and Pinaleno Forest units; the southeastern part includes the Dragoon, Peloncillo, and Chiricahua-Pedregosa Forest units; and the southwestern part includes the Santa Rita, Atascos–Cobre–Coches–Pajarito–San Luis–Tumacacori, Whetstone, and Patagonia-Huachuca-Canelo Forest units]

1. Maps showing key geologic features and geology-based mineral resource evaluation of Coronado National Forest

   Compiled by Harald Drewes

2–4. Geologic maps of the northern, southeastern, and southwestern parts of Coronado National Forest

   Compiled by Harald Drewes

   2. Northern part
   3. Southeastern part
   4. Southwestern part

5. Maps showing geology, sample localities, and distribution of samples containing anomalous abundances of selected elements, Coronado National Forest

   Compiled by Gary A. Nowlan

6–8. Maps showing geochemical anomalies and distribution of stream-sediment and soil samples containing high and anomalous abundances of Au, Ag, As, Sb, Cu, Pb, Zn, and Mo in the northern, southeastern, and southwestern parts of Coronado National Forest

   Compiled by Gary A. Nowlan

   6. Northern part
   7. Southeastern part
   8. Southwestern part

9–11. Complete Bouguer-gravity-anomaly maps of the northern, southeastern, and southwestern parts of Coronado National Forest

   Compiled by Mark E. Gettings

   9. Northern part
   10. Southeastern part
   11. Southwestern part

12–14. Terrain-clearance maps for NURE profiles for the northern, southeastern, and southwestern parts of Coronado National Forest

   Compiled by Mark E. Gettings

   12. Northern part
   13. Southeastern part
   14. Southwestern part

Summary and Introduction

By Harald Drewes *and* Mark W. Bultman

MINERAL RESOURCE POTENTIAL AND GEOLOGY OF CORONADO NATIONAL FOREST, SOUTHEASTERN ARIZONA AND SOUTHWESTERN NEW MEXICO

Edited by Edward A. du Bray

U.S. GEOLOGICAL SURVEY BULLETIN 2083–A

UNITED STATES GOVERNMENT PRINTING OFFICE, WASHINGTON : 1996

CONTENTS

FIGURES

TABLE

Summary and Introduction

By Harald Drewes *and* Mark W. Bultman

SUMMARY

This volume is a mineral resource assessment of Coronado National Forest, southeastern Arizona and southwestern New Mexico, synthesized from available geologic, geochemical, and geophysical data. The project was initiated in October 1989; data compilation, synthesis, and manuscript preparation were completed in December 1991. The assessment is provided to help the U.S. Forest Service comply with requirements of title 36, chapter 2, part 219.22, Code of Federal Regulations, which requires the Forest Service to provide information and interpretations so that mineral resources can be considered with other types of resources in land-use planning.

Coronado National Forest (referred to in this report as "the Forest") contains approximately 1,853,000 acres (7,500 km^2), most of which is in the high mountain ranges of southeastern Arizona and southwestern New Mexico. The geology of Coronado National Forest is highly variable and reflects the complex geologic history of this region. Much of the geologic record in this region is indicated by sedimentary and volcanic rocks composing seven major sequences that have been intruded by igneous rocks during at least five major magmatic episodes.

The geologic resources of the Coronado National Forest region probably have been prospected and mined by various cultures for thousands of years. Silver was produced from the oxidized mantos of vein deposits during early phases of mineral resource exploitation. Gold, silver, and lead were subsequently produced from contact-metasomatic and fissure-hosted replacement deposits. About $20 billion of metallic commodities, mostly lead, copper, zinc, gold, and silver, have been produced from the Coronado National Forest region, which includes five world-class porphyry copper deposits, all of which are still producing ore. Most production has come from areas outside the Forest; the main exceptions are in the Patagonia Mountains, the Santa Rita Mountains, and the Cobre Ridge part of the Arivaca area. Other productive sites within the Forest include the Dragoon, Chiricahua, Whetstone, Huachuca, and Santa Catalina Mountains. Leasable commodities have not been produced in the Coronado National Forest region. Industrial commodities have been produced from within the Forest; at least 31 ornamental- or construction-stone sites are being exploited and 12 sand and gravel pits are active.

Numerous tracts within the Forest are favorable for the presence of undiscovered deposits. Rocks favorable for the occurrence of undiscovered ore deposits are mainly lower Paleozoic and Upper Cretaceous to lower Tertiary andesitic to dacitic volcanic and volcaniclastic rocks. Quantitative assessments of metal tonnages contained in inferred, undiscovered deposits have been made for the following ore-deposit types: (1) tungsten skarn, (2) tungsten vein, (3) porphyry copper, (4) porphyry copper skarn-related, (5) copper skarn, (6) polymetallic replacement, (7) porphyry copper-molybdenum, (8) polymetallic vein, (9) Creede epithermal vein, (10) rhyolite-hosted tin, and (11) placer gold. These data (table 1) were used to compute total inferred, undiscovered metal in these types of deposits for the entire Forest. These estimates are derived from subjective estimates of numbers of undiscovered deposits, reflect knowledge available at the time of the assessment, and are subject to considerable uncertainty.

Exploration for oil and gas has been sporadic in the Coronado National Forest region; shows of oil or gas in several exploratory wells were reported, but no wells have been completed for production of oil or gas. The southeastern part of the Forest has moderate potential for undiscovered petroleum deposits, whereas the northern and western areas have low potential for such deposits. Coal and geothermal energy resource potential in the Forest are low.

Salable minerals within or directly adjacent to Coronado National Forest consist of sand and gravel, limestone, pumicite, dimension stone, and humacite. Sand and gravel deposits, available in most parts of the Forest, are in basin and valley fills, stream terraces, buried and active stream channels, and alluvial fans. Metamorphosed Mississippian Escabrosa Limestone suitable for industrial uses is available in many parts of the Forest.

Table 1. Estimates of metal contents in undiscovered deposits for all assessed mineral deposit models, Coronado National Forest, southeastern Arizona and southwestern New Mexico.

Metal	Mean of the simulated distribution of metal (tonnes, giving approximate 95-percent confidence interval)	Quantiles of the simulated distribution of metal (tonnes)		
		10 percent	50 percent	90 percent
Copper	2×10^7 (-2×10^7, $+7\times10^9$)	7×10^5	1×10^7	5×10^7
Gold	1×10^2 (-1×10^2, $+8\times10^4$)	2×10^0	4×10^1	3×10^2
Lead	1×10^5 (-1×10^5, $+1\times10^8$)	7×10^2	1×10^4	3×10^5
Molybdenum	5×10^5 (-5×10^5, $+6\times10^7$)	3×10^4	3×10^5	1×10^6
Silver	6×10^3 (-6×10^3, $+1\times10^6$)	2×10^2	3×10^3	1×10^4
Tin	3×10^1 (-3×10^1, $+2\times10^4$)	1×10^0	2×10^1	8×10^1
Tungsten	5×10^3 (-5×10^3, $+2\times10^5$)	9×10^2	4×10^3	1×10^4
Zinc	1×10^5 (-1×10^5, $+1\times10^8$)	4×10^2	7×10^3	2×10^5

INTRODUCTION

Federal land-use planners require periodically updated information to regulate effectively the development and multiple use of Federal lands. In 1988, the U.S. Forest Service identified the Coronado National Forest of southeastern Arizona and southwestern New Mexico (fig. 1) as a tract for which existing mineral resource potential data were no longer sufficiently current to facilitate land-use planning decisions. Accordingly, the U.S. Geological Survey was asked to provide a mineral resource assessment.

The need for resource data by land-use planners is ongoing and the present assessment will require periodic updating. Computer-based data files were prepared during the course of this study and will be available for future studies. These data bases include digital information, which can be readily augmented or improved, for the geology, geophysics, and geochemistry of Coronado National Forest.

Time and funding limitations necessitated this assessment be based almost entirely on currently available earth science data. New field and laboratory work were oriented toward resolution of only the most critical questions and involved approximately 6 person-months in the field. Previously completed mineral resource studies of wilderness and roadless areas within Coronado National Forest were a major asset to this review; extensive parts of the Forest region have not been as completely studied by the U.S. Geological Survey, however.

Available earth science data for the Forest region vary widely in kind and quality. Previous studies (fig. 2) of greatest use in this assessment are regional compilations of the Silver City $1^\circ \times 2^\circ$ quadrangle CUSMAP (Conterminous United States Minerals Assessment Program) (Drewes and others, 1985; Richter and others, 1986), as well as the geologic synthesis of the southern two-thirds of the Forest region (Drewes, 1980). Many quadrangle maps and thesis and dissertation maps were incorporated in these older syntheses. Data included in the pre-assessment studies of the Douglas (Hammarstrom and others, 1988) and Tucson and Nogales $1^\circ \times 2^\circ$ quadrangles (Peterson, 1990) were also utilized (fig. 2). The present synthesis includes data from recently completed quadrangle maps, particularly in the Chiricahua Mountains.

Whereas the majority of mineral resource assessments recently published by the U.S. Geological Survey identify tracts that are permissive for the occurrence of undiscovered mineral deposits of various types, in this report we identify tracts that are favorable for the occurrence of undiscovered mineral deposits. Permissive tracts are more areally inclusive but provide land-use planners with, at best, vague information as to the probable locations of lands that may potentially be subject to mineral entry. Favorable tracts are geographically more restrictive, provide much more definitive information with regard to lands that may potentially be subject to mineral entry, and probably contain most, if not all, of the undiscovered mineral deposits that would be inferred for associated permissive tracts.

Team members, specialists in each of the earth science disciplines represented by chapters in this report, established the favorability for undiscovered deposits throughout the Forest region using data from their respective fields. These favorability studies resulted in a series of maps that display tracts within the Forest that are considered favorable for the occurrence of undiscovered deposits of various types. During team meetings these discipline-specific favorability tract maps were used to compile a single set of favorabilty tract maps that display relative levels of favorabilty. The most favorable areas are those confirmed by data from the greatest number of disciplines.

Terminology expressing relative levels of mineral resource potential and associated levels of certainty assigned to these estimates are those identified by Goudarzi (1984). This terminology, defined in Appendix 1, is used throughout this report.

Acknowledgments.—We would like to thank the Douglas District of the U.S. Forest Service for logistical support during some of our field operations. The authors are indebted to C.H. Thorman and T.G. Theodore, whose thorough reviews helped sharpen this report. In addition, we benefitted from discussions with W.D. Menzie, D.H. Root, L.J. Drew, and D.A. Singer.

CHARACTER AND GEOLOGIC SETTING

Coronado National Forest contains approximately 1,853,000 acres (7,500 km^2), most of which is in the high mountain ranges that occupy parts of Cochise, Graham, Greenlee, Pima, and Santa Cruz counties in southeastern Arizona and Hidalgo County in southwestern New Mexico. The area shown on the accompanying plates includes many private inholdings and terranes around the Forest units; the Forest and adjacent or enclosed non-Forest lands cover about 9,070 km^2.

The Forest is in the Basin and Range Province, which is composed of alternating broad intermontane valleys and flanking high mountain ranges. The physiography and geology of this region are similar to those of many other areas of the Basin and Range Province. The Forest comprises 12 separate units, most of which are centered on a specific mountain range or a group of associated ranges (fig. 1). Elevation ranges from approximately 760 m in the valleys west and south of the Santa Catalina Mountains to 3,265 m at Mount Graham in the Pinaleno Mountains; relief between the range front and mountain tops exceeds 1,500 m in many of the ranges. This relief has facilitated development of a broad spectrum of climatic zones ranging from the semi-arid Sonoran Desert at the lower elevations to ponderosa pine and douglas fir forests found in the high-elevation alpine zone.

The geology of the 12 units that compose Coronado National Forest is highly variable and reflects the complex geologic history of this region. Land within the separate Forest units has been uplifted and eroded to varying degrees. Where uplift has been extreme, the geologic record has been truncated by deep erosion, whereas the record is largely concealed in areas that have subsided or have been affected by minor uplift and erosion. Much of the geologic record of the Coronado National Forest region is recorded in packages of sedimentary and volcanic rocks that compose seven major sequences. Major unconformities separate the sequences and represent periods of erosion or nondeposition, and possibly of tilting or other deformation. The combined thickness of these sequences is probably greater than 10 km, but nowhere are all seven present together because of irregularities in their initial thicknesses, in local erosion, and in their subsequent deformation. These layered rocks were intruded in many places by igneous rocks during at least five major magmatic episodes.

MINERAL RESOURCES

LOCATABLE MINERALS

The Coronado National Forest region has probably been prospected and mined by various cultures for thousands of years. Spanish settlers were mining silver by 1800 and Confederate miners exploited lead deposits in the 1860's. The area of the San Manuel porphyry copper deposit was noted as a potential source of minerals in 1870, and brightly colored (hydrothermally altered) rocks were noted near Bisbee in 1877, where ore was discovered in 1880. Early production was probably from oxidized mantos of vein deposits; early production records are nonexistent. Many other discoveries followed, culminating with the porphyry copper-related deposits of the Pima district (Sierrita Mountains),

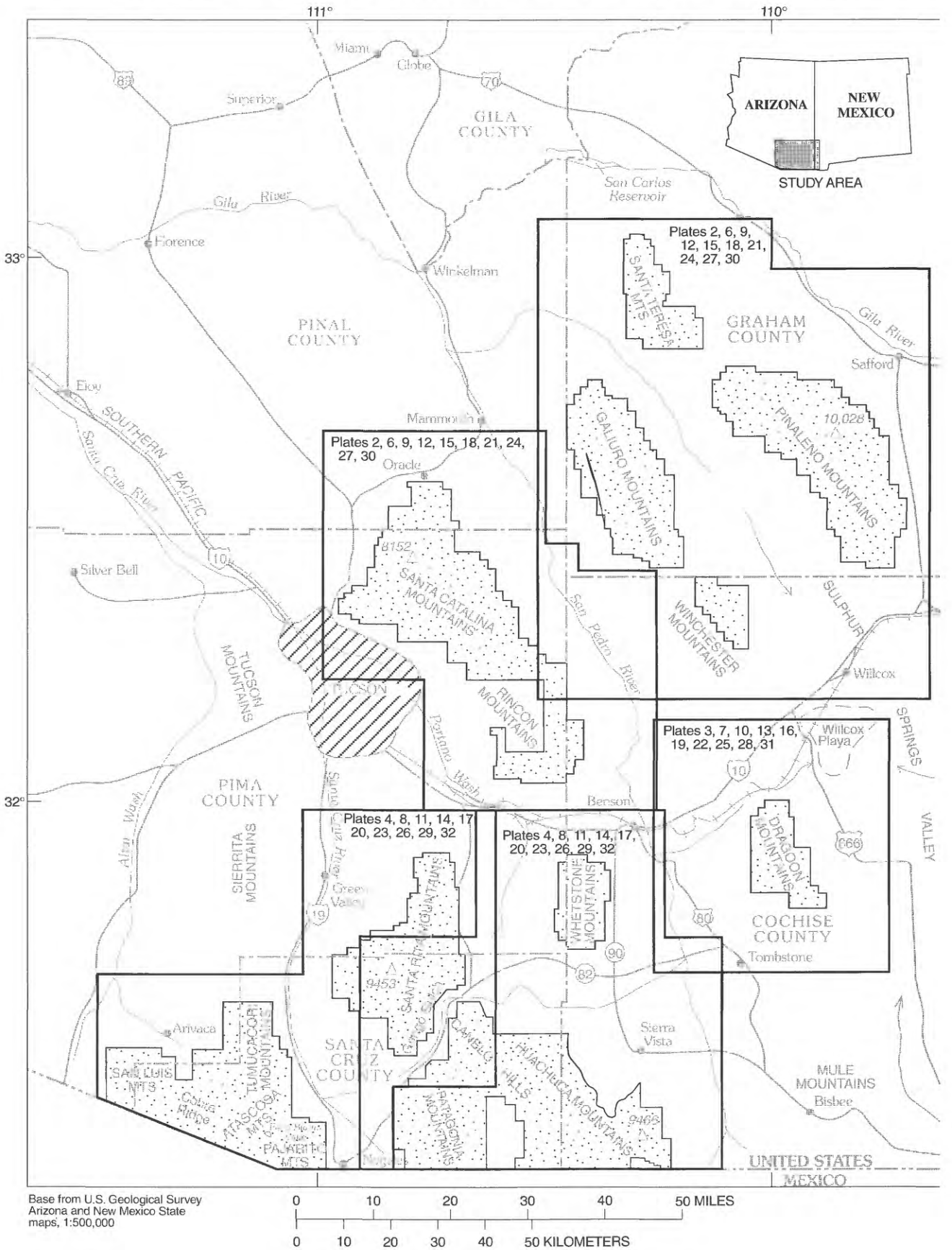
111°
110°
33°
32°
ARIZONA
NEW MEXICO
STUDY AREA
Miami
Globe
Superior
GILA COUNTY
Gila River
San Carlos Reservoir
Florence
Winkelman
PINAL COUNTY
Eloy
SOUTHERN PACIFIC
Santa Cruz River
Mammoth
Oracle
Silver Bell
Plates 2, 6, 9, 12, 15, 18, 21, 24, 27, 30
SANTA TERESA MTS.
GRAHAM COUNTY
Safford
GALIURO MOUNTAINS
PINALENO MOUNTAINS
10,028
8152
SANTA CATALINA MOUNTAINS
WINCHESTER MOUNTAINS
SULPHUR
San Pedro River
Wilcox
TUCSON MOUNTAINS
TUCSON
RINCON MOUNTAINS
Plates 3, 7, 10, 13, 16, 19, 22, 25, 28, 31
Wilcox Playa
SPRINGS
Pantano Wash
Benson
PIMA COUNTY
Plates 4, 8, 11, 14, 17, 20, 23, 26, 29, 32
Plates 4, 8, 11, 14, 17, 20, 23, 26, 29, 32
SIERRITA MOUNTAINS
Green Valley
SANTA RITA MOUNTAINS
WHETSTONE MOUNTAINS
DRAGOON MOUNTAINS
VALLEY
COCHISE COUNTY
Tombstone
9453
Arivaca
SAN LUIS MTS.
TUMACACORI MOUNTAINS
ATASCOSA MTS.
PAJARITO MTS.
SANTA CRUZ COUNTY
PATAGONIA MOUNTAINS
CANELO HILLS
HUACHUCA MOUNTAINS
9466
Sierra Vista
MULE MOUNTAINS
Bisbee
UNITED STATES
MEXICO
Base from U.S. Geological Survey
Arizona and New Mexico State
maps, 1:500,000
0 10 20 30 40 50 MILES
0 10 20 30 40 50 KILOMETERS

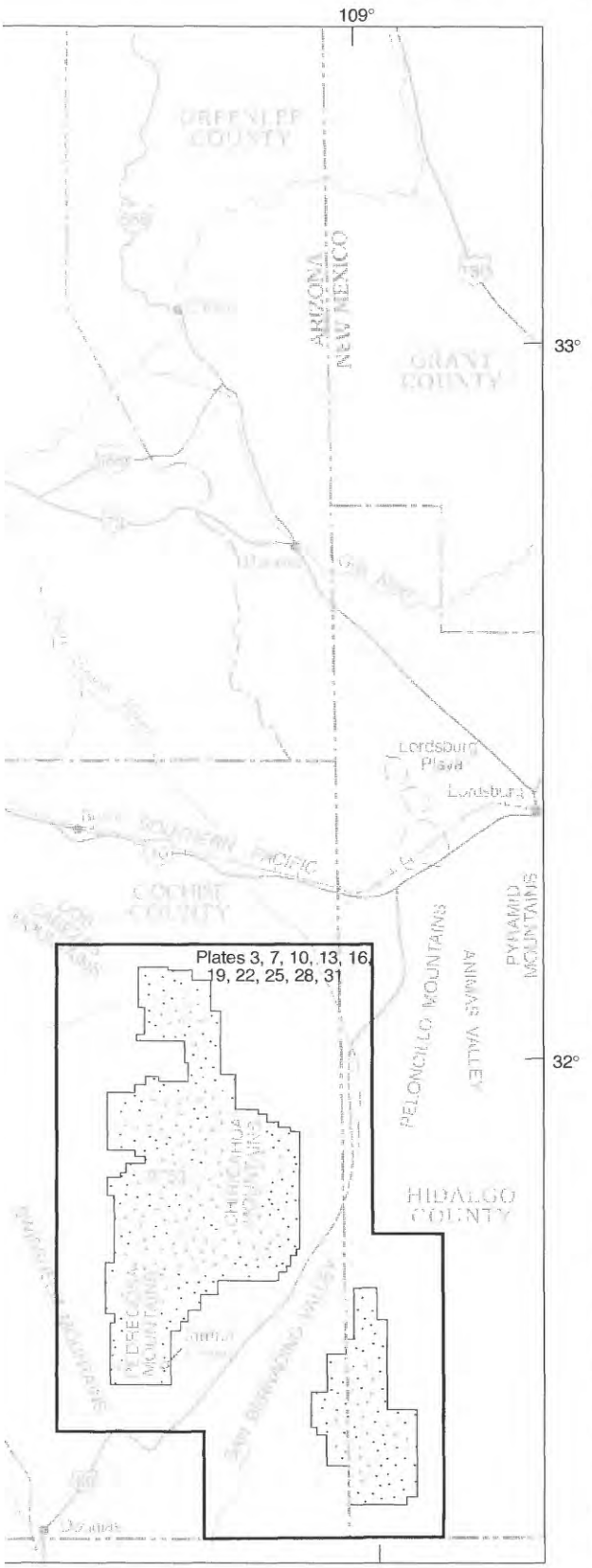

Figure 1 (left and facing page). Index map showing location of Coronado National Forest units and outlines of areas covered by plates 2–4 and 6–32, southeastern Arizona and southwestern New Mexico.

discovered between 1950 and 1970. Although additional discoveries have been made, few have been developed.

Most of the major mining districts were established or earlier workings were expanded during the last decades of the 19th century. Development of mass mining methods initiated a final spurt of mine expansion and new discoveries. Most of the large deposits discovered near the Forest, including several porphyry copper and porphyry copper-molybdenum deposits (Sierrita, San Manuel, Lakeshore, San Xavier, Silver Bell) and several porphyry copper skarn-related systems (Twin Buttes, Esperanza, Mission, and Johnson Camp), are all still in operation.

About $20 billion worth (Mardirosian, 1977) of metallic commodities have been produced from the region, including an area extending 80 km around Coronado National Forest. Most of this production has come from non-Forest lands, but there may be many sites favorable for the occurrence of undiscovered deposits within Forest units. This extended region includes five world-class porphyry copper deposits. The most productive of these copper deposits are composites of several mineral deposit types.

LEASABLE MINERALS

There is no recorded production of leasable commodities in the Coronado National Forest region.

SALABLE MINERALS

The Santa Catalina, Chiricahua, and Dragoon Mountains contain reserves of limestone well suited for all aggregate purposes. Marmarized limestone used as dimension stone and riprap is chiefly quarried from the Escabrosa Limestone and Pennsylvanian Naco Group in several locations within the Forest. Production of bright white marble stone from the Santa Rita and Dragoon Mountains continues to command the most interest; dimension stone, including riprap, is hand-picked or quarried from deposits in every district in the Forest. At least 31 stone sites are being exploited within the Forest, although several of these are areas not operated on a regular basis. The Ligier and Dragoon Marble quarries exploit varicolored limestone, dolomite, and marble. A single venture that produces aggregate limestone operates in the Santa Rita Mountains. The historic Helvetia mining district in the Santa Rita Mountains contains

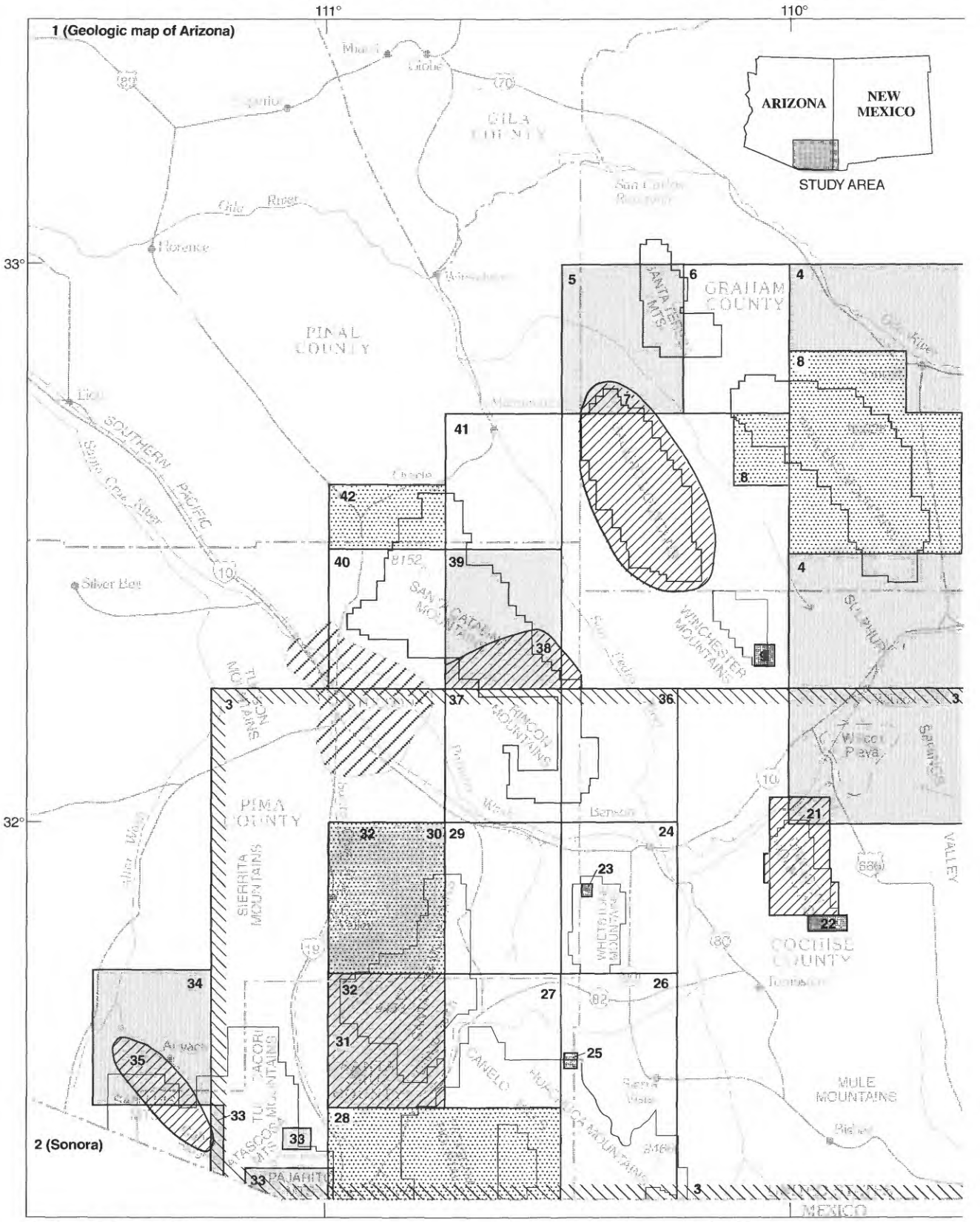
111°
110°
33°
32°
1 (Geologic map of Arizona)
2 (Sonora)
ARIZONA
NEW MEXICO
STUDY AREA
GILA COUNTY
GRAHAM COUNTY
PINAL COUNTY
PIMA COUNTY
COCHISE COUNTY
SANTA TERESA MTS.
SAN CAYETANO MOUNTAINS
VINCHESTER MOUNTAINS
RINCON MOUNTAINS
SIERRITA MOUNTAINS
WHETSTONE MOUNTAINS
MULE MOUNTAINS
SOUTHERN PACIFIC
Gila River
San Pedro River
Santa Cruz River
Florence
Silver Bar
Benson
MEXICO
Base from U.S. Geological Survey
Arizona and New Mexico State
maps, 1:500,000
0 10 20 30 40 50 MILES
0 10 20 30 40 50 KILOMETERS

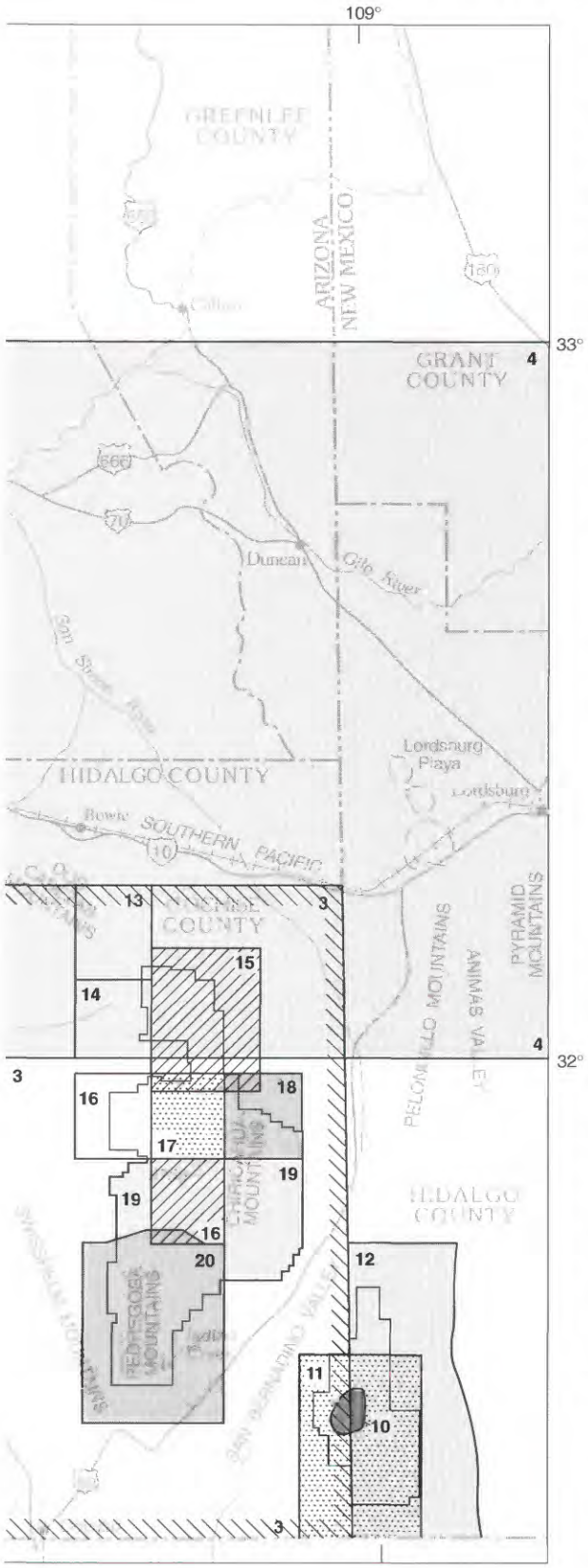

Figure 2 (left and facing page). Index to source maps used in the compilation of plates 2–4. 1, Wilson and others, 1969; 2, Lucarelli, 1967; 3, Drewes, 1980; 4, Drewes and others, 1985; 5, Simons, 1964; 6, Blacet and Miller, 1978; 7, Creasey and others, 1981; 8, C.H. Thorman, unpub. mapping of several 7½-minute quadrangles or parts thereof (1978–1982); 9, Drewes, 1981a, fig. 14; 10, McIntyre, 1988; 11, Hayes, 1982; 12, Wrucke and Bromfield, 1961; 13, Drewes, 1984; 14, Drewes, 1981b; 15, Drewes, 1982; 16, Pallister and du Bray, 1994; 17, Pallister and others, 1994; 18, Drewes and others, 1995; 19, Cooper, 1959; 20, Drewes and Brooks, 1988; 21, Drewes, 1987; 22, Gilluly, 1956; 23, Drewes, 1981a, fig. 11; 24, Creasey, 1967a; 25, Drewes, 1981a, pl. 6; 26, Hayes and Raup, 1968; 27, R.B. Raup (written commun., 1967); 28, Simons, 1974; 29, Finnell, 1971; 30, Drewes, 1971a; 31, Drewes, 1971b; 32, Drewes, 1972; 33, Drewes, 1981a, pl. 8; 34, Keith and Theodore, 1975; 35, Riggs and others, 1990 (sketch map); 36, Drewes, 1974; 37, Drewes, 1977; 38, Thorman and others, 1981; 39, Creasey and Theodore, 1975; 40, Banks, 1976; 41, Creasey, 1967b; 42, Budden, 1975

enormous reserves of recrystallized limestone (marble). Twelve small sand and gravel pits in alluvial deposits in the Forest are infrequently worked.

RESOURCE POTENTIAL

LOCATABLE MINERALS

A mineral resource assessment of Coronado National Forest was conducted by a team of U.S. Geological Survey earth scientists. The assessment process involved three steps. First, earth science data were used to help identify tracts in Coronado National Forest considered favorable for occurrence of various types of mineral deposits (figs. 3 and 4). Second, numbers of undiscovered deposits were estimated for each identified favorable tract. Third, a computer-based numerical simulation methodology was used to generate estimates of amounts of undiscovered metals (table 1). Although this information is presented in a quantitative format, we emphasize that these numbers are derived from subjective, consensus estimates of numbers of undiscovered deposits for each specific mineral deposit model considered (see Chapter J). These estimates are based solely on data and interpretations available at the time of the assessment and are subject to considerable uncertainty.

Rocks favorable for the occurrence of undiscovered ore deposits are mainly lower Paleozoic and Upper Cretaceous to lower Tertiary andesitic to dacitic volcanic and volcaniclastic rocks. Upper Cretaceous to lower Tertiary diorite to granite stocks, plugs, and dikes are most closely associated with ore deposits of the region. Jurassic and middle Tertiary stocks and plugs are less commonly associated with ore deposits. Ore deposits are localized along or near steeply

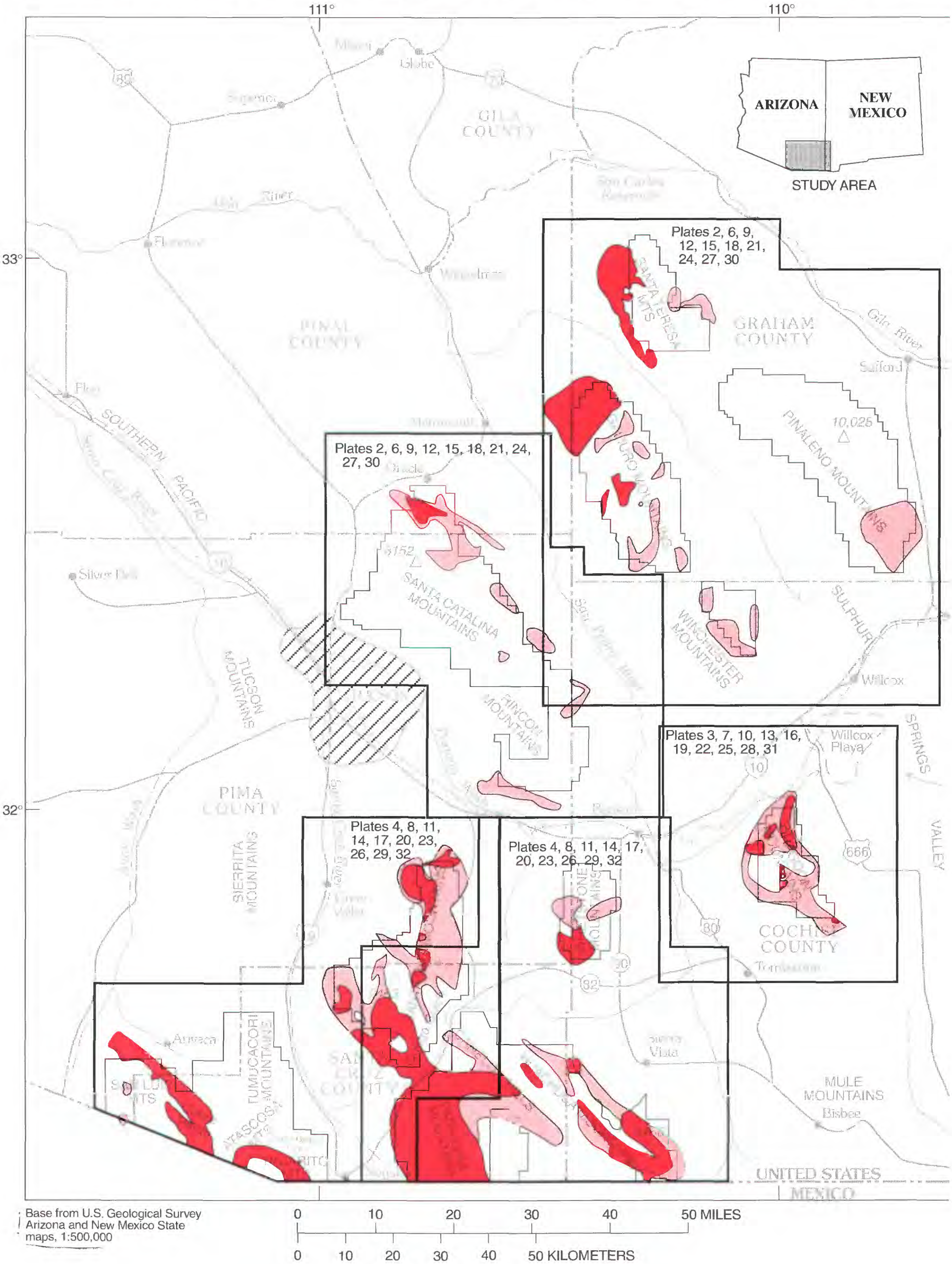
111°
110°
33°
32°
ARIZONA
NEW MEXICO
STUDY AREA
GILA COUNTY
PINAL COUNTY
GRAHAM COUNTY
PIMA COUNTY
COCHISE COUNTY
SANTA CRUZ COUNTY
Plates 2, 6, 9, 12, 15, 18, 21, 24, 27, 30
Plates 2, 6, 9, 12, 15, 18, 21, 24, 27, 30
Plates 3, 7, 10, 13, 16, 19, 22, 25, 28, 31
Plates 4, 8, 11, 14, 17, 20, 23, 26, 29, 32
Plates 4, 8, 11, 14, 17, 20, 23, 26, 29, 32
SANTA TERESA MTS
PINALENO MOUNTAINS
10,025
SANTA CATALINA MOUNTAINS
8152
RINCON MOUNTAINS
WINCHESTER MOUNTAINS
TUCSON MOUNTAINS
SIERRITA MOUNTAINS
TUMUCACORI MOUNTAINS
ATASCOSA MTS
MULE MOUNTAINS
SOUTHERN PACIFIC
SULPHUR SPRINGS VALLEY
Gila River
Safford
Willcox
Willcox Playa
Sierra Vista
Bisbee
Arivaca
Silver Bell
UNITED STATES
MEXICO
Base from U.S. Geological Survey Arizona and New Mexico State maps, 1:500,000
0 10 20 30 40 50 MILES
0 10 20 30 40 50 KILOMETERS

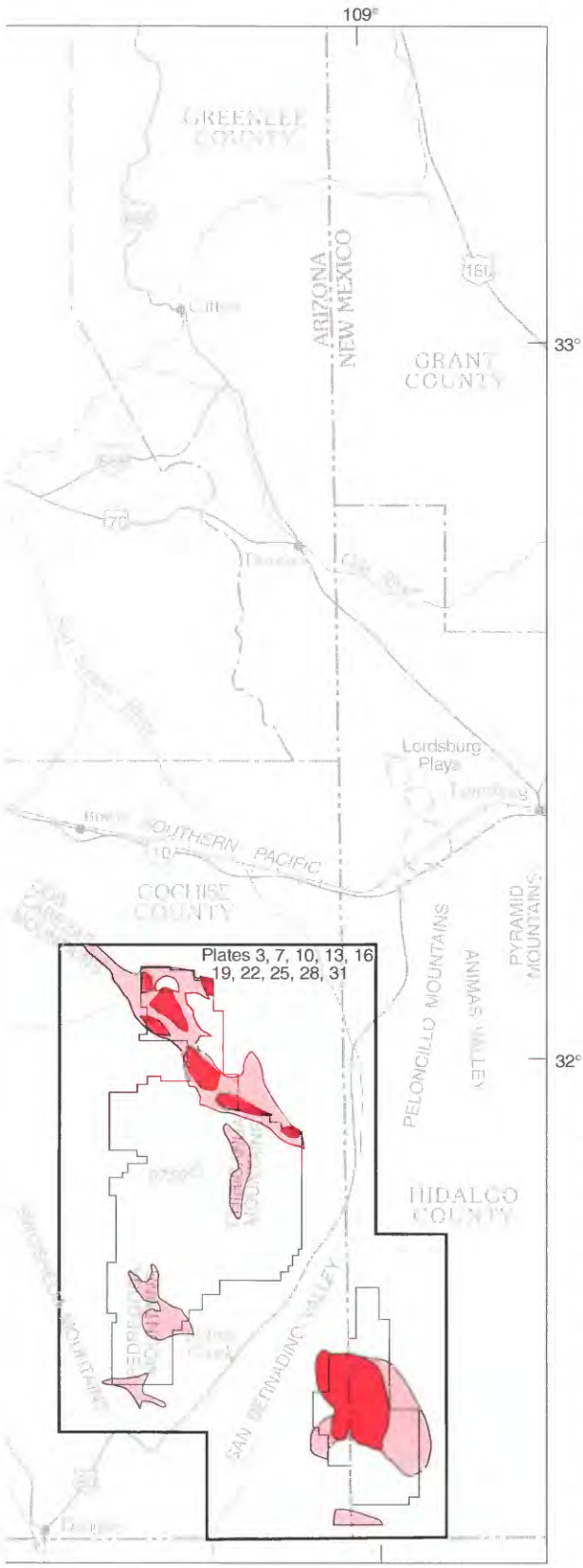

Figure 3 (left and facing page). Map showing tracts favorable for locatable lode minerals, Coronado National Forest, southeastern Arizona and southwestern New Mexico. Red and pink areas are subtracts having high and moderate to low mineral resource potential, respectively.

dipping, northwest-striking faults. In some places, steeply dipping structures that trend in directions other than northwest have also guided migration of ore-bearing fluids.

LEASABLE MINERALS

There has been sporadic exploration for oil and gas in the Coronado National Forest region, primarily since 1950. Target development followed successful development of plays in other regions believed to be geologically similar to the Forest region. An oil seep is present outside the Forest unit southwest of the Whetstone Mountains, and shows of oil or gas were reported from several exploratory wells drilled in the Forest region. Although some favorable shows were identified, none resulted in producing wells. At present, exploration activity is minimal or non-existent; renewed exploration activity is possible. Sufficient source rocks for oil and gas, reservoir rocks, and potential targets are present in the southeastern part of the Forest for this part of the region to be assigned moderate potential for undiscovered petroleum deposits; petroleum potential is low in the northern and western areas, however.

Coal has not been mined or prospected in the Forest region. The geologic environments indicated by rocks of the Forest region are such that coal resource potential in Coronado National Forest is low.

The Sulphur Springs and Animas Valleys contain playas that are geologic environments suitable for the occurrence of lithium brines. The Willcox playa, east of the Dragoon Mountains and outside the Forest, was drilled by the U.S. Geological Survey, and minor anomalous lithium concentrations were identified (Vine and others, 1979). The lithium brine content of the playa in the Animas Valley is unknown. Other playa deposits may be present in the subsurface, but little is known about most basins in this area. Coronado National Forest has low potential for lithium brine.

The potential for geothermal energy resources throughout the Coronado National Forest region is low. However, the Forest region contains two hot springs. Hookers Hot Springs is southeast of the Galiuro Mountains, and the other hot spring is in the northern part of the Animas Valley, east of the Peloncillo Mountains. Neither temperature nor volume of hot water at either site is sufficient for commercial power generation.

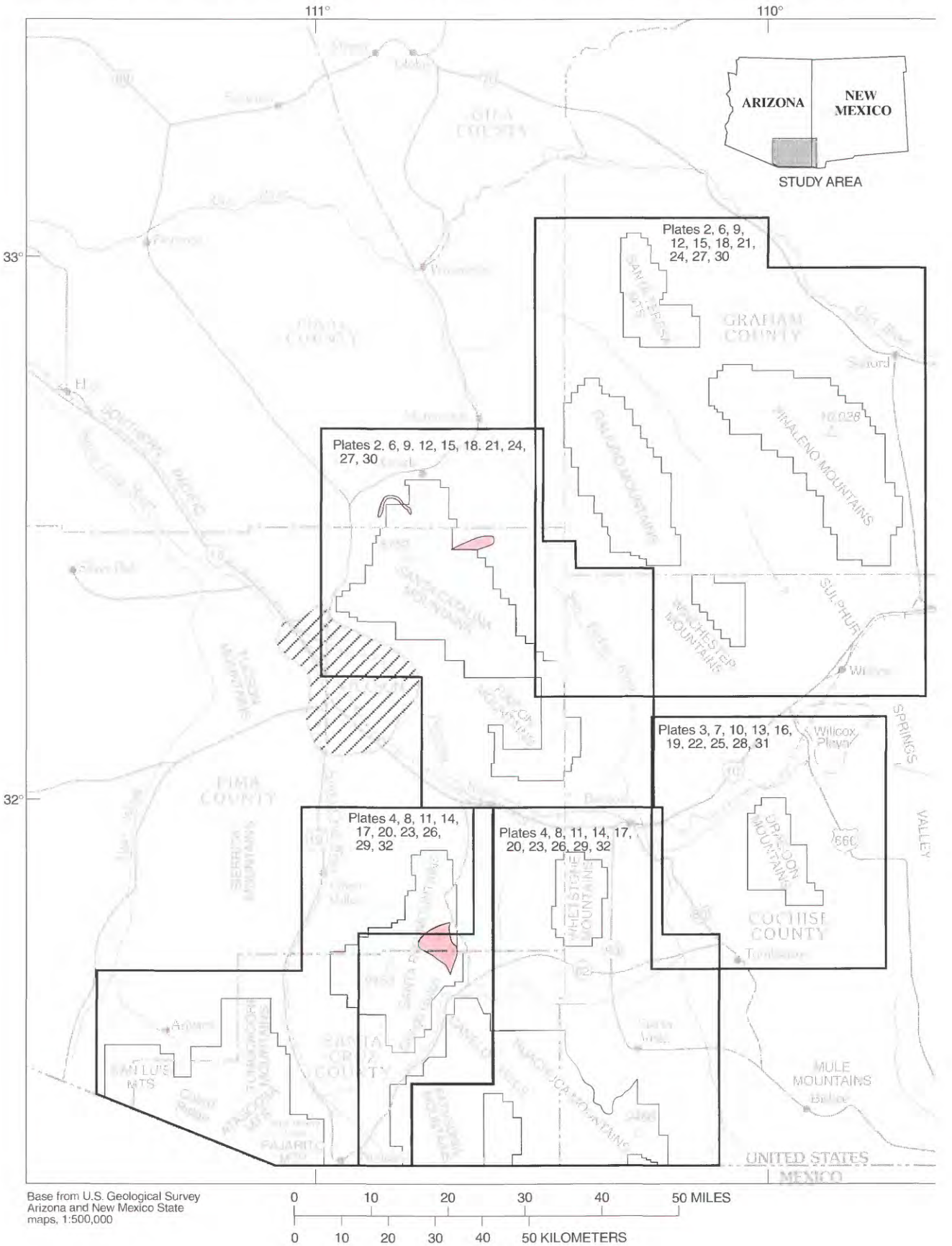
111°
110°
33°
32°
ARIZONA
NEW MEXICO
STUDY AREA
Plates 2, 6, 9, 12, 15, 18, 21, 24, 27, 30
Plates 2. 6, 9. 12, 15, 18. 21, 24, 27, 30
Plates 3, 7, 10, 13, 16, 19, 22, 25, 28, 31
Plates 4, 8, 11, 14, 17, 20. 23, 26, 29, 32
Plates 4, 8, 11, 14, 17, 20, 23, 26, 29, 32
GRAHAM COUNTY
PINALENO MOUNTAINS
SULPHUR SPRINGS VALLEY
COCHISE COUNTY
MULE MOUNTAINS
PIMA COUNTY
SANTA CRUZ COUNTY
UNITED STATES
MEXICO
Base from U.S. Geological Survey
Arizona and New Mexico State
maps, 1:500,000
0 10 20 30 40 50 MILES
0 10 20 30 40 50 KILOMETERS

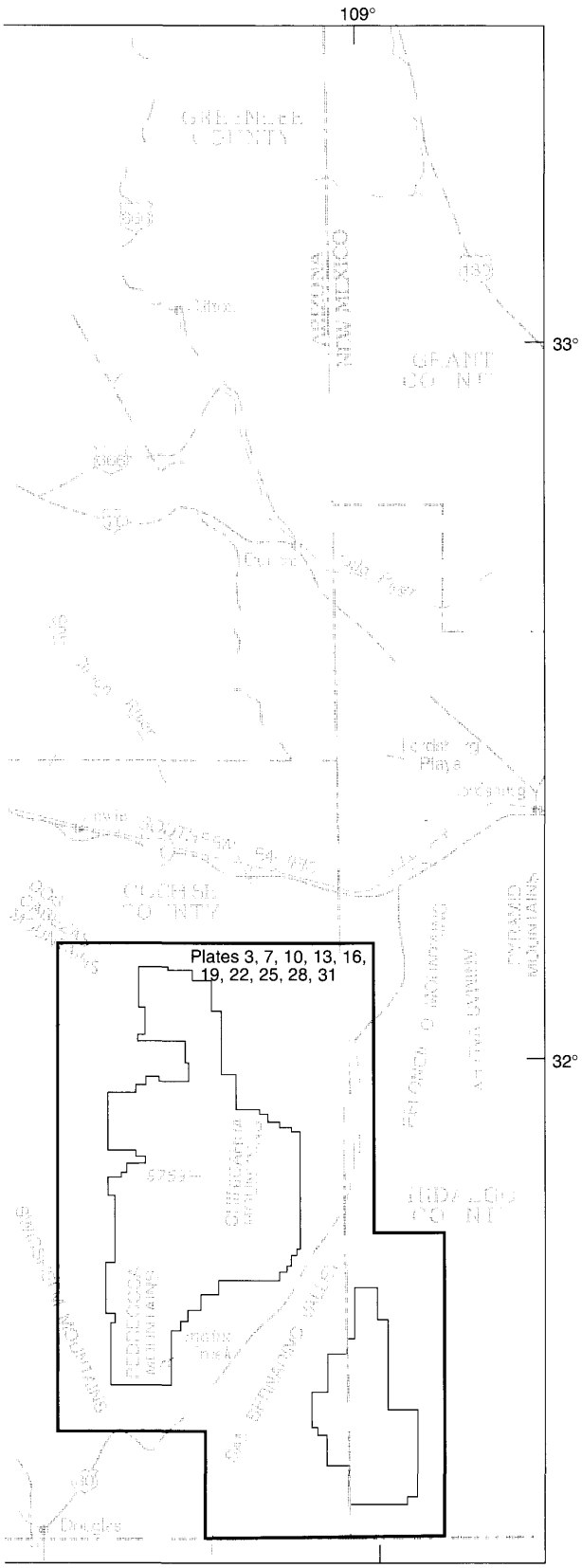

Figure 4 (left and facing page). Map showing tracts favorable for locatable placer deposits, Coronado National Forest, southeastern Arizona and southwestern New Mexico. Pink areas are subtracts having moderate to low mineral resource potential.

SALABLE MINERALS

Salable minerals within or directly adjacent to Coronado National Forest consist of sand and gravel, limestone, pumicite, dimension stone, and humacite. Sand and gravel are readily available in most parts of the Forest. However, abundant and more accessible deposits are in basin and valley fills, stream terraces, buried and active stream channels, and alluvial fans outside the Forest. Therefore, much of the Forest sand and gravel resources will remain unexploited. Sources of dimension stone and riprap are plentiful within the Forest; most exploitation occurs in the Nogales district. The majority of the dimension stone and riprap sources being worked are in middle Tertiary volcanic rocks, such as near Peña Blanca Lake, in the Pajarito Mountains. Metamorphosed Escabrosa Limestone is available in many of the Forest units. Cretaceous volcaniclastic rocks, such as found in the Gringo Gulch area, provide stone for structural purposes that is less indurated than middle Tertiary volcanic rock. The Whitetail Creek deposit in the Chiricahua Mountains, which has a long production record, is another source of white dimension stone. Pumicite crops out northeast of the Pajarito Mountains near Peña Blanca Lake, and a reported occurrence of pumiceous material is near Indian Creek at the southern end of the Pedregosa Mountains. Due to the presence of suitable substitutes and the lack of data concerning Forest pumicite resources, interest in pumicite deposits will remain low. Carbon-rich shale described as a humacite is found in Paleozoic metamorphic rocks in a small area within the Chiricahua Mountains; there is no indication that this occurrence has stimulated exploration activity.

REFERENCES CITED

Banks, N.G., 1976, Reconnaissance geologic map of the Mount Lemmon quadrangle, Pima County, Arizona: U.S. Geological Survey Miscellaneous Field Studies Map MF–747, scale 1:62,500.

Blacet, P.M., and Miller, S.T., 1978, Reconnaissance geologic map of the Jackson Mountain quadrangle, Graham County, Arizona: U.S. Geological Survey Miscellaneous Field Studies Map MF–939, scale 1:62,500.

Budden, R.T., 1975, The Tortolita–Santa Catalina Mountains complex: Tucson, Ariz., University of Arizona, M.S. thesis, 133 p.

Cooper, J.R., 1959, Reconnaissance geologic map of southeastern Cochise County, Arizona: U.S. Geological Survey Mineral Investigations Field Studies Map MF–213, scale 1:125,000.

Creasey, S.C., 1967a, Geologic map of the Benson quadrangle, Cochise and Pima Counties, Arizona: U.S. Geological Survey Miscellaneous Geologic Investigations Map I–470, scale 1:48,000.

———1967b, General geology of the Mammoth quadrangle, Pinal County, Arizona: U.S. Geological Survey Bulletin 1218, 94 p., map scale 1:48,000.

Creasey, S.C., Jinks, J.E., Williams, F.E., and Meeves, H.C., 1981, Mineral resources of the Galiuro Wilderness and contiguous further planning areas, Arizona, *with a section on* Aeromagnetic survey and interpretation, *by* W.E. Davis: U.S. Geological Survey Bulletin 1490, 94 p., 2 plates, map scale 1:62,500.

Creasey, S.C., and Theodore, T.G., 1975, Preliminary reconnaissance geologic map of the Bellota Ranch quadrangle, Pima County, Arizona: U.S. Geological Survey Open-File Report 75–295, scale 1:31,680.

Drewes, Harald, 1971a, Geologic map of the Sahuarita quadrangle, southeast of Tucson, Pima County, Arizona: U.S. Geological Survey Miscellaneous Geologic Investigations Map I–613, scale 1:48,000.

———1971b, Geologic map of the Mount Wrightson quadrangle, southeast of Tucson, Santa Cruz and Pima Counties, Arizona: U.S. Geological Survey Miscellaneous Geologic Investigations Map I–614, scale 1:48,000.

———1972, Structural geology of the Santa Rita Mountains, southeast of Tucson, Arizona: U.S. Geological Survey Professional Paper 748, 35 p.

———1974, Geologic map and sections of the Happy Valley quadrangle, Cochise County, Arizona: U.S. Geological Survey Miscellaneous Investigations Map I–832, scale 1:48,000.

———1977, Geologic map and sections of the Rincon Valley quadrangle, Pima County, Arizona: U.S. Geological Survey Miscellaneous Investigations Series Map I–997, scale 1:48,000.

———1980, Tectonic map of southeastern Arizona: U.S. Geological Survey Miscellaneous Investigations Series Map I–1109, scale 1:125,000.

———1981a, Tectonics of southeastern Arizona: U.S. Geological Survey Professional Paper 1144, 96 p.

———1981b, Geologic map and sections of the Bowie Mountain South quadrangle, Cochise County, Arizona: U.S. Geological Survey Miscellaneous Investigations Series Map I–1363, scale 1:24,000.

———1982, Geologic map and sections of the Cochise Head quadrangle and adjacent areas, southeastern Arizona: U.S. Geological Survey Miscellaneous Investigations Series Map I–1312, scale 1:24,000.

———1984, Geologic map and structure sections of the Bowie Mountain North quadrangle, Cochise County, Arizona: U.S. Geological Survey Miscellaneous Investigations Series Map I–1492, scale 1:24,000.

———1987, Geologic map and structure sections of the northern part of the Dragoon Mountains, southeastern Arizona: U.S. Geological Survey Miscellaneous Investigations Series Map I–1662, scale 1:24,000.

Drewes, Harald, and Brooks, W.E., 1988, Geologic map and sections of the Pedregosa Mountains quadrangle, Cochise County, Arizona: U.S. Geological Survey Miscellaneous Investigations Series Map I–1827, scale 1:48,000.

Drewes, Harald, du Bray, E.A., and Pallister, J.S., 1995, Geologic map of the Portal quadrangle and vicinity, Cochise County, southeast Arizona: U.S. Geological Survey Miscellaneous Investigations Series Map I–2450, scale 1:24,000.

Drewes, Harald, Houser, B.B., Hedlund, D.C., Richter, D.H., Thorman, C.H., and Finnell, T.L., 1985, Geologic map of the Silver City 1° × 2° quadrangle, New Mexico and Arizona: U.S. Geological Survey Miscellaneous Investigations Series Map I–1310–C, scale 1:250,000.

Finnell, T.L., 1971, Preliminary geologic map of the Empire Mountains quadrangle, Pima County, Arizona: U.S. Geological Survey Open-File Report 71–106, scale 1:48,000.

Gilluly, James, 1956, General geology of central Cochise County, Arizona, *with sections on* Age and correlation by A.R. Palmer, J.S. Williams, and J.B. Reeside, Jr.: U.S. Geological Survey Professional Paper 281, 169 p.

Goudarzi, G.H., compiler, 1984, Guide to preparation of mineral survey reports on public lands: U.S. Geological Survey Open-File Report 84–0787, 42 p.

Hayes, P.T., 1982, Geologic map of the Bunk Robinson and Whitmire Canyon Roadless Areas, Coronado National Forest, New Mexico and Arizona: U.S. Geological Survey Miscellaneous Field Studies Map MF–1425–A, scale 1:62,500.

Hayes, P.T., and Raup, R.B., 1968, Geologic map of the Huachuca and Mustang Mountains, southeastern Arizona: U.S. Geological Survey Miscellaneous Geologic Investigations Map I–509, scale 1:48,000.

Keith, W.J., and Theodore, T.G., 1975, Reconnaissance geologic map of the Arivaca quadrangle, Arizona: U.S. Geological Survey Miscellaneous Field Studies Map MF–678, scale 1:62,500.

Lucarelli, Ludano, 1967, Mapa geologico de la parte septemprional del estado de Sonora (Sheet 7): Unpublished map series of the Consejo de Recursos Naturales No Renovables and of the United Nations, scale 1:100,000.

Mardirosian, C.A., 1977, Mining districts and mineral deposits of Arizona (2nd ed.), private publication, press not identified, scale 1:1,000,000.

McIntyre, D.H., 1988, Volcanic geology in parts of the southern Peloncillo Mountains, Arizona and New Mexico: U.S. Geological Survey Bulletin 1671, 18 p.

Pallister, J.S., and du Bray, E.A., 1994, Geologic map of the Fife Peak quadrangle, Cochise County, Arizona: U.S. Geological Survey Geologic Quadrangle Map GQ–1708, scale 1:24,000.

Pallister, J.S., du Bray, E.A., and Latta, J.S., IV, 1994, Geologic map of the Rustler Park quadrangle, Cochise County, Arizona: U.S. Geological Survey Geologic Quadrangle Map GQ–1696, scale 1:24,000.

Peterson, J.A., ed., 1990, Preliminary mineral resource assessment of the Tucson and Nogales 1° × 2° quadrangles, Arizona: U.S. Geological Survey Open-File Report 90–276, 129 p., 24 pls., scale 1:250,000.

Richter, D.H., Sharp, W.N., Watts, K.C., Raines, G.L., Houser, B.B., and Klein, D.P., 1986, Maps showing mineral resource assessment of the Silver City 1° × 2° quadrangle, New Mexico and Arizona: U.S. Geological Survey Miscellaneous Investigations Series Map I–1310–F, scale 1:250,000.

Riggs, N.R., Haxel, G.B., and Busby-Spera, C.J., 1990, Paleogeography and tectonic setting of the Jurassic magmatic arc in southern Arizona—Progress and problems: Geological Society of America Abstracts with Programs, v. 22, no. 3, p. 78.

Simons, F.S., 1964, Geology of the Klondyke quadrangle, Graham and Pinal Counties, Arizona: U.S. Geological Survey Professional Paper 461, 173 p., map scale 1:62,500.

———1974, Geologic map and sections of the Lochiel and Nogales quadrangles, Santa Cruz County, Arizona: U.S. Geological Survey Miscellaneous Investigations Series Map I–762, scale 1:48,000.

Thorman, C.H., Drewes, Harald, and Lane, M.E., 1981, Mineral resources of the Rincon Wilderness Study Area, Pima County, Arizona: U.S. Geological Survey Bulletin 1500, 62 p., scale 1:48,000.

Vine, J.D., Asher-Bolinder, Sigrid, Morgan, J.D., and Higgins, Brenda, 1979, Lithologic log and lithium content of sediments penetrated in a test boring drilled on Willcox playa, Cochise County, Arizona: U.S. Geological Survey Open-File Report 79–397, 16 p.

Wilson, E.D., Moore, R.T., and Cooper, J.R., 1969, Geologic map of Arizona: U.S. Geological Survey map, scale 1:500,000.

Wrucke, C.T., and Bromfield, C.S., 1961, Reconnaissance geologic map of part of the southern Peloncillo Mountains, Hidalgo County, New Mexico: U.S. Geological Survey Mineral Investigations Field Studies Map MF–160, scale 1:62,500.

Geology of Coronado National Forest

By Harald Drewes

MINERAL RESOURCE POTENTIAL AND GEOLOGY OF CORONADO NATIONAL FOREST, SOUTHEASTERN ARIZONA AND SOUTHWESTERN NEW MEXICO

Edited by Edward A. du Bray

U.S. GEOLOGICAL SURVEY BULLETIN 2083–B

UNITED STATES GOVERNMENT PRINTING OFFICE, WASHINGTON : 1996

CONTENTS

FIGURE

Geology of Coronado National Forest

By Harald Drewes

ABSTRACT

The geology of the 12 units that compose Coronado National Forest is highly variable and reflects the complex geologic history of this area. In addition, the separate Forest units have been uplifted and eroded to varying degrees, exposing geologic features from various levels within the crust. Thus, the geologic record in areas that have been strongly uplifted and deeply eroded (mountain ranges) is well exposed, whereas the record is largely concealed in areas that have been downdropped (valleys).

In this chapter an overview of the geology of Coronado National Forest is followed by descriptions of the geology of each Forest unit. I have emphasized identification of the geologic features that are favorable for the occurrence of ore deposits. In particular, favorable host rocks, intrusive rocks and their associated hydrothermal systems, and structural features that acted as conduits for ore-forming fluids are described. Favorable host rocks are mainly lower Paleozoic and Upper Cretaceous to lower Tertiary andesitic to dacitic volcanic and volcaniclastic rocks. Late Cretaceous to early Tertiary intrusive rocks are most closely associated with ore deposits of the region and are typically multiphase, range in composition from diorite to granite, and form stocks, plugs, and dikes. Jurassic and middle Tertiary stocks and plugs are less commonly associated with ore deposits, and, with one exception, these deposits are small. Ore deposits are localized along or near steeply dipping, northwest-striking faults that have a long history of reactivation. At deep structural levels ore deposits and intrusive bodies are more likely to be localized by these structures, whereas at shallower levels deposits and intrusive rocks may spread laterally along subordinate structures. In some places, steeply dipping structures that trend in directions other than northwest have also guided ore-bearing fluids.

About $20 billion worth of metallic commodities have been produced from the region including and extending 80 km around individual Coronado National Forest units. Most of this production came from non-Forest lands, which reflects the fact that original Forest boundaries were drawn to exclude mining districts. Subsequently, mineral exploration and mining activity resulted in many mining districts extending into Forest units. In addition, Forest lands may include many sites favorable for undiscovered deposits.

The most prolific mineralizing systems are composites of several model types. Local characteristics of these deposits vary with proximity to the heat source, abundance of fluids, host rock, the variety of metals in the mineralizing fluids. Thus, skarn replacement deposits, which are present adjacent to porphyry and stockwork deposits in carbonate rocks that host the plutonic rocks, grade into more restricted stockwork and pipe deposits or diffuse fissure veins as distance to magmatic sources increases. Vein and hot spring silica replacement deposits commonly form on distal margins of many hydrothermal systems. Some parts of the Forest have been affected by multiple mineralizing events, which complicates categorization of ore deposit types.

INTRODUCTION

Much of the geologic record in the Coronado National Forest region is preserved in packages of sedimentary and volcanic rocks that compose seven major sequences (pls. 2–4). These sequences are separated from one another by major regional unconformities that represent periods of erosion or nondeposition and possibly of tilting or other deformation (fig. 1). Their combined thickness is probably more than 10 km, but nowhere do they all occur together because of irregularities in their initial thickness, in local erosion, and in their subsequent deformation. These layered rocks were intruded in many places by igneous rocks during at least five major magmatic episodes.

The oldest sequence consists of sedimentary and volcanic rocks known as the Pinal Schist and locally some gneiss, both of Early Proterozoic age (sedimentary sequence 1, fig. 1). This formation consists of graywacke, siltstone, shale, and quartzite; locally it includes pyroclastic rocks, lava flows, and rhyolitic to dioritic intrusive rocks. Commonly, the Pinal Schist is metamorphosed to a greenschist facies assemblage and its fabric is that of schist or phyllite. Although not abundantly mineralized, in some places the Pinal Schist hosts quartz veins and aplite pods, some of which contain gold, base metals, or thorium.

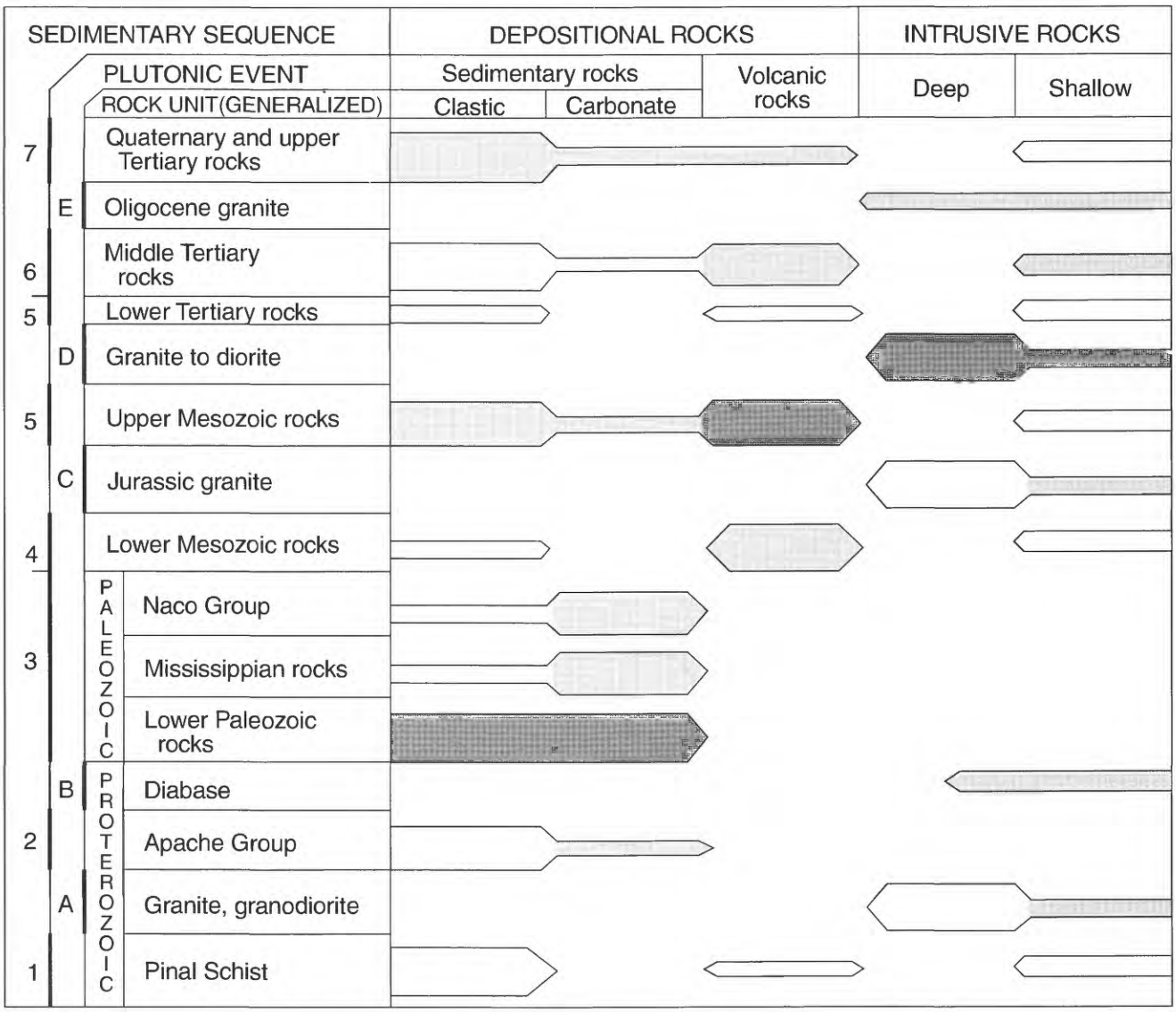

Figure 1. Summary of rocks in the Coronado National Forest region, southeastern Arizona and southwestern New Mexico, showing their relative abundance (thickness of bar) and relative importance to the occurrence of mineral deposits and economic materials (shading of bar, the darker being the more important rock).

Granitic rocks of the first major magmatic episode intruded the Pinal Schist (plutonic event A, fig. 1). These rocks are commonly very coarse grained, and many are porphyritic or porphyroblastic. Their compositions range from alaskite to granodiorite, and some host aplite and lamprophyre bodies. No contact metamorphic halos have been reported for the Pinal Schist. The Pinal Schist, granites, and gneiss make up the basement rocks; they have been strongly uplifted and deeply eroded.

The second sequence of sedimentary rocks is the Middle Proterozoic Apache Group, (sedimentary sequence 2, fig. 1), which unconformably overlies the basement rocks. Apache Group rocks, 305 m thick in the northern part of the Forest region, are marine and fluvial deposits that thin gradually southward, and just north of Interstate Highway 10 they have been completely removed by erosion. Apache Group rocks in the Forest region include the basal Pioneer Shale, the Dripping Spring Formation (typically a sandstone), and possibly, in one Forest unit, Mescal Limestone. The Pioneer Shale and Dripping Spring Formation are not known to host ore deposits in the region, but elsewhere in Arizona (Ray porphyry copper deposit, near Winkleman, see Chapter A, this volume, fig. 1) the Pioneer Shale hosts some ore. In addition, the Mescal Limestone could be a favorable host for skarn and replacement deposits and the thin conglomerate at the base of the Pioneer Shale may have potential for paleo-placer gold deposits.

A few small diabase or metadiorite intrusive bodies, associated with the Apache Group and nearby parts of the Pinal Schist, were emplaced during the second magmatic

event (plutonic event B, fig. 1). North of the Forest region, where these rocks intrude and alter dolomite, they were emplaced 1,050–1,200 Ma and are genetically associated with asbestos deposits. After intrusion of the diabase the region was strongly uplifted, tilted gently northward, and deeply eroded to a surface of very low relief.

The third sedimentary sequence, divided here into lower, middle, and upper parts, comprises Paleozoic clastic and carbonate rocks mainly of marine origin but including some of fluvial origin (sedimentary sequence 3, fig. 1). Some of these rocks are hosts for major mineral deposits, and some are potential source and reservoir rocks for oil and gas. Several disconformities, which are more numerous to the west than to the east, mark periods of nondeposition and (or) erosion. The sequence is about 1,500 m thick in much of the region and thickens slightly to the southeast.

The lower part of the Paleozoic sequence is the most common host to ore deposits in the region. In ascending stratigraphic order, it comprises the Middle Cambrian Bolsa Quartzite (or its partial correlative, the Middle and Upper Cambrian Coronado Sandstone), the Middle and Upper Cambrian Abrigo Formation (the Lower Ordovician and Upper Cambrian El Paso Formation in the eastern part of the Forest area), and the Upper Devonian Martin Formation (or its correlative units, the Swisshelm Formation, Portal Formation, or Percha Shale, in the eastern part of the Forest area). Quartzite, arkose, conglomerate, sandstone, siltstone, and calcareous or glauconitic beds characterize the Bolsa. The Abrigo is composed of thin beds of shale, siltstone, sandstone, and limestone, whereas the El Paso is commonly thin- to medium-bedded dolomitic limestone, dolomite, limestone, and some siltstone. The Martin Formation contains abundant limestone and dolomite and some shale and sandstone. In contrast, units correlative with the Martin contain more limestone and dolomite (Swisshelm Formation), consist of interbedded gray shale and thin limestone (Portal Formation), or are largely black shale (Percha Shale). The rocks of the lower part of the Paleozoic sequence were readily metamorphosed to skarn near stocks and in most Forest units are an excellent host rock for skarn and replacement deposits.

The middle part of the Paleozoic sequence is commonly a single thick formation composed of thick-bedded Mississippian Escabrosa Limestone that disconformably overlies Devonian rocks. In the eastern part of the Forest area the Upper Mississippian Paradise Formation is a thin shale and limestone unit that overlies the Escabrosa Limestone and is also part of the middle Paleozoic sedimentary rock unit. The Escabrosa Limestone is commonly recrystallized in many places, locally dolomitized, but rarely mineralized. A major exception is at the Bisbee porphyry copper deposit, where the Escabrosa is a major ore host. Locally, it is metamorphosed to marble that has been quarried for dimension stone, ornamental or roofing stone, or flux.

The upper part of the Paleozoic sequence comprises the Pennsylvanian and Lower Permian Naco Group, which disconformably overlies Mississippian rocks. At the base of the Naco Group is the Pennsylvanian and Lower Permian Horquilla Limestone, a thick formation of thin- to medium-bedded limestone and some interbedded siltstone. The Horquilla is the youngest Paleozoic formation in many of the Forest units. Elsewhere, however, especially in the central and eastern parts of the Forest region, the Horquilla Limestone is overlain, in ascending order, by Lower Permian formations including the Earp Formation (shale, marlstone, and some limestone), Colina Limestone, Epitaph Dolomite, Scherrer Formation (sandstone and sparse dolomite), Concha Limestone, and Rainvalley Formation (mostly limestone and some dolomite and sandstone) all of the Naco Group. In some Forest units, the Horquilla is mineralized; elsewhere it is a source for cement rock. The other formations are neither mineralized in many places nor otherwise commercially utilized.

The fourth sedimentary sequence comprises lower Mesozoic strata that mark a change from chiefly Paleozoic marine conditions to a subaerial environment in which clastic and volcanic rocks were deposited (sedimentary sequence 4, fig. 1). This deposition was preceded, accompanied, and followed by erosion; most of these rocks reflect regional conditions, but some are responses to local raising of blocks. The oldest rocks of this sequence include rhyolite welded ash-flow tuff and lava, some andesite lava, and minor wind-blown sandstone (Hayes and Raup, 1968; Drewes, 1971a, b, c, 1981a; Cooper, 1973; Riggs and others, 1990). The Triassic and Jurassic Mount Wrightson Formation is mainly rhyolite and subordinate andesite and sandstone and is at least 835 m thick. The Lower Jurassic Gardner Canyon Formation (red beds, sandstone, and some conglomerate) overlies the Mount Wrightson Formation (Drewes, 1971c; 1972b). The Canelo Hills Volcanics, of Late Triassic and Early Jurassic age, overlie the Gardner Canyon red beds and are primarily rhyolite tuff (Hayes and Raup, 1968). Locally, in the central part of the Forest region, clastic beds of the Triassic or Jurassic Walnut Gap Formation are rich in angular volcanic clasts and record nearby volcanism (Cooper and Silver, 1964; Drewes, 1987). Some intrusive rocks associated with these volcanic rocks are present in the western ranges of the Forest. In a few parts of the Forest region, some of these rocks are mineralized. Vents for the andesitic rocks of the Mount Wrightson Formation and brittle rhyolitic rocks in strongly faulted areas are moderately favorable as ore deposit hosts.

A third magmatic event is represented by a set of Late Jurassic granitic rocks that intruded the early Mesozoic and older rocks in the western and southern parts of the Forest region (plutonic event C, fig. 1). The first stocks were emplaced about 185 Ma; most were emplaced 165–140 Ma. These rocks are typically medium to coarse grained; the oldest bodies are monzonite and the others granite; one small

stock at Bisbee is composed of fine-grained granite. Except for scattered occurrences of pyrite, the stocks are barren. Areas of mineralized Late Jurassic stocks in other ranges are apparently associated with younger plutonism.

The fifth sedimentary and volcanic sequence is of late Mesozoic age and locally also includes some early Tertiary-age units (sedimentary sequence 5, fig. 1). These rocks unconformably overlie Jurassic granite and older rocks, and are primarily clastic marine, lacustrine, and fluvial deposits, including some subordinate limestone. A thin (0.3–9 m) basal conglomerate of the Bisbee Group of Early Cretaceous age indicates an environment dominated by low topography in a flood plain, but a few uplifts were present as indicated by locally thick conglomerate (Hayes, 1970a, b; Drewes, 1981a, 1991; Drewes and Dyer, 1989). During Bisbee Group time, an arm of the sea encroached upon the southern part of the Forest region from the southeast, resulting in deposition of reef limestone and lagoonal limestone and shale in the southeastern and central parts of the Forest area, respectively. Fluvial deposition, primarily of gray silt and mud derived from deformed, volcanic-capped mountains to the west, and augmented by some locally derived sand from nearby small uplifts formed in front of an advancing belt of deformed rocks (Drewes and Dyer, 1989; Drewes, 1991), and filled a basin with at least 2,130 m of sediment. Additional clastic beds, which include mostly fluvial beds that became coarser and richer in volcanic clasts upward and some intermontane lacustrine beds, all of Late Cretaceous age, unconformably overlie the Bisbee Group. These include the Fort Crittenden Formation to the west, the Pinkard Formation to the north, and the formation of Javelina Canyon of Epis (1956) to the east.

An advancing deformation front disrupted these depositional conditions, and andesitic to rhyolitic volcanic rocks were deposited on the deformed Cretaceous and older rocks. Andesitic lava and breccia derived from formations such as the lower member of the Salero Formation and the Silver Bell Formation formed a thick cover to the west and a more fragmentary one to the east, especially around composite and shield volcanos. Rhyolite tuffs, probably related to caldera formation about 70 Ma, were deposited around a few volcanic centers, but locally were contemporaneous with andesitic volcanism that largely followed caldera development. In the eastern Forest units, these tuffs thin markedly and have not been found in New Mexico. Locally, the volcanic rocks include coarse and (or) exotic-breccia deposits. To the west, the rhyolite tuffs are known as the upper member of the Salero Formation (Drewes, 1971c) or the Cat Mountain Tuff (Cooper, 1973; Drewes, 1981a; Hagstrum and Lipman, 1991).

During Late Cretaceous to Eocene time, a fourth set of granitic rocks was emplaced (plutonic event D, fig. 1). Igneous rocks of this age were emplaced during the Laramide (or Cordilleran) orogeny and are commonly referred to as "Laramide." These stocks are abundant, multistage, and variable in composition, having wide (hundreds of meters to kilometers) contact metamorphic halos, and are closely associated with major ore deposits. The rocks of this event range in age from 75 to 52 Ma; most are 71–65 Ma. The stocks to the east are slightly younger than those to the west, and they are generally smaller and have fewer igneous phases. Compositions of stocks range from granite to diorite, and plugs range from quartz latite to dacite. Stocks and related plugs of fine-grained rocks are associated with mineralized rock in some Forest units. In some places, the 69- to 67-Ma stocks are associated with mineralized rock, but in most places mineral deposits are associated with slightly younger intrusions. The types of mineral deposits associated with these rocks include skarn, porphyry, and extensive stockwork, breccia pipes, massive replacement deposits, and veins. Many of these types of mineral deposits have secondary enrichment capping zones and polymetallic manto-type deposits.

The sixth sequence of sedimentary and volcanic rocks is of mid-Tertiary (Oligocene and early Miocene) age (sedimentary sequence 6, fig. 1). The sedimentary rocks are mostly clastic, of local provenance, and rich in volcanic material. Some of them are local stream deposits within a volcanic sequence and mark a break in nearby volcanism. Others fill, or partly fill, large structural basins and characteristically have a coarse clastic facies along the basin margins and fine clastic facies elsewhere in the basins; they commonly have local evaporate facies toward the basin centers. The volcanic rocks form extensive sheets around dispersed volcanic centers, some of which are calderas. Many volcanic sequences have andesitic or dacitic rocks at the base, abundant rhyolite ash-flow tuff in the middle, and in some places, basaltic andesite at the top. Some of these rocks near certain vents or caldera margins are mineralized, typically with vein or pipe deposits that contain precious metals. Fluorite, industrial clays, and some building materials have been obtained from these rocks at scattered sites.

The fifth and youngest magmatic event involved emplacement of granitic rocks into rocks as young as the middle Tertiary volcanic rocks with which they are genetically associated (plutonic event E, fig. 1). Typically, these granites form small unevolved stocks. The large stock in the Dragoon Forest unit is of exceptional size, contains a low abundance of mafic minerals, and contains primary fluorite. Fine-grained rhyolitic plugs and dike swarms are associated with these stocks. Some mark volcanic vents and caldera ring structures. Pyrite is the most common sulfide mineral in these intrusive rocks; base metals are present but their abundances are unimportant compared to those of gold or silver. These precious metals are present mainly in vein systems and small stockwork or pipe deposits in highly fractured and altered volcanic rocks.

The seventh and youngest sequence of sedimentary and volcanic rocks overlies the middle Tertiary deposits and post-dates most Basin and Range faulting. These deposits are mainly sand and gravel along the margins of intermontane

valleys, where they form extensive alluvial-fan aprons, and silt and clay in the valley centers. Basalt lava flows and cinder cones are interbedded with, or overlie, the sand and gravel of the easternmost intermontane valleys. Two valleys also contain beach and lacustrine deposits. Gravel, sand, and cinder deposits are the chief source of road metal and aggregate material; most of the production and consumption of these materials is near Tucson.

ROCK ALTERATION

Sedimentary, volcanic, and intrusive rocks described in the preceding section are altered in some places; evaluation of this alteration bears on the Coronado National Forest resource assessment. Nearly all rock types of the Forest region are indurated sufficiently to fracture under stress and therefore are potential hosts to vein deposits. The chief exceptions are many of the sedimentary rocks and most of the tuffs of the sixth sequence (middle Tertiary), most sedimentary rocks of the youngest sequence, and, in a few places, marl beds of the Lower Permian Earp Formation. These unindurated deposits can be mined easily as placers where they contain mineral deposits.

Sequences of limestone are recrystallized, and some have been dolomitized by various processes. In most cases, recrystallization reduces rock permeability and thereby its favorability as a host for replacement deposits and as reservoir rock for hydrocarbon accumulations. The Escabrosa Limestone is coarsely recrystallized and rarely mineralized. However, the Escabrosa and overlying Horquilla Limestone of southwestern New Mexico contain dolomitized masses that are viewed as favorable sites for hydrocarbon accumulation because dolomitization greatly enhances rock porosity and permeabilty (Thompson and others, 1978; Thompson and Jacka, 1981). The thermal maturation index, indicated by the color of conodont fossils, provides a measure of a rock's thermal history. In a review of the Horquilla Limestone, Wardlaw and Harris (1984) showed that most of the Forest region has a maturation index of 2 or 3, which is viewed as adequate for generation of oil but is submarginal for natural gas. The samples that were studied were probably collected from sections that are tectonically undisturbed. If so, higher maturation indices may be anticipated in the abundant, tectonically disturbed rocks of the Forest region.

Rock alteration has included both thermal metamorphism and hydrothermal alteration. In the Forest region five types of alteration, of diverse intensity and age, have been documented. In some places rocks have been variably affected by several kinds of alteration. Some of these altered rocks have no relation to mineral deposits, whereas others are closely associated with certain types of deposits.

In the earliest form of alteration, a load- and deformation-generated, regional or nearly regional metamorphic process altered the oldest Proterozoic basement rocks to schist or phyllite (Pinal Schist), but in some places some Proterozoic granitic rocks were metamorphosed to gneiss. Typically, these rocks were metamorphosed to low-grade greenschist facies, and some subsequently underwent retrograde metamorphism. No mineral deposits are known to have been directly associated with this form of metamorphism, but low-sulfide gold-quartz veins can be associated with regional metamorphism.

Contact metamorphic halos around Mesozoic and Cenozoic intrusions constitute a second product of alteration. These altered rocks form sheaths or halos tens to hundreds of meters wide around intrusions. Contact metamorphic effects vary in intensity between intrusive centers and commonly decrease in intensity with increasing distance from the intrusive center. Within these halos, shale was converted to argillite or phyllite; pure limestone was metamorphosed to marble; and impure limestone, shale, and sandstone were metasomatically transformed to skarn, much of which contains concentrations of ore minerals.

A third kind of metamorphic condition resulted from tectonism. Rocks so affected may have a slaty cleavage. At two sites, in the Chiricahua and the Dragoon Mountains, metamorphism reached medium grade or amphibolite facies conditions; this metamorphism was not related to intrusive activity (Drewes, 1984a, 1987). Locally, carbonaceous shale was altered to graphite and the Escabrosa Limestone to marble.

A fourth kind of metamorphic environment is found in the gneiss-cored domes of the Pinaleno, Rincon, and Santa Catalina Mountains. The rocks in the cores of these domes are mainly Proterozoic. In the Rincon and Santa Catalina Mountains the core rocks were massively invaded by two-mica granite plutons of Late Cretaceous or Paleocene age. Overlying the core rocks are as many as three major thrust plates of Paleozoic and Cretaceous strata separated by low-angle faults (Drewes, 1974, 1977; Davis, 1975, 1979, 1983; Thorman and others, 1981). Core rocks and generally also the lower thrust plate were metamorphosed in response to both thermal and tectonic conditions. The core rocks are foliated, lineated, and in places protomylonitized and sheared, probably due to two tectonic events. Most lower-plate rocks (primarily Paleozoic) were altered to calc-silicate minerals or were recrystallized. Most of these changes took place beneath a thick cover, and hence are old (perhaps Paleocene or older). Following deep erosion of the cover and emplacement of the latest phases of the two-mica granites, tectonic overprinting occurred under a thin cover (Drewes, 1977, 1991; Drewes and Dyer, 1989). The core rocks are mostly barren of ore deposits and mineralized zones in the cover rocks are minor.

Hydrothermal alteration was pervasive in some mining districts. The primary characteristics of this alteration are best documented in those districts that contain porphyry copper deposits. Sericitic and kaolinitic alteration of feldspathic rock and propylitic alteration of andesitic rock are

evident in scattered localities throughout the Forest region. This type of alteration may represent either locations near volcanic vents or locations peripheral to more complex hydrothermal systems that may have affinities to porphyry copper systems. Potassic and ferric oxide alteration, particularly where associated with alunite, are of great interest because effects of this are typically well developed around disseminated sulphide systems.

STRUCTURAL FEATURES

Rocks of the Coronado National Forest region were deformed several times under various conditions, which resulted in an extremely complex geologic record. Small and medium-size folds are sparse, but faults of diverse displacement and kinds are abundant. Folds are of only local interest in the assessment of the region's mineral and energy resources. Faults, however, provided some key controls to the siting of mineral deposits. In particular, steeply dipping, northwest-striking faults have a recurrent and diverse (with respect to sense of offset) history of movement and are the master faults along which many magmas and hydrothermal fluids moved, especially at deep levels. Steeply dipping faults of other orientations, typically having a simpler history of movement, as well as thrust faults, further guided the upward and outward dispersal of hydrothermal fluids at shallow levels.

Folds in the study region but not within the Forest, such as the one southwest of the Whetstone Mountains and those southeast of Tombstone (Drewes, 1980), have been the target of a few wildcat oil wells. Folds in the Bisbee Group, especially shattered zones along anticline hinge lines, may have helped channel ore fluids at Tombstone (Butler and others, 1938). Other folds may assist exploration efforts at the local scale, but these structures are either too few, too small, or too poorly known to assist regional ore or energy resource exploration.

Faults in the Forest region played a major role in both regional and local controls in the accumulation of metals, and they may provide an unusual situation for entrapment of oil and gas. For the purpose of this study, faults are grouped into steeply dipping northwest-striking structures, steeply dipping faults of other orientations, gently dipping faults of compressional stress origin (thrust faults), and gently dipping faults of extensional origin (gravity, glide, or detachment faults).

Northwest-striking fault zones range in width from single planes and narrow zones to broad zones and sets of splay faults, many of which flare out to the southeast. Narrow fault zones are hosted most commonly by basement rocks, and the broadest fault zones and splay zones are in the overlying Paleozoic and Mesozoic rocks. This type of lateral variation may also reflect vertical variation, such that fluids moving in the fault zone would have been dispersed both laterally and vertically.

The evidence of age and direction of movement along the northwest-striking faults varies from place to place (Drewes, 1981a). In most cases the largest fault offsets are in basement rocks and the smallest ones are in the youngest cover rocks. Along several of these faults the thicknesses of Mesozoic sedimentary rocks indicate an abrupt increase or recurrent increases in local relief and thus imply normal faulting. Thus, evidence of early, major displacements are easily concealed beneath young rocks that depict subsequent, small displacements only.

That northwest-striking faults are loci for fluid movement is indicated by the many stocks, plugs, and dikes emplaced along or near them. The Apache Pass fault zone of the Chiricahua and Dos Cabezas Mountains, which contains 10 stocks, many plugs and dikes, and three volcanic centers, is the best example of fluid channelling by a northwest-trending fault. Indeed, in the Santa Rita Mountains so many large stocks were injected along one zone that for tens of kilometers the fault is obliterated and therefore referred to as a fault scar (Drewes, 1971b, 1972b, 1980). The association of mines or mining districts and northwest-trending faults is particularly well developed along the Apache Pass fault zone and the Santa Rita fault scar–Harshaw Creek fault zone. Most mines or mining camps not near northwest-trending faults are in young cover rocks, typically the volcanic rocks of sequence 6.

Rocks of the Forest units are also cut by high-angle faults that trend in directions other than northwest. Within some mining districts of the region, ore deposits are present along these structures, many of which are minor sympathetic structures that cut, or abut, the northwest-striking faults. Most are narrow fault zones or discrete fault planes and have a simple history of normal movement during the Mesozoic or Tertiary. Some of these fault zones acted as dispersal systems for fluids rising along the master faults.

Low-angle faults cut rocks of the Forest and include thrust faults of Late Cretaceous to early Tertiary age and low-angle normal faults (detachment, glide, or gravity faults) of middle Tertiary or younger age. The presence of both types of faults is generally accepted, but assignment of specific faults to compressional or extensional origins and amounts of movement attributed to these classes of faults receive various interpretation. The older of these structures caused dispersal of ore fluids near master faults. In some Forest areas extensional faults are interpreted to have utilized and reactivated older thrust faults (Drewes, 1976, 1977, 1978, 1981a).

Age and depth of cover beneath which low-angle faults of the Forest region formed are significant with regard to ore genesis. The low-angle normal faults are mostly Miocene or younger; a few may be Oligocene. The age of most ore deposition in the Forest region is Paleocene or older, but some is Oligocene. Therefore, the low-angle normal faults were not

available, with perhaps a few minor exceptions, to the hydrothermal systems of the Forest region. Extensional faults cut mineralized rock in many places, as has been inferred in the Sierrita Mountains, where the San Xavier (gravity) fault offsets a major porphyry copper deposit from its root (Cooper, 1973). These faults formed beneath a 0.8- to 1.6-km-thick cover over a broad region (Frost and Martin, 1982), whereas thrust faults formed as deep as 8 km, and so were more accessible to the many ore-associated stocks and related hydrothermal systems, emplaced at depth of 3–6 km.

AREA GEOLOGY

Each of the Forest areas has certain unique geologic features that bear on resource potential. Favorability for undiscovered deposits, as indicated by geologic factors, is partitioned into high, medium, and low categories, which have three or more, two, or one or zero, respectively, geologic factors that are favorable for the presence of undiscovered deposits. The geology of the 12 Forest units is described in this section, beginning with a geologically simple situation in the northernmost area, and continuing in clockwise order to areas of more complex geology and ore deposits.

SANTA TERESA MOUNTAINS

The geology of the Santa Teresa Mountains includes many features common to the Forest region but lacks the complications of several Forest units (pls. 1 and 2). Some rocks that underlie the Santa Teresa Mountains are favorable as hosts for ore deposits. These rocks are cut by northwest-trending steep faults and are intruded by a granite stock of Late Cretaceous or early Tertiary age (Ross, 1925; Simons, 1964; Blacet and Miller, 1978; Wilson and others, 1969). The Aravaipa mining district, on the western flank of the mountains, produced $1–10 million worth of copper, lead, zinc, and silver, largely from vein and polymetallic replacement deposits.

Paleozoic rocks crop out along the northwestern part of the Forest unit in fault-bounded and intrusive body-bounded blocks west of the stock, in remnants of fault plates (klippen) on the northeast mountain flank, and in scattered blocks along steep faults. The first of these, west of the stock, is by far the most intensely mineralized. The Abrigo Formation of the lower Paleozoic sedimentary rock unit (map unit PzI) is absent in this Forest unit, and the overlying Martin Formation is barren. The Escabrosa Limestone (Ms) and Horquilla Limestone (PIPn), next in ascending stratigraphic order, are the rocks most favorable as potential ore deposit hosts.

The Escabrosa Limestone contains large bodies of red silica rock (jasperoid) formed by massive replacement of the limestone, and the Horquilla Limestone contains smaller replacement skarn bodies. Replacement deposits are among the major ore deposits of this Forest unit. Subsurface projections of these formations beneath Cretaceous sedimentary and volcanic rocks (map unit Ksv) of the west flank of the mountains are also potential sites for ore deposits. The klippen northeast of the mountains appear to be unmineralized; this may reflect either inadequate data or the possibility that the klippen were not transported from a mineralized area. The blocks or fault slices of Paleozoic rock in or near the stock are possible sites of mineralized rock; those north of the stock are along a fault not known to be in contact with the stock and thus are less likely to have been mineralized.

Upper Cretaceous or lower Tertiary volcanic rocks may indicate the fragments of old volcanic centers, which are favorable as hosts to stockwork, breccia pipe, and vein deposits. Most of the mineral deposits of the Aravaipa district are vein deposits in rhyolitic rocks (pl. 2, map unit Kr). The andesitic unit (Ka) was described by Simons (1964) as containing plug-like bodies that may mark vent sites of ancient volcanos.

Northwest-trending, steeply inclined faults are predominant in the Santa Teresa Mountains, and, although they are not through-going structures, as in most other Forest units, they have served as the principal conduits for hydrothermal solutions (pl. 2). The Goodwin Canyon and Grand Reef faults are the major faults; the Tule Spring and Tule Canyon faults are important branches of the Grand Reef fault. Many major mines lie along these faults, and others lie along a maze of smaller northeast-trending faults near the Goodwin Canyon fault in the core of the Aravaipa mining district.

The faults coincident with the three major mines, Cobre Grande, Grand Reef, and Ben Hur mines, illustrate the various (proximal through distal relative to the heat source) types of ore deposits that may derive from a single large hydrothermal system. The Cobre Grande deposits are replacements in silicified limestone and skarn; sulfide ores of copper and lead are common, silver is sparse, gold is absent, and pyrite is minor. At the Grand Reef mine, ore is in a 45-m-wide silicified breccia reef. The ore includes sulfides of copper, lead, and zinc; silver is abundant; gold is minor; the gangue includes quartz and minor fluorite; and oxidized ore is abundant. The Ben Hur mine is in quartz veins at the intersection of several fault sets. Ore is partly sulfides of lead and zinc; silver concentrations are moderately high and gold abundance is 0.07 oz per ton; fluorite, specularite, and quartz are the gangue minerals; oxidized minerals are predominant. These three deposits represent, respectively, mesothermal metasomatic replacement deposits, upper-level mesothermal to lower-level epithermal vein deposits, and upper-level epithermal vein deposits. Ore deposition in each deposit was strongly controlled by northwest-striking master faults. Mesothermal metasomatic replacement deposits formed at deep intersections between the fault and the margin of the stock. Upper-level mesothermal to lower-level epithermal vein deposits represent the mid-level zone, in which the master fault zone is dominant.

Upper-level epithermal vein deposits formed as shallow deposits where the master fault zone is diffuse and splays upward to several subordinate faults.

The Santa Teresa stock is a multiphase granitic stock of Late Cretaceous age. It was emplaced following relatively mild compressive deformation of the host rocks. The magma evolved to granite and quartz monzonite phases. Its contact metamorphic halo is hundreds of meters to a few thousand meters wide. The associated polymetallic-replacement base-metal deposits contain silver and gold. Many dikes and plugs of rhyolite, quartz latite, and dacite cut Paleozoic sedimentary country rocks in the mining district but not the stock. The compositional variation among these fine-grained intrusive rocks is similar to that of the stock. The dikes appear to post-date ore deposition in that they are present at many mines but are not mineralized. The fine-grained intrusive rocks cut the andesite host but not the stock. These relations led Simons (1964) to infer that they are about the same age as, or a bit younger than, the stock and ore deposition and that all three features reflect one magmatic event. Some of the dikes may be middle Tertiary. Dikes and plugs associated with Late Cretaceous to Paleocene stocks are useful geologic features for locating magmatic centers and thus of possible associated ore deposits.

GALIURO MOUNTAINS

The geology of the northwestern Galiuro Mountains is similar to that of the Santa Teresa Mountains, whereas the central and southeastern part is underlain by middle Tertiary volcanic rocks (pls. 1 and 2). The Paleozoic rocks exposed in this area are the Martin Formation and Escabrosa Limestone. Small areas of these rocks are exposed stratigraphically below younger volcanic rocks and, although the Paleozoic rocks are silicified and altered, they are not mineralized. The Martin and Escabrosa underlie the volcanic rocks in much of the area. The Abrigo Formation, a highly favorable host for ore deposits, is probably beneath the Martin.

The geology of the rocks at the northwestern end includes andesitic rocks, which are favorable hosts for ore deposits; a granitic stock; northwest-striking faults; large tracts of altered rock; and intrusive plugs, dikes, and breccia pipes. These features were described by Darton (1925), Creasey and others (1961, 1981), Creasey and Krieger (1978), Krieger and others (1979), and Simons (1964).

The older rocks in the Bunker Hill, or Copper Creek, mining district are strongly mineralized; some of the middle Tertiary volcanic rocks are less intensely mineralized. A moderate amount of copper and molybdenum were produced from breccia pipes just outside the Forest in the Bunker Hill area. Creasey and others (1981) projected this favorable geologic environment into the Forest unit beneath the young volcanic cover. Minor mineral occurrences in the central part of the Galiuro Mountains, found near rhyolite plugs and in placers, contain base metals and gold.

The Upper Cretaceous Glory Hole Volcanics host mineralized rocks in the Bunker Hill mining district (pl. 2, map unit Ka). These volcanic rocks comprise lava flows and breccia sheets in a thick sequence interpreted to be part of a composite volcano (Creasey and others, 1981). Breccia pipes that contain andesitic clasts, but mostly lacking a volcanic matrix, cut the flows and breccia sheets; the pipes are not considered to be source vents for the flows and breccia sheets because of their nonvolcanic (sedimentary?) matrix and because of their younger, crosscutting relationships. One pipe cuts the stock that intrudes the Glory Hole Volcanics.

The age (68 Ma) and composition (granodiorite and subordinate quartz monzonite; Simons, 1964) of the Copper Creek Granodiorite (map unit TKg) are favorable for associated major mineral deposits. A contact metamorphic halo as much as 1.5 km wide surrounds the stock. Andesitic wallrock was altered to hornfels; amphibole replaced pyroxene, secondary biotite and chlorite was formed, and feldspar was sausseritized. Limestone was recrystallized and, locally, was silicified and metamorphosed to skarn. The granodiorite itself may be deuterically altered in places.

Northwest-striking steep faults are the main structures cutting the rocks of the Galiuro Mountains, but they are not as well developed as in other ranges. Mineralized rock is present along these faults, particularly the Rattlesnake fault, which extends for 30 km along the center of the range. For most of its length, this fault is a down-to-the-southwest normal fault of modest offset; to the northwest, en echelon faults extend the general zone of weakness into the terrane of older rocks. These structures may be a rejuvenated segment of a larger, deeper structure with a more complex history, comparable to certain segments of the Apache Pass fault (pl. 3). Most of the altered rock and mineralized tracts in the young volcanic rocks lie along the Rattlesnake fault (Creasey and others, 1981, pl. 1), which seems to have had a major influence on hydrothermal fluid movement.

In their resource study of the Galiuro Mountains, Creasey and others (1981, pl. 2) delineated four tracts of altered rock, some of which are beyond the limits of the Copper Creek district. Rocks in these altered tracts are pyritized, argillized, and sericitized, indicative of hydrothermal activity. In places, rocks in these tracts are enriched in base or precious metals, and to the southeast some anomalous abundances of tin and barium were reported (Creasey and others, 1981). These sites should be considered favorable for the presence of undiscovered deposits of the types associated with porphyry copper-molybdenum systems, and further study of them is needed.

The presence of small intrusive bodies, particularly of breccia pipes, further indicates a geologic environment favorable for undiscovered ore deposits. Only a few breccia pipes in the northwestern part of the Galiuro Mountains are mineralized; at least $0.5 million worth of copper and

molybdenum has been produced from four pipes in this area. Most of the pipes are in the Glory Hole Volcanics and along the contact between this andesite host rock and the intruding granodiorite, but one pipe is in the granodiorite. Clasts in the pipes are compositionally similar to the wallrocks, and the matrix is finely broken material also of similar composition. In a few places, latite porphyry dikes, like those in the adjacent volcanics, cut the pipe rocks. The more intensely mineralized pipes are those in the granodiorite and close to the stock, the localization suggesting a genetic link between the mineralized rock and the stock. The pipes are many tens to a few hundred meters across and appear to taper downward. Their richest ores comprise mainly hypogene minerals about 120–180 m beneath the present-day surface. These pipes and their mines were described in detail by Weed (1913), Kuhn (1941, 1951), and Denton (1947), who summarized the early studies.

Tracts favorable for the presence of ore deposits are indicated by the geologic factors just reviewed and are augmented by the studies of Creasey and others (1981). They proposed that favorable ground extends east of the core of the mining district because of alteration, pyritization, and copper "staining" in the area east of the mines along Copper Creek; a distal part of the hydrothermal system responsible for ore deposition in the Copper Creek district may be responsible for this alteration. However, the upper reaches of Fourmile Creek do not seem to be as favorable for the occurrence of undiscovered deposits because geochemical analyses of these altered rocks do not indicate an anomalous abundance of metal (see Chapter C).

WINCHESTER MOUNTAINS

The geology of the Winchester Mountains is simple (pls. 1 and 2), and geologic evidence indicates that most of the area has low mineral resource potential for the presence of undiscovered polymetallic replacement deposits (Keith and others, 1982). The entire Forest unit is underlain by Oligocene volcanic rocks; outside the area, to the southeast, older rocks and structures emerge from beneath the volcanic cover. A sequence of rhyolitic rocks, mostly welded ash-flow tuff and nonwelded air-fall tuff overlies an andesitic or dacitic volcanic unit and, in places, is overlain by basalt (Wilson and others, 1969; Cooper, 1960). These volcanic rocks are probably underlain throughout the area by faulted Paleozoic and Mesozoic rocks like those that crop out at the southeastern end of the mountains (Cooper and Silver, 1964; Drewes, 1981a, fig. 14).

The Paleozoic and Mesozoic rocks are cut by a major northwest-striking, steeply inclined fault. The fault may extend beneath the volcanic cover to the northwest to a point near Javelina Spring on the southwest flank of the mountains. A second northwest-striking fault cuts the Oligocene(?) volcanic cover 1.5 km northeast of the fault in the older rocks. These faults may merge near the spring and possibly continue from there to the northwest beneath the volcanic rocks. This suggested pattern of a basement flaw splaying to the southeast and having a simpler history in younger rocks than in older ones is consistent with that of the major faults.

A small area in the southeastern part of the Forest unit has moderate mineral resource potential for the presence of undiscovered polymetallic replacement deposits. Geologic features favorable for the occurrence of ore deposits outside the Forest unit can be projected beneath the volcanic rocks. These favorable conditions include northwest-trending faults, potential host rocks of Paleozoic age, and a rhyolite plug that intruded the fault.

PINALENO MOUNTAINS

The geology of the Pinaleno Mountains Forest unit is as varied as its topography (pls. 1 and 2). The main part of the unit, a high, rugged terrane, is underlain by gneiss and schist that are intruded by several Proterozoic granitic plutons. The low northwestern flank is underlain by Oligocene and Miocene sedimentary and volcanic rocks that are juxtaposed across a southwest-dipping, low-angle extensional fault; the footwall and hanging-wall rocks are cut by a Miocene and Oligocene rhyolite dike swarm. The moderately high southern foothills (Greasewood Mountain) are underlain by volcanic rocks of Oligocene and Miocene age plus late Oligocene granite and another rhyolite dike swarm (pl. 2). A southerly dipping low-angle fault juxtaposes the volcanic rocks against Proterozoic basement. A reconnaissance geologic map is available for the northwestern end of the mountains and its low foothills (Blacet and Miller, 1978), and Swan (1975) studied a major fault between the central mountains and southern foothills. The geology of the western three-fourths of the area is documented in a summary report (Thorman, 1981) and by unpublished maps, which were generalized for the Silver City $1^\circ \times 2^\circ$ quadrangle (Drewes and others, 1985). Superposed middle Tertiary extensional (detachment) faulting is denoted on the northeastern flank of the range by a veneer of northeast-dipping schist, gneiss and plutonic rock that contain a mylonitic fabric. Minor mineralized rock (mineral deposit model unknown) was reported for the two foothills areas of the Pinaleno Mountains. Geologic features of particular importance to the resource assessment are low-angle faults, a northwest-trending steep fault, a middle Tertiary igneous center, and dike swarms in both foothills areas.

In western Arizona some gold deposits are associated with low-angle normal (detachment) faults (Frost and Martin, 1982). The faults are considered to have been conduits for hydrothermal fluids responsible for formation of disseminated gold and (or) base-metal deposits. This type of ore deposit has not been recognized along or above

low-angle normal faults in southeastern Arizona. Mineralized rock near the Eagle Pass fault (pl. 1), in the northwestern foothills, is related to the dike swarm in its lower plate, and that near the Oak Draw fault, in the southern foothills, was attributed by C.H. Thorman (unpub. mapping, 1982) to a local volcanic center and its associated dike swarm (Richter and Lawrence, 1983). Systematic sampling of rocks along these faults in the Forest unit has not been undertaken, but they appear to be unmineralized (C.H. Thorman, unpub. data, 1982). The link between detachment faults and gold deposits in western Arizona may be incidental, in the sense that hydrothermal solutions may have been routed along any plane of weakness for dispersal, rather than genetic. Perhaps gold- or base-metal-bearing mineralizing fluids, similar to those responsible for deposits in western Arizona, were not generated in southeastern Arizona. Alternatively, the low-angle detachment faults of the Forest region may be geologically distinct from detachment structures of western Arizona.

The Stockton Pass fault is a high-angle, northwest-striking structure that separates the central dome of the Pinaleno Mountains from their southern foothills. Movement along this fault began in Proterozoic time, was recurrent, and was primarily strike-slip (Swan, 1976). Interpretations concerning the amount and sense of slip along this fault are diverse (Drewes, 1981a); the fault may have controlled magma emplacement and channelled hydrothermal fluid circulation. In particular, the granite magma that formed an Oligocene stock and the fluids that introduced uranium or other radioactive elements and gold may have been controlled by this structure (Richter and Lawrence, 1983, p. 47).

A volcanic center is genetically associated with base-metal and silver deposits (mineral deposit model unknown) at Greasewood Mountain in the southern foothills (pls. 1 and 2). The volcanic rocks include andesite lava flows and rhyolite tuff. Prospects and mines are present along fractures and small faults in these rocks; meager production records and unpublished geochemical data (C.H. Thorman, oral commun., 1992) indicate that copper, lead, zinc, molybdenum, and silver in fault gouge along the structures were concentrated by hydrothermal fluid flow. A swarm of northeast-trending rhyolite dikes cuts the volcanic rocks of Greasewood Mountain and older rocks; the dikes are considered (C.H. Thorman, oral commun., 1992) to be related both to the volcanic center and the nearby granite stock.

Another swarm of northeast-trending rhyolite dikes cuts the gneiss of the northwestern foothills; these dikes and a nearby diabase pod contain minor amounts of copper and gold (Richter and Lawrence, 1983; Richter and others, 1986). Mardirosian (1977) indicated the presence of anomalous concentrations of manganese at this site. The dikes are cut by the low-angle Eagle Pass fault.

PELONCILLO MOUNTAINS

The Peloncillo Mountains are underlain by middle Tertiary volcanic rocks that are cut by middle Tertiary or younger normal faults; the distribution and variety of these rocks and faults and the geologic relations in this Forest unit are poorly known (pls. 1 and 3). The central part of this Forest unit contains a few plugs, a tract of altered rocks, a few prospects, and a small mine. The geologic data are primarily of a reconnaissance nature and are from studies by Wrucke and Bromfield (1961), Erb (1979), Hayes (1982), and McIntyre (1988). Geologic features that bear on the mineral resource assessment are the plugs, altered rock, a few faults, and proposed calderas.

Paleozoic and Mesozoic strata that are favorable host rocks for replacement-type ore deposits do not crop out in this Forest unit, but are probably present in the subsurface. Middle Tertiary rhyolite ash-flow tuff and airfall tuff and tuffaceous sedimentary rocks comprise most of the rocks exposed in the Forest unit. Andesitic lava flows and breccia deposits are present low in the volcanic sequence and Pliocene basalt lava flows lap onto the rhyolite along the west flank of the mountains. A few basalt dikes cut the rhyolite and andesite near the eroded edge of the basalt flows. This entire volcanic pile probably overlies Lower Cretaceous Bisbee Group and upper Pennsylvanian-Permian Naco Group sedimentary rocks, which crop out a few kilometers southwest of the Forest unit. Farther to the north, the middle Tertiary volcanic pile may overlie younger Cretaceous rocks and older Paleozoic rocks.

Several plugs cluster within 3 km of a northwest-striking fault, and one plug is in the center of the altered rock tract (pl. 1). These rhyolite plugs apparently are not associated with any of the nearby tuffs. Inasmuch as one of the plugs may have a genetic tie to ore deposits, all of the plugs are considered as favorable hosts.

Caldera structures are favorable sites for certain kinds of mineral deposits, and thus their recognition is useful to the present assessment. One or more calderas have been proposed in the central part of the Peloncillo Forest unit, but available geologic map coverage is inadequate either to validate this interpretation or to show their proposed locations. The Geronimo Trail caldera was proposed by Erb, but its location is ill defined (compare Erb, 1979, with Erb *in* Deal and others, 1978, and McIntyre, 1988). In addition, McIntyre (1988) postulates another caldera, the Clanton Draw caldera.

A few northwest-striking, steep faults of moderate length and short, northeast-striking faults cut the rhyolite volcanic pile. One of the northwest-striking faults near the plugs and the altered rocks is arcuate and concave to the northeast. The northwest-striking faults may be near-surface reactivated segments of major deep-level master faults, a relationship seen along more deeply exposed faults of this trend. The cluster of rhyolite plugs near the arcuate fault lends some support to this evaluation. A segment of the margin of a proposed

caldera is also coincident with the arcuate fault, but the southwest block is shown as the downthrown side.

The tract of altered rock (pl. 1) includes mainly rhyolite low in the middle Tertiary volcanic sequence. Alteration is mainly kaolinization and oxidation of iron-bearing minerals. The small Silvertip Mine and a few prospects are along the western margin of the altered tract. McIntyre (1988, p. 17–18) mentioned that the rock is intensely leached and that the leaching process is ongoing, for waters of a seep in this area contain anomalously high abundances of aluminum, iron, manganese, and zinc. Some north-striking pyritized quartz veins as much as a few hundred meters long and 6 m wide and having slightly anomalous concentrations of base and precious metals were reported in the tract (Erb, 1979; Hayes and others, 1983; McIntyre, 1988). The resource potential for gold and silver are of greatest interest. Copper and zinc are sporadically present and probably are related to fractures and faults, such as those on which the workings of the Silvertip Mine are situated. Tin, as cassiterite, may have been derived as a primary mineral from one of the rhyolite ash-flow tuffs.

CHIRICAHUA AND PEDREGOSA MOUNTAINS

The geology of the Chiricahua and Pedregosa Mountains is highly variable (pls. 1 and 3). The high central part of this Forest unit is underlain largely by Oligocene and lower Miocene volcanic rocks in which one caldera has been identified and another proposed. The moderately high northern part is underlain by the entire sequence of rocks of the Forest region. These rocks are cut by a major northwest-striking fault zone and by other faults and are intruded by stocks, plugs, and dikes, mainly of Oligocene age. The lower Pedregosa Mountains to the south are underlain mainly by Oligocene and lower Miocene volcanic rocks. At several places Paleozoic and Cretaceous rocks are exposed in raised blocks that are cut by pre-Oligocene faults across which the Paleozoic and Cretaceous rocks are juxtaposed. Pliocene and Pleistocene basalt lava flows and plugs and dikes of several ages overlie and cut, respectively, older rocks in the area. Each of these geologic terranes (north, central, and southern) contains mineralized rock. That in the north is most abundant and varied and includes base metals, silver, and gold mined and prospected from polymetallic vein and stockwork deposits. The geology of this Forest unit was documented by Sabins (1957), Cooper (1959), Drewes (1981b, 1982), and Drewes and Brooks (1988), and the mapping was adapted and updated from the synthesis by Drewes (1980). New studies include those by Pallister and du Bray (1994), Pallister and others (1994), and Drewes and others (1995). Geologic features that indicate high favorability for associated polymetallic vein and replacement ore deposits include the presence of preferred lower Paleozoic and Cretaceous andesitic host rocks, major northwest-striking faults, granitic stocks, shallow intrusive bodies, caldera-margin structures, and altered rocks and veins.

Lower Paleozoic rocks are exposed discontinuously along the northern part of the Forest unit, and they also crop out or are near the surface in several of the raised blocks of the Pedregosa Mountains. Near intrusive bodies these rocks were metamorphosed to skarn and some are mineralized. The other Paleozoic map units, which less commonly host mineralized rock, are more widely distributed.

Upper Cretaceous andesitic rocks, also a favorable host for mineralized rock, are widespread in the Pedregosa Mountains and form limited outcrops in the northern part of the Chiricahua Mountains, typically in a strongly faulted terrane. Basalt is interbedded with, or intrudes, Lower Cretaceous Bisbee Group rocks (map unit Kb) and volcaniclastic andesite of Late Cretaceous and Eocene age (unit TKvs), and it is a favorable ore host.

The major northwest-striking, steeply dipping structure is the Apache Pass fault zone. The fault zone splays southeastward, where the offset rocks are mostly younger than those to the northwest. In the narrower northwestern part of the fault zone, offset rocks are older and are metamorphosed in a style more typical of a high-pressure (load or tectonism) environment than of a contact environment (Drewes, 1981a, 1984a, 1991; Drewes and others, 1988). During the Proterozoic, offset along the fault was primarily left slip. Smaller amounts of left slip occurred along some of its branch faults in Late Cretaceous and Paleocene time, and some segments in Oligocene time were reactivated as normal faults. Additionally, Late Cretaceous thrust faults interacted with segments of the Apache Pass fault zone, along which prior offsets may have established conditions for the development of thrust ramps. The importance of the northwest-striking faults in guiding magma and hydrothermal fluids is well illustrated along this fault zone.

Simple, one-phase granite stocks, most of Oligocene age, intrude rocks of the Apache Pass fault zone. One stock is composed of diorite and may be older, as are most diorite stocks in the region. Contact metamorphic halos are usually about 100-m wide, but, locally, near the large bodies of diorite, they widen to more than 1.5 km, possibly marking concealed shoulders to the bodies. Metamorphosed host rocks include recrystallized Paleozoic limestone, hornfelsed rocks of the lower Paleozoic (map unit Pzl), and some propylitized Upper Cretaceous andesite (map unit Ka). Many fine-grained rhyolitic plugs and dikes and some quartz veins are present near these stocks and may be genetically related to the stocks. Andesitic dikes are present near the diorite and may be genetically related to the diorite stock. A few of the granite stocks and the diorite are spatially associated with mineralized rock that includes skarn and vein deposits.

Rhyolite plugs and abundant quartz veins are found mainly along the Apache Pass fault zone, and most apparently are Oligocene, but some are probably Miocene. Most are barren of ore minerals, but a few contain pyrite. Rhyolite

breccia pipes in the Oligocene volcanic rocks of the northern part of the Forest unit and andesitic breccia pipes, probably of Late Cretaceous age, in the central part of the Pedregosa Mountains may mark vent sites for some of the associated volcanic piles. Finally, a crescent-shaped mass of coarsely and abundantly porphyritic dacite marks the structural boundary of the Turkey Creek caldera margin. This mass is believed to be mainly extrusive and to have vented through a ring fracture. Polymetallic gold- and silver-bearing quartz veinlets are present near this mass (Drewes and Williams, 1973, fig. 2 and p. A37). In the late 1980's, quartz smelter flux was produced in small amounts from El Tigre Mine; small amounts of gold and silver were recovered from this material.

Calderas are present in several parts of the Chiricahua Mountains, and their marginal structures are favorable sites for the types of ore deposits associated with calderas, such as epithermal veins and polymetallic vein and replacement deposits. However, structural margin faults are in many cases occupied by ring intrusions or concealed by post-caldera collapse deposits. The structural margin of the Turkey Creek caldera (Marjaniemi, 1968; Drewes and Williams, 1973; Pallister and du Bray, 1994; and Pallister and others, 1994) is largely concealed. Several varieties of calderas or volcanic collapse structures are present within the volcanic piles around Cochise Head and east of Paradise. In these places, old fault systems having linear or rectilinear surface traces guided collapse, and the resulting structure resembles a partly lowered trap door. Border faults are exposed in these areas. Vent breccias are present near border faults, and some of these are mineralized. The Portal caldera was proposed along the east flank of the high part of the Chiricahua Mountains (Bryan, 1988).

Altered and mineralized rock is also present in several large tracts along the Apache Pass fault zone (Drewes, 1981b, 1982; Drewes and others, 1983a; Watts and others, 1985). These rocks are commonly impregnated with pyrite that alters to red-oxide-coated and clay-mineral-rich rocks. In places this rock contains silicified pods or reefs, such as those found southeast of Cochise Head, east of Portal, and north of the Portal Paradise road (Drewes and others, 1995).

Altered rocks are also present in the central part of the Chiricahua Mountains (Drewes and Williams, 1973) and in the Pedregosa Mountains (Drewes and Brooks, 1988). Most of these are clay-mineral and iron-oxide-coated Tertiary volcanic rocks that appear to be unmineralized. There is an area of silicified rock and minor base-metal enrichment a few kilometers northwest of Limestone Mountain.

Several kinds of industrial materials have been mined or prospected near the Forest unit; geologic controls for these commodities are independent of those relevant to the metallic commodities. The Mural Limestone of the Bisbee Group (map unit Kb) is a source near Douglas of rock used to make cement. This limestone changes from its characteristic reef facies to a lagoonal facies just south of the Forest unit, where its composition changes to one not appropriate for use as cement rock. A tuff in the middle Tertiary sequence has been quarried for building stone for local use near the Mud Springs Ranch (Drewes and Brooks, 1988). Similar tuff may be present in the Forest unit. Marble has been mined from metamorphosed Escabrosa Limestone a few kilometers north of the Forest unit. Similar rock is less metamorphosed or unmetamorphosed in the Forest unit. Although abundance of fracturing in subsurface extensions of these marble occurrences is unknown, their locations along fault zones suggests that flaws due to fracturing may preclude its use as decorative stone. Basalt cinder deposits have been quarried for road metal along U.S. Highway 80 (Drewes and Brooks, 1988). Similar cinder deposits are present at many of the volcanic cones of the San Bernardino Valley and the adjacent part of the Pedregosa Mountains.

Tracts in the Pedregosa and Chiricahua Mountains are favorable for polymetallic vein, breccia pipe, polymetallic replacement, stockwork, and disseminated deposits in which gold and (or) silver are probably the most important metals. Tracts having high mineral resource potential for base and precious metals are clustered along the Apache Pass fault zone; these tracts are may contain some skarn deposits, but it is more likely they contain polymetallic vein, stockwork, and breccia pipe deposits.

DRAGOON MOUNTAINS

The Dragoon Mountains are underlain by some of the most complex geology in Coronado National Forest (pls. 1 and 3). This Forest unit contains several major thrust plates, a major overturned fold, tectonically telescoped sedimentary and metamorphic facies, and igneous stocks of three ages. Some of this mountain range is mineralized, but production from the many mines has been limited. The geology of this area is well known from several mapping studies (Gilluly, 1956; Drewes and Meyer, 1983; Drewes, 1987), geochemical studies (Drewes, 1984b; Watts and others, 1984), and a geophysical study (Klein, 1983), all of which were compiled previously in a mineral resource assessment (Drewes and others, 1983b; Kreidler, 1984). Geologic features favorable to ore deposition include suitable host rocks, favorably oriented faults, and abundant magma-related heat and fluid sources (pl. 3). Mineral deposit types include skarn and polymetallic vein and replacement deposits, particularly in fractured or sheared rock. These deposit types were described by Dale and others (1960), Wilson (1950), Stewart and Pfister (1960), and Keith (1973). Most mines produced copper, lead, and zinc; half also produced silver, a few produced gold, and others produced molybdenum and barite.

Nearly half of the mines in this area are in rocks of the Abrigo Formation (lower Paleozoic map unit PzI, pl. 3). The Martin Formation, also part of map unit PzI, the Horquilla Limestone of the Naco Group (map unit PPn), and the

Bisbee Group (unit Kb) are locally mineralized. Skarn deposits are most common in the Abrigo and Martin; polymetallic replacement and vein deposits are present in all host rocks.

A zone of northwest-striking, steeply inclined faults cut the rocks at the crest of the mountains south of a large Miocene stock. North of the stock these structures are obscured by numerous thrust faults. Many of the mines, such as the Hubbard and Black Diamond Mines, are present along or near this fault zone, which has had recurrent and diverse movement.

Locally, northeast-striking faults seem to have localized veins, some fine-grained intrusive bodies, and mineralized rocks. For example, the Golden Rule Mine is associated with rhyolite plugs along a branch fault of a major northeast-striking left-slip fault. Other prospects are on or near northeast-striking dikes, which were probably controlled by fractures east of Mount Glenn. Mineralized rock of the Black Diamond Mine also seems to have been localized by a northeast-striking fault; fluids may have circulated upward and northeastward from the nearby northwest-striking fault.

Within this Forest unit, granite stocks were emplaced during the Proterozoic, early Oligocene, and early Miocene; a late Paleocene stock was also emplaced a few kilometers north of the area, and a Jurassic stock was emplaced 16 km south of the area. A few rhyolite plugs and many dikes cut the sedimentary rocks, and some dikes cut the Miocene stock. The large Miocene Stronghold stock, plugs near the Golden Rule Mine, the dike swarm, and elongate plugs near the Black Diamond Mine are the intrusive bodies of greatest interest with regard to mineral potential.

The Stronghold stock (pl. 1) is an alkali-feldspar granite that forms two petrographically similar phases and is unique in the Forest region in that it contains primary fluorite. The broad contact metamorphic halo around the stock may reflect both its large size and (or) the presence of concealed apophyses in sites such as its northeastern side and the area south of the Abril and Sala Ranch Mines (pl. 3). The age of the rhyolite porphyry plugs near the Golden Rule Mine is unknown. These plugs are near a splay of the major northeast-striking left-slip fault separating highly deformed rocks from much less deformed rocks. A small amount of gold has been produced from the mine.

Tracts of moderate and high favorability for the occurrence of mineral deposits form an irregular pattern that reflects the complex deformation and magmatic history in this area; mutually reinforcing favorable geologic factors are present in spatially variable combinations. Tracts of high favorability are small, but those of moderate favorability are large. The geology of the Dragoon Mountains is most favorable for small, high-grade silver or gold-bearing, lead-rich vein, stockwork, or replacement deposits. Precious-metal vein or porphyry copper-molybdenum deposits and deposits of tin or fluorite in veins or skarn replacements are possible.

WHETSTONE MOUNTAINS

The geology of the Whetstone Mountains is simple relative to that in the surrounding mountains (pls. 1 and 4; Drewes, 1980). A sequence of Paleozoic and Lower Cretaceous sedimentary rocks overlies a largely granitic Proterozoic basement in a little-deformed and sparsely intruded, westward-dipping structural block (Tyrrell, 1957; Creasey, 1967a, Hayes and Raup, 1968; Drewes (1981a). Stratigraphic studies were conducted by Gilluly and others (1954), Bryant (1955), Bryant and McClymonds (1961), and Schumacher (1978), and a resource assessment was made by Wrucke and others (1983) and McColly and Scott (1982). Lower Paleozoic rocks crop out in a nearly continuous band from the southeast to the northwest side of the mountains.

Geologic features favorable to the occurrence of mineralized rock include lower Paleozoic host rocks, Late Cretaceous intrusive rocks, shallow fine-grained intrusive rocks, and two northwest-striking steep faults. The area is known to contain base-metal skarn and polymetallic vein deposits, a copper-molybdenum porphyry, a fluorite vein, flux quartz deposits, and occurrences of uranium, tungsten, and gypsum. Around a stock in Mine Canyon host rocks are contact metamorphosed. Sedimentary-hosted gypsum is present locally in marly beds of the Lower Permian Epitaph Dolomite (Gilluly and others, 1954; Graybeal, 1962; Keith, 1969; Creasey, 1967a). Whereas Creasey (1967a) indicated that gypsum is present in only one of his two stratigraphic sections, Wrucke and others (1983) projected high potential for gypsum continuously along the strike of that horizon (marly beds).

Two small granite stocks and a thick granite sill intrude the Paleozoic and Cretaceous rocks (pl. 1). These rocks were emplaced at 76 Ma and are among the oldest of the Cordilleran orogenic granites in this region. The stocks are moderately coarse grained, but the sill is fine grained. Geophysical evidence suggests the presence of a concealed extension of the stock that trends toward the sill (Wrucke and Armstrong, 1984); the bodies may join at depth. The granite is mineralogically homogeneous, and its texture varies from fine to moderately coarse grained to porphyritic.

Rhyolitic intrusive rocks form many sills in the Bisbee Group of the Whetstone Mountains. Several of the sills are as much as 460 m thick; they appear to be unmineralized.

Steeply inclined, northwest-striking faults cut the northern and southern ends of the tilted Whetstone Mountains block. A concealed fault has been inferred (Drewes, 1981a) to underlie the host rocks near the stock; this fault may extend from Silver Bell to Tombstone as indicated by the alignment of 73- to 76-Ma plugs in the region. Minor mineralized rock has been reported to exist where this fault intersects the Benson fault.

The paucity of mineral deposits in this Forest unit is noteworthy. Geologic factors favorable for the occurrence of ore deposits are not coextensive. Thus, only a few small

tracts are moderately favorable for the occurrence of undiscovered deposits.

PATAGONIA AND HUACHUCA MOUNTAINS AND CANELO HILLS

This large Forest unit (pl. 1) is underlain by many rock types that were affected by many kinds of geologic structures (pl. 4). The Canelo Hills are underlain mostly by volcanic and sedimentary rocks cut by a few small intrusive bodies and by many steep faults. The Huachuca Mountains are underlain mostly by Paleozoic and Mesozoic rocks that overlie a Proterozoic granitic basement and are cut by large Jurassic and small Late Cretaceous granitic bodies. These rocks are cut by thrust faults, by northwest-striking steep faults that are splays of the Sawmill Canyon–Kino Springs fault system, and by many other minor faults. Much of the Patagonia Mountains are a granitic terrane, chiefly of Proterozoic, Jurassic, and Late Cretaceous ages. Small areas (pl. 4) are underlain by Paleozoic and Mesozoic sedimentary rocks, and Cretaceous or early Tertiary volcanic rocks are common to the northeast.

The geology of the Canelo Hills has been extensively studied. The area was mapped by R.B. Raup (unpub. mapping, 1967) whose work was compiled by Drewes (1981a). Hayes and Raup (1968) mapped the Huachuca Mountains and southeastern end of the Canelo Hills. A key part of the northwestern end of the Huachuca Mountains was remapped by R.A. Dockweiler, as shown by Keith and Wilt (1978, fig. 79.9a) and by Drewes (1981a; pl. 6). The Patagonia Mountains and the southern part of the low terrain southeast of Patagonia were mapped by Simons (1974). Stratigraphic studies include those by Feth (1948), Hayes (1970a, b; 1972), Hayes and Cone (1975), Hayes and others (1965), Simons (1972), and Bilodeau and others (1987).

Mineralized rock is sparse in the Canelo Hills, moderately abundant in the Huachuca Mountains, and abundant in the Patagonia Mountains. The Hartfort (Huachuca) mining district (pl. 1) contains base and precious metals in polymetallic replacement deposits along minor northeast- to east-striking faults. Tungsten minerals (wolframite and scheelite) are present in northwest-striking quartz veins, and some stream gravels contain placer gold. In the Wakefield (Van Horn) mining district base metals, tungsten minerals, and gold occur in quartz veins. Deposits in the Coronado National Monument also contain base and precious metals; pyrite is abundant in sheared rock at the State of Texas Mine (Dale and others, 1960; Elsing and Heineman, 1936; Johnson, 1972; and Wilson, 1961). In the Patagonia Mountains copper, lead, zinc, molybdenum, manganese, silver, and gold are in vein, skarn, polymetallic replacement, and porphyry copper deposits. Some placer deposits have produced minor amounts of gold.

Geologic features favorable for ore deposition are abundant in the Huachuca and Patagonia Mountains but are less common in the Canelo Hills. These features include favorable host rocks, large, extensively altered areas, the presence of Late Cretaceous or early Tertiary stocks, the presence of fine-grained intrusive rocks that are the same age or slightly younger than the plutons, and the presence of steep, northwest-striking faults.

In this Forest unit, host rocks favorable for the presence of undiscovered deposits of several types vary from range to range. Lower Paleozoic rocks (unit Pzl), other Paleozoic units (units Ms and PPn), and andesitic or dacitic rocks of Late Cretaceous (Ka, Ksv) or early Tertiary age (TKvs) rocks are the predominant ore deposit hosts. Other Mesozoic volcanic and sedimentary rocks also host mineral deposits in the western part of the Forest region.

Lower Paleozoic rocks are sparsely exposed in the Patagonia Mountains and Canelo Hills but crop out extensively in the Huachuca Mountains. In the Hartfort mining district they contain base- and precious-metal replacement deposits.

The Naco Group, in particular, and other Paleozoic rocks, in general, are the preferred hosts for mineralized rock in the Patagonia (Duquesne-Washington) mining district and in the American Peak area of the Harshaw mining district. In both places, buried lower Paleozoic rocks may be attractive exploration targets.

Andesitic rocks of Late Cretaceous and early Tertiary age are favorable hosts for base metal and silver ore deposits in the Harshaw mining district; they are intensively altered at Red Mountain, where they host a concealed porphyry copper deposit (Corn, 1975). Some of the Triassic and Jurassic rhyolitic volcanic rocks are moderately favorable as host rocks because they are intensely fractured and thus could have channelled hydrothermal fluids effectively. Fractured rhyolite is present along the southeast end of the Dove Canyon fault, near dikes northeast of Ashburn Mountain, and near the major faults around the Coronado National Monument.

One large granite stock in the Patagonia Mountains and several smaller ones in the Patagonia and Huachuca Mountains are spatially associated with mineralized rock. Ages for these rocks range from 65 to 53 Ma; the large body has five compositional or textural phases (Simons, 1974). The Patagonia stock has a broad metamorphic halo in which garnetite skarn and marble are common; mineralized rock of the Washington and Duquesne mining camps are closely associated with these altered rocks. The stock near the Eureka (Sunnyside) Mine, in the Huachuca Mountains, is accompanied by dikes or sills of varied composition that are inferred to be the same age as stocks in this Forest unit. Their steep attitudes and compositional variations suggest that they may be apophyses of a large body having multiple compositional phases, as is typical of many Cordilleran stocks elsewhere. This inference implies that Paleozoic rocks, beneath widespread outcrops of the Bisbee Group, may be mineralized.

Two small granite bodies in the northwestern Huachuca Mountains are surrounded by hydrothermally altered host rocks (Drewes, 1981a, p. 67), are along or near a major northwest-striking fault (Kino Spring fault), and are known to be no older than Early Cretaceous. Likewise, at Saddle Mountain, southeast of Patagonia, a pyroxene monzonite stock that has central plugs of rhyolite breccia is considered a favorable host rock for undiscovered ore deposits. This stock may be genetically related to the extensive field of andesitic rocks that it intrudes.

Shallowly emplaced, fine-grained intrusive rocks form extensions of favorable geologic environments represented by plutonic rocks. Many dikes and some plugs of rhyolitic to andesitic rock are present in all parts of this Forest unit; the ages of these rocks are unknown, so they may include Jurassic and middle Tertiary rocks, as well as the most favorable Late Cretaceous and Paleocene intrusive pulses. One such body, at Red Mountain, is particularly noteworthy because it is present in an intensely altered terrane that was thoroughly drilled by the Kerr-McGee Corporation in the early 1970's (Corn, 1975). A hypogene copper-molybdenum porphyry deposit was identified at a depth slightly below the level of the nearby Sonoita Creek Valley by Kerr-McGee. Corn described the alteration zonation and mineralized rock and inferred that the geologic setting represents a combination of volcanic and subvolcanic terranes centered on a caldera.

Northwest-striking faults are prominent structures in this Forest unit; segments of the Harshaw Creek fault are closely associated with mineralized rock, but less intensely mineralized rock occurs along the Sawmill Canyon–Kino Spring fault and its several southeast-striking splays.

In summary, geologic factors combine to indicate many tracts of high and moderate mineral resource potential. Some tracts are centered around mining districts that include favorable geologic characteristics; others, however, are present in less mineralized areas.

SANTA RITA MOUNTAINS

In terms of geology, the Santa Rita Mountains are among the most thoroughly studied areas of Coronado National Forest. The exposed rocks span the full range of those present in the Forest region and include some that are generally absent elsewhere (pls. 1 and 4). Plutons of all five magmatic events crop out in these mountains. Although rocks throughout large parts of these mountains are only slightly deformed, as in homoclinally dipping, large structural blocks, rocks in other parts were strongly folded and faulted during recurrent periods of deformation. Base- and precious-metal production was moderate in two mining districts (Tyndall and Helvetia-Rosemont mining districts) and small from five others. Geologic map coverage was provided by Schrader (1915), Drewes, (1971a, 1972b) and Finnell (1971). Topical studies that support this assessment include Schrader (1915), Creasey and Quick (1955), and Drewes (1967, 1970, 1971c, 1972a, 1973, 1976). A compendium of copper occurrences was published by the U.S. Geological Survey (1973). These studies show the geologically favorable features to include selected host rocks, polyphase granitic stocks of Late Cretaceous to Paleocene age, certain shallow plugs and dikes, northwest-striking steep faults, variously altered and mineralized rock, and gypsum plugs (pl. 4).

Host rocks favorable for the presence of undiscovered deposits of several types include the lower Paleozoic sedimentary rocks and andesitic to dacitic rocks of Late Cretaceous or Paleocene age; they also include the Naco Group of Pennsylvanian and Permian age and the older Cretaceous andesitic and sedimentary rocks. Other rocks that may be favorable as deposit hosts include Cretaceous rhyolite and Triassic and Jurassic volcanic and sedimentary rocks.

The Abrigo and Martin Formations (of map unit Pzl, pl. 4) are commonly altered to skarn in the Helvetia and Rosemont areas near stocks and plugs, along the Sawmill Canyon fault zone, and near the Glove Mine, though no igneous bodies crop out near the last two sites. Similar rocks may underlie the upper reaches of Josephine Canyon, southwest of Mount Wrightson (Drewes, 1973). The Horquilla Limestone of the Naco Group is commonly mineralized in the Helvetia area and may also be present in the subsurface at the Josephine Canyon and Glove Mine sites. Many limestone blocks in the exotic-block member of the Upper Cretaceous Salero Formation (Drewes, 1971b, c; 1972a) are probably Horquilla Limestone, and where the andesitic host rock is mineralized the limestone blocks may be sites of rich polymetallic skarn ore.

Andesitic or dacitic volcanic rocks of Late Cretaceous to Paleocene age are also favorable as host rocks for polymetallic vein and replacement deposits. One such site is around Mount Fagan in the northern part of the Santa Rita Mountains, which may be a major volcanic center. Another volcanic center, possibly a caldera, is proposed for the Josephine Canyon site (Drewes, 1971c). Possible vent sites for pre-Bisbee Group andesite or dacite lava flows are not known. As outlined on figure 11, host rocks judged to have moderate favorability are widespread, particularly in the northern part of the Forest unit.

A large, northwest-striking composite granitic stock of Late Cretaceous age extends the length of the southern half of the Forest unit; eight other small stocks, most of which show no compositional variation and are of Paleocene age, also intrude the rocks of this area. The composition of the stocks was presented by Drewes (1976). The emplacement of the large stocks nearly obliterated a fault, the Santa Rita fault scar, whose upended faulted relicts are present between stocks and cover rocks (Drewes, 1972b). Around most of its circumference, the large stock is in contact with other granite, which is unmetamorphosed; the margin of the stock is locally concealed by alluvium. At Josephine Canyon, in the

Tyndall mining district, large country rock inclusions were metamorphosed. The contact between the composite stock and andesitic and Paleozoic rocks in the area south of the Salero Mine and near the Montosa Mine may have potential for contact metamorphic deposit types; where that contact is faulted, subsurface parts of the hanging wall may be mineralized. Most of the small granitic stock is unmineralized; the relationship of the 74-Ma stock at Mount Fagan to mineral resource potential remains unknown.

Of the many shallow plugs and dikes in this Forest unit, only a few plugs are known to have associated mineral resource potential. These plugs are of Paleocene age, have irregular shapes, and contain doubly terminated quartz phenocrysts (Drewes, 1971a, b; 1972b; 1976). These rocks are known as the "ore porphyries." Some Oligocene pyrite-bearing dikes and plugs are also of interest. In the Helvetia and Rosemont areas, however, the ore porphyries are associated with silver and base-metal ore in skarn, polymetallic replacement, and porphyry type deposits (Drewes, 1973). Locally, base-metal, gold, or gold-tellurium-quartz vein deposits are present in these rocks. Gold in the Greaterville placer deposits is derived from nearby gold-bearing quartz veins.

Most of the large ore deposits in the Santa Rita Forest unit are on or near major northwest-striking, steep faults. While some segments of these faults are characterized by altered rock or by intrusive bodies, other segments are barren. These faults were described by Drewes (1972b, 1981a) as branching to the southeast, being recurrently active, having diverse movement history from segment to segment, and probably having a large component of left slip at an early stage of development. The Sawmill Canyon fault zone, Salero fault, Santa Rita fault scar, and an unnamed fault northeast of the Helvetia-Rosemont mining district are all examples of these structures. Some of them controlled development of thrust and glide faults, which add to their complex history. Most importantly, at least some segments of these faults are mineralized and subordinate high-angle or low-angle faults near the major faults may also be mineralized, particularly at higher structural levels. Examples of such occurrences, given by Drewes (1973), include the Salero fault and some of the branches of the unnamed fault described above. The southeastward branching or flaring aspect of the major faults may indicate that these rocks have been tilted down and consequently protected from erosion; the Alto vein swarm may be a manifestation of this tilting. Uptilted rocks, to the northwest, have been eroded down to levels at which fault zones are narrower.

The Eocene(?) Alto vein swarm is present on both flanks of the southern part of the Santa Rita Mountains (Drewes, 1971b, 1973, pl. 1). More than 300 polymetallic quartz veins strike east-west and dip between 70° N. and 70° S. Most veins are about 600 m long and 1.5 m wide; the veins form low ribs of nearly white rock whose fracture surfaces are coated brown by iron oxides. To the south the tabular veins grade into more diffuse silicified reefs, a term used by miners rather than "coral reef." These quartz veins and reefs are mineralized and characterized by a systematic variation in mineral assemblage and metal content from north to south. Galena and copper minerals are common in the north; copper, lead, zinc, silver, and molybdenum are predominant in the center; and barite and zinc are abundant in the south. This distribution suggests a zoned hydrothermal system whose deep and shallow levels are exposed in the north and south, respectively. The variation in the host rocks, from stocks and their andesitic host rocks in the north to younger volcanic rocks and capping deposits in the south, provides support for the model of slight southward tilt of the Santa Rita fault block.

Other altered and mineralized ground is considered favorable for occurrence of undiscovered ore deposits. West of Greaterville and around Elephant Head, small vein swarms are less systematically oriented and less intensely mineralized. There are areas of clay-mineral-enriched and iron-oxide-coated altered rocks in the upper reaches of Josephine Canyon (pl. 1), between the Alto and Mansfield groups of mines, and around the Ivanhoe Mine along the Santa Rita fault scar (Drewes, 1971b, 1973, pl. 1). Around the Ivanhoe Mine these altered rocks are enriched in base metals and silver for as much as 760 m from veins (Drewes, 1967).

Rocks around the Glove Mine and along the Sawmill Canyon fault zone are contact metamorphosed and contain dikes. The presence of metamorphic rock and dikes in an area where no large intrusive bodies are exposed may indicate concealed stocks, which in turn may indicate a favorable setting for the occurrence of ore deposits in the subsurface.

In the Helvetia-Rosemont mining district, more than 15 gypsum plugs are present in deformed rocks of the Naco Group (Drewes, 1972b, pl. 4). These plugs are typically only tens of meters across and are commonly found near faults. Anhydrite(?) is admixed with gypsum, clay, and dolomitic marl. Although these plugs intrude Permian formations known to contain bedded gypsum in the Whetstone Mountains, the Permian rocks near the plugs do not contain salt casts or solution breccias, which might indicate a local source for the gypsum. This observation, combined with the intrusive form of these gypsum bodies, suggests a distant and likely deep structural level for gypsum mobilization. The amount of gypsum is small, and its structural form renders cost-effective extraction difficult.

In summary, the Santa Rita Mountains contain many geologic tracts having high mineral resource potential (pl. 1). Favorable host rocks, intrusive bodies, and tracts of altered rock are present along three major northwest-striking faults. Presence of skarn, polymetallic vein, and at least several porphyry deposits suggests that there may be more in the subsurface.

ATASCOSA, PAJARITO, SAN LUIS, AND TUMACACORI MOUNTAINS AND COBRE AND COCHES RIDGES

The geology of the Atascosa, Pajarito, San Luis, and Tumacacori Mountains and Cobre and Coches Ridges is the least well known of any part of Coronado National Forest (pls. 1 and 4) and suggests that parts of the area are favorable for the presence of undiscovered ore deposits. This area is large and geologically diverse, and access is poor over large regions. Reconnaissance or local studies in this area include those by Wilson and others (1969), Knight (1970), Keith and Theodore (1975), Drewes (1981a and pl. 4, this volume), and Riggs and others (1990).

The Atascosa–Cobre–Coches–Pajarito–San Luis–Tumacacori Forest unit is underlain by Mesozoic and Tertiary volcanic, sedimentary, and some plutonic rocks. The ages of many of these rocks are unknown, and correlation with rocks in other areas is uncertain. The older rocks are cut by faults, and, although a northwest-striking set is present, these faults appear discontinuous and are variously shown in the several studies; intrusive bodies have a strong northwest orientation.

Some of the older rocks in the Atascosa–Cobre–Coches–Pajarito–San Luis–Tumacacori area are strongly mineralized; principal production has come from the Oro Blanco mining district (includes the Ruby Mine). Silver, copper, and lead in polymetallic quartz veins along fractures or faults were the principal commodities that were produced (Wilson and others, 1934; Arizona Bureau of Mines, 1950; U.S. Geological Survey, 1973). Gold-bearing quartz veins are present in the Pajarito mining district, and local placer mining was recorded by Wilson and others (1969).

Most of the previously exploited mineral deposits in this area are polymetallic veins, which suggests that favorable host rocks are less important here than elsewhere. Vein location and orientation were not noted in the reconnaissance studies, but mines and mining districts are aligned northwest. Andesitic or dacitic volcanic rocks and volcaniclastic sedimentary rocks are present, however, and may be favorable as hosts for ore deposition. Paleozoic rocks may be present in the subsurface; where they are near faults and intrusive rocks, they may be favorable as host rocks.

A Late Cretaceous diorite stock extends between the Ruby and the Oro Blanco mining districts, and a second, smaller body is near the Dos Amigos Mine ("Dos Amigos district" on some maps) a few kilometers south of Ruby. The veins may be related to these stocks. Riggs and Haxel (1990) suggested that a granite stock in the San Luis Mountains of the Atascosa–Cobre–Coches–Pajarito–San Luis–Tumacacori Forest unit is middle Tertiary. The age of a swarm of rhyolite or latite dikes along the southwest side of the Oro Blanco mining district is unknown, and its relations to nearby mineralized rock is also unknown. Contact metamorphosed rock is present only locally.

The structural margin of a caldera may be present in the Pajarito Mountains in the eastern part of the Atascosa–Cobre–Coches–Pajarito–San Luis–Tumacacori Forest unit (Drewes, 1980, 1981a), and may extend south into Sonora, Mexico. The age of igneous rocks of the Pajarito Mountains is variously reported as Late Cretaceous (Wilson and others, 1969; Nelson, 1963; Drewes, 1981a) and as Jurassic (Riggs, 1987; Riggs and others, 1990). A thick pile of rhyolitic tuff underlies the central part of these mountains. Several large masses of exotic block breccia, whose clasts are not represented by exposures in the immediate region, are incorporated in the easternmost part of the tuff (Drewes, 1981a and pl. 4, this volume) and may indicate intracaldera megabreccia. Basin and Range-type faulting and surficial deposits conceal the structural margin of the caldera north of the United States–Mexico border; the area south of the border is unmapped except for the reconnaissance work of Lucarelli (1967).

The structural setting of the Tumacacori Mountains is different from that in the rest of the Atascosa–Cobre–Coches–Pajarito–San Luis–Tumacacori area. These mountains are underlain by Oligocene rhyolite that may be outflow ash-flow tuff. Although no source has been proposed for them, they may have been erupted from a volcanic center in the Grosvenor Hills southwest of the Santa Rita Mountains (Drewes, 1971b; 1972a). Along the west side and north end of the Tumacacori Mountains, the volcanic rocks form a thin cap on a basement of Mesozoic volcanic and plutonic rocks, some of which are mineralized. Tracts favorable for the occurrence of undiscovered deposits may underlie Oligocene volcanic rocks.

SANTA CATALINA AND RINCON MOUNTAINS

The Santa Catalina and Rincon Mountains are underlain by many of the rock types that are present elsewhere in the Forest units (pls. 1 and 2). Gently dipping faults (10°–30°) juxtapose younger rocks on older ones in many places. The structure in these ranges is typical of metamorphic core complexes, core complexes, or gneiss-cored domes. These complexes or domes typically have had a middle Tertiary thermal and magmatic history and episodes of structural deformation that overprinted Mesozoic and older events. Few ore deposits appear to be related to the younger events. Only those terranes most distal from the domes show weak effects of interaction with hydrothermal systems.

The geology of the Rincon Mountains is relatively well known; that of the Santa Catalina Mountains is less known. Geologic maps of the Rincon Mountains include those by Drewes (1974, 1977) and Thorman and others (1981). The geology for about 80 percent of the Santa Catalina Mountains was compiled from reconnaissance maps of Banks (1976) and by Creasey and Theodore (1975); the remaining

15 percent was compiled from detailed mapping by Creasey (1967b) or was adapted from Budden (1975). University theses were also incorporated in the geologic compilation of the Santa Catalina Mountains (pls. 1 and 4). Key topical studies of these mountains include those of Bykerk-Kauffman and Janecke (1987), Davis (1975, 1979, 1983), Dickinson (1981, 1991), and Reynolds and Lister (1990).

The central parts of the Santa Catalina and Rincon Mountains are underlain by plutonic and metamorphic rocks of Proterozoic, Late Cretaceous, and early to middle Tertiary ages (Creasey and others, 1977). These crystalline rocks form the cores of the two ranges and are present in the overlying and flanking terranes. Most of the overlying and flanking terranes are underlain by Paleozoic, Mesozoic, and middle Tertiary sedimentary formations and their metasedimentary equivalents. Very locally, middle Tertiary volcanic and shallow, fine-grained intrusive rocks crop out. The distribution of these sedimentary rocks is highly irregular because they have been affected by several structural events that caused development of various styles of faults and folds (Pashley, 1966; Drewes, 1974, 1977, 1981a, 1991; Davis, 1975, 1979; Thorman and others, 1981; Bykerk-Kauffman and Janecke, 1987). These rocks have been multiply metamorphosed. The youngest metamorphic event, of Tertiary age, appears to have lasted 30 m.y., and apparently overlaped several tectonic events. Some mineralized rock is attributed to events at the end of an early compressive deformation, about 75–55 Ma, and concurrent granitic intrusion; other mineralized rock is either associated with magmatic events following a later extensional deformation, about 25–15 Ma, or were emplaced during the earlier event and remobilized during the later one.

Most crystalline core rocks are foliated and lineated and are protoclastically mylonitized. The foliation and attitudes of the overlying cover rocks are arched into broad gentle domes whose southwestern flanks are folded into southwestward-plunging anticlines and synclines. The mylonitic foliation and lineation are more strongly developed on the southwest flanks of the domes than on the northeast. The lineation is primarily in the plane of foliation and is oriented N. 70° E. throughout most of the region, but over a large area north of the Rincon Mountains the lineation trends gradually past north to N. 10° W.

Core rocks are separated from structurally higher rocks by a low-angle outward-dipping fault (Santa Catalina complex fault), which is typically marked by a mylonite zone as much as several meters thick on the southwest flank of the domes; movement along the fault has occurred in several episodes. This fault may project over the Santa Catalina Mountains, where shearing is not as conspicuous and where metamorphism may have helped to obscure faults. From the Mount Lemon area the fault may project into the Samaniego stock through a zone that contains many rock inclusions that resemble the assortment of rock types found in the plate above the Santa Catalina fault (Banks, 1976).

The cover rocks are cut by many thrust faults, some low-angle gravity or extensional faults, and many normal faults. Some thrust faults were reactivated as low-angle extensional faults and have complex movement history (Drewes, 1991).

Folds of several scales and origins are present in this Forest unit. The domes and their flanking anticlines and synclines are large, open structures. The cover rocks contain medium-sized folds, commonly restricted to a single local fault block or thrust plate; the orientation of those around the Rincon dome indicate radial movement off the dome (Davis, 1975).

Four groups of plutonic rocks are found in the Santa Catalina and Rincon Mountains Forest unit, of which only the third group of plutons, of late intermediate (Paleocene) age, are associated with mineralized rock. The first and oldest group of plutonic rocks in the Santa Catalina and Rincon Mountains Forest unit are Proterozoic, very coarse grained granite to granodiorite, and contain zircon from which a U-Pb age of 1.4 Ga has been determined (Shakel and others, 1977). The second group is moderately coarse grained granite to diorite stocks that are assigned to the Tertiary and Cretaceous map unit (pl. 1, unit TKg). Of these stocks, several in the Santa Catalina Mountains are unfoliated, intrude the cover rocks, and may be Late Cretaceous. Rocks in the third group of stocks are foliated and faulted against the cover rocks, and they may be Paleocene. Plutons of the fourth group are Oligocene (Tg), but their chemical and petrographic attributes are similar to those of the third group, two-mica- and garnet-bearing peraluminous granite (Naruk and Bykerk-Kauffman, 1990).

Mineral deposits may have evolved in two geologic settings and during two or more times in the geologic development of the area. Following a peak time of thrust faulting at deep structural levels, granitic and dioritic stocks accompanied by large base-metal- and silver-bearing hydrothermal systems were emplaced (pl. 2). Then, the early phases of two-mica granite were emplaced and bowed up some core rocks, still under great cover and thus fairly ductile, before the last movement on the thrust faults occurred. Uplift and erosion throughout early Tertiary time caused much of the thick cover to be removed and, with continued uplift, now under less cover and thus fairly brittle, these stocks generated topographic domes centered above the earlier formed structural domes. Coincident with rapid erosion, the domes were tectonically stripped, possibly both by earlier unidirectional movement and later radial movement. Base metals and silver were mobilized in small hydrothermal systems, perhaps associated with the middle Tertiary late structural and thermal changes, along now-dormant low-angle faults; metals in some of the older deposits, farther from the domes, may have been redistributed at this time.

The geologic history of this Forest region is sufficiently dissimilar as compared to that of other Forest units that a different set of geologic factors indicative of mineral resource

potential must be applied. As late as Miocene time, rocks in the cores of the domes were hot enough to sustain hydrothermal circulation systems, but only limited quantities of mineralized rock formed during this period (pl. 1). Therefore, these rocks are not indicative of a favorable geologic environment. The Santa Catalina complex fault is only locally mineralized, and no apparent tie exists between mineralized rock and stocks or vertical faults. Thus, the Santa Catalina complex fault is not viewed as a favorable indicator, nor is it likely that the minor quantities of mineralized rock that are present along the fault represent the dismembered parts of other deposits. Finally, gypsum and uranium occurrences located just outside the Forest are in structures that project away from the Forest unit and thus do not bear on the mineral potential of the Forest.

The geology of the northernmost part of the Santa Catalina Mountains is marginal to the Santa Catalina core complex; geologic criteria applied to other parts of the Forest are used in this area. These factors include favorable host rocks, stocks of suitable age and composition, and strongly developed northwest-trending faults (pl. 2).

Favorable host rocks include lower Paleozoic formations and the Proterozoic Apache Group. Some Cretaceous andesite is also present; andesite may also underlie the flanking gravels of the San Pedro River valley.

The northern part of the Santa Catalina Mountains contains four stocks whose compositions indicate that these rocks are favorable for the occurrence of associated ore deposits; in some places these stocks contain copper ore. Three of the stocks are of the most favorable Late Cretaceous or Paleocene age. These three bodies crop out close together and may be cupolas of a single composite stock. Detailed study of the 70-Ma quartz diorite of the Leatherwood stock and the two granodiorite bodies (A and B, pl. 1), are lacking. However, observations at a few sites indicate that contact metamorphic aureoles are about 300 m wide, except to the southwest where metamorphic overprinting by the middle Tertiary two-mica granite event occurred. Rocks that contain anomalous base-metal abundances and recently have produced minor amounts of copper ore are associated with some parts of these stocks.

The Mogul and Geesaman Canyon faults are steep, major, northwest- to west-striking, steeply dipping structures and probably have a history of multiple movements. Moderate amounts of gold and tungsten have been produced from veins along second-order structures in the Camp Bonito (Maudina) mining district along the Mogul fault (Creasey, 1967b, p. 82–87). The Geesaman Canyon fault cuts Paleozoic rocks that are themselves cut by low-angle faults, most of which juxtapose younger rocks on older ones. Both low- and high-angle faults were intruded by the 70-Ma Leatherwood stock quartz diorite. The Paleozoic rocks host copper deposits, and minor amounts of gold have been produced (Wilson, 1961) from placer deposits in nearby Alder Canyon. East of the Forest, the Mogul and Geesaman Canyon faults may merge beneath alluvium. If the faults intersect, their junction may be accompanied by highly fractured rock that could indicate a site favorable for ore deposition. A similar fault, which may also have had strike-slip movement and been recurrently active, is a few kilometers northeast of the Forest, at San Manuel, a major porphyry copper district (Creasey, 1965).

Five tracts of moderate favorability for mineral deposits are located along the northeast flank of the Santa Catalina and Rincon Mountains; one of these tracts contains small tracts having high favorability. The southeastern three moderately favorable tracts and a fourth tract at the inferred junction of major faults, are wholly or largely outside the Forest unit. Furthermore, the southeastern tracts are near the crystalline rocks that form the core of the range, where repeated thermal events in the period postdating the most prolific mineralizing period (Late Cretaceous to Paleocene) are believed to have driven off, rather than causing accumulation of, metals. Deposit types that may be present include skarn, porphyry copper-molybdenum, and polymetallic vein deposits.

REFERENCES CITED

Arizona Bureau of Mines, 1950, Arizona zinc and lead deposits, part II: Arizona Bureau of Mines Bulletin 158, 115 p.

Banks, N.G., 1976, Reconnaissance geologic map of the Mount Lemmon quadrangle, Pima County, Arizona: U.S. Geological Survey Miscellaneous Field Studies Map MF–747, scale 1:62,500.

Bilodeau, W.L., Kluth, C.F., and Vedder, L.K., 1987, Regional stratigraphic, sedimentologic, and tectonic relationships of the Glance Conglomerate in southeastern Arizona: Arizona Geological Society Digest, v. 18, p. 229–256.

Blacet, P.M., and Miller, S.T., 1978, Reconnaissance geologic map of the Jackson Mountain quadrangle, Graham County, Arizona: U.S. Geological Survey Miscellaneous Field Studies Map MF–939, scale 1:62,500.

Bryan, C.R., 1988, Geology and geochemistry of mid-Tertiary volcanic rocks in the eastern Chiricahua Mountains, southeastern Arizona: Albuquerque, N. Mex., University of New Mexico, M.S. thesis, 137 p.

Bryant, D.L., 1955, Stratigraphy of the Permian System in southern Arizona: Tucson, Ariz., University of Arizona, Ph.D. dissertation, 209 p.

Bryant, D.L., and McClymonds, N.E., 1961, Permian Concha Limestone and Rainvalley Formation, southeastern Arizona: American Association of Petroleum Geologists Bulletin, v. 45, p. 1324–1333.

Budden, R.T., 1975, The Tortolita–Santa Catalina Mountains complex: Tucson, Ariz., University of Arizona, M.S. thesis, 133 p.

Butler, B.S., Wilson, E.D., and Rasor, C.A., 1938, Geology and ore deposits of the Tombstone district, Arizona: University of Arizona Bulletin, v. 9, no. 1, 114 p.

Bykerk-Kauffman, Ann, and Janecke, S.U., 1987, Late Cretaceous to early Tertiary ductile deformation, Catalina-Rincon

metamorphic core complex, southeastern Arizona: Geology, v. 15, no. 5, p. 462–465.

Cooper, J.C., and Silver, L.T., 1964, Geology and ore deposits of the Dragoon quadrangle, Cochise County, Arizona: U.S. Geological Survey Professional Paper 416, 196 p., map scale 1:31,680.

Cooper, J.R., 1959, Reconnaissance geologic map of southeastern Cochise County, Arizona: U.S. Geological Survey Mineral Investigations Field Studies Map MF–213, scale 1:125,000.

———1960, Reconnaissance geologic map of Willcox, Fisher Hills, Cochise, and Dos Cabezas quadrangles, Cochise and Graham Counties, Arizona: U.S. Geological Survey Mineral Investigations Field Studies Map MF–231, scale 1:62,500.

———1973, Geologic map of the Twin Buttes quadrangle, southwest of Tucson, Pima County, Arizona: U.S. Geological Survey Miscellaneous Investigations Series Map I–745, scale 1:48,000.

Corn, R.M., 1975, Alteration-mineralization zoning, Red Mountain, Arizona: Economic Geology, v. 70, no.8, p. 1437–1447.

Creasey, S.C., 1965, Geology of the San Manuel area, Pinal County, Arizona: U.S. Geological Survey Professional Paper 471, 64 p.

———1967a, Geologic map of the Benson quadrangle, Cochise and Pima Counties, Arizona: U.S. Geological Survey Miscellaneous Geologic Investigations Map I–470, scale 1:48,000.

———1967b, General geology of the Mammoth quadrangle, Pinal County, Arizona: U.S. Geological Survey Bulletin 1218, 94 p., map scale 1:48,000.

Creasey, S.C., Banks, N.G., Ashley, R.P., and Theodore, T.G., 1977, Middle Tertiary plutonism in the Santa Catalina and Tortolita Mountains, Arizona: U.S. Geological Survey Journal of Research, v. 5, no. 6, p. 705–718.

Creasey, S.C., Jackson, E.D., and Gulbrandsen, R.A., 1961, Reconnaissance geologic map of parts of the San Pedro and Aravaipa Valleys, south-central Arizona: U.S. Geological Survey Mineral Investigations Field Studies Map MF–238, scale 1:125,000.

Creasey, S.C., Jinks, J.E., Williams, F.E., and Meeves, H.C., 1981, Mineral resources of the Galiuro Wilderness and contiguous further planning areas, Arizona, *with a section* on Aeromagnetic survey and interpretation, *by* W.E. Davis: U.S. Geological Survey Bulletin 1490, 94 p., 2 pls., map scale 1:62,500.

Creasey, S.C., and Krieger, M.H., 1978, Galiuro Volcanics, Pinal, Graham, and Cochise Counties, Arizona: U.S. Geological Survey Journal of Research, v. 6, no. 1, p. 115–132.

Creasey, S.C., and Quick, G.L., 1955 [1956], Copper deposits of part of the Helvetia mining district, Pima County, Arizona: U.S. Geological Survey Bulletin 1027–F, p. 301–321.

Creasey, S.C., and Theodore, T.G., 1975, Preliminary reconnaissance geologic map of the Bellota Ranch quadrangle, Pima County, Arizona: U.S. Geological Survey Open-File Report 75–295, scale 1:31,680.

Dale, V.B., Stewart, L.A., and McKinney, W.A., 1960, Tungsten deposits of Cochise and Santa Cruz Counties, Arizona: Arizona Bureau of Mines Report of Investigations 5650, 132 p.

Darton, N.H., 1925, A résumé of Arizona geology: Arizona Bureau of Mines Bulletin 119, Geology Series 3, 298 p.

Davis, G.H., 1975, Gravity-induced folding of a gneiss dome complex, Rincon Mountains, Arizona: Geological Society of America Bulletin, v. 86, no. 7, p. 979–990.

———1979, Laramide folding and faulting in southeastern Arizona: American Journal of Science, v. 279, no. 5, p. 543–569.

———1983, Shear zone model of the origin of metamorphic core complexes: Geology, v. 11, p. 342–347.

Deal, E.G., Elston, W.E., Erb, E.E., Peterson, S.L., Reiter, D.E., Damon, P.E., and Shafiqullah, M., 1978, Cenozoic volcanic geology of the Basin and Range province in Hidalgo County, southwestern New Mexico, *in* Callender, J.F., Wilt, J.C., and Clemons, R.E., eds., Land of Cochise, southeastern Arizona: New Mexico Geological Society, Annual Field Conference Guidebook, no. 29, p. 219–229.

Denton, T.C., 1947, Aravaipa lead-zinc deposits, Graham County, Arizona: U.S. Bureau of Mines Report on Investigations 4007, 14 p.

Dickinson, W.R., 1981, Plate tectonic evolution in the southern Cordillera, *in* Dickinson, W.R., and Payne, W.D., eds., Relations of tectonics to ore deposits in the southern Cordillera: Arizona Geological Society Digest, v. 14, p. 113–135.

———1991, Tectonic setting of faulted Tertiary strata associated with the Catalina core complex in southern Arizona: Geological Society of America Special Paper 264, 106 p.

Drewes, Harald, 1967, A geochemical anomaly of base metals and silver in the southern Santa Rita Mountains, Santa Cruz County, Arizona, *in* Geological Survey Research 1967: U.S. Geological Survey Professional Paper 575–D, p. D176–D182.

———1970, Structure control of geochemical anomalies at the Greaterville mining district, southeast of Tucson, Arizona: U.S. Geological Survey Bulletin 1312–A, 49 p.

———1971a, Geologic map of the Sahuarita quadrangle, southeast of Tucson, Pima County, Arizona: U.S. Geological Survey Miscellaneous Geologic Investigations Map I–613, scale 1:48,000.

———1971b, Geologic map of the Mount Wrightson quadrangle, southeast of Tucson, Santa Cruz and Pima Counties, Arizona: U.S. Geological Survey Miscellaneous Geologic Investigations Map I–614, scale 1:48,000.

———1971c, Mesozoic stratigraphy of the Santa Rita Mountains, southeast of Tucson, Arizona: U.S. Geological Survey Professional Paper 658–C, 81 p.

———1972a, Cenozoic rocks of the Santa Rita Mountains, southeast of Tucson, Arizona: U.S. Geological Survey Professional Paper 748, 35 p.

———1972b, Structural geology of the Santa Rita Mountains, southeast of Tucson, Arizona: U.S. Geological Survey Professional Paper 748, 35 p.

———1973, Geochemical reconnaissance of the Santa Rita Mountains, southeast of Tucson, Arizona: U.S. Geological Survey Bulletin 1365, 67 p., 2 plates.

———1974, Geologic map and sections of the Happy Valley quadrangle, Cochise County, Arizona: U.S. Geological Survey Miscellaneous Investigations Map I–832, scale 1:48,000.

———1976, Plutonic rocks of the Santa Rita Mountains, southeast of Tucson, Arizona: U.S. Geological Survey Professional Paper 915, 75 p.

———1977, Geologic map and sections of the Rincon Valley quadrangle, Pima County, Arizona: U.S. Geological Survey

Miscellaneous Investigations Series Map I–997, scale 1:48,000.

———1978, The Cordilleran orogenic belt between Nevada and Chihuahua: Geological Society of America Bulletin, v. 89, no. 5, p. 641–657.

———1980, Tectonic map of southeastern Arizona: U.S. Geological Survey Miscellaneous Investigations Series Map I–1109, scale 1:125,000.

———1981a, Tectonics of southeastern Arizona: U.S. Geological Survey Professional Paper 1144, 96 p.

———1981b, Geologic map and sections of the Bowie Mountain South quadrangle, Cochise County, Arizona: U.S. Geological Survey Miscellaneous Investigations Series Map I–1363, scale 1:24,000.

———1982, Geologic map and sections of the Cochise Head quadrangle and adjacent areas, southeastern Arizona: U.S. Geological Survey Miscellaneous Investigations Series Map I–1312, scale 1:24,000.

———1984a, Geologic map and structure sections of the Bowie Mountains North quadrangle, Cochise County, Arizona: U.S. Geological Survey Miscellaneous Investigations Series Map I–1492, scale 1:24,000.

———1984b, Geochemical and mineralogic maps of the Dragoon Mountains Roadless Area, Cochise County, Arizona: U.S. Geological Survey Miscellaneous Field Studies Map MF–1521–E, scale 1:50,000.

———1987, Geologic map and structure sections of the northern part of the Dragoon Mountains, southeastern Arizona: U.S. Geological Survey Miscellaneous Investigations Series Map I–1662, scale 1:24,000.

———1991, Description and development of the Cordilleran orogenic belt in the southwestern United States and northern Mexico: U.S. Geological Survey Professional Paper 1512, 92 p.

Drewes, Harald, and Brooks, W.E., 1988, Geologic map and sections of the Pedregosa Mountains quadrangle, Cochise County, Arizona: U.S. Geological Survey Miscellaneous Investigations Series Map I–1827, scale 1:48,000.

Drewes, Harald, du Bray, E.A., and Pallister, J.S., 1995, Geologic map of the Portal quadrangle and vicinity, Cochise County, southeast Arizona: U.S. Geological Survey Miscellaneous Investigations Series Map I–2450, scale 1:24,000.

Drewes, Harald, and Dyer, Russ, 1989, Tectonics of the eastern part of the Cordilleran orogenic belt, Chihuahua, New Mexico, and Arizona: American Geophysical Union Field Trip Guidebook, T–121, 28th International Geologic Congress, 1989, 82 p.

Drewes, Harald, Houser, B.B., Hedlund, D.C., Richter, D.H., Thorman, C.H., and Finnell, T.L., 1985, Geologic map of the Silver City 1° × 2° quadrangle, New Mexico and Arizona: U.S. Geological Survey Miscellaneous Investigations Series Map I–1310–C, scale 1:250,000.

Drewes, Harald, Klein, D.P., and Birmingham, S.C., 1988, Volcanic and structural controls of mineralization in the Dos Cabezas Mountains of southeastern Arizona: U.S. Geological Survey Bulletin 1676, 45 p., 1 pl.

Drewes, Harald, Kreidler, T.J., Watts, K.C., Jr., and Klein, D.P., 1983a, Mineral resource potential of the Dragoon Mountains Roadless Area, Cochise County, Arizona: U.S. Geological Survey Miscellaneous Field Studies Map MF–1521–B, scale 1:50,000.

Drewes, Harald, and Meyer, G.A., 1983, Geologic map of the Dragoon Mountains Roadless Area, Cochise County, Arizona: U.S. Geological Survey Miscellaneous Field Studies Map MF–1521–A, scale 1:50,000.

Drewes, Harald, Moss, C.K., Watts, K.C., Jr., Forn, C.L., and Bigsby, P.R., 1983b, Mineral resource potential map of the North End Roadless Area, Chiricahua Mountains, Cochise County, Arizona: U.S. Geological Survey Miscellaneous Field Studies Map MF–1412–D, scale 1:50,000.

Drewes, Harald, and Williams, F.E., 1973, Mineral resources of the Chiricahua Wilderness area, Cochise County, Arizona: U.S. Geological Survey Bulletin 1385–A, 53 p., 1 pl.

Elsing, H.J., and Heineman, R.E., 1936, Arizona metal production: Arizona Bureau of Mines Bulletin 140, 112 p.

Epis, R.C., 1956, Geology of the Pedregosa Mountains, Cochise County, Arizona: Berkeley, Calif., University of California, Ph.D. dissertation, 263 p.

Erb, E.E., Jr., 1979, Petrologic and structural evolution of ash-flow tuff cauldrons and non-cauldron-related volcanic rocks in the Animas and southern Peloncillo Mountains, Hidalgo County, New Mexico: Albuquerque, N. Mex., University of New Mexico, Ph.D. dissertation, 286 p.

Feth, J.H., 1948, Permian stratigraphy and structure, northern Canelo Hills, Arizona: American Association of Petroleum Geologists Bulletin, v. 32, no. 1, p. 82–108.

Finnell, T.L., 1971, Preliminary geologic map of the Empire Mountains, Pima County, Arizona: U.S. Geological Survey Open-File Report 71–106, scale 1:48,000.

Frost, E.G., and Martin, D.L., eds., 1982, Mesozoic-Cenozoic tectonic evolution of the Colorado River region, California, Arizona, and Nevada: San Diego, Calif., Cordilleran Publishers, 608 p.

Gilluly, James, 1956, General geology of central Cochise County, Arizona, *with sections on* Age and correlation by A.R. Palmer, J.S. Williams, and J.B. Reeside, Jr.: U.S. Geological Survey Professional Paper 281, 169 p.

Gilluly, James, Cooper, J.R., and Williams, J.S., 1954, Late Paleozoic stratigraphy of central Cochise County, Arizona: U.S. Geological Survey Professional Paper 266, 49 p.

Graybeal, F.T., 1962, The geology and gypsum deposits of the southern Whetstone Mountains, Cochise County, Arizona: Tucson, Ariz., University of Arizona, M.S. thesis, 80 p.

Hagstrum, J.T., and Lipman, P.W., 1991, Late Cretaceous paleomagnetism of the Tucson Mountains—Implications for vertical axis rotations in south central Arizona: Journal of Geophysical Research, v. 96, B10, p. 16069–16081.

Hayes, P.T., 1970a, Mesozoic stratigraphy of the Mule and Huachuca Mountains, Arizona: U.S. Geological Survey Professional Paper 658–A, 28 p.

———1970b, Cretaceous paleogeography of southeastern Arizona and adjacent areas: U.S. Geological Survey Professional Paper 658–B, 42 p.

———1972, Stratigraphic nomenclature of Cambrian and Lower Ordovician rocks of easternmost southern Arizona and adjacent westernmost New Mexico: U.S. Geological Survey Bulletin 1372–B, 19 p.

———1982, Geologic map of the Bunk Robinson and Whitmire Canyon Roadless Areas, Coronado National Forest, New Mexico and Arizona: U.S. Geological Survey Miscellaneous Field Studies Map MF–1425–A, scale 1:62,500.

Hayes, P.T., and Cone, G.C., 1975, Cambrian and Ordovician rocks of southern Arizona and New Mexico and westernmost Texas: U.S. Geological Survey Professional Paper 873, 98 p.

Hayes, P.T., and Raup, R.B., 1968, Geologic map of the Huachuca and Mustang Mountains, southeastern Arizona: U.S. Geological Survey Miscellaneous Geologic Investigations Map I–509, scale 1:48,000.

Hayes, P.T., Simons, F.S., and Raup, R.B., 1965, Lower Mesozoic extrusive rocks in southeastern Arizona, the Canelo Hills Volcanics: U.S. Geological Survey Bulletin 1194–M, 9 p.

Hayes, P.T., Watts, K.C., Hassemer, J.R., and Brown, S.D., 1983, Mineral resource potential map of the Bunk Robinson Peak and Whitmire Canyon Roadless Area, Hidalgo County, New Mexico, and Cochise County, Arizona: U.S. Geological Survey Miscellaneous Field Studies Map MF–1425–B, scale 1:62,500.

Johnson, M.G., 1972, Placer gold deposits of America: U.S. Geological Survey Bulletin 1355, 103 p.

Keith, S.B., 1969, Gypsum and anhydrite, *in* Mineral and water resources of Arizona: Arizona Bureau of Mines Bulletin 180, p. 371–382.

———1973, Index of mining properties in Cochise County, Arizona: Arizona Bureau of Mines Bulletin 187, 98 p.

Keith, S.B., and Wilt, J.C., 1978, Second day road log from Douglas to Tucson via Bisbee, Tombstone, Charleston, Fort Huachuca, and Sonoita, *in* Callender, J.F., Wilt, J.C., and Clemons, R.E., eds., Land of Cochise, southeastern Arizona: New Mexico Geological Society, Annual Field Conference Guidebook, no. 29, p. 31–76.

Keith, W.J., Martin, R.H., and Kreidler, T.J., 1982, Mineral resource potential of the Winchester Mountains Roadless Area, Cochise County, Arizona: U.S. Geological Survey Open-File Report 82–1028, 7 p.

Keith, W.J., and Theodore, T.G., 1975, Reconnaissance geologic map of the Arivaca quadrangle, Arizona: U.S. Geological Survey Miscellaneous Field Studies Map MF–678, scale 1:62,500.

Klein, D.P., 1983, Geophysical maps of the Dragoon Mountains Roadless Area, Cochise County, Arizona: U.S. Geological Survey Miscellaneous Field Studies Map MF–1521–C, scale 1:50,000.

Knight, L.H., Jr., 1970, Structure and mineralization of the Oro Blanco mining district, Santa Cruz County, Arizona: Tucson, University of Arizona, Ph.D. dissertation, 251 p.

Kreidler, T.J., 1984, Mine and prospect map of the Dragoon Mountains Roadless Area, Cochise County, Arizona: U.S. Geological Survey Miscellaneous Field Studies Map MF–1521–F, scale 1:50,000.

Krieger, M.H., Johnson, M.G., and Bigsby, P.R., 1979, Mineral resources of the Arivaipa Canyon Instant Study Area, Pinal and Graham Counties, Arizona: U.S. Geological Survey Open-File Report 79–291, 183 p., 1 pl., map scale 1:24,000.

Kuhn, T.H., 1941, Pipe deposits of the Copper Creek area, Arizona: Economic Geology, v. 36, p. 512–538.

———1951, Bunker Hill district, *in* Arizona zinc and lead deposits: Arizona Bureau of Mines Bulletin 158, p. 56–65.

Lucarelli, Ludano, 1967, Mapa geologico de la parte septemprional del estado de Sonora (Sheet 7): Unpublished map series of the Consejo de Recursos Naturales No Renovables and of the United Nations, scale 1:100,000.

Mardirosian, C.A., 1977, Mining districts and mineral deposits of Arizona (2nd ed.), private publication, press not identified, scale 1:1,000,000.

Marjaniemi, D.K., 1968, Tertiary volcanics in the northern Chiricahua Mountains, Cochise County, Arizona, *in* Southern Arizona Guidebook 3: Tucson, Ariz., Arizona Geological Society, p. 209–214.

McColly, R.A., and Scott, D.C., 1982, Mineral investigations of the Whetstone Roadless Area, Cochise and Pima Counties, Arizona: U.S. Bureau of Mines Open-File Report MLA 129–82, 22 p.

McIntyre, D.H., 1988, Volcanic geology in parts of the southern Peloncillo Mountains, Arizona and New Mexico: U.S. Geological Survey Bulletin 1671, 18 p.

Naruk, S.J., and Bykerk-Kauffman, A., 1990, Late Cretaceous and early Tertiary deformation of the Santa Catalina metamorphic core complex, Arizona, *in* Gehrels, G.E., and Spencer, J.E., Geologic excursions through the Sonoran Desert region, Arizona and Sonora: Arizona Geological Survey Special Paper 7, p. 41–50.

Nelson, F.J., 1963, The geology of the Peña Blanca and Walker Canyon area, Santa Cruz County, Arizona: Tucson, University of Arizona, M.S. thesis, 105 p.

Pallister, J.S., and du Bray, E.A., 1994, Geologic map of the Fife Peak quadrangle, Cochise County, Arizona: U.S. Geological Survey Geologic Quadrangle Map GQ–1708, scale 1:24,000.

Pallister, J.S., du Bray, E.A., and Latta, J.S., IV, 1994, Geologic map of the Rustler Park quadrangle, Cochise County, Arizona: U.S. Geological Survey Geologic Quadrangle Map GQ–1696, scale 1:24,000.

Pashley, E.F., 1966, Structure and stratigraphy of the central northern and eastern parts of the Tucson Basin, Pima County, Arizona: Tucson, University of Arizona, Ph.D. dissertation, 273 p.

Reynolds, S.J., and Lister, G.S., 1990, Folding of mylonitic zones in Cordilleran metamorphic core complexes—Evidence from near the mylonitic front: Geology, v. 18, p. 216–219.

Richter, D.H., and Lawrence, V.A., 1983, Mineral deposit map of the Silver City 1° × 2° quadrangle, New Mexico and Arizona: U.S. Geological Survey Miscellaneous Investigations Series Map I–1310–B, scale 1:250,000.

Richter, D.H., Sharp, W.N., Watts, K.C., Raines, G.L., Houser, B.B., and Klein, D.P., 1986, Maps showing mineral resource assessment of the Silver City 1° × 2° quadrangle, New Mexico and Arizona: U.S. Geological Survey Miscellaneous Investigations Series Map I–1310–F, scale 1:250,000.

Riggs, N.R., 1987, Stratigraphy, structure, and geochemistry of Mesozoic rocks in the Pajarito Mountains, Santa Cruz County, Arizona, *in* Dickenson, W.R., and Klute, M.A., eds., Mesozoic rocks of southern Arizona and adjacent areas: Arizona Geological Society Digest, v. 18, p. 165–176.

Riggs, N.R., and Haxel, G.B., 1990, The early to middle Jurassic magmatic arc in southern Arizona—Plutons to sand dunes, *in* Gehrels, G.E., and Spencer, J.E., Geologic excursions through the Sonoran Desert region, Arizona and Sonora: Arizona Geological Survey Special Paper 7, p. 90–103.

Riggs, N.R., Haxel, G.B., and Busby-Spera, C.J., 1990, Paleogeography and tectonic setting of the Jurassic magmatic arc in southern Arizona—Progress and problems: Geological Society of America Abstracts with Programs, v. 22, no. 3, p. 78.

Ross, C.P., 1925, Geology and ore deposits of the Aravaipa and Stanley mining districts, Graham County, Arizona: U.S. Geological Survey Bulletin 763, 120 p.

Sabins, F.F., Jr., 1957, Geology of the Cochise Head and western part of the Vanar quadrangles, Arizona: Geological Society of America Bulletin, v. 68, no. 10, p. 1315–1342, map scale 1:62,500.

Schrader, F.C., 1915, Mineral deposits of the Santa Rita and Patagonia Mountains, Arizona, *with contributions by* J.M. Hill: U.S. Geological Survey Bulletin 582, 373 p.

Schumacher, Dietmar, 1978, Devonian stratigraphy and correlations in southeastern Arizona, *in* Callender, J.F., Wilt, J.C., and Clemons, R.E., eds., Land of Cochise, southeastern Arizona: New Mexico Geological Society, Annual Field Conference Guidebook, no. 29, 1978, p. 175–181.

Shakel, D.W., Silver, L.T., and Damon, P.E., 1977, Observations on the history of the gneissic core complex, Santa Catalina Mountains, southern Arizona: Geological Society of America Abstracts with Programs, v. 9, p. 1169–1170.

Simons, F.S., 1964, Geology of the Klondyke quadrangle, Graham and Pinal Counties, Arizona: U.S. Geological Survey Professional Paper 461, 173 p., map scale 1:62,500.

———1972, Mesozoic stratigraphy of the Patagonia Mountains and adjoining areas, Santa Cruz County, Arizona: U.S. Geological Survey Professional Paper 658–E, 23 p.

———1974, Geologic map and sections of the Lochiel and Nogales quadrangles, Santa Cruz County, Arizona: U.S. Geological Survey Miscellaneous Investigations Series Map I–762, scale 1:48,000.

Stewart, L.A., and Pfister, A.J., 1960, Barite deposits of Arizona: U.S. Bureau of Mines Report of Investigations 5651, p. 10–11.

Swan, N.M., 1975, The Texas lineament—Tectonic expression of a Proterozoic orogeny: Geological Society of America Abstracts with Programs, v. 7, no. 7, p. 1288–1289.

———1976, The Stockton Pass fault—An element of the Texas lineament: Tucson, University of Arizona, M.S. thesis, 119 p.

Thompson, Sam, III, and Jacka, A.D., 1981, Pennsylvanian stratigraphy, petrography, and petroleum geology of the Big Hatchet Peak section, Hidalgo County, New Mexico: New Mexico Bureau of Mines and Mineral Resources Circular 176, 125 p.

Thompson, Sam, III, Tovar, J.C., and Conley, J.N., 1978, Oil and gas exploration wells in the Pedregosa basin, *in* Callender, J.F., Wilt, J.C., and Clemons, R.E., eds., Land of Cochise, southeastern Arizona: New Mexico Geological Society, Annual Field Conference Guidebook, no. 29, p. 331–344.

Thorman, C.H., 1981, Geology of the Pinaleno Mountains, Arizona—A preliminary report: Arizona Geologic Society Digest v. 13, p. 5–12.

Thorman, C.H., Drewes, Harald, and Lane, M.E., 1981, Mineral resources of the Rincon Wilderness Study Area, Pima County, Arizona: U.S. Geological Survey Bulletin 1500, 62 p., 2 pls., map scale 1:48,000.

Tyrrell, W.W., Jr., 1957, Geology of the Whetstone Mountains area, Cochise and Pima Counties, Arizona: New Haven, Conn., Yale University, Ph.D. dissertation, 171 p.

U.S. Geological Survey, 1973, Map showing potential for copper deposits in the eastern three-quarters of the Nogales 2° quadrangle, Tucson area, Arizona: U.S. Geological Survey Miscellaneous Investigations Series Map I–844–G, scale 1:250,000.

Wardlaw, B.R., and Harris, A.G., 1984, Conodont-based thermal maturation of Paleozoic rocks in Arizona: American Association of Petroleum Geologists Bulletin, v. 69, p. 1101–1106.

Watts, K.C., Jr., Drewes, Harald, and Forn, C.L., 1985, Geochemistry of the North End Roadless area, Cochise County, Arizona: U.S. Geological Survey Miscellaneous Field Studies Map MF–1412–C.

Watts, K.C., Jr., Hassemer, J.R., Erickson, M.S., and Drewes, Harald, 1984, Geochemical and mineralogic maps of the Dragoon Mountains Roadless Area, Cochise County, Arizona: U.S. Geological Survey Miscellaneous Field Studies Map MF–1521–E, scale 1:50,000.

Weed, W.H., 1913,"Chimney" or "pipe" deposits in the porphyries: Mining and Engineering World, v. 38, p. 375–378.

Wilson, E.D., 1950, Fluorspar in Arizona: Arizona Bureau of Mines Circular 15, 13 p.

———1961, Gold placers and placering in Arizona: Arizona Bureau of Mines Bulletin 168, 124 p.

Wilson, E.D., Cunningham, J.B., and Butler, B.M., 1934 [revised 1967], Arizona lode mines and mining: Arizona Bureau of Mines Bulletin 137, 154 p.

Wilson, E.D., Moore, R.T., and Cooper, J.R., 1969, Geologic map of Arizona: U.S. Geological Survey map, scale 1:500,000.

Wrucke, C.T., and Armstrong, A.K., 1984, Geologic map of the Whetstone Roadless Area and vicinity, Cochise and Pima Counties, Arizona: U.S. Geological Survey Miscellaneous Field Studies Map MF–1614–B, scale 1,48,000.

Wrucke, C.T., and Bromfield, C.S., 1961, Reconnaissance geologic map of part of the southern Peloncillo Mountains, Hidalgo County, New Mexico: U.S. Geological Survey Mineral Investigations Field Studies Map MF–160, scale 1:62,500.

Wrucke, C.T., McColly, R.A., Werschky, R.S., Scott, D.C., Bankey, V.L., Kleinkopf, M.D., Staatz, M.H., and Armstrong, A.K., 1983, Mineral resource potential map of the Whetstone Roadless Area, Cochise and Pima Counties, Arizona: U.S. Geological Survey Miscellaneous Field Studies Map MF–1614–A, scale 1:48,000.

Geochemistry of Coronado National Forest

By Gary A. Nowlan

MINERAL RESOURCE POTENTIAL AND GEOLOGY OF CORONADO NATIONAL FOREST, SOUTHEASTERN ARIZONA AND SOUTHWESTERN NEW MEXICO
Edited by Edward A du Bray

U.S. GEOLOGICAL SURVEY BULLETIN 2083–C

UNITED STATES GOVERNMENT PRINTING OFFICE, WASHINGTON : 1996

CONTENTS

TABLES

Geochemistry of Coronado National Forest

By Gary A. Nowlan

ABSTRACT

Geochemical data for samples collected in Coronado National Forest and adjacent areas, southeastern Arizona and southwestern New Mexico, were compiled from existing U.S. Geological Survey data bases in order to characterize the geochemistry of the Forest and to aid in determining its mineral resource potential. The geochemical evaluation is based mainly on stream-sediment data because the stream-sediment sample coverage is much more extensive than are other sample media (rocks or panned concentrates) and is supplemented, in places, by data from rock and panned-concentrate samples. Existing data were supplemented for this study by additional stream-sediment sampling in areas of sparse sampling.

The routine analytical method for the samples considered in this study, including 3,874 stream-sediment, 1,355 panned-concentrate, and 1,782 rock samples, was 31-element, semiquantitative, direct-current arc emission spectrography. In addition, all of the new (approximately 150 samples) and a representative part (approximately 2,500 samples) of the existing stream-sediment samples were analyzed for Au by flameless atomic-absorption spectrophotometry and for Ag, As, Au, Bi, Cd, Cu, Mo, Pb, Sb, and Zn by inductively coupled plasma spectroscopy. Flameless atomic-absorption spectrophotometric and inductively coupled plasma spectroscopic analyses were conducted in order to obtain accurate, quantitative data for these elements; abundances of these elements are so low, in most cases, that they are below detection limits for direct-current arc emission spectrographic analysis. The geochemical evaluation is principally based on abundances of Ag, As, Au, Ba, Bi, Cd, Cu, Mn, Mo, Pb, Sb, Sn, W, and Zn because of their association with most hydrothermal ore deposits of the types present in the geologic environments represented in the Forest. The geochemical signature of certain parts of the Forest is compatible with signatures characteristic of several types of mineral deposits.

The Forest was subdivided into 35 areas that were delineated on the basis of geologic settings. These areas were ranked on a scale of 1 to 10 on the basis of geochemical intensity; the most and least geochemically anomalous areas were assigned geochemical intensity values of 10 and 1, respectively. Rankings are based on the number of elements present in anomalous concentrations, the proportion of samples having anomalous concentrations of these elements, and the magnitude of concentrations in individual samples. The outlines of these areas are shown on plate 5, and their rankings by geochemical intensity are listed below:

Area	*Rank*
Patagonia Mountains, southern part	10
Santa Teresa Mountains, west-central part	9
Dragoon Mountains, middle one-third	9
Patagonia Mountains, northern part	9
Santa Rita Mountains, western three-fourths	8
Tumacacori and Atascosa Mountains	8
Pinaleno Mountains, southeastern half	7
Chiricahua Mountains, northern part	7
Dragoon Mountains, northern one-third	7
Dragoon Mountains, southern one-third	7
Huachuca Mountains	7
Santa Rita Mountains, northern part	7
Cobre and Coches Ridges, Pajarito Mountains	7
Chiricahua Mountains, except northern part	6
Whetstone Mountains, northeastern one-third	6
Whetstone Mountains, southwestern one-third	6
Santa Rita Mountains, eastern part	6
Santa Catalina Mountains, northern part	6
Rincon Mountains, northern part; Santa Catalina Mountains, southern part	6
Galiuro Mountains	5
Pedregosa Mountains, western part	5
Whetstone Mountains, middle one-third	5
Area west of Nogales	5
Santa Catalina and Rincon Mountains, eastern part	5
Santa Teresa Mountains, northwestern part	4
Peloncillo Mountains	4
Pedregosa Mountains, eastern part	4
Santa Teresa Mountains, southern and southeastern parts	3
Winchester Mountains, eastern two-fifths	3
Pinaleno Mountains, northwestern half	3
San Rafael Valley	3
San Luis Mountains	3
Canelo Hills	2
Rincon Mountains, southern part	2
Winchester Mountains, western three-fifths	1

INTRODUCTION

Geochemical methods have been used in prospecting for metallic ores in the general area of Coronado National Forest since at least 1950 (Lovering and others, 1950). These methods are widely accepted and used as tools in the search for ore deposits in southeastern Arizona and elsewhere. Application of geochemical techniques and data in mineral resource evaluations is a consequence of (1) their acceptance as a valid prospecting method, (2) initiatives to preserve tracts of federal lands as wilderness, and (3) the need of government agencies to make land-use decisions.

Geochemical data used in this mineral resource evaluation of Coronado National Forest were obtained for samples collected as long ago as 1963. The comparability of data collected over such a long time span is assured, however, by the fact that analytical techniques, emission spectrography (ES) in particular, have changed very little since 1963. In addition, many of the analysts who were part of the southeastern Arizona geochemical surveys conducted in the 1960's are still employees of the U.S. Geological Survey (USGS) and either analyzed the samples themselves or trained others who performed the analyses.

Most of the USGS samples considered in this mineral resource evaluation were collected, beginning in the early 1960's, during investigations of geochemical zonation around known mineralized areas or as part of mineral resource evaluations of specific areas. The purpose, history, and procedures of U.S. Forest Service wilderness studies made from 1965 to 1983 were summarized by Brobst and Goudarzi (1984). Hundreds of samples were also collected as part of the Conterminous United States Mineral Assessment Program (CUSMAP) studies of the Silver City 1° × 2° quadrangle in the late 1970's and early 1980's (McDanal and others, 1983; Watts and Hassemer, 1988). Curtin (1985) summarized CUSMAP studies.

In addition to USGS samples, data for about 1,800 samples obtained during the National Uranium Resource Evaluation (NURE) program of the U.S. Department of Energy (Shannon, 1977) were included in the Coronado National Forest data base (U.S. Department of Energy, 1981a, b; 1982a–c).

Approximately 150 stream-sediment samples were collected in 1990 from the Chiricahua, Santa Teresa, and Santa Catalina Mountains to provide sample coverage where it was lacking. Also, about 2,500 samples of stream-sediment and soil were retrieved from sample archives of the USGS in 1990 and 1991 and were reanalyzed by sensitive, modern methods for low levels of gold and several other metals.

Retrieval and consolidation of data from these several sources has resulted in a geochemical data base for Coronado National Forest that is adequate, for the most part, to characterize regional geochemistry of the Forest and to allow a mineral resource evaluation, when combined with data from other earth science disciplines.

SOURCES OF DATA

Analytical data, summarized in table 1, for samples from Coronado National Forest and adjacent areas (the Coronado study area) stored in the USGS Rock Analysis Storage System (RASS), PLUTO (described below), and NURE computerized data bases were retrieved and examined by the STATPAC system (VanTrump and Miesch, 1977). The RASS and PLUTO data bases contain analytical and descriptive data for rock, stream-sediment, heavy-mineral-concentrate, and soil samples, and for other types of geologic material collected by the USGS. They also contain data for other sample types such as water and vegetation. The NURE data base contains analytical and other data for samples collected during the National Uranium Resource Evaluation program of the U.S. Department of Energy (Shannon, 1977; Sharp and Aamodt, 1978; Sharp and others, 1978; Cook and Fay, 1982).

Most of the USGS analytical data for the Coronado study area are stored in the RASS data base (VanTrump and Miesch, 1977). Some USGS data for samples from the Coronado study area are stored in the PLUTO data base (formerly the geochemical data base of the USGS Branch of Analytical Chemistry and subsequently adopted as the geochemical data base of the the USGS Branch of Geochemistry), but because the RASS and PLUTO data bases are operationally similar, reference to the RASS data base will hereafter include sample data from the PLUTO data base. Data for selected elements useful in mineral resource evaluations were studied and plotted. Data in the RASS and NURE computer data bases are available to the public. Some of the data had not been released as published or open-file reports before this mineral resource evaluation of Coronado National Forest; reports released before that time are listed in table 1. A tabulation of both previously released and unreleased geochemical data used in the mineral resource evaluation of Coronado National Forest is available (Nowlan and Chaffee, 1995).

SAMPLE TYPES

RASS data for stream-sediment samples, panned-concentrate samples derived from stream sediment, and rock samples were considered because the samples they represent have the widest areal distribution in the study area. The stream-sediment fraction analyzed was usually minus-80 (<0.177 mm) or minus-60 (<0.250 mm) mesh; the minus-30-mesh fraction (<0.595) was analyzed for about 40 samples. Panned-concentrate samples are the nonmagnetic heavy fraction of stream sediments and consist of nonmagnetic ore minerals and some accessory minerals such as sphene and zircon. The rock data are for unmineralized, mineralized, and altered rock samples.

Table 1. Published sources of geochemical data for Coronado National Forest and adjacent areas, southeastern Arizona and southwestern New Mexico.

Forest unit designation (fig. 1)	Name	Area sampled	Reference
A1	Santa Teresa Mountains	Black Rock Wilderness Study Area	Harms and others, 1985.
		Tucson 1°×2° quadrangle	U.S. Department of Energy, 1982d.
A2	Galiuro Mountains	Galiuro Wilderness and contiguous Further Planning Areas.	Creasey and others, 1981.
		Tucson 1°×2° quadrangle	U.S. Department of Energy, 1982d.
A3	Winchester Mountains	Winchester Roadless Area	Sutley and others, 1983.
		Tucson 1°×2° quadrangle	U.S. Department of Energy, 1982d.
A4	Pinaleno Mountains	Silver City 1°×2° quadrangle	McDanal and others, 1983.
		Tucson 1°×2° quadrangle	U.S. Department of Energy, 1982d.
B1	Peloncillo Mountains	Bunk Robinson Peak and Whitmire Canyon Roadless Areas.	Watts and others, 1983.
		New Mexico part of Douglas 1°×2° quadrangle.	U.S. Department of Energy, 1982a.
B2	Chiricahua and Pedregosa Mountains.	Chiricahua Wilderness Area	Drewes and Williams, 1973.
		Silver City 1°×2° quadrangle	McDanal and others, 1983.
C1	Dragoon Mountains	Dragoon Mountains Roadless Area	Drewes, 1984; Watts and others, 1984.
		Nogales 1°×2° quadrangle	U.S. Department of Energy, 1982b.
		Tucson 1°×2° quadrangle	U.S. Department of Energy, 1982d.
D1	Whetstone Mountains	Whetstone Roadless Area	Werschsky and others, 1983.
		Nogales 1°×2° quadrangle	U.S. Department of Energy, 1982b.
D2	Patagonia and Huachuca Mountains; Canelo Hills.	Nogales 1°×2° quadrangle	U.S. Department of Energy, 1982b.
E1	Santa Rita Mountains	Santa Rita Mountains	Drewes, 1967, 1970, 1973.
		Nogales 1°×2° quadrangle	U.S. Department of Energy, 1982b.
E2	Atascosa, Pajarito, San Luis, and Tumacacori Mountains; Cobre and Coches Ridges.	Nogales 1°×2° quadrangle	U.S. Department of Energy, 1982b.
F1	Santa Catalina and Rincon Mountains.	Pusch Ridge Wilderness Area	Hinkle and others, 1981a.
		Rincon Wilderness Study Area	Thorman and others, 1981.
		Tucson 1°×2° quadrangle	U.S. Department of Energy, 1982d.

NURE data consist of analyses of stream-sediment and soil samples. Evaluation of the stream-sediment and soil data separately indicates that the two media can be combined and treated as one data set. The analyzed fraction of NURE samples from the Coronado study area is the minus-100 mesh (<0.149 mm) fraction.

ANALYTICAL METHODS

Almost all RASS samples included in this investigation of the Coronado study area were analyzed for 31 or more elements by semiquantitative, direct-current arc emission spectrography (ES) (Grimes and Marranzino,1968; Myers and others, 1961). RASS samples from some areas were analyzed by atomic absorption or other methods; these additional analyses were considered but their usefulness is limited because of incomplete areal coverage.

Concentrations of elements determined by the emission spectrographic method are reported as six steps per order of magnitude that represent intervals of some power of 10 times 1.2–1.8, 1.8–2.6, 2.6–3.8, 3.8–5.6, 5.6–8.3, or 8.3–12 (Motooka and Grimes, 1976, p. 2). For most samples in this report, those intervals are represented by the values 1.5, 2, 3, 5, 7, and 10, respectively, or powers of 10 of these numbers. Reported values for some samples are somewhat different but still represent approximately the same intervals. The precision of the emission spectrographic method is approximately ± one reporting interval at the 83 percent confidence level and ± two reporting intervals at the 96 percent confidence level (Motooka and Grimes, 1976, p. 3).

NURE samples from New Mexico were analyzed for uranium by delayed neutron counting with a precision of 4 percent or better (Sharp and others, 1978, p. 18). NURE samples from the Nogales and Tucson 1° × 2° quadrangles were also analyzed for uranium by delayed neutron counting; coefficients of variation for control samples ranged from 0.03 to 0.24 (U.S. Department of Energy, 1982c, p. 15). All but two of the NURE samples were analyzed by inductively coupled plasma spectroscopy (ICP). NURE samples were analyzed by ICP for Ag, Al, B, Ba, Be, Ca, Ce, Co, Cr, Cu, Fe, Hf, K, La, Li, Mg, Mn, Mo, Na, Nb, Ni, P, Pb, Sc, Sr, Th, Ti, V, Y, Zn, and Zr; coefficients of variation for control samples ranged from 0.03 to 2.57 (U.S. Department of Energy, 1981a, p. 15; 1982c, p. 15).

In addition to existing USGS data, abundances of Au (determined by flameless atomic-absorption spectrophotometry, or FAA) and Ag, As, Au, Bi, Cd, Cu, Mo, Pb, Sb, and Zn (determined by inductively coupled plasma spectroscopy, or ICP) were determined for about 2,500 archived RASS and NURE samples. The FAA method was described by Meier (1980) and by O'Leary and Meier (1986); the precision of the method, based on five replicate analyses of six samples, was found to range from 3.7 to 21.1 percent relative standard deviation (O'Leary and Meier, 1986, p. 27). The ICP method was described by Motooka (1988); the precision of the method, based on 10 replicate analyses of four samples, ranged from 0.8 to 4.0 percent relative standard deviation (Motooka, 1988, table 3).

The archived samples selected for analyses by FAA and ICP were chosen to give reasonably uniform areal coverage of the mountainous and mountain-front areas of the Coronado study area. Approximately 150 additional samples collected in 1990 in the Chiricahua, Santa Teresa, and Santa Catalina Mountains were analyzed by FAA and ICP to provide coverage where none existed previously.

DATA COVERAGE

Map A, plate 5, shows the Coronado study area, which encompasses about 25,900 km^2, and the approximate boundaries of the 12 units that make up Coronado National Forest, which encompasses about 7,500 km^2. Sampling localities for the various sample media are shown on maps B–F, plate 5. Distribution of RASS stream-sediment sampling sites (map B, pl. 5) is adequate for a regional geochemical evaluation, but it is not of uniform density and is especially sparse in parts of the Santa Catalina–Rincon and Pinaleno Forest units (map B, pl. 5). The average sampling-site density for RASS stream-sediment samples in the Coronado study area is approximately one site per 6.5 km^2. The average sampling-site density within the 12 units that make up the Forest is somewhat greater because most of these sites are limited to the mountain ranges and nearby areas. Map C, plate 5, shows the sampling sites for samples analyzed by FAA and ICP expressly for this study; average sampling-site density for samples in the Coronado study area so analyzed is approximately one site per 10 km^2. The pattern is based on NURE samples from the Nogales and Tucson 1° × 2° quadrangles, basin samples being omitted, and the New Mexico part of the Douglas 1° × 2° quadrangle, a selected portion of RASS stream-sediment samples from the Douglas and Silver City 1° × 2° quadrangles, and the new stream-sediment samples collected in the Chiricahua, Peloncillo, Santa Catalina, and Santa Teresa Mountains. Panned-concentrate sampling sites (map D, pl. 5) are unevenly distributed in Coronado National Forest; coverage of the Forest units ranges from no samples in the Galiuro Mountains to heavy coverage in the southern Pinaleno Mountains. Distribution of rock sampling sites (map E. pl. 5) is spotty and tends to be heavily concentrated in several mining districts. NURE samples (map F, pl. 5) are limited to the Nogales and Tucson 1° × 2° quadrangles and to the small part of the Douglas 1° × 2° quadrangle that is in New Mexico. The Arizona parts of the Douglas and Silver City 1° × 2° quadrangles were apparently never sampled in the NURE program. However, the only parts of Coronado National Forest having no NURE coverage are the Chiricahua and Pedregosa Mountains, most of the Pinaleno Mountains, and the eastern part of the Dragoon Mountains.

NURE coverage of some of the other mountain ranges is somewhat poor because, apparently, sampling was largely limited to roads and well-established hiking trails.

GEOCHEMICAL EVALUATION

A large number of the interpretive geochemical studies of areas in and near Coronado National Forest augment mineral resource evaluations of wilderness areas and proposed wilderness areas. The mineral-resource potential, as of 1984, of wilderness study areas was cursorily summarized on a map by Peterson and others (1984); this map also shows the locations of potential wildernesses not studied by the USGS. Results of evaluations of National Forest wilderness and potential wilderness areas that were studied by the USGS and U.S. Bureau of Mines are summarized by Marsh and others (1984). Locations of wilderness study areas and established wildernesses as of 1986 are shown on wilderness status maps of Arizona and New Mexico published by the U.S. Bureau of Land Management (U.S. Bureau of Land Management, 1986a, b).

In addition to the many interpretive geochemical studies of selected areas in and near Coronado National Forest, three broad regional interpretive geochemical studies have been carried out by the USGS; two of the studies have been released. One of the released studies (Chaffee, 1990) is part of a preliminary mineral resource assessment of the Tucson and Nogales 1° × 2° quadrangles (Peterson, 1990) and is based entirely on a compilation of geochemical data obtained for other studies. The other released broad study is of the Silver City 1° × 2° quadrangle (Watts and others, 1986a–j; Watts and Hassemer, 1988) and is based on several thousand panned-concentrate, stream-sediment, rock, and water samples collected as part of a CUSMAP study of the Silver City 1° × 2° quadrangle.

In addition to the two released regional studies, a similar assessment of the Douglas 1° × 2° quadrangle was prepared as an administrative report. This report was prepared by J.M. Hammarstrom, Harald Drewes, J.D. Friedman, D.P. Klein, D.M. Kulik, K.C. Watts, Jr., J.A. Pitkin, S.L. Simpson, and T.G. Theodore, and will be referred to throughout this report as "J.M. Hammarstrom and others, unpub. data, 1988." The Tucson-Nogales, Silver City, and Douglas 1° × 2° quadrangle interpretive reports together cover most of Coronado National Forest; they and interpretive reports of smaller areas will be referred to in this geochemical evaluation.

Plots of abundances of selected elements in the various sample media were prepared in order to depict geochemical trends in the Coronado study area. The selected elements include Ag, As, Au, B, Ba, Be, Bi, Cd, Ce, Co, Cr, Cu, La, Mn, Mo, Nb, Ni, Pb, Sb, Sc, Sn, Th, U, V, W, Y, and Zn. The geochemical evaluation is based most heavily on existing data from RASS stream-sediment samples and the new FAA analyses of gold and the 10-element ICP because of the more complete and uniform coverage by these sample media.

Statistics for the selected elements are presented in table 2. Threshold (highest background) concentrations were selected by visual and statistical examination of the data and by reference to published reports of specific geochemical studies of areas in southeastern Arizona and southwestern New Mexico. Table 2 includes published threshold concentrations established for specific studies within or adjacent to the Coronado study area; these are included for reference and illustrate how threshold concentrations vary with the scale of the study, variations in local bedrock types as well as in types of mineralized rock present, and the judgment of the individual investigator.

Geochemical evaluations of geologic terrain must establish anomalous elemental concentrations relative to background. This issue is more difficult when a wide range of rock types is present. For example, the average concentration of cobalt in mafic rocks is 48 ppm (parts per million), but in granite it is 1 ppm (Rose and others, 1979, p. 554). If high concentrations of cobalt are accompanied by high concentrations of other common constituents of mafic rocks, such as nickel and chromium, high concentrations of cobalt might be due to the presence of mafic rocks and therefore are probably not anomalous. On the other hand, high concentrations of cobalt accompanied by high concentrations of base metals but not by nickel and chromium may indicate that hydrothermal activity is responsible for the high concentrations. Cobalt is part of the geochemical signature for a number of mineral deposit types that are not associated with mafic rocks, such as porphyry copper-molybdenum (Cox, 1986). Therefore, the recognition of geochemical signatures is an important part of the geochemical evaluation of Coronado National Forest in view of the wide range of bedrock types.

The geochemical evaluation in this study identifies geochemical signatures that may be related to hydrothermal processes. Obviously, the elements analyzed by 10-element ICP and FAA (Au, As, Ag, Bi, Cd, Cu, Mo, Pb, Sb, and Zn) are evidence of hydrothermal processes when they are present together in anomalous concentrations. Other elements such as barium, tungsten, and manganese can also be part of the geochemical signature for hydrothermal mineral deposits.

The 12 Coronado National Forest units, divided into 35 subareas on the basis of very generalized geology, are listed in table 3 and are shown on map A, pl. 5. The geology of each subarea is adapted from the Geologic Map of Arizona (Reynolds, 1988), the New Mexico Geologic Highway Map (New Mexico Geological Society, 1982), and from selected, more detailed geologic reports. These more detailed reports are referenced in the mineral resource or geologic reports for the Silver City, Douglas, and Tucson-Nogales 1° × 2° quadrangles (Drewes and others, 1985; J.M. Hammarstrom and others, unpub. data, 1988; Peterson and others, 1990, tables 1 and 2). Elements considered to be present in anomalous concentrations in samples from each subarea are listed in table 3.

Table 2. Geochemical statistics for selected elements in samples of stream sediment, soil, and heavy-mineral concentrate from Coronado National Forest and adjacent areas, southeastern Arizona and southwestern New Mexico.

[Concentrations in RASS/PLUTO stream-sediment and RASS heavy-mineral-cncentrate samples determined by emission spectrography; concentrations in RASS/NURE stream-sediment and soil samples determined by inductively coupled plasma spectroscopy, except gold, which was determined by flameless atomic-absorption spectrophotometry. ppm, parts per million; N, not detected at concentration shown; L, detected below concentration shown; G, greater than concentration shown; ---, no data. 50th percentile, concentrations in one-half of samples are equal to or lower than this number. Threshold: GW, Galiuro Wilderness and contiguous Further Planning Areas (Creasey and others, 1981); SC2, Silver City 1° × 2° quadrangle (Watts and Hassemer, 1988); D2, Douglas 1° × 2° quadrangle (J.M. Hammarstrom and others, unpub. data, 1988); CWA, Chiricahua Wilderness Area (Drewes and Williams, 1973); PM, Patagonia Mountains (Chaffee and others, 1981); TN2, Tucson and Nogales 1° × 2° quadrangles (Chaffee, 1990); PRWA, Pusch Ridge Wilderness Area (Hinkle and others, 1981); RWSA, Rincon Wilderness Study Area (Thorman and others, 1981)]

Element	Customary limits of determination (ppm)		Concentration (ppm)												No. of samples	No. of anomalous samples
						Threshold (highest background)										
	Lower	Upper	Minimum	Maximum	50th percentile	This study	GW	SC2	D2	CWA	TN2	PM	PRWA	RWSA		
RASS/PLUTO stream-sediment samples																
Ag	0.5	5,000	N(0.5)	200	N(0.5)	L(0.5)	L(0.5)	---	L(0.5)	L(0.5)	L(0.5)	1	---	L(0.5)	3,874	456
B	10	2,000	N(10)	1,500	20	50	---	---	30	---	---	50	---	---	3,874	451
Ba	20	5,000	20	G(5,000)	700	1,500	---	---	700	---	---	---	---	---	3,874	68
Be	1	1,000	N(1)	50	1.5	5	---	---	3	3	---	---	---	3	3,874	83
Co	5	2,000	N(5)	G(500)	10	30	---	---	15	---	---	---	---	---	3,874	86
Cr	10	5,000	N(2)	700	30	150	---	---	50	---	---	---	---	---	3,874	145
Cu	5	20,000	L(5)	G(1,000)	30	100	100-300	---	30	30	70	100	---	70	3,874	247
La	20	1,000	N(20)	G(1,000)	50	100	---	---	70	---	---	---	---	---	3,874	380
Mn	10	5,000	15	G(5,000)	1,000	2,000	---	---	1,000	---	---	2,000	---	3,000	3,874	158
Mo	5	2,000	N(1)	300	N(5)	5	L(5)	---	L(5)	---	5	5	---	5	3,874	317
Nb	20	2,000	N(10)	300	L(20)	30	---	---	30	---	---	---	---	---	3,761	108
Ni	5	5,000	N(1)	500	15	70	---	---	20	---	---	---	---	---	3,874	113
Pb	10	20,000	N(10)	G(20,000)	50	100	70	---	50	30	70	100	---	70	3,874	378
Sn	10	1,000	N(10)	1,000	N(10)	L(10)	L(10)	---	---	---	N(10)	---	---	---	3,871	219
V	10	10,000	L(10)	1,000	100	300	---	---	100	---	---	---	---	---	3,874	52
Y	10	2,000	N(5)	G(200)	30	100	---	---	50	---	---	---	---	---	3,874	277
RASS/NURE stream-sediment and soil samples																
Au	0.002	---	N(0.002)	4.6	N(0.002)	0.002	---	---	---	---	---	---	---	---	2,429	207
Ag	0.045	---	N(0.045)	24	N(0.045)	0.16	---	---	---	---	---	---	---	---	2,530	156
As	0.6	---	N(0.6)	400	2.6	7.9	---	---	---	---	---	---	---	---	2,530	236
Bi	0.6	---	N(0.6)	47	N(0.6)	1.6	---	---	---	---	---	---	---	---	2,530	235
Cd	0.03	---	N(0.03)	40	0.18	0.39	---	---	---	---	---	---	---	---	2,530	317
Cu	0.05	---	1.7	G(1,000)	22	59	---	---	---	---	---	---	---	---	2,530	184
Mo	0.09	---	N(0.09)	130	0.75	2.6	---	---	---	---	---	---	---	---	2,530	148
Pb	0.6	---	4.3	10,000	25	79	---	---	---	---	---	---	---	---	2,529	195
Sb	0.6	---	N(0.6)	250	0.6	1.6	---	---	---	---	---	---	---	---	2,530	265
Zn	0.05	---	4.3	G(1,400)	42	79	---	---	---	---	---	---	---	---	2,530	284

Element	Customary limits of determination (ppm)		Concentration (ppm)												No. of samples	No. of anomalous samples
						Threshold (highest background)										
	Lower	Upper	Minimum	Maximum	50th percentile	This study	GW	SC2	D2	CWA	TN2	PM	PRWA	RWSA		
RASS nonmagnetic heavy-mineral concentrate samples																
Ag	1	10,000	N(1)	2,000	N(1)	1.5	---	2	---	---	---	---	---	---	1,355	204
As	500	20,000	N(500)	G(20,000)	N(500)	L(500)	---	N(500)	---	---	---	---	---	---	1,355	65
Ba	50	10,000	N(50)	G(10,000)	500	5,000	---	1,000	---	---	---	---	---	---	1,355	203
Be	2	2,000	N(2)	2,000	L(2)	15	---	20	7	---	---	---	---	---	1,355	102
Bi	20	2,000	N(20)	G(2,000)	N(20)	200	---	20	---	---	---	---	---	---	1,353	144
Co	10	5,000	N(10)	700	10	50	---	---	15	---	---	---	---	---	1,355	42
Cu	10	50,000	N(10)	50,000	30	300	---	100	30	---	---	---	100	---	1,355	125
La	50	2,000	N(50)	G(2,000)	300	1,500	---	---	300	---	---	---	---	---	1,355	121
Mo	10	5,000	N(10)	G(5,000)	L(10)	30	---	20	L(10)	---	---	---	70	---	1,355	307
Nb	50	5,000	N(50)	1,000	50	150	---	---	70	---	---	---	300	---	1,346	173
Pb	20	50,000	N(20)	G(50,000)	100	2,000	---	100	100	---	---	---	500	---	1,355	180
Sn	20	2,000	N(20)	G(2,000)	30	500	---	50	50	---	---	---	300	---	1,355	114
Th	200	5,000	N(200)	G(5,000)	L(200)	1,000	---	---	---	---	---	---	---	---	1,342	231
V	20	20,000	N(20)	G(20,000)	100	300	---	---	150	---	---	---	300	---	1,355	113
W	100	20,000	N(50)	G(20,000)	N(100)	300	---	100	---	---	---	---	700	---	1,355	143
Zn	500	20,000	N(500)	G(20,000)	N(500)	L(500)	---	500	---	---	---	---	1,000	---	1,355	188

Table 3 ranks the subareas in terms of "geochemical intensity" on a scale of 1–10, 10 being the most geochemically anomalous area. Geochemical intensity is based on the number of elements present in anomalous concentrations, the proportion of samples having anomalous concentrations of selected elements, and the magnitude of anomalous concentrations in individual samples. The geochemical intensity is heavily weighted in favor of the elements Ag, As, Au, Bi, Cd, Cu, Mo, Pb, Sb, W, and Zn, lesser weight being given to Ba, Mn, and Sn. Other elements considered in this geochemical evaluation (B, Be, Ce, Co, Cr, La, Nb, Ni, Sc, Th, U, V, Y) may be related to bedrock type in many places, but are also considered because high concentrations can indicate mineral deposits normally associated with a specific rock type, such as the association of Be-Nb-Th-U-REE (rare-earth element)-bearing pegmatites with certain granites.

Distributions of concentrations of selected elements in stream-sediment and panned-concentrate samples are shown on maps G–Q, plate 5. These maps show the localities only of those samples that contain anomalous concentrations. Geochemically anomalous areas in each of the 12 Coronado National Forest units are shown on plates 6–8. The plates also show distributions of all samples analyzed for Au (by FAA) and for Ag, As, Cu, Mo, Pb, Sb, and Zn (by ICP). Concentration ranges shown on these plates are divided into anomalous, high background, and background categories. Elements present in anomalous abundances in a large proportion (at least 30 percent) of samples are considered to be part of the geochemical signature of their source area. FAA and ICP data were used principally to identify the elemental constituents of the geochemical signatures; elements present in anomalous abundances (as determined by emission spectrographic analysis) in stream-sediment and panned-concentrate samples are added to these elemental suites wherever these data present additional evidence concerning the presence of mineralized rock.

Rock samples were considered during preparation of this report, but their limited coverage reduces their utility. Geochemically anomalous rock samples tend to be samples of mineralized or altered rocks, which are anomalous by definition in terms of regional geochemistry. Nevertheless, the rock data are useful because they show elemental associations that may be used to characterize and distinguish various types of mineralizing systems, including zonation patterns indicative of such systems.

The remainder of this chapter examines geochemical relations in each of the 35 subareas established on the basis of geology. Each area is assigned a unique three-character code that consists of a capital letter, an Arabic number, and a lower case letter (map A, pl. 5). The capital letter designates the map area containing the subarea. The 12 Forest units are shown on plates 6–8: plate 6, Santa Catalina–Rincon and Santa Teresa, Galiuro, Winchester, and Pinaleno Forest units; plate 7, Dragoon, Peloncillo, and Chiricahua-Pedregosa Forest units; plate 8, Santa Rita, Atascosa–Cobre–Coches–Pajarito–San Luis–Tumacacori, Whetstone, and Patagonia-Huachuca-Canelo Forest units. All of the maps, with the exception of the one showing the Dragoon Forest unit, comprise more than one Forest unit. Forest units within map areas are given unique Arabic numbers. Areas within numbered Forest units, divided on the basis of geology, are assigned lower case letters. For instance, the area designated D2e is geologically subdivided area "e" in Forest unit 2, which can be found on plate 8; this area is on the east flank of the Patagonia-Huachuca-Canelo Forest unit.

SANTA TERESA MOUNTAINS (A1)

Published regional geochemical study of the Santa Teresa Mountains Forest unit is limited to a mineral resource evaluation of the Black Rock Wilderness Study Area (Simons and others, 1987), which adjoins the east side of the Forest. The Santa Teresa Wilderness covers about half of the Santa Teresa Mountains Forest unit (U.S. Bureau of Land Management, 1986a), but the USGS was never asked to undertake a study of this area.

Most of the Santa Teresa Mountains Forest unit (pl. 6) is underlain by Tertiary granitoid rocks (Simons, 1964; Blacet and Miller, 1978). Proterozoic granitoid and metasedimentary rocks, Paleozoic and Mesozoic sedimentary rocks, or Cretaceous to Tertiary intrusive and volcanic rocks occupy the northwest and southeast ends of the Forest unit.

The west side of the Santa Teresa Mountains Forest unit (pl. 6) is coincident with part of the Aravaipa mining district. The district contains middle Tertiary lead-zinc-silver polymetallic vein and replacement deposits (Keith, Gest, and DeWitt, 1983; Keith and others, 1983). In a preliminary mineral resource assessment of the Tucson and Nogales 1° × 2° quadrangles, Jones (1990) classified existing mineral deposits in the Santa Teresa Mountains Forest unit as zinc-lead skarns, polymetallic replacements, polymetallic veins, porphyry copper-molybdenum, and flat-fault gold. A beryllium-thorium-rare-earth-element-bearing pegmatite was reported for the Lucky Strike claim (U.S. Geological Survey and others, 1969, p. 247–249). On the basis of geologic, geochemical, and geophysical criteria, Jones (1990) outlined parts of the Santa Teresa Mountains Forest unit as being favorable for deposits of the preceding types and also for epithermal precious-metal deposits.

AREA A1a

Bedrock in area A1a, the northwestern part of the Santa Teresa Mountains Forest unit, is predominantly Paleozoic and Mesozoic sedimentary rocks that include some

carbonate units; Proterozoic granitoid and metasedimentary rocks and Cretaceous to Tertiary intrusive and volcanic rocks are also present. Part of the Aravaipa mining district extends into the southern part of area A1a. Polymetallic vein and replacement deposits were mined and prospected in the past (Simons, 1964, p. 124–127).

Stream-sediment samples contained anomalous concentrations of Bi, Cd, Cu, Mn, Mo, Pb, Sb, and Zn. Panned-concentrate samples contained anomalous concentrations of Ba, Bi, Cu, Mo, Sn, and W. Rock samples contained anomalous concentrations of silver, bismuth, molybdenum, and zinc. Ore minerals that are present in deposits of the area (Simons, 1964, p. 120–121) can account for all of the elements present in anomalous concentrations except for tin. The southern part of area A1a is part of a geochemically anomalous region characterized by the Ag-As-Au-Bi-Cd-Cu-Mo-Pb-Sb-Sn-Zn geochemical signature (pl. 6). In addition to the polymetallic replacement and polymetallic vein deposits known to be present, the geochemical signature may indicate a porphyry copper-molybdenum deposit at depth, as suggested by Chaffee (1990, p. 21); tin is part of the distal porphyry copper-molybdenum deposit signature (Cox, 1986). Other elements present in anomalous concentrations in samples from the area are boron, beryllium, cobalt, niobium, and thorium; these elements may indicate the presence of pegmatite, but only thorium is present in highly anomalous concentrations. Jones (1990) categorized parts of area A1a as favorable for the presence of skarn and replacement deposits, polymetallic vein deposits, and flat-fault gold deposits. The area is ranked 4 on the geochemical-intensity scale (table 3), but the southern part is strongly anomalous.

AREA A1b

Bedrock in most of the middle Santa Teresa Mountains Forest unit consists of Tertiary granitoid rock. The geology of area A1b is homogeneous, but geochemical data indicate that the area can be divided into small western and eastern parts, and a large central part. Hydrothermal alteration processes affected margins of the Tertiary granitoid rocks that make up most of the central part of the area.

Proterozoic granitoid and metamorphic rocks are present on the west side of area A1b. Proterozoic metamorphic and Tertiary volcanic rocks are present on the east side of the area. The center of area A1b was not sampled; however, the center is a topographic high and if geochemical anomalies are present they would probably be reflected in samples obtained from streams draining margins of the area.

Part of the Aravaipa mining district is coincident with area A1b. Polymetallic vein deposits associated with the Grand Reef fault near the western side of area A1b have been mined and prospected (Simons, 1964, p. 124–127). The area near the western border is one of the most geochemically anomalous parts of Coronado National Forest. Stream-sediment samples from near the western border contained strongly anomalous concentrations of Au, Ag, As, Bi, Cd, Cu, Mo, Pb, Sb, Zn, Sn, and W. The western part of area A1b is the most geochemically anomalous part of an area characterized by the Ag-As-Au-Bi-Cd-Cu-Mo-Pb-Sb-Sn-Zn geochemical signature that extends into area A1a to the north and A1c on the south. The geologic setting and geochemical signature are similar to area A1a, except for the lack of carbonate sedimentary rocks. Therefore, the west side of area A1b has potential for polymetallic vein deposits and possibly for porphyry copper-molybdenum deposits at depth. Jones (1990) indicated that the west side of area A1b is favorable for the occurrence of porphyry copper deposits, polymetallic vein deposits, and flat-fault gold deposits.

Stream-sediment samples near the east central border of area A1b contained anomalous concentrations of Ag, Cu, Mo, Pb, Zn, and Sn. Panned-concentrate samples had anomalous concentrations of bismuth. Rock samples from this area had anomalous concentrations of Ag, Bi, Cu, Mo, Pb, Zn, and Ba. In addition, stream-sediment samples from drainage basins that are slightly east of area A1b had anomalous concentrations of lanthanum, niobium, yttrium, and thorium; panned-concentrate samples had anomalous concentrations of yttrium and thorium; and rock samples had anomalous concentrations of beryllium, lanthanum, and niobium. The geochemical signature for the east-central part of area A1b is Bi-Co-Cr-La-Nb-Pb-Sn-Th-V-Y. These data and geologic criteria caused Simons and others (1987) to assign moderate potential for REE (based on analyses for lanthanum and yttrium), thorium, and tin deposits to the western part of the Black Rock Wilderness Study Area and adjoining parts of area A1b; these deposits might be present as vein, greisen, pegmatite, or contact-metamorphic deposits associated with Tertiary granitoid rocks. Jones (1990) indicated that the east part of area A1b is favorable for the occurrence of porphyry copper deposits, epithermal precious-metal deposits, and flat-fault gold deposits.

No panned-concentrate or rock samples were collected in the highly anomalous western part of the area but the high proportion of anomalous stream-sediment samples and the magnitude of the concentrations give area A1b an overall ranking of 9 on the geochemical-intensity scale.

AREA A1c

Bedrock in the south and southeast parts of the Santa Teresa Mountains (area A1c) consists of Proterozoic granitoid and metamorphic rocks cut by Tertiary rhyolite dikes. According to Jones (1990), the Lucky Strike claim, where a beryllium-thorium-REE bearing pegmatite crops out, is present in Proterozoic granite.

Stream-sediment samples contained anomalous concentrations of Ag, Bi, Cd, Cu, Mo, Pb, and Zn. Panned-

Table 3. Geochemical-intensity rankings, elements present in anomalous concentrations, and general geology, by area, Coronado National Forest, southeastern Arizona and southwestern New Mexico.

[NS, no samples. Based on emission spectrographic analyses of RASS and PLUTO stream-sediment, heavy-mineral concentrate, and rock samples, flameless atomic-absorption and inductively coupled plasma analyses of RASS/NURE stream-sediment and soil samples, and neutron-activation analyses of NURE stream-sediment/soil samples. Elements in boldface are present in highly anomalous concentrations; elements in normal print are present in moderately anomalous concentrations; elements in italics are present in weakly anomalous concentrations. Geology from Reynolds (1988) and New Mexico Geological Society (1982), with modifications from reports listed in reference list]

Area (plates 5-8)	Geochemical-intensity ranking	RASS/PLUTO stream-sediment samples	RASS/NURE stream-sediment and soil samples	NURE stream-sediment and soil samples	RASS nonmagnetic heavy-mineral-concentrate samples	RASS/PLUTO rock samples	General geology
Ala--Santa Teresa Mountains, northwest	4	B, *Bi*, Co, Cr, *Cu*, **Mn**, *Mo*, *Nb*, Pb, *Sn*, V, Zn	Bi, Cd, Cu, Mo, Pb, Sb, Zn	*Be*, Co, Cr, *Cu*, Mn, *Nb*, Ni, Pb, V, **Zn**	Ba, Bi, Cr, *Cu*, *Mo*, Sn, Th, **V**, W	*Ag*, *Bi*, Cr, Mo, *Ni*, *Zn*	Paleozoic-Mesozoic sedimentary rocks; Proterozoic granitoid rocks.
Alb--Santa Teresa Mountains, west-central	9	**Ag**, *B*, **Bi**, Cr, *Cu*, **La**, **Mn**, **Mo**, **Nb**, **Pb**, **Sn**, Th, V, W, Y, **Zn**	Ag, As, Au, **Bi**, **Cd**, **Cu**, **Mo**, **Pb**, **Sb**, **Zn**	Ag, *Be*, Ce, Cu, **La**, *Mn*, **Mo**, **Nb**, **Pb**, **Th**, U, Y, **Zn**	*B*, Bi, *Co*, Th, *Y*	Ag, B, Ba, Be, Bi, Co, Cr, Cu, La, Mo, Nb, Ni, Pb, Sc, V, Zn	Tertiary granitoid rocks.
Alc--Santa Teresa Mountains, south and southeast	3	Ag, B, *Bi*, Co, **Cr**, Cu, La, **Mn**, *Mo*, Ni, Pb, Sc, Sn, *V*, Y, *Zn*	Bi, Cd, Mo, *Zn*	*Ce*, La, Mn, *Nb*, Y, *Zn*	Ag, As, **Ba**, Bi, *Cu*, **Mo**, Pb, Sn, **Th**, V, **W**, Y, *Zn*	Ag, *As*, B, Ba, Bi, Cd, Co, Cr, Cu, La, Mo, Nb, Ni, Pb, V, W, Zn	Proterozoic granitoid and metamorphic rocks.
A2a--Galiuro Mountains	5	*Ag*, *B*, *Ba*, **Co**, **Cr**, *Mo*, **Ni**, Sn, *V*	Ag, As, **Au**, *Cd*, Cu, *Mo*, *Pb*, Sb, *Zn*	Ag, **B**, Ba, Co, Cr, *Cu*, *La*, *Mn*, **Ni**, *Pb*, Zn	NS	Ag, *As*, *B*, *Ba*, Be, *Co*, Cr, *Cu*, *Mn*, Ni, *Pb*, Sb, *Sn*, V, *W*, Zn	Tertiary volcanic rocks.
A3a--Winchester Mountains, west three-fifths	1	*La*, *Mo*, *Zn*	Sb, Zn	*Ba*, Co, Cr, Ni, *Zn*	*B*, *Co*, Cr, *Cu*, La, Ni, *Sc*, Sn, *Y*	*Co*, Cr, La, Ni	Tertiary andesite, dacite.
A3b--Winchester Mountains, east two-fifths	3	*Ba*, La, *Mn*, *Mo*, *Pb*, *Y*, *Zn*	**Sb**, Zn	Ba, *La*, *Mo*, *Zn*	La, *Mo*, Ni, Sc, Sn, *Y*	*Ba*, *Co*, *Cr*, **La**, *Ni*	Tertiary rhyolite.
A4a--Pinaleno Mountains, northwest one-half	3	*B*, *Be*, *La*, Mn, *Pb*, *Sc*, Sn, Y	Au, *Bi*, *Zn*	Ag, B, *Cr*, Ni, Y, Zn	*Ag*, *Ba*, *Bi*, *Co*, Mo, *Pb*, *Sn*, *V*, W	La, *Sn*, *W*	Proterozoic metamorphic rocks; Proterozoic granitoid rocks.
A4b--Pinaleno Mountains, southeast one-half	7	Ag, B, *Ba*, *Be*, Bi, *Co*, Cr, **La**, Mn, Nb, *Ni*, Pb, **Sn**, Th, V, **Y**, **Zn**	*Ag*, As, **Au**, **Bi**, *Cd*, *Cu*, **Mo**, Pb, **Sb**, Zn	NS	Ag, **As**, **Au**, *B*, **Ba**, **Be**, **Bi**, *Cd*, **Co**, Cr, Cu, *La*, **Mo**, **Nb**, **Pb**, **Sc**, Sn, **Th**, V, W, Y	*Ag*, *As*, B, *Ba*, Be, Bi, Co, **Cr**, Cu, **La**, *Mn*, Mo, *Nb*, **Ni**, Pb, Sc, Sn, **V**, W, Y, Zn	Proterozoic granitoid rocks; Tertiary volcanic and granitoid rocks.
B1a--Peloncillo Mountains	4	**Be**, *Co*, La, *Mn*, Nb, *Pb*, *Sn*, *V*, *Zn*	*Au*, Bi, *Cd*, *Cu*, Sb, *Zn*	*Be*, *Ce*, *Cr*, La, *Mo*, *Nb*, *Ni*, *Th*, *U*, *Zn*	**As**, **Ba**, **Be**, Co, **Cr**, **La**, Mn, *Mo*, **Nb**, **Ni**, *Pb*, **Sb**, **Sc**, **Sn**, V, *W*, Y, Zn	*Ba*, Be, *Bi*, *Zn*	Tertiary rhyolite with some Tertiary andesite and Tertiary-Quaternary basalt.

Area (plates 5-8)	Geochemical-intensity ranking	RASS/PLUTO stream-sediment samples	RASS/NURE stream-sediment and soil samples	NURE stream-sediment and soil samples	RASS nonmagnetic heavy-mineral-concentrate samples	RASS/PLUTO rock samples	General geology
B2a--Chiricahua Mountains, north	7	Ag, *B*, Ba, Cr, *Cu*, *La*, Mn, *Mo*, *Ni*, Pb, Sn, *V*, W, *Y*, Zn	Ag, **As**, Au, *Bi*, Cd, *Cu*, Mo, Pb, **Sb**, **Zn**	NS	Ag, As, **B**, **Ba**, *Be*, *Bi*, Cd, *Co*, *Cu*, *Mo*, Nb, Pb, **Sn**, Th, *W*, *Y*, Zn	**Ag**, As, Au, **B**, Ba, Be, **Bi**, **Cd**, **Co**, **Cr**, Cu, La, **Mn**, Mo, Nb, Ni, **Pb**, **Sc**, **Sn**, Th, V, **W**, Y, **Zn**	Paleozoic-Tertiary sedimentary rocks; Tertiary granitoid and volcanic rocks.
B2b--Chiricahua Mountains, except north	6	Ag, *B*, Be, *Bi*, *Co*, *Cr*, La, *Mo*, Nb, *Ni*, **Pb**, Sn, W, Y, *Zn*	Ag, **As**, Au, Bi, Cd, *Cu*, **Mo**, *Pb*, Sb, Zn	NS	*Ag*, *As*, B, *Ba*, Cd, *Co*, *Cu*, *Mo*, *Pb*, Sb, *Sc*, Sn, *V*, *Y*, Zn	Ag, *As*, *Ba*, Be, *Bi*, *Co*, *Cr*, **La**, *Mo*, **Nb**, *Ni*, *Sc*, Sn, Y	Tertiary volcanic rocks and subvolcanic intrusions.
B2c--Pedregosa Mountains, west	5	*Ag*, *Bi*, *Cu*, *Mo*, Pb, *Sn*, *V*, *Zn*	*As*, *Bi*, Cd, Cu, *Pb*, *Sb*, *Zn*	NS	NS	*Ag*, **Be**, *Bi*, Co, Cr, **La**, Mo, **Nb**, Ni, Sc, Sn, V, Y, *Zn*	Tertiary volcanic rocks; Cretaceous volcanic rocks.
B2d--Pedregosa Mountains, east	4	Ag, *Cr*, Pb, *Sn*, *Th*, *Y*, *Zn*	Au, *Bi*, Cd, Cu, *Sb*	NS	NS	*Ag*, As, *Ba*, **Co**, Cr, Mo, Nb, Ni, *Pb*, Sb, Sc, Sn, **V**, *Zn*	Paleozoic-Mesozoic sedimentary rocks; Cretaceous volcanic rocks.
C1a--Dragoon Mountains, north one-third	7	Ag, *B*, Be, *Bi*, *Cd*, La, *Nb*, Pb, Sn, *Th*, W, Zn	Ag, **Au**, Bi, Cd, Cu, Mo, *Pb*, *Sb*, *Zn*	**Be**, *Ce*, *Cr*, Cu, *La*, Mo, Nb, Th, U, Zn	Ag, Au, **B**, Ba, **Be**, **Bi**, **Co**, **Cr**, *Cu*, **Mo**, Nb, **Ni**, Pb, *Sb*, *Sn*, Th, *V*, **W**, Y	**Ag**, *As*, *B*, **Be**, **Bi**, **Cd**, **Co**, Cr, **Cu**, **Mn**, **Mo**, *Ni*, **Pb**, Sb, **Sn**, *V*, W, **Zn**	Mostly Paleozoic-Mesozoic sedimentary rocks.
C1b--Dragoon Mountains, middle one-third	9	*Ag*, *B*, **Be**, Bi, Cd, *Cu*, **La**, **Mn**, *Mo*, **Nb**, Pb, **Sn**, **Th**, *V*, **W**, **Y**, Zn	Au, Ag, **Bi**, Cd, Cu, **Mo**, Pb, *Sb*, **Zn**	*Ag*, Be, *Ce*, *La*, *Mo*, Nb, **Th**, U	*Ag*, As, B, **Be**, **Bi**, *Cd*, **Co**, Cr, *Cu*, **La**, Mn, **Mo**, **Nb**, Ni, *Pb*, Sc, **Sn**, **Th**, *V*, **W**, **Y**, *Zn*	**Ag**, *B*, **Be**, **Bi**, **Cd**, **Co**, Cr, **Cu**, **Mn**, **Mo**, *Nb*, **Pb**, **Sn**, V, **W**, **Y**, **Zn**	Tertiary granitoid rocks.
C1c--Dragoon Mountains, south one-third	7	Ag, B, *Be*, *Bi*, Cd, *Cu*, *La*, *Nb*, Pb, Sn, *Th*, W, Zn	Bi, Cd, Cu, Mo, *Pb*, *Sb*, Zn	NS	Ag, *As*, B, **Ba**, Be, Bi, Cd, Co, **Cr**, *Cu*, *La*, *Mn*, **Mo**, Nb, *Ni*, Pb, *Sb*, Sn, *Th*, **V**, W, Zn	**Ag**, *As*, B, **Be**, **Bi**, **Cd**, **Co**, Cr, **Cu**, *La*, **Mn**, **Mo**, *Nb*, *Ni*, **Pb**, Sb, **Sn**, V, W, **Zn**	Mostly Paleozoic-Mesozoic sedimentary rocks.
D1a--Whetstone Mountains, northeast one-third	6	**B**, Be, *Bi*, **Cr**, *Sn*, **W**, **Y**	Ag, Bi, Cd, *Cu*, *Mo*, *Pb*, *Sb*, Zn	**Be**, *Cr*, Cu, Mo, Nb, U, Y, Zn	B, *Be*, Bi, *W*	Bi, Cr, *W*	Proterozoic granitoid rocks.
D1b--Whetstone Mountains, middle one-third	5	*Ag*, **B**, Be, Cr	Au, Cd, Sb	Mo	*Ag*, **B**, Ba, Bi, Cd, *Cr*, *Cu*, Mo, *Nb*, *Ni*, *Pb*, *V*, W, Y, *Zn*	Cr, *Mo*, *V*	Paleozoic sedimentary rocks.

Table 3. Geochemical-intensity rankings, elements present in anomalous concentrations, and general geology, by area, Coronado National Forest, southeastern Arizona and southwestern New Mexico.—*Continued*

Area (plates 5-8)	Geochemical-intensity ranking	RASS/PLUTO stream-sediment samples	RASS/NURE stream-sediment and soil samples	NURE stream-sediment and soil samples	RASS nonmagnetic heavy-mineral-concentrate samples	RASS/PLUTO rock samples	General geology
D1c--Whetstone Mountains, southwest one-third	6	*Ag*, B, Ba, *Bi*, *Cu*, *Mo*, *V*	**Au**, As, Bi, Cu, Mo, Sb	Zn	*Ag*, B, **Ba**, *Bi*, *Co*, *Cu*, *La*, *Mo*, *Ni*, *Pb*, *Sb*, *Th*, *V*, *W*	Ag, B, Ba, Bi, Co, Cr, Cu, Mo, *Pb*, *Sb*, *Sn*, W, Zn	Cretaceous-Tertiary granitoid and sedimentary rocks.
D2a--Patagonia Mountains	10	**Ag**, **As**, **B**, **Ba**, **Bi**, **Cd**, **Co**, Cr, **Cu**, *La*, **Mn**, **Mo**, *Ni*, **Pb**, **Sb**, *Sn*, Th, V, W, **Zn**	**Ag**, **As**, **Au**, Bi, **Cd**, **Cu**, Mo, **Pb**, **Sb**, **Zn**	Ag, *Ba*, *Be*, Ce, **Co**, Cr, **Cu**, La, **Mn**, Ni, **Pb**, **Th**, U, V, **Zn**	**Ag**, **As**, Au, **B**, **Ba**, Bi, **Cd**, **Co**, **Cu**, *La*, Mn, **Mo**, Nb, Ni, **Pb**, **Sb**, Sn, *Th*, V, W, **Zn**	Ag, *As*, B, Bi, Cd, Co, Cr, Cu, La, Mo, *Ni*, Pb, Sb, **Sc**, *Sn*, V, *W*, Zn	Paleozoic-Mesozoic sedimentary rocks; Jurassic-Tertiary granitoid rocks.
D2b--Patagonia Mountains, north	9	**Ag**, B, Ba, *Co*, Cr, **Cu**, *Mn*, **Mo**, **Pb**, *Sn*, V, **Zn**	Ag, As, Au, *Bi*, **Cu**, *Mo*, Pb, **Sb**, **Zn**	Ag, *B*, Ba, Co, Cr, Cu, *Mn*, *Mo*, **Ni**, **Pb**, *U*, V, **Zn**	Ag, As, *B*, **Ba**, Cd, Co, **Cu**, *Mn*, Mo, *Ni*, Pb, Sb, *Sn*, V, *W*	Ba, Co, Cr, La, Mo, *Ni*, *Pb*, Sn, *Th*, *V*, *Zn*	Cretaceous volcanic rocks.
D2c--San Rafael Valley	3	*Ag*, Ba, *Mn*, *Sn*	Cd, *Cu*, *Pb*, Sb, *Zn*	*Cu*, Th, *U*, V, Zn	NS	Ba, *Co*, Sn	Tertiary sedimentary rocks.
D2d--Canelo Hills	2	Ag, *B*, *Pb*, *Sn*, *Th*, *Zn*	Sb, *Zn*	Ag, *Mn*, *Zn*	NS	La, Sn	Paleozoic sedimentary rocks; Jurassic volcanic rocks.
D2e--Huachuca Mountains	7	Ag, *B*, *Bi*, Cd, *Co*, *Cr*, *Cu*, *La*, *Mn*, *Ni*, Pb, *Sc*, *Sn*, **Th**, **W**, *Y*, *Zn*	Ag, Au, *Bi*, *Cd*, *Pb*, Sb, *Zn*	*Ag*, *Be*, *Cr*, *Mo*, *Pb*, **Th**, U, Y, *Zn*	Ag, *As*, Au, *B*, **Ba**, **Cd**, *Co*, Cu, Mo, **Pb**, Sb, Sn, *Th*, *V*, W, **Zn**	*Ag*, *Bi*, *Cu*, La, *Mo*, *Sn*, *V*, *Y*	Paleozoic-Mesozoic sedimentary rocks; Proterozoic and Jurassic granitoid and volcanic rocks; Proterozoic granitoid rocks.
E1a--Santa Rita Mountains, north	7	Ag, *Cu*, Mo, Sn, W, Zn	Ag, As, Au, Bi, Cd, Cu, Mo, Pb, Sb, Zn	*Ag*, Cu, Mn, Mo, Pb, Zn	NS	**Ag**, As, **Au**, B, Ba, **Be**, **Bi**, **Cd**, **Co**, **Cr**, **Cu**, La, **Mn**, **Mo**, **Ni**, **Pb**, **Sb**, **Sn**, V, **W**, **Y**, **Zn**	Cretaceous rhyolite, andesite; Jurassic-Cretaceous sedimentary rocks; Cretaceous-Tertiary granitoid rocks.
E1b--Santa Rita Mountains, west three-fourths	8	Ag, *As*, B, Ba, *Bi*, Cd, *Co*, Cu, *La*, **Mn**, Mo, Pb, Sb, Sn, *Th*, V, **W**, **Zn**	Ag, As, Au, Bi, Cd, Cu, **Mo**, Pb, **Sb**, **Zn**	*Ag*, *B*, Ba, *Be*, Ce, *Co*, *Cr*, Cu, **La**, Mn, Mo, *Nb*, *Ni*, Pb, **Th**, U, V, **Y**, **Zn**	Ag, As, *Au*, B, *Ba*, *Bi*, Cd, *Co*, Cu, *Mn*, Mo, Pb, Sb, *Sn*, *Th*, *V*, *W*, Zn	**Ag**, **As**, **Au**, **B**, **Ba**, Be, **Bi**, **Cd**, **Co**, **Cr**, Cu, **La**, **Mn**, **Mo**, **Nb**, Ni, **Pb**, **Sb**, Sc, **Sn**, **V**, **W**, **Y**, **Zn**	Jurassic-Tertiary granitoid rocks; Jurassic-Tertiary volcanic rocks; Jurassic-Cretaceous sedimentary rocks; undifferentiated Paleozoic rocks; Proterozoic granitoid rocks.

Area (plates 5-8)	Geochemical-intensity ranking	RASS/PLUTO stream-sediment samples	RASS/NURE stream-sediment and soil samples	NURE stream-sediment and soil samples	RASS nonmagnetic heavy-mineral-concentrate samples	RASS/PLUTO rock samples	General geology
E1c--Santa Rita Mountains, east	6	Ag, *B*, *Pb*, *W*, *Zn*	As, Au, *Cd*, Cu, *Mo*, Pb, Sb, Zn	*Ag*, *B*, Cu, *Mo*, *Ni*, *Pb*, Zn	*Ag*, *Ba*, *Cd*	NS	Tertiary sedimentary rocks.
E2a--San Luis Mountains	3	*Ba*, *Co*, *Cr*, **La**, Mo, *Th*, V, **W**, Zn	Au, *Zn*	Ba, *Th*, U, *Zn*	*Cu*, *La*, *Th*, *V*, *W*	Ag, *Mo*	Cretaceous-Tertiary granitoid rocks; Jurassic volcanic rocks.
E2b--Cobre and Coches Ridges, Pajarito Mountains	7	**Ag**, **B**, Ba, Be, **Bi**, **Cd**, *Co*, *Cr*, **Cu**, *La*, **Mn**, **Mo**, Ni, **Pb**, Sb, **Sn**, *V*, **W**, **Zn**	**Ag**, *As*, **Au**, Bi, Cd, *Cu*, Mo, **Pb**, Sb, **Zn**	Ag, B, **Ba**, *Co*, *Cr*, *Cu*, Mn, *Mo*, Ni, Pb, **Zn**	Ag, Au, B, *Ba*, *Bi*, Cd, Cu, *La*, *Mn*, Mo, **Pb**, Sb, Sn, *V*, *W*, Zn	**Ag**, *As*, **B**, **Ba**, Be, Bi, **Cd**, Co, Cr, Cu, La, Mn, Mo, *Ni*, Sb, *Sc*, *Sn*, *V*, **Zn**	Jurassic volcanic and granitoid rocks; Jurassic-Cretaceous sedimentary rocks.
E2c--Tumacacori and Atascosa Mountains	8	**Ag**, B, *Ba*, Be, *Bi*, *Cd*, *Co*, *Cu*, La, Mn, Mo, *Ni*, Pb, Sb, *Sc*, *Sn*, *Th*, *V*, **Zn**	Ag, Au, Cd, *Pb*, **Sb**, Zn	Ag, B, Ba, *Be*, *Co*, *Cr*, *Mn*, *Nb*, Ni, Pb, *Th*, Zn	*Ag*, *As*, *B*, *Ba*, *Cd*, *Co*, *Cr*, *Cu*, *Mo*, *Pb*, Sb, Sn, *V*, *Zn*	B, *La*, *Sn*	Tertiary volcanic rocks.
E2d--Area west of Nogales	5	Ag, **B**, *Ba*, Be, *Bi*, *La*, **Mn**, Mo, **Pb**, **Zn**	As, Au, *Cd*, *Mo*, Pb, **Sb**, *Zn*	Ag, B, *Ba*, Cr, Mn, Mo, *Ni*, **Pb**, *Th*, U, Zn	Ag, As, **B**, Ba, *Bi*, *Cu*, *Mn*, Mo, **Pb**, Sb, *Sn*, V, Zn	NS	Tertiary sedimentary rocks.
F1a--Santa Catalina Mountains, north	6	*Ag*, *Bi*, *Co*, *Cr*, *Cu*, La, *Mn*, Nb, *Ni*, *Pb*, *Sc*, Sn, **Th**, *V*, W, Y, *Zn*	*Ag*, *As*, Au, *Bi*, *Cd*, Cu, *Sb*, *Zn*	Ag, **Be**, Ce, *Co*, *Cr*, Cu, La, Mn, *Mo*, Nb, *Ni*, Th, U, **V**, **Y**, **Zn**	*Nb*, *Th*		Tertiary granitoid rocks; Proterozoic granitoid rocks; Paleozoic-Mesozoic sedimentary rocks. Proterozoic sedimentary rocks.
F1b--Rincon Mountains; Santa Catalina Mountains, south	6	*Ag*, **Ba**, *Be*, *Bi*, *Co*, *Cr*, *Cu*, **La**, **Mn**, **Mo**, Nb, *Ni*, Pb, Sn, **Th**, *V*, W, **Y**	*Ag*, *Au*, *Bi*, *Cd*, *Cu*, *Mo*, *Pb*, *Sb*, Zn	Ba, *Be*, Ce, *Co*, *Cu*, La, *Mn*, *Mo*, *Nb*, *Ni*, *Pb*, U, **Y**, Zn	*Ag*, *B*, Be, *Co*, *Cr*, *Cu*, **La**, **Mn**, Mo, **Nb**, *Pb*, *Sn*, Th, V, *W*, *Y*, Zn	Ag, *As*, *B*, Be, Bi, Cd, Co, Cr, Cu, *La*, Mn, Mo, Ni, Sn, *W*, Y, *Zn*	Cretaceous-Tertiary granitic rocks having mylonite fabric; Proterozoic granitoid rocks.
F1c--Santa Catalina and Rincon Mountains, east	5	*Ag*, *B*, *Cu*, *La*, Mn, Mo, Nb, Pb, Y	*Ag*, *As*, *Au*, *Cd*, *Cu*, *Mo*, *Sb*, *Zn*	Ag, Ba, **Be**, *Co*, Cu, Mn, Mo, U, Y, **Zn**	NS	Ag, As, B, Be, Bi, *Co*, Cu, Mn, Mo, *Pb*, Sb, Sn, *V*, W, Zn	Cretaceous-Tertiary granitic rocks; Paleozoic-Mesozoic sedimentary rocks; Proterozoic granitoid rocks.
F1d--Rincon Mountains, south	2	*Ba*, *Mo*, *Pb*	*Ag*, Au, *Sb*		NS	Be, Bi, Cr, Cu, *Mo*, Ni, *Pb*, Sb, W, *Zn*	Undifferentiated Paleozoic rocks; Cretaceous-Tertiary granitic rocks having mylonite fabric.

concentrate samples contained anomalous concentrations of Ag, As, Bi, Cu, Mo, and Pb. Rock samples contained anomalous concentrations of Ag, As, Bi, Cd, Cu, Mo, Pb, W, and Zn. In addition, Mn, Sn, La, Nb, and Y concentrations were anomalously high in stream-sediment samples; Ba, Sn, Y, and Th concentrations were anomalously high in panned-concentrate samples; and Ba, La, and Nb concentrations were anomalously high in rock samples. Three anomalous areas are outlined in area A1c (pl. 6). One of these, discussed above, is characterized by a Bi-Co-Cr-La-Nb-Pb-Sn-Th-V-Y geochemical signature and extends into area A1b. Of the other two anomalous areas, the northeastern one is characterized by a Ba-Bi-Co-Cr-La-Mo-Nb-Ni-Pb-Sn geochemical signature, whereas the southeastern one is characterized by a Co-Sn-Y-Zn geochemical signature. Simons and others (1987) assigned moderate potential for Th and Be resources, for Cu, Pb, Mo, Co, Sn, and V resources, and for W and Mo resources to parts of the Black Rock Wilderness Study Area, which adjoin the Forest on the northern border of area A1c. Jones (1990) included the area in a broad area that includes the Santa Teresa Mountains and indicated that the area is favorable for the occurrence of porphyry copper deposits. Jones (1990) indicated a small part of area A1c that is associated with a detachment fault (Simons and others, 1987) in Tertiary volcanic rocks as favorable for the occurrence of epithermal precious-metal deposits. However, the overall geochemical signature of area A1c includes weak anomalies and, except for Proterozoic rocks, units in the Black Rock Wilderness Study Area extend only a short distance into area A1c. Most of the samples that contained anomalous concentrations are in or near the Black Rock Wilderness Study Area and are primarily outside Coronado National Forest. Anomalous concentrations of molybdenum and tungsten are in samples from streams that drain area A1c and may reflect contact-metamorphic minerals (Simons and others, 1987, p. C8). Area A1c is ranked 3 on the geochemical-intensity scale.

GALIURO MOUNTAINS (A2)

AREA A2a

The entire Galiuro Forest unit (pl. 6) was studied (Creasey and others, 1981; Creasey and Jinks, 1984) during a mineral resource evaluation of the Galiuro Wilderness and contiguous Further Planning Areas. During the evaluation by Creasey and others (1981), the geology of the range was mapped and 481 stream-sediment and 46 rock samples were collected. Most of the rock samples were from altered zones.

Area A2a is underlain almost exclusively by Tertiary volcanic rocks whose compositions range from rhyolite to andesite. The Copper Creek (Bunker Hill) mining district, noted for its copper-molybdenum breccia-pipe deposits (Simons, 1964, p. 127–131), is adjacent to the northwest corner of the area. The breccia pipes were tentatively identified as part of a porphyry copper-molybdenum system (Creasey and others, 1981, p. 54–57, 64–65, 87, 92) associated with Cretaceous granodiorite. The Copper Creek district includes a porphyry copper deposit of Late Cretaceous to Tertiary age (Keith, Gest, and DeWitt, 1983; Keith and others, 1983). Jones (1990) indicated that deposits in the Copper Creek district are porphyry copper, polymetallic veins, flat-fault gold, and epithermal precious-metal vein deposits. Although the rocks that host the deposits at Copper Creek are almost entirely covered by Tertiary volcanic rocks in the Forest, mineralized rocks that are part of the Copper Creek system may extend for many kilometers into the Forest under volcanic cover.

The Rattlesnake district, the other mining district in the Galiuro Mountains Forest unit, is a vein- and replacement-silver type (without lead and zinc) of middle Tertiary age (Keith, Gest, and DeWitt, 1983; Keith and others, 1983). Jones (1990) considered the deposits in the Rattlesnake district to be epithermal precious-metal veins. These precious-metal deposits are in altered Tertiary volcanic rocks associated with faults (Creasey and others, 1981, p. 55–57, 92).

The bulk of ore production from the Galiuro Mountains was from the Copper Creek district. Gold was a byproduct of the production of base metals in the Copper Creek district but gold and silver were the primary commodities produced from the small mines in the Rattlesnake mining district in the central part of the Galiuro Mountains.

Stream-sediment samples from the Galiuro Mountains Forest unit contained anomalous concentrations of Au, Ag, As, Cd, Cu, Mo, Pb, Sb, Zn, Ba, Mn, and Sn. Rock samples contained anomalous concentrations of Ag, As, Cu, Pb, Sb, W, Zn, Ba, Mn and Sn. No panned-concentrate samples were collected. Five anomalous areas are outlined in area A2a (pl. 6). The geochemical signature for the area near Copper Creek is Cu-Zn. The northern part of area A2a is characterized by an As-Au-Cu geochemical signature. The geochemical signature near the Rattlesnake district is only gold. Two areas are outlined on the basis of this gold signature; they extend to the west and southeast for many kilometers beyond the Rattlesnake district. The fifth anomalous area is characterized by an As-Sb geochemical signature and adjoins one of the areas characterized by the gold signature. These geochemical features are consistent with the presence of known polymetallic vein deposits and with porphyry copper-molybdenum deposits. Creasey and others (1981) and Chaffee (1990, p. 21) suggested that scattered copper and silver anomalies in the Galiuro Mountains may be due to leakage through volcanic rocks from underlying porphyry copper-molybdenum systems.

Jones (1990) indicated that the northwestern part of the Galiuro Mountains Forest unit is favorable for the occurrence of porphyry copper deposits and that most of this Forest unit is favorable for the occurrence of epithermal precious-metal deposits. In this report, the area is assigned a

ranking of 5 on the geochemical-intensity scale because of the small proportion of anomalous samples. However, low but anomalous concentrations of gold (2–5 ppb) in stream-sediment samples without accompanying anomalous concentrations of other elements may be the signature of epithermal precious-metal systems.

WINCHESTER MOUNTAINS (A3)

Most of the Winchester Mountains Forest unit (pl. 6) was included in a mineral resource evaluation of the Winchester Roadless Area (Keith and others, 1982; Keith and Kreidler, 1984). Stream-sediment, panned-concentrate, and rock samples were analyzed as a part of that evaluation (Sutley and others, 1983; Chaffee, 1985). The Winchester Mountains are underlain by silicic Tertiary volcanic rocks that range in composition from rhyolite to latite and are partially covered by vesicular Tertiary basalt (Creasey and others, 1961; Keith and others, 1982). Evidence of mineralized rock or of prospecting in the Winchester Mountains is almost nonexistent (Keith and others, 1982). Jones (1990) included the Winchester Mountains and the Galiuro Mountains in a large tract that is considered to be favorable for the occurrence of deposits of epithermal precious metals.

AREA A3a

The central to western part of the Winchester Mountains Forest unit is underlain by Tertiary rhyolite, which is partially capped by Tertiary basalt. Some stream-sediment samples have anomalous concentrations of molybdenum, antimony, zinc, and barium. Panned-concentrate samples contained anomalous concentrations of copper and tin. An anomalous area characterized by an antimony geochemical signature (pl. 6) overlaps area A3b (described below). Except for antimony and possibly zinc, the elements present in apparently anomalous concentrations in drainage and rock samples from area A3a appear to reflect the two rock types in the area, rhyolite and basalt. Chaffee (1985) suggested that anomalous elemental abundances not related to bedrock type may result from human contamination. Overall, this area is the least anomalous noted in this study and is ranked 1 on the geochemical-intensity scale.

AREA A3b

The eastern part of the Winchester Mountains Forest unit is underlain by Tertiary rhyolite to latite. Stream-sediment samples contained anomalous concentrations of Mo, Pb, Sb, Zn, Ba, and Mn. Panned-concentrate samples contained anomalous concentrations of molybdenum and tin, and rock samples contained anomalous concentrations of barium. These geochemical features are similar to those of the central to western part (area A3a) of the Winchester Mountains Forest unit except that antimony abundances are anomalously high in several samples from the eastern part of area A3b; the only sample from the western part that contained an anomalous concentration of antimony is from near the border with the eastern part. The anomalous area characterized by the antimony signature covers most of area A3b and overlaps the east edge of area A3a (pl. 6). These anomalous concentrations of antimony may indicate that epithermal precious-metal deposits are present. The area is somewhat more anomalous than is the western part of the Winchester Mountains and is ranked 3 on the geochemical-intensity scale.

PINALENO MOUNTAINS (A4)

Most of the Pinaleno Mountains Forest unit (pl. 6) was included in CUSMAP studies of the Silver City 1° × 2° quadrangle; a geochemical study was an important part of that investigation (Watts and Hassemer, 1988). Data from panned-concentrate samples were the primary basis for interpretation of the geochemistry of the Silver City 1° × 2° quadrangle. No USGS geochemical studies of the Mount Graham (U.S. Bureau of Land Management, 1986a) or the Kane Springs Wilderness Study Areas (Peterson and others, 1984), both in the Pinaleno Mountains Forest unit, were undertaken.

Most of the Forest unit is underlain by Proterozoic rocks except the southern part, where Tertiary rocks of possible economic significance predominate (Blacet and Miller, 1978; Bergquist, 1979; Thorman, 1981; Drewes and others, 1985). Mining districts in the Pinaleno Mountains Forest unit are the Black Beauty (Proterozoic tungsten skarn and tungsten veins or pegmatites), the Black Hawk (middle Tertiary manganese veins), and the Clark (middle Tertiary polymetallic Pb-Zn-Ag vein and replacement deposits) (Keith, Gest, and DeWitt, 1983; Keith and others, 1983); these deposits are all in the Tucson 1° × 2° quadrangle. Deposits in the Black Beauty district are probably of the tungsten-vein type, whereas those in the Clark district are epithermal veins (Jones, 1990). Deposits in part of the Pinaleno Mountains Forest unit within the Silver City 1° × 2°° quadrangle include manganese oxides, uranium veins, and beryllium pegmatites (Richter and Lawrence, 1983).

AREA A4a

Area A4a comprises the northwest half of the Pinaleno Mountains Forest unit. The eastern part of area A4a was included in the Silver City 1° × 2° quadrangle study. Area A4a is underlain by Proterozoic metamorphic rocks, except for the western end and other scattered areas, where the bedrock consists of Proterozoic granitoid rocks. A detachment fault separates upper-plate Tertiary volcanic and

sedimentary rocks from lower-plate Proterozoic rocks immediately west of the northwestern end of the Forest unit (Peterson, 1990, pl. 1).

Stream-sediment samples contained anomalous concentrations of Au, Ag, Bi, Pb, Zn, Mn, and Sn. Panned concentrate-samples contained anomalous concentrations of Ag, Bi, Mo, Pb, W, Ba, and Sn. Rock samples contained anomalous concentrations of tin and tungsten. Most anomalous concentrations were in single samples from clusters of samples whose geochemistry was otherwise not anomalous. However, stream-sediment samples from streams draining the southwest side of the western part of area A4a consistently contained 6 ppb or greater gold; silver concentrations in most of these samples were high background levels, and zinc was anomalously high in a few samples. This anomalous area is shown as one characterized by a gold signature (pl. 6). The presence of gold and silver anomalies (along with some zinc) and the geology suggest that low-sulfide gold-quartz veins may be present in the western part of area A4a. Alternatively, the gold and silver may have been derived from altered and deformed rocks immediately below the detachment fault that extends a short distance to the north.

Manganese and tin abundances in sediment samples and molybdenum and tungsten abundances in panned-concentrate samples were anomalously high in the northern part of area A4a. The Black Hawk manganese district and the Clark epithermal-vein district are near this area. Jones (1990) included only the western end of area A4a in a large tract that is favorable for the occurrence of porphyry copper deposits because the Proterozoic rocks that underlie its eastern part pre-date Arizona porphyry copper deposits. Although areas of some geochemical interest are present, the geochemistry of area A4a is overall only mildly anomalous and is assigned a ranking of 3 on the geochemical-intensity scale.

AREA A4b

The southeastern half of the Pinaleno Mountains, area A4b, was included in the Silver City 1° × 2° quadrangle CUSMAP study. The area is underlain by Proterozoic gneiss and granitoid rocks, Tertiary volcanic rocks, and Tertiary granitoid rocks. Base- and precious-metal-vein and replacement, precious-metal (and uranium) vein, and manganese vein (Richter and others, 1986) deposits are known to be present in area A4b. Watts and Hassemer (1988) noted the occurrence of several geologic features that indicate considerable mineral resource potential in this area, including several major faults, a volcanic center, and specialized granitoid rocks. Abundant fluorite was noted by Watts and Hassemer (1988) in panned-concentrate samples from the area.

NURE samples were not collected in the area. RASS stream-sediment samples contained anomalous concentrations of Au, Ag, As, Bi, Cd, Cu, Mo, Pb, Sb, Zn, Ba, Mn, and Sn. Stream-sediment samples also contained anomalous concentrations of Be, La, Nb, V, Y, and Th; La and Y concentrations were especially anomalous. Panned-concentrate samples had anomalous concentrations of Au, Ag, As, Bi, Cd, Cu, Mo, Pb, W, Ba, and Sn. They also contained anomalous concentrations of B, Be, La, Nb, Sc, V, Y, and Th; Nb, Sc, V, Y, and Th were especially abundant. About two-thirds of area A4b is divided into three anomalous areas that have Be-Bi-Mo-Sn-W, Bi-La-Sn-Th-Y, and Ag-As-Bi-Cr-Cu-La-Mo-Nb-Ni-Pb-Sb-Th-V-Zn geochemical signatures, respectively.

The geochemical signatures and the geologic setting suggest that a number of mineral deposit types, including polymetallic veins, a variety of skarn types, Th-Nb-REE-bearing pegmatites, tin greisens, Climax-type molybdenum deposits, or epithermal gold deposits, could be present in area A4b. According to Richter and others (1986), parts of area A4b are favorable for stockwork molybdenum (Climax-type), manganese vein, and fluorite deposits. The proportion of anomalous samples and the magnitude of anomalous concentrations of some elements result in a ranking of 7 on the geochemical-intensity scale.

PELONCILLO MOUNTAINS (B1)

AREA B1a

Previous geochemical studies in and near the Peloncillo Forest unit (pl. 7) were conducted as part of mineral resource evaluations of potential wilderness areas. The Bunk Robinson Peak and Whitmire Canyon Roadless Areas (Hayes and others, 1983; Watts and others, 1983; Hayes and Brown, 1984) are within the Forest. Two U.S. Bureau of Land Management wilderness study areas are adjacent to the south side of the national forest (U.S. Bureau of Land Management, 1986a,b); the Baker Canyon Wilderness Study Area was included in the geochemical study of the Whitmire Canyon Roadless Area (Watts and others, 1983), and geochemical samples from the Guadalupe Canyon Instant Study Area were considered in the mineral resource evaluation of Coronado National Forest, but the data have not been published previously. The NURE program included the New Mexico part of the Peloncillo Mountains Forest unit (U.S. Department of Energy, 1981a; Sharp and others, 1978), and those geochemical data are included in the data base. The data base also includes data for 11 stream-sediment samples collected in 1990 specifically for the Coronado National Forest mineral resource evaluation.

The Peloncillo Mountains are underlain mostly by Tertiary rhyolite and minor Tertiary andesite (Cooper, 1959; Wrucke and Bromfield, 1961; Drewes, 1980; Hayes, 1982). Elston (1978) and Hayes and Brown (1984) suggested that the area is within a middle Tertiary caldera complex. The Cottonwood Basin mining district, containing middle Tertiary manganese vein deposits (Keith, Gest, and DeWitt, 1983; Keith and others, 1983), is in the center of the

Peloncillo Mountains Forest unit. According to Farnham and others (1961, p. 10, 40), the Jasper (Lucky Strike) claim is part of the district; manganese oxides at the claim are present as numerous seams, stringers, and pockets in a shear zone. The Jasper claim is considered to be an epithermal manganese deposit (J.M. Hammarstrom and others, unpub. data, 1988). The Silvertip Mine, which Elston and others (1979, p. 1, fig. 1) suggested contains minor silver, is also part of the district; the geochemical signature for epithermal manganese deposits (Mosier, 1986), may include silver. However, manganese is not present in anomalous abundances in any samples from the area of the Jasper claim–Silvertip Mine and silver abundances are not anomalous in any samples from the Peloncillo Mountains Forest unit.

Stream-sediment samples contained anomalous concentrations of Au, Bi, Cd, Cu, Mo, Pb, Sb, Zn, Mn, and Sn. An area underlain by Paleozoic and Mesozoic sedimentary rocks south of this Forest unit is characterized by a clustering of anomalous abundances in stream-sediment samples of the elements listed above. If these sedimentary rocks extend into the Forest unit beneath the Tertiary volcanic rocks, they are not reflected by the geochemical patterns, except that the patterns of bismuth and antimony anomalies seem to overlap the area of contact between sedimentary and volcanic rocks. Panned-concentrate samples contained anomalous concentrations of As, Mo, Pb, Sb, W, Zn, Ba, Mn, and Sn. Highly anomalous concentrations of arsenic, antimony, barium, and tin were found in panned-concentrate samples from the central to southern parts of the Peloncillo Mountains Forest unit. The only analyzed rock samples from the Peloncillo Mountains Forest unit appear to be from the mineralized areas mentioned above and they had anomalous concentrations of barium and beryllium.

In addition to the elements mentioned above, some samples from the Peloncillo Mountains contained highly anomalous abundances of beryllium, lanthanum, niobium, and scandium. Three anomalous areas are outlined on plate 7. The geochemical signature of the largest of these, which covers most of the central part of the Forest unit, is As-Be-Nb-Sn. An anomalous area that includes the Silvertip district is outlined (pl. 7) solely on the basis of barium. At the south end of the Peloncillo Forest unit an anomalous area is outlined (pl. 7) on the basis of a beryllium-antimony geochemical signature. Geochemical signatures of area B1a, coupled with the geology, suggest that undiscovered Climax-type molybdenum deposits that contain precious metals may be present in this area (J.M. Hammarstrom and others, unpub. data, 1988). Highly anomalous concentrations of arsenic and antimony in panned-concentrate samples suggest that epithermal precious-metal deposits may be present. Area B1a is ranked 4 on the geochemical-intensity scale because the proportion of samples having anomalous concentrations is low. However, the southwestern part is geochemically more anomalous than is area B1a as a whole.

CHIRICAHUA AND PEDREGOSA MOUNTAINS (B2)

The central part of the Chiricahua and Pedregosa Mountains Forest unit (pl. 7) was sampled as part of the mineral resource evaluation of the Chiricahua Wilderness (Drewes and Williams, 1973; Drewes and Williams, 1984). The areas east and north of Chiricahua National Monument were sampled as part of the mineral resource evaluation of the North End Roadless Area (Drewes, Moss, and others, 1983; Drewes and Bigsby, 1984) and as part of CUSMAP studies of the Silver City 1° × 2° quadrangle (Watts and Hassemer, 1988). In November of 1990, 95 stream-sediment samples were collected in the Chiricahua and Pedregosa Mountains, west, south, and east of the Chiricahua Wilderness. NURE samples were not collected in the Chiricahua and Pedregosa Mountains.

The entire Chiricahua and Pedregosa Mountains Forest unit is included on a 1:125,000-scale geologic map of southeastern Arizona (Drewes, 1980). Parts of the Forest unit were mapped, mostly at larger scales, by Sabins (1957), Cooper (1959), Drewes and Williams (1973), Drewes (1981, 1982), and Drewes and Brooks (1988). Rocks in the Chiricahua and Pedregosa Mountains Forest unit range in age from Proterozoic to Quaternary. The large central mass of the mountain range is underlain by Tertiary extrusive and intrusive rocks that are part of the Turkey Creek caldera (du Bray and Pallister, 1991). The northern and southern parts of the Forest unit are underlain by Proterozoic granitoid rocks and metamorphic rocks, Paleozoic, Mesozoic, and Cretaceous sedimentary rocks, Cretaceous and Tertiary intrusive and volcanic rocks, and Tertiary and Quaternary basalt.

Mining districts in the Chiricahua and Pedregosa Mountains Forest unit are the California (Chiricahua) and Rucker Canyon districts, which contain middle Tertiary lead-zinc-silver polymetallic vein and replacement deposits (Keith, Gest, and DeWitt, 1983; Keith and others, 1983). The Rucker Canyon district was a minor producer (200 tons of base and (or) precious metals) compared to the California district (30,000 tons). J.M. Hammarstrom and others (unpub. data, 1988) classified the deposits in that part of the California district that is in the Douglas 1° × 2° quadrangle (south of lat 32° N.) to be porphyry copper skarn-related, copper skarn, zinc-lead skarn, tungsten skarn, polymetallic vein, and polymetallic replacement deposits. The deposits in the Silver City 1° × 2° part of the California district (north of lat 32° N.) and north of the district are base- and precious-metal vein and polymetallic replacement deposits (Richter and Lawrence, 1983).

AREA B2A

The area north, east, and southeast of Chiricahua National Monument is underlain by Proterozoic granitoid

rocks, Paleozoic and Cretaceous sedimentary rocks and Tertiary intrusive and volcanic rocks. Area B2a includes most of the California mining district. This area is also the location of a thick accumulation of volcanic rocks centered on Cochise Head and may contain the source for some of the rhyolite flows and other volcanic rocks in the Chiricahua Mountains (Drewes and others, 1985).

Stream-sediment samples contained anomalous concentrations of Au, Ag, As, Bi, Cd, Cu, Mo, Pb, Sb, W, Zn, Ba, Mn, and Sn. Panned-concentrate samples contained anomalous concentrations of Ag, As, Bi, Cd, Cu, Mo, Pb, W, Zn, Ba, and Sn. High-density rock sampling was done in mineralized areas; rock samples contained anomalous concentrations of Ag, As, Au, Bi, Cd, Cu, Mo, Pb, Sb, W, Zn, Ba, Mn, and Sn. Two anomalous areas that include most of area B2a are outlined on plate 7. The geochemical signature of the northern part of area B2a is As-Au-Sb. Most of the remainder of area B2a has the signature Ag-As-Au-Ba-Cd-Co-Cr-Cu-Mo-Ni-Pb-Sb-Sn-Zn.

As discussed above, the California mining district is in area B2a. Base- and precious-metal vein and replacement deposits are present in the Silver City $1° \times 2°$ quadrangle (Richter and others, 1986), whereas skarn, porphyry copper skarn-related, and polymetallic vein and replacement deposits are present in the Douglas $1° \times 2°$ quadrangle (J.M. Hammarstrom and others, unpub. data, 1988). The part of the area within the Silver City $1° \times 2°$ quadrangle is also favorable for the occurrence of porphyry copper-molybdenum deposits of several types, tungsten vein deposits, and Spor Mountain–type beryllium deposits (Richter and others, 1986). The potential for beryllium deposits is presumably based on the presence of rhyolite tuffs and Paleozoic carbonate sedimentary rocks and the reasoning that by analogy these tuffs and sedimentary rocks may be similar to those at Spor Mountain, Utah (Shawe, 1968). The geochemical signatures are spatially coincident and compatible with known deposits in the area and indicate that other types of deposits may be present in area B2a. The area is ranked 7 on the geochemical-intensity scale because of the large number of anomalous samples and elements and magnitude of the anomalies.

AREA B2b

The middle half of the Chiricahua Mountains (area B2b) is underlain by Tertiary volcanic rocks and subvolcanic intrusive rocks; the center of the Turkey Creek caldera is in the western part of the area. The Rucker Canyon mining district (see above) is in this area; information concerning the district is sparse. Mineralized rock in the area may be related to the Turkey Creek caldera. Stream-sediment samples contained anomalous concentrations of Au, Ag, As, Bi, Cd, Cu, Mo, Pb, Sb, W, Zn, and Sn. Panned-concentrate samples contained anomalous concentrations of Ag, As, Cd, Cu, Mo, Pb, Sb, Zn, Ba, and Sn. Rock samples contained anomalous concentrations of Ag, As, Bi, Mo, Ba, and Sn. Geochemical anomalies in area B2b (pl. 7) extend well beyond the Rucker Canyon district. The geochemical signature of the northeastern part of area B2b is Ag-As-Au-Bi-Cd-Cu-Mo-Pb-Sb-Zn; the anomaly extends north into area B2a. Two smaller parts of area B2b have Mo-Zn and As-Au geochemical signatures, respectively.

The geologic setting and geochemical data suggest that porphyry tin, tin-polymetallic veins, or epithermal veins could be present. The geochemical signature is also appropriate for Climax-type porphyry molybdenum deposits (J.M. Hammarstrom and others, unpub. data, 1988). The area is ranked 6 on the geochemical-intensity scale.

AREA B2c

The west half of the Pedregosa Mountains is underlain mainly by Tertiary volcanic rocks ranging in composition from rhyolite to andesite. Stream-sediment samples contained anomalous concentrations of Ag, As, Bi, Cd, Cu, Pb, Sb, Zn, and Sn. Rock samples contained anomalous concentrations of Ag, Bi, Mo, Zn, and Sn. No panned-concentrate samples were collected in the area. Part of area B2c underlain by volcanic rocks is associated with a geochemically anomalous terrane that extends west from, and is coincident with, most of area B2d (described below). The southern part of area B2c is underlain by Paleozoic sedimentary rock and is characterized by an As-Cd-Cu-Pb-Sb-Zn geochemical signature.

As in other parts of Coronado National Forest where rhyolite is an important bedrock type, area B2c has potential for various types of tin deposits. Also, because of the band of Paleozoic rocks, many of which are carbonate sedimentary rocks, the area has potential for polymetallic vein and replacement, copper skarn, and lead-zinc skarn deposits; a geochemical signature for these types of deposits has, indeed, been noted in the southern part of area B2c, where carbonate sedimentary rocks crop out. J.M. Hammarstrom and others (unpub. data, 1988) included the Pedregosa Mountains in a large area, along with the Chiricahua and Swisshelm Mountains, where conditions are favorable for the occurrence of polymetallic vein and replacement and skarn deposits of various types. Area B2c is ranked 5 on the geochemical-intensity scale because only restricted areas are geochemically anomalous.

AREA B2d

The east half of the Pedregosa Mountains is underlain by Paleozoic (mostly carbonate) sedimentary rocks, Cretaceous volcanic and intrusive rocks, Cretaceous sedimentary rocks, Tertiary intrusive and volcanic rocks, and Tertiary to Quaternary basalt. Stream-sediment samples contained

anomalous concentrations of Au, Ag, Bi, Cd, Cu, Pb, Sb, Zn, and Sn. Rock samples contained anomalous concentrations of Ag, As, Mo, Pb, Sb, Zn, Ba, and Sn. Panned-concentrate samples were not collected in the area. Most of area B2d is coincident with an anomalous terrane characterized by a Ag-As-Au-Bi-Cd-Cu-Sb geochemical signature. Area B2d (and area B2c) is in the large tract that J.M. Hammarstrom and others (unpub. data, 1988) considered favorable for the occurrence of polymetallic vein and replacement and copper or lead-zinc skarn deposits; the geochemical signature is compatible with those deposit types. The area is ranked 4 on the geochemical scale because a small proportion of samples contained anomalous concentrations of most elements.

DRAGOON MOUNTAINS (C1)

The Dragoon Mountains Forest unit (pl. 7) is at the intersection of the Douglas, Nogales, Silver City, and Tucson 1° × 2° quadrangles. Therefore, this area was partially included in mineral resource assessments of each of the quadrangles (Richter and others, 1986; J.M. Hammarstrom and others, unpub. data, 1988; Peterson, 1990;). The geology of the entire area was published as part of a tectonic map of southeastern Arizona (Drewes, 1980), and most of the area was included in a mineral resource evaluation of the Dragoon Mountains Roadless Area (Drewes, Watts, and others, 1983; Drewes and Kreidler, 1984), which included geochemical studies of panned-concentrate samples (Watts and others, 1984) and mineralized rocks (Drewes, 1984).

The geology of the Dragoon Mountains area includes a sequence of sedimentary rocks that range in age from Proterozoic to Cretaceous (Drewes, 1980; Drewes and Meyer, 1983). Carbonate sedimentary rocks make up a large proportion of the Paleozoic sequence there and a small part of the Cretaceous sequence. The sedimentary rocks have been complexly folded and faulted. The northwest-striking grain of the sedimentary sequence is interrupted by the granitic Stronghold stock, which was intruded in Tertiary time (Drewes and Meyer, 1983). The Forest unit has been divided into three parts on the basis of geology and geochemistry; the northern and southern parts are underlain by a sequence of sedimentary rocks, and the middle part is mostly underlain by granite.

Mining districts in the Dragoon Mountains Forest unit are the Middle Pass district (middle Tertiary lead-zinc vein and replacement deposits) and the Golden Rule (Dragoon) district (Late Cretaceous gold and silver) (Keith, Gest, and DeWitt, 1983; Keith and others, 1983). The Middle Pass district produced 97,000 tons of base- and precious-metal ore before 1979, and the Golden Rule district produced 34,000 tons of ore before 1957 (Keith and others, 1983). Kreidler (1984) described the mines and prospects of the Dragoon Mountains Roadless Area and nearby areas.

Ore deposits in the Dragoon Mountains Forest unit are in carbonate sedimentary rocks near contacts with the Stronghold stock or rhyolite dikes (Kreidler, 1984). Deposits in the part of the Forest unit within the Silver City 1° × 2° quadrangle are base- and precious-metal vein and replacement deposits (Richter and others, 1986). Deposits in the Forest unit within the Douglas 1° × 2° quadrangle are copper skarns, zinc-lead skarns, and polymetallic replacement and vein deposits (J.M. Hammarstrom and others, unpub. data, 1988). Deposits in parts of the Forest within the Tucson and Nogales 1° × 2° quadrangles are zinc-lead skarns (Jones, 1990).

AREA C1a

The northern third of the Dragoon Mountains is primarily underlain by Proterozoic to Cretaceous sedimentary rocks and subordinate Proterozoic and Tertiary granitoid intrusive rocks. Zinc-lead skarn and base- and precious-metal vein and replacement deposits are known in this area (Richter and others, 1986; J.M. Hammarstrom and others, unpub. data, 1988; Jones, 1990).

Stream-sediment samples contained anomalous concentrations of Au, Ag, Bi, Cd, Cu, Mo, Pb, Sb, W, Zn, and Sn. Panned-concentrate samples contained anomalous concentrations of Ag, Au, Bi, Cu, Mo, Pb, Sb, W, Zn, Ba, and Sn. Rock samples contained anomalous concentrations of Ag, As, Bi, Cd, Cu, Mo, Pb, Sb, Zn, Mn, and Sn. Two-thirds of area C1a falls within an anomalous area (pl. 7) characterized by a Ag-Au-Ba-Be-Bi-Cd-Cu-La-Mo-Nb-Pb-Sn-Th-W-Y-Zn geochemical signature. This geochemical signature is compatible with known deposits in area C1a, although anomalous concentrations of molybdenum and tin probably correlate with granitoid rocks rather than indicate mineralized rock.

The part of the Dragoon Mountains Forest unit within the Douglas 1° × 2° quadrangle is favorable for the occurrence of tungsten and gold skarns because upper Paleozoic limestone was intruded by Tertiary granite and many of the skarns there include bismuth-bearing phases in their mineralized parts (J.M. Hammarstrom and others, unpub. data, 1988). In addition, reported production from the Dragoon mining district includes a high ratio of gold to silver (J.M. Hammarstrom and others, unpub. data, 1988). Jones (1990) included the parts of the Dragoon Mountains that are within the Nogales and Tucson 1° × 2° quadrangles in tracts that are favorable for the occurrence of porphyry copper deposits, replacement deposits, silver-bearing base-metal, and tungsten skarn deposits. Drewes and Kreidler (1984) suggested that area C1a may also be favorable for the occurrence of stockwork molybdenum deposits. The area is ranked 7 on the geochemical-intensity scale because anomalous concentrations of many elements are present in a moderate number of samples.

AREA C1b

The middle third of the Dragoon Mountains is underlain mostly by the Tertiary Stronghold granitic stock. Proterozoic to Cretaceous sedimentary rocks are also present, mostly in the center of area C1b, but also on the margins of the pluton. Here, as elsewhere in the Dragoon Mountains Forest unit, ore deposits are concentrated in the sedimentary rocks and not in the Stronghold pluton. Known mineral deposits are copper skarns, lead-zinc skarns, and polymetallic vein and replacement deposits (J.M. Hammarstrom and others, unpub. data, 1988).

Stream-sediment samples contained anomalous concentrations of Au, Ag, Bi, Cd, Cu, Mo, Pb, Sb, W, Zn, Mn, and Sn. Panned-concentrate samples contained anomalous concentrations of Ag, As, Bi, Cd, Cu, Mo, Pb, W, Zn, Mn, and Sn. Rock sampling was limited to mineralized rocks, for the most part (Drewes, 1984); rock samples represent mineralized carbonate sedimentary rocks because known mineral deposits are only in carbonate sedimentary rocks (Kreidler, 1984). Rock samples contained anomalous concentrations of Ag, Bi, Cd, Cu, Mo, Pb, Sn, W, Zn, Mn, and Sn. Anomalous abundances of Au, Ag, Cd, Pb, and Sb are limited to areas of sedimentary rocks, of Bi, Cu, Mo, Nb, W, Zn, and Sn to areas of sedimentary and granitic rocks, and of As and Mn to areas of granitic rocks. Other elements present in anomalous concentrations are almost exclusively from areas underlain by granitic rocks and include lanthanum, niobium, scandium, yttrium, and thorium. Beryllium abundances are anomalous in samples from areas of both rock types. Anomalous concentrations of tin in stream-sediment samples are present in an unusually large proportion of samples.

Elements present in anomalous abundances are clearly separated into two groups: one group consists of elements typically associated with known mineral deposits in carbonate sedimentary rocks (Au, Ag, Cd, Pb, and Sb) and the other consists of elements associated with granitic rocks (La, Sc, Y, and Th). The La-Sc-Pb-Sb signature, together with some elements that are not exclusively part of it (Be, Nb, and Sn) appears to be the signature for a specialized granite, as suggested by Watts and others (1984), although some specialized granite bodies are characteristically depleted in lanthanum and scandium (Reed, 1986; Reed and Cox, 1986). Area C1b is divided into two anomalous areas (pl. 7); the northern one also includes much of area C1a (discussed above) to the north and the southern one extends to the south and includes all of area C1c (discussed below).

In addition to the known deposit types in area C1b, the area is favorable for the occurrence of gold skarns and tungsten skarns, because of the intrusions of granitic rocks into carbonate sedimentary rocks, for tin greisens (J.M. Hammarstrom and others, unpub. data, 1988), tin skarns, and tin veins because of the specialized nature of the Stronghold stock. Area C1b is favorable for the occurrence of porphyry copper deposits (Jones, 1990).

The number of elements present in anomalous concentrations and the proportion of anomalous samples from the area are high relative to other Forest units and indicate a ranking of 9 on the geochemical-intensity scale.

AREA C1c

Geology in the southern third of the Dragoon Mountains Forest unit is similar to that in the northern third. The area is underlain by Proterozoic to Cretaceous sedimentary rocks, with some Proterozoic and Tertiary granitoid intrusive rocks. Known deposits are copper and lead-zinc skarns (J.M. Hammarstrom and others, unpub. data, 1988).

NURE samples were not collected in the area. Stream-sediment samples contained anomalous concentrations of Ag, Bi, Cd, Cu, Mo, Pb, Sb, W, Zn, and Sn. Panned-concentrate samples contained anomalous concentrations of Ag, As, Bi, Cd, Cu, Mo, Pb, Sb, W, Zn, Ba, Mn, and Sn. Rock samples contained anomalous concentrations of Ag, As, Bi, Cd, Cu, Mo, Pb, Sb, W, Zn, Mn, and Sn. The geochemical signature for area C1c and the southern part of area C1b is Ag-Be-Bi-Cd-Cu-La-Mo-Nb-Pb-Sn-Th-W-Y-Zn (pl. 7). A major difference between the northern and southern parts of area C1 is that the geochemical signature for the southern part of the area does not, for an unknown reason, include gold.

The geologic settings and geochemical signatures of the southern and northern parts of the Dragoon Mountains Forest unit are similar. Consequently, the southern part of this Forest unit is considered favorable for the occurrence of the same types of mineral deposits as the northern part. In addition to known copper and lead-zinc skarns, the area is favorable for the occurrence of porphyry copper, replacement, silver-bearing base-metal, gold and tungsten skarn, and stockwork molybdenum deposits (Drewes and Kreidler, 1984; J.M. Hammarstrom and others, unpub. data, 1988; Jones, 1990). This area is ranked 7 on the geochemical-intensity scale because a smaller proportion of samples than in area C1b contained anomalous concentrations of many elements.

WHETSTONE MOUNTAINS (D1)

The Whetstone Mountains Forest unit of Coronado National Forest (pl. 8) was included in the geochemical sampling program of the Whetstone Roadless Area mineral resource evaluation (Werschsky and others, 1983; Wrucke and others, 1983; Wrucke and McColly, 1984). Stream-sediment, panned-concentrate, and rock samples were collected for the resource evaluation. NURE samples were also collected in parts of the Forest unit.

A homoclinal sequence of Cambrian through Cretaceous sedimentary rocks that overlie Proterozoic granitoid

rocks and schist (Drewes, 1980; Wrucke and Armstrong, 1984) underlies the Whetstone Mountains Forest unit; Tertiary granitoid rocks are also present. Ordovician, Silurian, Triassic, and Jurassic rocks are not present in the sedimentary sequence.

The Forest unit contains the Whetstone and Mine Canyon mining districts (Keith, Gest, and DeWitt, 1983; Keith and others, 1983). Known deposits are Proterozoic tungsten veins and Late Cretaceous porphyry copper, base-metal vein and replacement, fluorite vein, and uranium vein deposits (Wrucke and McColly, 1984; Jones, 1990).

AREA D1a

The northeastern third of the Whetstone Mountains is underlain mostly by Proterozoic granitoid rocks. Mineral deposits include tungsten veins (Jones, 1990), uranium veins, and fluorite veins (Wrucke and McColly, 1984). Stream-sediment samples contained anomalous concentrations of Ag, Bi, Cd, Cu, Mo, Pb, Sb, W, Zn, and Sn. Panned-concentrate and rock samples contained anomalous concentrations of bismuth and tungsten. Except for bismuth, anomalous concentrations were found in samples from the southeastern part of area D1a. The anomalous area is near Paleozoic carbonate sedimentary rock outcrops and is confined to several drainage basins. The geochemical signature of this area is Ag-As-Au-B-Bi-Cd-Cu-Mo-Pb-Sb-W-Zn. Mesozoic or Cenozoic igneous rocks are not present in the area, but the geochemical signature suggests that they may be in the subsurface and could have been the source of the metals in the deposits mentioned above, which commonly are present in carbonate sedimentary rocks adjacent to intrusions. Anomalies in the southeastern part of the area rank 6 on the geochemical-intensity scale; the remainder of area D1a is only weakly anomalous.

AREA D1b

Area D1b, a northwest-striking band in the middle third of the Whetstone Mountains, is underlain by Paleozoic sedimentary rocks and small Cretaceous granitic intrusions. The only known mineral deposit in area D1b is the Gold Crystal prospect, a low-grade gold prospect (Wrucke and McColly, 1984) in Cambrian limestone and sandstone (Wrucke and others, 1983) at its eastern end.

Stream-sediment samples contained anomalous concentrations of gold, silver, cadmium, molybdenum, and antimony. Panned-concentrate samples appeared to be more anomalous overall than stream-sediment samples and contained anomalous concentrations of Ag, Bi, Cd, Cu, Mo, Pb, W, Zn, and Ba. Rock samples contained anomalous concentrations of molybdenum. Anomalous regions outlined in areas D1a (described above) and D1c (described below) extend into area D1b. Paleozoic carbonate sedimentary rocks intruded by Cretaceous granitoid rocks and the geochemical signature noted above suggest the presence of polymetallic vein and replacement deposits, and skarns of various types. A carbonate-hosted gold-silver deposit (Carlin-type, Berger, 1986), is also suggested by persistently anomalous, low-level gold abundances (the same is not generally true of other elements) in stream-sediment samples from the western part of the area and by the carbonate sedimentary rocks in the area. The area is ranked 5 on the geochemical-intensity scale.

AREA D1c

The southwestern third of the Whetstone Mountains Forest unit is underlain by Cretaceous sedimentary and Tertiary granitoid rocks. Known mineral deposits within area D1c include copper skarns (Jones, 1990), polymetallic veins, and a porphyry copper deposit associated with polymetallic base-metal veins (Wrucke and McColly, 1984).

Stream-sediment samples contained anomalous concentrations of Au, Ag, As, Bi, Cu, Mo, Sb, Zn, and Ba; low-level anomalous abundances of gold are ubiquitous in most of area D1c. Panned-concentrate samples contained anomalous concentrations of Ag, Bi, Cu, Mo, Pb, Sb, W, and Ba. Rock samples contained anomalous concentrations of Ag, Bi, Cu, Mo, Pb, Sb, W, Zn, Ba, and Sn. Most of area D1c is part of a geochemical anomaly characterized by a As-Au-B-Ba-Mo-Sb geochemical signature. The geochemical signature is compatible with known mineral deposits in the area. The persistent low-level gold anomaly is a continuation of the distribution pattern of gold in area D1b. Certain bedrock units, such as the Apache Canyon Formation (Wrucke and Armstrong, 1984), appear to be favorable for the occurrence of carbonate-hosted gold-silver deposits (Berger, 1986).

In addition to known deposits, area D1c is favorable for the occurrence of polymetallic replacement (Jones, 1990) and carbonate-hosted gold-silver deposits. Except for gold, relatively few samples contained anomalous elemental concentrations, so the area is ranked 6 on the geochemical-intensity scale.

PATAGONIA AND HUACHUCA MOUNTAINS AND CANELO HILLS (D2)

The geochemistry of the Patagonia Mountains was studied extensively and summarized by Chaffee and others (1981). Interpretations of the geochemistry of the Canelo Hills and Huachuca Mountains have not been published. Geology of the Patagonia-Huachuca-Canelo Forest unit is described in the discussion of each area.

Mining districts within the Patagonia-Huachuca-Canelo Forest unit (pl. 8) include the Harshaw, Palmetto, Patagonia, Querces, and Washington Camp districts (Late Cretaceous to early Tertiary porphyry copper districts), the Hartford district (early Tertiary lead-zinc-silver vein and replacement deposits), the Parker Canyon and Red Rock districts (Late Cretaceous lead-zinc-silver vein and replacement deposits), the Bluebird district (middle Tertiary manganese veins), and the Reef district (early Tertiary tungsten skarns and veins or pegmatites) (Keith, Gest, and DeWitt, 1983; Keith and others, 1983).

AREA D2a

This area includes all of the Patagonia Mountains except the northern part. Bedrock in the area consists of Cambrian to Cretaceous sedimentary rocks, Proterozoic to Tertiary granitoid rocks, and Jurassic to Tertiary volcanic rocks (Drewes, 1980; Simons, 1974). The Red Mountain porphyry copper deposit (Corn, 1975; Chaffee and others, 1981) is immediately north of area D2a, but the extensive hydrothermal system associated with the Red Mountain deposit strongly affected area D2a. Mining districts within area D2a are the Harshaw, Palmetto, Patagonia, Querces, and Washington Camp, which are all Late Cretaceous to early Tertiary porphyry copper deposits (Keith, Gest, and DeWitt, 1983; Keith and others, 1983). Polymetallic vein and replacement, porphyry copper-molybdenum, replacement manganese, copper skarn, zinc-lead skarn, and tungsten skarn deposits are known to be present in area D2a (Jones, 1990).

Area D2a is the most geochemically anomalous in Coronado National Forest. Anomalous abundances of Au, Ag, As, Bi, Cd, Cu, Mo, Pb, Sb, W, Zn, Ba, Mn, and Sn are present in most stream-sediment, panned-concentrate, and rock samples throughout the area. The anomalous nature of the area is evident despite contamination of drainage samples by extensive mining (Chaffee and others, 1981). Most of area D2a is highly anomalous (pl. 8) and is characterized by a Ag-As-Au-B-Ba-Bi-Cd-Co-Cr-Cu-Mo-Ni-Pb-Sb-V-W-Zn geochemical signature.

The geochemical signature reflects known deposits of area D2a and strongly suggests that additional undiscovered deposits may be present (Chaffee and others, 1981). In addition to being favorable for the known deposit types, the area is favorable for the occurrence of epithermal precious-metal deposits (Jones, 1990). Area D2a is ranked 10 on the geochemical-intensity scale.

AREA D2b

The northern Patagonia Mountains are underlain by Cretaceous volcanic rocks (Drewes, 1980). Mining districts wholly or partially within area D2b are the Harshaw district (porphyry copper) and the Red Rock district (Late Cretaceous manganese veins) (Keith, Gest, and DeWitt, 1983; Keith and others, 1983). The deeply buried (at least 3,500 ft) Red Mountain porphyry copper deposit is present in this area (Corn, 1975; Chaffee and others, 1981). Other known mineral deposits in area D2b are polymetallic veins (Jones, 1990). The area is very nearly as anomalous as the rest of the Patagonia Mountains (area D2a).

Stream-sediment samples contained anomalous concentrations of Au, Ag, As, Bi, Cu, Mo, Pb, Sb, Zn, Ba, Mn, and Sn. Panned-concentrate samples contained anomalous concentrations of the same elements, and cadmium and tungsten are also present in anomalous concentrations. Rock samples contained anomalous concentrations of molybdenum, lead, zinc, barium, and tin. Most of area D2b is coincident with part of an anomalous region that extends northeast from area D2a and has the Ag-As-Au-B-Ba-Bi-Cd-Co-Cr-Cu-Mo-Ni-Pb-Sb-V-W-Zn geochemical signature, indicating that the types of deposits present in area D2a may also be present in area D2b, although sedimentary rocks are largely absent. Parts of the area are favorable for the occurrence of porphyry copper, various types of skarn, polymetallic replacement, epithermal precious-metal, and polymetallic vein deposits (Jones, 1990). The area is ranked 9 on the geochemical-intensity scale.

AREA D2c

Areas of Coronado National Forest surrounding the San Rafael Valley are underlain by unconsolidated to poorly consolidated Tertiary and Quaternary sedimentary deposits (Drewes, 1980; Simons, 1974). Stream-sediment samples contained anomalous concentrations of Ag, Cd, Cu, Pb, Sb, Zn, Ba, Mn, and Sn. No panned-concentrate samples were collected in the area. Rock samples contained anomalous concentrations of barium and tin. Anomalous regions that cover parts of areas D2a, D2b, and D2d extend into area D2c.

The western part of the area is favorable for the occurrence of porphyry copper deposits (Jones, 1990). Detritus in the sedimentary deposits of area D2c is probably a composite of the adjoining four areas within this Forest unit because debris from all of them sheds into area D2c. The overall area is ranked 3 on the geochemical-intensity scale, although specific parts of the area are more anomalous than others and may deserve a higher rank.

AREA D2d

The Canelo Hills are underlain by Cambrian to Cretaceous sedimentary rocks, Triassic or Jurassic granitoid rocks, and Triassic to Tertiary volcanic rocks (Drewes, 1980). Part of the area was designated a wilderness study

area (Peterson and others, 1984) but was not studied by the USGS. The Bluebird (middle Tertiary manganese veins) and Parker Canyon (Late Cretaceous(?) lead-zinc-silver vein and replacement deposits) mining districts are on the western edge of area D2d (Keith, Gest, and DeWitt, 1983; Keith and others, 1983). Stream-sediment samples contained anomalous concentrations of Ag, Pb, Sb, Zn, Mn, and Sn. Panned-concentrate samples were not collected. Rock samples contained anomalous concentrations of tin. A large part of area D2d includes a region delineated by anomalous concentrations of antimony (pl. 8), the most widespread component of the geochemical signature in area D2d. The geochemical data are compatible with vein and replacement deposits associated with carbonate sedimentary rocks. The area is favorable for the occurrence of various types of skarn and polymetallic replacement deposits (Jones, 1990). The ranking on the geochemical-intensity scale is 2 because only a small proportion of the samples contained anomalous metal concentrations.

AREA D2e

The Huachuca Mountains are underlain by Proterozoic, Triassic, Jurassic, Cretaceous, and Tertiary granitoid rocks, Cambrian to Tertiary sedimentary rocks, and Triassic to Tertiary volcanic rocks (Hayes and Raup, 1968; Drewes, 1980). Two tracts were designated as wilderness study areas (Peterson and others, 1984), but only one of them, the Miller Peak Wilderness (U.S. Bureau of Land Management, 1986a), was studied by the USGS, in a literature-based investigation (Ludington, 1984a). Mining districts within area D2e are the Hartford district (early Tertiary lead-zinc-silver vein and replacement deposits) and the Reef district (early Tertiary tungsten skarn and veins or pegmatites) (Keith, Gest, and DeWitt, 1983; Keith and others, 1983). Polymetallic vein and replacement, tungsten skarn and vein, and epithermal precious-metal vein deposits are known to be present in area D2e (Jones, 1990).

Stream-sediment samples contained anomalous concentrations of Au, Ag, Bi, Cd, Cu, Mo, Pb, Sb, W, Zn, Mn, and Sn. Panned-concentrate samples contained anomalous concentrations of Au, Ag, Cd, Cu, Mo, Pb, Sb, W, Zn, Ba, and Sn. Rock samples contained anomalous concentrations of silver, bismuth, copper, molybdenum, and tin. The geochemical signature for most of the southern part of area D2e is Ag-Au-Cd-Pb-Sb-W-Zn (pl. 8). A single sample indicated that a drainage basin at the north end of area D2e (pl. 8) has a silver-gold geochemical signature. The geochemical signatures are compatible with known mineral deposits of area D2e. In addition to these deposits, the area is favorable for the occurrence of porphyry copper deposits (Jones, 1990). Ludington (1984a) considered the area, in particular the area around clustered tungsten-vein deposits associated with the rhyolite intrusive center at Sutherland Peak, to be favorable for the occurrence of disseminated tungsten deposits. The proportion of samples having anomalous concentrations is much less than in the Patagonia Mountains, and, therefore, the area is ranked 7 on the geochemical-intensity scale.

SANTA RITA MOUNTAINS (E1)

The Santa Rita Mountains were one of the first areas in Arizona to be systematically studied with exploration geochemistry techniques (Drewes, 1973). Areas of interest were studied in greater detail, although still on a reconnaissance basis (Drewes, 1967, 1970, 1973). Forest unit E1 is underlain by Proterozoic, Mesozoic, and Tertiary granitoid rocks, Cretaceous and Tertiary volcanic rocks, and Proterozoic, Paleozoic, and Mesozoic sedimentary rocks (Drewes, 1971a, b, 1980; Finnell, 1971).

Mining districts within the Santa Rita Mountains Forest unit (pl. 8) are Late Cretaceous to early Tertiary porphyry copper deposits (Cave Creek, Helvetia-Rosemont, and Jackson districts), Late Cretaceous lead-zinc-silver vein and replacement deposits (Greaterville, Ivanho, Mansfield, Old Baldy, Salero, Tyndall, and Wrightson districts), and Late Cretaceous uranium vein or fissure deposits (Duranium district) (Keith, Gest, and DeWitt, 1983; Keith and others, 1983). Copper skarn, porphyry copper, polymetallic vein and replacement, epithermal manganese, and gold placer deposits are present in this area (Ludington, 1984b; Jones, 1990).

AREA E1a

The north end of the Santa Rita Mountains is underlain by Paleozoic and Mesozoic sedimentary rocks, Cretaceous and Tertiary volcanic rocks, and Proterozoic, Cretaceous, and Tertiary granitoid rocks. The Helvetia-Rosemont district (Late Cretaceous and early Tertiary porphyry copper deposits) is partly in area E1a (Keith, Gest, and DeWitt, 1983; Keith and others, 1983). Also, copper skarn and polymetallic replacement deposits are present (Jones, 1990).

Stream-sediment samples contained anomalous concentrations of Au, Ag, As, Bi, Cd, Cu, Mo, Pb, Sb, W, Zn, Sn, and Mn. Panned-concentrate samples were not collected. Rock samples contained anomalous concentrations of Ag, As, Au, Bi, Cd, Cu, Mo, Pb, Sb, W, Zn, Ba, Mn, and Sn. About half of area E1a is part of an anomalous region that also covers the northern part of areas E1b and E1c (pl. 8). The geochemical signature of this anomalous area is Ag-As-Au-Bi-Cd-Cu-Mo-Pb-Sb-Sn-Zn. The geochemical signature is compatible with known deposits in area E1a. In addition to deposit types known to occur in the area, the area is favorable for the occurrence of other types of skarn (including gold) and replacement deposits (Jones, 1990).

The proportion of anomalous samples justifies ranking this area at 7 on the geochemical-intensity scale.

AREA E1b

The western three-fourths of the Santa Rita Mountains Forest unit forms the bulk of the mountain range and is underlain by Proterozoic, Triassic, Jurassic, Cretaceous, and Tertiary granitoid rocks, Cretaceous and Tertiary volcanic rocks, Proterozoic metamorphic rocks, and Paleozoic and Mesozoic sedimentary rocks. The Mt. Wrightson Wilderness (U.S. Bureau of Land Management, 1986a) was studied by the USGS (Ludington, 1984b); the study depended heavily on existing reports of the USGS, including geochemical studies by Drewes (1973). All mining districts in the Santa Rita Mountains Forest unit are wholly or partly in area E1b. Copper skarn, polymetallic vein and replacement, porphyry copper, epithermal manganese, and gold placer deposits are known to occur in this area.

Stream-sediment samples contained anomalous concentrations of Au, Ag, As, Bi, Cd, Cu, Mo, Pb, Sb, W, Zn, Ba, Mn, and Sn. Only a few panned-concentrate samples were collected in area E1b; their geochemistry is like that of the stream-sediment samples. Rock samples contained anomalous concentrations of Ag, As, Au, Bi, Cd, Cu, Mo, Pb, Sb, W, Zn, Ba, Mn, and Sn.

Ludington (1984b) recorded classic zonation, as indicated by the pattern of copper, lead, and zinc abundances in stream-sediment samples from the Mount Wrightson Wilderness, for a porphyry copper type deposit; a central area of anomalous copper concentrations is surrounded by a zone of anomalous lead and zinc concentrations. Most of the southern part of area E1b is part of an anomalous region that is characterized by the Ag-As-Au-B-Bi-Cd-Cu-Pb-Sb-Zn geochemical signature (pl. 8). As discussed above, the northern part of area E1b is part of an anomalous region characterized by the Ag-As-Au-Bi-Cd-Cu-Mo-Pb-Sb-Sn-Zn geochemical signature. These geochemical signatures are compatible with known deposits in the area. In addition to known deposits, area E1b may be favorable for the occurrence of gold skarn deposits (Jones, 1990). The geochemistry and the geologic setting for the southern Santa Rita Mountains are similar to those in the Patagonia Mountains (Jones, 1990). The area is ranked 8 on the geochemical-intensity scale.

AREA E1c

The eastern one-fourth of the Santa Rita Mountains Forest unit is covered by weakly indurated Tertiary and Quaternary gravel deposits. Thus, the geochemistry of samples collected in this area may reflect the mountains to the west, unless bedrock is near enough to the surface to be detected by geochemical methods. Only a few panned-concentrate samples were collected in area E1c. No rock samples were collected. Stream-sediment data are based on NURE data or on the re-analysis of NURE samples, except along the border with area E1b.

Stream-sediment samples contained anomalous concentrations of Au, Ag, As, Cd, Cu, Mo, Pb, Sb, W, and Zn. Panned-concentrate samples contained anomalous concentrations of silver, cadmium, and barium. Anomalous regions in areas E1a and E1b extend into the northern and southern parts of area E1c, respectively (pl. 8). The geochemical signatures are similar to those in the rest of the Santa Rita Mountains, and they may reflect similar mineral deposits beneath the gravel cover. The proportion of samples having anomalous concentrations of several elements gives the area a ranking of 6 on the geochemical-intensity scale.

ATASCOSA, PAJARITO, SAN LUIS, AND TUMACACORI MOUNTAINS AND COBRE AND COCHES RIDGES (E2)

The Atascosa–Cobre–Coches–Pajarito–San Luis–Tumacacori Forest unit (pl. 8) is underlain mostly by Jurassic, Cretaceous, and Tertiary granitoid, volcanic, and sedimentary rocks (Drewes, 1980; Peterson and others, 1990). Mining districts are limited to the Coches Ridge–Cobre Ridge–Pajarito Mountains area (area E2b). Several tracts of land were designated as wilderness study areas (Peterson and others, 1984) but were not studied by the USGS; a part of those tracts is now the Pajarito Wilderness (U.S. Bureau of Land Management, 1986a).

AREA E2a

The part of the San Luis Mountains in Coronado National Forest is underlain by Cretaceous to Tertiary granitoid rocks (including peraluminous granite) and Jurassic volcanic rocks (Peterson and others, 1990). Area E2a contains no mining districts (Keith, Gest, and DeWitt, 1983; Keith and others, 1983). Small wolframite-scheelite placers and at least one tungsten vein deposit are present in the San Luis Mountains (Jones, 1990). The tungsten vein deposit is near the intrusive contact of a peraluminous granite.

Stream-sediment samples contained anomalous concentrations of gold, molybdenum, tungsten, zinc, and barium. Panned-concentrate samples contained anomalous concentrations of copper and tungsten. Rock samples contained anomalous concentrations of silver and molybdenum. The geochemical data are compatible with tungsten deposits (tungsten is the most anomalous element from area E2a); also, molybdenum and zinc are part of the signature for tungsten veins (Cox and Bagby, 1986). The area is ranked 3 on the geochemical-intensity scale.

AREA E2b

Cobre Ridge, Coches Ridge, and the Pajarito Mountains are underlain by Jurassic, Cretaceous, and Tertiary granitoid rocks, Jurassic and Tertiary volcanic rocks, and Jurassic and Cretaceous sedimentary rocks (Peterson and others, 1990). The Pajarito Wilderness is in area E2b (U.S. Bureau of Land Management, 1986a). Mining districts in the area are the Easter (Late Cretaceous tungsten skarns and veins or pegmatites), Oro Blanco and Pajarito (Late Cretaceous lead-zinc-silver vein and replacement deposits), Cerro de Fresnal and Austerlitz (middle Tertiary gold deposits), and Arivaca (late Tertiary lead-zinc-silver vein and replacement deposits) (Keith, Gest, and DeWitt, 1983; Keith and others, 1983). These districts contain tungsten vein, polymetallic vein, and epithermal precious-metal vein deposits (Jones, 1990).

Stream-sediment samples contained anomalous concentrations of Au, Ag, As, Bi, Cd, Cu, Mo, Pb, Sb, W, Zn, Ba, Mn, and Sn. Panned-concentrate samples contained anomalous concentrations of Au, Ag, Bi, Cd, Cu, Mo, Pb, Sb, Zn, Ba, Mn, and Sn. Rock samples contained anomalous concentrations of Ag, As, Bi, Cd, Cu, Mo, Sb, Zn, Ba, Mn, and Sn. About two-thirds of area E2b falls within an anomalous region (pl. 8) characterized by the Ag-Au-B-Cd-Cu-Mo-Pb-Sb-Zn geochemical signature. The geochemical signature for the eastern part of area E2b is As-B-Pb-Sb-Zn (pl. 8). These geochemical signatures are compatible with known deposits in area E2b. The area is also favorable for occurrence of porphyry copper deposits (Jones, 1990). Area E2b is ranked 7 on the geochemical-intensity scale.

AREA E2c

The Atascosa and Tumacacori Mountains making up area E2c are underlain by Jurassic granitoid and Tertiary volcanic rocks (Drewes, 1980); there are no mining districts in area E2c (Keith, Gest, and DeWitt, 1983; Keith and others, 1983). Stream-sediment samples contained anomalous concentrations of Au, Ag, Bi, Cd, Cu, Mo, Pb, Sb, Zn, Ba, Mn, and Sn. Panned-concentrate samples contained anomalous concentrations of Ag, As, Cd, Cu, Mo, Pb, Sb, Zn, Ba, and Sn. Rock samples contained anomalous concentrations of tin. The geochemical anomaly that includes much of area E2b, characterized by the Ag-Au-B-Cd-Cu-Mo-Pb-Sb-Zn signature (pl. 8), includes the southwestern part of area E2c as well. The northern part of area E2c is in a geochemically anomalous region characterized by the As-B-Sb geochemical signature. In view of the geology, the geochemical signature suggests that polymetallic vein, porphyry copper, and epithermal precious-metal deposits may be present. The Atascosa Mountains are favorable for the occurrence of epithermal precious-metal deposits (Jones, 1990). The proportion of samples having anomalous concentrations suggests that additional mineral deposits may be present. The area is ranked 8 on the geochemical-intensity scale.

AREA E2d

Area E2d is west of the city of Nogales and comprises the eastern part of the Atascosa–Cobre–Coches–Pajarito–San Luis–Tumacacori Forest unit. Weakly indurated Tertiary and Quaternary gravels underlie the entire area (Drewes, 1980); no mining districts are present (Keith, Gest, and DeWitt, 1983; Keith and others, 1983). Stream-sediment samples contained anomalous concentrations of Au, Ag, As, Cd, Mo, Pb, Sb, Zn, Ba, and Mn. Panned-concentrate samples contained anomalous concentrations of Ag, As, Bi, Cu, Mo, Pb, Sb, Zn, Ba, Mn, and Sn. No rock samples were collected. Area E2d is part of an anomalous region characterized by the As-B-Pb-Sb-Zn geochemical signature (pl. 8).

As in other Forest units where bedrock is covered by weakly indurated gravels, the geochemistry may reflect gravel source areas rather than underlying bedrock. Assuming that the bedrock units of nearby source areas extend underneath the gravels, possible deposit types could be polymetallic vein and epithermal precious-metal deposits. Jones (1990) included parts of area E2d in tracts favorable for the occurrence of porphyry copper and epithermal precious-metal deposits. The area is ranked 5 on the geochemical-intensity scale, but parts near the range front to the west may be more highly anomalous.

SANTA CATALINA AND RINCON MOUNTAINS (F1)

Geochemical studies were conducted in the Santa Catalina–Rincon Forest unit (pl. 6) as part of mineral resource evaluations of two wilderness study areas. Stream-sediment and rock samples were collected and analyzed as part of the evaluation of the Rincon Wilderness Study Area, which adjoins Saguaro National Monument on its north, east, and south sides (Thorman and others, 1981). Stream-sediment and panned-concentrate samples were collected as part of the mineral resource evaluation of the Pusch Ridge Wilderness Area (Hinkle and others, 1981b,c; Hinkle and Ryan, 1982), which includes a large tract of the Santa Catalina Mountains.

Bedrock geology was compiled by Peterson and others (1990) from maps by Banks (1976), Creasey (1967), Creasey and Theodore (1975), Drewes (1974, 1977), and Reynolds (1988). Sedimentary and metasedimentary rocks in the Forest unit range in age from Proterozoic to Tertiary. Granitoid intrusive rocks are Proterozoic, Cretaceous, and Tertiary in age. Crustal extension during the Tertiary formed detachment faults in the Santa Catalina and Rincon Mountains and produced mylonitic rocks.

Mining districts in the Santa Catalina–Rincon Forest unit are Late Cretaceous to early Tertiary porphyry copper (Burney, Catalina, Little Hills, Marble Peak, and Redington), early Tertiary tungsten skarns and veins or pegmatites (Oracle), early Tertiary(?) uranium in veins or fissures (Blue Rock), middle Tertiary gold (Canada del Oro), and middle Tertiary copper veins (Rincon) (Keith, Gest, and DeWitt, 1983; Keith and others, 1983). Jones (1990) suggested that copper skarn and polymetallic vein and replacement deposits also are present in this Forest unit.

The Santa Catalina–Rincon Forest unit was subdivided into four areas on the basis of predominant rock types. Area F1a is north of an east-west line through Mount Lemmon and is underlain mainly by Proterozoic granite and by Cretaceous and Tertiary granitoid rocks; Paleozoic sedimentary rocks underlie much less area than the granitic rocks but are important hosts for mineral deposits. Area F1b is most of the area south of Mount Lemmon and is underlain by Cretaceous to Tertiary mylonitized peraluminous granite. Area F1c is a narrow strip along the east side of the Forest unit that is mostly underlain by Paleozoic and Mesozoic sedimentary rocks; carbonate sedimentary rocks are common. Area F1d is a small strip along the southern edge of the Forest unit where Paleozoic sedimentary rocks crop out.

AREA F1a

This area comprises the Santa Catalina Mountains north of Mount Lemmon. Proterozoic granitoid and sedimentary rocks, Paleozoic and Mesozoic sedimentary rocks, and Cretaceous to Tertiary granitoid rocks underlie the area. The granitoid rocks predominate areally, but most mineral production has been from deposits associated with Paleozoic sedimentary rocks. Mining districts in area F1a are the Burney, Little Hills, and Marble Peak districts (porphyry copper), Oracle (tungsten skarns and veins or pegmatites), and Cañada del Oro (gold) (Keith, Gest, and DeWitt, 1983; Keith and others, 1983).

Stream-sediment samples contained anomalous concentrations of Au, Ag, As, Bi, Cd, Cu, Mo, Pb, Sb, W, Zn, Mn, and Sn. Only a few panned-concentrate and rock samples were collected in this area and they contained no anomalous elemental concentrations. Samples that contained anomalous concentrations of the preceding elements are generally from the eastern part of area F1a and are associated with sedimentary rocks and known mineral deposits. The eastern part of area F1a (pl. 6) contains two anomalous regions. The geochemical signature for the northern one consists solely of zinc. The geochemical signature for the southern one is Ag-Au-Cu-Mo-Sb-Zn. As previously indicated, the abundances of many elements are anomalous in selected samples. However, geochemical signatures and abundances are compatible with known mineral deposits. Parts of area F1a are favorable for the occurrence of porphyry copper, skarn, and replacement deposits (Jones, 1990). The area is ranked 6 on the geochemical-intensity scale as indicated by the high proportion of anomalous samples and the number of elements present in anomalous concentrations.

Some additional elements present in anomalous concentrations are lanthanum, niobium, scandium, yttrium, and thorium; samples having anomalous concentrations of these elements are present in areas underlain by granitoid rocks. The highly anomalous abundances of these elements in samples from area F1b may be a lithologic signature.

AREA F1b

Area F1b includes most of the Santa Catalina and Rincon Mountains south of Mount Lemmon. Proterozoic metasedimentary rocks, Proterozoic granite, Paleozoic and Mesozoic sedimentary rocks, and Cretaceous to Tertiary granitoid rocks underlie the area; Cretaceous to Tertiary peraluminous granite is the predominant rock type. Much of the granite is mylonitic gneiss that was deformed during late Mesozoic to middle Tertiary contractional and extensional faulting, respectively; this mountain range is one of the many metamorphic core complexes in the region (Reynolds, 1988). The Catalina mining district (Late Cretaceous to early Tertiary porphyry copper) is within the southwestern part of the area (Keith, Gest, and DeWitt, 1983; Keith and others, 1983).

The distribution of panned-concentrate samples is limited to the Pusch Ridge Wilderness. Stream-sediment samples contained anomalous concentrations of Au, Ag, As, Bi, Cd, Cu, Mo, Pb, Sb, W, Zn, Ba, Mn, and Sn. Panned-concentrate samples contained anomalous concentrations of Ag, Cu, Mo, Pb, W, Zn, Mn, and Sn. Rock samples contained anomalous concentrations of Ag, As, Bi, Cd, Cu, Mo, W, Zn, Mn, and Sn. The southernmost anomalous region of area F1a is characterized by the Ag-Au-Cu-Mo-Sb-Zn geochemical signature and extends into area F1b (pl. 6). Other small parts of area F1b are geochemically anomalous, but the number of elements whose abundances are geochemically anomalous is three or fewer (Sb; Cu-Mo-Zn; Cu-Zn; Au). Some of the samples that contained anomalous concentrations of the preceding elements are from areas underlain by sedimentary rocks, such as the east side of the area. Many of the anomalous concentrations are compatible with known mineral deposits associated with sedimentary rocks throughout the Santa Catalina and Rincon Mountains, but the significance of some of the anomalies is not known.

Some of the anomalous elements (Ba, Mn, Mo, Sn) may be part of a lithologic signature that also includes anomalous concentrations of Be, La, Nb, Y, and Th. Because barium abundances are anomalously high in stream-sediment samples but not in panned-concentrate samples, barium must be present in a mineral such as feldspar or mica, rather than as barite. This signature suggests that beryllium-niobium-thorium-REE pegmatites could be present. The northern fringe of area F1b is favorable for the occurrence of

porphyry copper, skarn, and polymetallic replacement deposits, and the southeastern part is favorable for the occurrence of flat-fault gold deposits (Jones, 1990). The number of geochemically anomalous samples in this area supports a rank of 6 on the geochemical-intensity scale.

AREA F1c

This area is a narrow strip along the east side of the Santa Catalina and Rincon Mountains that is mostly underlain by Paleozoic and Mesozoic sedimentary rocks. Proterozoic granitoid and metamorphic rocks are also present. Area F1c borders, and is partly underlain by, the large masses of Cretaceous and Tertiary granitoids and peraluminous granite that underlie areas F1a and F1b. The Redington (Late Cretaceous to early Tertiary porphyry copper) and Blue Rock (early Tertiary(?) uranium veins and fissures) mining districts are within or on the border of the area (Keith, Gest, and DeWitt, 1983; Keith and others, 1983). A known deposit near the center of area F1b is a copper skarn (Jones, 1990).

No panned-concentrate samples were collected. Stream-sediment samples contained anomalous concentrations of Au, Ag, As, Cd, Cu, Mo, Pb, Sb, Zn, Ba, and Mn. Rock samples contained anomalous concentrations of Ag, As, Be, Cu, Mo, Pb, Sb, W, Zn, Mn, and Sn. A small anomalous region near the center of area F1c is limited to a single drainage basin (pl. 6); the geochemical signature is Ag-As-Au-Cu-Mo-Sb-Zn. Two small regions characterized by Cu-Mo-Zn and Cu-Zn geochemical signatures, respectively, extend into area F1c from area F1b. These geochemical signatures are compatible with known copper skarn and with other skarns and polymetallic vein and replacement deposits that may occur in an area where abundant carbonate sedimentary rocks are present. The north end of area F1c is favorable for the occurrence of porphyry copper, skarn, and replacement deposits, and the south end is favorable for the occurrence of flat-fault gold (Jones, 1990). Because the proportion of anomalous samples is relatively low, the area is ranked 5 on the geochemical-intensity scale.

AREA F1d

A small area within Coronado National Forest and adjacent to the south side of the Forest on the southern slopes of the Rincon Mountains is underlain by Paleozoic and Tertiary sedimentary rocks, Proterozoic granite, and Cretaceous and Tertiary peraluminous granite. Thorman and others (1981, p. 17–19) described prospect pits in mineralized rock characterized by copper and iron minerals; mineralized areas are associated with faults.

No panned-concentrate samples were collected. Stream-sediment samples contained anomalous concentrations of Au, Ag, Mo, Pb, Sb, and Ba. Rock samples contained anomalous concentrations of Bi, Cu, Mo, Pb, Sb, W, and Zn. The geochemical data are compatible with the existence of skarn, vein, and replacement deposits in carbonate sedimentary rocks. The area is ranked 2 on the geochemical-intensity scale. However, area F1d is part of a larger anomalous region (pl. 6) in which the geochemical signature is gold only. The area is favorable for the occurrence of flat-fault gold (Jones, 1990); anomalous gold concentrations may support this inference.

REFERENCES CITED

Banks, N.G., 1976, Reconnaissance geologic map of the Mount Lemmon quadrangle, Arizona: U.S. Geological Survey Miscellaneous Field Studies Map MF–747, scale 1:62,500.

Berger, B.R., 1986, Descriptive model of carbonate-hosted Au-Ag, *in* Cox, D.P., and Singer, D.A., eds., Mineral deposit models: U.S. Geological Survey Bulletin 1693, p. 175.

Bergquist, J.R., 1979, Reconnaissance geologic map of the Blue Jay Peak quadrangle, Graham County, Arizona: U.S. Geological Survey Miscellaneous Field Studies Map MF–1083, scale 1:24,000.

Blacet, P.M., and Miller, S.T., 1978, Reconnaissance geologic map of the Jackson Mountain quadrangle, Graham County, Arizona: U.S. Geological Survey Miscellaneous Field Studies Map MF–939, scale 1:62,500.

Brobst, D.A., and Goudarzi, G.H., 1984, Introduction, *in* Marsh, S.P., Kropschot, S.J., and Dickinson, R.G., eds., Wilderness mineral potential; assessment of mineral-resource potential in U.S. Forest Service lands studied 1964–1984: U.S. Geological Survey Professional Paper 1300, p. 1–10.

Chaffee, M.A., 1985, Geochemical evaluation of the Winchester Roadless Area, Cochise County, Arizona: U.S. Geological Survey Open-File Report 85–113, 8 p.

———1990, Geochemistry, *in* Peterson, J.A., ed., Preliminary mineral resource assessment of the Tucson and Nogales 1°° × 2° quadrangles, Arizona: U.S. Geological Survey Open-File Report 90–276, p. 19–40.

Chaffee, M.A., Hill, R.H., Sutley, S.J., and Watterson, J.R., 1981, Regional geochemical studies in the Patagonia Mountains, Santa Cruz County, Arizona: Journal of Geochemical Exploration, v. 14, p. 135–153.

Cook, J.R., and Fay, W.M., 1982, Data report, Western United States, hydrogeochemical and stream sediment reconnaissance: U.S. Department of Energy, Savannah River Laboratory, National Uranium Resource Evaluation Program, 33 p.

Cooper, J.R., 1959, Reconnaissance geologic map of southeastern Cochise County, Arizona: U.S. Geological Survey Mineral Investigations Field Studies Map MF–213, scale 1:125,000.

Corn, R.M., 1975, Alteration-mineralization zoning, Red Mountain, Arizona: Economic Geology, v. 70, no. 8, p. 1437–1447.

Cox, D.P., 1986, Descriptive model of porphyry Cu-Mo, *in* Cox, D.P., and Singer, D.A., eds., Mineral deposit models: U.S. Geological Survey Bulletin 1693, p. 115.

Cox, D.P., and Bagby, W.C., 1986, Descriptive model of W veins, *in* Cox, D.P., and Singer, D.A., eds., Mineral deposit models: U.S. Geological Survey Bulletin 1693, p. 64.

Creasey, S.C., 1967, General geology of the Mammoth quadrangle, Pinal County, Arizona: U.S. Geological Survey Bulletin 1218, 94 p., map scale 1:48,000.

Creasey, S.C., Jackson, E.D., and Gulbrandsen, R.A., 1961, Reconnaissance geologic map of parts of the San Pedro and Aravaipa Valleys, south-central Arizona: U.S. Geological Survey Mineral Investigations Field Studies Map MF–238, scale 1:125,000.

Creasey, S.C., and Jinks, J.E., 1984, Galiuro Wilderness and contiguous roadless areas, Arizona, *in* Marsh, S.P., Kropschot, S.J., and Dickinson, R.G., eds., Wilderness mineral potential; assessment of mineral-resource potential in U.S. Forest Service lands studied 1964–1984: U.S. Geological Survey Professional Paper 1300, p. 65–68.

Creasey, S.C., Jinks, J.E., Williams, F.E., and Meeves, H.C., 1981, Mineral Resources of the Galiuro Wilderness and contiguous further planning areas, Arizona; *with a section on* Aeromagnetic survey and interpretation, *by* W.E. Davis: U.S. Geological Survey Bulletin 1490, 94 p., 2 pls., map scale 1:62,500.

Creasey, S.C., and Theodore, T.G., 1975, Preliminary reconnaissance geologic map of the Bellota Ranch quadrangle, Pima County, Arizona: U.S. Geological Survey Open-File Report 75–295, scale 1:31,680.

Curtin, G.C., 1985, The Conterminous United States Mineral Assessment Program, *in* Krafft, Kathleen, ed., USGS Research on Mineral Resources—1985, Program and Abstracts: U.S. Geological Survey Circular 949, p. 61–63.

Drewes, Harald, 1967, A geochemical anomaly of base metals and silver in the southern Santa Rita Mountains, Santa Cruz County, Arizona: U.S. Geological Survey Professional Paper 575–D, p. D176–D182.

———1970, Structure control of geochemical anomalies in the Greaterville mining district, southeast of Tucson, Arizona: U.S. Geological Survey Bulletin 1312–A, 49 p., 1 plate.

———1971a, Geologic map of the Mount Wrightson quadrangle, southeast of Tucson, Santa Cruz and Pima Counties, Arizona: U.S. Geological Survey Miscellaneous Geologic Investigations Map I–614, scale 1:48,000.

———1971b, Geologic map of the Sahuarita quadrangle, southeast of Tucson, Pima County, Arizona: U.S. Geological Survey Miscellaneous Geologic Investigations Map I–613, scale 1:48,000.

———1973, Geochemical reconnaissance of the Santa Rita Mountains, southeast of Tucson, Arizona: U.S. Geological Survey Bulletin 1365, 67 p., 2 pls.

———1974, Geologic map and sections of the Happy Valley quadrangle, Cochise County, Arizona: U.S. Geological Survey Miscellaneous Investigations Series Map I–832, scale 1:48,000.

———1977, Geologic map and sections of the Rincon Valley quadrangle, Pima County, Arizona: U.S. Geological Survey Miscellaneous Investigations Series Map I–997, scale 1:48,000.

———1980, Tectonic map of southeast Arizona: U.S. Geological Survey Miscellaneous Investigations Series Map I–1109, scale 1:125,000.

———1981, Geologic map and sections of the Bowie Mountain South quadrangle, Cochise County, Arizona: U.S. Geological Survey Miscellaneous Investigations Series Map I–1363, scale 1:24,000.

———1982, Geologic map and sections of the Cochise Head quadrangle and adjacent areas, southeastern Arizona: U.S. Geological Survey Miscellaneous Investigations Series Map I–1312, scale 1:24,000.

———1984, Reconnaissance geochemical maps of mineralized rocks in the Dragoon Mountains Roadless Area, Cochise County, Arizona: Miscellaneous Field Studies Map MF–1521–D, scale 1:50,000.

Drewes, Harald, and Bigsby, P.R., 1984, North End Roadless Area, Arizona, *in* Marsh, S.P., Kropschot, S.J., and Dickinson, R.G., eds., Wilderness mineral potential; assessment of mineral-resource potential in U.S. Forest Service lands studied 1964–1984: U.S. Geological Survey Professional Paper 1300, p. 90–93.

Drewes, Harald, and Brooks, W.E., 1988, Geologic map and cross sections of the Pedregosa Mountains, Cochise County, Arizona: U.S. Geological Survey Miscellaneous Investigations Series Map I–1827, scale 1:48,000.

Drewes, Harald, Houser, B.B., Hedlund, D.C., Richter, D.H., Thorman, C.H., and Finnell, T.L., 1985, Geologic map of the Silver City 1° × 2° quadrangle, New Mexico and Arizona: U.S. Geological Survey Miscellaneous Investigations Series Map I–1310–C, scale 1:250,000.

Drewes, Harald, and Kreidler, T.J., 1984, Dragoon Mountains Roadless Area, Arizona, *in* Marsh, S.P., Kropschot, S.J., and Dickinson, R.G., eds., Wilderness mineral potential; assessment of mineral-resource potential in U.S. Forest Service lands studied 1964–1984: U.S. Geological Survey Professional Paper 1300, p. 58–61.

Drewes, Harald, and Meyer, G.A., 1983, Geologic map of the Dragoon Mountains Roadless Area, Cochise County, Arizona: Miscellaneous Field Studies Map MF–1521–A, scale 1:50,000.

Drewes, Harald, Moss, C.K., Watts, K.C., Jr., Forn, C.L., and Bigsby, P.R., 1983, Mineral resource potential map of the North End Roadless Area, Chiricahua Mountains, Cochise County, Arizona: Miscellaneous Field Studies Map MF–1412–D, scale 1:50,000.

Drewes, Harald, Watts, K.C., Jr., Klein, D.P., and Kreidler, T.J., 1983, Mineral resource potential map of the Dragoon Mountains Roadless Area, Cochise County, Arizona: U.S. Geological Survey Miscellaneous Field Studies Map MF–1521–B, scale 1:50,000.

Drewes, Harald, and Williams, F.E, 1973, Mineral resources of the Chiricahua Wilderness Area, Cochise County, Arizona: U.S. Geological Survey Bulletin 1385–A, 53 p., 1 pl., scale 1:62,500.

———1984, Chiricahua Wilderness, Arizona, *in* Marsh, S.P., Kropschot, S.J., and Dickinson, R.G., eds., Wilderness mineral potential; assessment of mineral-resource potential in U.S. Forest Service lands studied 1964–1984: U.S. Geological Survey Professional Paper 1300, p. 55–58.

du Bray, E.A., and Pallister, J.S., 1991, An ash-flow caldera in cross section—Ongoing field and geochemical studies of the mid-Tertiary Turkey Creek caldera, Chiricahua Mountains, SE Arizona: Journal of Geophysical Research, v. 96, p. 13435–13457.

Elston, W.E., 1978, Mid-Tertiary cauldrons and their relationship to mineral resources, southwestern New Mexico; A brief review, *in* Field guide to selected cauldrons and mining districts of the Datil-Mogollon volcanic field, New Mexico: New Mexico Geological Society Special Publication No. 7, p. 107–113.

Elston, W.E., Erb, E.E., and Deal, E.G., 1979, Tertiary geology of Hidalgo County, New Mexico; guide to metals, industrial

minerals, petroleum, and geothermal resources: New Mexico Geology, v. 1, no. 1, p. 1, 4–6.

Farnham, L.L., Stewart, L.A., and DeLong, C.W., 1961, Manganese deposits of eastern Arizona: U.S. Bureau of Mines Information Circular 7990, 178 p.

Finnell, T.L., 1971, Preliminary geologic map of the Empire Mountains quadrangle, Pima County, Arizona: U.S. Geological Survey Open-File Report 71–106, scale 1:48,000.

Grimes, D.J., and Marranzino, A.P., 1968, Direct-current arc and alternating-current spark emission spectrographic field methods for the semiquantitative analysis of geologic materials: U.S. Geological Survey Circular 591, 6 p.

Harms, T.F., Bradley, L.A., Tidball, R.R., Motooka, J.M., and Conklin, N.M., 1985, Analytical results and sample locality maps of stream sediments, heavy-mineral concentrates, and plant samples from Black Rock, Fishhooks, and Needles Eye Wilderness Study Areas, Graham and Gila Counties, Arizona: U.S. Geological Survey Open-File Report 85–462, 49 p., 3 pls., scale 1:24,000.

Hayes, P.T., 1982, Geologic map of Bunk Robinson Peak and Whitmire Canyon Roadless Areas, Coronado National Forest, New Mexico and Arizona: Miscellaneous Field Studies Map MF–1425–A, scale 1:62,500.

Hayes, P.T., and Brown, S.D., 1984, Bunk Robinson Peak and Whitmire Canyon Roadless Areas, New Mexico and Arizona, *in* Marsh, S.P., Kropschot, S.J., and Dickinson, R.G., eds., Wilderness mineral potential; assessment of mineral-resource potential in U.S. Forest Service lands studied 1964–1984: U.S. Geological Survey Professional Paper 1300, p. 798–800.

Hayes, P.T., and Raup, R.B., 1968, Geologic map of the Huachuca and Mustang Mountains, southeastern Arizona: U.S. Geological Survey Miscellaneous Geologic Investigations Map I–509, scale 1:48,000.

Hayes, P.T., Watts, K.C., Hassemer, J.R., and Brown, S.D., 1983, Mineral resource potential map of the Bunk Robinson Peak and Whitmire Canyon Roadless Areas, Hidalgo County, New Mexico, and Cochise County, Arizona: Miscellaneous Field Studies Map MF–1425–B, scale 1:62,500.

Hinkle, M.E., Kilburn, J.E., Eppinger, R.G., III, and Speckman, W.S., 1981a, Geochemical analysis of samples of stream sediments, panned heavy-mineral concentrates, rocks, and waters of the Pusch Ridge Wilderness Area, Arizona: U.S. Geological Survey Open-File Report 81–435, 44 p.

———1981b, Statistical analyses of data on stream sediments, panned heavy-mineral concentrates, rocks, and waters of the Pusch Ridge Wilderness Area, Arizona: U.S. Geological Survey Open-File Report 81–436, 183 p.

Hinkle, M.E., Kilburn, J.E., Eppinger, R.G., III, and Tripp, R.B., 1981c, Geochemical maps of the Pusch Ridge Wilderness Area, Pima County, Arizona: U.S. Geological Survey Miscellaneous Field Studies Map MF–1356–A, scale 1:50,000.

Hinkle, M.E., and Ryan, G.S., 1982, Mineral resource potential map of the Pusch Ridge Wilderness Area, Pima County, Arizona: U.S. Geological Survey Miscellaneous Field Studies Map MF–1356–B, scale 1:62,500.

Jones, G.M., 1990, Mineral resources, *in* Peterson, J.A., ed., Preliminary mineral resource assessment of the Tucson and Nogales 1° × 2° quadrangles, Arizona: U.S. Geological Survey Open-File Report 90–276, p. 68–101.

Keith, S.B., Gest, D.E., and DeWitt, Ed, 1983, Metallic mineral districts of Arizona: Arizona Bureau of Geology and Mineral Technology Map 18, scale 1:1,000,000.

Keith, S.B., Gest, D.E., DeWitt, Ed, Toll, N.W., and Everson, B.A., 1983, Metallic mineral districts and production in Arizona: Arizona Bureau of Geology and Mineral Technology Bulletin 194, 58 p.

Keith, W.J., and Kreidler, T.J., 1984, Whetstone Roadless Area, Arizona, *in* Marsh, S.P., Kropschot, S.J., and Dickinson, R.G., eds., Wilderness mineral potential; assessment of mineral-resource potential in U.S. Forest Service lands studied 1964–1984: U.S. Geological Survey Professional Paper 1300, p. 130–132.

Keith, W.J., Martin, R.A., and Kreidler, T.J., 1982, Mineral resource potential of the Winchester Roadless Area, Cochise County, Arizona: U.S. Geological Survey Open-File Report 82–1028, 7 p.

Kreidler, T.J., 1984, Mine and prospect map of the Dragoon Mountains Roadless Area, Cochise County, Arizona: Miscellaneous Field Studies Map MF–1521–F, scale 1:50,000.

Lovering, T.S., Huff, L.C., and Almond, H., 1950, Dispersion of copper from the San Manuel Copper deposit, Pinal County, Arizona: Economic Geology, v. 45, no. 6, p. 493–514.

Ludington, S.D., 1984a, Preliminary mineral resource assessment of the proposed Miller Peak Wilderness, Cochise County, Arizona: U.S. Geological Survey Open-File Report 84–293, 9 p.

———1984b, Preliminary mineral resource assessment of the proposed Mt. Wrightson Wilderness, Santa Cruz and Pima Counties, Arizona: U.S. Geological Survey Open-File Report 84–294, 11 p.

McDanal, S.K., Forn, C.L., Hassemer, J.R., and Watts, K.C., 1983, Analytical results for stream-sediment concentrates, sieved stream sediments, water, rock, and soils, Silver City, New Mexico–Arizona quadrangle: U.S. Geological Survey Report NTIS USGS–GD–83–003 [magnetic tape available from the National Technical Information Service, U.S. Department of Commerce, Springfield, VA 22161].

Marsh, S.P., Kropschot, S.J., and Dickinson, R.G., eds., 1984, Wilderness mineral potential; assessment of mineral-resource potential in U.S. Forest Service lands studied 1964–1984: U.S. Geological Survey Professional Paper 1300, 1183 p.

Meier, A.L., 1980, Flameless atomic-absorption determination of gold in geological materials: Journal of Geochemical Exploration, v. 13, p. 77–85.

Mosier, D.L., 1986, Descriptive model of epithermal Mn, *in* Cox, D.P., and Singer, D.A., eds., Mineral deposit models: U.S. Geological Survey Bulletin 1693, p. 165.

Motooka, J.M., 1988, An exploration geochemical technique for the determination of preconcentrated organometallic halides by ICP–AES: Applied Spectroscopy, v. 42, no. 7, p. 1293–1296.

Motooka, J.M., and Grimes, D.J., 1976, Analytical precision of one-sixth order semiquantitative spectrographic analysis: U.S. Geological Survey Circular 738, 25 p.

Myers, A.T., Havens, R.G., and Dunton, P.J., 1961, A spectrochemical method for the semiquantitative analysis of rocks, minerals, and ores: U.S. Geological Survey Bulletin 1084–I, p. 207–229.

New Mexico Geological Society, 1982, New Mexico geologic highway map: Socorro, N. Mex., scale 1:1,000,000.

Nowlan, G.A., and Chaffee, M.A., eds., 1995, Analytical results, sample locations, and other information for stream-sediment, soil, heavy-mineral-concentrate, and rock samples used in mineral resource studies of Coronado National Forest and adjacent areas, southeastern Arizona and southwestern New Mexico: U.S. Geological Survey Open-File Report 95–615, one 3.5-inch, 1.44-M diskette; 10-p. description of diskette contents available separately.

O'Leary, R.M., and Meier, A.L., 1986, Analytical methods used in geochemical exploration, 1984: U.S. Geological Survey Circular 948, 48 p.

Peterson, J.A., ed., 1990, Preliminary mineral resource assessment of the Tucson and Nogales 1° × 2° quadrangles, Arizona: U.S. Geological Survey Open-File Report 90–276, 129 p., 24 pls., scale 1:250,000.

Peterson, J.A., Bergquist, J.R., Reynolds, S.J., and Page-Nedell, S.S., 1990, Geology, *in* Peterson, J.A., ed., Preliminary mineral resource assessment of the Tucson and Nogales 1° × 2° quadrangles, Arizona: U.S. Geological Survey Open-File Report 90–276, p. 8–18.

Peterson, J.A., Page-Nedell, S.S., and Bergquist, J.R., 1984, Map showing mineral resource potential of U.S. Forest Service and Bureau of Land Management wilderness study areas in Arizona: U.S. Geological Survey Open-File Report 84–408, 15 p., map scale 1:1,000,000.

Reed, B.L., 1986, Descriptive model of Sn veins, *in* Cox, D.P., and Singer, D.A., eds., Mineral deposit models: U.S. Geological Survey Bulletin 1693, p. 67.

Reed, B.L., and Cox, D.P., 1986, Descriptive model of Sn skarn deposits, *in* Cox, D.P., and Singer, D.A., eds., Mineral deposit models: U.S. Geological Survey Bulletin 1693, p. 58.

Reynolds, S.R., 1988, Geologic map of Arizona: Tucson, Ariz., Arizona Geological Survey, scale 1:1,000,000.

Richter, D.H., and Lawrence, V.A., 1983, Mineral deposit map of the Silver City 1° × 2° quadrangle, New Mexico and Arizona: U.S. Geological Survey Miscellaneous Investigations Series Map I–1310–B, scale 1:250,000.

Richter, D.H., Sharp, W.N., Watts, K.C., Raines, G.L., Houser, B.B., and Klein, D.P., 1986, Maps showing mineral resource assessment of the Silver City 1° × 2° quadrangle, New Mexico and Arizona: U.S. Geological Survey Miscellaneous Investigations Series Map I–1310–F, scale 1:250,000.

Rose, A.W., Hawkes, H.E., and Webb, J.S., 1979, Geochemistry in mineral exploration (2nd ed.): New York, Academic Press, 657 p.

Sabins, F.L., Jr., 1957, Geology of the Cochise Head and western part of the Vanar quadrangles, Arizona: Geological Society of America Bulletin, v. 68, no. 10, p. 1315–1342, map scale 1:62,500.

Shannon, S.S., Jr., 1977, The hydrogeochemical and stream-sediment reconnaissance program and its relation to the NURE, *in* HSSR symposium papers: Symposium on hydrogeochemical and stream-sediment reconnaissance for uranium in the United States, Grand Junction, Colo., March 16–17, 1977: Grand Junction, Colo., U.S. Department of Energy, p. 3–4.

Sharp, R.R., Jr., and Aamodt, P.L., 1978, Field procedures for the uranium hydrogeochemical and stream sediment reconnaissance as used by the Los Alamos Scientific Laboratory: U.S. Department of Energy National Uranium Resource Evaluation Program Open-File Report LA–7054–M [GJBX–68(78)], U.S. Department of Energy, Los Alamos Scientific Laboratory, Los Alamos, N. Mex., April 1978, 64 p.

Sharp, R.R., Jr., Morris, W.A., and Aamodt, P.L., 1978, Uranium hydrogeochemical and stream sediment data release for the New Mexico portions of the Douglas, Silver City, Clifton, and Saint Johns NTMS quadrangles, New Mexico/Arizona: U.S. Department of Energy National Uranium Resource Evaluation Program Open-File Report LA–7180–MS [GJBX–69(78)], U.S. Department of Energy, Los Alamos Scientific Laboratory, Los Alamos, N. Mex., March 1978, 123 p.

Shawe, D.R., 1968, Geology of the Spor Mountain beryllium district, Utah, *in* Ridge, J.D., ed., Ore deposits of the United States, 1933–1967 (Graton-Sales Volume): New York, American Institute of Mining, Metallurgical, and Petroleum Engineers, Inc., p. 1148–1161.

Simons, F.S., 1964, Geology of the Klondyke quadrangle, Graham and Pinal Counties, Arizona: U.S. Geological Survey Professional Paper 461, 173 p., map scale 1:62,500.

———1974, Geologic map and sections of the Nogales and Lochiel quadrangles, Santa Cruz County, Arizona: U.S. Geological Survey Miscellaneous Investigations Series Map I–762, scale 1:48,000.

Simons, F.S., Theobald, P.K., Tidball, R.R., Erdman, J.A., Harms, T.F., Griscom, Andrew, and Ryan, G.S., 1987, Mineral resources of the Black Rock Wilderness Study Area, Graham County, Arizona: U.S. Geological Survey Bulletin 1703–C, 9 p.

Sutley, S.J., Chaffee, M.A., Fey, D.L., and Hill, R.H., 1983, Chemical analyses and statistical summaries for samples of rock, minus-60-mesh (0.25 mm) stream sediment, and nonmagnetic heavy-mineral concentrate, Winchester Roadless Area, Cochise County, Arizona: U.S. Geological Survey Open-File Report 83–648, 18 p.

Thorman, C.H., 1981, Geology of the Pinaleno Mountains, Arizona—A preliminary report: Arizona Geological Society Digest, v. 13, p. 5–12.

Thorman, C.H., Drewes, Harald, and Lane, M.E., 1981, Mineral resources of the Rincon Wilderness Study Area, Pima County, Arizona: U.S. Geological Survey Bulletin 1500, 62 p., 2 pls., map scale 1:48,000.

U.S. Bureau of Land Management, 1986a, Wilderness status map, State of Arizona: U.S. Bureau of Land Management, scale 1:1,000,000.

———1986b, Wilderness status map, State of New Mexico: U.S. Bureau of Land Management, scale 1:1,000,000.

U.S. Department of Energy, 1981a, Hydrogeochemical and stream sediment reconnaissance basic data for Douglas quadrangle, Arizona, New Mexico: U.S. Department of Energy National Uranium Resource Evaluation Program Open-File Report K/UR–315 [GJBX–244(81)]; U.S. Department of Energy, Oak Ridge Gaseous Diffusion Plant, Oak Ridge, Tenn., May 29, 1981, 57 p.

———1981b, Hydrogeochemical and stream sediment reconnaissance basic data for Silver City quadrangle, New Mexico, Arizona: U.S. Department of Energy National Uranium Resource Evaluation Program Open-File Report K/UR–345[GJBX–320(81)]; U.S. Department of Energy, Oak Ridge Gaseous Diffusion Plant, Oak Ridge, Tenn., June 30, 1981, 113 p.

———1982a, Hydrogeochemical and stream sediment reconnaissance basic data for Nogales quadrangle, Arizona: U.S.

Department of Energy National Uranium Resource Evaluation Program Open-File Report K/UR–420 [GJBX–65(82)], U.S. Department of Energy, Oak Ridge Gaseous Diffusion Plant, Oak Ridge, Tenn., April 1982, 1 fiche, 92 p.

———1982b, Hydrogeochemical and stream sediment reconnaissance basic data for the Tucson quadrangle, Arizona: U.S. Department of Energy National Uranium Resource Evaluation Program Open-File Report K/UR–419 [GJBX–64(82)]; U.S. Department of Energy, Oak Ridge Gaseous Diffusion Plant, Oak Ridge, Tenn., April 1982, 1 fiche, 138 p.

———1982c, Supplement to hydrogeochemical and stream sediment reconnaissance basic data reports K/UR–405 and K/UR–408 through K/UR–443 [GJBX–52(82) through GJBX–88(82)]: U.S. Department of Energy National Uranium Resource Evaluation Program Open-File Report K/UR–444 [GJBX–88(82)]; U.S. Department of Energy, Oak Ridge Gaseous Diffusion Plant, Oak Ridge, Tenn., March 1982, 25 p.

U.S. Geological Survey, Arizona Bureau of Mines, and U.S. Bureau of Reclamation, 1969, Mineral and water resources of Arizona: Arizona Bureau of Mines Bulletin 180, 638 p.

VanTrump, George, Jr., and Miesch, A.T., 1977, The U.S. Geological Survey RASS-STATPAC system for management and statistical reduction of geochemical data: Computers and Geosciences, v. 3, p. 475–488.

Watts, K.C., Jr., Erickson, M.S., Day, G.W., and Hassemer, J.R., 1984, Statistical analysis, and listing of spectrographic analyses of alluvial heavy-mineral concentrates and sieved stream-sediment samples, Dragoon Mountains Roadless Area and contiguous areas, Cochise County, Arizona: U.S. Geological Survey Open-File Report 84–013, 41 p.

Watts, K.C., Jr., and Hassemer, J.R., 1988, Geochemical interpretive and summary maps, Silver City 1° × 2° quadrangle, New Mexico and Arizona: U.S. Geological Survey Miscellaneous Investigations Series Map I–1310–E, scale 1:250,000.

Watts, K.C., Jr., Hassemer, J.R., and Day, G.W., 1983, Geochemical maps of Bunk Robinson Peak and Whitmire Canyon Roadless Areas, Hidalgo County, New Mexico, and Cochise County, Arizona: U.S. Geological Survey Miscellaneous Field Studies Map MF–1425–C, scale 1:125,000.

Watts, K.C., Jr., Hassemer, J.R., Erickson, M.S., and Drewes, Harald, 1984, Geochemical and mineralogic maps of the Dragoon Mountains Roadless Area, Cochise County, Arizona: U.S. Geological Survey Miscellaneous Field Studies Map MF–1521–E, scale 1:50,000.

Watts, K.C., Jr., Hassemer, J.R., Forn, C.L., and Siems, D.F., 1986a, Geochemical maps showing distribution and abundance of barium in two fractions of stream-sediment concentrates, Silver City 1° × 2° quadrangle, New Mexico and Arizona: U.S. Geological Survey Miscellaneous Field Studies Map MF–1183–K, scale 1:250,000.

———1986b, Geochemical maps showing distribution and abundance of bismuth and beryllium in the nonmagnetic fraction of stream-sediment concentrates, Silver City 1° × 2° quadrangle, New Mexico and Arizona: U.S. Geological Survey Miscellaneous Field Studies Map MF–1183–H, scale 1:250,000.

———1986c, Geochemical maps showing distribution and abundance of copper in two fractions of stream-sediment concentrates, Silver City 1° × 2° quadrangle, New Mexico and Arizona: U.S. Geological Survey Miscellaneous Field Studies Map MF–1183–B, scale 1:250,000.

———1986d, Geochemical maps showing distribution and abundance of lead in two fractions of stream-sediment concentrates, Silver City 1° × 2° quadrangle, New Mexico and Arizona: U.S. Geological Survey Miscellaneous Field Studies Map MF–1183–A, scale 1:250,000.

———1986e, Geochemical maps showing distribution and abundance of manganese in two fractions of stream-sediment concentrates, Silver City 1° × 2° quadrangle, New Mexico and Arizona: U.S. Geological Survey Miscellaneous Field Studies Map MF–1183–J, scale 1:250,000.

———1986f, Geochemical maps showing distribution and abundance of molybdenum in two fractions of stream-sediment concentrates, Silver City 1° × 2° quadrangle, New Mexico and Arizona: U.S. Geological Survey Miscellaneous Field Studies Map MF–1183–E, scale 1:250,000.

———1986g, Geochemical maps showing distribution and abundance of silver in two fractions of stream-sediment concentrates, Silver City 1° × 2° quadrangle, New Mexico and Arizona: U.S. Geological Survey Miscellaneous Field Studies Map MF–1183–F, scale 1:250,000.

———1986h, Geochemical maps showing distribution and abundance of tin in two fractions of stream-sediment concentrates, Silver City 1° × 2° quadrangle, New Mexico and Arizona: U.S. Geological Survey Miscellaneous Field Studies Map MF–1183–I, scale 1:250,000.

———1986i, Geochemical maps showing distribution and abundance of tungsten in two fractions of stream-sediment concentrates, Silver City 1° × 2° quadrangle, New Mexico and Arizona: U.S. Geological Survey Miscellaneous Field Studies Map MF–1183–G, scale 1:250,000.

———1986j, Geochemical maps showing distribution and abundance of zinc in two fractions of stream-sediment concentrates, Silver City 1° × 2° quadrangle, New Mexico and Arizona: U.S. Geological Survey Miscellaneous Field Studies Map MF–1183–D, scale 1:250,000.

Werschsky, R.S., Detra, D.E., Meier, A.L., and McDougal, C.M., 1983, Analytical and statistical results for stream sediment, panned concentrate, water, and rock samples collected from the Whetstone Roadless Area, Pima and Cochise counties, Arizona: U.S. Geological Survey Open-File Report 83–242, 110 p., 1 pl.

Wrucke, C.T., and Armstrong, A.K., 1984, Geologic map of the Whetstone Roadless Area and vicinity, Cochise and Pima Counties, Arizona: U.S. Geological Survey Miscellaneous Field Studies Map MF–1614–B, scale 1:48,000.

Wrucke, C.T., and Bromfield, C.S., 1961, Reconnaissance geologic map of part of the southern Peloncillo Mountains, Hidalgo County, New Mexico: U.S. Geological Survey Mineral Investigations Field Studies Map MF–160, scale 1:62,500.

Wrucke, C.T., and McColly, R.A., 1984, Whetstone Roadless Area, Arizona, *in* Marsh, S.P., Kropschot, S.J., and Dickinson, R.G., eds., Wilderness mineral potential; assessment of mineral-resource potential in U.S. Forest Service lands studied 1964–1984: U.S. Geological Survey Professional Paper 1300, p. 126–129.

Wrucke, C.T., McColly, R.A., Werschsky, R.S., Scott, D.C., Bankey, V.L., Kleinkopf, M.D., Staatz, M.H., and Armstrong, A.K., 1983, Mineral resource potential map of the Whetstone Roadless Area, Cochise and Pima Counties, Arizona: Miscellaneous Field Studies Map MF–1614–A, scale 1:48,000.

Aeromagnetic, Radiometric, and Gravity Data for Coronado National Forest

By Mark E. Gettings

MINERAL RESOURCE POTENTIAL AND GEOLOGY OF CORONADO NATIONAL FOREST, SOUTHEASTERN ARIZONA AND SOUTHWESTERN NEW MEXICO
Edited by Edward A. du Bray

U.S. GEOLOGICAL SURVEY BULLETIN 2083–D

UNITED STATES GOVERNMENT PRINTING OFFICE, WASHINGTON : 1996

CONTENTS

FIGURES

Aeromagnetic, Radiometric, and Gravity Data for Coronado National Forest

By Mark E. Gettings

ABSTRACT

This chapter presents the results of studies of the gravity, magnetic, and gamma-ray spectrometric anomaly fields of Coronado National Forest and adjacent areas in southeastern Arizona and southwestern New Mexico. Because of the diverse and complex geologic history of the lands included within the Forest, investigations at characteristic scales ranging from hundreds of kilometers to hundreds of meters were necessary in order to define the structures responsible for observed geophysical anomalies. Regional-scale relationships in the part of southeastern Arizona that encompasses the Forest are described first and are followed by presentation of geophysical data and interpretations for each of the individual Forest units. In order to facilitate future evaluations, all data assembled in this evaluation are presented in map form at a uniform scale. Because this work was completed as part of a mineral resource evaluation, the interpretive models presented here are not comprehensive but are instead focused on features of geophysical data that delineate geologic features that are favorable for occurrence of mineralized rock or indicate features that might have inhibited or precluded ore genesis.

INTRODUCTION

The geophysical data used in this study consist of gravity (plates 9–11), terrain-clearance (plates 12–14), aeromagnetic (plates 15–17), and airborne gamma-ray spectrometer (plates 18–26) data. Regional aeromagnetic data from constant-altitude surveys (Sauck and Sumner, 1970) were employed in digital and map forms. Gravity data were compiled from U.S. Defense Mapping Agency, University of Arizona, and U.S. Geological Survey (USGS) sources. Most of the geophysical data used in this assessment were retrieved from archives of the National Uranium Resource Evaluation (NURE) (Texas Instruments Inc., 1979). Reduced single-point data files were retrieved and reprocessed. These files consist of final-survey, point-by-point data for latitude; longitude; terrain clearance; aeromagnetic field value; gamma-ray total count; equivalent uranium, thorium, and potassium; and other data. The sample interval for NURE data is about 15 m between points along flight lines, and a nominal 5-km spacing between flight lines. Most lines are oriented north-south and have east-west tie lines every 50 km. In the New Mexico part of Coronado National Forest, the lines are oriented east-west and have north-south tie lines. The NURE data are strongly biased in the direction of the flight lines and are not suitable for constructing contour maps except to display regional-scale anomalies having half-wavelengths of 10 km or more. In order to show the information to be gained from the data more fully, the data are plotted as profiles along the flight lines projected onto maps at the scale of compilation of the geologic maps. For these plots, a base level was chosen for each area that approximates the average value of the data; base-level values plot on the flight-line location.

In examining spectrometric or aeromagnetic data, terrain-clearance maps (plates 12–14) must be considered to determine whether radiometric or magnetic anomalies have been strongly distorted by large variations in terrain clearance. Data for points having terrain-clearance values less than 100 m or greater than 200 m were deleted; the data profile across such an interval is shown as a straight line between points having acceptable terrain-clearance values. Several intervals of this type are present on the two westernmost, north-south flight lines of plate 17. Gamma-ray emissions depicted by the radiometric profiles are produced by material in the upper few meters of the Earth's crust. The source of magnetic-field signals ranges from material at the surface to that at depths of many kilometers. Variations in terrain clearance of as little as 50 m have much more effect on radiometric signals than on aeromagnetic signals.

Gamma-ray radiometric data "noise" (for example, compare the two central profiles coincident with the Whetstone Mountains, plate 23) can be caused by other than geologic factors, including instrument response time and sensitivity, and by seasonal variations due mostly to soil moisture content. In many cases it is customary to smooth radiometric data to minimize these effects. However, the

same smoothing can be accomplished visually during analysis of the data; presenting data that have not been smoothed, as in this report, allows the quality of the data and the information conveyed to be evaluated without concern for effects of filtering.

Regional gravity data were compiled from U.S. Defense Mapping Agency unclassified data and from University of Arizona and USGS sources. In addition, 779 additional stations were established in the Santa Catalina, Santa Teresa, Pinaleno, Galiuro, and Chiricahua Mountains, and in the Canelo Hills. Data were collected by M. Bultman, M. Gettings, G.S. Pitts, and K. Schwartz. A total of 15,613 stations were compiled within the area between lat 33°15′ N. and the Mexico border and between long 111°30′ W. to long 108°50′ W. These data were corrected for errors, reduced to a common datum (International Gravity Standardization Network 71, International Association of Geodesy, 1971; Morelli and others, 1974), and terrain corrected. Data for stations located in very rugged terrain were adjusted by manually calculated terrain corrections near stations and computer calculated corrections (Plouff, 1977) from the outer radius of the manual corrections to a radius of 167 km. Data for all other stations were adjusted by terrain corrections computed entirely by computer techniques. Standard USGS gravity reduction formulae (Cordell and others, 1982) were used to compute complete Bouguer gravity-anomaly values, which were then used to prepare the gravity-anomaly maps presented in this report. A minimum-curvature gridding algorithm (Briggs, 1974; Webring, 1981) and a computer program (Godson and others, 1988) that generates contour maps were both used in production of the gravity maps.

Previous compilations and interpretations of data covering parts of the Coronado National Forest may be found in Hammarstrom and others (unpub. data, 1988), Ponce (1990), Hummer-Miller and Knepper (1990), Wynn (1981), and Klein (1987), and in references contained therein.

Available drillhole data (Oppenheimer and Sumner, 1980) were used in conjunction with gravity data from near drillholes to estimate the average density contrast between valley fill and bedrock. Data for three holes in the Aravaipa Valley indicate contrasts in the range of –0.3 to –0.4 g/cc; these values have been used to estimate the thicknesses of basin fill for areas discussed elsewhere in this report.

REGIONAL RELATIONSHIPS AND TECTONIC FRAMEWORK

A complete Bouguer gravity-anomaly map for the area of Coronado National Forest and adjacent basins is shown in figure 1. The most obvious pattern on this map is a rectangular system of gravity-anomaly gradients that trend approximately N. 40° W. and N. 45° E. The northwest trends are more penetrative in their character than the northeast trends are. This pattern is disrupted along the western edge of the map north of 32° by the eastern boundary of a large regional gravity high that extends westward from approximately long 111°25′ W. across southern Arizona south of a line approximately from Phoenix to the northwest. This regional anomaly may be the gravity signature of a previously unrecognized accreted terrane. Examination of the state geologic map shows that the boundary reflects outcrop patterns: the amount of bedrock cropping out relative to basin fill is much greater in southeastern Arizona than it is west of the boundary, and the relative amount of Cretaceous and Tertiary granitic intrusive rock is much greater in the southeast. The effect is not due to a more mature terrain to the west or lower average elevation, that is, a filling of the basins at the expense of mountain ranges, because a depth-to-bedrock map (Oppenheimer and Sumner, 1980) shows that deep basin fills are rare west of the boundary, especially in the south-central area centered on Ajo, Ariz. The depth-to-bedrock map suggests that the erosional maturity of the Basin and Range province in southern Arizona is approximately the same throughout the province. Together with the gravity-anomaly map, the depth-to-bedrock map suggests that the extension in southeastern Arizona that caused development of alternating basins and ranges has occurred primarily along a northeast-southwest trend; crustal blocks have extended by tilting of blocks across surprisingly continuous northwest-trending block boundaries. The structures controlling these boundaries may be related to an orogenic belt formed during the Mesozoic accretion of the terrains to the southwest (for example, Coney and Harms, 1984, and Drewes, Chapter B, this volume), or may be due to a pre-existing Proterozoic fabric as suggested by Sumner (1985).

Trends on the gravity-anomaly map are defined mainly from traces of gradient midpoints, but offsets of anomalies, such as an apparently down-dropped part of a relative anomaly maximum, were also used. Figure 1 shows only the major trends. It appears that the northwest trends are more continuous and that northeast trends are less continuous. Northerly and easterly trends are much less common. A circular gravity low (fig. 1) is associated with the Galiuro volcanic center, which is itself extended by northwest-striking normal faults whose gravity-anomaly trends are discernible (fig. 1). Differential extension may have occurred along segments of some of northwest-striking faults (fig. 1); presumably, accommodation occurred by strike slip on northeast-striking faults coincident with northeast trends on the gravity-anomaly map. Northeast of Safford, trend patterns change (fig. 1) and easterly and more northerly trends are much more evident.

Figure 2 shows the regional aeromagnetic field extracted from the digital data set of Sauck and Sumner (1970) for the same area as the gravity-anomaly map (fig. 1). Figure 2 shows strong northwest and northeast trends in the aeromagnetic data similar to those of the gravity-anomaly

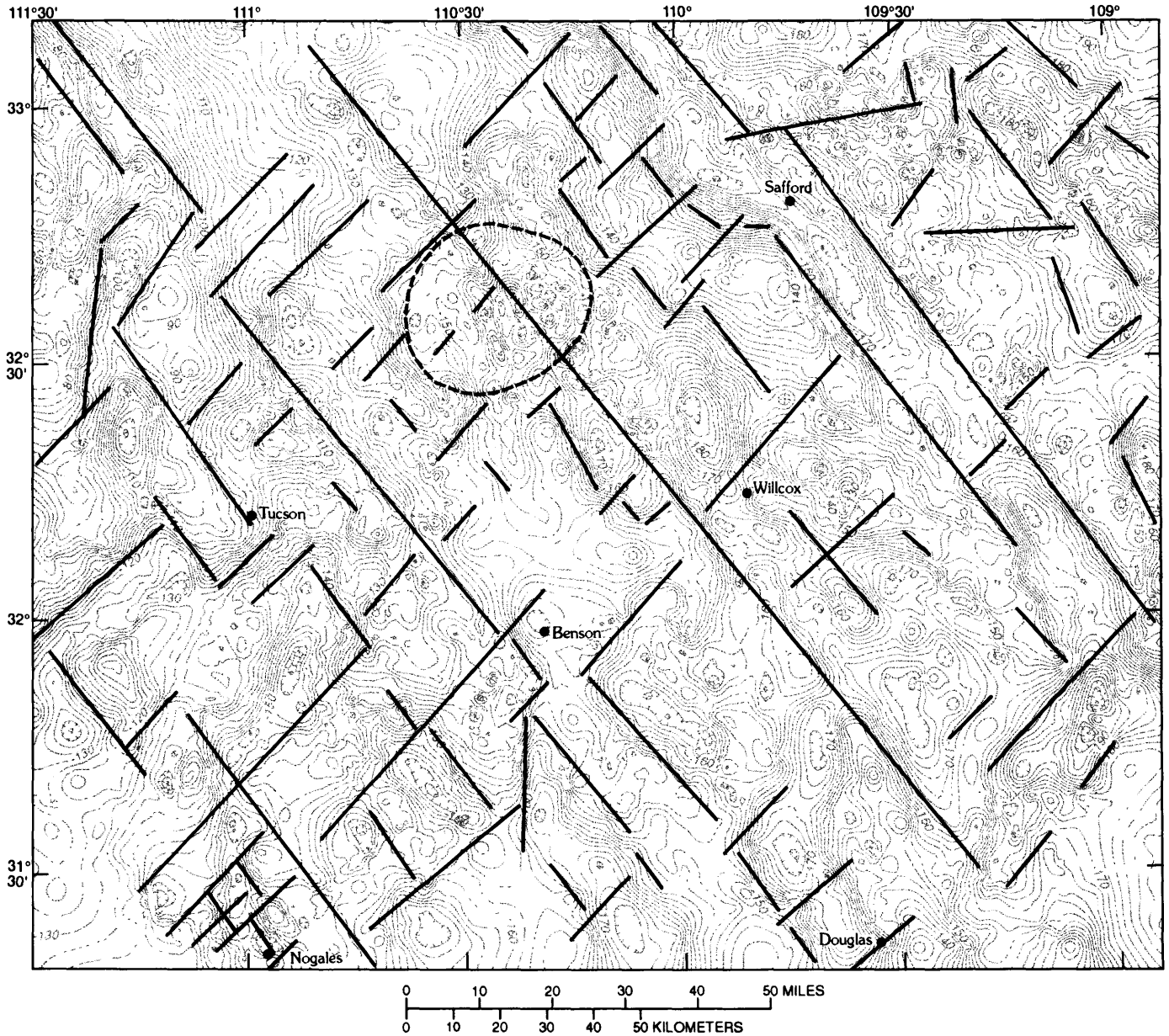

Figure 1. Complete Bouguer-gravity-anomaly map showing major gravity-anomaly trends (heavy black lines) in Coronado National Forest and adjacent areas, southeastern Arizona and southwestern New Mexico. Contour interval 2 mGal; hachured lines are closed gravity lows. Area enclosed by dashed black line is the inferred Galiuro volcanic center.

field, but the trends are not as continuous and easterly trends are more abundant in more places than in the gravity data. The lack of continuity and more numerous trends in the magnetic data are in part due to the dipolar nature and large dynamic range of the magnetic field and the consequent difficulty in distinguishing major from minor trends. In contrast to the gravity trends, the northeasterly magnetic anomaly trends tend to be more continuous than the northwest trends are. This may indicate that the gravity data depict deep, more spatially uniform variations in density, whereas magnetic data indicate shallow, well-defined though variable structures.

The correlation between gravity- and magnetic-anomaly trends is variable. In most cases, gravity-anomaly trends are reflected in magnetic trends either by coincident but less continuous trends, or by terminations of nearby cross trends. Both sets of data suggest differential extension; the greatest amount of extension is along a N. 45° E.-striking belt about 100 km wide centered on Tucson.

Comparison of the aeromagnetic and geologic maps indicates that many troughlike anomaly minima are apparently axes of weakly magnetic Cretaceous-Tertiary intrusions. The minima are not coincident, in most places, with basin fill; their trends cross range, basin, and pediment

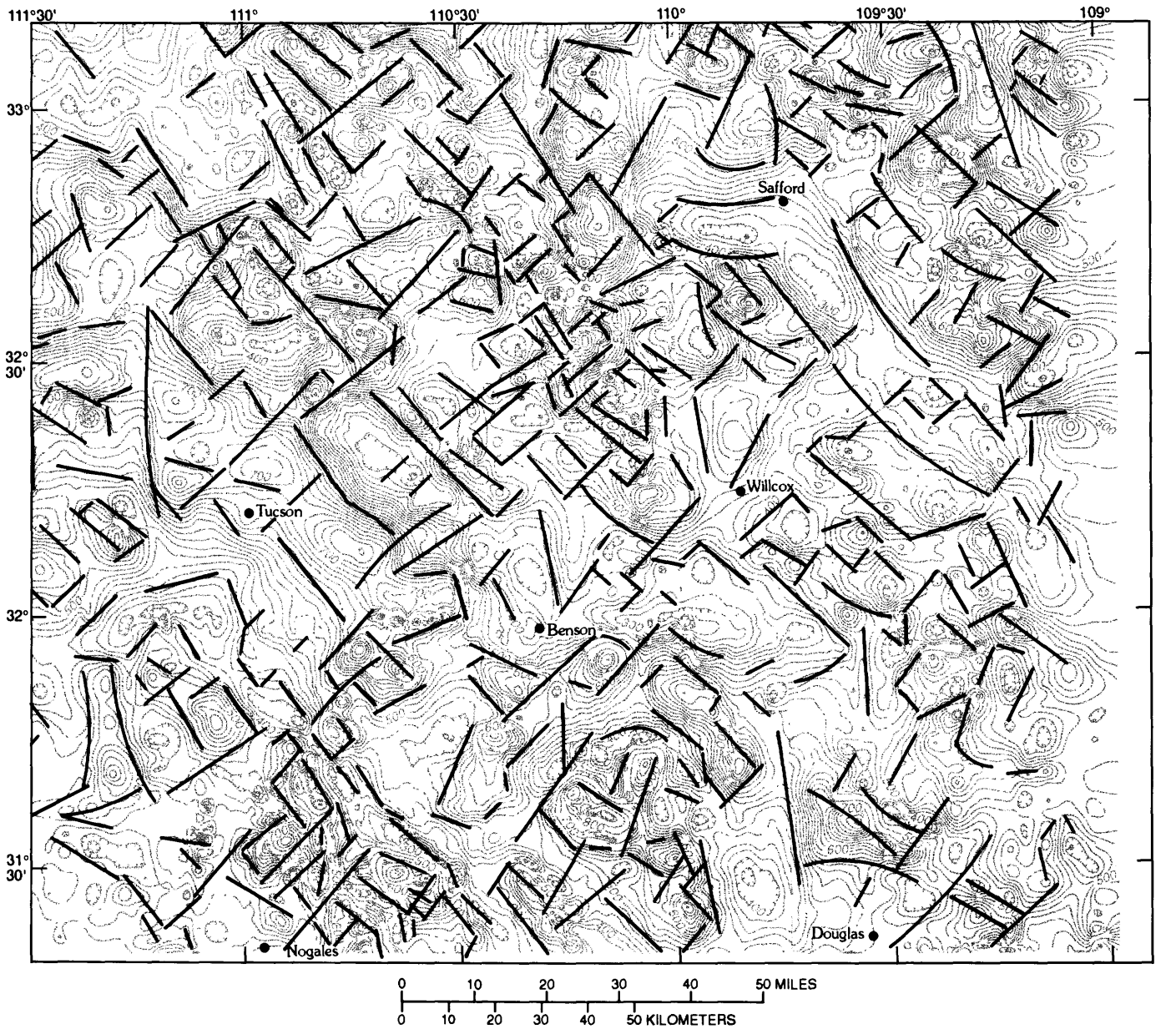

Figure 2. Residual-aeromagnetic-anomaly map showing aeromagnetic anomaly trends (heavy black lines) in southeastern Arizona extracted from Sauck and Sumner (1970). Contour interval 20 nanoteslas; hachured lines are closed magnetic lows.

trends. These intrusions may have originated in response to the latest phases of compressional orogeny or to early phases of extension. If the aeromagnetic minima do, in fact, indicate unexposed areas of intrusive rock, then the amount of intrusive rock present in the shallow subsurface is large relative to the amount of exposed intrusive rock shown on the geologic map.

Similarly, regional aeromagnetic anomaly maxima cross both basins and ranges; the most prominent example is the large, northwest-striking high that is approximately centered on Tucson. Preliminary estimates of depth indicate that the source of this anomaly is within several kilometers or less of the surface in most places. Young volcanic rocks interlayered with sedimentary rocks, identified in a deep borehole drilled in the Tucson Basin (Eberly and Stanley, 1978), have been suggested as a source. However, the extent of young volcanic rocks in the southern Rincon and northern Empire Mountains, an area coincident with the aeromagnetic anomaly, is insufficient to explain the anomaly (fig. 2). In this area, at least part of the anomaly coincides with outcrops of early Tertiary granodiorite, which implies that the source of much of the anomaly may be Cretaceous-Tertiary

intrusive rocks. These considerations are important to the Coronado National Forest mineral resource appraisal because intrusive rocks indicated by aeromagnetic data constitute heat sources that could have had associated mineralizing hydrothermal circulation systems. The recognition that these intrusions appear to be distributed differently in the subsurface than would be predicted by outcrop patterns has influenced us to expand the outlines of favorable tracts within Coronado National Forest in several cases to include the entire area coincident with aeromagnetic anomalies.

Extensional tectonics have played a major role in the geologic evolution of southeastern Arizona. Accordingly, we modeled gravity and magnetic anomalies that would result from a hypothetical, N. 50° E.-striking fault that crosses a pediment, a basin, a range, and another basin, and continues up onto a plateau (fig. 3). Extension can result from either antithetic steeply dipping block faults and accompanying block rotation (that is, the steeply dipping boundaries are faults), or by detachment faulting (the more gently dipping boundaries are faults). Figure 3 shows the magnetic-anomaly profile for a top-to-the-southwest detachment fault, such as is postulated for the Santa Catalina Mountains contrasted with the profile for a top-to-the-north detachment, such as is postulated for the Pinaleno Mountains. The gravity anomaly profile is the same, regardless of the sense of fault offset. Both aeromagnetic and gravity profiles have maxima over bedrock and minima over basin fill, which is assumed to be nonmagnetic and less dense than bedrock.

The model is obviously too crude to explain observed gravity and aeromagnetic anomalies; the northern Tucson Basin and Tucson Mountains are part of major regional gravity- and magnetic-anomaly highs (figs. 1 and 2), whereas the Santa Catalina Mountains are part of a large magnetic low and have a complex gravity field. A large gravity-anomaly high coincides with the Pinaleno Mountains and lows are coincident with the flanking basins, but the magnetic field over both the mountains and basins is a mixture of anomaly highs and lows. On a regional scale, neither aeromagnetic nor gravity anomalies directly correlate with traces of hypothesized large-scale detachment faults; geophysical-anomaly trends cut across both upper and lower fault plates. Lithologic variations both within and between detachment plates seem to cause larger anomalies than do the detachment faults themselves. The lack of a good correlation between geophysical anomalies and detachment faults in southeastern Arizona is problematic, especially considering that anomalies predicted by the model (fig. 3) are similar in magnitude to those associated with detachment faults in eastern California and western Arizona. This could be a consequence of the magnitude of detachment in southeastern Arizona being much less than the tens of kilometers of displacement suggested for detachment faults in western Arizona and eastern California.

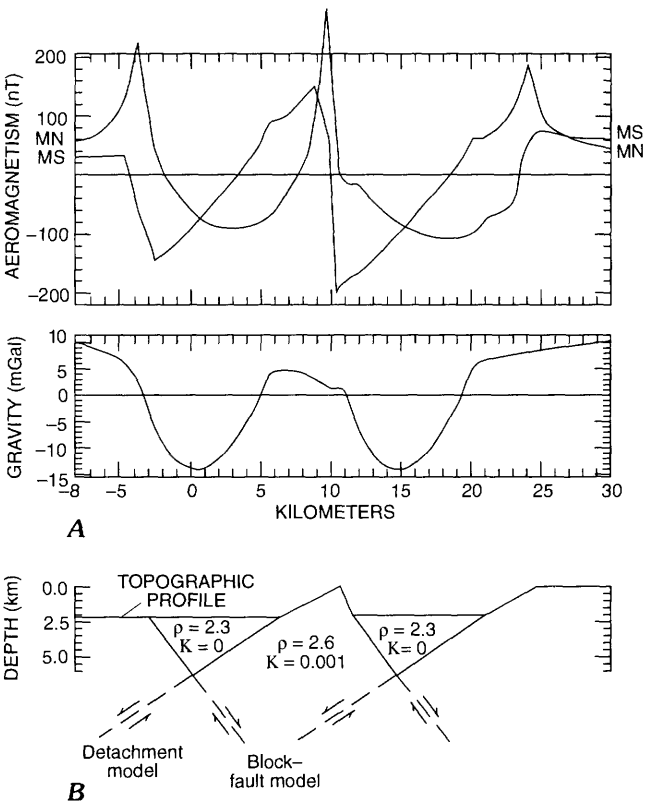

Figure 3. Hypothetical normal-fault or detachment-fault model for extension, showing modeled gravity and aeromagnetic responses. *A*, aeromagnetic (top) and gravity (bottom) profiles calculated for the model. *B*, Hypothetical cross section showing the density (ρ) and magnetic-susceptibility contrast (K) of blocks that compose the model. MN and MS refer to magnetic north and south, respectively.

GEOPHYSICS OF CORONADO NATIONAL FOREST UNITS

SANTA TERESA MOUNTAINS

Gravity data coverage for areas within the Santa Teresa Mountains varies from moderate to sparse; most observations were made near main roads (pl. 9). Although poorly defined because of wide station spacing, anomaly A (a single-station anomaly, pl. 9) may indicate an apophysis of Tertiary granite beneath the pre-Tertiary section; as such, it constitutes an exploration target if verified by additional observations. In areas for which an adequate number of gravity measurements have been made, the gravity-anomaly field over the Santa Teresa Granite and its host rocks appears very similar to that in the Santa Catalina Mountains, where a narrow gravity low is coincident with the youngest granite in the complex and relative gravity highs coincide with older rocks (fig. 1, pl. 9). The analogy to the Santa Catalina–Rincon core complex can be extended in that the approximately north-striking

gravity-anomaly high (B, pl. 9) is identical in its geologic setting to the gravity-anomaly high coincident with Tucson. In both cases, the high is coincident with all mapped segments of a detachment fault. Accordingly, geophysical evidence suggests that a detachment fault crosses the south end of the Santa Teresa Mountains at Eagle Pass and is offset to the left (southeast), perhaps along the Stockton Pass fault (a high-angle strike-slip fault having a history of multiple slip; Swan, 1976) to Kane Spring Mountain south of Mount Graham. If so, the Stockton fault is young (detachment age) and therefore was not available, unless it has been reactivated, as a conduit for mineralizing fluids associated with early and middle Tertiary mineralizing events. Alternatively, the gravity high coincident with the Santa Teresa Mountains may continue southward, across the Aravaipa Valley (C, pl. 9). In this case, the Stockton fault may have been active during early and middle Tertiary time; the potential occurrence of mineralized rock along the fault is enhanced accordingly. At present, these alternatives cannot be distinguished.

Three principal aeromagnetic anomalies are associated with rocks of the Santa Teresa Mountains. Anomaly A (pl. 15) has two parts, a more intense southern peak, which coincides with Proterozoic rocks, and a second, smaller northern peak, which is apparently related to the Goodwin Canyon fault and possibly to mineralized rock. Anomaly B (pl. 15) is not obviously related to the rocks with which it coincides, but small outcrops of Proterozoic diabase are present nearby and similar diabase is associated with positive anomalies in the Stockton Pass area (30 km south-southeast of Safford). Anomaly C (pl. 15) defines the edge between Tertiary volcanic rocks and basin fill at Eagle Pass. The central, straight line segment of anomaly C is due to a lack of data; the sensor was too close to the ground (pl. 12).

Uranium abundances in the Santa Teresa Mountains, as indicated by the radiometric survey, are relatively homogeneous; Early and Middle Proterozoic metamorphic gneiss (map unit YXm; pl. 2) contains less uranium than the Middle Proterozoic and younger granitic plutonic rocks do. These data may be useful in delineating large-scale plutonic granite and gneissic phases, but only the high-amplitude anomalies have been examined in this analysis. Paleozoic sedimentary rocks exposed on the west flank of the Santa Teresa Mountains are the least radiogenic rocks in this Forest unit; Cretaceous rocks exposed there (D, pl. 18) are slightly more radiogenic.

Thorium abundances in the Santa Teresa Mountains (pl. 21) seem to be much more variable than those of uranium (pl. 18). Cretaceous rhyolite (A, pl. 21) clearly contains anomalous thorium abundances, while thorium abundances in Tertiary granite (B, pl. 21) are elevated but highly variable. The anomaly high (C, pl. 21) is very important because it is centered on a fault that cuts Tertiary granite; the fault could have served as a conduit for circulating hydrothermal solutions and may be the locus of mineralized rock. The Pinal Schist is coincident with a radiometric-thorium low (D, pl. 21), whereas most outcrops of Middle Proterozoic granite (map unit Yg) are coincident with moderate, but highly variable, thorium abundances (E, pl. 21).

NURE radiometric data indicate that Cretaceous rhyolite on the west side of the Santa Teresa Mountains is highly potassic (A, pl. 24); all of the granitic plutonic rocks and metamorphic gneiss have base-level potassium abundances. The Pinal Schist (B, pl. 24) is potassium poor, whereas Tertiary rhyolite is associated with a strong positive radiometric-potassium anomaly (C, pl. 24). Anomaly C is noteworthy and requires field examination because the potassium anomaly there is larger than that associated with possibly correlative rocks across the Aravaipa Valley in the Galiuro Mountains (Creasey and others, 1981).

GALIURO MOUNTAINS

Gravity (pl. 9) and magnetic data (pl. 15, fig. 4) for the Galiuro Mountains are contained in reports by Schwartz (1990) and Creasey and others (1981). The most striking gravity feature in the Galiuro Mountains is the approximately circular regional gravity low that surrounds all near-vent facies of volcanic rocks (G, pl. 9). The Galiuro volcanic field has apparently been tectonically extended by displacements along a set of northeast-striking normal faults (F, pl. 9) that includes the western range front fault, the central Galiuro fault, and several smaller faults. Measured fault dips and exposed stratigraphic thicknesses indicate at least 5 km of extension. The faults are reflected in a dipole-like pattern of relative gravity highs and lows in the hanging wall and footwall, respectively, of each fault block. The highs are coincident with andesite and the lows with rhyolite; the same andesite-rhyolite stratigraphic sequence is repeated across each fault. Gravity trends (F, pl. 9) north of boundary G are collinear with their extensions to the south, and the central Galiuro fault cuts across boundary G; consequently, extension was more recent than the development of circular gravity low G.

The aeromagnetic responses of rhyolite and andesite in the Galiuro Mountains, as depicted by NURE data, are typical of responses observed for these rock types elsewhere in the Forest. Andesite coincides with anomalies of approximately 400 nanoteslas (nT), whereas those that coincide with rhyolite are much smaller in most cases. Most of the apparent, large-amplitude anomalies associated with rhyolite may, in fact, be attributable to andesite that is hypothesized to be present at a shallow depth beneath rhyolite. Intrusive rocks (unit Tri) are also associated with anomaly highs in many places. The fault block east of Sombrero Butte, which includes Proterozoic, Paleozoic, Cretaceous, and Tertiary rocks, is strongly magnetic (F, pl. 15). Young, extremely magnetic (pl. 15) Tertiary basalt extends into the southeastern part of the Galiuro Mountains but does not seem to extend into circular gravity low G (pls. 9 and 15). These

rocks produce some strong negative and positive anomalies, which suggests that some of the basalt may be reversely polarized. The source of anomaly J (pl. 15) is unknown, but it may be related to anomalies J1 (pl. 15). The character of anomaly J appears to be different from that associated with basalt, but a source having basaltic composition is not precluded. Anomaly gradients for J and J1 suggest that the top of the source is about 400 m below the surface. Thus, if the source is of basaltic composition, it is probably composed of gabbro or diorite. Anomaly K (pl. 15) does not have an obvious source either. The steep gradient on the south side of the anomaly suggests a shallow source; the source may be exposed in the walls or floor of Redfield Canyon.

Areas underlain by rhyolite in the Galiuro Mountains produce a radiometric-uranium response (pl. 18) of about 50–100 counts per second (CPS), whereas andesite, basalt, and older rocks east of Sombrero Butte produce 10–30 CPS. All radiometric-uranium anomalies correlate with map units. Radiometric uranium responses are highly variable between flight lines because of instrumental variations. Some anomalies could be masked along lines that have low variability in apparent response.

Most areas underlain by rhyolite produce a radiometric thorium response of about 75–150 CPS (L, pl. 21), whereas areas underlain by andesite and basin fill yield responses of 30–50 CPS (K, pl. 21) and 50–100 CPS, respectively. Pre-Tertiary rocks and Cretaceous and Tertiary intrusions in the Copper Creek area east of Sombrero Butte (M, pl. 21) are less radiogenic than the andesite.

The radiometric-potassium map for the Galiuro Mountains area (pl. 24) is similar to that for thorium. Areas underlain by rhyolite produce a radiometric-potassium response of about 300 CPS. Areas underlain by andesite and the Copper Creek area produce 200 CPS responses, though the latter yields more variable responses (G, pl. 24). The north end of the Copper Creek Granodiorite (G1, pl. 24) is associated with a major high; rock in this area may be enriched in potassium. Two large highs (H, pl. 24), whose sources are unknown, are located north of the mouth of Keilberg Canyon and about 3 km north of Cherry Spring Peak. Numerous prospects are present in both of these areas; the anomalies coincide with altered and mineralized rock.

WINCHESTER MOUNTAINS

Gravity and magnetic data for the Winchester Mountains Forest unit are contained in Martin (1986) and U.S. Geological Survey (1982). In the Winchester Mountains, a prominent gravity high (H, pl. 9) is associated with a basement high composed of Proterozoic and Paleozoic rocks; the gravity high north of anomaly I (pl. 9) may indicate an extension of the basement high. However, a strong east-west trend (J, pl. 9) could reflect a major structural boundary; the high north of anomaly I is probably an extension of the same source as that producing anomaly C (pl. 9). The intervening low (I, pl. 9) coincides with rhyolite and may indicate a locally thicker body of rhyolite, as might be present in a vent area. Areas east of I (pl. 9) that are underlain by basalt (Keith and others, 1982) are approximately correlative with a low-amplitude gravity-anomaly high.

NURE aeromagnetic data for areas underlain by rhyolite and andesite in the Winchester Mountains are similar to those for the Galiuro Mountains. Young Tertiary basalt in the northwestern part of the Winchester Mountains is extremely magnetic (pl. 15). These rocks exhibit some very strong negative and positive anomalies, which indicate that some of the basalts may be reversely polarized. The east-west structural trend identified in the gravity-anomaly field (J, pl. 9) is also present in aeromagnetic data (H, pl. 15). East-west-striking anomaly I (pl. 15) beneath the basement uplift discussed above suggest that the uplift may be underlain by young intrusive rock similar to that in the Whetstone Mountains as described below.

Aeromagnetic maps (fig. 5) from the wilderness study of the Winchester Mountains (U.S. Geological Survey, 1982; Martin, 1986) also indicate that positive anomalies strongly correlate with areas underlain by basalt and that areas underlain by rhyolite are associated with lows. Anomaly highs along the east edge of the Winchester Mountains suggest several buried mafic intrusions.

Radiometric uranium (pl. 18), thorium (pl. 21), and potassium (pl. 24) response levels for areas underlain by various types of rock are similar to those observed in the Galiuro Mountains. Uranium anomalies correlate well with map units. Relative thorium abundances indicated by the radiometric survey in areas labeled I (pl. 21) are unusually low for an area underlain by rhyolite, whereas those for area J are very high for an area underlain by andesite. The radiometric potassium response for areas underlain by rhyolite is about 300 CPS, except along the easternmost flight line across the Winchester Mountains; anomalies labeled F (pl. 21) indicate an area underlain by rhyolite for which the radiometric response exceeds 400 CPS. These rocks are either very potassic rhyolite or they have been potassium metasomatized. An anomaly low on the easternmost line crossing the Winchester Mountains and the one adjacent to the west (E, pl. 24) suggests, as do radiometric thorium data, that rhyolite at E is capped by unmapped basalt.

PINALENO MOUNTAINS

Gravity data coverage for areas within the Pinaleno Mountains varies from moderate to sparse; most observations were made on or near main roads (pl. 9). The source of local gravity-anomaly high D (pl. 9) is unknown, but the anomaly implies that depth to bedrock beyond the range front (to the southwest) in this part of the Forest is small. Gravity high E is not centered on the highest topography of

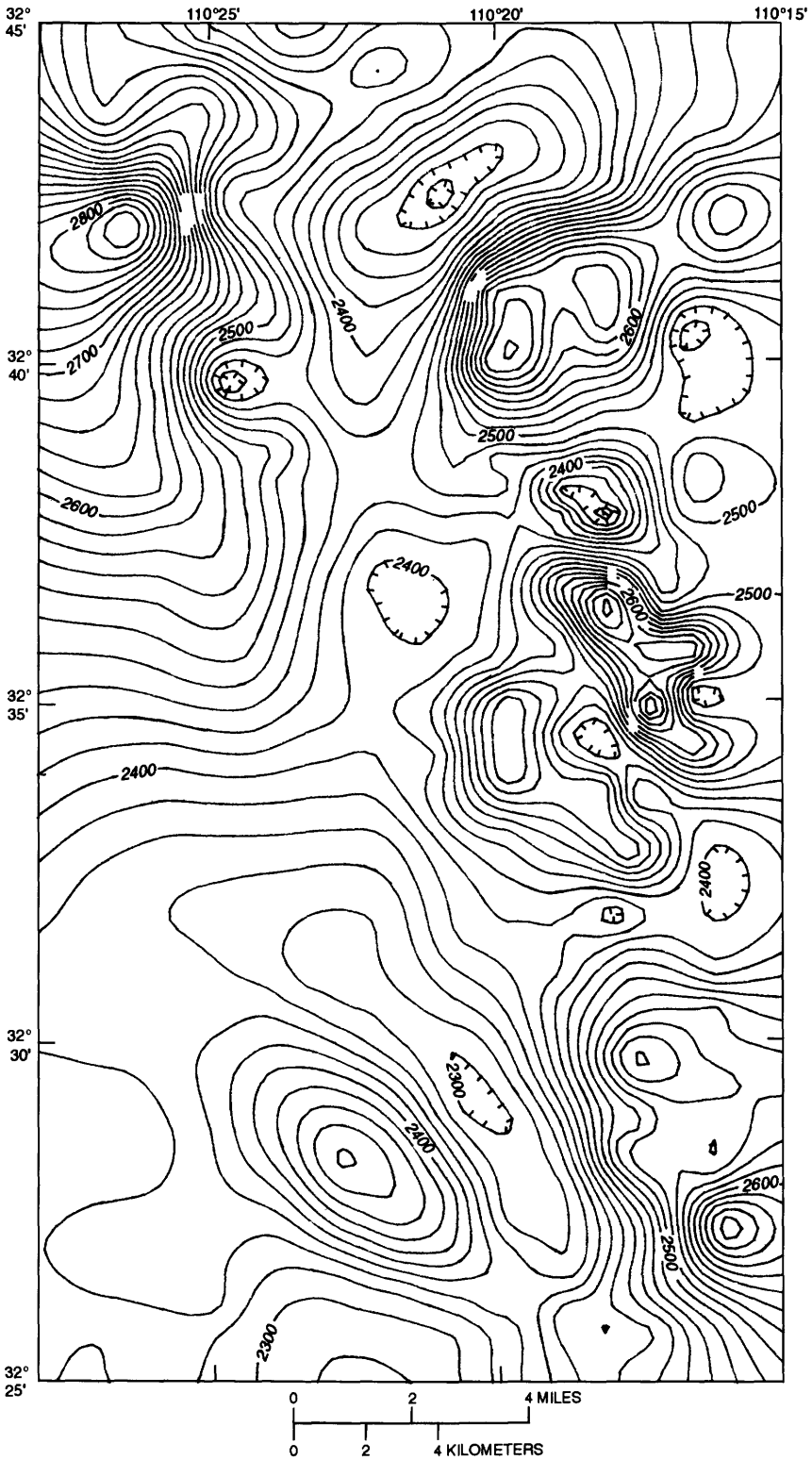

Figure 4. Aeromagnetic-anomaly map of the Galiuro Mountains Wilderness Study Area, southeastern Arizona (U.S. Geological Survey, 1982). Contour interval 20 nanoteslas; hachured lines are closed magnetic lows.

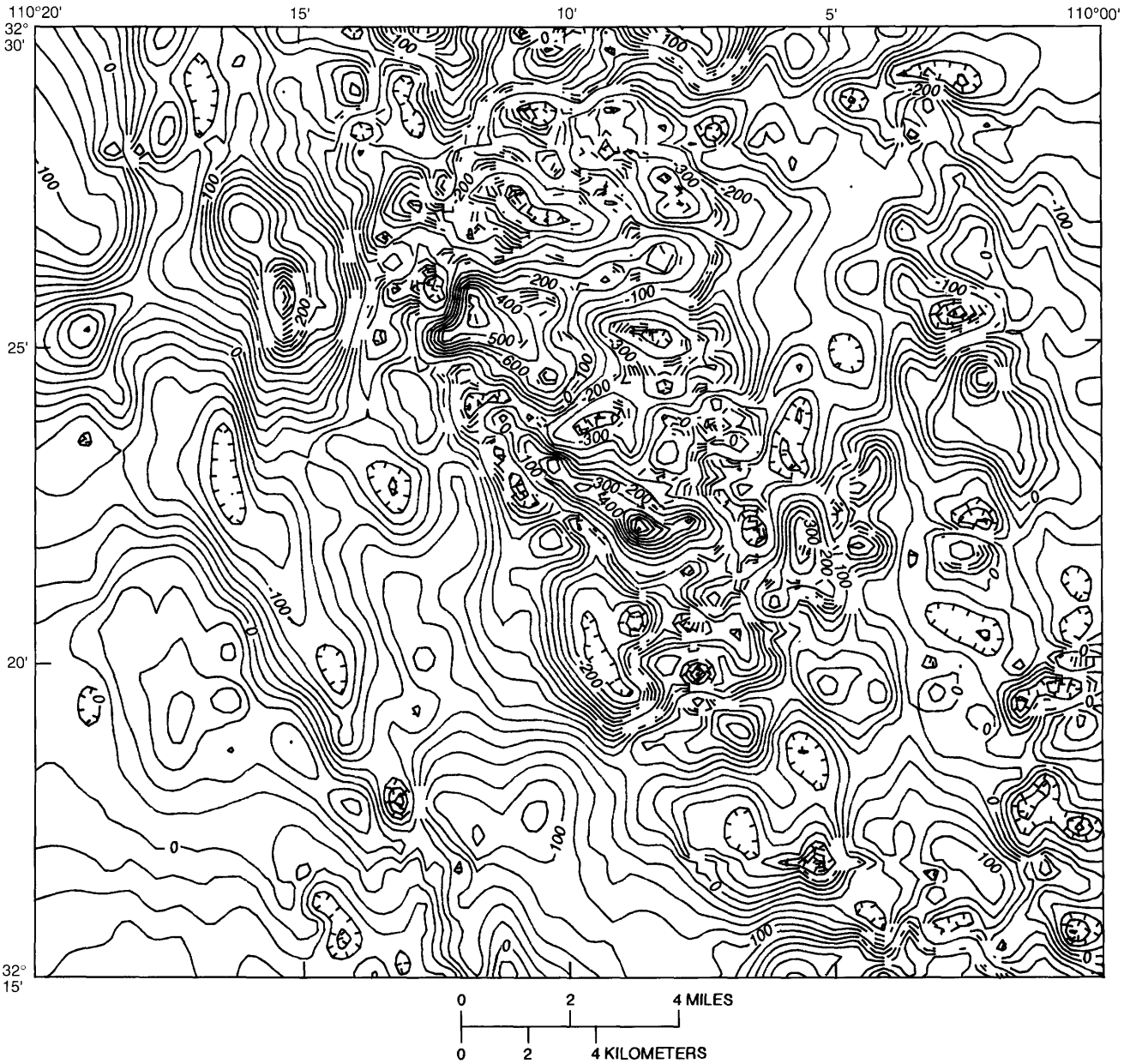

Figure 5. Aeromagnetic-anomaly map of the Winchester Mountains Wilderness-Study Area, southeastern Arizona (U.S. Geological Survey, 1982). Contour interval 20 nanoteslas; hachured lines are closed magnetic lows.

the Pinaleno Mountains, but the westward extension of the anomaly includes the high peaks. The high is centered instead over the eastern side of the range and correlates closely with the Middle Proterozoic granitic unit (Yg, pl. 2). The implication that granitic rock causes the high is probably incorrect, however, since similar rocks 8 km to the west (approximately north of Stockton Pass) coincide with a local gravity low. As is the case on the south side of the Santa Catalina Mountains, the gravity high coincides with forerange rocks, which are all granitic.

Aeromagnetic anomalies labeled D (pl. 15) are caused by unknown, shallow sources and may indicate mafic zones in the Proterozoic rocks. Some of the anomalies labeled D are due to low terrain clearance (pl. 12). The shapes and relative amplitudes of anomalies coincident with Tertiary volcanic rocks (E, pl. 15) suggest that these rocks are reversely polarized. The characteristic texture of profiles coincident with the Pinaleno Mountains east of long 110° is much smoother than to the west and in the area of the Santa Teresa Mountains. Consequently, the average magnetic character of rocks east of about long 110° may be different from that of rocks to the west.

The radiometric uranium response coincident with the Pinaleno Mountains is relatively monotonous and similar to that described above for the Santa Teresa Mountains. The southern of two anomalies labeled A (pl. 18) coincides with

Tertiary rhyolite tuff and the northern one coincides with Proterozoic granite. Both are extensive anomalies and imply large expanses of relatively radiogenic rock. Anomaly B (pl. 18) also coincides with exposures of rhyolite tuff, which indicates that the radiogenic unit is in the uppermost part of the sequence because the tuffs dip to the southwest. A strong uranium anomaly (C, pl. 18) coincides with fill in a dry wash and a small outcrop of Proterozoic granite. The source of the anomaly is probably alluvial material that has been transported down the wash because the granite is not anomalous elsewhere.

The radiometric thorium response (pl. 21) for the Pinaleno Mountains is considerably more variable than that for uranium. In the southeastern Pinaleno Mountains, unit Yg is associated with abrupt and very large thorium anomalies (F, pl. 21). The response that coincides with the upper part of Tertiary rhyolite tuff south of Stockton Pass (H, pl. 21) is anomalous, as is the uranium response. Metamorphic gneiss in the central Pinaleno Mountains is characterized by a fairly uniform thorium response at about base level (pl. 21). The radiometric thorium response of Tertiary granite (G, pl. 21) is high in most places, but highly variable.

Strong positive potassium radiometric anomalies coincide with the top of the rhyolite tuff south of the Stockton Pass area (D, pl. 24); uranium and thorium responses are also anomalous in this area, as discussed above.

PELONCILLO MOUNTAINS

Gravity data coverage for areas within the Peloncillo Mountains (pl. 10) is extremely sparse. The only conclusion that can be drawn is that bedrock in area F (pl. 10) is shallow.

NURE magnetic data (pl. 16) depict typical responses for rhyolite flows and tuffs. Boundary G (pl. 16) encircles an area of rhyolite that coincides with a low magnetic response; some rock in this area may be reversely polarized. Sources for the large positive anomalies H and I are unknown; they may indicate mafic rock at depth beneath volcanic cover.

Radiometric-uranium responses in the Peloncillo Mountains (pl. 19) are similar to those for rhyolite in the Chiricahua Mountains described below. The western boundary of the rhyolite corresponds with positive anomalies marked C (pl. 19), which, in turn, approximately correspond to boundary G defined on the aeromagnetic map (pl. 16). A similar relationship is shown on the radiometric-thorium-response map (D, pl. 22), which effectively discriminates rhyolite flows (unit Tr) from rhyolite tuff (unit Trt). The response of unit Tr in the Peloncillo Mountains (D, pl. 22) is similar to that of unit Trt south of Portal in the Chiricahua Mountains (C, pl. 22). Radiometric-potassium response (pl. 25) also discriminates between rhyolite flows and tuffs (units Tr and Trt) (D, pl. 25), although not as effectively; in addition, the potassium response for unit Tr in the Peloncillo Mountains is not obviously similar to that of unit Trt in the Chiricahua Mountains.

CHIRICAHUA AND PEDREGOSA MOUNTAINS

Geophysical data for the Chiricahua and Pedregosa Mountains are limited. The North End Roadless Area study (Moss and Abrams, 1985) provides good gravity and magnetic coverage from Chiricahua National Monument northward. South of the Monument, gravity stations are sparsely distributed and they are mostly restricted to basins, valleys, and pediments at the edges of the range. In this same area, the only low-level aeromagnetic and radiometric data available are those from NURE surveys.

The gravity-anomaly map (pl. 10) for the Chiricahua and Pedregosa Mountains is controlled by a sufficient number of stations to reasonably suggest that a gravity-anomaly minimum is associated with the Turkey Creek caldera of du Bray and Pallister (1991). A 12-mGal decrease in gravity coincides with the change from Bisbee Group rocks, outside the caldera to the north and south, to intracaldera rhyolite tuff (approximately along line A, pl. 10). Dacite porphyry that intrudes intracaldera tuff (du Bray and Pallister, 1991), yields a positive anomaly of about 4 mGal relative to tuff. Modeling the caldera as a vertical cylinder filled by tuff that was intruded by a smaller cylinder of dacite indicates that the tuff is at least 1.5 km thick (assuming a –0.2 g/cc density contrast with Bisbee Group rocks), and the dacite porphyry is at least 500 m thick (assuming a 0.2 g/cc density contrast with the tuff). Together, these estimates suggest that collapse of the Turkey Creek caldera resulted in 2 km of subsidence. The estimated thickness of the tuff agrees well with the results of Senterfit and Klein (1992), and Klein (Chapter E, this volume), who studied caldera structures using audio-magnetotelluric data; the thickness of the dacite porphyry was not estimated.

Gravity data do not indicate a large offset along the rangefront west of the Turkey Creek area. A 4-mGal low extends from the mouth of Turkey Creek for 15 km to the south and implies that bedrock is probably shallowly covered in this area and, by inference, that the caldera wall is just west of the westernmost outcrops.

In the northern Chiricahua Mountains, anomaly highs labeled B (pl. 10) correspond to Mesozoic and older sedimentary rocks, whereas lows labeled C correspond to Tertiary rhyolite and andesite. The north and south strands of the Apache Pass fault zone define boundaries of anomaly B reasonably well, but gravity and magnetic anomalies (Moss and Abrams, 1985) indicate that the southern strand probably has an unexposed substrand to the south. Both Tertiary and Proterozoic granitic rocks produce anomaly lows in this region. Strong geophysical signatures confirm that the Apache Pass fault zone is a major structure in this area. Tertiary intrusions in or near the fault zone in association with favorable

Paleozoic host rocks between the fault strands indicate an environment geologically favorable for the presence of undiscovered polymetallic vein and replacement deposits.

The east and southeast sides of the Chiricahua Mountains appear to be fault bounded as evidenced by steep gravity-anomaly gradients and by estimates of depth to bedrock, which increase rapidly toward the basin. Estimates of basin-fill thickness for density contrasts of 0.4 and 0.3 g/cc at anomaly D (pl. 10) are 700 and 1,000 m, respectively, and 650 and 900 m, respectively, at anomaly E (pl. 10). Thus, the amount of shallowly covered pediment on the east and south edges of the range is probably small.

Northwest and northeast structural grains and prominent anomaly highs are apparent in both the aeromagnetic map of the North End Roadless Area (fig. 6) and the NURE aeromagnetic field data (anomalies labeled D, pl. 16). Moss and Abrams (1985) attributed highs to intrusions related to Tertiary volcanic rocks. The potential for mineralized rock along major strands of the Apache Pass fault zone (fig. 6) is enhanced by nearby fault-hosted intrusions that were potential sources of circulating hydrothermal fluids and favorable host rocks; these characteristics indicate an environment geologically favorable for the presence of undiscovered polymetallic vein and replacement deposits. Another boundary, marked by the steep gradient labeled A on figure 6, is apparently a major structure, perhaps a fault, beneath Tertiary volcanic rocks of the Monument area; the magnetic field decreases by about 200 nT crossing the boundary to the southwest. Although part of this boundary correlates with a mapped fault, geologic evidence indicates that throw on the fault is small and not sufficient to cause the magnetic anomaly. Presumably, as suggested by Moss and Abrams (1985), the exposed fault reflects a reactivation of an old, major structure at depth.

Dacite porphyry within the Turkey Creek caldera, inferred by du Bray and Pallister (1991) to be a laccolithic intrusion, is relatively magnetic and is clearly manifested on aeromagnetic profiles (A, pl. 16) as a positive anomaly on the south and a small negative anomaly on the north. Noise between these two anomalies corresponds to areas covered by alluvium. The reason for the very large amplitudes at A1 and A2 are unknown, but they may indicate dacite porphyry feeder zones. The source of large anomalies labeled B (pl. 16) coincident with rhyolite tuff and flows is also unknown; these anomalies may indicate the northern ring-dike phase of the porphyry concealed by young rhyolite flows. The change in magnetic character labeled C coincides with the northern part of the caldera topographic margin, whereas a similar boundary on the south (C1) is not as well defined. Boundary C1 also coincides with the caldera topographic margin, but this feature is geologically more complex here than in the north. Anomaly E has a gentle southern gradient, which suggests that the causative source dips southward; the source is almost certainly the Tertiary intrusive rock to the west coincident with a magnetic anomaly high (fig. 6, extreme southeastern part of map).

Anomalies labeled F (pl. 16) have peculiar shapes characterized by intense negative anomalies north of positive anomalies. If these positive-negative pairs are a dipole effect, then the source is probably reversely polarized. However, these anomalies also mark the approximate southeast terminus of a large regional, northwest-striking anomaly that extends sinuously from about 50 km northwest of Tucson to the junction of the Swisshelm and Chiricahua Mountains. As such, the area at anomaly F may provide data needed to unravel the nature of this major geophysical feature. However, the area requires further study on a large scale with regard to its mineral resource potential and its bearing on interpretation of regional structure. East and south of area F, Quaternary basalt is the source of most of the observed short-wavelength anomalies.

With regard to radiometric-uranium response, the most anomalous rock type in the Chiricahua-Pedregosa Forest unit is the Middle Proterozoic granitic intrusion at its north end (A, pl. 19). Rhyolite Canyon Tuff in Chiricahua National Monument produces a fairly uniform positive anomaly (B, pl. 19). Elsewhere, the unit produces a positive, though more variable anomaly. The radiometric-uranium response of dacite porphyry in the Turkey Creek caldera is variable; in most places it yields positive anomalies having amplitudes somewhat less than that of the Rhyolite Canyon Tuff. Rhyolite flows on the north side of the caldera produce a response similar to that of the Rhyolite Canyon Tuff. The radiometric-uranium response of rhyolite south of Portal is not distinct from that in the Turkey Creek area. Most of the pre-Tertiary rocks yield low radiometric-uranium responses, whereas that for Quaternary gravel deposits are consistently high. The response of Quaternary basalt in the southern part of the area is consistently low and homogeneous.

The radiometric-thorium response (pl. 22) in the Chiricahua-Pedregosa Forest unit is similar in most places to that of uranium. The Middle Proterozoic granite is strongly anomalous in thorium (A, pl. 22) and the rhyolite of the Turkey Creek caldera is moderately responsive. A very strong anomaly coincides with alluvium in Tex Canyon (B, pl. 22), but the source in the upper reaches of the canyon does not appear to have been crossed by a flight line. Large thorium anomalies coincide with rhyolite tuff south of Portal, which suggests a composition distinct from those of the Turkey Creek area (C, pl. 22). Pre-Tertiary rocks yield low, but variable responses, whereas Quaternary basalt yields a low, homogeneous response.

The Middle Proterozoic intrusive rock in the northern Chiricahua Mountains is also characterized by an anomalous radiometric-potassium response (A, pl. 25). Dacite porphyry in the Turkey Creek area and that south of Portal yield higher radiometric-potassium responses than do associated tuffs. Some rhyolite flows, particularly those southwest of Portal, are associated with high potassium anomalies. Pre-Tertiary

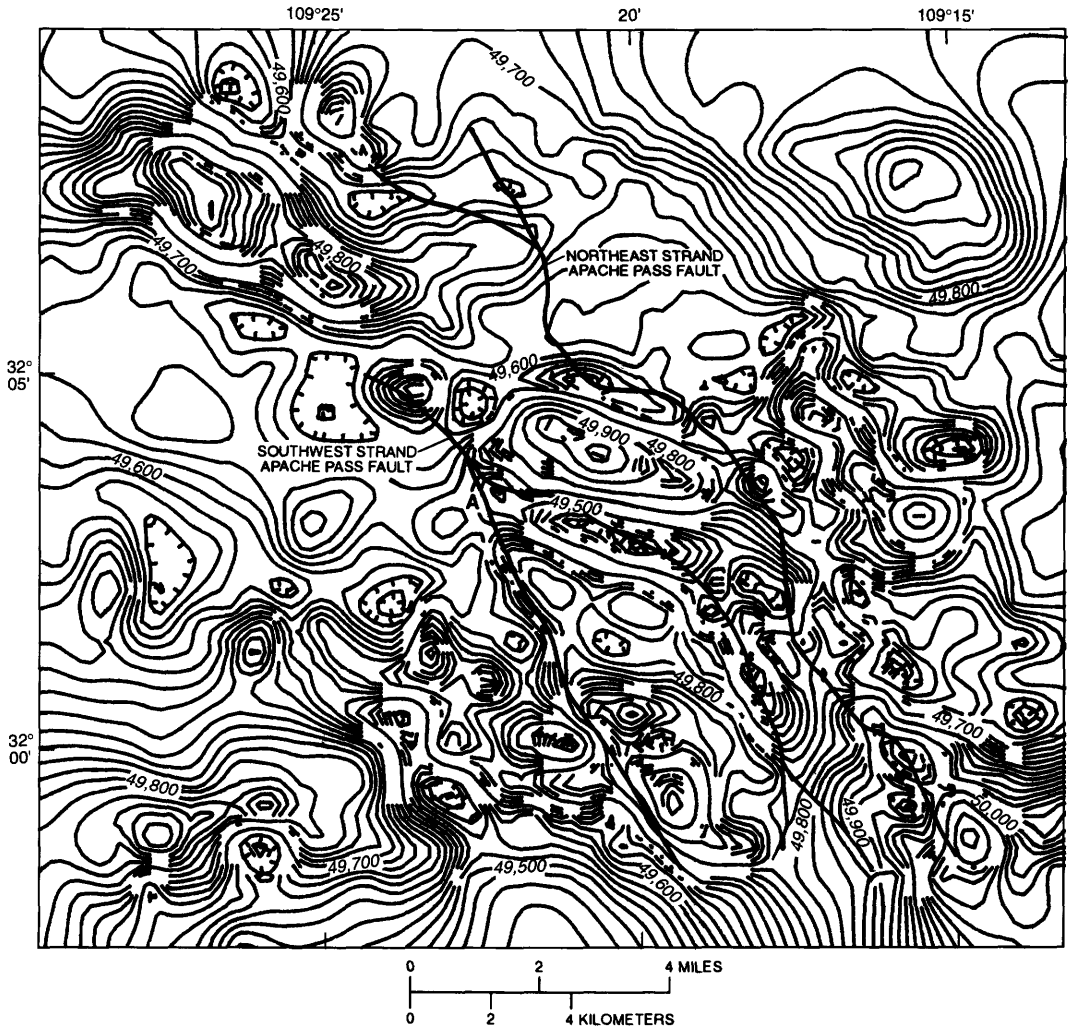

Figure 6. Aeromagnetic-anomaly map of the North End Roadless Area, northern Chiricahua Mountains, southeastern Arizona. Contour interval 20 nanoteslas; hachured lines are closed magnetic lows.

units and Quaternary basalt have uniformly low potassium responses. Gravel in Tex Canyon coincides with a strong anomaly (C, pl. 25), and, once again, no source in the upper reaches of the canyon is obvious; rhyolite flows and tuff to the east are likely source rocks.

DRAGOON MOUNTAINS

Thorough gravity and magnetic field anomaly studies of the Dragoon Mountains roadless area were conducted by Klein (1983); remarks presented here supplement that work. In addition to areas of known mineralized rock, Klein concluded that the area beneath alluvial deposits at the mouth of Stronghold Canyon West, near the inferred western contact of the Stronghold stock, and the area at the southeast edge of the Stronghold stock, east of the mouth of Grapevine Canyon, require further examination for mineralized rock.

Persistent northwest gravity trends and crosscutting northeast-trending gravity-gradient trends represent the predominant structural directions in the Dragoon Mountains and surrounding areas (pl. 10). The Dragoon Mountains block appears to have an abrupt northwest-striking termination along the southwest edge except in the southeast corner of the map. The bounding gravity anomaly gradient is displaced basinward from the bedrock-alluvium contact, which suggests that a significant area of shallowly buried pediment may be present within the Forest. Calculations indicate that basin fill is probably between 600 m (density contrast of 0.4 g/cc) and 800 m (density contrast of 0.3 g/cc) deep at point A (pl. 10); a large area covered by 100 m or less alluvium may be present in the southwestern part of the Forest unit.

The Stronghold stock does not have a strong gravity signature; in fact, the west lobe coincides with a ridgelike gravity maximum (B, pl. 10), whereas the east lobe coincides with a gravity minimum. Close inspection of gravity and aeromagnetic anomaly fields (pl. 10, fig. 7) relative to geology indicates that the Stronghold stock superposes a gravity minimum on the rest of the anomaly field. The overall

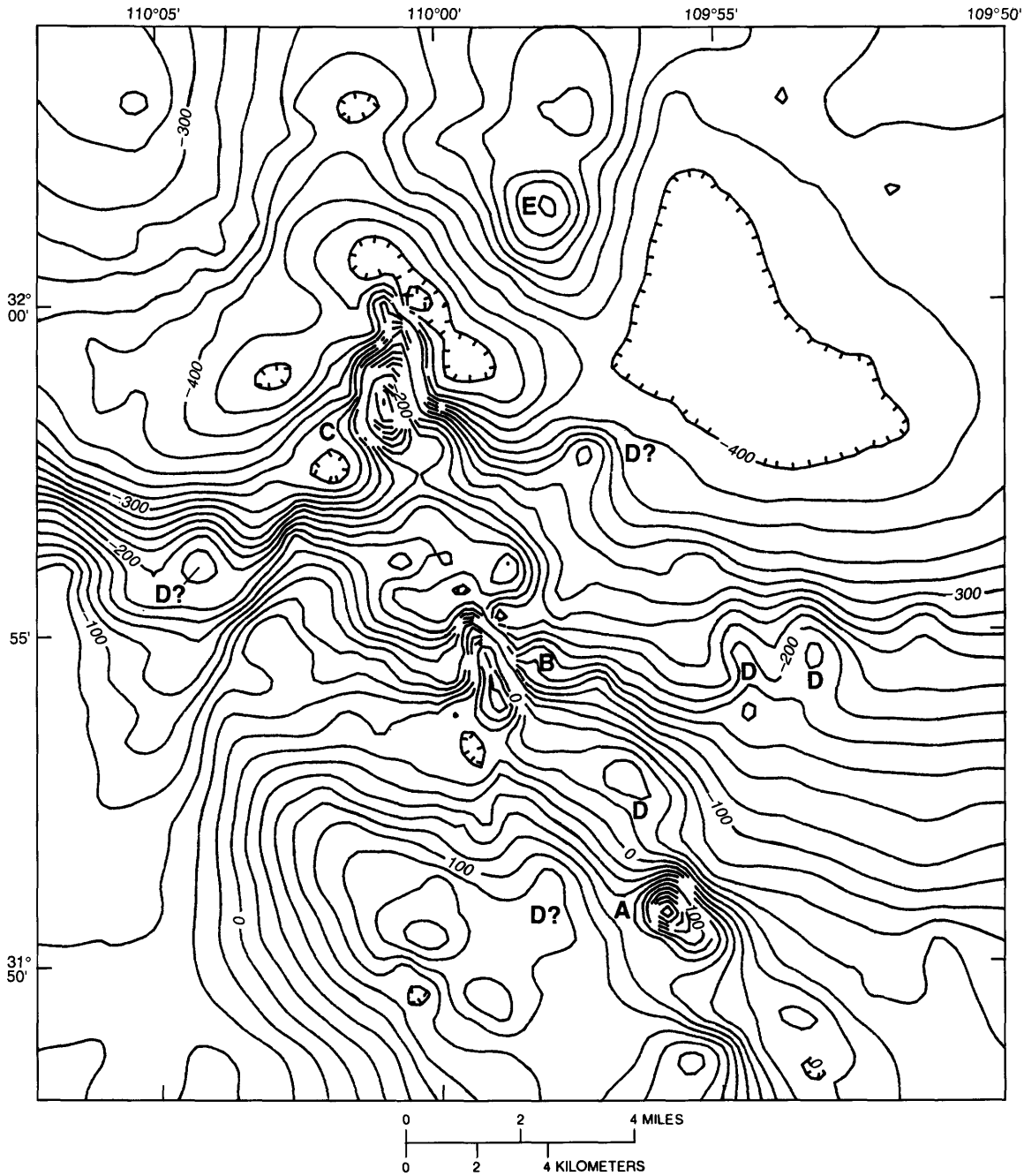

Figure 7. Aeromagentic-anomaly map of the Dragoon Mountains area, southeastern Arizona (U.S. Geological Survey, 1980a). Contour interval 20 nanoteslas; hachured lines are closed magnetic lows. Letter symbols correspond to anomalies discussed in the text.

gravity pattern in this Forest unit is that of a gravity high coincident with the Dragoon Mountains and a gravity low coincident with surrounding pediments and basins. In addition, a gravity-anomaly low is superposed on the area underlain by the granite stock in the central part of the range, which strongly suggests that the granite is less dense than the other rocks in the range.

Accordingly, a vertical extent of 0.8 km was calculated for the east lobe (C, pl. 10) by assuming a –6 mGal gravity effect for a vertically oriented circular cylinder having a radius of 4 km, a depth to its top of 10 m, and a density contrast of –0.2 g/cc. For the west lobe, a –3 mGal gravity effect is appropriate because both gravity maxima to the southeast and northeast are at least 4 mGal higher than the high at B (pl. 10). A vertical extent of 0.4 km was calculated for the west lobe assuming a cylinder having a radius of 3 km, a depth to its top of 10 m, and a density contrast of –0.2 g/cc. These models assume that the granite is significantly less

dense than its host rock; a contrast of only –0.1 g/cc causes estimates of thickness to approximately double. Accordingly, gravity data impose some limits on the subsurface configuration of the stock lobes and provide information with regard to the location and depth of potentially mineralized rock adjacent to the stock.

A small gravity high (D, pl. 10) is defined by only one station and thus needs to be verified by additional data. If the anomaly is real it can be interpreted as a compact source whose center of mass is 1.6 km below the surface and having a minimum density contrast of 0.16 g/cc (assuming that the source extends nearly to the surface).

The most conspicuous aeromagnetic anomalies in the Dragoon Mountains (U.S. Geological Survey, 1980a) are intense positive anomalies labeled A, B, and C (fig. 7). The anomalies are associated with Paleozoic limestone; Proterozoic amphibolite, granodiorite, or metasedimentary rocks; and Tertiary granite or granodiorite (Klein, 1983). Klein (1983) attributed these anomalies to Proterozoic rocks, but also suggested contact metamorphosed rock as a possible source. The close spatial association between limestone outcrops and anomaly gradients (especially anomaly C) and known occurrences of magnetite in skarn suggests that the source of these anomalies is magnetite in limestone-hosted skarn. Magnetic susceptibilities for Proterozoic rocks of the Whetstone Mountains (Bankey and Kleinkopf, 1985) and the Santa Catalina Mountains (M.E. Gettings, unpub. data, 1992) are not high enough to account for anomalies such as A, B, and C. However, without susceptibility data for samples from anomalies A, B, and C, the possibility of the Proterozoic rocks as sources for some of the anomalies cannot be dismissed.

Small magnetic highs (D, fig. 7) may be similar to a magnetic high (E, fig. 7) coincident with Cretaceous-Tertiary rhyolitic intrusions hosted by Paleozoic limestone at the Golden Rule Mine. Consequently, anomalies labeled D are possible targets for shallowly buried mineralized rock associated with the borders of intrusions. Most of these localities were identified by Klein (1983).

No NURE aeromagnetic data (pl. 16) are available for the high part of the Dragoon Mountains because the sensor was almost continuously more than 200 m above terrain (pl. 13) along this flight line. Small estimates of the thickness of basin fill (pl. 16) corroborate gravity interpretations that a significant area of shallowly buried pediment may be present within the Forest. The easternmost estimate of the thickness of basin fill, 0.5 km, suggests that the Stronghold stock, if it extends below the basin fill, must thin to about 0.38 km (that is, 0.50 km minus 0.12 km, terrain clearance), assuming that it is nonmagnetic.

NURE radiometric-uranium response data coincident with the Stronghold stock (A, pl. 19) show that the stock is relatively radiogenic and that its host rocks are characterized by a fairly homogenous, nonradiogenic response. However, Paleozoic rocks south of the east lobe of the Stronghold stock (B, pl. 19) are characterized by an intermediate-level radiometric-uranium response that may indicate altered or mineralized rock. Tertiary rhyolite dikes in the southeast corner of the Forest unit are associated with a positive uranium anomaly (C, pl. 19), but the anomaly is not as strong as that for most of the Stronghold Granite. The flight path crossed only the northwest end of the dikes, so the aeroradiometric data may represent a minimum response for the dikes.

The Stronghold Granite is clearly highly anomalous in thorium (A, pl. 22) as are Tertiary rhyolite dikes southeast of the Forest (B, pl. 22). Radiometric-thorium responses for Bisbee Group and Proterozoic rocks are approximately at background levels, whereas the Paleozoic rock response is substantially lower. The strong thorium response of the Stronghold Granite facilitates identification of outwash sheets, which in turn accurately portray the alluvial-outwash pattern for alluvial deposits forming the upper 1 m or so of alluvium.

The Stronghold Granite is the rock most anomalous in potassium in the Dragoon Mountains (A, pl. 25). In addition, a radiometric-potassium anomaly coincides with Paleozoic rocks just south of their contact with the stock (B, pl. 25). Rhyolite dikes in the southeastern part of the Forest unit are associated with a positive radiometric-potassium anomaly very similar to that of the Stronghold Granite, which implies that compositions of the dikes and the Stronghold Granite are similar; the two rock types may be genetically related. Most Bisbee Group and Paleozoic rocks are characterized by low radiometric-potassium responses. Proterozoic Pinal Schist coincides with a moderate potassium anomaly (D, pl. 25) that may be related to its elevated white-mica content. A small body of Jurassic granite yields a very low radiometric-potassium response (E, pl. 25).

WHETSTONE MOUNTAINS

The USGS conducted a Wilderness Study Area evaluation, including a geophysical study (Bankey and Kleinkopf, 1985) of the Whetstone Mountains. An aeromagnetic survey, having a terrain clearance of 300 m and a nominal 800-m flight-line spacing was completed (U.S. Geological Survey, 1980b). Existing gravity data were supplemented by 118 additional stations; the data set for the Whetstone area is relatively good. Additional geophysical data are contained in the NURE data set.

The gravity-anomaly field within the Whetstone Forest unit (pl. 11) consists of a broad high of about 10 mGal amplitude bounded on the south-southwest and northeast, north of the Forest, by northwest-striking gradients and on the east by northeast- and north-striking gradients. The western boundary is not well defined, but a northeast-striking gradient cuts diagonally across the central and northeastern part of

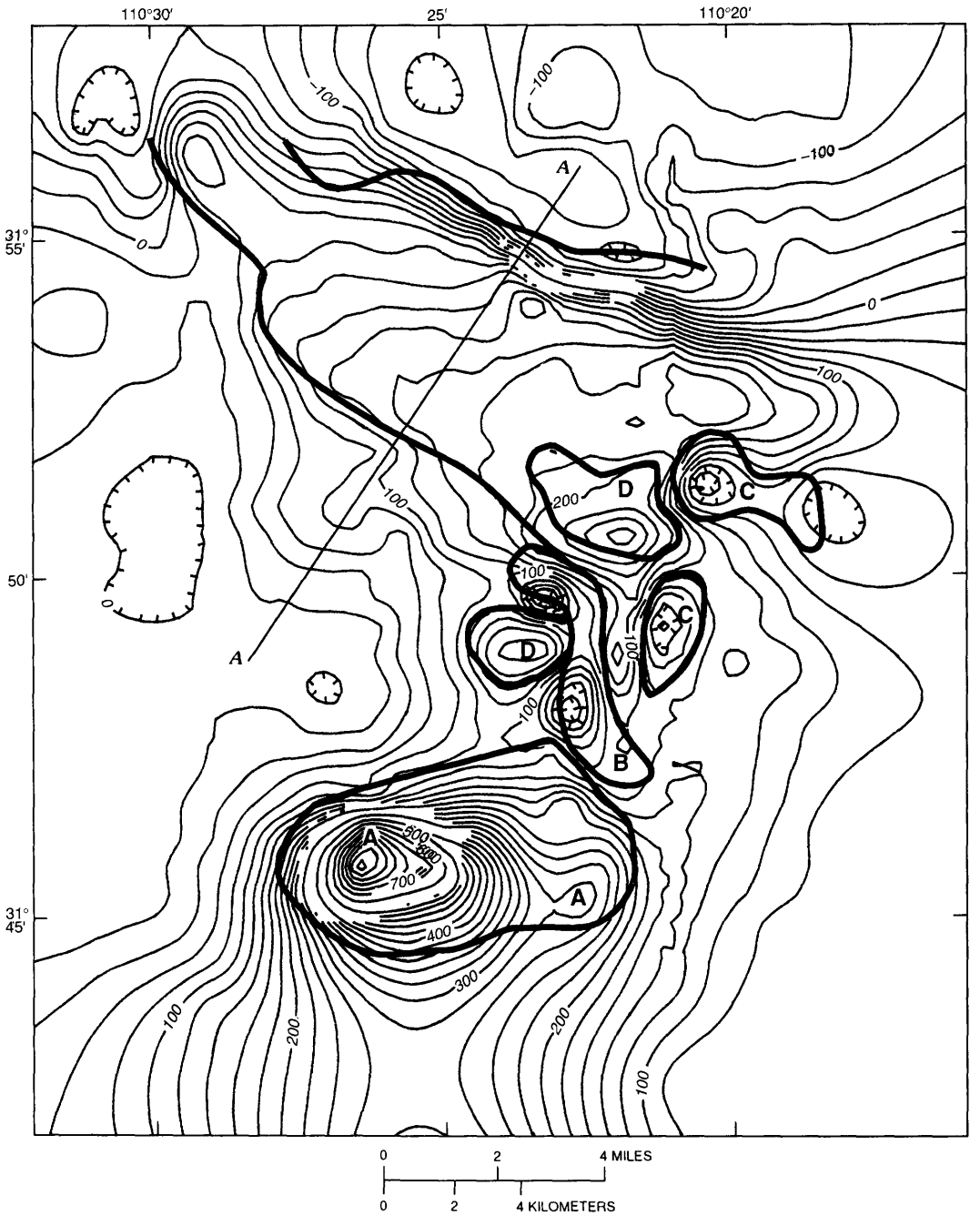

Figure 8. Aeromagentic-anomaly map of the Whetstone Mountains area, southeastern Arizona (U.S. Geological Survey, 1980b). Contour interval 20 nanoteslas; hachured lines are closed magnetic lows. Letter symbols correspond to anomalies discussed in the text; *A–A'*, profile across the Benson fault modeled in figure 9.

the area. Several small positive anomalies coincide with Proterozoic rocks along the northeast edge of the Forest. The Benson fault, just north of the Forest, does not correlate strongly with the gravity field, but the number of stations in this area is small; the fault may have a stronger gravity signature than shown. Density measurements reported by Bankey and Kleinkopf (1985) suggest that the density contrast between Proterozoic quartz monzonite and Bisbee Group rocks across the Benson fault may not be large, thereby precluding a strong gravity signature. The northwest-striking gradient north of the Benson fault and extending northwest through the Tucson area is probably a fault boundary associated with the large gravity high to the south and low to the north. The complexly shaped gravity high in the southern part of the Whetstone Mountains does not correlate well with geologic boundaries and is probably due to

Cretaceous-Tertiary granite (granodiorite of Bankey and Kleinkopf, 1985) and its buried extensions.

Modeling the southern gravity high, in the area of granodiorite outcrops (A, pl. 11), as a spherical source indicates a maximum depth to the center of the mass of about 2.6 km and a density contrast of 0.06 g/cc for a source having a 2.5-km radius. A vertical cylinder model having a radius of 2.5 km, a density contrast of 0.06 g/cc, and a depth to the top of the source of 0.1 km gives a thickness of 3.3 km; this estimate is considerably more than that of Bankey and Kleinkopf (1985), who modeled the aeromagnetic anomaly. The derived density contrast is in fair agreement with the measurements of Bankey and Kleinkopf (1985), who suggested a density contrast of about 0.03 g/cc for the granodiorite relative to Bisbee Group rocks.

Applying the simple sphere model to two small highs in the east-central area (B, pl. 11) yielded a depth to the center of the mass of about 0.8 km; assuming a density contrast of less than 0.2 g/cc, the calculated radius of the sphere would be greater than the depth to the center of the mass, which suggests that both sources, if not exposed, are only shallowly buried. The peak amplitudes of both anomalies are defined by one station each; the anomaly should be verified by several more measurements.

The northeast gradient across the central part of the Forest unit (pl. 11) is not reflected in the geology, but part of it does correspond to a southwestward step in the high topography of the range front. The gradient may be related to changes in thickness of intrusive masses, perhaps including the granodiorite exposed in the southern part of the Forest unit. Aeromagnetic data described below suggest that extensions of the granodiorite underlie the entire Whetstone Mountains area.

The most prominent feature of the aeromagnetic map of the Whetstone Mountains (fig. 8) is a large positive anomaly (A) associated with granodiorite exposed in the southern part of the area. A series of small positive and negative anomalies, some of which correlate with exposed granodiorite sills, are present to the north-northeast. In the northern half of the area the aeromagnetic field is a broad high that drops abruptly to a minimum at the Benson fault.

The large southern anomaly (A, fig. 8) was modeled by Bankey and Kleinkopf (1985), who found that the magnetic susceptibility of the granodiorite must be at least 0.006 cgs, that the one specimen measured is described as "severely weathered and altered," and that the intrusion must extend eastward in the subsurface.

Anomaly B (fig. 8) is a negative anomaly that was interpreted by Bankey and Kleinkopf (1985) to be due to either reversely polarized granodiorite or hydrothermally altered rock. The hypothesis of reverse polarization seems most plausible because an episode of hydrothermal alteration capable of completely demagnetizing the sill, whose outcrop area is larger than that of anomaly A (fig. 8), would have severely altered the host rocks as well. Therefore, the sources of anomalies B and C are inferred to be a series of sills, stocks, or cupolas emanating from a large underlying intrusion having reversed magnetic polarity.

The sources of anomalies labeled D (fig. 8) are inferred to be normally polarized stocks or, perhaps, cupolas connected to the intrusive body responsible for anomaly A. Estimates of the depth to the top of the source, calculated from the horizontal extent of steepest gradient, for anomalies B and C yield nearly the survey terrain clearance, implying that the sources are close to the surface, whereas an estimate for anomaly D indicates 100 m as the depth to the top of the source.

A profile across the Benson fault (*A–A′*, fig. 8) was digitized and modeled (fig. 9) with a Marquardt inversion program (Webring, 1985). The model shown in figure 9 is the result of several attempts in which magnetic susceptibilities and body geometries were varied to match the observations by assuming that the Proterozoic quartz monzonite basement is the magnetic source. No solution could be found that fits this hypothesis; the best fitting model is that of a buried source having a magnetic susceptibility of about 0.001 cgs and a nearly conformable geometry. The source could be a layer of more magnetic material in the basement below the quartz monzonite, or it could be a young intrusive rock. Considering that Cretaceous-Tertiary intrusive rocks are exposed in the southern part of the Whetstone Mountains, the most reasonable model would seem to include igneous rocks similar to those that are exposed. Magnetic-susceptibility measurements reported by Bankey and Kleinkopf (1985) support this interpretation. The Tertiary granodiorite is the only rock having a comparable susceptibility; those for older rocks are two to three orders of magnitude too small. If this interpretation of the gravity and magnetic anomalies is correct, then, essentially, the entire Whetstone Mountains block is underlain by Cretaceous or younger intrusions, which could be related to the uplift of the Whetstone block.

NURE aeromagnetic data, specifically the east-west line (pl. 17) across the southern Whetstone Mountains, clearly depict the large positive anomaly associated with the granodiorite. Points labeled A show the anomaly associated with the Benson fault (fig. 9) and analyzed by Bankey and Kleinkopf (1985). The points labeled R? (pl. 17) indicate locations at which a NURE flight line coincided with the granodiorite sill, interpreted herein to be reversely polarized, along the east edge of the range.

The radiometric-uranium response of Proterozoic quartz monzonite in the Whetstone Mountains is considerably higher than that of Bisbee Group rocks, whereas the response of Paleozoic sedimentary rocks is lower (pl. 20). The response of Cretaceous-Tertiary rhyolite (B, pl. 20) is about the same as that of the Paleozoic rocks. Cretaceous-Tertiary granodiorite intrusions have nearly the same response as the Bisbee Group rocks. The Pinal Schist may be highly uraniferous relative to Bisbee Group rocks (C, pl. 20), especially considering that the sensor was considerably

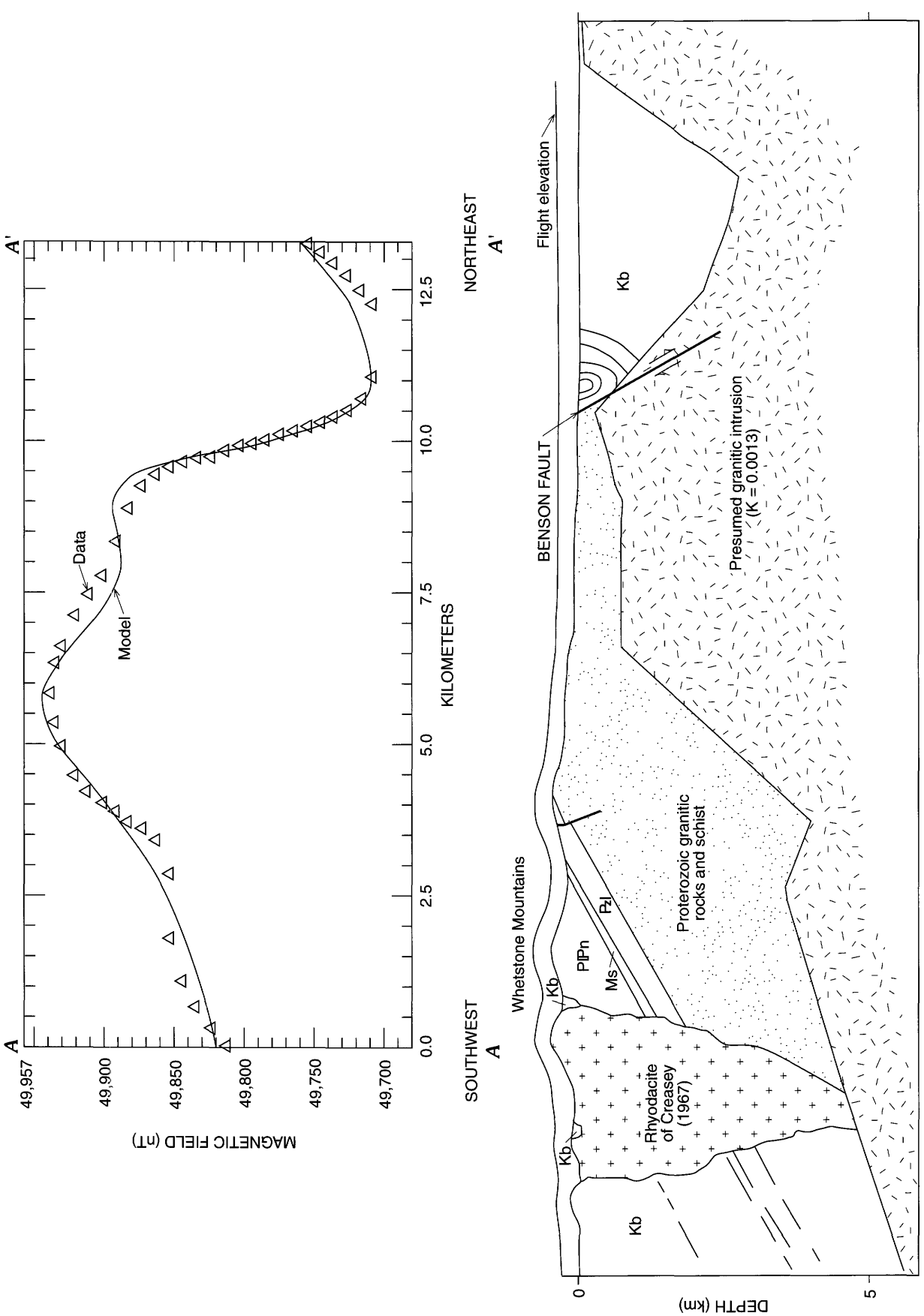

Figure 9. Aeromagnetic-anomaly profile, modeled magnetic response, and geologic cross section combined with the magnetic model, for section *A–A'* (fig. 8) across the Whetstone Mountains area, southeastern Arizona. K, magnetic-susceptibility contrast value used in the modelling procedure. Kb, Bisbee Group; PIPn, Naco Group; Ms, Mississippian sedimentary rocks; PzI, lower Paleozoic rocks.

above the specified 120-m terrain clearance (pl. 14) for much of the interval coincident with the schist. Anomalies that denote the intersection of the Benson fault with flight lines are indicated by points labeled A (pl. 20).

The most interesting radiometric-thorium anomaly is the series of highs associated with a zone about 0.5 km wide that coincides with the Benson fault (A, pl. 23). These anomalies suggest that altered or mineralized rock is present in the fault zone. Paleozoic rocks and the Cretaceous-Tertiary rhyolite have the lowest radiometric-thorium responses; Bisbee Group rocks, Cretaceous-Tertiary granodiorite, and Proterozoic quartz monzonite have progressively higher responses. The Pinal Schist appears to be thorium-poor (B, pl. 23).

The narrow strip of Bisbee Group rocks north of the Benson fault (A, pl. 26) coincides with a radiometric-potassium low, whereas the Proterozoic quartz monzonite south of the fault yields a positive anomaly. Paleozoic rocks are less potassic than Bisbee Group rocks, and the radiometric-potassium response of the Cretaceous-Tertiary rhyolite is slightly less than the base value. The Cretaceous-Tertiary granodiorite response is about at the base value, whereas the Pinal Schist (B, pl. 26) is quite strongly potassic. The variable response of the Pinal Schist in the three radiometric channels suggests that it might be hydrothermally altered where crossed by flight lines.

In summary, the potential for undiscovered mineralized rock in the Whetstone Mountains, as suggested by extensive and episodic intrusive activity, block fault patterns consistent with intrusion-related uplift, and the presence of favorable host rocks, is significant. Areas particularly worthy of future examination include the east-central area, in the vicinity of the positive and negative magnetic anomalies, and the western part of the Forest unit where Paleozoic rocks crop out north of Bisbee Group rocks and rhyolite.

PATAGONIA AND HUACHUCA MOUNTAINS AND CANELO HILLS

Gravity data coverage ranges from adequate in the northern Canelo Hills and basins to the north to none in much of the Patagonia Mountains and most of the Huachuca Mountains (pl. 11). Gravity data indicate that the San Rafael Basin (C, pl. 11), largely within the Forest, is a large, 750- to 1,000-m-deep bowl-shaped basin, assuming a density contrast of –0.4 or –0.3 g/cc and a vertical, circular cylinder model. The shape of the gravity anomaly associated with the part of the basin in the Forest indicates that this part of the basin is shallow, probably not more than 300–500 m deep. Gravity data coverage for the basin between the Santa Rita Mountains and the Patagonia Mountains and Canelo Hills (D, pl. 11) is adequate; the basin appears to be fault bounded only on its east side. The west side of the basin appears to be an extension of the east-dipping Santa Rita Mountains bedrock surface. Simple gravity models predict that the basin is about 300 m deep. Areas labeled F (pl. 11) are gravity-anomaly highs coincident with an extensive area of shallow cover, much of which is within the Forest. These areas and the San Rafael Basin are considered good prospects for future exploration.

The mountainous parts of this area coincide with gravity-anomaly highs that either are closed or form shelves within steep gradients (anomalies E, pl. 11). Anomaly G is probably related to dense Paleozoic carbonate sedimentary rocks; many additional gravity stations are needed to confirm that the high coincides with Paleozoic outcrops. Anomaly H is a moderately strong high superposed on the gradient at the edge of the San Rafael Basin. The anomaly also coincides with an aeromagnetic anomaly and a strong magnetic anomaly observed from truck-mounted magnetometer measurements. A spherical model indicates a maximum depth and a depth to the center of the mass of 1.6 km. Various assumptions for a vertical cylinder model give a depth-to-top of about 0.5 km, using radii of 1–2 km, thicknesses of the cylinder of 1–4 km, and density contrasts of 0.25–0.35 g/cc. Another, similar, more deeply buried body may be present at I (pl. 11); more gravity observations are required to confirm anomaly I. The area of Cretaceous-Tertiary volcanic and volcaniclastic rocks north of anomaly H and between the Patagonia Mountains and the Canelo Hills, an area having moderate potential for the presence of undiscovered porphyry copper skarn, polymetallic replacement, tungsten vein, and tungsten skarn deposits, deserves further examination with regard to buried mineral resources.

A number of aeromagnetic anomalies coincide with rocks of the Patagonia–Huachuca Mountains–Canelo Hills area. The contact of Cretaceous-Tertiary volcanic and volcaniclastic rocks with steeply northeast-dipping Cretaceous andesite and rhyolite coincides with a strong negative aeromagnetic anomaly (B, pl. 17). Strong magnetic-anomaly highs coincide with Cretaceous-Tertiary volcanic and volcaniclastic rocks (C and D, pl. 17). Anomaly C may be associated with gravity anomaly H (pl. 11). Intrusive rocks exposed at Saddle Mountain and in the body 2 km to the south at the edge of the San Rafael Basin appear to be plausible sources for the very large anomaly labeled D (pl. 17); this anomaly is similar to that correlated with Cretaceous-Tertiary granodiorite in the Whetstone Mountains. Anomaly E clearly reflects a deep source, part of which is beneath the Paleozoic and Cretaceous rocks. The source is probably associated with the Red Mountain porphyry-copper system, which has been intersected, at depths greater than 700 m, by exploration drilling (Corn, 1975). In the Huachuca Mountains, Middle Proterozoic granite is variably magnetized; the mass is associated with positive anomalies, anomalies having both polarities, negative anomalies, and, on the westernmost line across this unit (F, pl. 17), no anomaly at all. This suggests either that these rocks are underlain by variably magnetized rocks, or that variably magnetized,

unmapped bodies are present within this unit. A number of anomalies having unknown sources are present (G, pl. 17) in areas that may be favorable for the occurrence of undiscovered mineral deposits; implications of these anomalies for mineral resource potential of associated rocks requires further evaluation.

NURE radiometric-uranium anomalies coincident with Middle Proterozoic granite in the Huachuca Mountains are markedly more radiogenic to the west (D, pl. 20). Most Cretaceous-Tertiary volcanic and volcaniclastic rocks in this Forest unit are moderately radiogenic (E, pl. 20), and thus reflect the fact that most are composed of rhyolite. The Cretaceous-Tertiary granite has a similar response (F, pl. 20), and an area of Triassic-Jurassic volcanic rocks also exhibits a positive anomaly (G, pl. 20). The Paleozoic rocks respond almost uniformly at about 20 CPS, whereas the Triassic-Jurassic volcanic and sedimentary rocks (areas H, pl. 20) are associated with a positive anomaly.

NURE radiometric-thorium data for Middle Proterozoic granite depicts a uniform, strong, positive thorium anomaly (C, pl. 23), and Tertiary granitic intrusions display small-amplitude, positive anomalies. Most of the Paleozoic and Mesozoic rocks of the Huachuca Mountains respond at about 30 CPS. Cretaceous-Tertiary volcanic and volcaniclastic rocks, Tertiary granite intrusions in the Patagonia Mountains, and the Triassic-Jurassic volcanic unit have strong positive anomalies (D–F, pl. 23). Positive relative anomalies coincide with Triassic-Jurassic volcanic rocks in the southern Canelo Hills (G, pl. 23) and in a narrow belt, labeled H (pl. 23), in the northern Canelo Hills.

Middle Proterozoic granite in the Huachuca Mountains is characterized by a positive radiometric-potassium response at about 350–400 CPS (C, pl. 26). Tertiary granite in the Huachuca Mountains responds at about local base level, whereas responses of most other rock types are well below base level. A small area underlain by Bisbee Group rocks and associated with a very strong potassium anomaly (G, pl. 26) is an exception, however. North of the San Rafael Valley, Cretaceous-Tertiary volcanic and volcaniclastic rocks respond slightly below base level, except around the Red Mountain and Saddle Mountain intrusions, where negative anomalies, perhaps indicative of altered rock, are present. Triassic-Jurassic volcanic rocks (E, pl. 26) are strongly potassic. Triassic-Jurassic volcanic and sedimentary rocks in the northern (G, pl. 26) and southern (F, pl. 26) Canelo Hills are extremely anomalous.

Comparison of radiometric uranium, thorium, and potassium anomalies in the Canelo Hills area (H, pl. 20; G and H, pl. 23; and F and G, pl. 26) suggests relative anomaly zonation, especially in the southern Canelo Hills, among anomalies for the various elements. Uranium anomalies are not as extensive as overlapping thorium anomalies, which in turn are overlapped by larger potassium anomalies. This apparent zonation requires verification. The anomalies may indicate altered rock rather than the original rock; as such, zonation of altered rock, if found, would provide the most sensitive indicator of intensely altered areas.

SANTA RITA MOUNTAINS

Gravity data coverage in most parts of the Santa Rita Mountains Forest unit is poor, and little is known of the gravity-anomaly field, especially in the central part of the range (pl. 11). Areas labeled A (pl. 11) are tracts within or near the Forest that are covered by thin accumulations of unconsolidated surficial deposits; these areas may contain concealed deposits. Surficial deposits at A1 and A2 are about 500 m thick. Toward the range front from these points, gravity data indicate a continuously decreasing thickness of surficial cover.

The Sawmill Canyon fault zone, which crosses the Santa Rita Mountains at about lat 31°45′ N., appears to continue across the Tucson Basin to the northwest (line B, pl. 11); however, the fault is apparently truncated to the southeast by a well-defined, east- or east-northeast-striking structure (line D, pl. 11). Line D is part of a lineament identified on satellite images. The lineament forms a morphologic trace from near Gardiner Canyon on the east to Montosa Canyon on the west. South of this lineament, geophysical trends and linear features seen on satellite images are rotated slightly clockwise from northeast trends toward west trends. These features are consistent with a rotational couple associated with Tertiary northwest-directed extension. Such a rotational couple would produce a north-south dilatancy south of the Montosa-Gardiner lineament and provide a mechanism for emplacement of the east-striking, polymetallic Alto vein system in the southern Santa Rita Mountains. Gravity data are consistent with southward offset of the Sawmill Canyon fault system and splaying out of faults to the southeast (the area between lines labeled C, pl. 11).

The northeasternmost of two anomalies labeled G is north of the Forest but defines bedrock highs that project into the Forest. Anomaly I (pl. 11) is interpreted as a felsic intrusion in the northwest-striking fault zone that cuts across the northern part of the Santa Rita Mountains. A maximum estimate of depth for this anomaly is 800 m, and the depth to the top of source is probably substantially less; mineralized rock may be present in the shallow subsurface near anomaly I.

Aeromagnetic anomaly A (pl. 17) correlates with a Cretaceous-Tertiary granite, but the anomaly extends considerably beyond the contacts of the granite into an area underlain by Cretaceous andesite, and implies that the granite broadens with depth to the north and south. Aeromagnetic anomaly B is attributed to another mostly buried granite, a small exposure of which is exposed beneath the flight line. Anomalies labeled C are due to a reversely polarized, but unknown source. These two anomalies are particularly puzzling because they coincide with Proterozoic granite. Anomalies

labeled D have no obvious source. The anomaly labeled D in the central Santa Rita Mountains clearly correlates with Middle Proterozoic granite north of the Sawmill Canyon fault, but it is unclear why the anomaly is so variable north of the fault. Anomalies labeled E are due to shallow sources and seem to strike east. They are present in the area of the Alto vein swarm (Drewes, Chapter B, this volume) and may be related to magmatism that produced the swarm.

The radiometric-uranium response (pl. 20) of Cretaceous-Tertiary granite north of the Sawmill Canyon fault and Cretaceous rocks is about 30 CPS. The same rock responds much more strongly (about 65 CPS or more) south of the Sawmill Canyon fault (A, pl. 20). Jurassic granite (B, pl. 20) also has a signature similar to that of the Cretaceous-Tertiary granite. Cretaceous rhyolite (C, pl. 20) responds at about base levels.

Radiometric-thorium data (pl. 23) show strong differences among the various Cretaceous-Tertiary and Tertiary granite stocks. North of the Sawmill Canyon fault, Cretaceous-Tertiary stocks and Cretaceous rocks respond at about 50 CPS, whereas the radiometric-thorium response of Cretaceous-Tertiary granite in the southwest Santa Rita Mountains is 150-200 CPS (B, pl. 23). Middle Proterozoic granite north of the Sawmill Canyon fault produces about 85 CPS, and Jurassic granite in the southern Santa Rita Mountains (A, pl. 23) is nearly as responsive (about 150 CPS) as the Cretaceous-Tertiary granite. The lack of correlation along flight lines between a possible source for anomalies labeled C (pl. 23) and nearby granite outcrops having the same width as the anomaly suggests that location errors along some flight lines may be as much as 700 m. However, on both flight lines that intercept anomalies labeled C, the correlations between other anomalies and geologic contacts are within 100 m or less.

Radiometric-potassium responses in the Santa Rita Mountains are in accord with geologic units exposed therein (pl. 26). Anomaly A (pl. 26) indicates a particularly potassic zone within the Triassic volcanic and sedimentary unit. Jurassic granite (B, pl. 26) and Cretaceous-Tertiary granite (C, pl. 26) in the southwestern Santa Rita Mountains are characterized by moderate, but unexpectedly variable, radiometric-potassium responses, possibly indicating compositional zoning within these granites.

ATASCOSA, PAJARITO, SAN LUIS, AND TUMACACORI MOUNTAINS AND COBRE AND COCHES RIDGES

Gravity station coverage in the Atascosa–Cobre–Coches–Pajarito–San Luis–Tumacacori area is generally poor, and, with few exceptions, little is known of the gravity-anomaly field in the central parts of these mountain ranges (pl. 11). Moderate to good coverage exists for surrounding basins, however, and basin-defined trends can be used to trace regional structures across the ranges. The area labeled A3 (pl. 11) is covered by only about 300 m of alluvium; a relatively shallow pediment area such as this is amenable to exploration by drilling. The southwestern of the two anomalies labeled G (pl. 11) is north of the Forest boundary, but defines another bedrock high that projects into the Forest unit.

The shape of the gravity low in Bear Valley west of the Atascosa Mountains (E, pl. 11) correlates poorly with the distribution of valley fill; the gravity low may depict a structural depression. If anomaly E is interpreted along with the gravity high to the southwest (F, pl. 11) as indicating a fault block, the calculated structural relief of this block is 1.4–1.7 km, assuming a mean density contrast of 0.2 g/cc for the older rocks relative to Tertiary rhyolite. The fault-block model is consistent with a resurgent dome in a rhyolitic caldera; existing data are equally well explained by northwest-striking block faulting. The common association of ore deposits and calderas suggests that this area is favorable for the occurrence of undiscovered mineral deposits at depth.

The gravity-anomaly field along the eastern edge of the Tumacacori Mountains is consistent with a pediment surface dipping shallowly beneath valley fill. This inference is consistent with scattered bedrock outcrops exposed through valley fill in the southern part of the area; gravity-anomaly data do not require a major fault between the Tumacacori Mountains and the valley at least as far north as Diablito Mountain.

Sources for aeromagnetic anomalies labeled C (pl. 17) are unknown but are apparently due to reversely polarized sources. Anomalies labeled D have no obvious source either. Anomaly E, in the Tumacacori Mountains, correlates with exposed andesite, but the same andesite 5 km west does not produce a similar, strong positive anomaly. The terrain-clearance record (pl. 14) shows that at E the sensor was about 75 m above the base level, whereas on the line to the west it was, on the average, at the base level; thus, correction for terrain clearance would make the anomaly at E stronger.

North of the Sawmill Canyon fault the radiometric-uranium responses of Cretaceous-Tertiary granite and Cretaceous rocks are all similar, about 30 CPS (pl. 20). Cretaceous rhyolite in the Pajarito Mountains responds at about 60 CPS (G, pl. 20). Strong anomalies labeled D are coincident with Tertiary rhyolite in the Tumacacori Mountains and areas to the west; the cause of these anomalies is unknown. Cretaceous-Tertiary granite coincident with anomaly E responds at only about 10 CPS, which is an extremely low value for granite. Tertiary granite plugs (F, pl. 20) respond at about 60–90 CPS.

Radiometric-thorium responses indicate strong differences among various Cretaceous-Tertiary and Tertiary granite stocks. Cretaceous-Tertiary granite west of Bear Valley (G1, pl. 23) responds at about 40 CPS, whereas the northern (F, pl. 23) and southern (G, pl. 23) Tertiary granite stocks in the San Luis Mountains respond at about 150 and 80 CPS,

respectively. Cretaceous rhyolite in the Pajarito Mountains (D, pl. 23) also responds at approximately 150 CPS. Tertiary rhyolite west of the Tumacacori Mountains coincides with strong anomalous thorium responses in some areas (E, pl. 23) compared to the same rock in the Tumacacori Mountains and in areas to the west. Radiometric-uranium data for this area show similar patterns, which suggest that these anomalies may indicate several different rhyolite flows.

Most of the radiometric-potassium responses correlate with map units (pl. 26). Tertiary rhyolite in the Tumacacori Mountains and in areas to the west have fairly uniform responses, about 300 CPS (pl. 26); rocks on the flight line coincident with the Tumacacori Mountains may be somewhat less potassic than those to the west. An exception is anomaly D, for which the source of potassium enrichment is unknown. Cretaceous rhyolite in the Pajarito Mountains (E, pl. 26) responds at about 450 CPS. The radiometric-potassium response of Cretaceous-Tertiary granite at anomaly F is again very low for granite; low radiometric responses and the magnetic-anomaly coincident with this body suggest a dioritic composition. The Jurassic volcanic and sedimentary rocks in the San Luis Mountains seem to contain some potassium-enriched rocks (G, pl. 26) as was the case for Triassic rocks in the Santa Rita Mountains (A, pl. 26). Jurassic granite in the western San Luis Mountains is relatively potassic (H, pl. 26) and has a response similar to that of Jurassic granite in the southern Santa Rita Mountains (B, pl. 26).

SANTA CATALINA AND RINCON MOUNTAINS

Gravity data coverage within the Santa Catalina–Rincon Forest unit is very sparse in the central part of both ranges, especially the Rincon Mountains. The Bouguer gravity-anomaly field consists of a gravity high along the southwest edge of the range (A, pl. 9), a central gravity-anomaly low coincident with the granitic core of the range (B, pl. 9), and another high coincident with pre-Tertiary rocks along the northeast edge of the range (C, pl. 9).

Gravity-anomaly high A (pl. 9) is a strong (20–mGal) anomaly coincident with mylonitic rocks in the southwestern forerange of the Santa Catalina and Rincon Mountains. In the northwest, the anomaly maximum coincides with mylonitized Wilderness Granite and some Proterozoic Oracle Granite xenoliths or roof pendants at the southwest end of Pusch Ridge. Farther southeast, some of the Paleozoic and Mesozoic sections, as well as Proterozoic rocks, coincide with the anomaly. Types of rock coincident with the less intense high on the northeast side of the range are similar except that more of the Phanerozoic section is exposed. The trend of anomaly A (pl. 9) is strongly curvilinear, from east-west in the northwest to north-south in the southeast.

Gravity-anomaly lows B (pl. 9) coincide with the youngest granite, the 27-Ma Catalina Granite or Samaniego stock and with the 49-Ma Wilderness Granite along the axis of the range. Currently available data indicate that the trend of the low leaves the range south of Redington. In areas where gravity stations are sufficient to justify interpretation, the northwest gravity low labeled B does not indicate the transition from bedrock to valley fill, and thus suggests that the Pirate fault may not offset units that have an appreciable density contrast along the northwest edge of the Santa Catalina Mountains. Central low B indicates thicknesses of low-density material from 1 to 3.0 km for the Wilderness Granite in the core of the range, assuming density contrasts of 0.1–0.2 g/cc and depending on the type of model used. These thicknesses imply that the granite may not extend below sea level and that most of the pluton is exposed. Thus, the granite body has the form of a tabular, subhorizontal sheet, as opposed to a body having a depth comparable to its horizontal dimensions. Mylonitic foliation dips southwest at the southwest edge of the Santa Catalina Mountains and is horizontal to northeast dipping in the core of the range at the northeast edge of the Sabino Basin.

Anomaly highs labeled C (pl. 9) on the northeast edge of the Santa Catalina Mountains coincide with a magnetic-anomaly high that is most intense at its northwest end where it is spatially associated with Oracle Granite. Sinistral offset of anomalies C (pl. 9) between the northwesternmost anomaly C and the next one to the southeast correlate, at least in part, with exposed faults, including the Mogul fault. Alternatively, offset could be along right-slip faults that trend northeast but are not exposed.

Aeromagnetic anomalies labeled A (pl. 15) coincide with Wilderness Granite (Tertiary) and are immediately north of areas of Middle Proterozoic granite (Oracle Granite in most places). The depth estimated on the basis of the horizontal extent of the steepest gradient indicates that the sources of these anomalies are shallow, probably within 200 m of the surface, if not exposed. This method of depth estimation is subject to error but overestimates depth in most cases. Thus, the sources of the anomalies labeled A are probably in Tertiary granite. One possibility is that granite was chilled at its contact with Middle Proterozoic rock during intrusion. Chilling would result in finer grain size, and could produce a mineral enriched in refractory components; both of these conditions would result in more magnetic granite at or near the chilled margins. Assuming a north-dipping contact between Middle Proterozoic and Tertiary rocks near areas labeled A, contact metamorphism or alteration may have produced magnetic minerals in the contact zone that could result in the observed aeromagnetic signature.

Anomalies labeled B (pl. 15) coincide with Middle Proterozoic granite blocks, most of which are along the northeast or southwest borders of the mountain range. Anomaly sources are enigmatic because, in some cases, correlations between anomaly highs and granite bodies are clear, whereas

in others, one side of an anomaly correlates with a contact and the other side of the same anomaly correlates with Tertiary granite or Proterozoic granite. Presumably, because these granite bodies are associated with negative anomalies, if with any at all, the anomalies may indicate magnetic zones within the granite.

Anomalies labeled C (pl. 15) appear to reflect a deep source, but some of these include superposed shallow anomalies. The anomalies coincide with the core of the range and, considering the maximum estimated thicknesses for the Wilderness Granite from gravity data discussed above, the sources could be below the Wilderness Granite.

Estimates of depth (pl. 15) include the terrain clearance of the sensor above the surface. The specified clearance was about 0.12 km, but variations between 0.1 and 0.21 km occurred routinely, so that estimates of depth of 0.1–0.2 indicate anomaly sources exposed at the surface in many cases.

Anomalies labeled D (pl. 15) are centered on the Mogul fault and extend both to the north and south, in a pattern that suggests a northward-dipping sheet. Shallow anomalies are superposed on anomalies labeled D, especially north of the fault, but the main source of the anomaly seems to be at a depth of 200–800 m. As was the case in the Whetstone Mountains (discussed above), these anomalies may indicate a Tertiary intrusive mass beneath the Oracle Granite. Magnetic-susceptibility measurements for samples of Oracle Granite yielded values that are five times too small to explain the observed anomaly, even assuming an infinitely thick slab of Oracle Granite.

Anomalies labeled E (pl. 15) coincide with the south edge of the mountains, along the bajada, and have an unknown source. The depth to the base of the basin fill (base of upper plate in the detachment model) is 200 m below the surface, based on extrapolation of drillhole data.

The radiometric-uranium response of the Wilderness Granite (pl. 18) is about 20 CPS, whether mylonitized or not; responses for Paleozoic and Mesozoic rocks are similar or slightly lower and less variable. Proterozoic granite on the northeast side of the range is the most anomalous (A, pl. 18); the response of the Samaniego stock, the youngest intrusive rock, is also highly anomalous (B, pl. 18). The Proterozoic granite is highly anomalous in uranium only where intruded by the Wilderness or Samaniego plutons, an important factor to be considered in modelling the genesis of any associated uranium deposits. Proterozoic granite north of the Mogul fault, although more anomalous than Wilderness Granite, is not as strongly anomalous as areas labeled A (pl. 18). These relations suggest that Tertiary magmatism may have mobilized or concentrated uranium in the Proterozoic granite, but other explanations are possible. Proterozoic rocks on the southwest and west sides of the range, north of Rincon Valley, are not anomalous in uranium, except where intruded by Wilderness Granite, again regardless of their association with mylonitic rock. The radiometric-uranium response of valley fill (for example, C, pl. 18) is highly anomalous west of the west face of the Santa Catalina Mountains.

The radiometric-thorium response of the Samaniego stock is by far the most anomalous in the area (A, pl. 21); valley fill to the west, derived as outwash from the stock, is also highly anomalous. Proterozoic granite is anomalous (B, pl. 21) in most places, though not all; there is no obvious pattern for thorium anomalies associated with this rock type. The Oracle Granite north of the Mogul fault has a distinct signature. The Paleozoic rocks have a uniformly low response at less than 20 CPS; the Wilderness Granite has a mean response of about 20 CPS, but its response is highly variable on the east side of the Rincon Mountains (C, pl. 21).

The radiometric-potassium response of the Proterozoic and Wilderness granites is about 250–325 CPS; that of the Samaniego stock is a little higher (pl. 24). Paleozoic rocks have a low response in most places, except where associated with anomalies labeled A (pl. 24). The source of these anomalies is unknown, but they coincide with Proterozoic Apache Group metasedimentary rocks and the lower part of the Paleozoic section. A distinct, but small, potassium low coincides with the forerange fault (B, pl. 24).

REFERENCES CITED

Bankey, Viki, and Kleinkopf, M.D., 1985, Geophysical maps of the Whetstone Roadless Area, Cochise and Pima Counties, Arizona: U.S. Geological Survey Miscellaneous Field Studies Map MF–1614–C, scale 1:48,000.

Briggs, I.C., 1974, Machine contouring using minimum curvature: Geophysics, v. 39, p. 39–48.

Coney, P.J., and Harms, T.A., 1984, Cordilleran metamorphic core complexes—Cenozoic extensional relics of Mesozoic compression: Geology, v. 12, p. 550–554.

Cordell, L., Keller, G.R., and Hildenbrand, T.G., 1982, Bouguer gravity map of the Rio Grande rift: U.S. Geological Survey Geophysical Investigations Map GP–949, scale 1:1,000,000.

Corn, R.M., 1975, Alteration-mineralization zoning, Red Mountain, Arizona: Economic Geology, v. 70, no. 8, p. 1437–1447.

Creasey, S.C., 1967, Geologic map of the Benson quadrangle, Cochise and Pima Counties, Arizona: U.S. Geological Survey Miscellaneous Geologic Investigations Map I–470, scale 1:48,000.

Creasey, S.C., Jinks, J.E., Williams, F.E., and Meeves, H.C., 1981, Mineral resources of the Galiuro Wilderness and contiguous further planning areas, Arizona, *with a section on* Aeromagnetic survey and interpretation, *by* W.E. Davis: U.S. Geological Survey Bulletin 1490, 94 p., 2 pls., map scale 1:62,500.

du Bray, E.A., and Pallister, 1991, An ash-flow caldera in cross section—Ongoing field and geochemical studies of the mid-Tertiary Turkey Creek caldera, Chiricahua Mountains, southeast Arizona: Journal of Geophysical Research, v. 96, p. 13435–13457.

Eberly, L.D., and Stanley, T.B., Jr., 1978, Cenozoic stratigraphy and geologic history of southwestern Arizona: Geological Society of America Bulletin, v. 89, p. 921–940.

Godson, R.H., Bracken, R.E., and Webring, M.W., 1988, PCCONTUR version 1.0, a microcomputer general purpose contouring program: U.S.Geological Survey Open File Report 88–593A–D.

Hummer-Miller, Susanne, and Knepper, D., 1990, Geophysics-remote sensing, *in* Peterson, J.A., ed., Preliminary mineral resource assessment of the Tucson and Nogales 1° × 2° quadrangles, Arizona: U.S. Geological Survey Open-File Report 90–276, 219 p., 33 pls., scale 1:250,000.

International Association of Geodesy, 1971, Geodetic Reference System 1967: Bureau Centrale de l'Association Internationale de Geodesie Special Publication 3, 116 p.

Keith, W.J., Martin, R.A., and Kreidler, T.J. 1982, Mineral Resource potential of the Winchester Roadless Area, Cochise County, Arizona: U.S. Geological Survey Open-File Report 82–1028, 9 p.

Klein, D.P., 1983, Geophysical maps of the Dragoon Mountains roadless area, Cochise County, Arizona: U.S. Geological Survey Miscellaneous Field Studies Map MF–1521–C, scale 1:50,000.

———1987, Aeromagnetic map of the Silver City 1° × 2° quadrangle, New Mexico and Arizona: U.S. Geological Survey Miscellaneous Investigations Series Map I–1310–D, scale 1:250,000.

Martin, R.A., 1986, Geophysical maps of the Winchester Roadless Area, Cochise County, Arizona: U.S.Geological Survey Miscellaneous Field Studies Map MF–1851, scale 1:24,000.

Morelli, C., Gantar, C., Honkasala, T., McConnel, R.K., Tanner, J.G., Szabo, B., Uotila, U.A., and Whalen, G.T., 1974, The International Gravity Standardization Net 1971 (IGSN71): Bureau Centrale de l'Association Internationale de Geodesie Special Publication 4, 194 p.

Moss, C.K., and Abrams, G.A., 1985, Geophysical maps of the North End Roadless Area, Chiricahua Mountains, Cochise County, Arizona: U.S.Geological Survey Miscellaneous Field Studies Map MF–1412–C, 2 sheets, scale 1:50,000.

Oppenheimer, J.M., and Sumner, J.S., 1980, Depth to bedrock map, Basin and Range province, Arizona: Tucson, Ariz., Department of Geosciences, University of Arizona, scale 1:1,000,000.

Plouff, Donald, 1977, Preliminary documentation for a Fortran program to compute terrain corrections based on topography digitized on a geographic grid: U.S. Geological Survey Open-File Report 77–535.

Ponce, D.A., 1990, Geophysics-gravity and magnetic methods, *in* Peterson, J.A., ed., Preliminary mineral resource assessment of the Tucson and Nogales 1° × 2° quadrangles, Arizona: U.S. Geological Survey Open-File Report 90–276, 219 p., 24 pls., scale 1:250,000.

Sauck, W.A., and Sumner, J.S., 1970, Residual aeromagnetic map of Arizona: Tucson, Ariz., Department of Geosciences, University of Arizona, scale 1:1,000,000.

Schwartz, K.L., 1990, A geohydrologic investigation of volcanic rocks using the gravity survey method—Galiuro Mountains, Graham, Pinal and Cochise Counties, Arizona: Tucson, Ariz., University of Arizona, M.S. thesis, 138 p.

Senterfit, R.M., and Klein, D.P., 1992, Audiomagnetotelluric investigation at Turkey Creek caldera, Chiricahua Mountains, southeastern Arizona: U.S. Geological Survey Bulletin 2012, p. K1–K9.

Sumner, J.S., 1985, Crustal geology of Arizona as interpreted from magnetic, gravity, and geologic data, *in* Hinze, W.H., ed.: The utility of regional gravity and magnetic anomaly maps: Tulsa, Okla., Society of Exploration Geophysicists, p. 164–180.

Swan, M.M., 1976, The Stockton Pass fault—An element of the Texas lineament: Tucson, Ariz., University of Arizona, M.S. thesis, 119 p.

Texas Instruments, Inc., 1979, Aerial radiometric and magnetic reconnaissance survey of parts of Arizona–New Mexico: U.S. Department of Energy Report GJBX–23(79), 7 vols.

U.S. Geological Survey, 1980a, Aeromagnetic map of the Dragoons area, Arizona: U.S. Geological Survey Open-File Report 80–996, scale 1:62,500.

———1980b, Aeromagnetic map of the Whetstone Mountains area, Arizona: U.S. Geological Survey Open-File Report 80–1126, scale 1:62,500.

———1982, Aeromagnetic map of the Winchester area, Arizona: U.S. Geological Survey Open-File Report 82–554, scale 1:62,500.

Webring, M., 1981, MINC—A gridding program based on minimum curvature: U.S. Geological Survey Open-File Report 81–1224.

———1985, SAKI—A Fortran program for generalized linear inversion of gravity and magnetic profiles: U.S. Geological Survey Open-File Report 85–122.

Wynn, J.C., 1981, Complete Bouguer gravity anomaly map of the Silver City 1° × 2° quadrangle, New Mexico–Arizona: U.S. Geological Survey Miscellaneous Investigations Series Map I–1310–A, scale 1:250,000.

Electrical Geophysical Surveys of Coronado National Forest

By Douglas P. Klein

MINERAL RESOURCE POTENTIAL AND GEOLOGY OF CORONADO NATIONAL FOREST, SOUTHEASTERN ARIZONA AND SOUTHWESTERN NEW MEXICO
Edited by Edward A. du Bray

U.S. GEOLOGICAL SURVEY BULLETIN 2083–E

UNITED STATES GOVERNMENT PRINTING OFFICE, WASHINGTON : 1996

CONTENTS

FIGURES

TABLE

Electrical Geophysical Surveys of Coronado National Forest

By Douglas P. Klein

ABSTRACT

Ground electrical traverses using the audiomagnetotelluric method have been performed within and adjacent to several units of Coronado National Forest, southeastern Arizona. Areas studied were the Winchester Mountains, the northern Dragoon Mountains, the northern Chiricahua Mountains near Emigrant Pass, and the Turkey Creek caldera in the central Chiricahua Mountains. These reconnaissance surveys provide information concerning the electrical structure in the depth range of about 10–3,000 m. The purpose of these surveys was to assist in mineral or geothermal assessment studies by providing information on thickness of volcanic or alluvial cover (overburden) and inferences as to rock types and structures beneath the overburden. These data are helpful for generalized mapping of location and extent of buried low-resistivity geothermal water, or of hydrothermally altered rock, low-resistivity brecciated rock, or lithologic contrasts associated with faults, and the location and extent of high-resistivity intrusions.

INTRODUCTION

Audiomagnetotelluric (AMT) surveys within or adjacent to Coronado National Forest have been performed by the U.S. Geological Survey (USGS) for various investigations related to the characterization of mineral or geothermal potential of Federal lands. These AMT studies have been performed primarily to assist in the subsurface mapping of geologic environments that are favorable for the occurrence of mineral or geothermal resources rather than for direct detection of economic concentration of such resources. This report reviews the potential of these data to provide information on the mineral appraisal of the land in or bordering Coronado National Forest.

Areas covered by AMT investigations reviewed here are shown on figure 1 (areas 2, 3, 4A, and 4B). Also shown for reference are the location of areas covered by electrical geophysical surveys northeast of the Pinaleno Mountains (areas 1A, 1B, and 1C; Vozoff, 1972; Strangway and others, 1973; Bell, 1979; Klein and Baer, 1983). The surveys reviewed here are (1) on the west flank of the Winchester Mountains (area 2: Martin and others, 1982; Martin, 1986); (2) across the northern Dragoon Mountains (area 3: Baer and Klein, 1984); (3) in the northern Chiricahua Mountains in the area of Emigrant Pass (area 4A: Nervick and Boler, 1981); and (4) across parts of the Turkey Creek caldera of the central Chiricahua Mountains (area 4B: Senterfit and Klein, 1992). In some cases, this review includes new modeling and interpretative observations that supplement the original reports.

ELECTRICAL GEOPHYSICS IN MINERAL EXPLORATION

Electrical geophysical surveys, including the AMT survey method, are usually designed to map the physical property of resistivity (ohm-meters, ohm-m), a measure of impedance to electrical current flow (Keller and Frischknecht, 1966, chapter 1). Conductivity (Siemens/m), the inverse of resistance, is often used as an equivalent physical measure instead of resistivity. In many electromagnetic surveys over dikelike bodies or veins, the conductance of a unit (Siemens: thickness/resistivity for the layer or dike) is employed as well (Strangway, 1966).

Resistivity surveys have had wide usage in the exploration for mineral deposits because rocks containing massive or interconnected metallic sulfides have been found to have anomalously low resistivity. Part of the anomaly is caused by the low resistivity of the metallic sulfide minerals, typically less than 0.1 ohm-m (Ward, 1966), but a significant part of the lowered bulk resistivity may be associated with alteration minerals (clay) associated with mineralized rock (Keller and Frischknecht, 1966, p. 22–27). Except in unusual cases, sulfide-bearing rock forms small volumes and surveys must be quite detailed to locate such bodies. The possibility that zones of low resistivity, when found, are related to mineralized rock and not to other secondary effects must be carefully evaluated. The various sources of low resistivity that may not be associated with mineralized rock, discussed below,

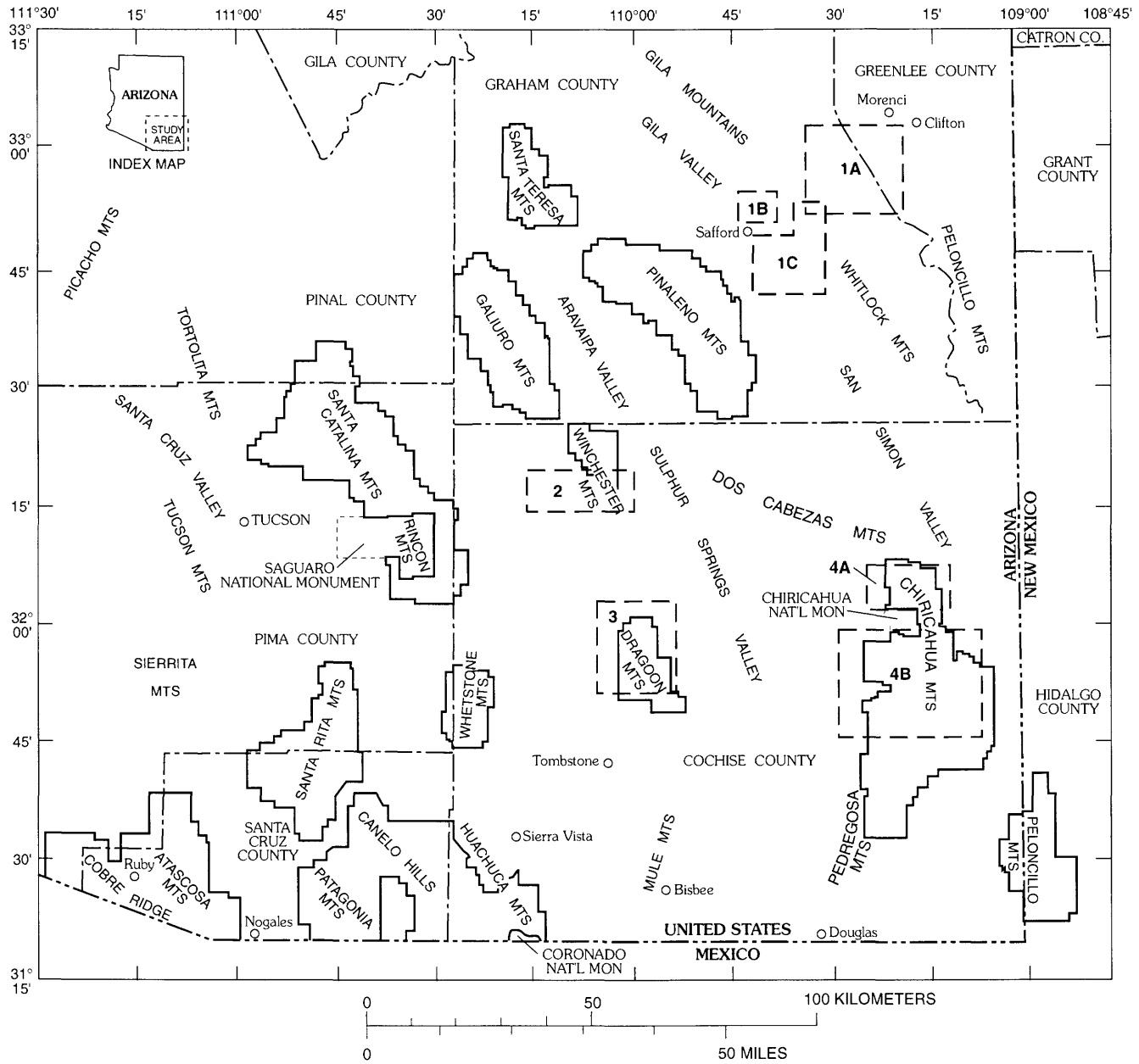

Figure 1. Map showing location of AMT electrical surveys in southeastern Arizona (dashed lines) and Coronado National Forest units. Areas 2, 3, 4A, and 4B are discussed in this report; electrical geophysical surveys of areas 1A, 1B, and 1C northeast of the Pinaleno Mountains are described by Vozoff (1972), Strangway (1973), Bell (1979), and Klein and Baer (1983).

contribute considerable uncertainty in the interpretation of electrical surveys.

The resistivity of rocks and minerals spans a large range in which there is considerable overlap between rock types and compositions (fig. 2) (Brant, 1966b). Except for localized concentrations of metallic minerals, and in some cases graphite, resistivity is much more dependent on composition and temperature of pore fluid than it is on a particular mineralogical composition. Ground water is quite conductive (fig. 2), thus, variation in porosity, as it affects the fluid fraction, is a primary factor affecting variations in resistivity. Resistivity surveys are, in fact, often applied to ground-water investigations as well as mineral and geothermal resource studies; examples for southeastern Arizona can be found in Zohdy and others (1974, p. 60) and Tucci (1984; 1989). Most common silicate minerals, for instance, are highly resistive, on the order of 10,000 ohm-m (Keller, 1982), and variations in silicate mineralogy has very little influence on the bulk resistivity of dry rocks. The chief conductive solids include the metallic sulfides and native metals, graphite, and clay and zeolite minerals. The latter exert a strong influence on the lowered resistivity of basin

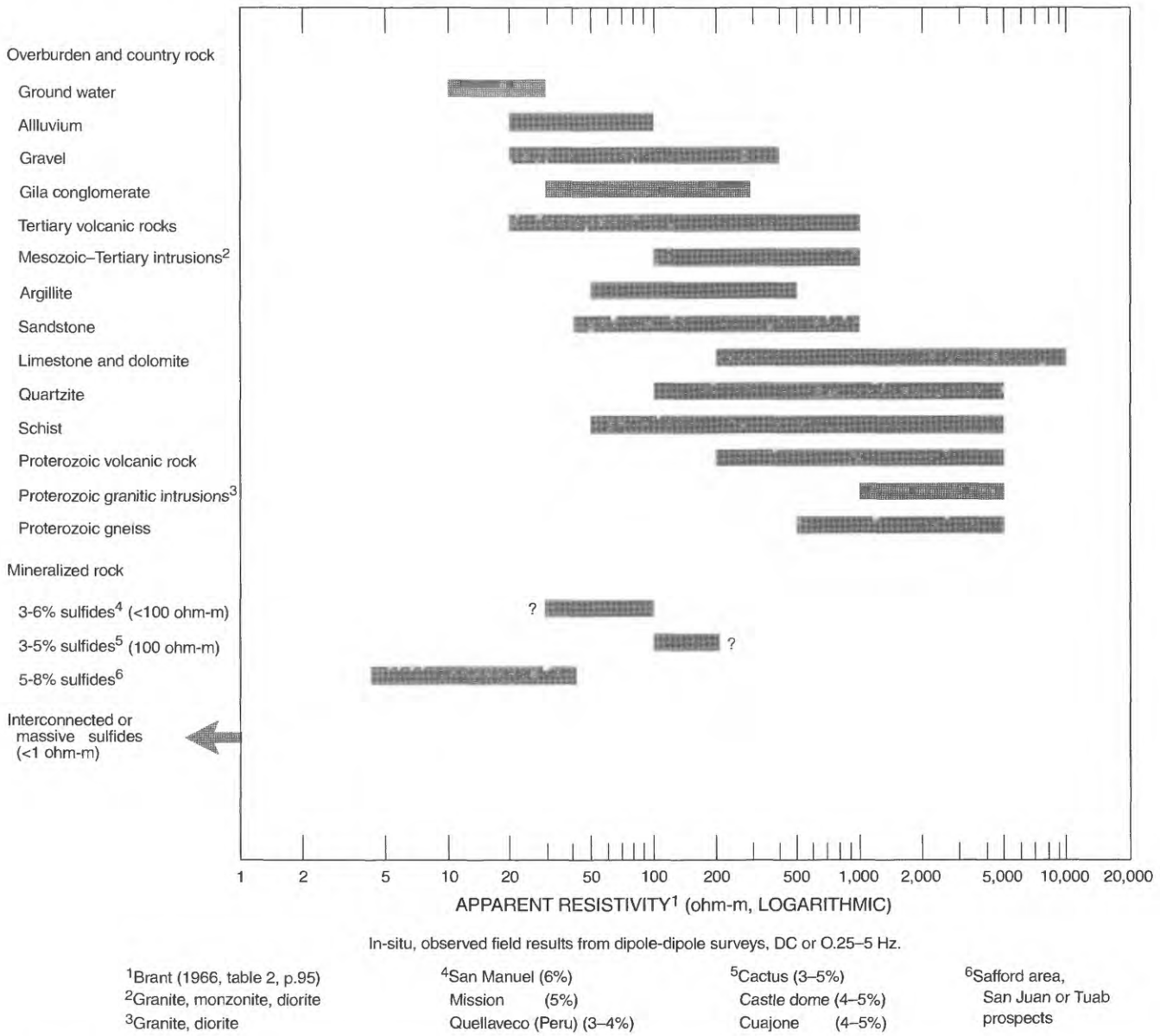

Figure 2. Typical ranges of resistivity in overburden, country rock, and mineralized rock for south-central and southeastern Arizona (Brant, 1966b, table 2, p. 95).

sediments and altered rocks (Keller and Frischknecht, 1966, Chapter 1). Inasmuch as higher temperature greatly decreases the resistivity of ionic fluids, saturated rocks in geothermal areas are also characterized by anomalously low resistivity (Hoover and others, 1978). An illustrative example of electrical geophysics for geothermal resource investigations in the Lightning Dock area, about 45 km east of area 4B (fig. 1), was provided by Jiracek and others (1976) and Smith (1978).

Rock fabrics and geologic structures can have a significant influence on porosity and fluid content and therefore on resistivity. Faults and breccia or fracture zones may have anomalous porosity and contain sufficient (a few percent) fluids along with clay gouge or hydrothermally altered material to have substantially lower resistivity than the surrounding wall rock. Thus, identification of structural features that may indicate areas favorable for mineral exploration is perhaps the most important contribution from electrical geophysics.

Two electrical survey approaches have been utilized in mineral exploration. The first, and the traditional, approach is the direct detection of rock masses containing a substantial fraction, 1 volume percent or more, of sulfides that have low resistivity or high chargeability. Difficulty results from the alternative explanations for an anomaly, which include non-economic, for instance pyrite-impregnated rock, or

non-mineralized alteration zones. Inasmuch as most mineral deposits have dimensions of tens or hundreds of meters (porphyry copper deposits can be larger), direct exploration techniques commonly employ relatively detailed and high-resolution methods that generally do not penetrate very far (10 m to a few hundred meters). These surveys focus on specific areas previously inferred as favorable and the surveys are closely coupled to exploration drilling. Such surveys may be quite costly.

In the second approach, electrical geophysics is utilized in mineral exploration as an aid to geological mapping of structures or rock units. Inferences concerning the potential for a mineral deposit are indirect in this application and rely on supplementary information. These studies are aimed largely at inferring the potential for mineral deposits within particular structural and lithological settings partly on the basis of the context of known mineral deposits within the region. The studies reviewed here all fall within this category. Electrical geophysics as an indirect mapping tool is useful largely as part of an integrated exploration effort that combines geologic mapping and various other geophysical techniques. The geophysical data provide information on the vertical dimension of mapped geological structures or rock types and on rocks or structures beneath alluvial or volcanic cover. Strangway (1970) discussed various approaches of indirect exploration through overburden, giving considerable attention to the area of southern Arizona. Electrical surveys that approach the problem of geologic setting are typically less detailed than those conducted in direct exploration for resource targets; they may commonly penetrate quite deeply and have spacing that may exceed the dimensions of mineral deposits. In terms of area covered, these surveys are relatively inexpensive, but sacrifice resolution, including the likelihood of directly detecting a deposit or its surrounding alteration halo.

In addition to the Earth's resistivity, which is sought by AMT, and most other electrical surveys, another electrical parameter defined in dipole-dipole, induced-polarization (IP) surveys is chargeability or polarizeability. This property is a measure of the ability of a rock unit to accumulate electrical charge (Ward and Fraser, 1967). IP surveys are the principal technique in the search for disseminated-sulfide ore deposits (Rogers, 1966, Brant, 1966a,b). Disseminated metallic sulfides may have the characteristic of quite high resistivity because the conducting fraction is small and not interconnected, while having significantly larger chargeability (Rogers, 1966; Madden and Cantwell, 1967) than unmineralized rock.

Illustrative discussions on IP work in southern Arizona were provided by Hallof (1966) in the Miami area, Maillot and Sumner (1966) in the Ajo and Morenci and Bisbee deposits, Hallof and Winniski (1971) for the Lakeshore deposit, Elliot and Maclean (1978) for the Silver Bell deposit, and Nelson and others (1982) in the San Pedro Valley. IP surveys also routinely provide resistivity information, from the dipole-dipole array, that can be used in the same way as other electrical survey data. The results of Strangway and others (1973) are of interest in providing an example of both dipole-dipole and AMT resistivity data over an area of known mineralized rock in the Safford area, northeast of the Pinaleno Mountains (area 1B on fig. 1). Other dipole-dipole resistivity data for near the Pinaleno Mountains are available for the Safford Valley (area 1C, fig. 1; Bell, 1979, contract work for the Arizona Geological Survey). The latter dipole-dipole resistivity survey partly crosses into bedrock in the area of a USGS AMT survey (Klein and Baer, 1983) in the northern Peloncillo Mountains (area 1A, fig. 1).

AUDIOMAGNETOTELLURICS

The audiomagnetotelluric (AMT) method (Strangway and others, 1973) is a high-frequency variation on the MT method (Vozoff and others, 1963; Vozoff, 1972); both utilize naturally occurring source fields. The AMT and MT methods contrast with controlled-source, direct-current (DC, such as IP surveys) or electromagnetic (EM) methods that utilize mobile generators for producing artificial electric or electromagnetic fields. AMT is commonly utilized for investigating the upper 1–2 km of the crust (Long, 1985; Frischknecht and others, 1986), whereas MT is utilized for investigating to depths of 20 or 30 km. MT surveys usually focus on the large-scale tectonic setting of a region (Ander, 1981; Ander and others, 1984; Kechet and Hermance, 1986; Klein, 1991).

The MT-AMT method measures two perpendicular components of the horizontal electric and magnetic fields at the surface of the earth. Signals are measured, or processed, in a manner that provides estimates of the field ratios (as apparent resistivity, explained below) at many discrete frequencies; in most cases, data are averages across frequency bands a few hertz wide. The "audio" frequencies of AMT for the USGS system (Hoover and others, 1978) range from 4.5 to 27,000 Hz, whereas typical MT frequencies range from about 0.001 to 100 Hz. "Scaler AMT," which was used for the investigations described here, varies from the general MT-AMT method in that scaler AMT utilizes only the amplitudes of the time-varying electric and magnetic field (full AMT or MT also measure phase). The scaler AMT approach simplifies the operation and instrumentation, but neglects one of the components of information available. Scaler AMT surveys are rapidly and inexpensively deployed and interpreted, but they sacrifice some interpretative capability. A two-person field crew can typically acquire scaler AMT soundings in about 1 hr. The field equipment is compact enough to be transported by helicopter.

AMT data, as well as many other electrical survey data, are reduced from the observed quantities (voltage, magnetic field intensity and frequencies) to a parameter called "apparent resistivity" which here shall be called the "data." The

MT-AMT reduction is given by $|E_i/H_j|^2/5f$, where E_i is the electric field measured in mV/km (millivolts/kilometer), H_j is the magnetic field measured in nanoteslas (gammas) and f is the frequency in hertz. The subscripts (i,j) indicate that orthogonal azimuths are used in the ratio. The MT-AMT sounding curve consists of plotting apparent resistivity versus frequency. Because two components of both E and H are measured, there are two curves for each sounding. Relationships between these curves provide information on the dimensions of the resistivity structure being sensed. In a one-dimensional environment, where resistivity varies only with depth, the two curves are the same and the sounding curve approximately "tracks" the variations in true resistivity. This tracking is in the sense that apparent resistivity varies with lower frequency as the Earth's resistivity varies with greater penetration distances.

The frequency band of AMT measurement (4.5–27,000 Hz) allows a range of penetration typically from tens of meters at higher frequencies to several kilometers at lower frequencies, dependent on the resistivity of the terrane traversed. Penetration, in meters, for a particular frequency is approximately estimated by an apparent penetration depth $356\sqrt{r/f}$ where f is the frequency in hertz and r is the measured apparent resistivity at that frequency (Bostick, 1977). This apparent penetration depth is the electromagnetic skin depth divided by the square root of 2.

Resistivity-depth sections from AMT sounding data are generally evaluated by deriving a model of the Earth's resistivity structure whose computed response fits the observed sounding curve. Methods of fitting a model to observed responses include simple trial and error "forward" computation, various error-minimizing inversion techniques, and depth-resistivity transforms such as the Bostick "inversion" (Bostick, 1977). The latter consists of a simple transformation from points on the curve showing apparent resistivity versus frequency to points on a curve showing resistivity versus depth (distance). One-dimensional modeling is most commonly employed for AMT data, but two-dimensional modeling is becoming the normal approach for processing MT data, and it can also be used for AMT data. Three-dimensional modeling is feasible but expensive in terms of time and resources. The Bostick one-dimensional transform is used extensively by the USGS because it is highly efficient in terms of computation time and the resulting model can reproduce (generally to within 10 percent) a sounding curve in most cases.

For scaler AMT data, one-dimensional modeling commonly uses the geometric average of the two observed curves at each station, corresponding to the E_x/H_y and E_y/H_x data. However, when these two curves differ substantially, the data indicate lateral changes in resistivity. In such cases, inferences as to the resistivity structure would benefit by two- or three-dimensional modeling to evaluate the consistency of the computed response of inferred structure with the observed response. Such modeling can provide estimates of the uncertainty in the inferred model and can, in some cases, provide information on electrical structure at lateral distances approximately equal to penetration depths. However, because of the cost involved relative to the cost and aims of the survey, such modeling is the exception rather than the rule for scalar AMT data.

AMT SURVEYS IN SOUTHEASTERN ARIZONA

The areas covered by AMT investigations in southeastern Arizona are shown on figure 1. The investigations discussed here are in the Winchester Mountains (area 2), the Dragoon Mountains (area 3), and the Chiricahua Mountains (areas 4A and 4B). Data for these areas cover part of Coronado National Forest. Areas 1A, 1B, and 1C are not discussed, but are relatively close to the Pinaleno unit of Coronado National Forest, and as mentioned above, may be of supplementary value in understanding the use and limitations of the AMT method.

WINCHESTER MOUNTAINS

The Winchester Mountains are a southeast-striking extension of the Galiuro Mountains. These ranges are chiefly underlain by the Oligocene and Miocene Galiuro Volcanics, lava flows and ash-flow tuffs of silicic to intermediate composition that are locally capped by basalt (Wilson and others, 1969; Martin, 1986). The central part of the Winchester Mountains is in the Coronado National Forest.

Ten AMT soundings (fig. 3) were acquired on the west slope of the Winchester Mountains and across the northern part of Allen Flat, an adjoining sedimentary depression separated from the San Pedro Basin by low hills (Martin and others, 1982; Martin, 1986). Two of the soundings (6 and 9) are within the Forest, and three other soundings (5, 7 and 10) are 1–3 km west and south of the Forest. The remaining soundings are on a profile extending westward from the range to the area of Hookers Hot Springs across Allen Flat. Soundings along the profile were spaced at about 1–3 km, whereas the soundings south of the profile, which are within or near the Forest, are about 3–5 km apart.

On the basis of the observed apparent resistivities (fig. 4), which are higher near or within the Winchester Mountains (soundings 6, 9, and 10), Martin and others (1982) suggested that a northwest-striking basin fault flanks the western part of the Winchester Mountains along a line between soundings 7 and 6, 5, and 9, and 5 and 10. The anomalously low apparent resistivities at the lower frequencies (deeper) for soundings 7, 5, and 8 are inferred to represent significant hydrothermally altered rock at depth (Martin and others, 1982) or a thick alluvial section (Martin, 1986).

In order to provide a more quantitative estimate of the resistivity distribution for this report, the observed data

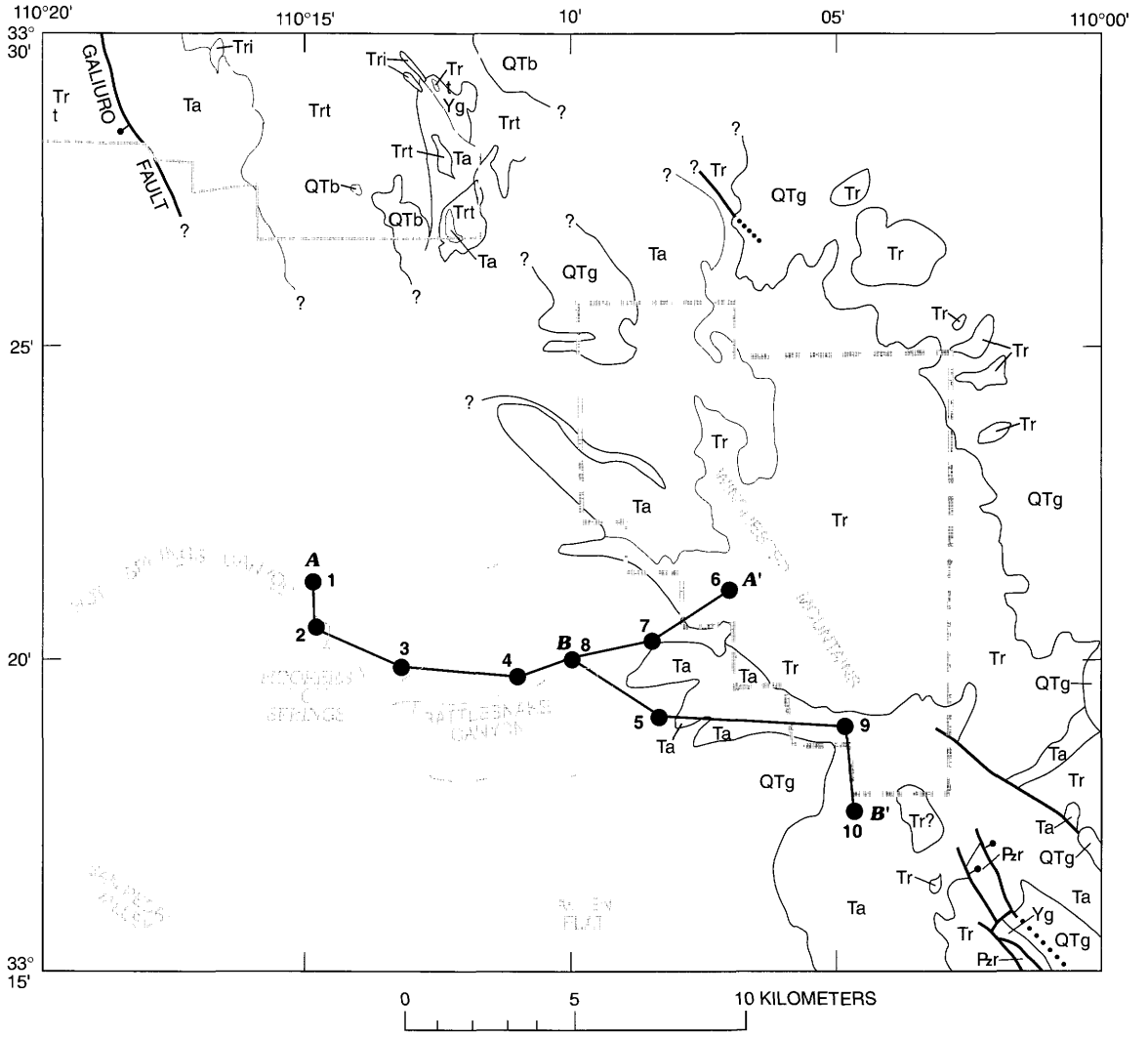

EXPLANATION

- **Boundary of Coronado National Forest**
- ●3 **AMT sounding**
- QTg **Gravel, sand, and conglomerate (Holocene to Miocene)**
- QTb **Basalt (Pleistocene to Miocene)**—Lava flows and cinder deposits
- Tr **Rhyolitic rocks (Miocene and Oligocene)**—Includes lava flows, tuffs, and tuffaceous sandstones
- Tri **Rhyolitic intrusion (Miocene and Oligocene)**
- Trt **Rhyolitic tuffs (Miocene and Oligocene)**—Airfall tuff, ash-flow tuff, tuff breccia, welded tuff, and some sedimentary rocks
- Ta **Andesitic rocks (Oligocene)**—Lava flows, breccia deposits, and interbedded sedimentary rocks
- Pzr **Sedimentary rocks (Paleozoic)**
- Yg **Intrusive rocks (Middle Proterozoic)**—Granite, granodiorite, and some alaskite, aplite, and lamprophyre
- **Contact**—Dotted where concealed; queried where uncertain
- **Fault**—Dotted where concealed; bar and ball on downthrown side

Figure 3. Geologic map showing location of AMT soundings on west flank of the Winchester Mountains, southeastern Arizona (Martin and others, 1982; Martin, 1986). Geology from plate 2; compiled by Harald Drewes, 1991. *A–A′* and *B–B′* are AMT lines of section discussed in text.

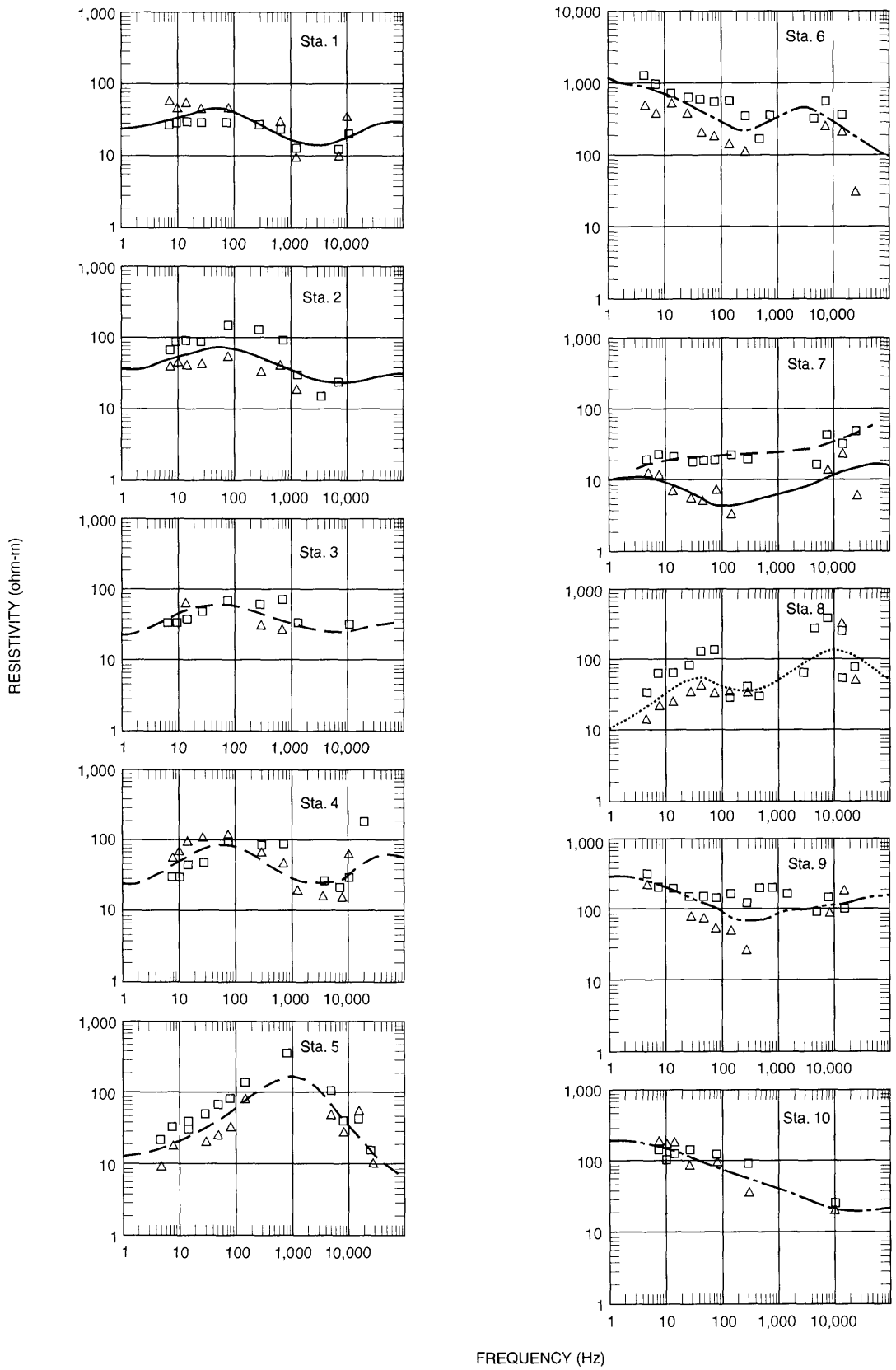

Figure 4. AMT sounding curves for the Winchester Mountains area, southeastern Arizona (Martin and others, 1982). Observed sounding curves shown as triangles and squares (apparent resistivity plotted against frequency for perpendicular electric-line orientations); computed sounding curves from one-dimensional modeling shown as lines. Station locations for sounding curves shown on figure 3.

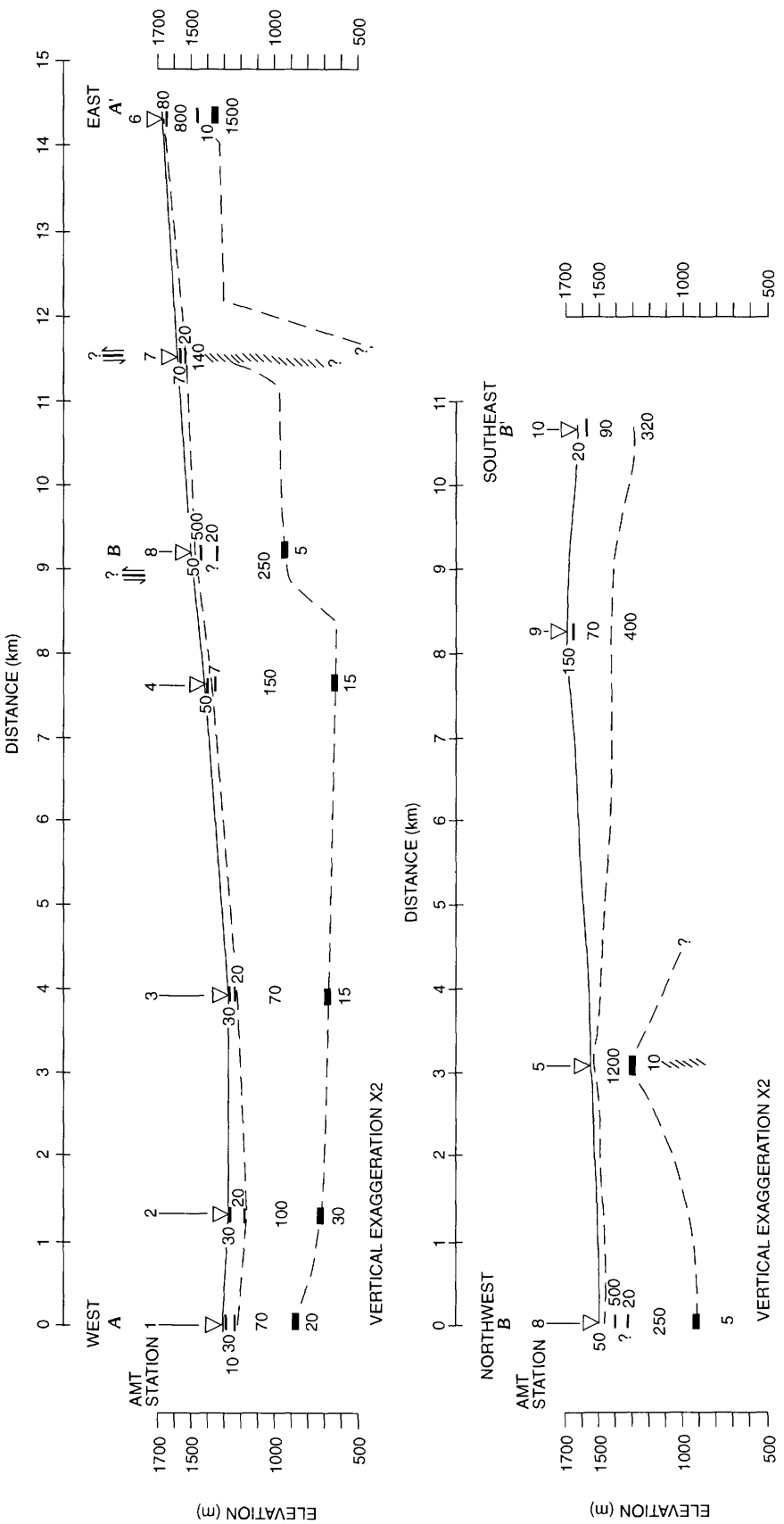

Figure 5. Resistivity-versus-depth cross sections of west flank of the Winchester Mountains, southeastern Arizona. Sections are based on composited one-dimensional modeling of data from Martin and others (1982). The derived one-dimensional models are indicated beneath each sounding (triangle). Dashed lines are interpretive extrapolations between soundings. Numbers within sections (below sounding points) give inferred resistivity (in ohm-m) at the indicated depth intervals.

from each station were modeled. The models for each sounding were generated by one-dimensional forward modeling, by trial and error, to find a resistivity-depth layering that approximately fit the log-average of all data points. The resulting models were composited along two profiles (fig. 5) whose locations are indicated on figure 3. The computed sounding curves for the models are shown with the data on figure 4.

The depth-resistivity sections (fig. 5, profile *A–A′*, soundings 4, 8, 7, and 6) agree in general with the pattern of faults mapped along the west flank of the Winchester Mountains (Martin and others, 1982; Martin, 1986). The depth-resistivity section also allows additional interpretation. From Hookers Hot Springs (stations 1 and 2) to station 7, section *A–A′* shows a fairly uniform 70- to 250-ohm-m layer having a thickness of 400–800 m. This layer is underlain by quite low resistivity material (5–30 ohm-m). The 70- to 250-ohm-m layer is probably volcanic and volcaniclastic bedrock beginning at a relatively shallow depth of several tens of meters. The resistivity of this layer appears too large to represent alluvial basin fill, but it could be conglomerate. The low-resistivity zone beneath this layer may indicate one or a combination of possibilities. The zone may represent rather widespread thermal fluids, perhaps trapped at depth by an impermeable layer that developed by mineral precipitation in the pores of the volcanic rock (or conglomerate). Alternatively, it may indicate a lithologic change to a significantly greater amount of more porous, unwelded and altered tuff. A third possibility is that the volcanic rock overlies older mudstone or clayey sedimentary rock. It is considered most likely that volcanic rocks, combined with fluids probably at an elevated temperature, form this low-resistivity basal zone.

The low-resistivity basal layer rises gently in the vicinity of soundings 1 and 2, a finding that is consistent with upward percolation of thermal fluids to the Hookers Hot Springs area. The low-resistivity zone becomes shallow more abruptly at soundings 7 and 8. These two soundings may be in a fault zone, as postulated by Martin and others (1982). Within this several-kilometer-wide zone it appears that the major splay of the fault zone may be at or near sounding 7, as indicated by the low resistivity there (40 ohm-m or less) and extending upward through all types of rock. In addition, hydrothermally altered rock and pore-fluid content along the fault zone may be responsible for this low resistivity. East of sounding 7, the layer of 70- to 250-ohm-m material is replaced by rock having a resistivity of about 800 ohm-m and underlain by even more resistive basement (1,500 ohm-m). The 800-ohm-m rock is probably volcanic rock equivalent to that inferred for the 70- to 250-ohm-m layer in the basin, but less altered; it is well drained above the water table and perhaps contains a larger fraction of resistive lava flows.

Section *B–B′* (fig. 5) shows a distinct increase in resistivity for the second layer from sounding 5 eastward; data are sparse but consistent. This change in resistivity may partly be related to the northwest-striking range-front fault postulated by Martin and others (1982), where higher resistivities of the deepest layer conform to lava flows or basement rock and perhaps equally resistive overlying Paleozoic carbonate sedimentary rocks. Except for sounding 5, the modeled resistivities along the near flank of the Winchester Mountains (soundings 9 and 10) show two layers. The upper layer is predominantly 70–90 ohm-m (typical of volcanic rocks) and is 400 m thick at sounding 10; it appears to thin toward sounding 5. The underlying higher resistivity layer appears to have resistivity values of 300–400 ohm-m, except at sounding 5, where the value is 1,200 ohm-m. The higher resistivity values, 300–1200 ohm-m, are consistent with Paleozoic sedimentary rocks and Proterozoic granite, which crop out in a horst a few kilometers east of sounding 10.

An unusual feature of the model for profile *B–B′* at sounding 5 is a high-resistivity zone extending from near the surface to about 400 m depth; the zone is overlain and underlain by very low resistivity material (fig. 5). This anomalous sounding is on the border of a complex magnetic anomaly, generally high, which forms a northeast-striking gradient normal to the postulated range-front fault (Martin, 1986). Inasmuch as sounding 5 is about equidistant from the range as sounding 8, the geophysical signature of the range-front fault at sounding 5 may be overwhelmed by another structure. The high resistivity zone, coincident with a magnetic anomaly, indicates the possible existence of a magnetic and resistive outflow ash-flow tuff or intrusion. Most unaltered lava flows are resistive independent of composition, but the magnetic anomaly may indicate a basaltic to dacitic composition of a probable source rock. The lowered resistivity at a depth of about 400 m suggests an altered basal zone of the intrusion or flow unit.

DRAGOON MOUNTAINS

The northern Dragoon Mountains (fig. 6) comprise one of a series of ranges extending south-southwest from the Galiuro Mountains. In the more northerly parts of the Dragoon Mountains, outcrops are intensely faulted Paleozoic and Cretaceous sedimentary rock (Drewes and Meyer, 1983) that is intruded by small Miocene granitic bodies and dikes. The Golden Rule Mine, at the extreme northern part of the range, is near one of these intrusions. South of Mount Glenn, outcrops are predominantly composed of a large Miocene granitic pluton. A northwest-striking septum of Proterozoic through Lower Cretaceous rocks separates the outcropping pluton into two major lobes. The eastern lobe of the pluton is intruded by a swarm of northwest-striking rhyolitic dikes.

Exposed Paleozoic and Cretaceous sedimentary and Tertiary granitic rocks in the northern Dragoon Mountains contrast significantly in lithology with volcanic rocks traversed by AMT soundings discussed for the Winchester

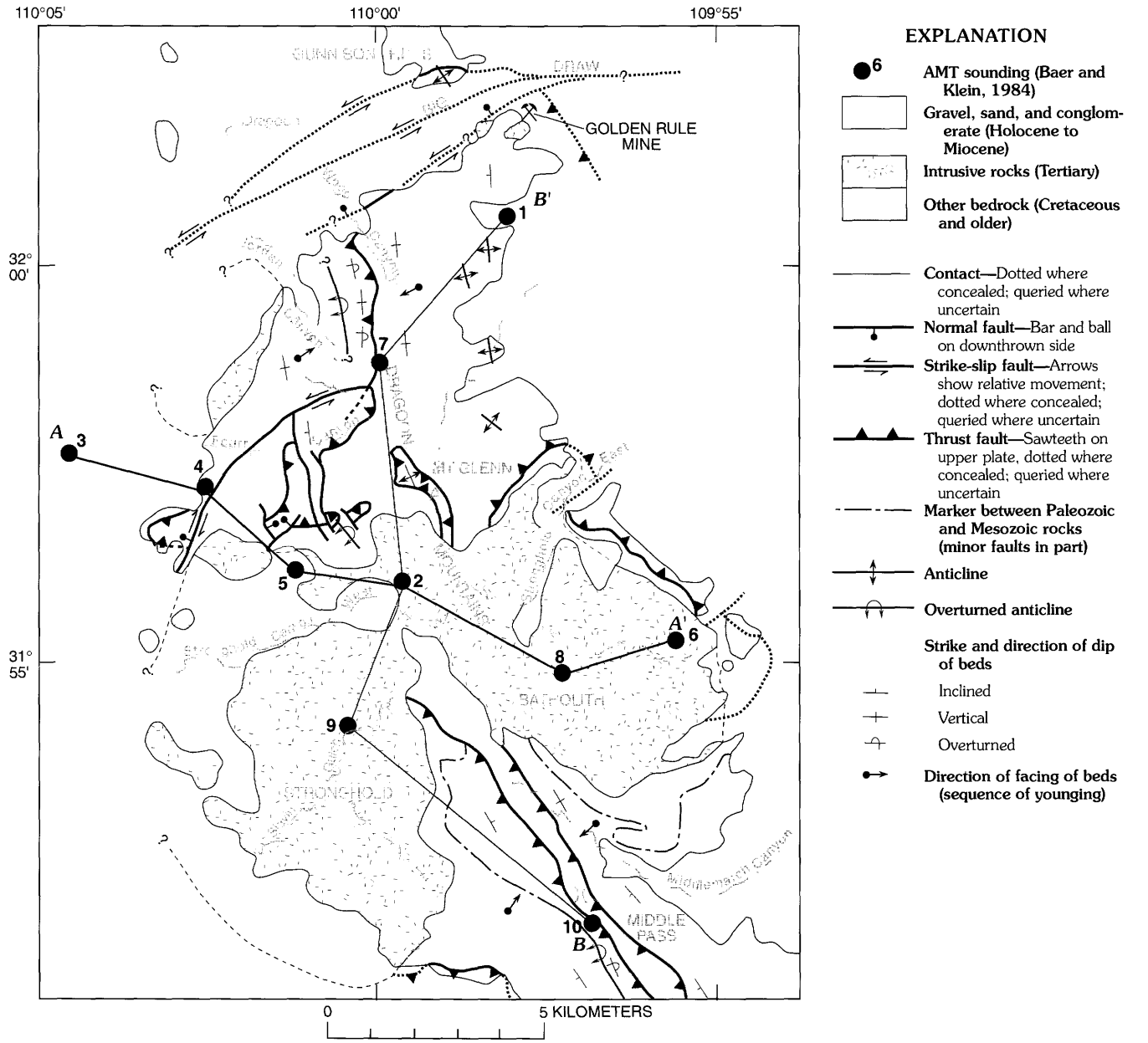

Figure 6. Geologic map showing location of AMT soundings in the northern Dragoon Mountains, southeastern Arizona (Baer and Klein, 1984). Generalized geologic structure from Drewes and Meyer (1983). *A–A'* and *B–B'* are AMT lines of section discussed in text.

Mountains. This geologic contrast is strongly reflected in resistivity data.

Figure 6 shows the location of 10 AMT soundings acquired across the northern Dragoon Mountains (Baer and Klein, 1984) spaced approximately 5 km apart. Most of the soundings are within the Dragoon Forest unit. The report by Baer and Klein (1984) provides contoured cross sections of modeled resistivity values and contoured planar maps of observed apparent resistivity values; however, little is offered in the way of interpretation of these data.

Sounding curves from the northern Dragoon Mountains are summarized on figure 7. In this representation, which is modified from that presented in Baer and Klein (1984), crosses represent the spread of apparent resistivity and frequency values for the two observed apparent-resistivity curves across three independent frequencies. The soundings are arranged in order corresponding to the east-west (*A–A'*) and south-north (*B–B'*) profiles shown on figure 6. The one-dimensional depth-resistivity models (from table 2 of Baer and Klein, 1984) along the profiles are shown along a cross section (fig. 8). Shallow modeled layers for soundings 4, 5, and 6 are not shown on figure 8. The uppermost layers for these three stations have high resistivity (700–5,000 ohm-m) and are less than 15 m thick. These layers may be

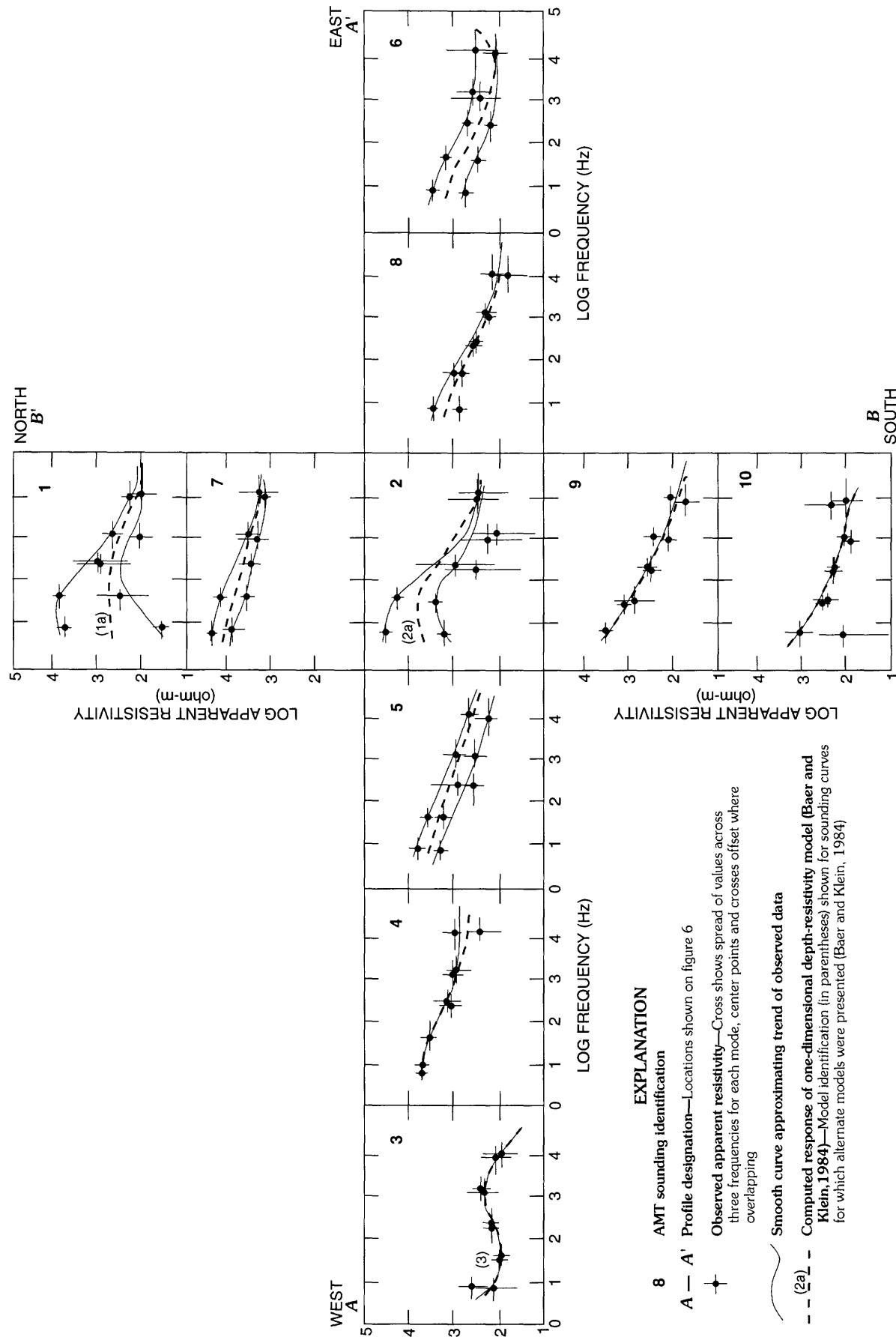

Figure 7. Summary of AMT sounding curves 1–10 (see fig. 6) in the northern Dragoon Mountains, southeastern Arizona (Baer and Klein, 1984). For soundings 1, 2, and 3, Baer and Klein (1984) showed two models; models shown here are their models 1a, 2a, and 3. Lines of section *A–A'* and *B–B'* are shown on figure 6.

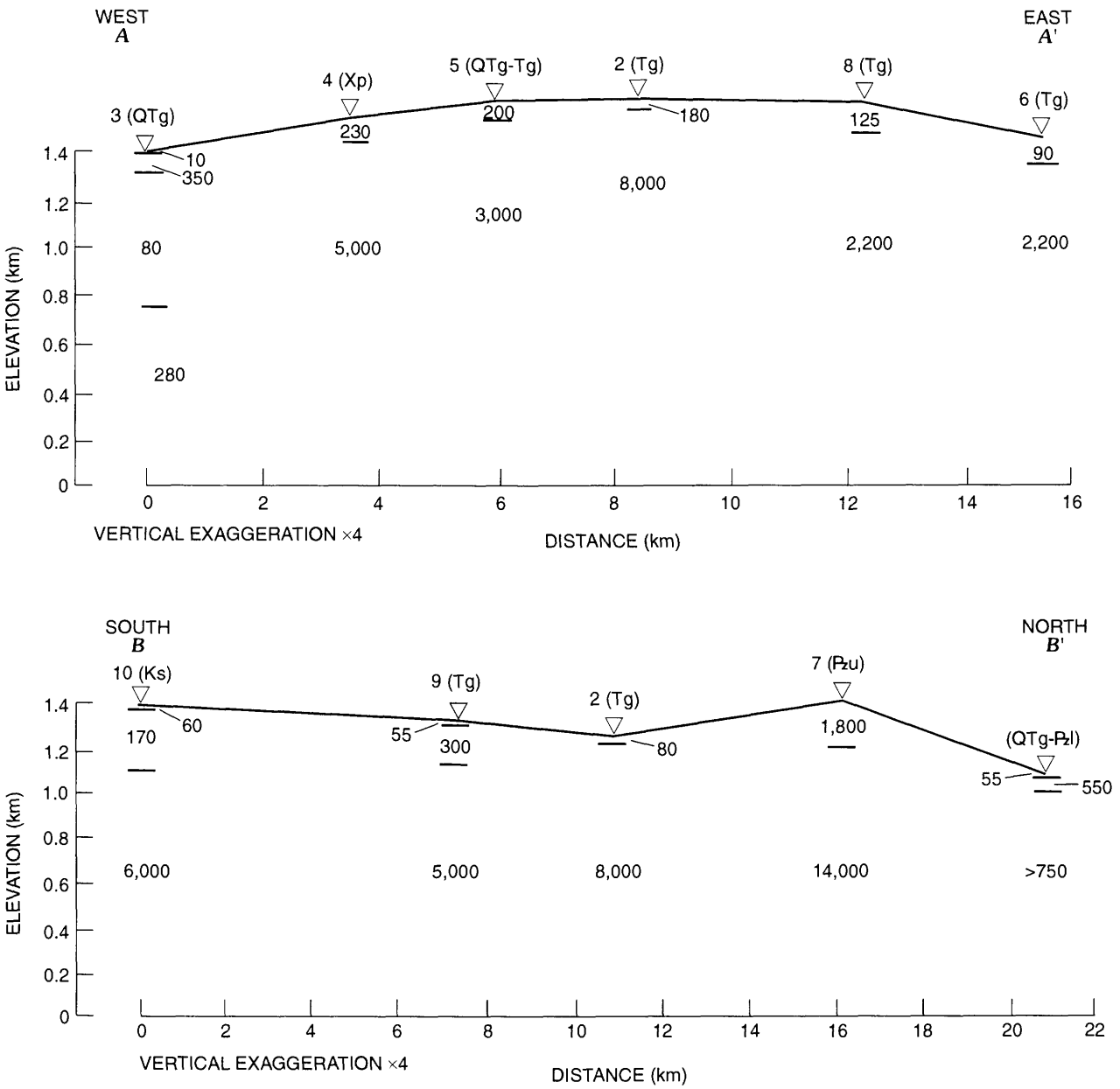

Figure 8. Resistivity-versus-depth cross sections from AMT soundings (triangles) in the northern Dragoon Mountains, southeastern Arizona. Lines of section *A–A'* and *B–B'* are shown on figure 6. The models of Baer and Klein (1984) neglect the surface layer for soundings 4, 5, and 6 (see text). Geologic units modified from Drewes and Meyer (1983): QTg, Holocene to Miocene gravel, sand, and conglomerate; Tg, Tertiary granite; Ks, Cretaceous sedimentary rocks, chiefly clastic; Pzu, upper Paleozoic sedimentary rocks, chiefly carbonate; Pzl, lower Paleozoic sedimentary rocks, chiefly clastic; Xp, Early Proterozoic metasedimentary rocks. Numbers within sections (below sounding points) give inferred resistivity (in ohm-m) at the indicated depth intervals.

artifacts of the modeling method of Baer and Klein (1984) inasmuch as the trends of the data (fig. 7) do not seem to require them. Several of the sounding curves (1, 2, 5, 6 and 7) show a significant and consistent separation between the two curves (fig. 7). This separation between curves, nearly a constant shift across all frequencies on soundings 5 and 6 (fig. 7), indicates resistivity contrasts whose sources lie at some distance from the sounding location and cannot be accounted for in one-dimensional modeling. Such separations are fairly common in MT-AMT data, particularly for resistive terrane where lateral and vertical penetration of electromagnetic fields is large (Sternberg and others, 1988; Klein, 1991).

Two primary characteristics of the resistivity distribution are indicated by nearly all of the models (fig. 8); soundings 1 and 3 on profiles *B–B'* and *A–A'*, respectively, were acquired on alluvium and are exceptions that will be

discussed below. The first characteristic of the models is extremely high resistivity (2,200–14,000 ohm-m; averaging about 5,000 ohm-m) at a depth greater than about 300 m. This high resistivity is typical of dry bedrock composed of compact, unaltered gneiss, granitic intrusions, or carbonate sedimentary rocks.

The second characteristic of the models for the northern Dragoon Mountains is that the highly resistive rock is overlain by a zone of lower resistivity, ranging from 50 to 300 ohm-m (except at station 7, 1,800 ohm-m). The resistivity of this upper layer is about an order of magnitude lower than the resistivity of deeper rock; its interpretation is partly dependent on the geologic setting of each sounding. This uppermost zone of low resistivity for soundings on granite outcrops (Tertiary intrusive rocks, fig. 6) probably represents the more fractured, weathered, or altered zone of this rock and may include a thin layer of talus or soil. The uppermost layer for soundings over sedimentary rock (4, 7, and 10) is believed to represent the combined thickness of the sedimentary rock and an altered and fractured zone at the intrusive contact. At sounding 7, the upper layer has a resistivity of 1,800 ohm-m, but this is still relatively low compared to the underlying 14,000-ohm-m zone. This 1,800-ohm-m layer is consistent for rock composed largely of massive limestone of the Pennsylvanian and Permian Naco Group (Drewes and Meyer, 1983). As indicated, the uppermost modeled layer at soundings 4, 10, and 7 represents in part the thickness of sedimentary or metasedimentary overburden above plutonic rock whose presence is inferred from geologic relations. However, as illustrated (fig. 8), the resistivity values for these layers are not much different from those for the upper layer seen for soundings on granite. Therefore, this layer is best interpreted as showing an upper limit to the thickness of the associated (exposed) sedimentary or metasedimentary rock.

Soundings 1 and 3, both acquired on alluvium, contrast significantly with the pattern discussed above. The model at sounding 1 on profile *B–B′*, near the northeastern part of the range, is consistent with a thin alluvial layer (58 ohm-m) overlying Paleozoic clastic sedimentary rock (550 ohm-m). Most rocks within 1 km of this sounding consist of lower Paleozoic formations (unit Pzl of Drewes and Meyer, 1983). Presumably, this is the unit represented by the 550-ohm-m layer; its maximum thickness here is inferred to be about 100 m. The shift between the two curves at this sounding is large (fig. 7) and results in considerable uncertainty as to the maximum thickness. The second layer is underlain by more resistive rock, at least 750 ohm-m, assumed to be metamorphic or intrusive rock. The large shift between the two observed apparent-resistivity curves indicates a major lateral-resistivity contrast, which may imply a nearby fault associated with altered rock having low resistivity or may simply imply conductive alluvium against resistive bedrock. Without additional nearby soundings, the shift precludes an accurate estimate of the geometry and properties of deep interfaces at either a vertical or lateral distance from the sounding. This sounding, however, is enclosed by an area having significant aeromagnetic and gravity gradients, both of which seem to attain maxima near the intrusions at the Golden Rule Mine (Klein, 1983). The gradients are consistent with either a shallow intrusion or Proterozoic basement in the northernmost part of the Dragoon Mountains.

Sounding 3 on profile *A–A′* (fig. 7) was made about 5 km west of the range. The model (fig. 8) indicates an upper, thin 10-ohm-m unit, a second layer of more resistive 350-ohm-m rock in the upper 100 m, which is underlain by a conductive zone, and finally a high resistivity unit, at least 350 ohm-m at the lowest observed frequency. The uppermost 10- and 350-ohm-m units probably represent fine-grained basin deposits and conglomerate, respectively. The deep resistive rock (350 ohm-m) may be metamorphic, intrusive, or carbonate sedimentary rock. A band of Cretaceous and Tertiary granitic intrusive rock along the northwestern edge of the northern Dragoon Mountains may underlie the basin to the west. Neither aeromagnetic nor gravity data show a distinctive signature for the intrusive rock along the northwestern edge of the Dragoon Mountains (Klein, 1983). However, this intrusion is associated with gravity and aeromagnetic gradients that decrease westward into the basin toward a pronounced aeromagnetic low in the vicinity of sounding 3. Klein (1983) suggested that this aeromagnetic low is consistent with a silicic intrusion in bedrock below basin fill.

The conductive unit (80 ohm-m, about 500 m thick) starting at a depth near 100 m, is an intriguing part of the model for sounding 3. The data require a conductive unit, but the only well-resolved parameter is its conductance (thickness divided by resistivity). For instance, there may be a much more conductive (10 ohm-m), thinner (70 m) layer at a depth of about 230 m that would be equally consistent with the data. Possible constituents of this conductive zone are a layer of wet volcanic ash, brine at the base of the inferred conglomerate, or a zone of altered rock at the top of an intrusion. The latter is preferred, inasmuch as similar conductivity is seen on the upper parts of intrusions exposed in the Dragoon Mountains (discussed above). At depth, the weathered and altered zone would be wet and probably more conductive than a geologically similar zone in the well-drained environments high in the range.

NORTHERN CHIRICAHUA MOUNTAINS

The northern Chiricahua Mountains are composed of a geologically complex terrane having similarities to the northern Dragoon Mountains and the volcanic terrane of the central Chiricahua Mountains (discussed below) (Drewes, 1980; Drewes and others, 1988). Exposed rocks include Proterozoic gneiss, Paleozoic sedimentary rocks, Cretaceous and Tertiary volcanic rocks, and Cretaceous–early Tertiary

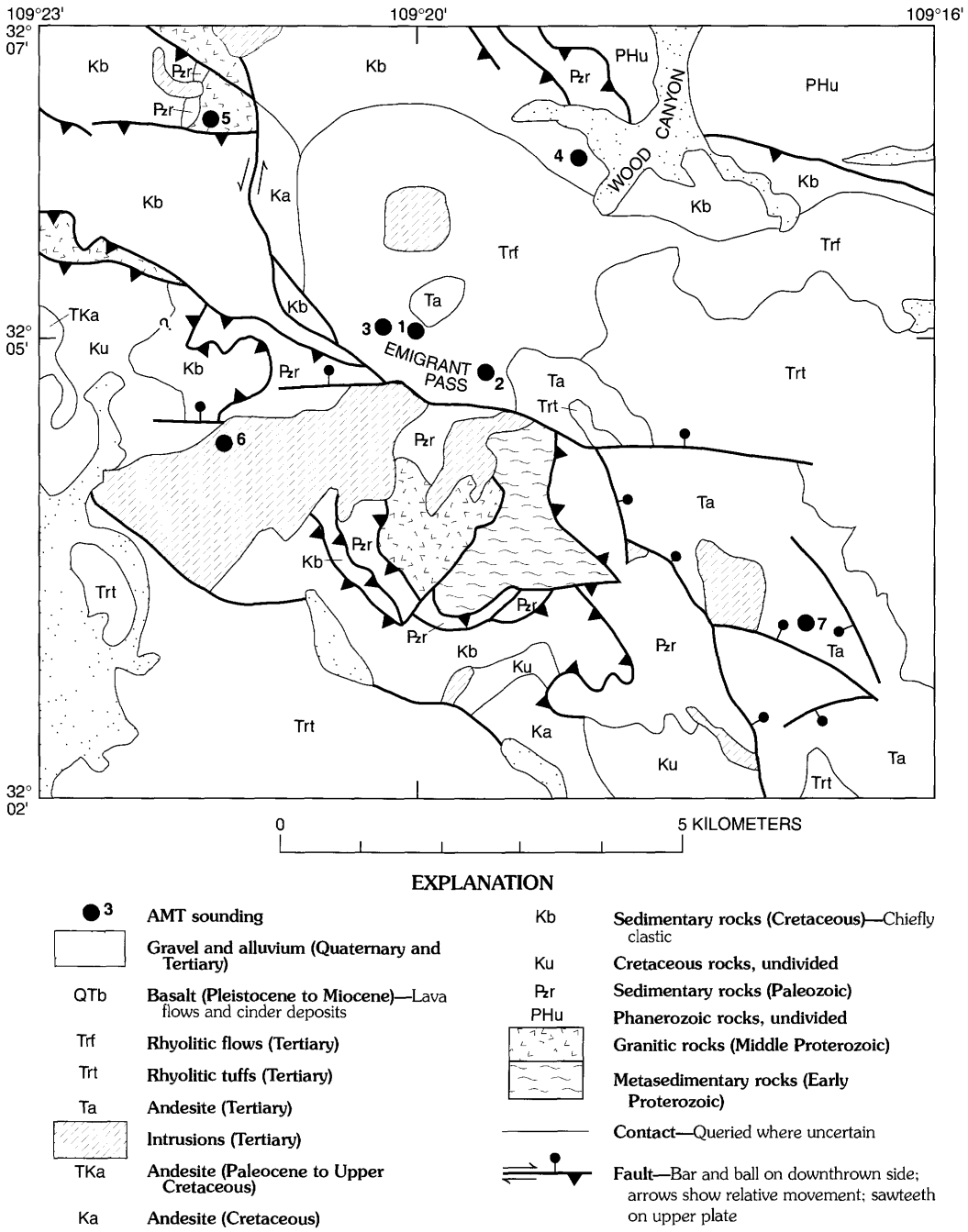

Figure 9. Geologic map showing location of AMT soundings in the northern Chiricahua Mountains (Emigrant Pass area), southeastern Arizona (Nervick and Boler, 1981). Generalized geology from Drewes (1980) and from Drewes and others (1988).

and middle Tertiary granitic intrusions. Structures include thrust faults that juxtapose rocks of various lithologies similar to those in the northern Dragoon Mountains. This part of the Chiricahua Mountains (fig. 9) extends east-southeast along the trend of the Doz Cabezas Mountains and is probably quite similar to the Dos Cabezas geologic environment described by Drewes and others (1988). This area is at the east end of the Dos Cabezas Mountains, which trend more westerly than most ranges in southeastern Arizona. This trend may have been influenced by the dominant

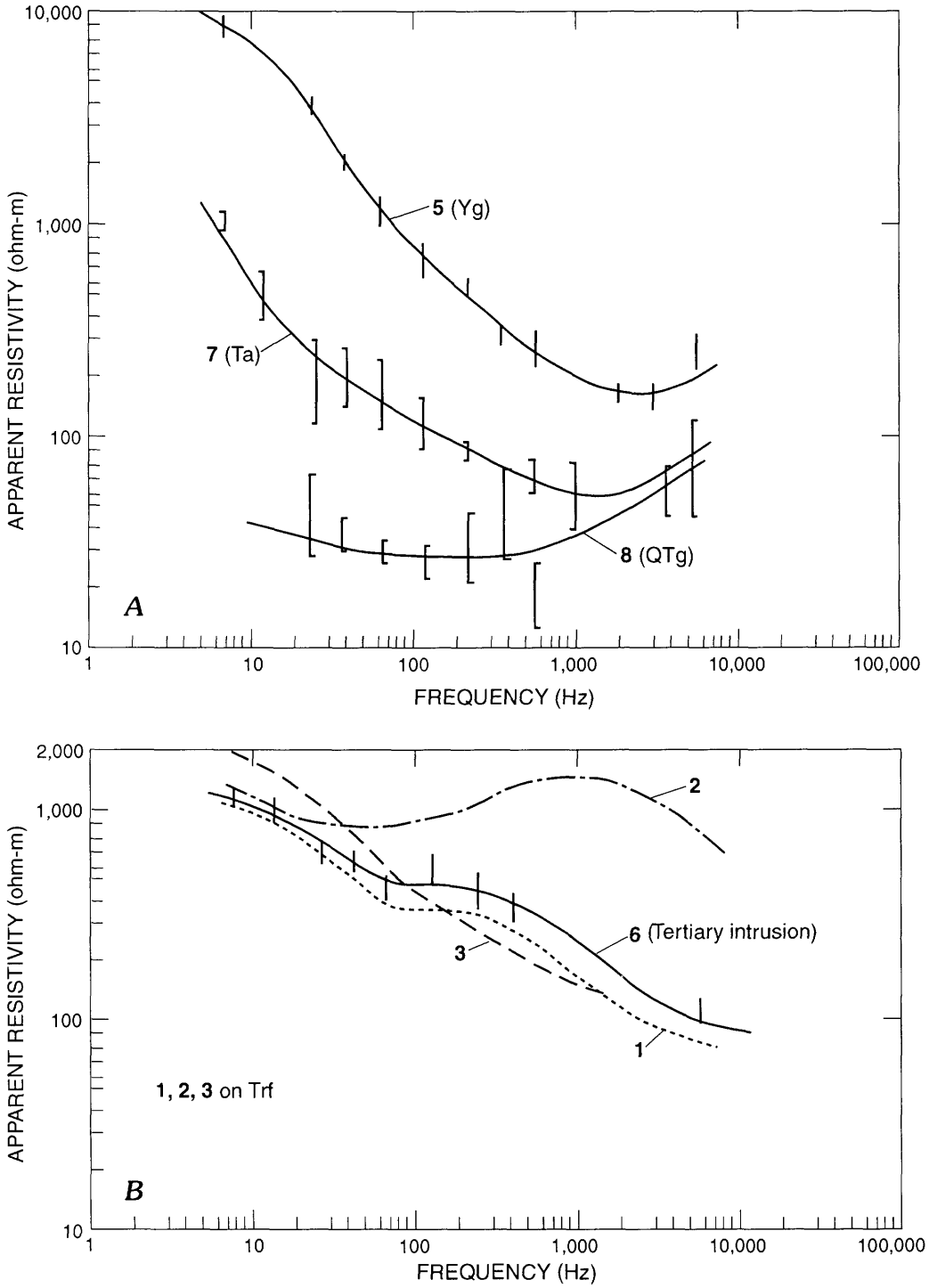

Figure 10. Examples of AMT sounding curves in the northern Chiricahua Mountains (Nervick and Boler, 1981), southeastern Arizona. Bars indicate the spread of values for the two apparent resistivity modes at each frequency except for soundings 1, 2, and 3, whose curves are shown schematically. Sounding locations are shown on figure 9, except for sounding 8, which is located on alluvium to the northeast, off the map. *A*, Soundings on various lithologic types surrounding the Emigrant Pass area. *B*, Soundings on volcanic rock in the Emigrant Pass area. QTg, Quaternary and Tertiary gravel and alluvium; Trf, Tertiary rhyolite flows; Ta, Tertiary andesite; Yg, Middle Proterozoic intrusive rocks.

Table 1. Resistivity-versus-depth models for AMT data for the northern Chiricahua Mountains, southeastern Arizona.

[Models shown here are representative of the Bostick transform (Bostick, 1977) of the sounding curves for each data set from Nervick and Boler (1981). Layers are queried where they may be in question due to possible lateral resistivity contrasts. Outcrop lithology is based on Drewes (1980) and Drewes and others (1988). Qa, Quaternary gravel and alluvium; Tv, Tertiary volcanic rocks, undivided; Tg, Tertiary granite; Pzu, upper Paleozoic carbonate sedimentary rocks; Yg, middle Proterozoic granitic rock]

Station No.	Rock unit	Resistivity (ohm-m)	Depth range (m)
Outlying soundings			
4	(Pzu)	170	Surface to 170
		250	120-360
		1,250	360 to more than 1,500
5	(Yg)	80	Surface to 90
		18,000	90 to more than 3,000
7	(Tv)	60	Surface to 110
		300	110-280
		6,500	280 to more than 3,000
8	(Qa)	60	Surface to 30
		15	30-80
		60	80 to more than 300
6	(Tg)	140	Surface to 40
		1,800	40-400 (or 900)
		400?	400-900
		2,500	900 to more than 3,000
Soundings on Emigrant Pass			
1	(Tg)	130	Surface to 90
		1,500	90-380 (or 530)
		500?	380-530
		1,800	530 to more than 3,000
2	(Tg)	800	Surface to 60
		2,500	60-580 (or 1,500)
		500?	580-1,500
		1,900	1,500 to more than 3,000
3	(Tg)	100	Surface to 70
		2,000	70-380 (or 890)
		700?	380-890
		4,000	890 to more than 3,000

structure along strike, the Apache Pass fault zone (Drewes and others, 1988). The more northerly striking faults shown on figure 9 merge into the Apache fault zone of the Dos Cabezas Mountains. This south-southeast trend of the northern Chiricahua range abruptly changes to a more northerly trend just south of the area shown on figure 9.

The seven AMT soundings whose locations are shown on figure 9 were acquired by the USGS as part of an investigation of the Northend Wilderness area (Nervick and Boler, 1981). These soundings are largely within Coronado National Forest (area 4A of fig. 2). Three closely spaced soundings are on volcanic rock in the Emigrant Pass area, and four more widely spread soundings are on various lithologic units (fig. 9). The three soundings on Emigrant Pass are just north of a Tertiary intrusion. One additional sounding is eastward of the map area on alluvium in the San Simon Valley.

Figure 10 summarizes the observed AMT data acquired in the northern Chiricahua Mountains (Nervick and Boler, 1981). The bars (fig. 10) indicate the spread of data for both modes at each observed frequency. Soundings on Proterozoic gneiss (sounding 5), on Tertiary volcanic or sedimentary rock in the southeastern area of the survey (sounding 7), and on alluvium (sounding 8, out of the map area of fig. 9) are compared on figure 10*A*. Sounding 4, not shown on figure 10, is on Cretaceous sedimentary rock, and the data are similar to sounding 7 except for higher apparent resistivity at the higher frequencies (a near-surface layer). Soundings on Tertiary granitic rock (sounding 6) or that are believed to be influenced by Tertiary granitic rock (soundings 1, 2, and 3) are compared on figure 10 *B*.

Nervick and Boler (1981) inspected the apparent-resistivity sounding curves and noted the high resistivity (greater than 1,000 ohm-m) of basement rocks implied by the rapid increase in the apparent resistivity at lower frequencies for all soundings except 8 (on alluvium). They also noted generally low surface resistivities implied by the higher frequency apparent-resistivity values, which in most cases are considerably less than 100 ohm-m. The lower near-surface resistivities were attributed to possible alteration along intrusive contacts or fault zones.

For this report, a Bostick transform (Bostick, 1977) was applied to the data to obtain an indication of the resistivity relations at depth implied by the data in the northern Chiricahua Mountains. Table 1 summarizes results of the analysis. The models show representative resistivities across a range of depths rather than listing the full transform, which provides depth and resistivity values for each frequency.

Sounding 5 (figs. 9 and 10; table 1), on Proterozoic gneiss, suggests that most of this rock has a resistivity exceeding 10,000 ohm-m. The high-resistivity unit is overlain by a body of low resistivity rock about 90 m thick that is believed to be a zone of surficial fracturing and weathering. This upper layer is characteristic of weathered, exposed granitic rock such as the previously described Tertiary granite of the Dragoon Mountains. Except for sounding 8 (on alluvium), other soundings on various types of rock also show a high-resistivity basement, varying from about 1,250 to 6,500 ohm-m. The curves do not show an appreciable leveling at the low frequencies, which suggests that resistivities at depths of a few hundred meters or more may approach that modeled for sounding 5. The uppermost layers in soundings on sedimentary or volcanic rock (for instance, soundings 4 and 7) indicate an approximate upper limit for the thickness of such rock (see table 1).

Soundings 1, 2, and 3 are important in that they were acquired north of the Apache Pass fault zone, and are relatively near a fault-bounded intrusion just to the southwest (fig. 9). Data for these soundings at Emigrant Pass are compared to sounding 6, located directly on outcrops of Tertiary granite (fig. 10). The data for soundings 1, 2, and 3 differ significantly from other soundings on sedimentary or volcanic cover; they show a rapid rise of apparent resistivity from 10,000 to 1,000 Hz and indicate a buried layer at intermediate depth in a zone of lower resistivity at a frequency of about 100 Hz (a depth of about 300–500 m, table 1). On table 1 the layer of lower resistivity is queried as possibly being related to a lateral contrast; however, all of the data in this subset show the apparent conducting layer (fig. 13, bottom). The layer having lower resistivity (conductance values from 0.3 to 1.8 siemens) probably occurs in the range of 300–900 m (perhaps 600–1,500 m at sounding 2) deep. The data may indicate an altered zone within fractured or brecciated parts of an intrusive rock or a basal contact of the intrusion.

CENTRAL CHIRICAHUA MOUNTAINS

The central Chiricahua Mountains, which are south of the area discussed above, are underlain by a volcanic terrane, part of which includes the middle Tertiary Turkey Creek caldera (Pallister and du Bray, 1988). Investigations of this caldera have included AMT traverses (Senterfit and Klein, 1992).

The location of 32 AMT soundings and the traverse designations within or peripheral to the Turkey Creek caldera are shown on fig. 11. Most of these soundings are within Coronado National Forest and are closely spaced, roughly 0.5 km apart, composing a more detailed AMT investigation than those previously discussed. The soundings acquired in this area allow fairly accurate lateral correlation of near-surface resistivity structure with geologic mapping and more reliable inferences concerning the continuity of possible relations between geology and geoelectric structure.

The goals of these soundings were to define the electrical signature of the well-mapped eastern boundary of the caldera and to attempt to recognize similar signatures to the north and west, where the geologically inferred boundaries of the caldera (fig. 11) are speculative. On the east, geologic mapping clearly shows an elongate body of dacite porphyry, inferred to overlay a ring-fracture intrusion in the structural margin of the caldera. Similar dacite porphyry is mapped in the center of the caldera (fig. 11) and is inferred to comprise an intrusive, resurgent laccolith (Pallister and du Bray, 1988). On the north, the inferred boundary of the caldera is largely covered by rhyolite moat deposits and intracaldera tuff, whereas the inferred boundary on the west is largely beneath alluvium. The geologic setting here, particularly on the east where Cretaceous sedimentary rocks outcrop and Paleozoic rocks may be concealed at depth, is favorable for the occurrence of epithermal vein deposits associated with hydrothermal activity and hosted by faulted or brecciated rocks.

Figure 12*A* shows a composite resistivity cross section for the northeastern section of the Turkey Creek caldera. This figure merges sections *A–A′*, *B–B′*, and *D–D′* (Senterfit and Klein, 1992) to provide an overall view of the resistivity structure. This cross section was constructed as a composite of Bostick transforms as was described earlier in this chapter. Figure 12*B* shows a schematic interpretative section in which representative resistivities are keyed to possible lithology and structure. Profile *C–C′* (fig. 11) is not shown here. Section *C–C′* showed some similarity to the western part of *D–D′*, but it also displayed more variability, which suggested distortions in the one-dimensional modeling that may have been related to topographic relief along this profile rather than geologic associations.

Outcrops along the profile define geologic relations to a depth of 100 m (fig. 12*B*). Although the interpretation is less certain at greater depth, the resistivity structure is believed to be well constrained. However, possible distortions due to two- and three-dimensional structures have not yet been defined by modeling, so this electric structure remains tentative. The mapped intrusive area on the northeast boundary was traversed by soundings 15, 13, 4, 14, and 9. As seen near the surface at sounding 4 and deeper at other soundings, unaltered intrusive rock in this area has resistivity of about 1,600 ohm-m or more. Variability across this zone is discussed below.

A significant thickness of near-surface welded tuff having relatively low resistivity (less than 160 ohm-m) is indicated by soundings 23, 22, 19, and 21 in the far north. The resistivity increases to perhaps 400 ohm-m at a depth of 1–2 km and may indicate more densely welded units. The apparent smoothness of the increase in resistivity to a depth of 2 km, and possibly deeper, is not constrained; sharp contrasts (layers) are not defined by Bostick transform. Alternative layered models, similar to the schematic (fig. 12*B*), that are also consistent with the data could be developed. The data, however, do not allow high-resistivity units (exceeding 1,000 ohm-m; such as unaltered dacite porphyry intrusions or basement) above a depth of at least 2 km. The data indicate gradually varying structure along this section of the profile and suggest that lateral effects are not likely to have caused significant distortion in the one-dimensional modeling.

Strong lateral changes in electrical structure along the section from soundings 20–8 (fig. 12) make for more uncertainty in details concerning the deeper structure, but the major features are probably resolved adequately for generalized conclusions. A fault between soundings 21 and 20 is reflected in the data by the disappearance of the upper 100- to 160-ohm-m unit (moat rhyolite lava flows and tuff) and the presence of an inferred zone of fractures, brecciation, and altered rock at a depth greater than about 1.5 km. A similar deep zone is inferred from the low resistivities beneath sounding 13, near the mapped ring structure. A landslide

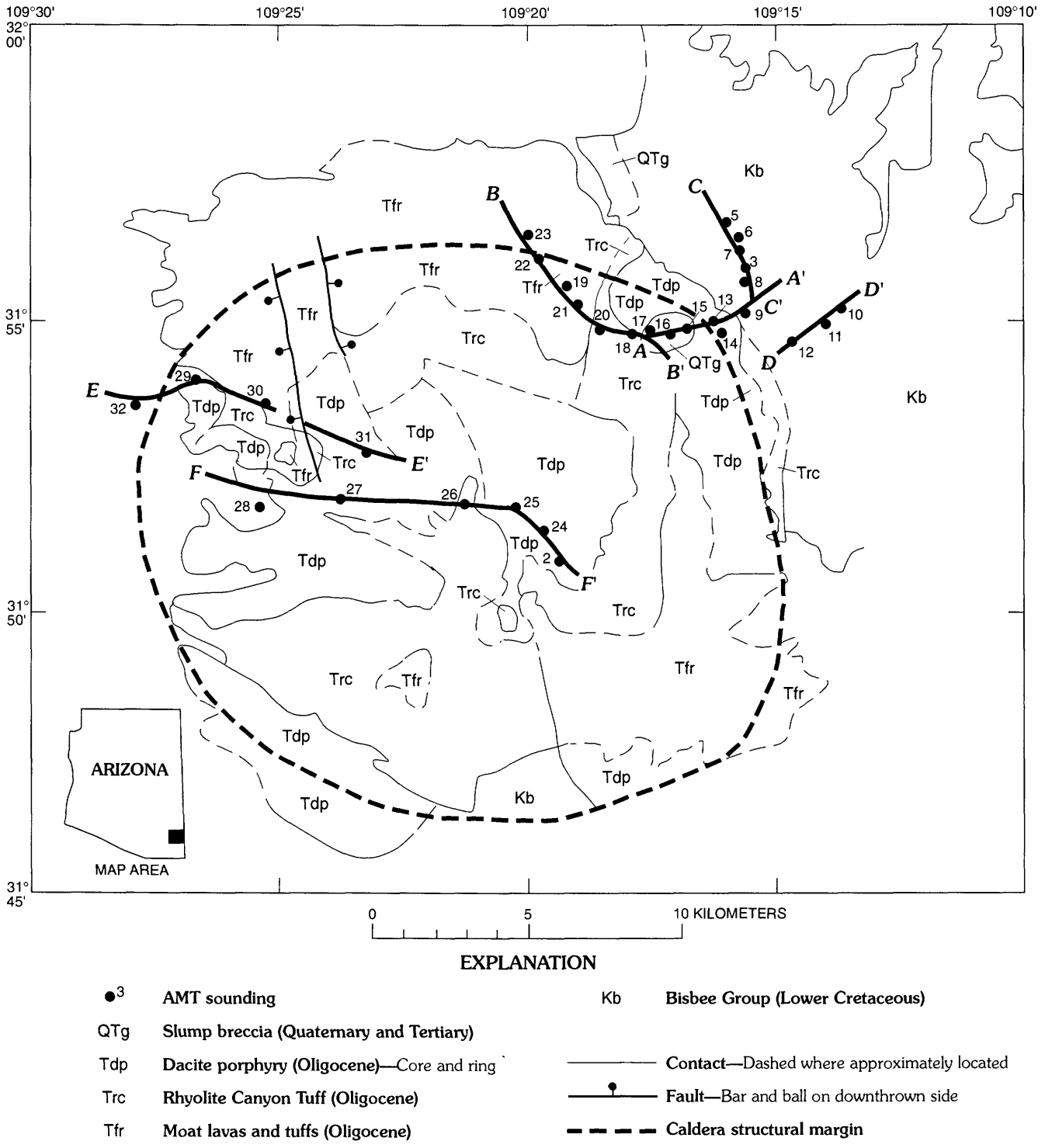

Figure 11. Geologic map showing location of AMT soundings and traverses in the Turkey Creek caldera, central Chiricahua Mountains, southeastern Arizona (Senterfit and Klein, 1991). Generalized geology from Pallister and du Bray (1988). *A–A′* through *F–F′* are AMT lines of section discussed in text.

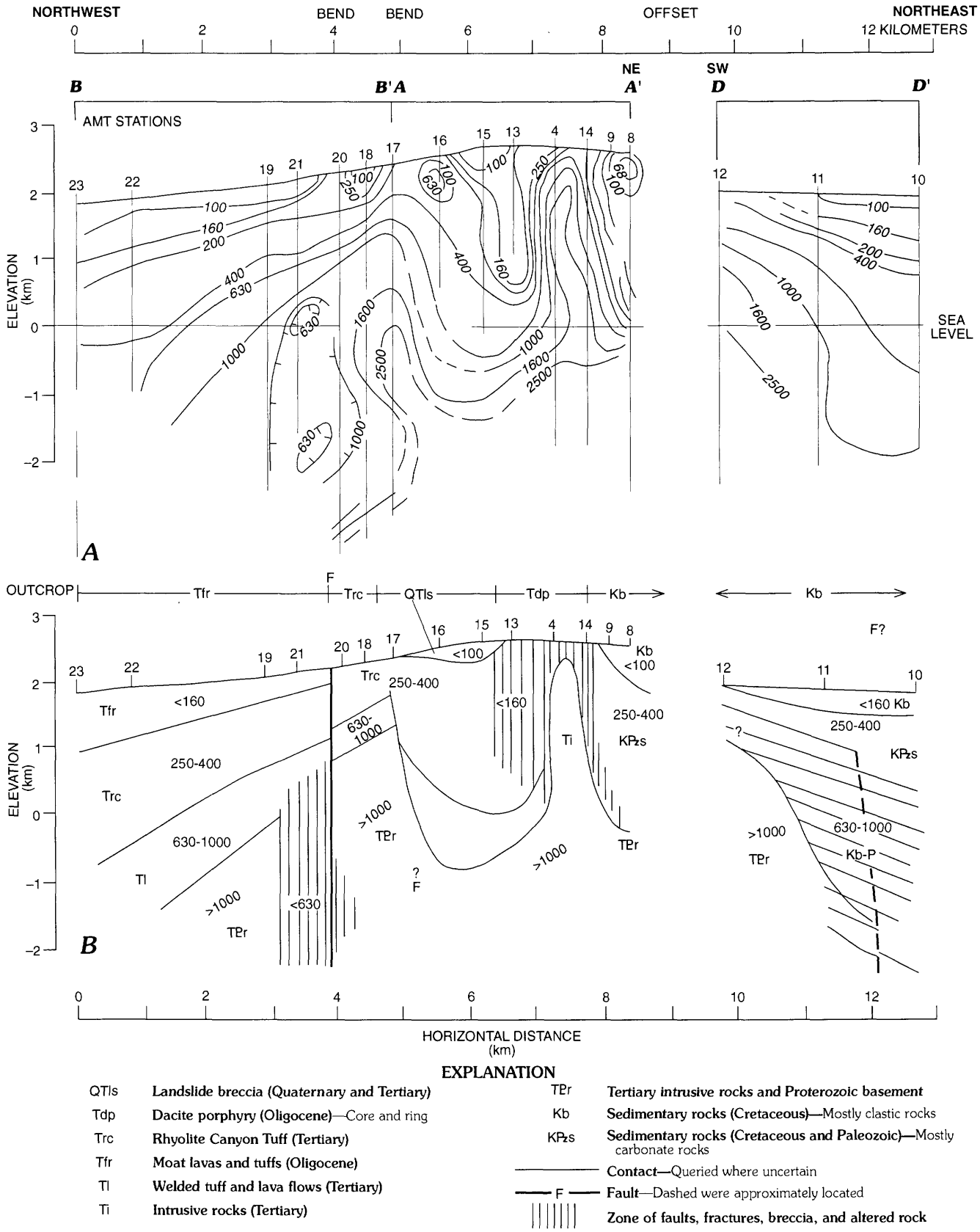

Figure 12. Depth-versus-resistivity cross sections from AMT soundings across the northern and eastern margins of the Turkey Creek caldera, central Chiricahua Mountains, southeastern Arizona (Senterfit and Klein, 1991). *A*, Composite section compiled for soundings along AMT sections *A–A′*, *B–B′*, and *D–D′*. Contours show lines of equal resistivity (indicated values in ohm-m), dashed where uncertain. *B*, Hypothetical geologic-resistivity section constructed by interpretation of sounding data along AMT profile *F–F′*.

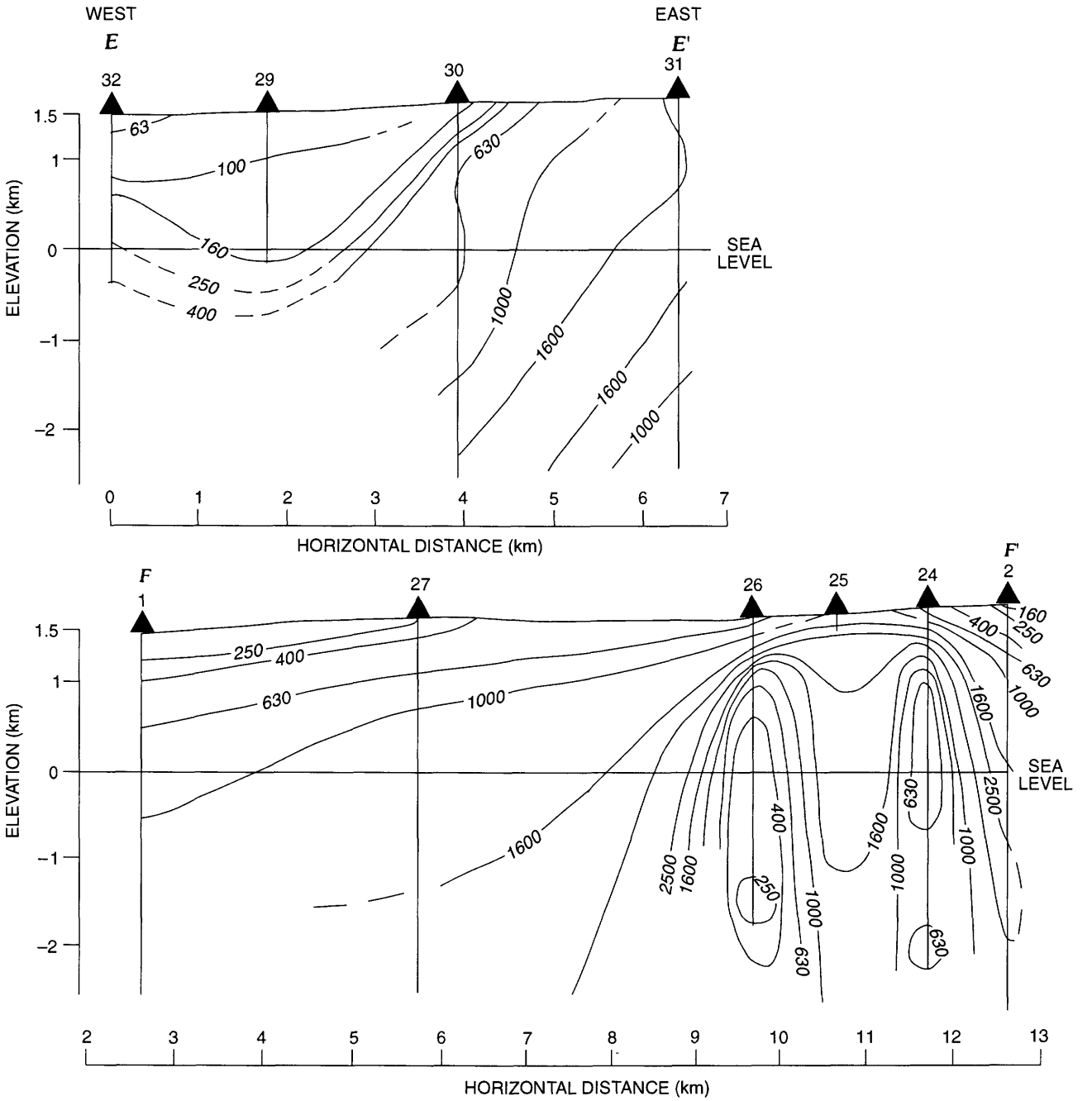

Figure 13. Depth-versus-resistivity cross sections from AMT soundings (triangle) across the western edge of the central Chiricahua Mountains, southeastern Arizona (Senterfit and Klein, 1991). Contours show lines of equal resistivity (indicated values in ohm-m), dashed where uncertain.

breccia in the vicinity of soundings 15–17 has low resistivities (less than 100 ohm-m) at shallow depth for soundings 15 and 16 and is interpreted to be underlain by a fairly thick (2 km) zone of welded tuff. The relatively narrow zone of high resistivity over the dacite porphyry on the northeast of the caldera (soundings 4 and 14) is inferred to be the core of this intrusion, which is mapped across a greater width. Bordering fractures and altered rock surrounding the core of the intrusion are believed to be responsible for the relatively low resistivity, particularly toward the center of the caldera. This zone between soundings 15 and 4 is considered to be an exploration target for epithermal ore deposits.

East of the inferred caldera (sounding 9, including section *D–D'*, fig. 12), the upper part of the Cretaceous sedimentary rocks shows resistivities of 63 to perhaps 250 or 400 ohm-m to a depth of about 1 km. Units below about 1 km having higher resistivity probably indicate carbonate sedimentary rocks that comprise Paleozoic strata. The

resistivity range of 630–1,000 ohm-m is permissible for carbonate sedimentary rocks or Proterozoic basement, but it is high for strata containing a large proportion of clastic sedimentary rock. The resistivity increases to more than 1,000 ohm-m at greater depth, and this higher range is more likely to represent most of the metamorphic and granitic basement. This high-resistivity unit merges westward at sounding 12 (on section *D–D'*, fig. 12) with the highly resistive intrusive rocks inferred at depth beneath Turkey Creek. The schematic diagram (fig. 12) shows inferred faulting along the east flank of the central Chiricahua Mountains. This inference is based on the rapid increase in thickness of the units having resistivities less than 1,000 ohm-m, mainly at sounding 11. This change in slope may be related to tilting of the deep rocks due to resurgent intrusion in the Turkey Creek area.

The profiles across the western side of the caldera are shown on fig. 13. Here, as on the far northwest of the previous section (fig. 12), a resistivity structure suggestive of caldera ring intrusion was not detected west of sounding 27. At soundings 32, 29, 1, and 27 (fig. 13; compare the section of fig. 12, soundings 23–21) a thick section of tuff (1 km or more) is inferred to cover deeper, more resistive rock. The deep resistive rock (1,000 ohm-m or greater) is shown to rise to shallow depths near soundings 31 (section *E–E'*) and 26 (section *F–F'*). This high-resistivity unit is inferred to be the resurgent laccolith that crops out in the center of the caldera (Pallister and du Bray, 1988).

In the vicinity of soundings 26, 25, and 24, an unexpected low-resistivity zone is shown at a depth of about 200–500 m. The lowest resistivities appear at soundings 26 and 24. The enhanced low-resistivity anomalies at 26 and 24 suggest fracturing and altered rock in these areas that could be associated with faulting.

SUMMARY

Resistivity data from scaler AMT surveys, which were acquired primarily in volcanic or plutonic terranes in or adjoining various Forest units, allow numerous inferences concerning large-scale geologic, especially structural, relations. Additional detailed studies, similar to that conducted in and around the Turkey Creek caldera, could lead to discovery of many more targets at depth in other Forest units. Inferred relationships that may lead to further investigations aimed at revealing mineralized rock are presented below. In most cases, the associations of interest are low resistivities possibly related to intrusion, faulting, brecciation, or alteration. Rocks thus affected are favorable hosts for mineral deposits; however, electrical data alone do not predict mineralized rock, nor, except in the central Chiricahua Mountains, were the soundings spaced closely enough to allow an estimate of the probable extent of the favorable hosts along profile.

For the Winchester Mountains area, a few kilometers west of Coronado National Forest, AMT data suggest the location of a fault or fracture zone in the vicinity of soundings 8 and 7 (fig. 5). At sounding 7 low-resistivity rock was found at depths of less than 200 m. To the southwest, also just west of Coronado National Forest, sounding 5 was found to be anomalous as well. Aeromagnetic data over sounding 5 indicates that this sounding is along a trend of anomalous magnetization, which leads to the inference of a possible buried intrusion.

In the northern Dragoon Mountains, all data, except those over alluvium, reflect the high-resistivity intrusion in this area, and in several cases allowed estimates of the probable maximum thickness of overlying Paleozoic through Cretaceous rock. Sounding 6, on alluvium near the northeast end of the range (figs. 7 and 8), indicated a large electrical contrast located lateral to the sounding. There is a low probability that the resistivity data indicate a zone of enhanced alteration; more likely the data indicate the alluvium-bedrock contrast. Sounding 3, on alluvium about 5 km west of Coronado National Forest, combined with inferences from aeromagnetic data, is consistent with the possibility of intrusive rock at about 350 m below basin fill.

In the Emigrant Pass area of the northern Chiricahua Mountains (fig. 9), soundings 1, 2, and 3 are inferred to indicate a buried intrusion. Data from soundings 1 and 3 are consistent with, but do not strongly require, that this inferred intrusion is either altered at a depth of 300–500 m or that the intrusion bottoms near this depth. Sounding 2 is considerably more anomalous (fig. 10) and more diagnostic of a low-resistivity zone at such a depth. The extent to which all of these soundings are affected by lateral variations that may produce such one-dimensional models is uncertain.

Detailed traverses on the northeast border of Turkey Creek caldera (figs. 11 and 12) reveal rock having moderately low resistivity peripheral to the inferred core of the mapped intrusion (sounding 13 in particular, fig. 12). This low-resistivity rock is within tens of meters of the surface. Deep (greater than 1 km), low-resistivity rock, associated with faults (near sounding 18), is also indicated. In the western part of the caldera, inward from the geologically inferred caldera margin, soundings 26, 25, and 24 (fig. 13) indicate rock having moderately low resistivity at a depth of about 300 m. This anomaly may relate to faulting. As above, the effect of lateral contrasts in surface resistivity on the model have not been quantitatively evaluated.

REFERENCES CITED

Ander, M.E., 1981, Magnetotelluric exploration in Arizona and New Mexico for hot dry rock geothermal energy using squid magnetometers, *in* Weinstock, Harold, and Overton, W.C., eds., SQUID applications to geophysics: Tulsa, Okla., Society of Exploration Geophysicists, p. 61–65.

Ander, M.E., Gross, Ron, and Strangway, D.W., 1984, A detailed magnetotelluric audio-magnetotelluric study of the Jemez volcanic zone, New Mexico: Journal of Geophysical Research, v. 19, p. 3335–3353.

Baer, M.J., and Klein, D.P., 1984, Audio–magnetotelluric data in the Dragoon Mountains Roadless Area, Cochise County, Arizona: U.S. Geological Survey Open-File Report 84–417, 59 p.

Bell, B.S., 1979, Report on the reconnaissance resistivity and VLF-EM surveys of the Safford Valley area, Graham County, Arizona, Tucson, and Phoenix: Geophysics, Inc., report for Arizona Bureau Geology and Mineral Technology, 9 p. plus data and appendix.

Bostick, F.X., Jr., 1977, A simple almost exact method of MT analysis, *in* Workshop of evaluation of electrical methods in the geothermal environment (WEEMGE), Snowbird, Utah, November, 1977: Salt Lake City, University of Utah Report, p.175–177.

Brant, A.A., 1966a, Examples of induced-polarization field results in the time domain, *in* Mining geophysics, v. 1, Case histories: Tulsa, Okla., Society of Exploration Geophysicists, p. 288–305.

———1966b, Geophysics in the exploration for Arizona porphyry coppers, *in* Titley, S.R., and Hicks, C.L., eds., Geology of the porphyry copper deposits, southwestern North America: Tucson, Ariz., University of Arizona Press, p. 87–110.

Drewes, Harald, 1980, Tectonic map of southeastern Arizona: U.S. Geological Survey Miscellaneous Investigations Series Map I–1109, scale 1:125,000.

Drewes, Harald, Klein, D.P., and Birmingham, S.D., 1988, Volcanic and structural controls of mineralization in the Dos Cabezas Mountains of southeastern Arizona. U.S. Geological Survey Bulletin 1676, 45 p., 1 pl.

Drewes, Harald, and Meyer, G.A., 1983, Geologic map of the Dragoon Mountains Roadless Area, Cochise County, Arizona. U.S. Geological Survey Miscellaneous Field Studies Map MF–1521–A, scale 1:50,000.

Elliot, C.L., and MacLean, H.D., 1978, Induced-polarization depth penetration in exploring for porphyry coppers, *in* Proceedings of the porphyry copper symposium, Tucson, Ariz., March 18–20, 1976: Arizona Geological Society Digest, v. 11, p. 37–48.

Frischknecht, F.C., Smith, B.D., Hoover, D.B., and Long, C.L., 1986, New applications of geoelectric methods in mineral resource assessment, *in* Cargill, S.M., and Green, S.B., eds., Prospects for mineral resource assessments on public lands; Proceedings of the Leesburg workshop: U.S. Geological Survey Circular 980, p. 221–247.

Hallof, P.G., 1966, Induced-polarization and resistivity results from the Cactus Deposit, Miami, Arizona, *in* Mining Geophysics, v. 1, Case Histories: Tulsa, Okla., Society of Exploration Geophysicists, p. 313–316.

Hallof, P.G., and Winniski, E., 1971, A geophysical case history of the Lakeshore ore body: Geophysics, v. 36, no. 6, p. 1232–1249.

Hoover, D.B., Long, C.L., and Senterfit, R.M., 1978, Some results from audiomagnetotelluric investigations in geothermal areas: Geophysics, v. 43, p.1501–1514.

Jiracek, G.R., Smith, Christian, and Ander, M.E., 1976, Deep resistivity investigations at two known geothermal resource areas (KGRAs) in New Mexico: Radium Springs and Lightning Dock, *in* Tectonics and mineral resources of southwestern North America, N.M.: New Mexico Geological Society Special Publication, p. 71–76.

Kechet, Y., and Hermance, J.F., 1986, A new regional electrical model for the southern section of the Rio Grande Rift and the adjacent Basin and Range and Great Plains: Journal of Geophysical Research, v. 91, no. B6, p. 6359–6366.

Keller, G.V., 1982, Electrical properties of rocks and minerals, *in* Carmichael, R.S., II, CRC handbook of physical properties of rocks: Boca Raton, Fla., CRC Press, p. 217–293.

Keller, G.V., and Frischknecht, F.C., 1966, Electrical methods in geophysical prospecting: New York, Pergamon Press, 517 p.

Klein, D.P., 1983, Geophysical maps of the Dragoon Mountains Roadless Area, Cochise County, Arizona. U.S. Geological Survey Miscellaneous Field Studies Map MF–1521–C, scale 1:50,000.

———1991, Crustal resistivity structure from magnetotelluric soundings in the Colorado Plateau–Basin and Range provinces, central and western Arizona: Journal of Geophysical Research, v. 96, no. B7, p. 12313–12331.

Klein, D.P., and Baer, M.J., 1983, Geoelectric structure of the Gila–San Francisco Wilderness Area, Graham and Greenlee counties, Arizona from audio-magnetotelluric data: U.S. Geological Survey Open-File Report 83–815, 107 p.

Long, C.L., 1985, Regional audio-magnetotelluric study of the Questa caldera, New Mexico: Journal of Geophysical Research, v. 90, no. B13, p. 11270–11274.

Madden, T.R., and Cantwell, T., 1967, Induced polarization, a review, *in* Mining Geophysics, v. 2: Tulsa, Okla., Society of Exploration Geophysicists, p. 373–400.

Maillot, E.E., and Sumner, J.S., 1966, Electrical properties of porphyry deposits at Ajo, Morenci, and Bisbee, Arizona, *in* Mining Geophysics, v. 1, Case Histories: Society of Exploration Geophysics, Tulsa, Okla., p. 273–287.

Martin, R.A., 1986, Geophysical maps of the Winchester Roadless Area, Cochise County, Arizona: U.S. Geological Survey Miscellaneous Field Studies Map MF–1851, scale 1:24,000.

Martin, R.A., Sherrard, M.S., and Tippens, C.L., 1982, Station location map and audio-magnetotelluric data log for an area between Hooker's Hot Springs and the Winchester Mountains, Arizona: U.S. Geological Survey Open-File report 82–779, 8 p.

Nelson, P.H., Hansen, W.H., and Sweeney, M.J., 1982, Induced-polarization responses of zeolitic conglomerate and carbonaceous siltstone: Geophysics, v. 47, no. 1, p. 71–88.

Nervick, K.H., and Boler, F.M., 1981, Audio-magnetotelluric investigations of the North End Study Area, Cochise County, Arizona: U.S. Geological Survey Open-File Report 81–774, 6 p.

Pallister, J.S., and du Bray, E.A., 1988, A field guide to volcanic and plutonic features of the Turkey Creek caldera, Chiricahua Mountains, southeast Arizona, *in* Pallister, J.S., and Sawyer, D.A., Excursion 7A—From silicic calderas to mantle nodules—Cretaceous to Quaternary volcanism, southern Basin and Range province, Arizona and New Mexico: New Mexico Bureau of Mines and Mineral Resources Memoir 46, p. 138–152.

Rogers, G.R., 1966, Introduction—The search for disseminated sulfides, *in* Mining Geophysics, v. 1, Case Histories: Tulsa, Okla., Society of Exploration Geophysicists, p. 265–272.

Senterfit, R.M., and Klein, D.P., 1992, Audiomagnetotelluric investigation at Turkey Creek Caldera, Chiricahua Mountains, southeastern Arizona: U.S. Geological Survey Bulletin 2012, p. K1–K9.

Smith, Christian, 1978, Geophysics, geology, and geothermal leasing status of the Lightning Dock KGRA, Animas Valley, New Mexico, *in* Callender, J.F., Wilt, J.C., and Clemons, R.E., eds., Land of Cochise, southeastern Arizona: New Mexico Geological Society, Annual Field Conference Guidebook, no. 29, p. 343–348.

Sternberg, B.K., Washburne, J.C., and Pellerin, Louise, 1988, Correction for the static shift in magnetotellurics using transient electromagnetic soundings: Geophysics, v. 53, p. 1459–1468.

Strangway, D.W., 1966, Electromagnetic parameters of some sulfide ore bodies, *in* Mining Geophysics, v. 1: Tulsa, Okla., Society of Exploration Geophysicists, p. 227–242.

———1970, Geophysical exploration through geologic cover, Geothermics Special Issue 2: Proceedings of U.N. Symposium on the Development and Utilization of Geothermal Resources, Piza, v. 2, pt. 2., p. 1231–1243.

Strangway, D.W., Swift, C.M., Jr., and Holmer, R.C., 1973, The application of audio-frequency magnetotellurics (AMT) to mineral exploration: Geophysics, v. 38, no. 6, p. 1159–1175.

Tucci, Patrick, 1984, Surface resistivity studies for water resources investigations near Tucson, Arizona, *in* Nielson, D.M., and others, eds., Surface and borehole geophysical methods in ground water investigations: Worthington, Ohio, National Water Well Association, p. 92–106.

———1989, Geophysical methods for water-resources studies in southern and central Arizona: Society of Engineering and Mineral Exploration Geophysicists, Proceedings of the Symposium on the application of geophysics to engineering and environmental problems, Golden, Colo., Colorado School of Mines, 1989, p. 370–381.

Vozoff, Keeva, 1972, The magnetotelluric method in the exploration of sedimentary basins. Geophysics, v. 37, p. 98–141.

Vozoff, Keeva, Hasegawa, H., and Ellis, R.M., 1963, Results and limitations of magnetotelluric surveys in simple geologic situations: Geophysics v. 28, p. 778–792.

Ward, S.H., 1966, Introduction, *in* Mining Geophysics, v. 1, Chapter III: Tulsa, Okla., Society of Exploration Geophysicists, p.117–129.

Ward, S.H., and Fraser, D.C., 1967, Conduction of electricity in rocks, *in* Mining geophysics, v. II: Tulsa, Okla., Society of Exploration Geophysicists, p. 197–223.

Wilson, E.D., Moore, R.T., and Cooper, J.R., 1969, Geologic map of Arizona. U.S. Geological Survey map, scale 1:500,000.

Zohdy, A.A.R., Eaton, G.P., and Mabey, D.R., 1974, Application of surface geophysics to ground water investigations, *chapter D1 in* Techniques of water-resource investigations of the U.S. Geological Survey: Washington, D.C., U.S. Government Printing Office, 116 p.

Remote Sensing and Its Use in Identification of Altered Rocks in Coronado National Forest

By Mark W. Bultman

MINERAL RESOURCE POTENTIAL AND GEOLOGY OF CORONADO NATIONAL FOREST, SOUTHEASTERN ARIZONA AND SOUTHWESTERN NEW MEXICO
Edited by Edward A. du Bray

U.S. GEOLOGICAL SURVEY BULLETIN 2083–F

UNITED STATES GOVERNMENT PRINTING OFFICE, WASHINGTON : 1996

CONTENTS

FIGURES

TABLE

Remote Sensing and Its Use in Identification of Altered Rocks in Coronado National Forest

By Mark W. Bultman

ABSTRACT

Digitally enhanced Landsat Thematic Mapper imagery for Coronado National Forest was used to identify minerals that may be the products of hydrothermal alteration systems. Landsat Thematic Mapper imagery provides information on energy reflected from the Earth's surface in seven spectral bands. These data allow delineation of areas that may be underlain by ferric oxide minerals and by clay minerals that are commonly produced by hydrothermal alteration associated with mineralizing systems and may be indicative of, and associated with, ore-forming processes. Numerous, diversely altered areas were identified in Coronado National Forest by analysis of Thematic Mapper imagery.

INTRODUCTION

Knowledge of the location, number, and size of altered areas is important to mineral resource assessments and to mineral exploration. This chapter presents the results of a remote-sensing study of Coronado National Forest using Landsat Thematic Mapper imagery to delineate areas that may be underlain by ferric oxide and clay minerals. Areas of inferred altered rock are outlined on 1:500,000-scale maps of the Forest units (figs. 1–4). The geology and inferred alteration minerals of each tract are described.

SPECTRAL BAND RESPONSE AND THE DELINEATION OF ALTERED AREAS BY THEMATIC MAPPER IMAGERY

Landsat Thematic Mapper imagery is an excellent tool for the study of Earth processes having electromagnetic manifestations that are detectable at its surface. This imagery presents an accurate representation of landforms, vegetation, geology, and culture. The Thematic Mapper satellite collects radiation reflected from the Earth's surface in seven spectral bands at a spatial resolution of 30 m. The spectral response characteristic of the seven Landsat Thematic Mapper bands are presented in table 1.

The wide spectral width of Thematic Mapper bands and the absence of data from other spectral ranges render identification of specific rock types impossible. Fortunately, the spectral positions of the seven bands does enable a large amount of lithologic and mineralogic discrimination.

Bands 3, 5, and 7 provide the best information for lithologic discrimination because the lower frequency energy characteristic of these bands enhances deeper penetration due to the spectral response of various minerals. Shorter wavelength bands (1 and 2) are more affected by surface processes, including weathering, and are useful in regolith studies or for correlating weathering products with bedrock lithology (Spatz and Taranik, 1989).

The spectral location of band 7 was selected, at least in part, for delineation of hydrothermal alteration products. Electromagnetic energy in the band 7 spectral region is absorbed by clays and micas due to overtones of fundamental hydroxyl (OH) bond stretching and bending (Hunt and Salisbury, 1970). The exact spectral location of the absorption depends on the coordination of OH radicals and cations in mineral lattices (Segal and others, 1984). Absorption is not present in band 5, which also receives a strong reflectance from high-silica rocks (Hunt and Ashley, 1979). Thus, the 5/7 band ratio indicates the abundance of hydroxyl-bearing minerals, such as micas and clays, in non-vegetated areas. Unaltered rock and soil have nearly equal reflectance in the two bands (Elvidge and Lyon, 1984). Areas underlain by clay and mica minerals are denoted by bright areas on images created from the 5/7 band ratio. High concentrations of these minerals are generally related to hydrothermal-alteration systems or weathering of hydrothermal-alteration systems.

Unfortunately, other minerals also display absorption in the spectral range of band 7 and could be mistaken for clays and micas. For example, carbonate minerals absorb electromagnetic energy in band 7 due to overtones of CO_3^{2-} vibration. The broad spectral width of band 7 precludes determination of specific mineral assemblages that absorb in band 7.

The 5/7 band ratio also responds to water content of leaves. Consequently, this ratio cannot be directly applied in the evaluation of heavily vegetated areas. Densely vegetated

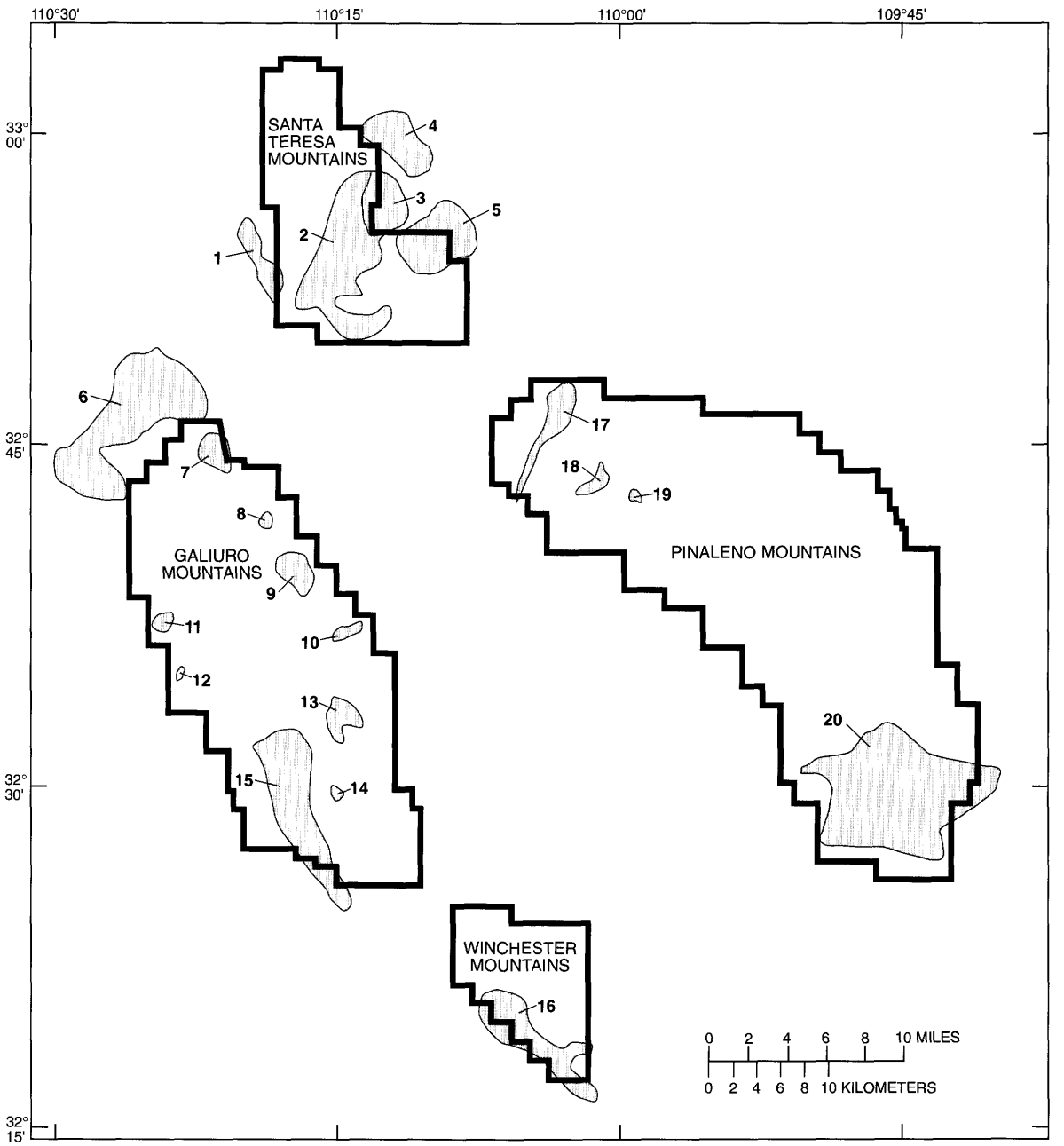

Figure 1. Map showing tracts of possibly altered rock in the Santa Teresa, Galiuro, Winchester, and Pinaleno Mountains, Coronado National Forest, southeastern Arizona, as inferred from analysis of Thematic Mapper imagery. Numbers keyed to tract identifiers in text.

areas have high values in the 4/3 band ratio, which can be used to minimize the influence of vegetation on the 5/7 band ratio. Elvidge and Lyon (1984) found a linear relationship between 4/3 and 5/7 band ratios in unaltered areas and in densely vegetated areas. Thus, subtracting the 4/3 ratio from the 5/7 ratio creates an image that has very low DN (data number) values in densely vegetated areas and high DN values in altered areas.

Limonitic minerals are ferric oxides, such as goethite, hematite, and jarosite, that are commonly associated with hydrothermally altered rock but also can be present as primary minerals or as weathering products. These minerals are characterized by intense absorption, depicted in band 1 data, at the very low end of the visible spectrum (< 0.6 micro-meters) and in ultraviolet wavelengths due to electron transitions (Hunt and Ashley, 1979). The 1/3 band ratio results in a large DN for areas underlain by rocks that contain abundant ferric oxides.

Areas underlain by rocks having high ferrous iron contents can be identified from the 5/4 band ratio (Ford and

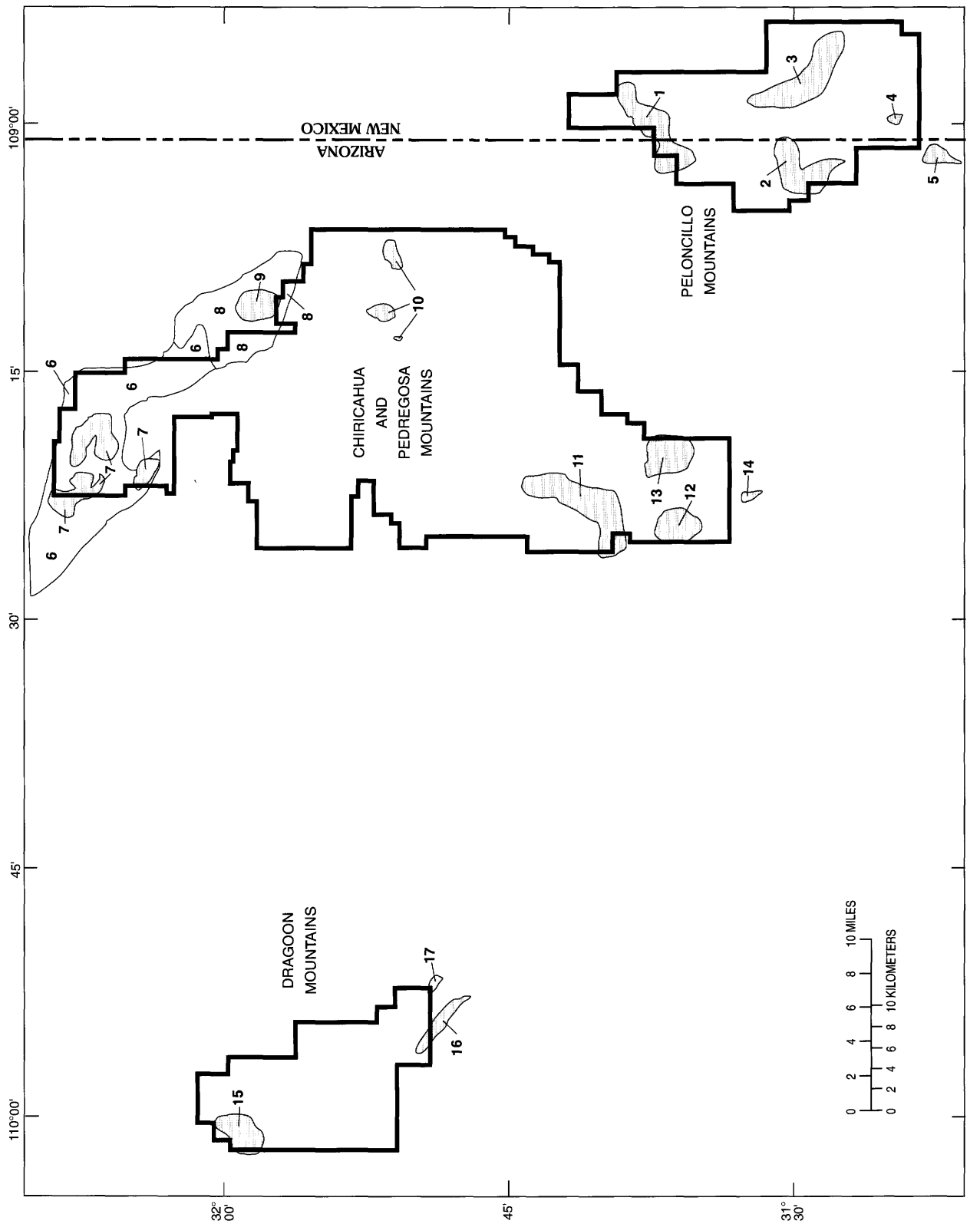

Figure 2. Map showing tracts of possibly altered rock in the Peloncillo, Chiricahua, Pedregosa, and Dragoon Mountains, Coronado National Forest, southeastern Arizona and southwestern New Mexico, as inferred from analysis of Thematic Mapper imagery. Numbers keyed to tract identifiers in text.

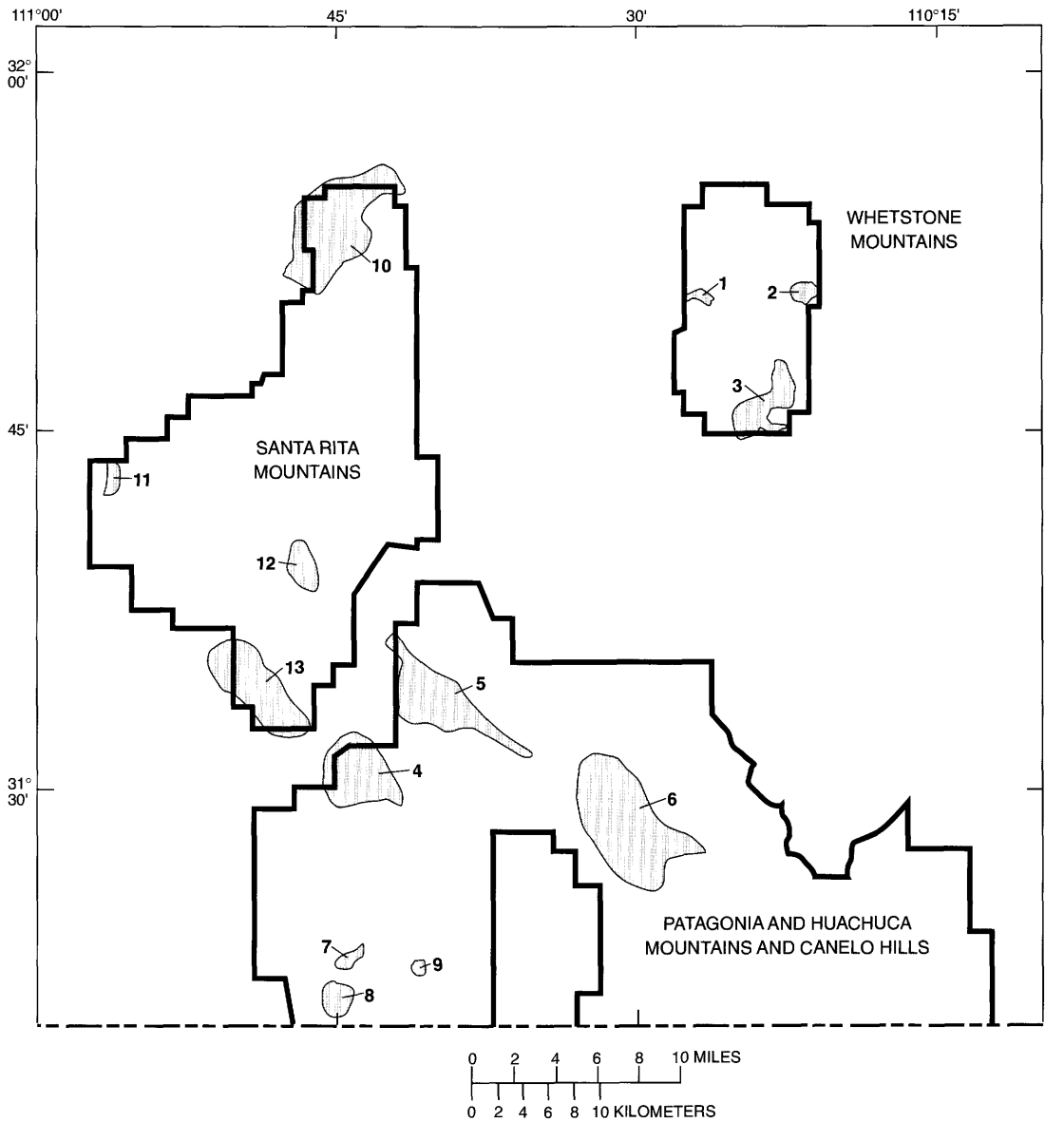

Figure 3. Map showing tracts of possibly altered rock in the Whetstone, Patagonia, Huachuca, and Santa Rita Mountains, Coronado National Forest, southeastern Arizona, as inferred from analysis of Thematic Mapper imagery. Numbers keyed to tract identifiers in text.

others, 1990). Many other rock-forming mineral assemblages may also result in high reflectivities in 5/4 band-ratio images; these images are useful indicators of compositional differences among rocks.

METHODS FOR PROCESSING THEMATIC MAPPER DATA

A mosaiked image for the Coronado National Forest area was assembled from data from four Landsat Thematic Mapper scenes that are available in the U.S. Geological Survey and FOLD (Federally owned Landsat database) Landsat imagery libraries. Acquisition dates of the imagery vary from June 1982 to November 1985; large seasonal differences between images exist. Seasonal and other differences were minimized by normalizing image data numbers to a standard image.

Images were not corrected for atmospheric effects, with the result that image data numbers do not represent true reflectance values (Chavez, 1989). Reflectance values therefore vary across Thematic Mapper quarter-scenes due to elevation differences. From the perspective of the data-collection satellite, the atmosphere is thicker at low elevations than at high elevations. Most high elevations within the Forest are densely vegetated and consequently

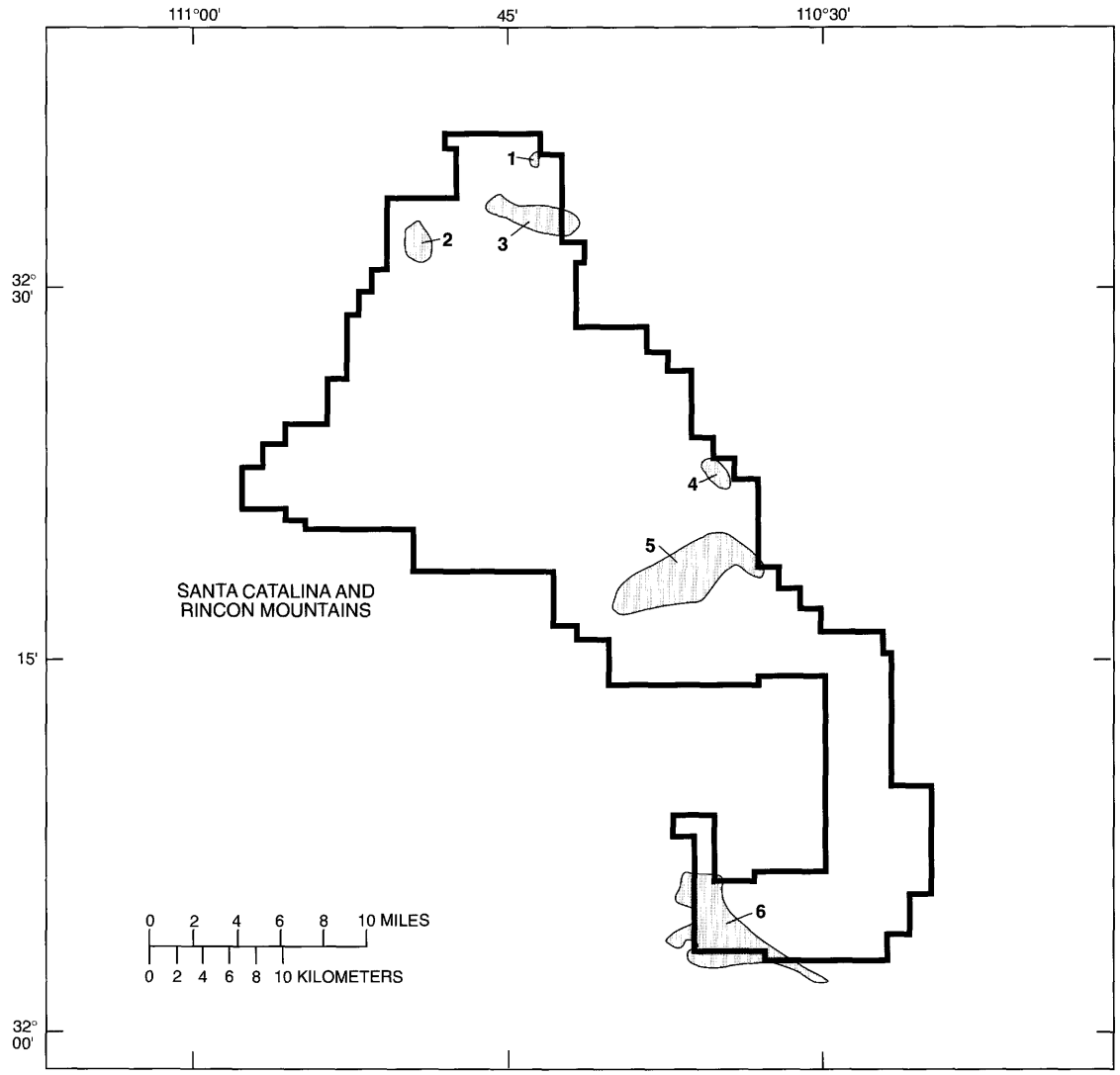

Figure 4. Map showing tracts of possibly altered rock in the Santa Catalina and Rincon Mountains, Coronado National Forest, southeastern Arizona, as inferred from analysis of Thematic Mapper imagery. Numbers keyed to tract identifiers in text.

were not studied. Atmospheric effects can vary dramatically between Landsat images and cause reflectance values of the same feature in different scenes to be quite different. However, the effects due to atmospheric phenomena are not likely to be important in a qualitative data analysis.

Several band-ratio images were produced to enable generation of a color composite image. Values for the 3/1 band ratio were assigned to blue. This band ratio has high DN values in areas of ferric oxide minerals that may be the products of hydrothermal alteration. Values for the 5/4 band ratio were assigned to green. This band ratio has high DN values that correspond to high ferrous iron abundances and it helps emphasize compositional variations among rocks. Values for the 5/7 band ratio delineate vegetated areas and areas of clay and mica minerals that may be products of hydrothermal alteration. Values for the 4/3 band ratio were subtracted from values for the 5/7 band ratio to remove effects of vegetation; resulting data values were assigned to red. The resulting image has high DN values in areas inferred to contain abundant clay and mica minerals and low DN values in densely vegetated areas.

The resultant color composite image shows possible ferric oxide minerals in blue, rocks that contain ferrous iron in green (a number of other mineral assemblages may also appear as green), and possible clay minerals as red. Combinations of these mineral assemblages are depicted by combinations of the primary colors. These images, collectively referred to as the inferred alteration image, were registered to Universal Transverse Mercator Grid Zone 12 and composited to form a single image that covers all units of the Forest. This large image was eventually subdivided into five smaller images for ease of handling. The alteration images were

Table 1. Spectral bands of the Landsat Thematic Mapper.

[Adapted from Earth Observation Satellite Company (1985, p. 2–3)]

Thematic mapper band	Spectral range (micrometers)	Principal applications
1	0.45–0.52	Coastal water mapping. Soil and vegetation differentiation. Deciduous and coniferous differentiation. Hydrothermal-alteration mapping.
2	0.52–0.60	Green reflectance by healthy vegetation.
3	0.63–0.69	Chlorophyll absorption for plant-species differentiation.
4	0.76–0.90	Biomass surveys. Water-body delineation.
5	1.55–1.72	Vegetation-moisture measurement. Snow-cloud differentiation.
6	10.4–12.5	Plant heat-stress measurement. Thermal mapping.
7	2.08–2.35	Hydrothermal-alteration mapping.

entered into a geographic information system (GIS) to enable integration with vector, point, and other imagery databases.

In addition to the color image used to map altered rock, gray-scale images of bands 5 and 7 helped distinguish lithology and may have identified unmapped, but unknown, rock types.

INTERPRETATION OF THEMATIC MAPPER IMAGERY FOR CORONADO NATIONAL FOREST

In order to help delineate altered areas on Thematic Mapper imagery, other types of earth science data, including digital renditions of the Coronado National Forest geologic map (pl. 2–4), a Bouguer anomaly map, NURE aeromagnetic flight-path profiles, NURE aerial gamma-ray flight-path profiles, side-looking synthetic aperture radar (SLAR), the USGS Mineral Resource Documentation System (MRDS, U.S. Geological Survey, 1986) mines and prospects data base, and profiles from a truck-mounted proton precession magnetometer, were combined with the geographic information system that contained Thematic Mapper data. Consequently, information on the Thematic Mapper alteration image could be directly compared to geology, mineral resource data, and geophysical data.

Tracts or areas inferred to contain alteration minerals that may be the products of hydrothermal alteration are delineated on a series of line drawings (figs. 1–4). Tract delineation follows from recognition of inferred altered areas on the inferred alteration image, though Thematic Mapper data does not provide sufficient data to distinguish alteration minerals directly. Many alteration products can result from surficial processes; minerals derived by weathering and those that are products of hydrothermal alteration cannot be distinguished except by field examination. Areas that contain many small areas of inferred altered rock are generalized to a single enclosing polygon because it is not possible to accurately represent all such areas at the scale of this study. Brief descriptions of areas in Coronado National Forest (by Forest unit), in which the presence of hydrothermally altered rock was inferred from Landsat Thematic Mapper imagery, follow.

SANTA TERESA MOUNTAINS

Tract 1.—Tract 1 (fig. 1) delineates an area of possible ferric oxide mineral occurrence on the west side of the Santa Teresa Mountains. It is underlain by Early Proterozoic Pinal Schist, Middle Proterozoic granitic intrusive rocks, Paleozoic sedimentary rocks, and Cretaceous rhyolite. The area of inferred altered rock is spatially associated with known mineralized rock in the Aravaipa mining district (Simons, 1964) and is aligned along the Grand Reef fault (pl. 1)

Tract 2.—Tract 2 (fig. 1) delineates an area of possible ferric oxide minerals in the southern and central part of the Late Cretaceous to Paleocene Santa Teresa granitic stock. The tract coincides with part of the granitic stock and may be associated with distinctive weathering of one or more of its phases. Mineralized rock is not known in this tract.

Tract 3.—Tract 3 (fig. 1) delineates an area of possible ferric oxide and clay minerals in the eastern Santa Teresa Mountains. Rock in this tract appears white on the image and may be intensely altered. The tract is underlain by the eastern part of the Santa Teresa stock (granite) and is associated with highly anomalous concentrations of Au, Ag, As, Bi, Cd, Cu, Mo, Pb, Sb, Zn, Mn, Sn, and W in stream-sediment samples.

Tract 4.—Tract 4 (fig. 1) delineates an area of possible ferric oxide minerals in the northeastern part of the Santa Teresa Mountains outside Coronado National Forest. This tract is underlain by Middle Proterozoic granite, Paleozoic sedimentary rocks, and Late Cretaceous to Paleocene granite.

Tract 5.—Tract 5 (fig. 1) delineates an area of possible clay minerals in the southeastern part of the Santa Teresa

Mountains. This tract is underlain by Pinal Schist, Early to Middle Proterozoic schist and gneiss, Late Cretaceous to Paleocene granite, and Tertiary rhyolite. This image anomaly may be due to the high mica content of Proterozoic metamorphic rocks.

GALIURO MOUNTAINS

Tract 6.—Tract 6 (fig. 1) delineates an area of inferred altered rock in the northwestern part of the Galiuro Mountains. The tract is mostly outside Coronado National Forest and is underlain by Middle Proterozoic Apache Group sedimentary rocks, Cretaceous andesite, and the Late Cretaceous to Paleocene Samaniego granitoid stock. The area that includes the Samaniego stock and immediately adjacent rocks appears to contain ferric oxide and clay minerals. White patches in the area may represent highly altered rock or mine dumps. Northeast of the Samaniego stock, the tract contains several circular and annular patches that appear green on the image, are spatially associated with volcanic rock, and have reflectivities that are quite distinct from adjacent areas. These areas may indicate pyritized breccia pipes.

Tract 7.—Tract 7 (fig. 1) delineates an area of possible clay minerals in the northeastern Galiuro Mountains. It is underlain entirely by Tertiary andesite and appears as scattered areas of white, pink, and red on the alteration image.

Tracts 8–11.—Tracts 8–11 (fig. 1) delineate areas of possible ferric oxide minerals in the central Galiuro Mountains. These tracts are underlain by Tertiary andesite and rhyolite. They appear as areas of blue containing small patches of white on the alteration image and are quite distinct from the surrounding areas.

Tract 12.—Tract 12 (fig. 1) delineates an area of possible clay minerals in the western Galiuro Mountains, which is underlain by Tertiary andesite and rhyolite flows.

Tracts 13 and 14.—Tracts 13 and 14 (fig. 1) delineate areas in the southeastern part of the Galiuro Mountains that appear green with small areas of white on the image. These tracts are underlain by Tertiary andesite and rhyolite tuff. Tract 14 is coincides with an andesite unit, and tract 13 may represent an unmapped andesite. The tracts are quite distinct from the surrounding areas and may indicate andesitic rocks, which generally have a higher ferrous-iron content than does rhyolite tuff. Alternatively, these areas may be related to pyritized rock or other types of altered rock. Tract 13 in part coincides with an area identified by Creasey and others (1981) as one containing altered and pyrite-bearing rocks, whereas no such identification was made for the area containing tract 14.

Tract 15.—Tract 15 (fig. 1) delineates a region that appears as scattered green and red areas on the image in the southwestern Galiuro Mountains. This area is aligned with the southern part of the Rattlesnake fault. The image may distinguish Tertiary andesite and rhyolite tuff that crop out in this area, but the reflectivity patterns do not correspond to units mapped by Creasey and others (1981). Some of the red areas may represent clay minerals; a thorough field investigation of this area is warranted.

WINCHESTER MOUNTAINS

Tract 16.—Tract 16 (fig. 1) delineates an area of possible clay minerals that is underlain almost entirely in Tertiary rhyolite and andesite in the southwestern Winchester Mountains. The southeastern tip of the tract is underlain by Paleozoic sedimentary rocks. This tract is also aligned with a northwest striking fault system.

PINALENO MOUNTAINS

Tract 17.—Tract 17 (fig. 1) delineates an area of possible ferric oxide minerals in the northwestern Pinaleno Mountains. The tract is underlain by Proterozoic granite, metamorphosed granite, schist, and gneiss.

Tracts 18 and 19.—Tracts 18 and 19 (fig. 1), in the northwestern Pinaleno Mountains, appear on the alteration image as green and are quite different from surrounding areas. The geologic compilation (pl. 2) indicates that these areas are underlain by metamorphosed Proterozoic granite, schist, and gneiss, whereas remote-sensing data indicate that they may be areas underlain by a different, unmapped lithology.

Tract 20.—Tract 20 (fig. 1) delineates an area of ferric oxide and (or) clay minerals in the southern Pinaleno Mountains. The tract is underlain by Early Proterozoic granite, Tertiary granite, Tertiary rhyolite flows and tuff, and Tertiary andesite. It contains several northwest-striking high-angle faults. The Proterozoic granite and the Tertiary granite may be associated with ferric oxide minerals, whereas the Tertiary volcanic rocks may be associated with clay minerals.

PELONCILLO MOUNTAINS

Tract 1.—Tract 1 (fig. 2) delineates an area of possible ferric oxide and (or) clay minerals in the northern part of the Peloncillo Mountains that is within Coronado National Forest. The tract is underlain by Tertiary rhyolite and is aligned with several north- and northeast-striking faults. South of this tract, the area of a thin band of green on the image is underlain by Tertiary rhyolite. This area may delineate an unmapped lithology.

Tract 2.—Tract 2 (fig. 2) delineates an area of possible ferric oxide and (or) clay minerals in the western Peloncillo Mountains. The tract is underlain by Tertiary andesite and Tertiary rhyolite tuff and plugs. It also contains several northeast-striking faults.

Tract 3.—Tract 3 (fig. 2) delineates scattered areas of possible clay minerals in the eastern Peloncillo Mountains. The tract is underlain by Tertiary rhyolite and represents a high density of small, possibly altered areas.

Tract 4.—Tract 4 (fig. 2) delineates a region of possible clay minerals in the southern Peloncillo Mountains. This tract is underlain by Tertiary rhyolite tuff.

Tract 5.—Tract 5 (fig. 2) delineates an area of possible clay minerals southwest of the Peloncillo Mountains part of Coronado National Forest. The tract is underlain by Tertiary rhyolite flows and tuff and is bounded on the north and west by faults.

CHIRICAHUA AND PEDREGOSA MOUNTAINS

Tracts 6–9.—Tracts 6–9 (fig. 2) are all aligned with the northwest-striking high-angle Apache Pass fault system in the northern Chiricahua Mountains. Displacement along the fault system began in the Proterozoic and has strongly influenced subsequent emplacement of igneous rocks and circulation of hydrothermal fluids in this area. The Chiricahua Mountains and the Apache Pass fault area are at moderate to high elevations, at which vegetation may obscure reflectivity patterns characteristic of altered rock.

Tracts 6 and 7.—Tract 6 and tracts labeled 7 (fig. 2) delineate areas of possible ferric oxide and (or) clay minerals. These tracts are underlain by Early Proterozoic Pinal Schist; Middle Proterozoic intrusive rocks; Paleozoic sedimentary rocks; Cretaceous andesite, rhyolite, and sedimentary rocks; Tertiary andesite and rhyolite lava flows, granite, rhyolite plugs and dikes, and quartz veins; and Quaternary alluvium. Tracts labeled 7 appear white on the alteration image and may be highly altered; they were mapped (Drewes, 1982) as areas of pyritic alteration (pl. 3).

Tract 8.—Tract 8 (fig. 2) delineates an area of narrow, northwest-trending zones of possible clay minerals in Paleozoic sedimentary rocks and Quaternary alluvium.

Tract 9.—Tract 9 (fig. 2) delineates an area of possible ferric oxide and (or) clay minerals. The tract is underlain by Tertiary andesite. It appears white in the alteration image and was mapped (Drewes and others, 1995) as a pyritized zone.

Tract 10.—Tracts labeled 10 (fig. 2) delineate areas of possible clay minerals in the eastern Chiricahua Mountains. These tracts are underlain by Tertiary rhyolite flows, tuff, and plugs and are present at high elevation. Reflectivities in the area are obscured by dense vegetation, and the indicated tracts may be more extensive than shown.

Tract 11.—Tract 11 (fig. 2) delineates a possible area of scattered clay minerals in the western Pedregosa Mountains. The tract is underlain by Paleozoic sedimentary rocks, Tertiary andesite, and Tertiary rhyolite flows and tuff, and it is cut by numerous northwest-striking faults.

Tract 12.—Tract 12 (fig. 2) delineates possible scattered areas of ferric oxide and (or) clay minerals in the southwestern Pedregosa Mountains. The tract is underlain by Tertiary andesite and rhyolite, Tertiary plugs, and Quaternary alluvium, and it includes several northwest-striking faults.

Tract 13.—Tract 13 (fig. 2) delineates a possible area of clay minerals in the southeastern Pedregosa Mountains. The tract is underlain by Paleozoic sedimentary rocks, Cretaceous and Tertiary undivided volcanic and sedimentary rocks, Tertiary rhyolite plugs, and northwest-striking faults.

Tract 14.—Tract 14 (fig. 2) delineates an area of possible ferric oxide and clay minerals associated with a Tertiary rhyolite plug south of the Chiricahua Mountains part of Coronado National Forest. The tract appears white on the alteration image.

DRAGOON MOUNTAINS

Tract 15.—Tract 15 (fig. 2) delineates an area of possible clay minerals in the northern Dragoon Mountains. This tract is underlain by Pinal Schist, Paleozoic sedimentary rocks, Cretaceous sedimentary rocks, and Tertiary granite. The tract is also cut by several northwest-striking faults. The apparent altered-rock anomaly may be due to mica in the Pinal Schist.

Tract 16.—Tract 16 (fig. 2) delineates an area of possible clay minerals in the southern Dragoon Mountains. The tract is underlain by the Pinal Schist, Paleozoic sedimentary rocks, and Jurassic granite. Again, mica in the Pinal Schist may cause the anomalous reflectivity in this area.

Tract 17.—Tract 17 (fig. 2) delineates an area of possible ferric oxide and (or) clay minerals and is underlain by undivided Cretaceous sedimentary rocks and volcanic rocks, Cretaceous sedimentary rocks, Tertiary granite, and northwest-trending faults. The tract is south of the Dragoon Mountains part of Coronado National Forest and appears white on the alteration image.

WHETSTONE MOUNTAINS

Tract 1.—Tract 1 (fig. 3) delineates an area of possible clay minerals in the western Whetstone Mountains. The tract coincides with Cretaceous sedimentary rocks and Upper Cretaceous to Paleocene rhyolite flows.

Tract 2.—Tract 2 (fig. 3) delineates an area of possible ferric oxide and (or) clay minerals in the eastern Whetstone Mountains. The tract is underlain by Early Proterozoic Pinal Schist and Middle Proterozoic granite.

Tract 3.—Tract 3 (fig. 3) delineates an area of potential ferric oxide and (or) clay minerals in the southern Whetstone Mountains. The tract is underlain by Paleozoic sedimentary rocks, Cretaceous sedimentary rocks, a Late Cretaceous to Paleocene granite stock, and Quaternary alluvium.

PATAGONIA AND HUACHUCA MOUNTAINS AND CANELO HILLS

Tract 4.—Tract 4 (fig. 3) delineates an area of known ferric oxide minerals in the Red Mountain area of the Patagonia Mountains. The tract is underlain by Jurassic granite and undivided Jurassic volcanic and sedimentary rocks. This zone of altered rock is a high-level manifestation of a known, but unexposed porphyry copper-molybdenum deposit at Red Mountain (Corn, 1975). The main ore body is roughly 600 m below the peak of Red Mountain.

Tract 5.—Tract 5 (fig. 3) delineates an area of possible clay minerals northeast of the Patagonia Mountains. The tract is underlain by undivided Tertiary volcanic and sedimentary rocks and a Tertiary rhyolite plug.

Tract 6.—Tract 6 (fig. 3) delineates an area of possible ferric oxide minerals with scattered possible clay mineral occurrences in the Canelo Hills. The tract is underlain by undivided Jurassic sedimentary and volcanic rocks, Jurassic rhyolite plugs, and Quaternary alluvium. It is aligned with the northwest-striking Dove Canyon fault system.

Tract 7.—Tract 7 (fig. 3) delineates an area of possible ferric oxide minerals in the southern Patagonia Mountains. The tract is underlain by Cretaceous to Paleocene granite.

Tract 8.—Tract 8 (fig. 3) delineates an area of possible ferric oxide and (or) clay minerals in the southern Patagonia Mountains. The tract is underlain by Cretaceous to Paleocene granite.

Tract 9.—Tract 9 (fig. 3) delineates an area of possible clay minerals in the southwestern Patagonia Mountains. The tract is underlain by undivided Jurassic volcanic rocks and sedimentary rocks, Paleozoic sedimentary rocks, and Cretaceous to Paleocene granite. The tract coincides with a northwest-striking high-angle fault.

SANTA RITA MOUNTAINS

Tract 10.—Tract 10 (fig. 3) delineates an area of possible clay minerals in the northern Santa Rita Mountains. The tract is underlain by Pinal Schist, Middle Proterozoic granite, Paleozoic sedimentary rocks, undivided Jurassic volcanic and sedimentary rocks, Cretaceous sedimentary rocks, Late Cretaceous to Paleocene granite, and Tertiary rhyolite.

Tract 11.—Tract 11 (fig. 3) delineates an area of possible clay minerals in the western Santa Rita Mountains. The tract is underlain by Late Cretaceous to Paleocene granite. The region south of tract 11 is cloud-covered in the Thematic Mapper imagery used in this study. Consequently, remote sensing did not help identify altered rock in this area.

Tract 12.—Tract 12 (fig. 3) delineates an area of possible clay minerals in the central Santa Rita Mountains. The tract is underlain by undivided Lower Cretaceous volcanic and sedimentary rocks.

Tract 13.—Tract 13 (fig. 3) delineates an area of possible ferric oxide minerals in the southern Santa Rita Mountains. The tract is underlain by Jurassic granite, Late Cretaceous to Paleocene granite, and northwest-striking high-angle faults.

ATASCOSA, PAJARITO, SAN LUIS, AND TUMACACORI MOUNTAINS AND COBRE AND COCHES RIDGES

Unfortunately, the Atascosa–Cobre–Coches–Pajarito–San Luis–Tumacacori unit of Coronado National Forest is cloud-covered in the Thematic Mapper imagery used in this study. Consequently, remote sensing did not help identify altered rock in this area.

SANTA CATALINA AND RINCON MOUNTAINS

Tract 1.—Tract 1 (fig. 4) delineates an area of possible ferric oxide and (or) clay minerals in the northern Santa Catalina Mountains. The tract is underlain by Middle Proterozoic granite and Middle Proterozoic diabase dikes.

Tract 2.—Tract 2 (fig. 4) delineates an area of possible ferric oxide and (or) clay minerals in the northern Santa Catalina Mountains. The tract is underlain by Tertiary granite.

Tract 3.—Tract 3 (fig. 4) delineates an area of possible ferric oxide minerals in the northern Santa Catalina Mountains. The tract is underlain by Apache Group sedimentary rocks, Middle Proterozoic diabase dikes, Paleozoic sedimentary rocks, Upper Cretaceous volcanic rocks and sedimentary rocks, and a Late Cretaceous to Paleocene granitic intrusion.

Tract 4.—Tract 4 (fig. 4) delineates scattered areas of possible clay minerals in the eastern Santa Catalina Mountains. The tract is underlain by Apache Group sedimentary rocks, Cretaceous sedimentary rocks, and Late Cretaceous to Paleocene granitic intrusive rocks.

Tract 5.—Tract 5 (fig. 4) delineates scattered areas of possible ferric oxide and clay minerals in the northern part of the Rincon Mountains. The tract is underlain by Middle Proterozoic granite, Paleozoic sedimentary rocks (Italian Trap klippe; pl. 2), and Late Cretaceous to Paleocene granitic intrusive rocks. Parts of the tract appear white on the alteration image.

Tract 6.—Tract 6 (fig. 4) delineates an area of possible ferric oxide and (or) clay minerals in the southern Rincon Mountains. The tract is underlain by Paleozoic sedimentary rocks, Late Cretaceous to Paleocene intrusive rocks, and Tertiary sedimentary and volcanic rocks. The northern part of this tract is on the south side of a Late Cretaceous to Paleocene granite body and appears white on the alteration image. It looks very different from the granite that is immediately to the north. This area is north of the Santa Catalina fault system, and some of the apparently altered rock may

be related to mylonitization and high phyllosilicate content of rocks so deformed.

REFERENCES CITED

Chavez, P.S., Jr., 1989, Radiometric calibration of Landsat Thematic Mapper multispectral images: Photogrammetric Engineering and Remote Sensing, v. 55, no. 9, September 1989, p. 1285–1294.

Corn, R.M., 1975, Alteration-mineralization zoning, Red Mountain, Arizona: Economic Geology, v. 70, no. 8, p. 1437–1447.

Creasey, S.C., Jinks, J.E., Williams, F.E., and Meeves, H.C., 1981, Mineral resources of the Galiuro Wilderness and contiguous further planning areas, Arizona, *with a section on* Aeromagnetic survey and interpretation, *by* W.E. Davis: U.S. Geological Survey Bulletin 1490, 94 p., 2 pls., scale 1:62,500.

Drewes, Harald, 1982, Geologic map and sections of the Cochise Head quadrangle and adjacent areas, southeastern Arizona: U.S. Geological Survey Miscellaneous Investigations Series Map I–1312, scale 1:24,000.

Drewes, Harald, du Bray, E.A., and Pallister, J.S., 1995, Geologic map of the Portal quadrangle and vicinity, Cochise County, southeast Arizona: U.S. Geological Survey Miscellaneous Investigations Series Map I–2450, scale 1:24,000.

Earth Observation Satellite Company, 1985, User's guide for Landsat Thematic Mapper computer-compatible tapes, p. 2–3.

Elvidge, C.D., and Lyon, R.J., 1984, Mapping clay alteration in the Virginia Range–Comstock lode, Nevada with airborne Thematic Mapper imagery: Proceedings, International Symposium on Remote Sensing of Environment, Third Thematic Conference, Remote Sensing for Exploration Geology, Colorado Springs, Colo., April 16–19, 1984.

Ford, J.P., Dokka, R.K., Crippen, R.E., and Blom, R.G., 1990, Faults in the Mojave Desert, California, as revealed on enhanced Landsat images: Science, v. 248, p. 1000–1003.

Hunt, G.R., and Ashley, R.P., 1979, Spectra of altered rocks in the visible and near infrared: Economic Geology, v. 74, 1979, p. 1613–1629.

Hunt, G.R., and Salisbury, J.W., 1970, Visible and near-infrared spectra of minerals and rocks; I. Silicate minerals: Modern Geology, v. 1, p. 283–300.

Segal, D.B., Ruth, M.D., Merin, I.S., Watanabe, H., Soda, K., Takano, O., and Sano, M., 1984, Spectral remote sensing investigation of Lisbon Valley, Utah: Proceedings, International Symposium on Remote Sensing of the Environment, Third Thematic Conference, Remote Sensing for Exploration Geology, Colorado Springs, Colo., April 16–19, 1984, p. 273–292.

Simons, F.S., 1964, Geology of the Klondyke quadrangle, Graham and Pinal Counties, Arizona: U.S. Geological Survey Professional Paper 461, 173 p.

Spatz, D.M., and Taranik, J.V., 1989, Regional analysis of Tertiary Volcanic calderas (western U.S.) using Landsat Thematic Mapper imagery: Remote sensing of the environment, v. 28, p. 257–272.

Mineral Resources, Ore Deposit Models, and Resource Potential of Coronado National Forest—Locatable Minerals

By Mark W. Bultman *and* Harald Drewes

MINERAL RESOURCE POTENTIAL AND GEOLOGY OF CORONADO NATIONAL FOREST, SOUTHEASTERN ARIZONA AND SOUTHWESTERN NEW MEXICO

Edited by Edward A. du Bray

U.S. GEOLOGICAL SURVEY BULLETIN 2083–G

UNITED STATES GOVERNMENT PRINTING OFFICE, WASHINGTON : 1996

CONTENTS

FIGURES

TABLES

Mineral Resources, Ore Deposit Models, and Resource Potential of Coronado National Forest—Locatable Minerals

By Mark W. Bultman *and* Harald Drewes

ABSTRACT

This report is a mineral resource assessment of Coronado National Forest prepared by a team of U.S. Geological Survey earth scientists. The assessment process involved three steps. In step one, known and potential ore deposits in Coronado National Forest were classified according to mineral deposit models and earth science data were used to help identify tracts whose characteristics are favorable for the occurrence of undiscovered deposits. In order to provide land-use planners with the most useful information, the parts of favorable tracts that have high potential for undiscovered deposits are specially noted. The results of step one, including a discussion of industrial commodity resource potential, are described herein. The results of steps two and three are presented in Chapter J of this volume.

INTRODUCTION

Locatable minerals include all minerals subject to exploration, development, and production under the Federal General Mining Law of 1872. Most metals and industrial minerals are included in this group. This chapter presents an assessment of the potential for locatable mineral resources of Coronado National Forest, and includes a discussion concerning industrial mineral resources of the Forest. This information will assist the U.S. Forest Service in complying with title 36, chapter 2, part 219.22, Code of Federal Regulations, which requires the U.S. Forest Service to provide information and interpretations so that mineral resources can be considered with other types of resources in land-use planning.

The method used to estimate the metallic mineral resources of Coronado National Forest involves three steps (Singer and Cox, 1988; Reed and others, 1989), the first of which is described in this chapter. In the first step, all known and possible mineral occurrences are identified and classified according to appropriate mineral deposit models. One of the principal sources of information concerning mines and prospects in the Forest is the USGS Mineral Resource Documentation System (MRDS) data base. Data comprising types of deposits, history, and production statistics for many of the deposits and occurrences described in the following sections are presented therein; additional information concerning these mineralized systems can be obtained from the MRDS data base. The mineral deposit models used are those of Cox and Singer (1986) and consist of systematically arranged information that describes the essential earth science attributes of a particular group or class of mineral deposits and their accompanying grade-tonnage models. Mineral resource assessment tract maps, showing areas that are favorable for the presence of various ore deposit types, are the product of this step. Tracts delineated on these maps (figs. 1–4; pls. 27–29) have been subdivided to show subtracts that have high mineral resource potential (as defined in appendix 1), as indicated by consideration of all available earth science data, for occurrence of undiscovered mineral deposits classified according to the ore deposit models defined in step one.

Tracts favorable for the occurrence of undiscovered deposits of the various mineral deposit model types were delineated by a team of U.S. Geological Survey earth scientists in June of 1991. The process began by definition of areas favorable for the occurrence of undiscovered mineral deposits as indicated by geologic evidence (Chapter B, this volume). These tract boundaries were modified through consideration of geochemical, geophysical, remote-sensing, and mineral resource data. In many cases, geologic and geophysical evidence were used to extend tracts beyond bedrock into areas where potential host rocks are concealed by basin fill. These favorable tracts were further subdivided to highlight areas having high mineral resource potential and a level of certainty determined by available information was assigned (see appendix 1 for definitions of mineral potential categories and certainty levels).

The mineral resource assessment presented in this chapter is based on the geologic, geochemical, geophysical, and remote-sensing data presented in this volume. Time and budget constraints greatly limited collection of new data, but a number of important new products were created specifically for this assessment by processing or reprocessing existing information. These include a compilation of geology at 1:126,770 and its relationship to mineralized areas (Chapter B, this volume); a compilation of existing and some new exploration geochemical data with accompanying interpretation (Chapter C, this volume); an aeromagnetic

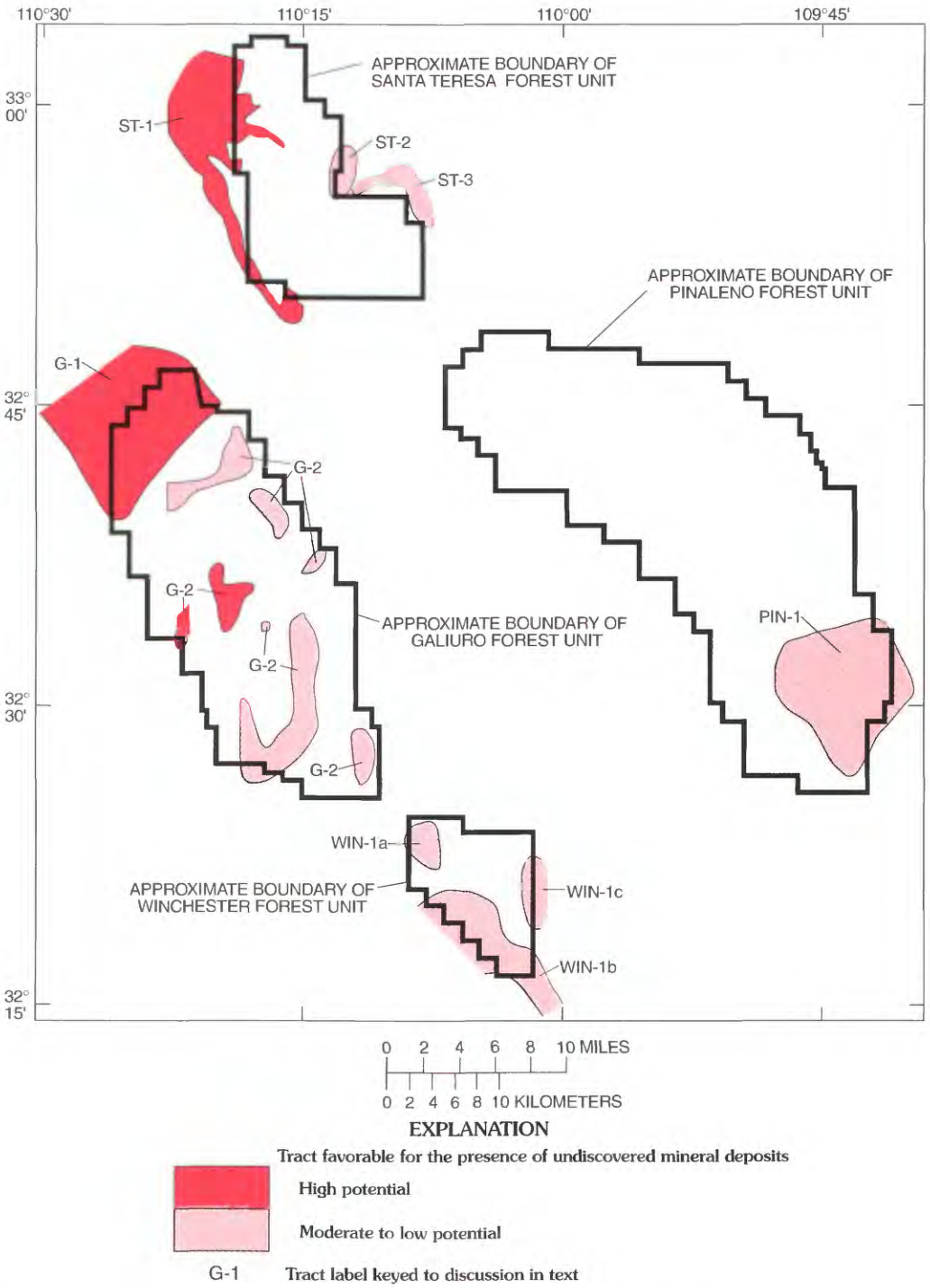

Figure 1. Mineral resource tracts in the northeastern part of Coronado National Forest, southeastern Arizona.

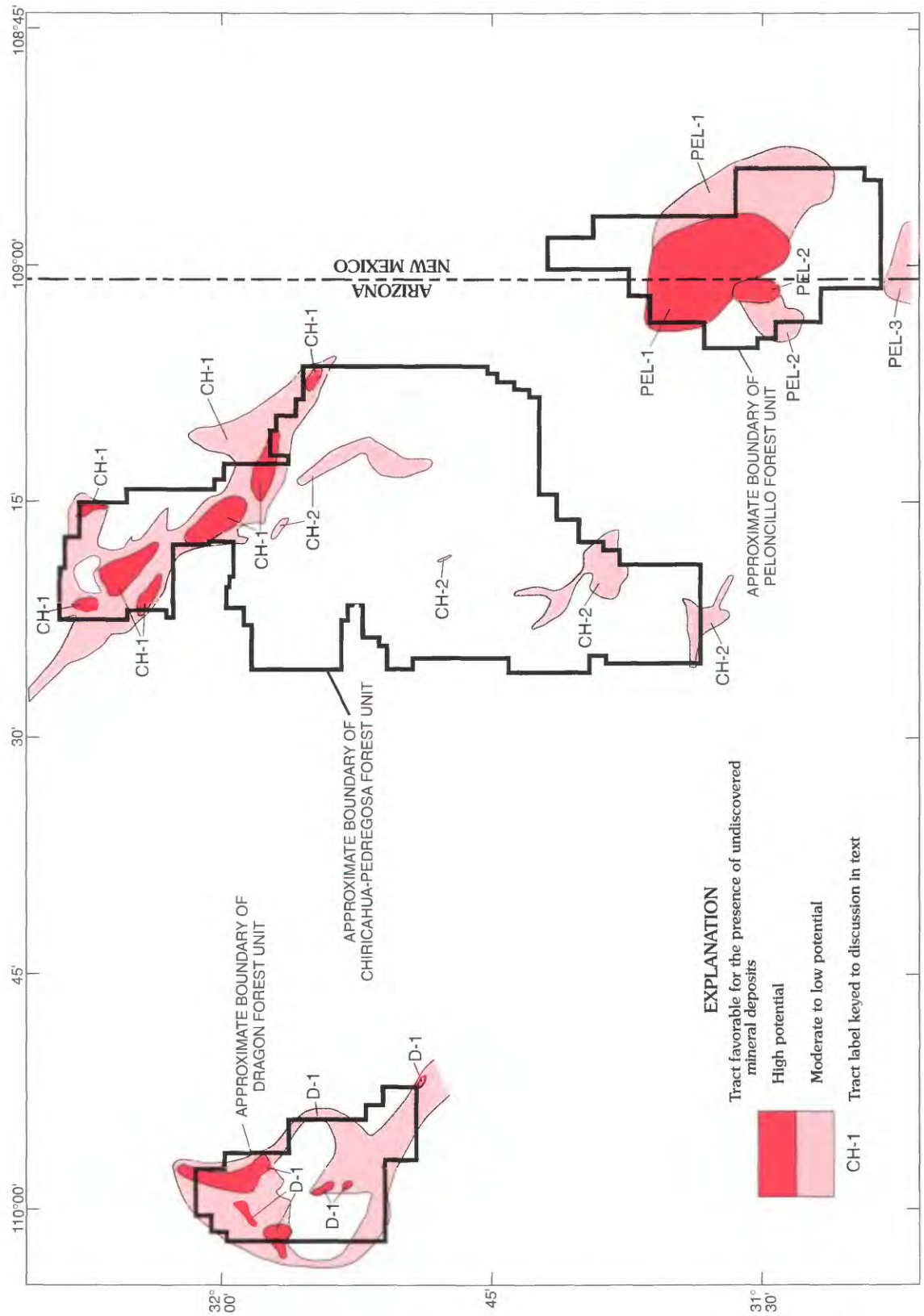

Figure 2. Mineral resource tracts in the southeastern part of Coronado National Forest, southeastern Arizona and southwestern New Mexico.

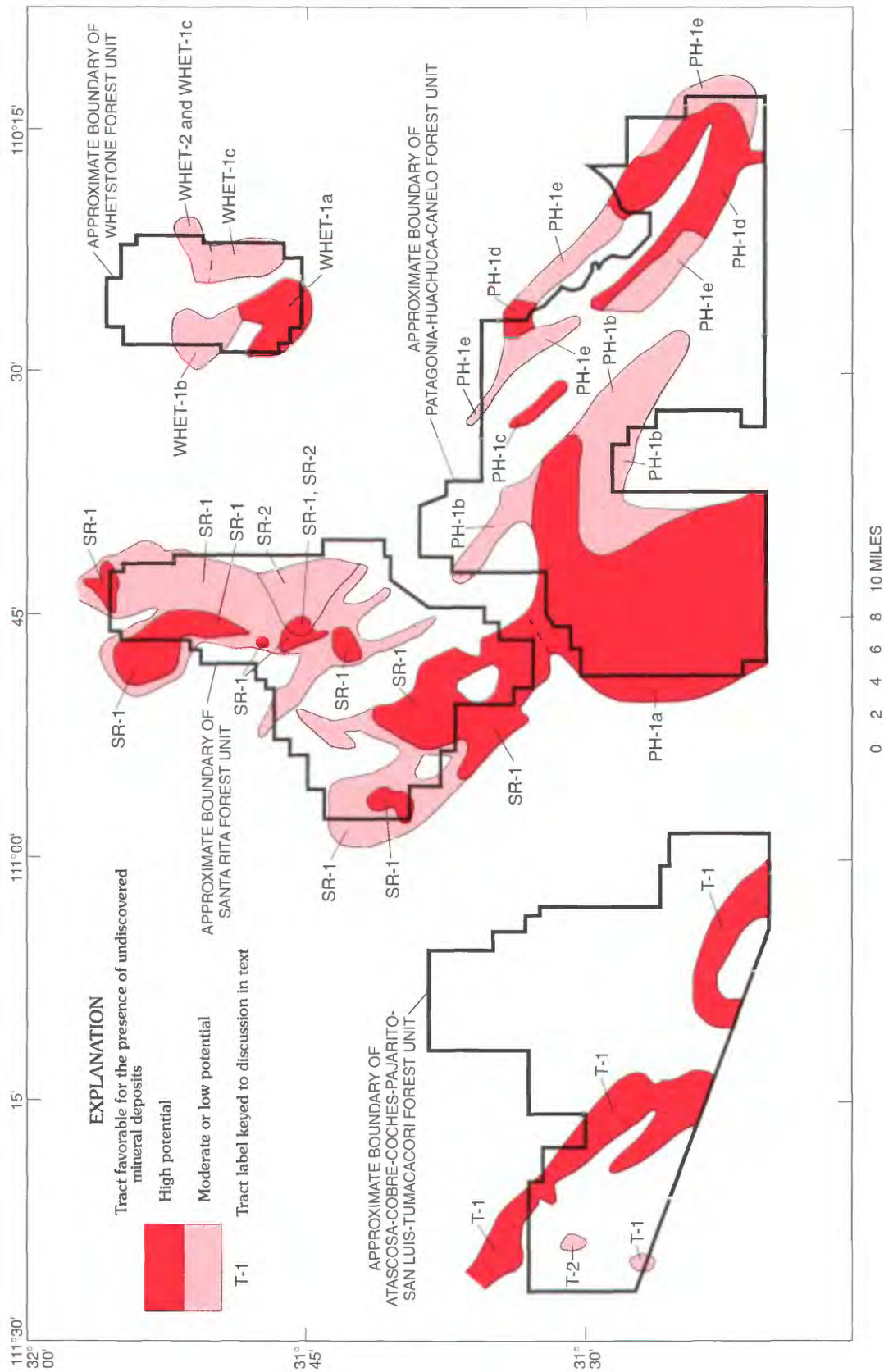

Figure 3. Mineral resource tracts in the southwestern part of Coronado National Forest, southeastern Arizona.

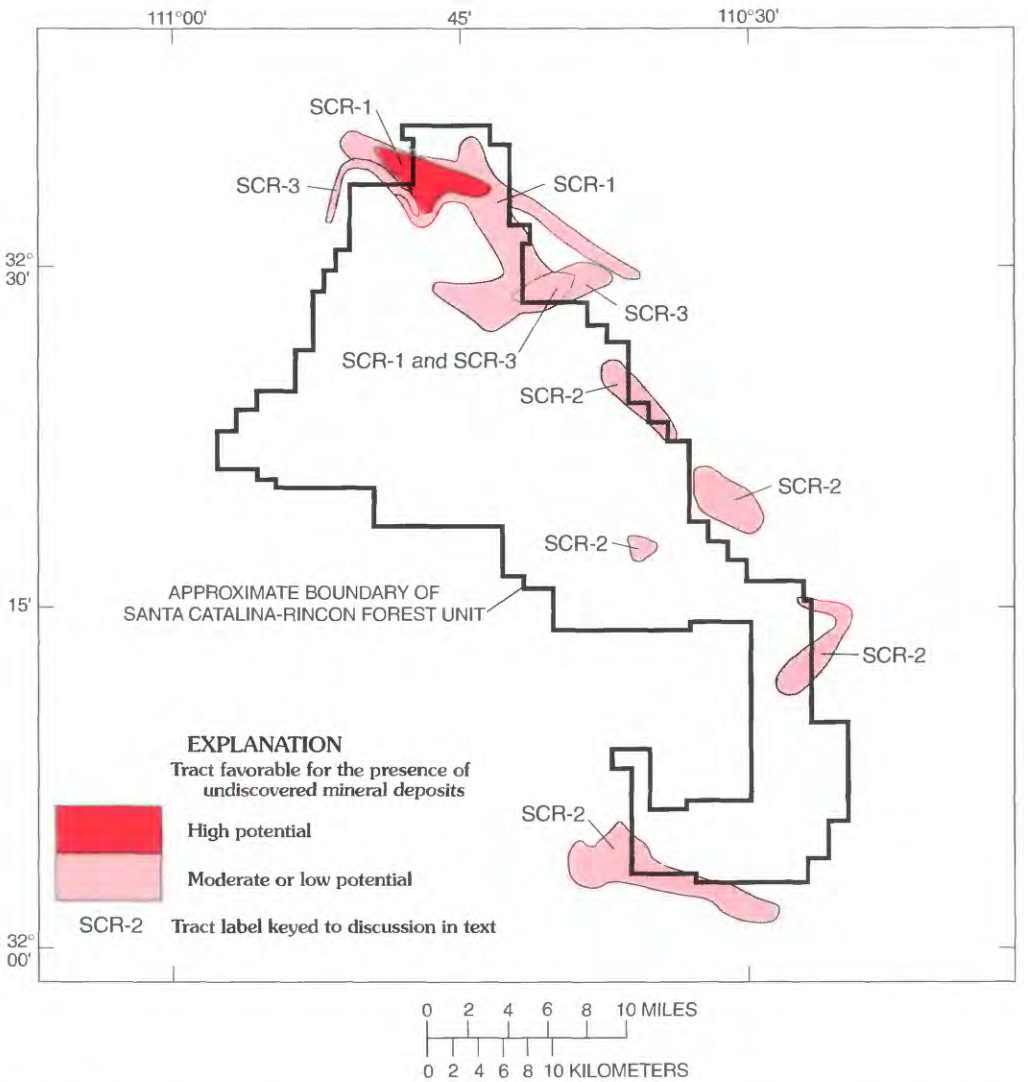

Figure 4. Mineral resource tracts in the northwestern part of Coronado National Forest, southeastern Arizona.

map, a Bouguer anomaly map, and gamma-ray spectrometer profiles and interpretations thereof (Chapter D, this volume); a compilation and interpretation of electrical geophysical data (Chapter E, this volume); and a Landsat-thematic-mapper-based remote-sensing study (Chapter F, this volume).

MINERAL EXPLORATION AND EXPLOITATION IN CORONADO NATIONAL FOREST

The Coronado National Forest has probably been prospected and mined by various cultures for thousands of years. The earliest prospectors and miners were the Native Americans whose needs were chiefly stone for tools, clay and stone for pottery and construction purposes, and certain minerals used for ornamentation.

With the influx of European explorers and missionaries, beginning in the early 16th century, the search for metals in and near the present-day Coronado National Forest was initiated (Drewes and Dyer, 1989). Father Eusebio Kino is known to have prospected for silver near the Mexican border as early as 1705 (Arizona Bureau of Mines, 1969). The Planches de Plata silver deposits near Nogales, in Sonora, Mexico, were reportedly worked about 1736 (Knight, 1958). The Spaniards established Tubac Presidio and Tumacacori Mission about 1752 and doubtless had discovered and begun mining silver in the surrounding areas by 1800. Butler (1936) wrote, "There is a tradition that $60,000 worth of silver utensils once decorated the altar of the San Xavier Mission (built 1783) and that this metal was mined in the Santa Rita Mountains." Early production was probably from the oxidized mantos of vein deposits. The replacement deposits along fissures and some contact replacement deposits, especially self-fluxing occurrences

hosted by carbonate rock, were among the first to be exploited. Production records are unavailable.

During the U.S. Civil War, lead mines in the Patagonia Mountains, such as the Mowry Mine, were developed to bolster Confederate munitions production, and some mines in the Arivaca and Santa Rita areas were also developed, only to be abandoned about 1868 as a result of conflicts with Native Americans. Mining activity was firmly re-initiated with the establishment of military control about 1875 and the coming of the railroad a few years later. The area of the present San Manuel porphyry copper deposit was noted as a potential source of minerals in 1870, but no ore was identified until 1944 (Arizona Bureau of Mines, 1969). An Army scout from Fort Huachuca noted brightly colored rocks near Bisbee in 1877, and ore was discovered there (the Copper Queen Mine) in 1880 (Arizona Bureau of Mines, 1969).

Most of the major mining districts were established or workings were greatly expanded during the last decades of the 19th century; boom towns such as Tombstone, Bisbee, Miami, Clifton-Morenci, San Manuel, Pierce, Courtland-Gleeson, and Ruby assumed roles as major ore producers. The development of mass mining methods for porphyry copper deposits initiated the most recent spurt of mine expansion and new discoveries in southern Arizona, particularly at Tyrone, Silver Bell, and Sacaton. The porphyry copper-related deposits of the Pima district (Sierrita Mountains) were discovered by geophysical methods about 1950. Ore production rates also benefitted from mass mining methods. The latest major innovations, including leach methods and computerized control of ore extraction and blending, has further extended the life of existing mines.

Most of the large porphyry copper–related deposits discovered within approximately 80 km of Coronado National Forest are still in operation. This includes several porphyry copper and porphyry copper-molybdenum deposits (Sierrita, San Manuel, Lakeshore, San Xavier, Silver Bell) and several skarn deposits related to porphyry copper systems (Twin Buttes, Esperanza, Mission, and Johnson Camp). The area has been a major supplier of ore metals for the Nation. The total metal production from Coronado National Forest and the adjacent region within 80 km of the Forest units is approximately $20 billion (Mardirosian, 1977).

Most of the mining districts are outside the Forest units because the Forest boundaries were determined, in part, by distribution of mining activity, location of mining towns, and distribution of patented ground. The main exceptions are in the Patagonia Mountains, Santa Rita Mountains, and the Cobre Ridge part of the Arivaca area. Other sites of moderate production from the Forest are in the Dragoon, Chiricahua, Whetstone, Huachuca, and Santa Catalina Mountains. While much of this mining has produced lead, copper, zinc, gold, and silver, other commodities have been locally mined in response to specific national needs, such as during times of war (tungsten, manganese, clay, diatomite, uranium, and flux rock). As technology has changed, old mines have reopened and mine dumps of earlier workings have been reprocessed. These developments will doubtless continue in the Coronado National Forest region.

MINERAL RESOURCES

METALS

Metals in the Coronado National Forest are produced from a variety of mineral deposit types of differing ages. The metallogeny of the Forest region can be described as having two aspects: a porphyry copper zone and a gold- and silver-bearing vein zone. Each zone contains types of mineral deposits that are unique to that zone in addition to types of deposits that are common to both zones; the overall character of mineralized rock in each zone is distinctive.

The porphyry copper zone (fig. 5) coincides with a northwest-striking belt of world-class porphyry copper deposits. The 160-km-wide by 800-km-long belt passes through the Tucson area and the southwestern part of the Forest. Its northwest end is near a structurally complex zone at the southwest side of the Colorado Plateau, and its southeast end is near the young magmatic province of the Sierra Madre Occidental, Mexico. The belt crosses a zone of Cordilleran deformation.

North of the Forest region, between Phoenix and Silver City, the porphyry copper zone seems to have an east-southeast-striking pronglike extension (fig. 5) in which similar types of ore deposits are present. This extension is aligned approximately with the northeast margin of the Cordilleran orogen, a zone of structural complexity (Drewes, 1991).

The porphyry copper zone is characterized by large, multiphase dispersed deposits for which the value of copper produced far outweighs the value of other metals. This zone also contains small and medium deposits, including polymetallic vein deposits, that have produced a variety of base and precious metals. Other base metals, including molybdenum, antimony, and arsenic, have been produced from some copper districts. Gold and silver have been important byproducts of many porphyry copper deposits. Production from some deposits in the porphyry copper zone is dominated by gold and silver, whereas production is dominated by tungsten in others.

The large, complex, dispersed deposits include not only typical porphyry deposits but also stockwork deposits, diffuse breccia pipes, and large composite ore deposit types. Contact metasomatic deposits are commonly present in broad, continuous metamorphic haloes around large, multiphase stocks.

Most deposits in the porphyry zone are of Late Cretaceous to Paleocene age. These deposits have been considered Laramide but deposits older and younger than the Laramide orogeny are present in this zone. More accurately, these deposits should be considered Cordilleran, to reflect other phases of deformation. The most prominent exception

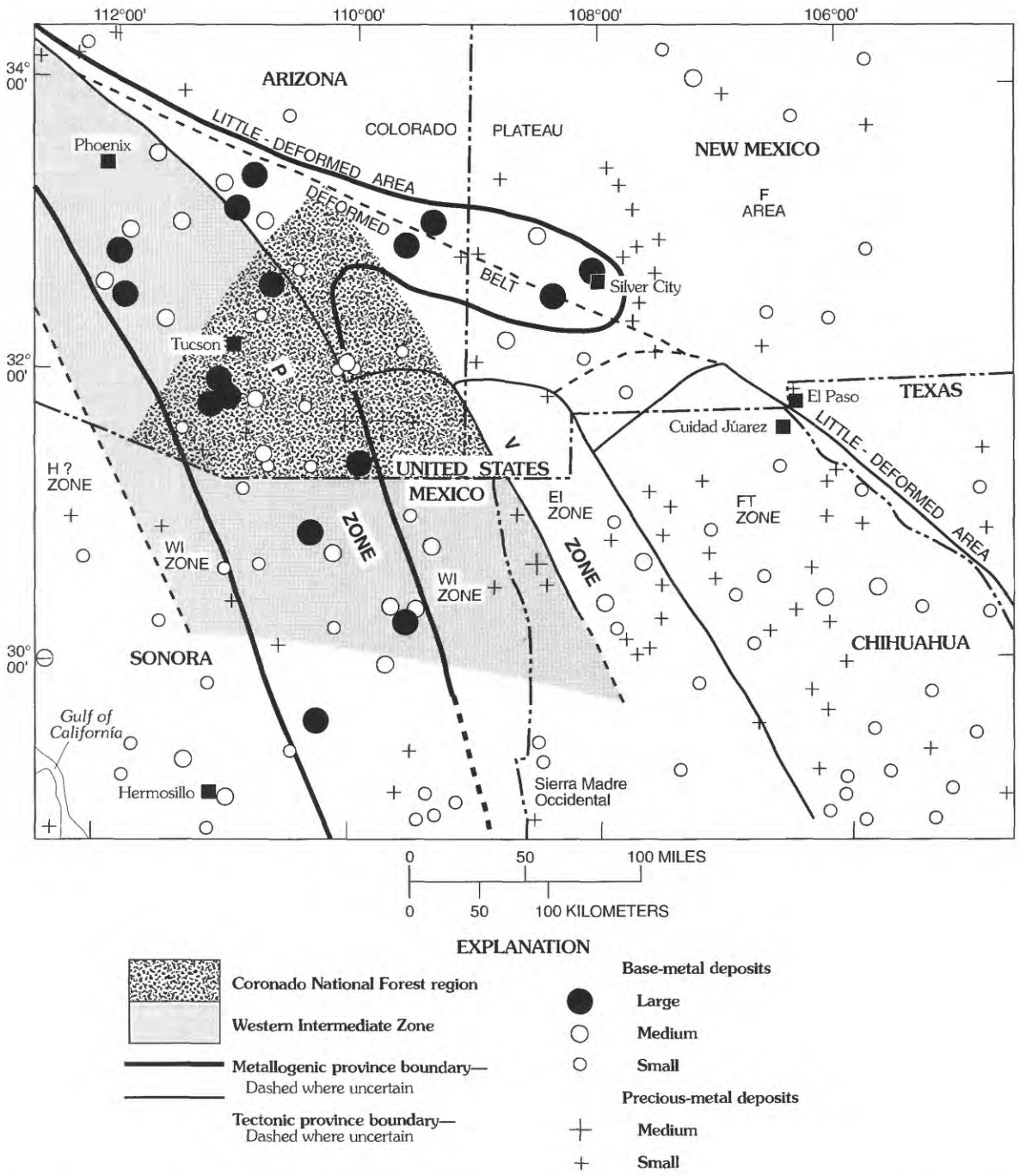

Figure 5. Metallogenic and tectonic setting of Coronado National Forest, southeastern Arizona and southwestern New Mexico. Metallogenic terranes: P zone, porphyry copper deposits and many large mining districts; V zone, vein gold and silver deposits and many small mining districts. Tectonic terranes: F area, foreland area; FT zone, fold and thrust zone; EI zone, eastern intermediate zone; WI zone, western intermediate zone; H? zone, hinterland (?) zone.

to a Cordilleran age for these deposits is the Jurassic porphyry copper district at Bisbee, Ariz., just outside the Forest.

The second metallogenic zone, which is east of the porphyry copper belt and south of its east-southeast-striking prong (fig. 5), contains gold- and silver-bearing veins, pipes, and contact metasomatic deposits. This region covers the eastern part of the Forest region and extends to the east into New Mexico and southeast into Chihuahua, Mexico.

Characteristically, the gold- and silver-bearing zone contains small or, in a few cases, medium deposits. They are mostly vein deposits but include some small pipes and contact metasomatic deposits. Locally, some stockwork deposits that are closely tied to veins and structures intersected by veins are present. Contact metamorphic deposits are fewer and smaller than in the porphyry copper zone, and they are commonly discontinuous. Although copper and other base

metals have been produced from deposits in this zone, gold and silver have been the major commodities produced from these deposits. Manganese and fluorite have also been produced from several of these deposits.

Deposits of the gold- and silver-bearing zone are mostly Tertiary in age; only a few deposits in the western part of the zone are slightly older. While these latest Cretaceous deposits and the Paleocene and Eocene deposits can be termed Laramide in age, many other deposits in the gold- and silver-bearing zone are Oligocene or Miocene in age and thus may reflect independent magmatic-tectonic event.

In a general way, copper-rich, complex and dispersed ore deposits are most likely in the southwestern part of the Forest region. Lead, zinc, silver, and gold, mostly in polymetallic vein deposits, may be present throughout the Forest region; the more complex and dispersed types of deposits are most typical of the southwestern part of the Forest. Fluorite and manganese are present in small, but minable concentrations in the eastern part of the Forest. Minable tungsten deposits are most likely to be present in the southwestern part of the Forest. While these generalizations represent an oversimplification of metallic mineral deposits in the Forest, they offer a useful framework for consideration of distribution of metallic mineral resources in the Forest.

INDUSTRIAL COMMODITIES

In the Forest region silica rock has been produced as an industrial commodity. This material can be used as a flux in smelting processes. Flux rock is a bulk commodity that is usually obtained relatively close to where it is used. Silica rock that contains subeconomic amounts of gold and silver has been preferred because these metals can be recovered or left with the melt to form lake copper, which is of premium value due to its high ductility.

Silica rock has been obtained from quartz sandstone beds in the upper part of the Bisbee Group in areas outside the Forest. Bisbee Group sandstone, although present in many areas of the Forest, has not been mined from any of these areas. Silica flux has also been produced from selected quartz vein and silica replacement deposits at scattered mines and prospects outside the Forest. Silica rock has been shipped for flux from at least one small mine (El Tigre) in the Chiricahua Mountains area of the Forest.

TYPES OF METALLIC MINERAL DEPOSITS KNOWN OR INFERRED TO EXIST IN CORONADO NATIONAL FOREST

Coronado National Forest hosts a variety of base- and precious-metal mineral deposits. Brief descriptions, modified from those presented by Cox and Singer (1986), of the mineral deposit models applicable to deposits known or inferred to exist in the Forest are presented herein. A list of mineral deposit types known to be present in Coronado National Forest was established by classifying known mineral deposits and prospects according to the deposit models of Cox and Singer (1986). The list of inferred mineral deposit types was established by comparing the earth science attributes, particularly geology, of prospective terranes to those of specific mineral deposit models.

The mineral deposit model descriptions presented here are adapted from Cox and Singer (1986) as modified by Fisher and Johnson (1987) and Worl and others (1989); ore deposit model numbers appended to model names in the following section are those of Cox and Singer (1986). The descriptions presented here are synopses and are not deposit models in a strict sense. These synopses include descriptions of important characteristics of deposits in Coronado National Forest; a representative deposit in the Forest is indicated for each mineral deposit model. More information concerning the ore deposit models was presented by Cox and Singer (1986). Lists of mineral deposit models applicable to known or inferred deposits in Coronado National Forest and type deposits for each mineral deposit model are presented in table 1, whereas tables 2 and 3 are cross-referenced tabulations of mineral deposit models and favorable tracts in the Forest.

Many mineral deposits in the Forest have characteristics typical of several ore deposit models, which suggests that the ore-forming process may have been a composite of overprinted signatures of superposed hydrothermal systems. The Cox and Singer (1986) deposit model that best accounts for all features of each mineral deposit in the Forest is used in this assessment; model numbers shown in parentheses are those assigned by Cox and Singer.

TUNGSTEN SKARN DEPOSITS (MODEL 14a)

Commodities.—Tungsten, copper, and zinc are the primary commodities produced from tungsten skarn deposits; gold and silver may be present as trace metals.

Deposit Description.—Tungsten skarn deposits are found at or near the contact between felsic igneous intrusions and reactive carbonate country rocks. Deposits consist of silicate and ore minerals that have replaced reactive carbonate minerals. Ore deposits are generally localized along the contact between intrusive bodies and carbonate host rocks, local faults, bedding planes, and breccia zones. Deposit ages are controlled by ages of related intrusive bodies, most of which are Cretaceous to Miocene.

Mineralogy and Alteration.—Scheelite is the principal ore mineral in these deposits, but molybdenite, pyrrhotite, sphalerite, chalcopyrite, bornite, arsenopyrite, pyrite, and magnetite may also be present. Trace amounts of wolframite,

Table 1. Known and inferred mineral deposit types[1] in Coronado National Forest, southeastern Arizona and southwestern New Mexico.

Mineral deposit model	Mineral deposit model number[1]	Type deposit in Coronado National Forest
Tungsten skarn	14a	Coronado Mine, Catalina Mountains.
Tungsten veins	15a	Lucky Strike Mine, Huachuca.
Climax-type molybdenum.	16	None known.
Porphyry copper	17	Mine Canyon district, Whetstone Mountains.
Porphyry copper skarn-related.	18a	King in Exile Mine, Santa Rita Mountains.
Copper skarn	18b	Elgin Mine, Santa Rita Mountains.
Polymetallic replacement.	19a	Mowry Mine, Patagonia Mountains.
Porphyry copper-molybdenum.	21a	Childs-Aldwinkle Mine, Galiuro Mountains.
Polymetallic vein	22c	Montana Mine, Cobre Ridge, Tumacacori Mountains.
Hot-springs gold-silver.	25a	Powers Mine, Galiuro Mountains.
Creede-type epithermal precious-metal.	25b	None known.
Rhyolite hosted tin	25h	None known.
Gold placer	39a	Greaterville placer, Santa Rita Mountains.

[1]Cox and Singer, 1986.

fluorite, cassiterite, and native bismuth may also be present. Reactive carbonate sedimentary rocks are altered to Fe-Mg-Mn-Ca silicate mineral assemblages that may include diopside-hedenbergite, grossularite-andradite, wollastonite, and possibly spessartine and almandine. An inner zone of massive quartz may be present.

Geophysical and Geochemical Signatures.—Most intrusive bodies associated with these deposits are discernible in regional gravity and magnetic data. Magnetite associated with many tungsten skarn deposits may produce a magnetic anomaly that can help indicate the location of an ore body. The geochemical signature of tungsten skarn deposits includes anomalous abundances of W, Mo, Zn, Cu, Sn, Bi, Be, and As.

Tungsten Skarn Deposits in Coronado National Forest.—Potential host rocks for tungsten skarn deposits in the Forest include (1) carbonate sedimentary rocks of the Middle Proterozoic Apache Group, especially the Mescal Limestone, in the northern part of the Forest; (2) Paleozoic carbonate sedimentary rocks including the Upper and Middle Cambrian Abrigo Formation, the Mississippian Escabrosa Limestone, and carbonate facies of the Permian and Pennsylvanian Naco Group; and (3) Lower Cretaceous carbonate facies of the Bisbee Group. The type tungsten skarn deposit in Coronado National Forest is the Coronado Mine, in the Marble Peak mining district, Santa Catalina Mountains.

TUNGSTEN VEIN DEPOSITS (MODEL 15a)

Commodities.—Tungsten is the primary commodity produced from tungsten vein deposits; molybdenum, copper, lead, and zinc are possible byproducts.

Deposit Description.—Tungsten-bearing vein deposits are associated with Tertiary monzogranite to granite stocks and form fissure-filling quartz veins that contain wolframite, scheelite, molybdenite, and minor base-metal sulfides. Quartz-vein emplacement was controlled by local shears or tension fractures present in granitic intrusive bodies or in adjacent wall rocks.

Table 2. Selected mineral deposit types[1] and tracts considered favorable for their occurrence, Coronado National Forest, southeastern Arizona and southwestern New Mexico.

[CH, Chiricahua Mountains; D, Dragoon Mountains; G, Galiuro Mountains; PEL, Peloncillo Mountains; PH, Patagonia-Huachuca Mountains; PIN, Pinaleno Mountains; SCR, Santa Catalina–Rincon Mountains; SR, Santa Rita Mountains; ST, Santa Teresa Mountains; T, Tumacacori Mountains; WHET, Whetstone Mountains; WIN, Winchester Mountains; ---, not applicable]

Mineral deposit model	Mineral deposit model number	Mineral resource tracts
Tungsten skarn	14a	D-1, PH-1, SR-1, SCR-1.
Tungsten veins	15a	WHET-2, PH-1, T-2, SCR-1.
Climax-type molybdenum.	16	Not delineated, see Peloncillo Mountains section.
Porphyry copper	17	WHET-1.
Porphyry copper skarn-related.	18a	CH-1, SR-1.
Copper skarn	18b	SCR-2, SCR-3.
Polymetallic replacement.	19a	ST-1, WIN-1, CH-1, D-1, PH-1.
Porphyry copper-molybdenum.	21a	G-1, PH-1, SCR-1, SCR-2.
Polymetallic vein	22c	CH-1, CH-2, SR-1, T-1.
Hot-springs gold-silver	25a	G-2.
Creede-type epithermal precious-metal.	25b	PEL-2.
Rhyolite-hosted tin	25h	PEL-1.
Gold placer	39a?	SR-2, SCR-3.
Unknown models	--	ST-2, ST-3, PIN-1, PEL-3.

[1]Cox and Singer, 1986.

Table 3. Tracts considered favorable for the occurrence of indicated mineral deposit types, Coronado National Forest, southeastern Arizona and southwestern New Mexico.

[CH, Chiricahua Mountains; D, Dragoon Mountains; G, Galiuro Mountains; PEL, Peloncillo Mountains; PH, Patagonia-Huachuca Mountains; PIN, Pinaleno Mountains; SCR, Santa Catalina–Rincon Mountains; SR, Santa Rita Mountains; ST, Santa Teresa Mountains; T, Tumacacori Mountains; WHET, Whetstone Mountains; WIN, Winchester Mountains; ---, not applicable]

Tract	Mineral deposit model	Mineral deposit model number[1]	Area (km^2)	Location
CH-1	Polymetallic replacement	19a	170	Chiricahua Mountains
	Polymetallic vein	22c		
	Porphyry copper skarn related	18a		
CH-2	Polymetallic vein	22c	73	Chiricahua Mountains
D-1	Polymetallic replacement	19a	91	Dragoon Mountains
	Tungsten skarn	14a		
G-1	Porphyry copper-molybdenum	21a	135	Galiuro Mountains
G-2	Hot-springs gold-silver	25a	98	Galiuro Mountains
PEL-1	Rhyolite-hosted tin	25h	213	Peloncillo Mountains
PEL-2	Creede-type epithermal vein	25b	27	Peloncillo Mountains
PEL-3	Unknown	---	15	Peloncillo Mountains
PEL	Climax-type molybdenum	16	---	Peloncillo Mountains
PIN-1	Unknown	---	111	Pinaleno Mountains
PH-1	Porphyry copper-molybdenum	21a	751	Patagonia-Huachuca Mountains
	Polymetallic replacement	19a		
	Tungsten vein	15a		
	Tungsten skarn	14a		
SCR-1	Tungsten skarn	14a	109	Santa Catalina-Rincon Mountains
	Tungsten vein	15a		
	Copper skarn	18b		
	Porphyry copper-molybdenum	21a		
SCR-2	Copper skarn	18b	77	Santa Catalina-Rincon Mountains
	Porphyry copper-molybdenum	21a		
SCR-3	Gold placer deposits	39a	21	Santa Catalina-Rincon Mountains
SR-1	Tungsten skarn	14a	410	Santa Rita Mountains
	Polymetallic vein	22c		
	Porphyry copper-skarn	18a		
SR-2	Gold placer deposits	39a	41	Santa Rita Mountains
ST-1	Polymetallic replacement	19a	85	Santa Teresa Mountains
ST-2	Unknown	---	9	Santa Teresa Mountains
ST-3	Specialized granite-related deposits for which model is unknown	---	15	Santa Teresa Mountains
T-1	Polymetallic vein	22c	159	Tumacacori Mountains
T-2	Tungsten veins	15a	6	Tumacacori Mountains
	Tungsten placer deposits			
WHET-1	Porphyry copper	17	98	Whetstone Mountains
WHET-2	Tungsten vein	15a	14	Whetstone Mountains
WIN-1	Polymetallic replacement	19a	75	Winchester Mountains

[1]Cox and Singer, 1986.

Mineralogy and Alteration.—These deposits can contain wolframite, scheelite, molybdenite, bismuthinite, pyrite, pyrrhotite, arsenopyrite, bornite, tennantite, chalcopyrite, cassiterite, beryl, and fluorite. Some deposits may include tetrahedrite-tennantite, sphalerite, galena, and enargite. Wallrock alteration ranged from pervasive albitization, potassium feldspar replacement, and disseminated rare-earth-element mineralization in the lower parts of deposits, to greisenization, chloritization, and sericitization in the upper parts; tourmaline may be present in the upper parts of some deposits.

Geophysical and Geochemical Signatures.—Intrusive rocks related to the deposits, as well as faults that may localize deposits may be produce gravity and (or) magnetic anomalies. Geochemical indicators include anomalous abundances of W, Mo, Sn, Bi, As, Cu, Pb, Zn, Be, F.

Tungsten Vein Deposits in Coronado National Forest.—Tungsten vein deposits in Coronado National Forest are associated with altered Late Cretaceous to middle Tertiary granitic plutons and the Paleozoic and Mesozoic sedimentary and metasedimentary rocks they intrude. Many of the deposits are quartz-scheelite veins rather than quartz-wolframite veins, but these are assumed to be a variant of this deposit type. The type tungsten vein deposit in the Forest is the Lucky Strike Mine, in the Reef district of the Huachuca Mountains.

CLIMAX-TYPE MOLYBDENUM DEPOSITS (MODEL 16)

Commodities.—Molybdenum is the primary commodity produced from Climax-type molybdenum deposits; tin and tungsten are possible byproducts.

Deposit Description.—Climax-type molybdenum deposits consist of quartz-molybdenite stockworks, with associated fluorite, that are present in multistage, hypabyssal, high-silica, multi-phase granite porphyry stocks, usually in rifted cratonic environments. Most of these stocks are small (less than 1 km^2 in plan view), have radial dikes, and are middle Tertiary in age (Ludington, 1986). Most ore zones are draped over late-stage phases of these stocks.

Mineralogy and Alteration.—The mineral assemblage associated with Climax-type molybdenum deposits is molybdenite and quartz, possibly accompanied by fluorite, potassium feldspar, pyrite, wolframite, cassiterite, and topaz. Alteration includes intense quartz or quartz and potassium feldspar veining in the ore zone. Upper phyllic and propylitic zones are present in most deposits. A halo of rhodochrosite, rhodonite, and spessartine garnet and a zone of greisen veins is generally present below the ore body.

Geophysical and Geochemical Signatures.—Intrusive bodies associated with this deposit type may coincide with gravity and (or) magnetic anomalies. Larger scale surveys may be needed to resolve these intrusions because most are small. Geochemical anomalies above the ore body include Mo, Sn, W, and Rb. Anomalous abundances of Pb, Zn, F, and U are found in the wall rocks as much as a few kilometers from the deposit. Anomalous abundances of Sn, W, Mo, and F may be present in panned concentrates derived from drainage basins peripheral to these deposits.

Climax-Type Molybdenum Deposits in Coronado National Forest.—No known Climax-type molybdenum deposits have been reported to exist in Coronado National Forest. The southern part of the Peloncillo Mountains may host this type of deposit at depth. The geology of this area is similar to that of the rifted cratonic environment that prevailed during development of the Climax porphyry molybdenum deposits of Colorado.

PORPHYRY COPPER DEPOSITS (MODEL 17)

Commodities.—Copper is the primary commodity produced from porphyry copper deposits; molybdenum, lead, zinc, silver, and gold are possible byproducts.

Deposit Description.—Porphyry copper deposits consist of chalcopyrite and bornite in quartz-feldspar-biotite stockwork veinlets hosted by intensely fractured, hydrothermally altered porphyry and adjacent country rock. Most deposits are associated with high-level tonalite to monzogranite or syenite porphyry intrusions and contemporaneous dikes, breccia pipes, and faults. Many deposits are hosted by Mesozoic to Cenozoic batholiths but these deposits may be of any age. Stockwork veins are present in the porphyry intrusion and along its contact with country rocks. Secondarily enriched parts of porphyry copper systems contain ore-grade concentrations of chalcocite and form ore bodies that formed by surficial copper leaching, downward percolation in solution, and reprecipitation at the water table.

Mineralogy and Alteration.—Ore minerals found in porphyry copper deposits include chalcopyrite, bornite, molybdenite, chalcocite, and gold. Gangue minerals include pyrite, quartz, potassium feldspar, biotite, white mica, and possibly anhydrite and clay minerals. Late veins of enargite, tetrahedrite, sphalerite, and galena are present in some deposits. From the lowest and innermost alteration zones outward and upward, alteration assemblages are arranged as follows: sodic-calcic, potassic, phyllic, and argillic to propylitic. Aluminum-metasomatized rock are present in the upper part of some deposits.

Geophysical and Geochemical Signatures.—Porphyry copper deposits are associated with gravity and magnetic anomalies produced by associated igneous intrusions. Anomalous abundances of Cu, Mo, Au, Ag, W, B, and Sr are present in the central parts of mineralized areas and grade outward to anomalous abundances of Pb, Zn, Au, Sb, Se, Te,

Mn, Co, Ba, and Rb; anomalous abundances of Bi and Sn are present in the distal parts of these systems.

Porphyry Copper Deposits in Coronado National Forest.—The type porphyry copper deposit in the Forest is the Mine Canyon deposit, in the Whetstone Mountains. This deposit is in a Late Cretaceous to Paleocene (Laramide) granitic stock, the Mine Canyon stock, exposed in the southwestern part of the Whetstone Mountains and is associated with a large aeromagnetic high. The stock may be an apophysis of a large batholith inferred to form the core the Whetstone Mountains (Chapter D, this volume); other porphyry copper deposits may be associated with the inferred batholith. The occurrence of numerous porphyry copper deposits in and near the western part of the Forest and of very few to no deposits in its eastern part implies that the favorabilty for undiscovered deposits of this type is greatest in the western part of the Forest. Exploration for undiscovered porphyry copper systems has been especially intense during the last three decades; these programs have essentialy exhausted the potential for discovery of exposed or shallowly buried porphyry copper systems in the Forest.

PORPHYRY COPPER SKARN-RELATED DEPOSITS (MODEL 18a)

Commodities.—Copper is the primary commodity produced from porphyry copper skarn-related deposits; lead, tungsten, zinc, silver, gold, uranium, and rhenium are possible byproducts.

Deposit Description.—Porphyry copper skarn-related deposits are found in the epizonal levels of tonalite to monzogranite stocks that intrude carbonate sedimentary rocks. Chalcopyrite is the principal ore mineral; it is present in stockwork veinlets in intensely fractured parts of hydrothermally altered intrusions and in skarn that displays extensive retrograde alteration. Porphyry copper skarn-related deposits may be present where igneous sytems of an Andean-type arc are superimposed on older continental shelf carbonate terrane; the deposits are mainly Mesozoic and Tertiary but may be of any age.

Mineralogy and Alteration.—Ore minerals associated with porphyry copper skarn-related deposits include chalcopyrite in the inner zone of the deposit and bornite, chalcopyrite, and possibly sphalerite and tennantite in the outer zone, if present. Pyrrhotite is the predominant ore mineral in some deposits of this type. Most stocks display potassic alteration associated with andradite and diopside in calcareous rocks. With increasing distance from the intrusive contact, hydrothermally altered rock changes from an assemblage that includes wollastonite and tremolite along with minor garnet, idocrase, and clinopyroxene to marble. Phyllitic alteration in the stock is associated with retrograde actinolite, chlorite, and clay in skarn.

Geophysical and Geochemical Signatures.—These deposits correlate with geophysical anomalies that result from the associated igneous intrusion. The skarn may be discernible in magnetic data if it contains abundant magnetite and (or) pyrrhotite. The geochemical signature of porphyry copper skarn-related deposits includes anomalous abundances of Cu, Mo, Pb, Zn, Au, Ag, W, Bi, Sn, As, and Sb.

Porphyry Copper Skarn-Related Deposits in Coronado National Forest.—Most porphyry copper skarn-related deposits in the Forest are associated with Laramide-age intrusions of granitic composition. Most of these porphyry systems are present in the western part of the Forest in association with non-porphyry copper skarn-related deposits. These porphyry copper skarn-related deposits may also be localized by northwest-striking, medium- to regional-scale faults and fault systems in association with structurally controlled intrusions. Potential host rocks for porphyry copper skarn-related deposits in the Forest include (1) carbonate sedimentary rocks of the Apache Group in the northern part of the Forest; (2) Paleozoic carbonate sedimentary rocks, including the Abrigo Formation, the Escabrosa Limestone, and carbonate facies of the Naco Group; and (3) Lower Cretaceous carbonate facies of the Bisbee Group. The type porphyry copper skarn-related deposit in the Forest is the King in Exile Mine, in the northern Santa Rita Mountains.

COPPER-SKARN DEPOSITS (MODEL 18b)

Commodities.—Copper is the primary commodity produced from copper-skarn deposits; zinc, lead, molybdenum, silver, and gold are possible byproducts.

Deposit Description.—Copper-skarn deposits are associated with tonalite to monzogranite stocks that intrude carbonate sedimentary rocks. Most deposits form irregular or tabular bodies along the intrusive contact or in xenoliths within the igneous rock. Ore is present in irregular or tabular ore bodies and in stockwork veins in intensely fractured and hydrothermally altered igneous rocks and skarn. Mineralization and skarn formation are directly related to emplacement of stocks, most of which are Mesozoic, but they can be any age.

Mineralogy and Alteration.—Chalcopyrite, bornite, and pyrrhotite are the ore minerals in copper-skarn deposits, but molybdenite, bismuthinite, sphalerite, galena, cosalite, arsenopyrite, enargite, tennantite, loellingite, cobaltite, gold, silver, and tetrahedrite may be present. Pyrite is a ubiquitous gangue mineral; hematite and magnetite may also be present. Host rocks are altered to diopside and andradite in areas proximal to the deposit, wollastonite and possibly tremolite are present in the outer parts of the deposit, and marble is peripheral to the deposit. The igneous rocks contain epidote, pyroxene, and garnet as alteration products. Retrograde alteration may produce epidote, actinolite, chlorite, and clay.

Geophysical and Geochemical Signatures.—Most intrusive bodies associated with these deposits are discernible in regional gravity and magnetic data. Magnetite associated with some of these skarns may produce a magnetic anomaly that can help locate the ore body. The geochemical signature of copper-skarn deposits includes anomalous abundances of Cu, Zn, Pb, Co, Au, Ag, As, Sb, and Bi.

Copper-Skarn Deposits in Coronado National Forest.—Potential host rocks for copper skarn deposits in Forest include (1) carbonate sedimentary rocks of the Apache Group in the northern part of the Forest; (2) Paleozoic carbonate sedimentary rocks, including the Abrigo Formation, the Escabrosa Limestone, and carbonate facies of the Naco Group; and (3) Lower Cretaceous carbonate facies of the Bisbee Group. The type copper-skarn deposit in the Forest is the Elgin Mine, in the northern Santa Rita Mountains.

POLYMETALLIC REPLACEMENT DEPOSITS (MODEL 19a)

Commodities.—Silver, lead, and zinc are the primary commodities produced from polymetallic replacement deposits; copper and gold are possible byproducts.

Deposit Description.—Polymetallic replacement deposits are present in carbonate sedimentary rocks through which solutions derived from volcanic centers and epizonal plutons have circulated and caused replacement of soluble country rock components by ore minerals and silicates. Most of these deposits are present in calcareous sedimentary rocks, including limestone, dolomite, and shale. In many places, these sedimentary rocks are overlain by volcanic rocks and intruded by calc-alkaline plutons. Ore bodies, located near igneous intrusions, vary from elongate or massive lenses to pods, pipes, and veins. They are localized by faults or by bedding in host rocks; most deposits are late Mesozoic to early Tertiary in age.

Mineralogy and Alteration.—Mineral assemblages in these deposits are zoned. The inner zone includes enargite, sphalerite, argentite, and digenite, along with possible chalcopyrite and rare bismuthinite. Galena, sphalerite, and argentite, and possibly tetrahedrite, proustite, pyrargyrite, rare jamesonite, jordanite, bournonite, stephanite, and polybasite occur in intermediate zones. The outer zone contains sphalerite and rhodochrosite. Gold, sylvanite, and calaverite are present locally. Quartz, pyrite, marcasite, barite, calcite, and fluorite are widespread gangue minerals; rhodochrosite is present in the outer zone. Alteration included dolomitization and silicification of wallrocks to jasperoids. Shale and igneous rocks were chloritized and argillized; where syngenetic iron oxide is present, rocks are pyritized.

Geophysical and Geochemical Signatures.—Faults that localize these deposits may be discernible in regional geophysical data. Deposits may be delineated by detailed electrical surveys. The geochemical signature for polymetallic replacement deposits includes anomalous abundances of Cu, Zn, Pb, Mn, Ag, Au, As, Sb, Bi, and Ba. Stream sediments contained anomalous abundances of As, whereas most panned concentrates contained anomalous abundances of B, Ag, Cu, Zn and Pb; heavy-mineral fractions contained anomalous abundances of Ba, Bi, Mo, Cd, Sn, and W.

Polymetallic Replacement Deposits in Coronado National Forest.—Potential host rocks for polymetallic replacement deposits in the Forest include (1) carbonate sedimentary rocks of the Apache Group in the northern part of the Forest; (2) Paleozoic carbonate sedimentary rocks, including the Abrigo Formation, the Escabrosa Limestone, and carbonate facies of the Naco Group; and (3) Lower Cretaceous carbonate facies of the Bisbee Group. Deposits were localized by major northwest-striking faults in several areas, including the Santa Teresa, Winchester, Patagonia, and Santa Catalina Mountains. The type polymetallic replacement deposit in the Forest is the Mowry Mine, in the Patagonia Mountains.

PORPHYRY COPPER-MOLYBDENUM DEPOSITS (MODEL 21a)

Commodities.—Copper and molybdenum are the primary commodities produced from porphyry copper-molybdenum deposits; lead, zinc, silver, uranium, rhenium, and gold are possible byproducts.

Deposit Description.—Porphyry copper-molybdenum deposits consist of a quartz-veinlet stockwork that contains chalcopyrite and molybdenite in or near a porphyritic tonalite to monzogranite stock and (or) breccia pipes emplaced in batholithic, volcanic, or sedimentary rocks. The ratio of gold (in parts per million) to molybdenum (in percent) in these deposits is less than 3. The porphyry intrusions, most of which are Mesozoic to early Tertiary in age, may be cut by abundant contemporaneous faults, dikes, or breccia pipes. In the upper parts of these deposits, ore grade is positively correlated with veinlet and mineralized-fracture spacing. Secondarily enriched parts of porphyry copper-molybdenum systems contain ore-grade concentrations of chalcocite and constitute ore bodies that formed by surficial copper leaching, downward percolation in solution, and reprecipitation at the water table.

Mineralogy and Alteration.—Ore minerals in porphyry copper-molybdenum deposits consist of chalcopyrite and molybdenite; pyrite is the principal gangue sulfide mineral. Peripheral polymetallic veins and associated replacement deposits contain chalcopyrite, sphalerite, galena, and possibly gold. Outer zones may contain veins of Cu-Ag-Sb sulfides, barite, and gold. Altered rock varies from a quartz-potassium feldspar-chlorite assemblage, along with possible anhydrite, in proximal zones to propylitically

altered rock in distal zones. A zone of white mica and phyllic alteration may cap and (or) encircle the entire deposit. Some deposits have high-alumina alteration at upper deposit levels.

Geophysical and Geochemical Signatures.—Most intrusive bodies associated with this deposit type are discernible in regional geophysical data; magnetic lows are associated with many deposits of this type. The geochemical signature for these deposits includes anomalous abundances of Cu, Mo, and Ag, and possibly anomalous abundances of W, B, and Sr in the center of the deposit. Anomalous abundances of Pb, Zn, Au, As, Sb, Se, Te Mn, Co, Ba, and Rb are found in the outer zones, and anomalous abundances of Bi and Sn are in distal zones; abundances of S are anomalous in all zones.

Porphyry Copper-Molybdenum Deposits in Coronado National Forest.—Porphyry copper-molybdenum deposits in the Forest are associated with Late Cretaceous to Paleocene (Laramide) felsic intrusions of granitic composition, most of which are in the western half of the Forest. Localization of these deposits may be controlled by northwest-striking, medium- to regional-scale faults. The type porphyry copper-molybdenum deposit in the Forest is the Childs-Aldwinkle deposit, in the northern Galiuro Mountains.

POLYMETALLIC VEIN DEPOSITS (MODEL 22c)

Commodities.—Silver, lead, and zinc are primary commodities produced from polymetallic vein deposits; gold may be a byproduct.

Deposit Description.—Polymetallic vein deposits consist of quartz-carbonate veins that contain silver, lead, zinc, and gold and are associated with felsic, hypabyssal intrusions composed of calc-alkaline and alkaline diorite to granodiorite, monzonite, and monzogranite of any age. The deposits are hosted by sedimentary and metamorphic rocks and are present near surface fractures and breccias within the thermal aureole of the associated intrusions; commonly, these types of deposits are peripheral to porphyry systems.

Mineralogy and Alteration.—Ore minerals in polymetallic vein deposits include native gold and electrum along with sphalerite, and possibly chalcopyrite, galena, arsenopyrite, tetrahedrite-tennantite, silver sulfosalts, and argentite in veins of pyrite, hematite, quartz, chlorite, calcite, and possibly dolomite, ankerite, siderite, rhodochrosite, barite, fluorite, chalcedony, and adularia. A wide propylitic alteration zone and narrow sericitic and argillic alteration zones surround most deposits. Many carbonate sedimentary rocks were silicified to jasperoid.

Geophysical and Geochemical Signatures.—These deposits can be directly detected by electrical methods. They may also be associated with lineaments or steep gradients in gravity and magnetic data. The geochemical signature of these deposits includes anomalous abundances of Zn, Cu, Pb, As, Au, Ag, Mn, and Ba; Cu and Au abundances are especially anomalous at the deposit center, whereas Zn, Pb, Ag, and Mn abundances are especially anomalous at its periphery.

Polymetallic Vein Deposits in Coronado National Forest.—Polymetallic vein deposits are present in a wide variety of rock types in the Forest. Specific host-rock composition is less important than is the presence of felsic hypabyssal intrusions whose emplacement seems to be genetically related to formation of these deposits. Favorable geologic settings are present in the northern Chiricahua and Santa Rita Mountains and in the Cobre Ridge and Pajarito Mountain regions of the Tumacacori Mountains. The type polymetallic vein deposit in the Forest is the Montana Mine, in the Tumacacori Mountains.

HOT-SPRINGS GOLD-SILVER DEPOSITS (MODEL 25a)

Commodities.—Gold and silver are the only commodities produced from hot springs gold-silver deposits in the region.

Deposit Description.—Ore in hot-springs gold-silver deposits is fine-grained chalcedonic and (or) opaline sinters and quartz in silicified breccia, veins, or stockworks that contain gold, pyrite, and antimony and arsenic sulfides. The deposits are hosted by subaerial Tertiary through Quaternary rhyolite centers, including rhyolite lava dome complexes and the shallow parts of related geothermal systems. Most deposits are related to through-going fracture systems.

Mineralogy and Alteration.—The mineral assemblage in hot-springs gold-silver deposits includes native gold, pyrite, stibnite, and realgar or arsenopyrite, and possibly sphalerite, chalcopyrite, fluorite, native gold, and silver selenides or tellurides, and pyrite. Some deposits contain alunite and pyrophyllite; ammonium feldspar may be present. Altered rock, from the top to the bottom of such a geothermal system, includes chalcedonic sinter, massively silicified rock, stockworks and quartz-adularia veins, and quartz- or quartz-chlorite-cemented breccia.

Geophysical and Geochemical Signatures.—The deposits themselves have no geophysical expression, but most are related to faults that may be discernible on regional magnetic and gravity surveys. The geochemical signature includes anomalous abundances of Au, As, Sb, Hg, and Ti near the top of the system. Ag abundances increase with depth, whereas As, Sb, Tl, and Hg abundances decrease with depth.

Hot-Springs Gold-Silver Deposits in Coronado National Forest.—The preferred host rock for this deposit

type in the Forest is Tertiary rhyolite associated with a proposed volcanic center in the Galiuro Mountains. Many of the deposits are associated with major to minor north- to north-northwest-striking faults. The type hot-springs gold-silver deposit in the Forest is the Powers Mine, in the Galiuro mountains.

CREEDE-TYPE EPITHERMAL VEIN DEPOSITS (MODEL 25b)

Commodities.—Gold and silver are the primary commodities produced from Creede-type epithermal vein deposits; lead, copper, and zinc are potential byproducts.

Deposit Description.—Creede-type epithermal vein deposits are commonly referred to as alkali-chloride or quartz-adularia epithermal vein deposits. They consist of galena, sphalerite, chalcopyrite, sulfosalts, and possibly tellurides and gold in quartz-carbonate veins hosted by felsic to intermediate composition volcanic rocks; type examples are Tertiary, but these deposits may be of any age. The host rocks must be underlain by prevolcanic evaporites or rocks with entrapped seawater to act as sources of saline fluids for the deposit. Host rocks for Creede-type epithermal vein deposits are porphyritic andesite, dacite, quartz latite, rhyodacite, rhyolite, and associated sedimentary rocks. Volcanic rocks related to the deposit can be classified as calc-alkaline or bimodal.

Mineralogy and Alteration.—The mineral assemblage of Creede-type epithermal vein deposits includes galena, sphalerite, chalcopyrite, copper sulfosalts, and silver sulfosalts, and possibly gold tellurides, bornite, and arsenopyrite. Gangue minerals are quartz, chloride, calcite, pyrite, rhodochrosite, and barite, and possibly fluorite, siderite, ankerite, sericite, adularia, specularite, and alunite. Altered rock at the top of the deposit contains quartz and montmorillonite, and possibly kaolinite, zeolites, barite, and calcite. Towards the bottom, quartz and possibly illite become the predominant alteration minerals. Specularite and alunite may also be present.

Geophysical and Geochemical Signatures.—The deposits have no geophysical expression, but the fault systems with which they are generally associated may be identifiable on regional magnetic and gravity surveys. High in the system, the geochemical anomaly is Au, As, Sb, and Hg, or Au, Ag, Pb, Zn, and Cu, or Ag, Pb, Zn, or Cu, Pb, and Zn; W and Bi may be present. Base-metal ore grades are generally higher in silver-bearing deposits.

Creede-Type Epithermal Vein Deposits in Coronado National Forest.—Creede-type epithermal vein deposits are unknown in the Forest but may be present in the Peloncillo Mountains, where there is a favorable geologic setting and geochemical anomalies are favorable for the occurrence of undiscovered deposits of this type.

RHYOLITE-HOSTED TIN DEPOSITS (MODEL 25h)

Commodities.—Tin is the primary commodity produced from rhyolite-hosted tin deposits.

Deposit Description.—Rhyolite-hosted tin deposits are characterized by cassiterite in discontinuous veinlets in high-silica rhyolite flow complexes and in related epiclastic and pyroclastic rocks; known deposits are Tertiary, but these deposits may be of any age. Deposits are present in the high-permeability, fractured and brecciated outer parts of flow complexes as narrow, discontinuous veins and veinlets that are generally less than 75 m long and 10 cm wide; veins and veinlets may be clustered in somewhat larger zones. These deposits can also be present as cassiterite disseminated in the matrix of rhyolite flows or fault breccias. Rhyolite-hosted tin deposits may be a high-level expression of Climax-type molybdenum deposits.

Mineralogy and Alteration.—The mineral assemblage for rhyolite-hosted tin deposits includes cassiterite and hematite, and possibly cristobalite, fluorite, tridymite, opal, chalcedony, beudantite, mimetite, adularia, durangite, and zeolite minerals. Tin occurrences may be associated with large areas of rock altered (tridymite, sanidine, hematite, pseudobrookite) by a vapor phase. Alteration minerals directly associated with mineralization include cristobalite, fluorite, smectite, kaolinite, and other clay minerals.

Geophysical and Geochemical Signatures.—The deposits have no geophysical signature; however, the deposits may be localized by high-angle faults, which may be discernible on regional gravity and magnetic surveys. The geochemical signature of rhyolite-hosted tin deposits is similar to that of Climax-type molybdenum deposits; in addition, cassiterite is abundant in stream sediments. Abundances of Mo, Sn, W, and Rb in rock overlying Climax-type molybdenum deposits are anomalous; Pb, Zn, F, and U abundances are anomalous in wall rock as much as a few kilometers from these deposits. Sn, W, Mo, and F abundances in panned concentrates may be anomalous.

Rhyolite-Hosted Tin Deposits in Coronado National Forest.—Rhyolite-hosted tin deposits are unknown in the Forest. A favorable geologic setting and appropriate geochemical anomalies indicate that these deposits may be present in the extensive Tertiary high-silica rhyolite flows and tuffs of the Peloncillo Mountains.

GOLD PLACER DEPOSITS (MODEL 39a)

Commodities.—Gold and silver are the primary commodities produced from gold placer deposits; radioactive minerals and rare-earth-elements are potential byproducts.

Deposit Description.—Gold placer deposits consist of elemental gold grains and, rarely, large nuggets concentrated in fluvial accumulations of gravel, silt, clay, and their

consolidated equivalents. Gold particles range from a few microns to as much as 1 m in diameter. These deposits are usually found downstream from precious-metal lode deposits and are formed where turbulent and irregular flow patterns have segregated light from heavy bedload components. Gold and other heavy ore minerals are erratically concentrated in small-volume fractions of gravel deposited immediately above the bedrock interface. Both free gold and electrum may be present. Most gold placer deposits are Cenozoic; older deposits may have formed but are unlikely to have been preserved.

Mineralogy and Alteration.—Gold and electrum are the ore minerals. Ilmenite, magnetite, euxenite, brannerite, monazite, cinnabar, stibnite, and garnet also are present in some placer deposits. No altered host rock is associated with these deposits.

Geophysical and Geochemical Signatures.—Ground-based magnetometer surveys may detect magnetite concentrations that may contain associated gold accumulations. Panned concentrates of stream sediment from an area favorable for the occurrence of placer gold deposits may contain anomalous abundances of native gold and (or) silver, electrum, ilmenite, magnetite, euxenite, and other black-sand minerals.

Gold Placer Deposits in Coronado National Forest.—Gold placer deposits are present in the Santa Catalina and Santa Rita Mountains, and trace amounts of gold have been recovered from other Forest units. The type gold placer deposit in the Forest is the Greaterville Placer Mine, in the Santa Rita Mountains.

RESOURCE POTENTIAL OF CORONADO NATIONAL FOREST

METALS

The earth science assessment team considered all available information in order to delineate mineral resource tracts for Coronado National Forest. No formula for a minimum number of favorable earth science criteria was used in delineating tracts or in assigning categories of mineral resource potential (high, moderate, or low) or levels of certainty (A, B, C, or D) (appendix 1). Tracts were delineated in accord with the local geologic environment and its relationship to the mineralization process.

Specific details concerning tract delineation and assignment of resource potential categories and levels of certainty for those categories are included in the sections that follow. Tracts having high mineral resource potential are specially indicated; other delineated areas have moderate to low mineral resource potential, whereas undelineated areas are considered to have no potential for the indicated deposit types. No area was assigned an unknown potential. Tracts that intersect known mining districts are noted; mining district names are from Keith and others (1983). Delineated tracts for the 12 Forest units are presented as page-size illustrations at 1:500,000 (figs. 1–4) as well as on the plates at 1:126,720 (pl. 27–29). The order in which the mineral resource potential of the Forest units is presented follows that used by Drewes (Chapter B, this volume).

Tract names reflect the name of the principal mountain range in that Forest unit. Subtracts are designated in cases for which parts of a tract were delineated for different reasons. Tract ST–1, for instance, refers to tract 1 in the Santa Teresa Mountains and tract ST–1a refers to subtract "a" of tract ST–1.

SANTA TERESA MOUNTAINS

TRACT ST–1—POLYMETALLIC REPLACEMENT DEPOSITS

Tract ST–1 (fig. 1 and pl. 27) has high potential, certainty level C, for the occurrence of undiscovered polymetallic replacement deposits. Mineral resource potential in this tract is indicated by proximity to the Santa Teresa Granite, the presence of faults that may have served as conduits for hydrothermal fluids (the Grand Reef fault system and the Goodwin Canyon fault), coincidence with the Aravaipa mining district, occurrence of numerous rock types that are favorable as hosts for polymetallic replacement deposits, and anomalous abundances of Bi, Cd, Cu, Mn, Mo, Pb, Sb, and Zn (stream-sediment) and Ba, Bi, Cu, Mo, Sn, and W (panned-concentrate) in samples collected from this area (Chapter C, this volume).

The two most favorable rock types within the tract are the Escabrosa Limestone and Horquilla Limestone of the Naco Group. Other rock types within the tract that can host these deposits include the Martin Formation (the Abrigo Formation is absent in this area), Cretaceous rhyolite and andesite, and Cretaceous volcaniclastic rocks. The areas having the most potential for polymetallic replacement deposits include intersections of faults with favorable host rock types. The tract includes areas concealed by alluvium that are west of favorable, exposed host rocks. Although geophysical evidence indicates that bedrock dips gently beneath the alluvium, the westward extent of the tract is limited to the area near the Grand Reef fault system and the Santa Teresa stock. The tract extends northwest for an indeterminate distance.

TRACT ST–2—DEPOSITS FOR WHICH A CORRESPONDING MODEL IS UNKNOWN

Tract ST–2 (fig. 1 and pl. 27) has moderate to low potential, certainty level A, for the occurrence of undiscovered deposits for which a corresponding model is unknown. The earth science attributes for this tract suggest that the area

is the locus of several superimposed mineralizing systems of different types. The mineral resource potential in this tract is indicated by anomalous abundances of Au, Ag, As, Bi, Cd, Cu, Mo, Pb, Sb, Zn, Mn, Sn, and W in stream-sediment samples. The area has a ranking of 9 (out of 10) on the geochemical intensity scale (Chapter C, this volume). An area of possible clay and ferric oxide alteration detectable on Landsat Thematic Mapper imagery (Chapter F, this volume) coincides with the geochemically anomalous area. The tract is entirely within the Late Cretaceous Santa Teresa Granite and includes one known copper occurrence. This occurrence is not well documented and evidence of mineralization is insufficient to delineate a high-potential tract.

TRACT ST–3—DEPOSIT RELATED TO HIGHLY SPECIALIZED GRANITE FOR WHICH A CORRESPONDING MODEL IS UNKNOWN

The boundary of tract ST–3 (fig. 1 and pl. 27) was taken directly from the U.S. Bureau of Land Management Black Rock Wilderness Study Area study (Simons and others, 1987). The tract has moderate to low resource potential, certainty level C, for the presence of undiscovered deposits related to highly specialized granite. Mineral resource potential in the tract is indicated by geochemically anomalous stream-sediment samples and mesquite leaves. These samples contained anomalous abundances of La, Th, Y, Ba, B, Sn, Th, Be, Pb, Mo, V, Cu, Co, W, and Ag. Commodities that may be present include thorium, rare-earth elements, tin, beryllium, copper, lead, molybdenum, cobalt, vanadium, and tungsten. Rock types within the tract include Proterozoic metamorphic rocks, Tertiary granite, Tertiary volcanic rocks of various compositions; the tract also contains areas in which potential host rocks are concealed by Cenozoic fanglomerate. Northwest- and northeast-striking faults having moderate dips also are present within the tract.

GALIURO MOUNTAINS

TRACT G–1—PORPHYRY COPPER-MOLYBDENUM DEPOSITS

Tract G–1 (fig. 1 and pl. 27) has high potential, certainty level D, for the presence of undiscovered porphyry copper-molybdenum deposits. The tract is underlain by Paleozoic sedimentary rocks (Martin Formation and Escabrosa Limestone), Upper Cretaceous andesite (Glory Hole Volcanics), the Laramide (68 Ma) Copper Creek Granodiorite, Tertiary andesite, and rhyolite lava and tuff and is cut by northwest-striking faults, plugs, and breccia pipes. The Tertiary volcanic rocks are not potential hosts for this deposit type, but they unconformably overlie and conceal potential host rocks. The tract includes the Bunker Hill mining district, which contains several medium to large porphyry copper-molybdenum deposits. The mineral resource potential in this tract is indicated by favorable geologic environment, coincidence with the Bunker Hill mining district, the observed and inferred extent of the Copper Creek Granodiorite, and location along a circular feature that is discernible on the Bouguer anomaly map (Chapter D, this volume) and may have controlled emplacement of intrusions. The northeastern extent of the tract is indicated by anomalous abundances of Au, Ag, As, Cd, Cu, Mo, Pb, Sb, Zn, Ba, Mn, and Sn (Chapter C, this volume).

Possible areas of favorable host rock east and southeast of the Copper Creek Granodiorite are concealed by Tertiary volcanic rocks. In these areas geophysical and structural interpretations indicate that the Tertiary andesite and rhyolite cover is less than 1 km thick.

Many of the porphyry copper-molybdenum deposits in the Bunker Hill district are associated with breccia pipes that are slightly younger that the Upper Cretaceous Glory Hole andesite they intrude. The northern part of the tract, especially, includes numerous breccia pipes; the extent of mineralized rock in the tract is not known.

TRACT G–2—HOT SPRINGS GOLD-SILVER DEPOSITS

Tracts labeled G–2 (fig. 1 and pl. 27) have high or moderate potential, certainty level B, for the occurrence of undiscovered hot springs gold-silver deposits. These tracts include the Rattlesnake mining district, which is composed of several small hot-springs precious-metal mines. Tracts having moderate or low potential were indicated by at least two of the following five attributes; tracts having high potential also contain known ore mineral occurrences:

(1) Areas are associated with, or inferred to be associated with, Tertiary rhyolite dome complexes; dome complexes may be associated with widespread hydrothermal circulation of fluids that resulted in deposition of ore related to hot-springs systems;

(2) Areas are near faults or geophysical evidence indicates the presence of faults; most faults, including the Rattlesnake fault, strike north-northwest;

(3) Areas were the source of stream-sediment samples that contained anomalous abundances of gold, arsenic, and antimony;

(4) Areas are aligned with a circular feature discernible on the Bouguer gravity map of the Galiuro Mountains (Chapter D, this volume);

(5) Areas display evidence of possible ferric oxide and (or) clay alteration on Landsat Thematic Mapper imagery.

All of these tracts coincide with Tertiary lava flows and tuffs whose compositions range from rhyolite to andesite, and all are within or along the circular gravity feature mentioned above.

WINCHESTER MOUNTAINS

TRACT WIN–1—POLYMETALLIC REPLACEMENT DEPOSITS

Tracts labeled WIN–1 (fig. 1 and pl. 27) have moderate to low potential, certainty level B, for the presence of

undiscovered polymetallic replacement deposits. Three subtracts were delineated on the basis of different evidence. Most of the area delineated by these tracts is underlain by Tertiary volcanic rocks, including rhyolite flows and tuff and andesite; rocks considered to be favorable hosts for polymetallic replacement deposits, however, are hypothesized to be present in the shallow subsurface. Only in the southeastern part of tract WIN–1b are these host rocks exposed.

Tract WIN–1a was delineated on the basis of an aeromagnetic anomaly and slightly anomalous abundances of zinc and barium in stream-sediment samples. The magnetic anomaly may represent a concealed felsic intrusion that may have had an associated hydrothermal system.

Tract WIN–1b was delineated on the basis of a northwest-striking, steeply dipping fault system that may have been a conduit for the inferred hydrothermal system. Paleozoic host rocks, including the Escabrosa Limestone and Naco Group rocks including the Horquilla Limestone, are exposed in the southeastern part of this tract. This region includes a poorly documented copper occurrence; evidence of mineralized rock is insufficient to classify the tract as having high potential. Landsat Thematic Mapper imagery shows strong evidence of possible ferric oxide and (or) clay alteration associated with Paleozoic rocks in the southern part of tract W–1b.

Tract WIN–1c was delineated on the basis of anomalous abundances of Mo, Pb, Sb, Zn, Ba, and Mn in stream-sediment samples, a north-striking aeromagnetic anomaly, and Landsat Thematic Mapper imagery indicates moderate levels of ferric oxide and (or) clay alteration in this area.

PINALENO MOUNTAINS

TRACT PIN–1—COMPOSITE MINERAL DEPOSIT FOR WHICH A CORRESPONDING MODEL IS UNKNOWN

Tract PIN–1 (fig. 1 and pl. 27) has moderate to low potential, certainty level B, for the occurrence of undiscovered composite deposits that incorporate two or more unknown mineral deposit model types. The tract was delineated on the basis of stream-sediment samples that contained anomalous abundances of Sn, Th, U, Be, Mo, Cu, Bi, As, Sb, Pb, and Zn (Chapter C, this volume); the presence of high-angle, northwest-striking faults; indications of mineralized rock (uranium occurrences); favorable host rocks (Tertiary rhyolite and andesite); scattered areas of possible ferric oxide and clay alteration, as indicated by Landsat Thematic Mapper imagery (Chapter F, this volume); and presence of Tertiary stocks. The uranium occurrences are poorly documented and insufficient to delineate a high-potential tract or to influence designation of a deposit model. Complex and diverse evidence indicates that an unknown type of mineralizing system or, more likely, two or more mineralizing systems affected this area. The effects of multiple, superimposed mineralizing events makes it impossible to designate an individual ore deposit model or to separate their respective manifestations.

PELONCILLO MOUNTAINS

TRACT PEL–1—RHYOLITE-HOSTED TIN DEPOSITS

Tracts labeled PEL–1, (fig. 2 and pl. 28) have high or moderate to low potential, certainty level B, for the occurrence of undiscovered rhyolite-hosted tin deposits. The tracts are underlain by Tertiary high-silica rhyolite flows, tuff, and plugs. High-potential tracts were delineated on the basis of suitable host rocks and on anomalous abundances of Au, Bi, Cd, Cu, Mo, Pb, Sb, Zn, Mn, and Sn (stream-sediment) and As, Mo, Pb, Sb, W, Zn, Ba, Mn, and Sn (panned-concentrate) collected in this area (Chapter C, this volume). The moderate- to low-potential tract, which lacks strong geochemical anomalies, extends into the Animas Valley east of the Peloncillo Mountains, where bedrock beneath alluvium is presumed to be similar to that exposed in the range; concealed rhyolite-hosted tin deposits are possible. Geophysical data suggest a shallow dip to bedrock beneath the basin sediments in this region, which indicates that this part of the tract contains less than 1 km of alluvium.

NONDELINEATED TRACT HAVING POTENTIAL FOR CLIMAX-TYPE MOLYBDENUM DEPOSITS

Rhyolite-hosted tin deposits are a possible high level manifestation of Climax-type molybdenum deposits; deposits of this type may be present at depth in the Peloncillo Mountains. While geologic, geophysical, and geochemical data are insufficient for delineation of a tract for this deposit model, all of the Peloncillo Mountains can be considered favorable for the occurrence of undiscovered Climax-type molybdenum deposits.

TRACT PEL–2—CREEDE-TYPE EPITHERMAL VEIN DEPOSITS

Tracts labeled PEL–2 (fig. 2 and pl. 28) have high or moderate to low potential, certainty level B, for the occurrence of undiscovered Creede-type epithermal vein deposits. The tracts were delineated on the basis of favorable host rock types, including Tertiary rhyolite tuff and plugs and andesite. The high-potential tract coincides with an area for which samples contained anomalous abundances of Au, Bi, Cd, Cu, Mo, Pb, Sb, Zn, Mn, and Sn (stream sediment) and As, Mo, Pb, Sb, W, Zn, Ba, Mn, and Sn (panned concentrate) (Chapter C, this volume). The moderate- to low-potential tract contains fewer, less geochemically anomalous samples. A small silver prospect is located in the moderate to low-potential tract, but indications of widespread, intensely mineralized rock are absent.

TRACT PEL–3—DEPOSITS FOR WHICH A CORRESPONDING MODEL IS UNKNOWN

Tract PEL–3 (fig. 2 and pl. 28) has moderate to low potential, certainty level A, for the occurrence of undiscovered deposits for which there is no known model. This area may represent a composite of several mineralizing events. The tract was delineated on the basis of a large magnetic low over which it is centered and that coincides with an area for which geochemical samples contained anomalous abundances of Sb, Ba, As, Co, V, Be, Zn, Y, and Bi. A magnetic high is directly north of the tract.

CHIRICAHUA AND PEDREGOSA MOUNTAINS

TRACT CH–1—POLYMETALLIC VEIN, POLYMETALLIC REPLACEMENT, AND PORPHYRY COPPER SKARN-RELATED DEPOSITS

Tract CH–1 (fig. 2 and pl. 28) has high or moderate to low potential, certainty level C, for the occurrence of undiscovered polymetallic vein, polymetallic replacement, and porphyry copper skarn-related deposits. The tract is underlain by Pinal Schist; Middle Proterozoic felsic intrusions; Paleozoic sedimentary rocks (including the Abrigo Formation, the Escabrosa Limestone, and the Naco Group); Cretaceous andesite, rhyolite, and sedimentary rocks; Tertiary andesite, rhyolite flows and tuff, granite, rhyolite plugs and dikes, and quartz veins; and it includes areas in which these host rocks are concealed by shallow Quaternary alluvium. The tract encompasses an area along the Apache Pass fault zone and includes the California mining district. The fault zone, which contains host rocks favorable for the occurrence of three mineral deposit types, has localized the emplacement of plutons and hydrothermal-fluid flow in this area. Tracts having moderate to low potential were delineated on the basis of spatial association with the Apache Pass fault system and anomalous abundances of Au, Ag, As, Bi, Cd, Cu, Mo, Pb, Sb, W, Zn, Ba, Mn, and Sn (stream sediment) and Ag, As, Bi, Cd, Cu, Mo, Pb, W, Zn, Ba, and Sn (panned concentrate) (Chapter C, this volume). High-potential tracts include areas that have all of the above characteristics and contain altered areas (Chapter B, this volume), possible clay and (or) ferric oxide alteration (Chapter F, this volume), or ore-mineral occurrences.

TRACT CH–2—POLYMETALLIC VEIN, PORPHYRY COPPER SKARN-RELATED, AND POLYMETALLIC REPLACEMENT DEPOSITS

Tracts labeled CH–2 (fig. 2 and pl. 28) have moderate to low potential, certainty level C, for occurrence of undiscovered polymetallic vein deposits. The potential for discovery of porphyry copper skarn-related deposits and polymetallic replacement deposits in these areas is low, certainty level C. The tracts are part of the central and southern Chiricahua Mountains and the Pedregosa Mountains and are underlain by a variety of rocks, including Paleozoic sedimentary rocks (including the lower Paleozoic Abrigo Formation, the middle Paleozoic Escabrosa Limestone, and the upper Paleozoic Naco Group); Cretaceous andesite, rhyolite, and sedimentary rocks; and Tertiary andesite, rhyolite flows and tuff, granite, rhyolite plugs and dikes, and quartz veins, and areas concealed by shallow Quaternary alluvium. The tracts were delineated on the basis of host rock types, and at least one of the following attributes:

(1) Ore minerals are present;

(2) possible ferric oxide and (or) clay alteration are indicated by Thematic Mapper imagery (Chapter F, this volume);

(3) stream-sediment samples had anomalous abundances of Au, Ag, As, Bi, Cd, Cu, Mo, Pb, Sn, Zn, and W in and (or) panned-concentrate samples had anomalous abundances of Ag, As, Cd, Cu, Mo, Pb, Sb, Zn, Ba, and Sn in (Chapter C, this volume).

DRAGOON MOUNTAINS

TRACT D–1—POLYMETALLIC REPLACEMENT AND TUNGSTEN SKARN DEPOSITS

Tracts labeled D–1 (fig. 2 and pl. 28) have high or moderate to low potential, certainty level C, for the occurrence of undiscovered polymetallic replacement and tungsten skarn deposits. The tracts are underlain by Paleozoic and Mesozoic sedimentary rocks, including the highly favorable Abrigo Formation, the Escabrosa Limestone, the Naco Group, and the Bisbee Group. Moderate- to low-potential tracts are underlain by favorable host rocks that crop out near the middle Tertiary Stronghold stock, an alkali-feldspar granite, and samples from these areas contained anomalous abundances of Au, Ag, Bi, Cd, Cu, Mo, Pb, Sb, W, Zn, and Sn (stream sediment) and Ag, As, Bi, Cd, Cu, Mo, Pb, Sb, W, Zn, Ba, Mn, and Sn (panned concentrate), respectively (Chapter C, this volume). Areas of favorable host rocks on the east and west flanks of the Dragoon Mountains that are concealed by Quaternary alluvium also have moderate to low potential, certainty level C. Geophysical evidence indicates that alluvium is shallow in these areas and that a shallow apophysis of the Stronghold stock may be on its northeast side (Chapter D, this volume).

High-potential tracts have the attributes listed above and contain mines and prospects of the Middle Pass and Golden Rule mining districts, are associated with large aeromagnetic highs (which may reflect magnetite accumulations in skarn and replacement deposits), or are areas that display possible clay or ferric oxide alteration on Landsat Thematic Mapper imagery. The Stronghold stock is the presumed source of heat and fluid for these deposits, but the stock itself is unmineralized.

WHETSTONE MOUNTAINS

TRACT WHET–1—PORPHYRY COPPER DEPOSITS

Tracts labeled WHET–1a–c (fig. 3 and pl. 29) have high or moderate to low potential, certainty level B, for the occurrence of undiscovered porphyry copper deposits. The tract is underlain by Pinal Schist; Paleozoic sedimentary rocks (including the Abrigo Formation), the Escabrosa Limestone, and the Naco Group rocks; Bisbee Group sedimentary rocks; Late Cretaceous and early Tertiary (Laramide) granite and rhyolite flows, and includes areas where favorable host rocks are concealed by Quaternary alluvium.

Subtract WHET–1a (fig. 3 and pl. 29) has high mineral resource potential, as indicated by the presence of a Late Cretaceous-age granitic stock (the Mine Canyon stock) exposed in the southwest corner of the Whetstone Mountains; a large aeromagnetic high; samples that contain anomalous abundances of Au, Ag, As, Bi, Cu, Mo, Sb, Zn, and Ba (stream sediment) and Ag, Bi, Cu, Mo, Pb, Sb, W, and Ba (panned concentrate); and the presence of mineralized rock in the Mine Canyon district, which includes a porphyry copper deposit. Wrucke and McColly (1984) reported that the porphyry copper deposit contains substantiated resources amounting to 32 million tons of ore at 0.28 weight percent copper and 0.01 weight percent molybdenum.

Subtract WHET–1b (fig. 3 and pl. 29) has moderate to low potential, as indicated by rhyolite flows and sills inferred to be associated with the Late Cretaceous-age intrusion; by highly anomalous gold abundances in stream-sediment samples; and by samples from this area that also contain anomalous abundances of Ag, Cd, Mo, and Sb (stream sediment) and Ag, Bi, Cd, Cu, Mo, Pb, W, Zn, and Ba (panned concentrate) (Chapter C, this volume).

Subtract WHET–1c (fig. 3 and pl. 29) has moderate to low potential, as indicated by the occurrence of Laramide-age granitic rocks, a sill possibly related to the Mine Canyon stock, and geochemical anomalies similar to those of subtract WHET–1a. The entire Whetstone range may be underlain by a granitic batholith of which only a small part is exposed as the Mine Canyon stock and associated sills (Chapter D, this volume). Subtract WHET–1c extends into the area occupied by tract WHET–2 and includes areas in which favorable host rocks are concealed by shallow alluvium.

TRACT WHET–2—TUNGSTEN VEIN DEPOSITS

Tract WHET–2 (fig. 3 and pl. 29) has moderate to low potential, certainty level B, for the occurrence of undiscovered tungsten vein deposits. It is underlain by Pinal Schist; lower Paleozoic sedimentary rocks (including the Abrigo Formation), Escabrosa Limestone, Naco Group sedimentary rocks; and Late Cretaceous (Laramide) granite. The tract was delineated on the basis of known deposits in the Whetstone mining district and because of the nearby presence of a Late Cretaceous-age granite that may be present at depth in the tract.

PATAGONIA AND HUACHUCA MOUNTAINS AND CANELO HILLS

TRACT PH–1—PORPHYRY COPPER-MOLYBDENUM, POLYMETALLIC REPLACEMENT, TUNGSTEN VEIN, AND TUNGSTEN SKARN DEPOSITS

Tracts labeled PH–1a–d (fig. 3 and pl. 29) have high or moderate to low potential, certainty level C, for the occurrence of undiscovered porphyry copper skarn, polymetallic replacement, tungsten vein, and tungsten skarn deposits. Host rocks within these include Paleozoic sedimentary rocks (including the Abrigo Formation, the Escabrosa Limestone, and the Naco Group); Jurassic granite (a rock type that hosts a porphyry copper deposit to the east, at Bisbee); Triassic and Jurassic volcanic rocks, including rhyolite tuff and flows, andesite flows, and volcaniclastic rocks; Cretaceous rhyolite (flows and tuff) and Bisbee Group sedimentary rocks; and Tertiary rhyolite tuff, andesite flows, volcaniclastic rocks, and intrusions (granite).

Tract PH–1a, (fig. 3 and pl. 29), in and northeast of the Patagonia Mountains, has high mineral resource potential and was delineated on the basis of favorable host rocks, anomalous abundances of Au, Ag, As, Bi, Cd, Cu, Mo, Pb, Sb, W, Zn, Ba, Mn, and Sn in stream-sediment samples from this area (Chapter C, this volume), known ore deposits, and a through-going, high-angle fault system (Harshaw Creek fault). This is the most geochemically anomalous area in Coronado National Forest and is ranked 10 out of 10 on the geochemical-intensity scale (Chapter C, this volume). Extensive mineralized rock is present within the tract in the Washington Camp, Harshaw, Palmetto, Patagonia, and Red Rock mining districts. The region of high potential extends beyond the contact between bedrock and basin fill north, east, and west of the Patagonia Mountains. Geophysical evidence indicates that alluvial cover in these regions is thin. The extension of the Harshaw Creek fault into the San Raphael basin east of the Patagonia Mountains is an especially promising area.

Tract PH–1b (fig. 3 and pl. 29) has moderate to low potential as indicated by the presence of favorable host rocks and the Dove Canyon fault, which may have acted as a conduit for hydrothermal fluids. This tract lacks the mineralized rock and intense geochemical anomalies found in tract PH–1a. Much of this tract is concealed by alluvium in the San Raphael basin; geophysical data suggest that alluvium is thin and may conceal at least one intrusion.

Tract PH–1c (fig. 3 and pl. 29) has high potential as indicated by a known silver occurrence, favorable host rocks, and the presence of the high-angle Sawmill Canyon

fault. Most of the favorable host rocks in this area and the fault are concealed by a thin alluvial cover.

Tracts labeled PH–1d (fig. 3 and pl. 29) have high potential as indicated by the presence of favorable host rocks, known mineralized rock in the Reef and Hartford mining districts, and anomalous abundances of Au, Ag, Bi, Cd, Cu, Mo, Pb, Sb, W, Zn, Mn, and Sn (stream-sediment) and by Au, Ag, Cd, Cu, Mo, Pb, Sb, W, Zn, Ba, and Sn (panned-concentrate) in samples from this area (Chapter C, this volume).

Tracts labeled PH–1e (fig. 3 and pl. 29) have moderate to low potential as indicated by the presence of favorable host rocks and geochemical anomalies similar to that in tract PH–1d. Mineralized rock is absent in this tract.

SANTA RITA MOUNTAINS

TRACT SR–1—TUNGSTEN SKARN DEPOSITS, POLYMETALLIC VEIN DEPOSITS, AND PORPHYRY COPPER SKARN DEPOSITS

Tracts labeled SR–1 (fig. 3 and pl. 29) have high or moderate to low potential, certainty level C, for the occurrence of undiscovered tungsten skarn, polymetallic vein, and porphyry copper skarn deposits. The tracts are underlain by Pinal Schist, Middle Proterozoic granite, Abrigo Formation, Escabrosa Limestone, Naco Group carbonate sedimentary rocks, Jurassic granite, Triassic and Jurassic volcanic rocks (including rhyolite tuff and flows and andesite flows) and volcaniclastic rocks, Cretaceous andesite and rhyolite and Bisbee Group sedimentary rocks, and Tertiary rhyolite, sedimentary rocks, and felsic intrusions. The tracts include a large area concealed by a thin cover of Quaternary alluvium. Most of this area is east of the Santa Rita Mountains, where geophysical data indicate that the thickness of alluvium is less than 1 km. The Helvetia-Rosemont, Jackson, Old Baldy, Tyndall, Duranium, Salero, Ivanhoe, Mansfield, Wrightson, Cave Creek, and Greaterville mining districts are within these tracts.

Moderate- to low-potential tracts contain rocks that host the indicated types of mineral deposits and are characterized by at least one of the following attributes:

(1) They contain areas that coincide with steeply dipping, northwest-striking faults;

(2) they contain areas in which favorable host rocks and felsic intrusions are juxtaposed; and

(3) they contain areas for which stream-sediment and panned-concentrate samples have anomalous abundances of Au, Ag, As, Bi, Cd, Cu, Mo, Pb, Sb, W, Zn, Ba, Mn, and Sn.

High-potential tracts are areas that possess all of these criteria and (or) contain known mineral occurrences.

TRACT SR–2—GOLD PLACER DEPOSITS

Tract SR–2 (fig. 4 and pl. 29) consists of areas in which fluvial deposits of sand and gravel have moderate to low potential, certainty level C, for the presence of undiscovered gold placer deposits hosted by stream gravels. Tracts were delineated on the basis of historic placer mining in the Greaterville mining district, the presence of known and potential lode deposits upstream, and anomalous abundances of Au, Ag, As, Cd, Cu, Mo, Pb, Sb, W, and Zn (stream-sediment) and Ag, Cd, and Ba (panned-concentrate) in samples from the area. The degree to which previous placer mining operations extracted all recoverable gold, thereby exhausting the resource potential, is indeterminate; therefore the tract has been assigned a moderate to low potential.

ATASCOSA, PAJARITO, SAN LUIS, AND TUMACACORI MOUNTAINS AND COBRE AND COCHES RIDGES

TRACT T–1—POLYMETALLIC VEIN DEPOSITS

Tracts labeled T–1 (fig. 3 and pl. 29) have high or moderate to low potential, certainty level B, for the occurrence of undiscovered polymetallic vein deposits. These tracts include the Oceanic, Arivaca, Austerlitz, and Oro Blanco mining districts and are underlain by Jurassic granite and rhyolite intrusions; Triassic and Jurassic rhyolite tuff and flows, andesite, and volcaniclastic rocks; Cretaceous andesite, rhyolite, and Bisbee Group sedimentary rocks; and Tertiary rhyolite, andesite, sedimentary rocks, and intrusions (rhyolite and granite). The tracts were delineated on the basis of favorable host rocks, known ore mineral occurrences, alignment along extensive, if somewhat discontinuous, northwest-striking faults, and anomalous abundances of Au, Ag, As, Bi, Cd, Cu, Mo, Pb, Sb, W, Zn, Ba, Mn, and Sn (stream sediment) and Au, Ag, Bi, Cd, Cu, Mo, Pb, Sb, Zn, Ba, Mn, and Sn (panned concentrate) in samples from the area (Chapter C, this volume).

TRACT T–2—TUNGSTEN VEIN AND TUNGSTEN PLACER DEPOSITS

Tract T–2 (fig. 3 and pl. 29) has moderate to low potential, certainty level B, for the occurrence of undiscovered tungsten vein and placer deposits for which there is no deposit model. The tract is primarily indicated by the presence of the Easter mining district, which includes placer and vein tungsten deposits. Information concerning the degree to which rock in this area is mineralized is sparse; therefore, the tract has been classified as having moderate to low potential. Mineralized rock may be associated with a peraluminous Tertiary granite that crops out within the tract or may be related to a buried intrusion.

SANTA CATALINA AND RINCON MOUNTAINS

TRACT SCR–1—TUNGSTEN VEIN DEPOSITS, TUNGSTEN SKARN DEPOSITS, COPPER SKARN DEPOSITS, AND PORPHYRY COPPER-MOLYBDENUM DEPOSITS

Tracts labeled SCR–1 (fig. 4 and pl. 27) have high or moderate to low potential for the occurrence of undiscovered tungsten vein (certainty level B), tungsten skarn (certainty level B), copper skarn (certainty level C), and porphyry copper-molybdenum deposits (certainty level B). The tracts are underlain by Middle Proterozoic granite to granodiorite; Apache Group sedimentary rocks; Paleozoic sedimentary rocks, including the Escabrosa Limestone and Naco Group; Late Cretaceous to Paleocene granite; and areas in which favorable host rocks are concealed by a thin cover of Quaternary alluvium. Moderate- to low-potential tracts were delineated on the basis of favorable host rocks, proximity to the northwest-striking Mogul fault system, and anomalous abundances of Au, Ag, As, Bi, Cd, Cu, Mo, Pb, Sb, W, Zn, Mn, and Sn in stream-sediment samples from these areas (Chapter C, this volume). High-potential tracts are characterized by having attributes of moderate to low potential tracts and also containing areas of mineralized rock, including the Burney, Canada del Oro, Marble Peak, and Redington mining districts.

TRACT SCR–2—COPPER SKARN AND PORPHYRY COPPER-MOLYBDENUM DEPOSITS

Tracts labeled SCR–2 (fig. 4 and pl. 27) have moderate to low potential for the occurrence of undiscovered copper skarn (certainty level C) and porphyry copper-molybdenum (certainty level B) deposits. The tracts are underlain by Pinal Schist; Middle Proterozoic granite to granodiorite; Apache Group sedimentary rocks; lower Paleozoic sedimentary rocks; Escabrosa Limestone; Naco Group; Bisbee Group sedimentary rocks; Late Cretaceous to Paleocene granite; Tertiary andesite and rhyolite flows, tuff, and some interbedded sedimentary rocks; and areas in which host rocks are concealed by a thin cover of Quaternary alluvium. The tracts are indicated by the presence of favorable host rock, anomalous abundances of Au, Ag, Cu, Mo, Pb, Sb, Zn, Ba, and Mn in stream-sediment samples from these areas (Chapter C, this volume), and structural features, such as numerous northwest-striking faults, conducive to ore deposition.

TRACT SCR–3— PLACER GOLD DEPOSITS

Tracts labeled SCR–3 (fig. 4 and pl. 27) are areas in which stream gravels and sand have moderate to low potential, certainty level C, for the occurrence of undiscovered gold placer deposits. Tracts were delineated on the basis of historic placer mining and on the presence of known and potential lode deposits upstream. The degree to which previous placer mining operations extracted all recoverable gold (thereby exhausting the resource potential) is indeterminate; therefore the tracts have been assigned a moderate to low potential.

RESOURCE POTENTIAL FOR OTHER METALS PRESENT IN CORONADO NATIONAL FOREST

Three other metallic mineral commodities have been reported in Coronado National Forest. Due to a lack of information, they cannot be assessed in the fashion or at the level of detail applied to the major metallic mineral deposits. Brief descriptions of their occurrence in the Forest follow.

BERYLLIUM

Beryl occurs in the Dragoon Mountains Stronghold stock (Drewes, 1987). Helvite and beryllium-bearing epidote are present in tactite associated with lead-zinc replacement deposits in limestone at the Gordon mine (Drewes, 1987), also associated with the Stronghold stock. Data available for these occurrences are insufficient to allow designation of a corresponding mineral deposit model or offer an assessment of resource potential.

MANGANESE

A manganese deposit was identified in a small outcrop of Jurassic volcanic rocks west of the Canelo Hills at the Bluebird mine (MRDS). Sparse data available for this deposit suggest that it is an epithermal vein deposit. Manganese is also present as a byproduct in the Mowry and Bender Mines, in the Harshaw district of the Patagonia Mountains.

URANIUM

Uranium occurrences have been noted at several locations in the Forest (MRDS). The Duranium claims in the Santa Rita Mountains consist of disseminated kasolite, uranophane, and autunite in an arkosic sandstone within Cretaceous conglomerate (table 24 and fig. 43, Arizona Bureau of Mines, 1969). Uranium has also been reported to exist on the east and south flanks of the Rincon Mountains, in the northeastern part of the Whetstone Mountains, in the southern Pinaleno Mountains, in the northern Tumacacori Mountains, and on Cobre Ridge west of the Tumacacori Mountains. Data available (MRDS) for these occurrences are insufficient to allow designation of a corresponding mineral deposit model or offer an assessment of resource potential.

INDUSTRIAL COMMODITIES

Silica deposits, like those present at El Tigre Mine, are in many areas of the Forest and could be exploited as sources of flux for smelters in southeastern Arizona.

Diatomite or diatomaceous earth is used as fillers or filters in various commercial processes. Diatomite occurs interbedded with other Tertiary rocks a few kilometers from the northwest end of the Galiuro Mountains. These rocks probably represent lake deposits in which diatoms flourished. Tertiary rock sequences of this type are also present within some Forest units, but exposed Tertiary lake deposits have not been identified.

Zeolites form a group of hydrous aluminosilicate minerals that are analogous to feldspars; a few are used commercially as filters or absorbants. Zeolites can form where rhyolite ash was deposited in an alkaline lake. There is a zeolite quarry having intermittent production southeast of the southern end of the Pinaleno Mountains Forest unit. Again, whereas Tertiary rhyolite-ash deposits are common in many of the Forest units, associated lacustrine beds are not known to exist in the mountains but do occur in some of the intermontane valleys between Forest units.

Graphite has been reported to be present in two sites northwest of the Chiricahua-Pedregosa Forest unit. Both are related to unusual metamorphism of thin beds of highly carbonaceous shale of Paleozoic and Mesozoic formations along a major fault zone. The first site is 3–5 km northwest of the Forest boundary in the Fort Bowie National Historic Site; graphite is present in a gully immediately south of the service facility. There are graphite lentils about 15 cm long and 5–10 cm thick in fault gouge between Permian limestone and metamorphosed Lower Cretaceous shale (Drewes, 1984). The second, nearby site is 6–300 m west of the Forest boundary near a saddle on the range crest about 1.5 km northwest of Dug Road Mountain (Drewes, 1981). Carbonaceous beds of Lower Cretaceous shale are metamorphosed at one prospect; a second prospect appears to be barren. Both occurrences are small; the likelihood of finding additional, higher purity material nearby seems to be limited.

Small, low-grade occurrences of semiprecious gemstones, including opal, turquoise, and fire agate, have been reported (John Gutierrez, U.S. Forest Service, written commun., 1991) to exist at four locations within Forest units. These areas are (1) northwest of Red Rock Tank, in the Arivaca area; (2) at Corral Nuevo, also in the Arivaca area; (3) at Aztec Gulch, at the north end of the Patagonia Mountains; and (4) at Deer Creek, on the east side of the Galiuro Mountains. A material reputed to be precious opal has been reported to exist at the two Arivaca sites. Mining claims are reportedly located on a rhyolite welded tuff in which fractures are filled with chalcedony veinlets. These veinlets are reported to grade locally into white or blue opal (John Gutierrez, U.S. Forest Service, written commun., 1991). No data are available to determine whether this material is opal or chatoyant chalcedony. Little information is available for the other two occurrences.

Alunite is a clay mineral that has the potential to become a source of aluminum, but the commercial process by which aluminum is extracted from alunite is not currently in use. Alunite is present at the northern end of the Patagonia Mountains in an area of heavily oxidized rock mineralized with disseminated sulfides.

Fluorite, a nonmetallic mineral that is in substantial commercial demand, is found in several geologic settings within the Forest. It is present as an accessory mineral in the Stronghold granite stock of the Dragoon Mountains (Drewes, 1987). Fluorite occurs in widely scattered veinlets in some Tertiary volcanic rocks of the Forest region. Sulfide-bearing veins in various mining districts of the Forest region contain fluorite. The feasibility of mining fluorite in these districts has not been evaluated.

REFERENCES CITED

Arizona Bureau of Mines, 1969, Geology and mineral resource of Arizona: Arizona Geological Survey Bulletin 180, pt. 1, 467 p.

Butler, G.M., 1936, Mineral industries in Arizona and its heritage: Tucson, Ariz., University of Arizona Press, 385 p.

Cox, D.P., and Singer, D.A., eds., 1986, Mineral deposit models: U.S. Geological Survey Bulletin 1693, 379 p.

Drewes, Harald, 1981, Geologic map and sections of the Bowie Mountain South quadrangle, Cochise County, Arizona: U.S. Geological Survey Miscellaneous Investigations Series Map I–1363, scale 1:24,000.

———1984, Geologic map and structure sections of the Bowie Mountain North quadrangle, Cochise county, Arizona: U.S. Geological Survey Miscellaneous Investigations Series Map I–1492, scale 1:24,000.

———1987, Geologic map and structure sections of the northern part of the Dragoon Mountains, southeastern Arizona: U.S. Geological Survey Miscellaneous Investigations Series Map I–1662, scale 1:24,000.

———1991, Description and development of the Cordilleran orogenic belt in the southwestern United States and northern Mexico: U.S. Geological Survey Professional Paper 1512, 92 p.

Drewes, Harald, and Dyer, Russ, 1989, Tectonics of the eastern part of the Cordilleran orogenic belt, Chihuahua, New Mexico, and Arizona: American Geophysical Union 28th International Congress Field Trip Guidebook T–121, 82 p.

Fisher, F.S., and Johnson, K.M., eds., 1987, Preliminary manuscript for mineral resource potential and geology of the Challis 1° × 2° quadrangle, Idaho, U.S. Geological Survey Open-File Report 87–480, 251 p.

Keith, S.B., Gest, D.E., and DeWitt, Ed, 1983, Metallic mineral districts of Arizona: Arizona Bureau of Geology and Mineral Technology Map 18, scale 1:1,000,000.

Knight, F.P., 1958, Mining in Arizona: Phoenix, Ariz., Arizona Department of Mineral Resources, 28 p.

Ludington, S.D., 1986, Descriptive model of Climax Mo deposits, *in* Cox, D.P., and Singer, D.A., eds., Mineral deposit models: U.S. Geological Survey Bulletin 1693, p. 73.

Mardirosian, C.A., 1977, Mining districts and mineral deposits of Arizona (2nd ed.): Private publication, press not identified, scale 1:1,000,000.

Reed, B.L., Menzie, W.D., McDermott, M., Root, D.H., Scott, W., and Drew, L.J., 1989, Undiscovered lode tin resources of the Seward Peninsula, Alaska: Economic Geology, v. 84, p. 1936–1947.

Simons, F.S., Theobald, P.K., Tidball, R.R., Erdman, J.A., Harms, T.F., Griscom, Andrew, and Ryan, G.S., 1987, Mineral resources of the Black Rock Wilderness Study Area, Graham County, Arizona: U.S. Geological Survey Bulletin 1703–C, 9 p.

Singer, D.A., and Cox, D.P., 1988, Applications of mineral deposit models to resource assessments: U.S. Geological Survey Yearbook 1987, p. 55–57.

U.S. Geological Survey, 1986, Mineral Resources Data System (MRDS; formerly Computer Resources Information Bank, CRIB): active computer file; data available from U.S. Geological Survey, Branch of Resource Analysis, Building 25, Denver Federal Center, Denver, CO 80225.

Worl, R.G., Wilson, A.B., Smith, C.L., and Kleinkopf, M.D., 1989, Mineral resource potential and geology of the Challis National Forest, Idaho, U.S. Geological Survey Bulletin 1873, 101 p.

Wrucke, C.T., and McColly, R.A., 1984, Whetstone Roadless Area, Arizona: U.S. Geological Survey Professional Paper 1300, p. 126–129.

Mineral Resources and Resource Potential of Coronado National Forest—Leasable Minerals

By Harald Drewes

MINERAL RESOURCE POTENTIAL AND GEOLOGY OF CORONADO NATIONAL FOREST, SOUTHEASTERN ARIZONA AND SOUTHWESTERN NEW MEXICO
Edited by Edward A. du Bray

U.S. GEOLOGICAL SURVEY BULLETIN 2083–H

UNITED STATES GOVERNMENT PRINTING OFFICE, WASHINGTON : 1996

CONTENTS

FIGURE

Mineral Resources and Resource Potential of Coronado National Forest—Leasable Minerals

By Harald Drewes

ABSTRACT

Leasable minerals have not been produced in the Coronado National Forest region. However, there has been considerable exploration for oil and natural gas. In addition, two small occurrences of noncommercial hot water are present in the Forest region, but resource potential for geothermal energy is considered low. Coal has not been mined or prospected in the Forest region, and the potential for discovery of coal resources in Coronado National Forest is low. A single exploratory hole drilled in the Willcox playa identified a 72-m-thick interval that contained anomalous lithium abundances, but the resource potential for lithium in the Forest is considered low.

The Forest region is a frontier for oil and gas exploration. Many factors critical for accumulation of petroleum products, including source and reservoir rocks, are present in the region. In addition, thermal maturation studies indicate that conditions were suitable for petroleum formation.

Oil and gas plays in southeastern Arizona have developed around three kinds of traps. A conventional play targeting structures in Mesozoic and Paleozoic reservoirs at depths of 300–2,100 m resulted in the drilling of about a dozen wells in southeastern Arizona. Oil and gas shows were reported in some of the holes. A play in an intermontane-valley Tertiary deposit led to critical examination of several larger valleys, and one hole was drilled to a depth of 3,660 m; no shows were encountered. An overthrust play aimed at subthrust fault grabens involved drilling three holes to depths of 1.5–3 km, and many deep seismic surveys were conducted. The first and third types of targets are viable in some Forest units, particularly in the southeastern part of the region, where igneous activity is unlikely to have destroyed potential hydrocarbon accumulations. The second type of target is unlikely to be present in the Forest units, most of which are mountainous.

INTRODUCTION

Oil, natural gas, oil shale, lithium brine, potash, sodium, native asphalt, bitumen or bituminous rock, phosphate, and coal are leasable commodities, or "mining act minerals." They were excluded from the General Mining Law of 1872 by the Mineral Leasing Act of 1920, which set up laws requiring prospect permits and leases to control their exploration, development, and production. Geothermal energy sources were added to the list of leasable commodities by the Geothermal Steam Act of 1970.

MINERAL RESOURCES

There is no recorded production of leasable commodities in the Coronado National Forest region. However, there has been considerable exploration for oil and gas, and small occurrences of hot water have been identified within the region.

RESOURCE POTENTIAL

OIL AND NATURAL GAS

An oil seep is present outside the Forest unit southwest of the Whetstone Mountains, and shows of oil or gas were reported in several exploratory wells drilled in the Forest region (Thompson and others, 1978, table 2; Butler, 1989, table 3 and fig. 45).

There has been sporadic exploration for oil and gas in the Coronado National Forest region, primarily since 1950; these plays were aimed at three kinds of targets. Each play followed the successful development of a play in other regions believed to be geologically similar to the Forest region. Although some favorable shows were identified, none resulted in producing wells. During the last 10 years, exploration activity has been minimal or nonexistent. Thus, because the exploration effort is still in its infancy (Nydegger, 1982; Pierce, 1982; Stark and Gordon, 1982), renewed exploration activity is possible.

Basic data sources bearing on oil and gas potential are at least as difficult to assess as are those for the mining industry because of conflicting needs of play promotion and company confidentiality. Basic data are much scarcer than

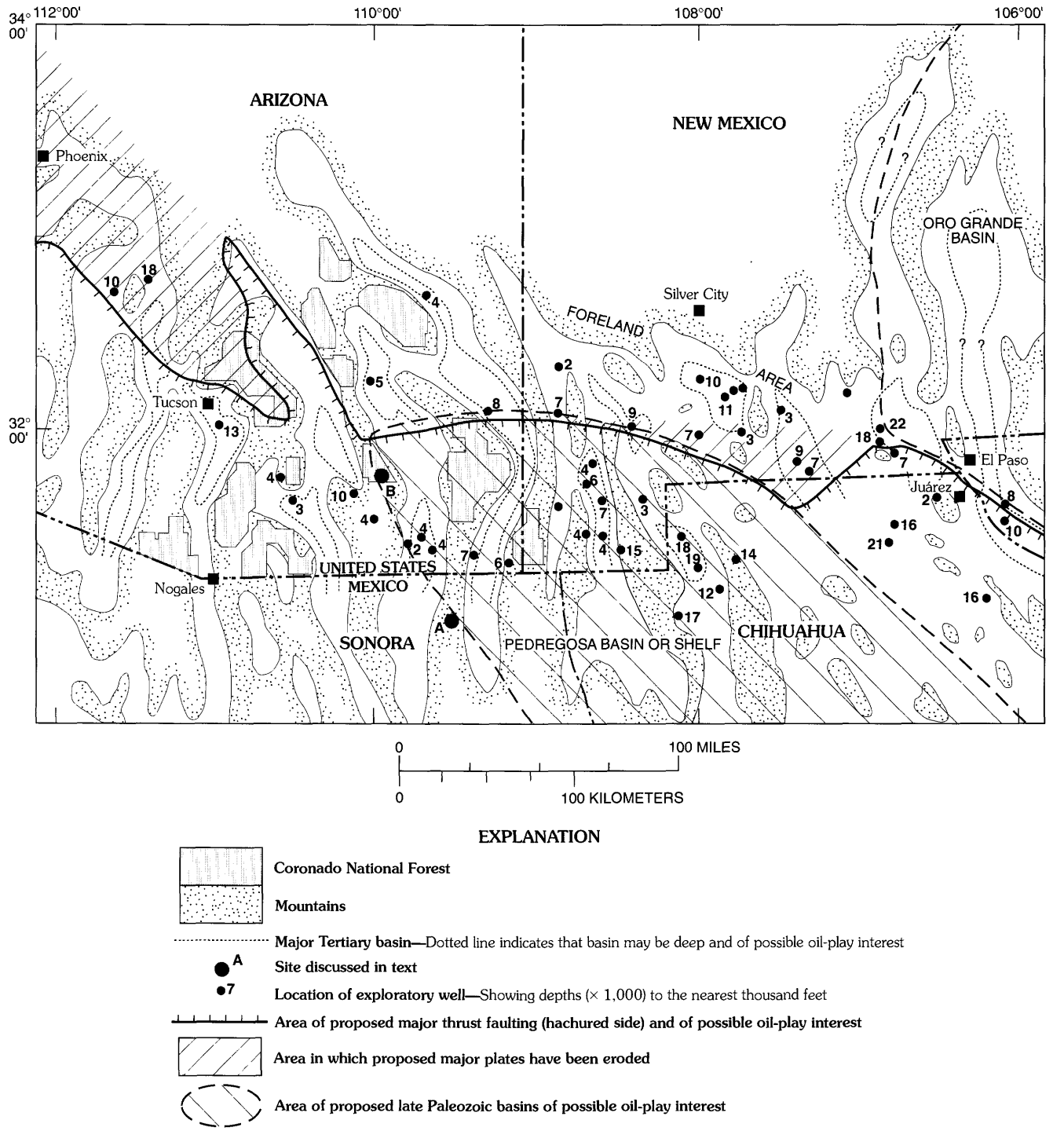

Figure 1. Map of southeastern Arizona–southwestern New Mexico–north-central Mexico region showing geologic features related to oil plays. The area of the Paleozoic-Mesozoic rock play discussed in text is not delineated but is considered in some reviews as equivalent to the proposed Pedregosa Basin play. Deep Tertiary basins and overthrust plates provide additional plays.

is the reiteration of selected parts of this data, typically by geologists far more familiar with oil plays in general than in local geology. Key data, such as deep-seismic records, are not generally available in most cases.

The earliest and longest lasting play involved exploration for oil and gas in conventional structural and stratigraphic traps in Paleozoic and Mesozoic rocks. These sequences were 3–8 km thick before deep Tertiary erosion, and are generally several kilometers thick thereafter. The focal concept of this play is a proposed upper Paleozoic Pedregosa Basin (Kottlowski, 1977), a broad sag in which units thicken inward; the proposed basin (fig. 1) may be

analogous to the West Texas Permian basin. The Pedregosa Basin and south-central Cochise County plays of Butler (1989) are conventional-trap plays. The structural and stratigraphic traps of the well-established West Texas Permian basins to the east were prolific oil producers; therefore, the southward- and westward-thickening deposits of southwestern New Mexico and southeastern Arizona are considered promising plays, provided that the geologic setting in these areas is similar to that of West Texas.

However, the basin-facies requirement of the latter play is inadequately substantiated by available geologic data. Meager evidence from a single site (fig. 1, site A) in northeastern Sonora suggests that this sequence of rocks is thin, but this interpretation is questionable. The area of thinned Pennsylvanian and Permian rocks is aligned with a belt of tectonically thinned rocks (fig. 1, site B) in Arizona (Drewes, 1980, 1981). Furthermore, postulated stratigraphic thinning is unsupported by any geologic synthesis that demonstrates the absence of structural disruption near the studied section. In addition, thickness of Pennsylvanian and Permian rocks in Arizona and New Mexico may have been measured inconsistently between studied sections because a major lithologic boundary in rocks near the Pennsylvanian-Permian boundary is time transgressive. Regardless of whether these key rocks are in a basin or are simply part of a southwestward-thickening shelf sequence, the potential for conventional structural traps exists because source and reservoir rocks are present and their geothermal maturity is appropriate for petroleum formation (Butler, 1989; Wardlaw and Harris, 1984). Young igneous intrusive rocks are not believed to have been sufficiently voluminous to have driven off oil and gas in most of southwestern New Mexico (Thompson, 1976); conditions in southeasternmost Arizona are similar. Thus, parts of the Peloncillo Mountains and the Chiricahua-Pedregosa Mountains areas may contain suitable structural and stratigraphic targets. Farther west, however, intrusive masses are larger and more abundant and suitable targets may have been faulted or heated to an extent that entrapped hydrocarbons were lost.

A second oil and gas play focused on the Tertiary deposits of the intermontane valleys where they may form structural or stratigraphic traps. Hydrocarbons may have been derived from the underlying older rocks or from swampy facies of the basin deposits themselves. This play was modelled on the oil discoveries in the fault-block basins of east-central Nevada, largely between 1976 and 1983 (Foster and Vincelette, 1991). These discoveries followed a nearly 20-year-long exploration period. Much less effort has been devoted to this Tertiary basin play in Arizona. Humble Oil Company (now EXXON) culminated the effort by drilling a 3,827-m-deep exploratory well southwest of the Rincon Mountains Forest unit (Drewes, 1977; Thompson and others, 1978).

Most of the Tertiary basins are outside the Forest units, and all of the more attractive deep basins are outside the Forest units; possible exceptions include the east flank of the Peloncillo Mountains, the west side of the Chiricahua Mountains, and parts of the Winchester and Galiuro Mountains Forest units, where Tertiary volcanic rocks may overlie older Tertiary basin deposits. Narrow flanking zones in the Chiricahua and the Tumacacori Mountains (Arivaca area) cannot be dismissed, but range-bounding faults that are mountainward of the Forest unit boundaries are not present at any of these sites.

The third, and most recent, oil and gas play in the Forest region involved potential targets at great depth beneath hypothesized thrust plates. This play was encouraged by the success in developing large natural gas fields in such a structural environment in the Idaho-Wyoming overthrust belt. In Arizona this play of the late 1970's and early 1980's had two target alternatives. Moulton and others (1978) and Keith (1979) suggested the possible presence of early Mesozoic grabens, which might contain entrapped hydrocarbons, beneath Cretaceous thrust plates. Available regional geologic data provide no support for such grabens. Drewes (1980, 1981) and Woodward and Duchene (1981), however, inferred the presence of multiple thrust plates, and hydrocarbons could be entrapped in lower plate structures that are concealed by upper plates. Multiple-plate structures have been mapped in many ranges of the Forest region, and they have been interpreted from some of the few deep seismic lines that are available to the public.

Large-scale overthrust plates have been proposed for the mountains of the southern and western parts of the Forest region; the northeastern part, essentially the Winchester, Galiuro, Santa Teresa, and Pinaleno Mountains, is less severely deformed (Drewes, 1981, 1991). Proterozoic basement rock forms parts of the large-scale thrust plates of Arizona but may not be part of the thrust plates of southwestern New Mexico. The rocks of the western Forest units are less likely to contain deep overthrust targets than are rocks in the southeastern areas, especially the Chiricahua-Pedregosa, Dragoon, and Whetstone Mountains Forest units, because they have a strong post-thrusting thermal history. An exploratory well drilled southwest of the Dragoon Mountains encountered Proterozoic rocks overlying Cretaceous sedimentary rock at a depth greater than 10,000 ft, which verifies the presence of overthrust structural settings in this area (Betton, 1982).

Sufficient oil and gas source rocks, reservoir rocks, and potential targets are present in the southeastern part of the Forest for this region to be assigned a moderate potential for undiscovered petroleum deposits; petroleum potential is low in the northern and western areas, however. A more definitive assessment may be possible when deep-seismic data become available.

COAL

Coal has not been mined or prospected in the Forest region. Descriptions of two speculative occurrences of coal have been published. One site consists of black carbonaceous shale, and the other is probably black volcanic glass. However, a small lens of coaly shale that contains anthracite chips are present in the Lower Jurassic Gardner Canyon Formation of the Santa Rita Mountains Forest unit (Drewes, 1971, p. C20).

The likelihood of finding coal in Coronado National Forest is low. Typical coal-bearing rock of the Western United States consists of organic-rich fluvial deposits of Cretaceous or early Tertiary age. These rocks are facies of an interior North American seaway. In contrast, the rocks of Cretaceous age of southeastern Arizona are foreland basin deposits, whose black or gray color more likely reflects accumulation of volcanic detritus than organic material (Drewes, 1991).

LITHIUM BRINE

Lithium-bearing material has recently become of commercial interest. Lithium production comes mainly from pegmatites, the appropriate type of which is not abundant in this region, and playa brines. Coronado National Forest has low potential for lithium brine. The Willcox and Animas Valleys contain the two playas exposed in the Forest region. Other playa deposits may be present in the subsurface covered by deposits of the present intermontane valleys or by Tertiary volcanic deposits; little is known about most basins in this area.

The Willcox Playa, located outside the Forest boundary east of the Dragoon Mountains, was drilled by the U.S. Geological Survey to determine the lithium content of its brine. Anomalous lithium concentrations were found between 35 and 137 m in a hole drilled to a total depth of 360 m (Vine and others, 1979).

GEOTHERMAL ENERGY

Geothermal energy is typically obtained from circulating groundwater where shallow young volcanic rocks or deep plutonic bodies are accessible to the water. The potential for hot-water or steam-energy resources throughout the Forest region is low.

The Coronado National Forest region contains two hot springs, however. Hookers Hot Springs are southeast of the Galiuro Mountains, and the other hot spring is in the northern part of the Animas Valley, east of the Peloncillo Mountains. Neither the temperature nor the volume of hot water at either site is sufficient for commercial power generation, although the hot water may be usable for small-scale greenhouse applications (Witcher, 1979).

Volcanic rocks young (hot) enough to heat ground water are present in the San Bernardino Valley, between the Pedregosa and Peloncillo Mountains, but springs are not present. The extension of this basalt system into adjacent Forest land involves its older (3-Ma) parts, which are likely to have cooled sufficiently that very little heat is available to heat circulating water (Swanberg, 1978).

REFERENCES CITED

Betton, C.W., 1982, Phillips' Tombstone State A–1 exploration well, Cochise County, Arizona, *in* Powers, R.B., ed., Geologic studies of the Cordilleran thrust belt: Rocky Mountain Association of Geologists Symposium, p. 675.

Butler, W.C., 1989, The geologic setting of southern Arizona and southwestern New Mexico, with a rationale for assessment of undiscovered, economically recoverable oil and gas—A summary of four potential plays: U.S. Geological Survey Open-File Report 88–450–M, 150 p.

Drewes, Harald, 1971, Mesozoic stratigraphy of the Santa Rita Mountains, southeast of Tucson, Arizona: U.S. Geological Survey Professional Paper 658–C, 81 p.

———1977, Geologic map and sections of the Rincon Valley quadrangle, Pima County, Arizona: U.S. Geological Survey Miscellaneous Investigations Series Map I–997, scale 1:48,000.

———1980, Tectonic map of southeastern Arizona: U.S. Geological Survey Miscellaneous Investigations Series Map I–1109, scale 1:125,000.

———1981, Tectonics of southeastern Arizona: U.S. Geological Survey Professional Paper 1144, 96 p.

———1991, Description and development of the Cordilleran orogenic belt in the southwestern United States and northern Mexico: U.S. Geological Survey Professional Paper 1512, 92 p.

Foster, N.H., and Vincelette, R.R., 1991, Petroleum potential of the Great Basin, *in* Gluskoter, H.J., Rice, D.D., and Taylor, R.B., eds., Economic geology, U.S.: Geological Society of America, The Geology of North America, v. P–2, p. 403–416.

Keith, S.B., 1979, The great southwestern Arizona oil and gas play: Arizona Bureau of Geology and Mineral Technology: Field notes, v. 9, no. 1, p. 10–15.

Kottlowski, F.E., 1977, New Mexico geology and petroleum potential: Interstate Oil Compact Committee Bulletin, v. 19, no. 2, p. 26–30.

Moulton, F.C., Owings, B.F., and Hanson, A.R., 1978, Utah-Arizona hingeline thrust belt—Potential new hydrocarbon province [abs.]: American Association of Petroleum Geologists Bulletin, v. 62, pt. 1, p. 2357–2358.

Nydegger, G.L., 1982, The Las Vegas–El Paso gap—A review of the southern part of the Cordilleran Overthrust Belt, *in* Powers, R.B., ed., Geologic studies of the Cordilleran Thrust Belt, v. I: Denver, Colo., Rocky Mountain Association of Geologists, p. 391–407.

Pierce, H.W., 1982, The search for petroleum in Arizona: Arizona Bureau of Geology and Mineral Technology Fieldnotes, v. 12, no. 2, p. 1–5.

Stark, P.H., and Gordon, M.S., 1982, Exploratory drilling and distribution of hydrocarbon shows in the western Thrust Belt of the U.S., *in* Powers, R.B., ed., Geologic studies of the Cordilleran Thrust Belt, v. II: Denver, Colo., Rocky Mountain Association of Geologists, p. 507–519.

Swanberg, C.A., 1978, Chemistry, origin and potential of geothermal resources in southwestern New Mexico and southeastern Arizona, *in* Callender, J.F., Wilt, J.C., and Clemons, R.E., eds., Land of Cochise, southeastern Arizona: New Mexico Geological Society, Annual Field Conference Guidebook, no. 29, p. 349–351.

Thompson, Sam, III, 1976, Tectonic and igneous effects on petroleum accumulation in southwestern New Mexico, *in* Woodward, L.A., and Northrop, S.A., eds., Tectonics and mineral resources of southwestern North America: New Mexico Geological Society Special Publication 6, p. 122–126.

Thompson, Sam, III, Tovar, J.C., and Conley, J.N., 1978, Oil and gas exploration wells in the Pedregosa basin, *in* Callender, J.F., Wilt, J.C., and Clemons, R.E., eds., Land of Cochise, southeastern Arizona: New Mexico Geological Society, Annual Field Conference Guidebook, no. 29, p. 331–344.

Vine, J.D., Asher-Bolinder, Sigrid, Morgan, J.D., and Higgins, Brenda, 1979, Lithologic log and lithium content of sediments penetrated in a test boring drilled on Willcox playa, Cochise County, Arizona: U.S. Geological Survey Open-File Report 79–397, 15 p.

Wardlaw, B.R., and Harris, A.G., 1984, Conodont-based thermal maturation of Paleozoic rocks in Arizona: American Association of Petroleum Geologists Bulletin, v. 69, p. 1101–1106.

Witcher, J.C., 1979, Proven, potential, and inferred geothermal resources of Arizona and their heat contents: Arizona Bureau of Mines and Mineral Resources Open-File Report 79–5, 64 p.

Woodward, L.A., and Duchene, H.R., 1981, Overthrust belt of southwestern New Mexico: Comparison with Wyoming-Utah overthrust belt: American Association of Petroleum Geologists Bulletin, v. 65, p. 722–729.

Mineral Resources and Resource Potential of Coronado National Forest—Salable Minerals

By John Gutierrez
U.S. Forest Service

MINERAL RESOURCE POTENTIAL AND GEOLOGY OF CORONADO NATIONAL FOREST, SOUTHEASTERN ARIZONA AND SOUTHWESTERN NEW MEXICO
Edited by Edward A. du Bray

U.S. GEOLOGICAL SURVEY BULLETIN 2083–I

UNITED STATES GOVERNMENT PRINTING OFFICE, WASHINGTON : 1996

CONTENTS

Mineral Resources and Resource Potential of Coronado National Forest—Salable Minerals

By John Gutierrez, U.S. Forest Service

INTRODUCTION

Salable minerals, comprising mostly nonmetallic industrial minerals, are those that are mined or quarried chiefly for their value as industrial materials and generally require little to no processing before use (pl. 30–32). In contrast, metallic ores must first be metallurgically treated to recover the metals of interest. Salable mineral materials, although they may contain small amounts of metals, are valued because of their physical properties, which remain unchanged after the material has been used. Generally, salable minerals are used in the form in which they are removed from the ground. Several nonmetallic industrial minerals within the Forest, such as high-calcium limestone, fluorite, graphite, and gemstones are considered valuable minerals subject to the General Mining Law of 1872; however, this section refers only to those mineral materials that are salable by regulation.

The Materials Act of July 31, 1947, as amended by Public Law 167 (30 U.S.C. 611) authorized the Secretary of Agriculture, under such rules and regulations as he may prescribe, to dispose of mineral materials, which include common varieties of sand, stone, gravel, pumice, pumicite, cinder, and clay. The Act removed these categories of mineral material from location under the 1872 Mining Law and classified them as "common" or "salable." However, the Act went on to provide for an exception to "uncommon variety" minerals. Exceptions include those deposits of such materials "which are valuable because the deposit has some property giving it distinct and special value."

Because of ambiguity in the definition of common variety minerals, the U.S. Forest Service recently amended regulations in 36 CFR 228, Subpart C, which covers disposal of salable mineral materials. The new regulations are designed to provide additional criteria for sale of mineral materials in view of the judicial interpretations of the Materials Act. Salable mineral commodities generally have low unit value (value per ton). Exploitation is usually dependent upon access to transportation and most mineral materials are used near production sites.

RESOURCES

Salable minerals present within, or directly adjacent to, Coronado National Forest consist of sand and gravel, limestone, pumicite, dimension stone, and humacite. Sand and gravel for general construction purposes, road construction, road resurfacing, and aggregate are readily available in most parts of the Forest. However, only 12 sand and gravel pits are currently active and these operations are small and infrequently worked. Exploitation of dry stream channels and alluvial deposits along the mountain ranges provides most of these resources.

Paleozoic sedimentary rocks within the Forest are major sources of salable dolomite and limestone minerals. Limestone, dolomite, and marble are calcium and calcium-magnesium carbonate sedimentary rocks that are very important and useful in the construction industry and for chemical and industrial use. Crushed and broken limestone and dolomite are important products used for general construction materials, ballast, riprap, cast stone, roofing granules, landscaping rock, building stone, and stone veneer. Plates 30–32 indicate limestone deposits that have either been worked in the past or are currently active. The Santa Catalina, Chiricahua, and Dragoon Mountains contain reserves of limestone well suited for all aggregate purposes. The Ligier (pl. 32) and Dragoon (pl. 31) marble quarries exploit varicolored limestone, dolomite, and marble and produce material that ranges from friable to extremely indurated. The whitest, most coarsely crystalline layers of the Mississippian Escabrosa Limestone are most desirable for decorative rock and other common uses.

Currently, the Forest has one active aggregate limestone operation in the Santa Rita Mountains and one operation being proposed for the Dragoon Mountains. The historic Helvetia Mining district in the Santa Rita Mountains contains enormous reserves of recrystallized limestone (marble). Calcium Products of Arizona is producing a common limestone aggregate product and landscaping rock in conjunction with mining bright white, high-calcium limestone suitable for the mineral filler and extender industry.

Pumice and pumicite are volcanic glassy pyroclastic rocks formed by explosive volcanism. Pumicite and pumice are useful for various construction purposes because the material is light weight and vesicular, and it forms angular fragments. Pumicite outcrops are found northeast of the Pajarito Mountains near Peña Blanca Lake (pl. 32), and a reported occurrence of pumiceous material is near Indian Creek, on the southern end of the Chiricahua Mountains.

Dimension stone, including riprap, is hand-picked or quarried from deposits in every unit of the Forest. Currently, at least 31 stone sites are being exploited within the Forest, but a number of these sites are not being used on a regular basis. Most dimension stone within the Forest is collected, rather than quarried, from weathered volcanic, granitic, and sedimentary bedrock sources. Numerous collection areas are concentrated along stream and valley drainages. Marmarized limestone used as dimension stone and riprap is chiefly quarried from outcrops of the Escabrosa Limestone and the Pennsylvanian and Permian Naco Group in several locations within the Forest. Although Forest dimension stone is varied in color, the brilliant white stone is most desirable for crushed stone, decorative rock, riprap, and terrazzo.

A low-quality carbonaceous material found in the southeastern part of the Forest has been described as a humacite. Because the humic material is unusually high in ash content, it does not qualify as a fuel coal but could have potential as a soil amendment.

RESOURCE POTENTIAL

The mineral resource potential for sand and gravel, limestone, pumicite, dimension stone, and humates are evaluated in the following sections. Income from the sale of salable mineral commodities varies according to accessibility, unit value, cost, and amount produced. Environmental factors, such as impacts on other resources, are site specific and have not been considered in this report.

SAND AND GRAVEL

Sand and gravel deposits result from the natural disintegration and abrasion of bedrock through the combined action of weathering and erosion. While most rocks yield sand and (or) gravel, products from the different rock types vary greatly in quality and size and shape of particles. In the Forest, deposits are in basin and valley fills, stream terraces, buried and active stream channels, and alluvial fans. Special needs for aggregate are met by crushing coarse alluvium and colluvial material. The majority of deposits being worked were derived from granitic rocks of Late Cretaceous to early Tertiary age. The remaining sand and gravel deposits consist of volcanic, sedimentary, and granitoid materials derived from middle Tertiary bedrock sources. Granite, where coherent and not disintegrated, is a potential source of general-purpose crushed aggregate. Sand and gravel deposits originating from volcanic and sedimentary bedrock sources provide a general-purpose aggregate if not contaminated with clay or carbonate cement. Siliceous volcanic fragments contained in nearly all Arizona sand and gravel deposits limit the use of reactive aggregates from these deposits.

Due to the isolated nature (poor and distant access) of much of the Forest, significant sand and gravel resources will remain unexploited. Although abundant sand and gravel sources are more accessible on private and other public lands nearby (U.S. Bureau of Land Management), deposits within the Forest will continue to be utilized locally. Demand for developing new sand and gravel resources will remain high near populated areas adjacent to Forest boundaries.

Distribution of all the alluvial and colluvial deposits on the Forest cannot be shown at 1:126,720 scale. Plates 30–32 show existing mineral material sites presently (1992) being worked; the maps do not inventory all potential sources of these materials.

LIMESTONE

Within the Forest, local use of limestone resources, especially in construction applications, is expected to remain constant. Salable limestone from Forest resources is being quarried continuously to meet growing urban demands. Because known limestone resources are easily reached from major highways, future exploitation of new deposits is likely. Metamorphosed Escabrosa Limestone is available in many of the Forest units; however, its metallurgical properties are unknown. Most of the metamorphosed Escabrosa Limestone in the Forest region is in halos around stocks; these halos are generally narrow and do not have large reserves of uniformly metamorphosed limestone (marble). However, where the Escabrosa Limestone is more highly metamorphosed (converted to marble), near large or clustered stocks and along certain fault zones, its exploitation as flux may be feasible.

PUMICITE

The pumicite deposits found in the Forest consist of upper to middle Miocene basaltic rocks. The difference between pumice and pumicite is a matter of particle size: pumice is coarse (>2–3 mm) and pumicite is fine (<2–3 mm). Finely ground pumicite and unground pumicite are used in scouring powders and for fine-polishing agents. Pumicite is also used as an ingredient in acoustical plaster, insulation, filter aids, poultry litter, soil conditioner, insecticide carrier, and highway blacktopping. Due to the presence of suitable substitutes and the lack of knowledge about Forest pumicite resources, interest in pumicite deposits will remain low. Plates 30–32 indicate two reported Forest pumicite occurrences.

DIMENSION STONE

Sources of dimension stone and riprap are plentiful within the Forest; most exploitation occurs within the Nogales district. The majority of the dimension stone and riprap sources being worked are located in middle Tertiary volcanic rocks, such as near Peña Blanca Lake. The material, derived from silicic to mafic lava flows, is suitable for selected uses, such as decorative purposes only. Gravels formed from these rocks are generally soft and of poor quality for commercial use. Cretaceous sedimentary rocks, such as found in the Gringo Gulch area, provide better stone for structural purposes. Production of the bright white marble stone from the Santa Rita and Dragoon Mountains continues to command the most interest. The Whitetail Creek deposit in the Chiricahua Mountains, which has a history of stone production, is another source of white dimension stone.

Stone resources must be evaluated according to the proposed use and value of the material. The appearance, aesthetic qualities, and physical characteristics of the material must be appropriate to the use. Extrinsic factors such as distance to market, ease of quarrying, and utilization determine the economic viability of a deposit. The potential for development of collection and quarry sites within the Forest remains good along existing transportation corridors. There is high potential for continued development of dimension stone and riprap in conjunction with the mining of major limestone deposits easily reached from developed areas adjacent to Forest boundaries (pl. 30–32).

HUMACITE

Organic-rich shale described as a humacite is found in Paleozoic metamorphic rocks in a small area within the Chiricahua Mountains. Although possibly suitable as a soil amendment, there is no indication that this occurrence has stimulated significant exploration activity, and thus potential for exploitation is low. Plates 30–32 show the location of the humacite occurrence.

Quantitative Mineral Resource Assessment of Coronado National Forest

By Mark W. Bultman *and* Mark E. Gettings

MINERAL RESOURCE POTENTIAL AND GEOLOGY OF CORONADO NATIONAL FOREST, SOUTHEASTERN ARIZONA AND SOUTHWESTERN NEW MEXICO

Edited by Edward A. du Bray

U.S. GEOLOGICAL SURVEY BULLETIN 2083–J

UNITED STATES GOVERNMENT PRINTING OFFICE, WASHINGTON : 1996

CONTENTS

TABLES

Quantitative Mineral Resource Assessment of Coronado National Forest

By Mark W. Bultman *and* Mark E. Gettings

ABSTRACT

This chapter presents a quantitative assessment of the metallic mineral resource potential of Coronado National Forest based on existing geologic, geochemical, and geophysical data and on subjective estimates of numbers of undiscovered deposits in tracts favorable for several types of mineral deposits. The subjective estimates of numbers of undiscovered deposits reflect the expected sizes of undiscovered deposits in the Forest for each deposit type. Consequently, the size of some inferred, undiscovered deposits are comparable to known deposits in and around all units of the Forest. In other cases, the use of world-wide deposit tonnage distributions to model the size of inferred, undiscovered deposits was deemed appropriate.

Quantitative assessments of metal tonnages contained in inferred, undiscovered deposits are summed for the entire Forest, for the following deposit types: (1) tungsten skarn; (2) tungsten vein; (3) porphyry copper; (4) porphyry copper skarn-related; (5) copper skarn; (6) polymetallic replacement; (7) porphyry copper-molybdenum; (8) polymetallic vein; (9) Creede-type epithermal vein; (10) rhyolite-hosted tin; and (11) placer gold. Estimated mean amounts (with approximately 95-percent confidence intervals given in parentheses) of undiscovered metal (in tonnes) for the entire Forest are as follows: copper, 2×10^7 (-2×10^7, $+7\times10^9$); gold, 1×10^2 (-1×10^2, $+8\times10^4$); lead, 1×10^5 (-1×10^5, $+1\times10^8$); molybdenum, 5×10^5 (-5×10^5, $+6\times10^7$); silver, 6×10^3 (-6×10^3, $+1\times10^6$); tin, 3×10^1 (-3×10^1, $+2\times10^4$); tungsten, 5×10^3 (-5×10^3, $+2\times10^5$); and zinc, 1×10^5 (-1×10^5, $+1\times10^8$). These estimates, based solely on knowledge available at the time of the assessment and subjective estimates of numbers of undiscovered deposits for each specific mineral deposit model considered, are subject to considerable uncertainty, greater than those indicated by confidence intervals.

The subjective estimates were processed in two computer simulations that employ the grade and tonnage models for each appropriate mineral deposit type to generate a distribution of estimates of metals in inferred, undiscovered deposits. One simulation procedure, MARK3, uses tonnage and grade models based on worldwide data (although these models can be appropriately modified with some difficulty) and includes many tonnage and grade models that are based on mining districts and are awkward to interpret. The second simulation procedure, developed by the authors, uses tonnage models designed to reflect the sizes of undiscovered mineral deposits in Coronado National Forest as a function of tonnage and grade distributions of known deposits in and around the Forest from which major amounts of ore have been produced. In many cases, the assessment team considered estimates of metals in inferred, undiscovered deposits generated by MARK3 to be implausibly large; these implausibly large estimates probably resulted from the use of worldwide grade and tonnage data distributions, which are inappropriate to the size and grade of deposits known or likely to be present in southeastern Arizona. In order to refine the mineral resource assessment of Coronado National Forest, the second set of simulations were processed by a routine in which it is easier to specify appropriate parts of worldwide grade and tonnage models and that provides rapid, on-site results. The results of the second simulation procedure probably provide a more accurate quantitative assessment of undiscovered mineral resources in the Forest and are those discussed in this chapter; the results of both procedures are presented in table 1.

INTRODUCTION

This chapter presents a quantitative assessment of the metallic mineral resource potential of Coronado National Forest ("the Forest"). The assessment is provided to help the U.S. Forest Service comply with requirements of title 36, chapter 2, part 219.22, Code of Federal Regulations, which requires the Forest Service to provide information and interpretations so that mineral resources, both discovered and undiscovered, can be considered with other types of resources in land-use planning. The quantitative mineral resource assessment presented in this chapter is principally based on compilations of existing geologic, geochemical, and geophysical data presented in this volume; new data generated specifically for this study are extremely limited.

Table 1. Results of simulations based on estimates of numbers of undiscovered deposits in Coronado National Forest, southeastern Arizona and southwestern New Mexico.

[The simulations differ in application of appropriate grade and tonnage models for the simulations.The simulations are of two types depending on the tonnage models and numerical simulator used. The simulation using tonnage models taken directly from Cox and Singer (1986) is prefixed with C&S; this simulation was conducted using the MARK3 program developed by the U.S. Geological Survey Branch of Resource Analysis in Reston, Va. Simulations that used tonnage models that have been adjusted to match presumed sizes of inferred, undiscovered deposits in Coronado National Forest are prefixed with AT (adjusted tonnage); this simulation was made using a procedure developed for this study (see text)]

A.—Estimated tonnages of metals in undiscovered tungsten skarn deposits. The C&S grade and tonnage model for tungsten skarn deposits (Menzie and Jones, 1986) is based on districts (defined as all mines within 10 km of one another or mines associated with an intrusion). The C&S-based estimates must be divided by the number of mines expected in a district to be valid. Adjusted tonnage (AT) estimates are based on tonnages centered around the 10-percent quantile of the C&S tonnage model and include the four smallest tonnages in that model. Adjusted tonnage estimates probably most accurately reflect tonnages of undiscovered tungsten skarn deposits in Coronado National Forest.

Simulation method	Mean tonnage	Quantiles of simulated metal distribution			Mean number of deposits
		10 percent	50 percent	90 percent	
			Tungsten		
C&S-MARK3	2.15×10^5	9.11×10^3	1.37×10^5	5.28×10^5	5.89
AT	3.17×10^3	3.27×10^2	1.62×10^3	8.15×10^3	5.88
			Ore		
C&S-MARK3	2.95×10^7	1.49×10^6	2.17×10^7	6.74×10^7	5.89

B.—Estimated tonnages of metals in undiscovered tungsten vein deposits. The C&S grade and tonnage model for tungsten vein deposits is based on vein systems. The C&S-based estimates must be divided by the number of deposits expected in a vein system to be valid. Adjusted tonnage (AT) estimates are based on tonnages centered around the 10-percent quantile of the C&S tonnage model and include the four smallest tonnages in that model. The adjusted tonnage simulations are thought to accurately reflect tonnages of undiscovered tungsten vein deposits in the Coronado National Forest.

Simulation method	Mean tonnage	Quantiles of simulated metal distribution			Mean number of deposits
		10 percent	50 percent	90 percent	
			Tungsten		
C&S-MARK3	9.72×10^4	1.89×10^3	6.52×10^4	2.35×10^5	4.66
AT	2.28×10^3	5.62×10^2	2.10×10^3	4.42×10^3	4.66
			Ore		
C&S-MARK3	1.28×10^7	2.04×10^5	8.55×10^6	3.03×10^7	4.662

C.—Estimated tonnages of metals in undiscovered Climax-type molybdenum deposits. The C&S grade and tonnage model (Singer, Theodore, and Mosier, 1986) is used in this simulation. Because the tonnage model of Climax-type molybdenum deposits is built from world-class deposits, it is considered inappropriate to estimate molybdenum contained in inferred Climax-type molybdenum deposits in the Forest. The simulation procedure was completed for this model, but the results are not deemed applicable as an estimate in the Coronado National Forest and are not included in tonnage sums.

Simulation method	Mean tonnage	Quantiles of simulated metal distribution			Mean number of deposits
		10 percent	50 percent	90 percent	
			Molybdenum		
C&S-MARK3	1.74×10^5	0	0	6.30×10^5	0.30
			Ore		
C&S-MARK3	9.12×10^7	0	0	3.57×10^8	0.30

Table 1. Results of simulations based on estimates of numbers of undiscovered deposits in Coronado National Forest, southeastern Arizona and southwestern New Mexico.—*Continued*

[The simulations differ in application of appropriate grade and tonnage models for the simulations.The simulations are of two types depending on the tonnage models and numerical simulator used. The simulation using tonnage models taken directly from Cox and Singer (1986) is prefixed with C&S; this simulation was conducted using the MARK3 program developed by the U.S. Geological Survey Branch of Resource Analysis in Reston, Va. Simulations that used tonnage models that have been adjusted to match presumed sizes of inferred, undiscovered deposits in Coronado National Forest are prefixed with AT (adjusted tonnage); this simulation was made using a procedure developed for this study (see text)]

D.—Estimated tonnages of metals in undiscovered porphyry copper deposits. The C&S grade and tonnage model (Singer, Mosier, and Cox, 1986) includes many world-class deposits having sizes (tonnages) unlikely for undiscovered deposits in Coronado National Forest, if not in the contiguous United States. The probability of finding such deposits in Coronado National Forest is nil. To account for this, adjusted tonnage (AT) simulations were based on the C&S model truncated below 2 billion tonnes.

Simulation method	Mean tonnage	Quantiles of simulated metal distribution			Mean number of deposits
		10 percent	50 percent	90 percent	
			Copper		
C&S-MARK3	3.07×10^{6}	0	5.16×10^{6}	6.53×10^{6}	1.01
AT	1.37×10^{6}	0	5.43×10^{5}	3.70×10^{6}	1.00
			Molybdenum		
C&S-MARK3	9.08×10^{4}	0	0	1.53×10^{5}	1.01
AT	2.12×10^{4}	0	0	5.44×10^{4}	1.00
			Gold		
C&S-MARK3	2.84×10^{1}	0	0	7.76×10^{1}	1.01
AT	3.41×10^{1}	2.06×10^{-2}	1.01×10^{1}	9.50×10^{1}	1.00
			Silver		
C&S-MARK3	5.94×10^{2}	0	0	1.49×10^{3}	1.01
AT	9.07×10^{1}	0	0	1.74×10^{2}	1.00
			Ore		
C&S-MARK3	4.72×10^{8}	0	1.10×10^{8}	1.17×10^{9}	1.01

E.—Estimated tonnages of metals in undiscovered porphyry copper skarn-related deposits. The C&S grade and tonnage models (Singer, 1986) are not representative of undiscovered porphyry copper skarn-related deposits inferred in Coronado National Forest. Available production data suggest that the estimates of numbers of undiscovered deposits be based on tonnages centered around the 10-percent quantile of the C&S tonnage model. The adjusted tonnage (AT) simulations are derived from the four smallest tonnages in the C&S model. These four tonnages probably accurately reflect the tonnages of undiscovered porphyry copper skarn-related deposits in Coronado National Forest.

Simulation method	Mean tonnage	Quantiles of simulated metal distribution			Mean number of deposits
		10 percent	50 percent	90 percent	
			Copper		
C&S-MARK3	2.01×10^{6}	0	7.40×10^{5}	5.88×10^{6}	1.30
AT	3.95×10^{5}	0	3.32×10^{5}	9.48×10^{5}	1.30
			Molybdenum		
C&S-MARK3	1.86×10^{4}	0	0	7.50×10^{4}	1.30
AT	1.79×10^{3}	0	0	6.65×10^{3}	1.30
			Gold		
C&S-MARK3	9.80×10^{0}	0	0	3.57×10^{1}	1.30
AT	2.78×10^{0}	0	0	8.64×10^{0}	1.30
			Silver		
C&S-MARK3	7.88×10^{2}	0	0	2.80×10^{3}	1.30
AT	5.93×10^{1}	0	0	2.16×10^{2}	1.30
			Ore		
C&S-MARK3	1.89×10^{8}	0	7.62×10^{7}	5.66×10^{8}	1.30

Table 1. Results of simulations based on estimates of numbers of undiscovered deposits in Coronado National Forest, southeastern Arizona and southwestern New Mexico.—*Continued*

[The simulations differ in application of appropriate grade and tonnage models for the simulations.The simulations are of two types depending on the tonnage models and numerical simulator used. The simulation using tonnage models taken directly from Cox and Singer (1986) is prefixed with C&S; this simulation was conducted using the MARK3 program developed by the U.S. Geological Survey Branch of Resource Analysis in Reston, Va. Simulations that used tonnage models that have been adjusted to match presumed sizes of inferred, undiscovered deposits in Coronado National Forest are prefixed with AT (adjusted tonnage); this simulation was made using a procedure developed for this study (see text)]

F.—Estimated tonnages of metals in undiscovered copper skarn deposits. The C&S copper skarn grade and tonnage models (Jones and Menzie, 1986b) are, in part, based on districts and are not representative of undiscovered copper skarn deposits inferred in Coronado National Forest. Adjusted tonnage (AT) simulations use the C&S model truncated above 75,000 tonnes. The tonnages used in the adjusted tonnage simulations probably accurately reflect tonnages of undiscovered copper skarn deposits in Coronado National Forest.

Simulation method	Mean tonnage	Quantiles of simulated metal distribution			Mean number of deposits
		10 percent	50 percent	90 percent	
		Copper			
C&S-MARK3	1.61×10^{5}	5.54×10^{3}	6.44×10^{4}	4.33×10^{5}	2.90
AT	2.31×10^{3}	2.50×10^{2}	1.45×10^{3}	5.53×10^{3}	2.88
		Gold			
C&S-MARK3	2.68×10^{0}	0	1.08×10^{-1}	6.12×10^{0}	2.90
AT	4.34×10^{-2}	0	0	0	2.88
		Silver			
C&S-MARK3	2.51×10^{1}	0	1.02×10^{0}	7.04×10^{1}	2.90
AT	6.16×10^{-1}	0	0	2.34×10^{0}	2.88
		Ore			
C&S-MARK3	1.23×10^{7}	3.45×10^{5}	4.51×10^{6}	4.12×10^{7}	2.90

G.—Estimated tonnages of metals in undiscovered polymetallic replacement deposits. The C&S polymetallic replacement deposit grade and tonnage models (Mosier, Morris, and Singer, 1986) are based on districts and are not representative of undiscovered polymetallic replacement deposits inferred in Coronado National Forest. Adjusted tonnage (AT) simulations use a tonnage model composed of data for polymetallic replacement deposits in Coronado National Forest. The tonnages of these deposits probably accurately reflect the tonnages of undiscovered copper skarn deposits in Coronado National Forest. Also, gold grades in the C&S grade model for these deposits are too high and would predict gold contents much larger than is likely for deposits inferred for Coronado National Forest. A local gold-grade model was used for all gold simulations for this deposit model except the MARK3 simulation.

Simulation method	Mean tonnage	Quantiles of simulated metal distribution			Mean number of deposits
		10 percent	50 percent	90 percent	
		Copper			
C&S-MARK3	1.73×10^{5}	1.38×10^{4}	1.05×10^{5}	4.11×10^{5}	11.67
AT	4.83×10^{2}	0	1.41×10^{-1}	8.39×10^{2}	11.73
		Gold			
AT	4.52×10^{-2}	0	0	2.30×10^{-3}	11.73
		Silver			
C&S-MARK3	1.50×10^{4}	1.93×10^{3}	1.12×10^{4}	3.27×10^{4}	11.67
AT	2.24×10^{1}	0	2.69×10^{-2}	9.09×10^{0}	11.73
		Lead			
C&S-MARK3	4.06×10^{6}	6.33×10^{5}	3.29×10^{6}	8.34×10^{6}	11.67
AT	6.56×10^{4}	5.10×10^{2}	7.14×10^{3}	1.58×10^{5}	11.73
		Zinc			
C&S-MARK3	4.33×10^{6}	6.38×10^{5}	3.54×10^{6}	9.06×10^{6}	11.67
AT	5.67×10^{4}	4.08×10^{2}	6.22×10^{3}	1.58×10^{5}	11.73
		Ore			
C&S-MARK3	7.38×10^{7}	1.31×10^{7}	6.59×10^{7}	1.44×10^{8}	11.67

Table 1. Results of simulations based on estimates of numbers of undiscovered deposits in Coronado National Forest, southeastern Arizona and southwestern New Mexico.—*Continued*

[The simulations differ in application of appropriate grade and tonnage models for the simulations.The simulations are of two types depending on the tonnage models and numerical simulator used. The simulation using tonnage models taken directly from Cox and Singer (1986) is prefixed with C&S; this simulation was conducted using the MARK3 program developed by the U.S. Geological Survey Branch of Resource Analysis in Reston, Va. Simulations that used tonnage models that have been adjusted to match presumed sizes of inferred, undiscovered deposits in Coronado National Forest are prefixed with AT (adjusted tonnage); this simulation was made using a procedure developed for this study (see text)]

H.—Estimated tonnages of metals in porphyry copper-molybdenum deposits. The C&S grade and tonnage estimates (Singer, Cox, and Mosier, 1986) are used. Many of the porphyry copper-molybdenum deposits in southeastern Arizona are included in this model. This model is probably an accurate portrayal of porphyry copper-molybdenum deposits in Coronado National Forest.

Simulation method	Mean tonnage	Quantiles of simulated metal distribution			Mean number of deposits
		10 percent	50 percent	90 percent	
Copper					
C&S-MARK3	1.61×10^{7}	7.00×10^{5}	9.07×10^{6}	4.22×10^{7}	3.20
Molybdenum					
C&S-MARK3	4.35×10^{5}	3.24×10^{4}	3.06×10^{5}	1.04×10^{6}	3.20
Gold					
C&S-MARK3	5.57×10^{1}	1.65×10^{0}	3.00×10^{1}	1.44×10^{2}	3.20
Silver					
C&S-MARK3	4.96×10^{3}	2.13×10^{2}	2.87×10^{3}	1.20×10^{4}	3.20
Ore					
C&S-MARK3	3.15×10^{9}	2.18×10^{8}	2.04×10^{9}	7.53×10^{9}	3.20

I.—Estimated tonnages of metals in undiscovered polymetallic vein deposits. The polymetallic vein deposit tonnage model in C&S (Bliss and Cox, 1986) is based on districts and is not representative of tonnages of polymetallic vein deposits in Coronado National Forest. The adjusted tonnage (AT) simulations were performed using the C&S tonnage model truncated above 50,000 tonnes. That model is probably accurate for tonnages of polymetallic vein deposits inferred for Coronado National Forest.

Simulation method	Mean tonnage	Quantiles of simulated metal distribution			Mean number of deposits
		10 percent	50 percent	90 percent	
Copper					
C&S-MARK3	1.54×10^{3}	1.13×10^{1}	3.34×10^{2}	3.06×10^{3}	14.01
AT	3.23×10^{2}	0	0	3.52×10^{2}	13.93
Gold					
C&S-MARK3	3.68×10^{0}	3.29×10^{-2}	1.06×10^{0}	1.04×10^{1}	14.01
AT	2.13×10^{-1}	0	1.59×10^{-3}	3.74×10^{-1}	13.93
Zinc					
C&S-MARK3	7.87×10^{4}	2.59×10^{3}	4.41×10^{4}	2.07×10^{5}	14.01
AT	3.86×10^{3}	0	4.02×10^{2}	1.12×10^{4}	13.93
Silver					
C&S-MARK3	1.37×10^{3}	6.11×10^{1}	5.96×10^{2}	4.02×10^{3}	14.01
AT	1.16×10^{2}	6.04×10^{-1}	1.37×10^{1}	2.82×10^{2}	13.93
Lead					
C&S-MARK3	1.12×10^{5}	8.05×10^{3}	7.51×10^{4}	2.55×10^{5}	14.01
AT	1.71×10^{4}	1.65×10^{2}	2.81×10^{3}	4.46×10^{4}	13.93
Ore					
C&S-MARK3	1.54×10^{6}	1.01×10^{5}	1.14×10^{6}	3.48×10^{6}	14.01

Table 1. Results of simulations based on estimates of numbers of undiscovered deposits in Coronado National Forest, southeastern Arizona and southwestern New Mexico.—*Continued*

[The simulations differ in application of appropriate grade and tonnage models for the simulations.The simulations are of two types depending on the tonnage models and numerical simulator used. The simulation using tonnage models taken directly from Cox and Singer (1986) is prefixed with C&S; this simulation was conducted using the MARK3 program developed by the U.S. Geological Survey Branch of Resource Analysis in Reston, Va. Simulations that used tonnage models that have been adjusted to match presumed sizes of inferred, undiscovered deposits in Coronado National Forest are prefixed with AT (adjusted tonnage); this simulation was made using a procedure developed for this study (see text)]

J.—Estimated tonnages of metals in undiscovered hot-springs gold-silver deposits. Only the four smallest deposits in the C&S grade and tonnage model of hot-springs gold-silver deposits (Berger and Singer, 1992) were used in the adjusted tonnage (AT) estimates. Three of these deposits have tonnages approximately two orders of magnitude larger than any of the deposits in Coronado National Forest. While the results of the simulation are presented, they are not included in the tonnage sums because of the large discrepancy in tonnage between the model and the inferred tonnages of hot-springs gold-silver deposits in the Forest.

Simulation method	Mean tonnage	Quantiles of simulated metal distribution			Mean number of deposits
		10 percent	50 percent	90 percent	
			Gold		
C&S-MARK3	9.58×10^{1}	3.80×10^{0}	5.49×10^{1}	2.33×10^{2}	1.95
AT	3.94×10^{0}	6.73×10^{-1}	2.25×10^{0}	1.06×10^{1}	1.93
			Silver		
C&S-MARK3	3.83×10^{2}	0	1.68×10^{2}	9.90×10^{2}	1.95
AT	4.93×10^{1}	0	2.11×10^{1}	1.88×10^{2}	1.93
			Ore		
C&S-MARK3	7.01×10^{7}	2.30×10^{6}	3.78×10^{7}	1.91×10^{8}	1.95

K.—Estimated tonnages of metals in undiscovered Creede-type epithermal vein deposits. The C&S grade and tonnage model (Mosier, Sato, and Singer, 1986) is thought to resemble the tonnages and grades of Creede-type epithermal vein deposits inferred for Coronado National Forest. No data are available to confirm or reject the hypothesis concerning grade and tonnage of inferred deposits because no deposits of this type are known to occur in the Forest.

Simulation method	Mean tonnage	Quantiles of simulated metal distribution			Mean number of deposits
		10 percent	50 percent	90 percent	
			Copper		
C&S-MARK3	3.49×10^{3}	0	0	5.37×10^{3}	0.30
			Gold		
C&S-MARK3	5.98×10^{0}	0	0	7.92×10^{0}	0.30
			Zinc		
C&S-MARK3	4.80×10^{4}	0	0	6.60×10^{4}	0.30
			Silver		
C&S-MARK3	6.90×10^{2}	0	0	5.52×10^{2}	0.30
			Lead		
C&S-MARK3	2.61×10^{4}	0	0	6.44×10^{4}	0.30
			Ore		
C&S-MARK3	2.53×10^{6}	0	0	5.03×10^{6}	0.30

L.—Estimated tonnages of metal in undiscovered rhyolite-hosted tin deposits. The C&S grade and tonnage model for rhyolite-hosted tin deposits (Singer and Mosier, 1986) is probably accurate for tonnages and grades of rhyolite-hosted tin deposits inferred for Coronado National Forest. No data are available to confirm or reject the hypothesis concerning grade and tonnage of inferred deposits because no deposits of this type are known to occur in the Forest.

Simulation method	Mean tonnage	Quantiles of simulated metal distribution			Mean number of deposits
		10 percent	50 percent	90 percent	
			Tin		
C&S-MARK3	3.17×10^{1}	1.01×10^{0}	1.78×10^{1}	8.00×10^{1}	2.95
			Ore		
C&S-MARK3	5.41×10^{3}	4.03×10^{2}	4.08×10^{3}	1.26×10^{4}	2.95

Table 1. Results of simulations based on estimates of numbers of undiscovered deposits in Coronado National Forest, southeastern Arizona and southwestern New Mexico.—*Continued*

[The simulations differ in application of appropriate grade and tonnage models for the simulations. The simulations are of two types depending on the tonnage models and numerical simulator used. The simulation using tonnage models taken directly from Cox and Singer (1986) is prefixed with C&S; this simulation was conducted using the MARK3 program developed by the U.S. Geological Survey Branch of Resource Analysis in Reston, Va. Simulations that used tonnage models that have been adjusted to match presumed sizes of inferred, undiscovered deposits in Coronado National Forest are prefixed with AT (adjusted tonnage); this simulation was made using a procedure developed for this study (see text)]

M.—Estimated tonnages of metal in undiscovered placer gold deposits. The gold placer deposit tonnage model in C&S (Orris and Bliss, 1986) is based on districts and is not representative of the placer gold deposits in Coronado National Forest. Adjusted tonnage (AT) simulations were performed using the C&S tonnage model truncated above 34,000 tonnes. That tonnage model is probably accurate for tonnages of placer gold deposits inferred for Coronado National Forest.

Simulation method	Mean tonnage	Quantiles of simulated metal distribution			Mean number of deposits
		10 percent	50 percent	90 percent	
		Gold			
C&S-MARK3	4.14×10^{-1}	9.52×10^{-3}	2.22×10^{-1}	9.74×10^{-1}	2.92
AT	4.52×10^{-3}	6.00×10^{-4}	2.86×10^{-3}	1.05×10^{-2}	2.93
		Silver			
AT	1.46×10^{-4}	0	0	4.30×10^{-4}	2.93
		Ore			
C&S-MARK3	5.74×10^{5}	2.28×10^{3}	3.16×10^{5}	1.58×10^{6}	2.92

The technique used to assess metallic mineral resources in the Forest involves three steps (Singer and Cox, 1988); results of the first step were presented in Chapter G, this volume; those for the second and third steps are presented in this chapter. In the first step, tracts were delineated on the basis of all available earth science data and with reference to descriptive ore deposit models (Cox and Singer, 1986) and according to the types of undiscovered deposits for which the tracts are favorable. In order to provide land-use planners with the most useful information, the parts of favorable tracts that have high potential for undiscovered deposits are specially noted (pls. 27–29). In the second step, subjective estimates of the number of undiscovered deposits of appropriate mineral deposit types were inferred for each favorable tract. These estimates reflect the plausible sizes (tonnage) of undiscovered deposits in the Forest. In step three, a computer simulation that uses the estimates of numbers of undiscovered deposits and grade and tonnage models for selected mineral deposit models as input is used to generate probabilistic estimates of quantities of metals in each of the deposit types. Selected mineral deposit types include only those already known to be present in the Forest region. The inferred quantities of metals in each mineral deposit type are summed, separately for each metal, to produce an estimate of the total metal in undiscovered mineral deposits in the Forest.

The quantitative metallic-mineral resource assessment presented here is based on the concept of the mineral deposit model, which can be defined as systematically arranged earth science information that describes the essential attributes of a particular group or class of mineral deposits (Cox and Singer, 1986). The mineral deposit models of Cox and Singer (1986) were used because they also include grade and tonnage models that are necessary as input for the computer simulation to generate quantitative estimates of metal in various mineral deposit types.

APPLICATION OF THE THREE-STEP METHOD TO THE QUANTITATIVE MINERAL RESOURCE ASSESSMENT OF CORONADO NATIONAL FOREST

Known mineral deposits in the Forest were assigned to appropriate mineral deposit models; deposits were categorized by deposit model after consideration of available geologic, geochemical, and geophysical evidence. Geologic relations were used to tentatively delineate mineral resource tracts. Tract boundaries were subsequently modified according to geochemical, geophysical, and remote-sensing data and locations of mines and prospects. In many cases, geologic and geophysical evidence was used to extend tracts beyond exposed bedrock into favorable areas concealed by thin veneers of surficial deposits. The results of tract delineation are described in Chapter G, this volume; table 1 (Chapter G) categorizes known deposits in the Forest by mineral deposit type, whereas table 2 (Chapter G) indicates which of the mineral deposit types (of table 1) are likely to be represented by undiscovered deposits in each of the favorable tracts.

Subjective estimates of numbers of undiscovered deposits presented here were made by a group of seven U.S. Geological Survey (USGS) earth scientists (Mark W. Bultman, Harald Drewes, Edward A. du Bray, Frederick S. Fisher, Mark E. Gettings, Douglas P. Klein, and Gary A. Nowlan) and are based on earth science data available for the

Forest region and knowledge of the various deposit models that were considered. The group also had direct access to the USGS Mineral Resource Data System (MRDS) and to a mineral production database provided by the Arizona Geological Survey. Each assessor brought to the group their own personal knowledge of Coronado National Forest geology, geochemistry, geophysics, and mineral deposits.

Quantitative estimates of numbers of undiscovered deposits were prepared following delineation of favorable tracts. The estimates presented in this report represent the least number of undiscovered deposits likely at 90-, 50-, and 10- (or greater, respectively) percent probabilities. For example, an estimate of five deposits at the 90-percent level implies that the probability of at least five undiscovered deposits is at least 90 percent; conversely, this estimate implies that the probability of five or fewer deposits is at most 10 percent.

Following much discussion concerning the mineral resource implications of geologic, geochemical, and geophysical data for each permisive tract, assessors offered undiscovered deposit estimates for each deposit model whose occurrence is favored within delineated tracts. Consensus estimates of numbers of undiscovered deposits of each appropriate deposit type, at each of the three certainty levels, were arbitrated from the estimates of individual assessors. From this subjective, and we cannot sufficiently emphasize the term "subjective," yet probabilistic estimate, a probability mass function of the number of undiscovered deposits was derived by the MARK3 numerical simulation procedure (Root and others, 1992).

The MARK3 simulation procedure then combined the probability mass function of the number of undiscovered deposits with appropriate grade and tonnage data for specific mineral deposit types (Root and others, 1992). The result is a simulated distribution of metals in such deposits. Statistics that describe this distribution are estimators of metallic endowment within favorable tracts. These statistics include the 10, 50 (the median value), and 90 percent quantiles of the simulated distribution as well as the mean value of the simulated distribution. For example, an estimate of 10 tons of undiscovered metal at the 90th quantile indicates that in at least 90 out of 100 cases the amount of metal in the inferred, undiscovered deposits will be 10 tons or less.

SIMULATION PROCEDURE USED IN THE QUANTITATIVE MINERAL RESOURCE ASSESSMENT OF CORONADO NATIONAL FOREST

The standard procedure in step three of quantitative mineral resource assessments made by the USGS involves inputting undiscovered deposit estimates into MARK3. The program, which is installed on a computer in the USGS offices in Reston, Va., is designed to build simulated distributions of metal from deposit grade and tonnage data and estimated numbers of undiscovered deposits (Drew, 1990). This procedure was followed, but the resulting estimates of metal in inferred undiscovered deposits in Coronado National Forest seem implausible in light of grades and tonnages of the expected sizes of undiscovered deposits in this area. In addition, mineral resource exploration in this area during the last 100 years has been sufficiently thorough that the likelihood of discovering deposits having tonnages like those predicted by MARK3 output is low. A thorough discussion of the workings of MARK3 was presented by Root and others (1992), whereas Bultman and others (1993) provide a critical evaluation of assumptions inherent in the three-step method of quantitative assessment, including MARK3.

The principal cause of implausibly high quantitative estimates of metals is probably the use of worldwide and district-based grade and tonnage models. Root and others (1992) stated, "Eighty percent of the estimated deposits should lie between the 90th and 10th percentiles of the tonnages and grades depicted in the models used." This is not the case for inferred, undiscovered deposits in the Forest. In some cases, the size (tonnage) of inferred, undiscovered mineral deposits within the Forest is probably commensurate with the size of known southeastern Arizona deposits. The subjective estimates of undiscovered deposits were therefore based on the sizes of known major producers, of each considered mineral deposit type, in and aound the Forest. Therefore, the parts of tonnage models delimited by tonnages of known deposits and occurrences in southeastern Arizona were used in cases for which the worldwide tonnage model for a given mineral deposit model (Cox and Singer, 1986) does not correspond to the size of known and inferred deposits.

In order to refine the mineral resource assessment, we developed a simple simulation procedure within a commercially available statistical package and ran additional simulations. These simulations were run in order to more easily specify grade and tonnage models appropriate to those for inferred, undiscovered deposits in the Forest. In addition, running the simulations in our own work environment precluded the problems inherent in the non-interactive mode dictated by the fact that MARK3 is installed only on a computer in Reston, Va.

The method we developed emulates MARK3, but its numerical output is slightly different because the grades and tonnages of a given deposit model are not modelled as in MARK3 (Root and others, 1992). Instead, actual grades and tonnages from the appropriate parts of grade and tonnage distributions are sampled in the simulation. Curves modeled through tonnage or grade data, especially lognormally distributed data (such as that for mineral deposit tonnage and grade), in the right-hand tail of the distribution may not be well fit, with the result that the models may underestimate or overestimate the quantity of undiscovered metal.

In summary, in all but three cases, quantitative assessment results reported in this chapter are the result of "adjusted tonnage" simulations. Nonetheless, MARK3 results are presented for comparison (table 1). The mean estimates are probably the most reliable "single number" estimator of metals but they represent a distribution that may have a very large variance for most of the deposit types; they should be used only if an appropriate confidence interval is stated. Because distributions of metals built by the simulation procedure are positively skewed (they are built from positively skewed distributions), the median is a more conservative estimator, but it may not reflect the properties of the distribution.

ANALYSIS OF UNCERTAINTY IN THE SIMULATION PROCEDURE

Assumptions and procedures in the quantitative assessment method may result in inaccurate estimates of mineral endowment. Demonstrably accurate methods of numerical mineral resource assessment do not yet exist; the assessment presented here is the most plausible estimate we can offer from available subjective data concerning the quantity of undiscovered metals present in the Forest. Table 2 presents an analysis of the uncertainties inherent in our estimates.

Two types of uncertainty are present. One type involves uncertainty in numbers of estimated, undiscovered deposits. These uncertainty levels have been propagated through to estimates of metal content (table 2). The second type of uncertainty is that resulting from the use of grade and tonnage distributions and numerical simulation. Many of the uncertainties of the second type are represented by the variance of the hypothetical distribution of metal content and are used as the basis for the construction of the confidence intervals stated in this chapter.

A complete analysis of the interactions of these uncertainties is beyond the scope of this report. Clearly, different components of uncertainty within each of the two forms of uncertainty can be additive and uncertainties between the two forms are multiplicative. Uncertainty concerning grade and tonnage estimates are multiplied just as grade and tonnage are multiplied to obtain a quantity of metal in a deposit of known grade and tonnage.

The magnitude of these uncertainties can have a major impact on the accuracy of the final mineral resource assessment. While not all forms of uncertainty are present at all times, the accuracy of estimates of undiscovered mineral resources developed according to existing numerical methods is considerably uncertain. In this report, we present our best estimates, based on existing earth science data and using prescribed methods of numerical mineral resource assessment, of undiscovered metals in the Forest. We have used the 10- and 90-percent quantiles to estimate the variance of the logarithms of the summed metal contents. The estimate of variance was then used to construct a 95-percent confidence region around the median of the log transformed data. The final quantitative estimates of metal contents are given as a mean for the summed metal content and accompanied by the 95-percent confidence region, which has been adjusted to the mean. There is a 95-percent chance that the one particular sum of results from the Monte Carlo procedures used to generate estimates for a specific metal will fall within the given confidence region. The confidence regions so generated are quite large due to the large variance in the distribution of the estimates of metal content. Yet, the confidence limits represent only uncertainties due to the variance in the grade and tonnage distributions used and in the range of the subjective estimates of undiscovered deposits; the confidence limits do not fully represent all of the possible uncertainty (table 2) in the methodology.

QUANTITATIVE ESTIMATES, BY ORE DEPOSIT MODEL, OF METAL IN THOSE DEPOSITS SUBJECTIVELY INFERRED TO OCCUR IN CORONADO NATIONAL FOREST

Discussions concerning estimates for each mineral deposit model follow. Table 3 presents estimates of the number of undiscovered deposits within favorable tracts of the Forest. Table 4 presents estimates of numbers of undiscovered deposits for each mineral deposit model. Table 5 presents estimates of undiscovered metal for each deposit model, and table 6 presents estimates of undiscovered metals in the entire Forest.

TUNGSTEN SKARN DEPOSITS

The Menzie and Jones (1986) grade and tonnage model for tungsten skarn deposits is based on districts (defined as all mines within 10 km or mines associated with one intrusive). The assessment offered here is based instead on the sizes of local tungsten skarn deposits.

Production statistics for tungsten are available, but in most cases insufficient information is available for classification of mines as a skarn or vein deposit. The tungsten production from all deposits in southeastern Arizona is small, totalling less than 1,000 tonnes of WO_3 (Arizona Geological Survey, 1989). The largest tungsten skarn mines produced approximately 12,000 short ton units, or about 110 tons, of WO_3 (one short ton unit equals 20 lbs WO_3). A grade of 0.9 percent WO_3 results in a 120,000-tonne ore deposit. The four smallest tonnages of tungsten skarn "deposits" (Menzie and Jones, 1986) vary from 16,000 tonnes to 164,000 tonnes WO_3. The sizes of these deposits are centered around the 10-percent quantile of the tonnage distribution (50,000

Table 2. An analysis of uncertainties inherent in the three-step quantitative mineral resource assessment method.

A.—Uncertainty in the estimation of number of deposits based on mineral deposit models as the basis for the assessment and on procedures used to estimate undiscovered deposits.

Source of uncertainty	Over (+) or under (-) estimation of number of deposits	Maximum uncertainty[1] factor of the estimate of metal content	Justification
Lack of rigorous mineral deposit models.	+/-	?	Could lead to large overestimation or underestimation of deposits due to a poor understanding of the deposit model and its relationship to occurrence. Insufficient data to attempt uncertainty-factor quantification.
Arbitrary boundaries between deposit models.	+/-	10?	May lead to uncertainty in estimation based on wrong model type. Similar models often display difference in tonnage of at least one order of magnitude.
Lack of sufficient conditions to predict the occurrence of ore deposits.	+	10?	Will lead to an overestimate of number of undiscovered deposits due to necessary (but not sufficient) conditions being chosen to indicate deposit occurrence. Maximum uncertainty factor of 10 is assumed.
The imprint of mineralized rock on geologic data sets.	+/-	10?	May lead assessors to estimate deposits that are not there or to miss deposits that actually exist. Maximum uncertainty factor of 10 is assumed.
Clustering and the spatial distribution of mineral deposits.	+	10?	May lead to overestimate of undiscovered deposits by assuming that barren areas can be modeled by areas where mines are clustered. Maximum uncertainty factor of 10 is assumed.
Spatial and temporal variations in mineral deposits.	+/-	?	May lead to overestimation or underestimation of deposit numbers due to difference in mineral deposition from one location to another or over time. Insufficient data to attempt uncertainty-factor quantification.
Interpretation of the estimate of number of undiscovered deposits.	+	5	Many assessors may not fully understand how Monte Carlo numerical simulations interpret subjective estimates of undiscovered deposits. For instance, an estimate of at least 0, 0, 1 deposits at 90, 50, and 10 percent probabilities or more, respectively, results in a 30-percent chance of the occurrence of one deposit.
Lack of ability to model ore-deposit formation.	+	?	As in lack of sufficient conditions for formation of an ore deposit, a set of requirements for ore deposit formation that is less restrictive than the actual requirements will be used to estimate the number of undiscovered deposits. This will lead to some unquantifiable level of uncertainty.

Table 2. An analysis of uncertainties inherent in the three-step quantitative mineral resource assessment method.—*Continued*

B.—Uncertainty in the estimation of metal content due to the use of mineral deposit models as the basis for the assessment and due to the use of grade and tonnage distributions and simulations for the assessment.

Source of uncertainty	Over (+) or under (-) estimation of metal content	Uncertainty factor[2] of the estimate of metal content	Justification
Lack of accounting for exploration intensity.	+	10	The lack of quantitative information about exploration could possibly lead to over-estimation of the number of undiscovered deposits and to uncertainty factor of 10.
Underrepresentation of unconventional deposits.	-	2-5	Unconventional and unrecognized deposit models are not well represented in Bulletin 1693 (Cox and Singer, 1986).
Lack of consideration of all known deposit models.	-	?	Mineral deposits that are not considered cannot add to estimates of metal contents.
Lack of statistical stationarity in grade and tonnage models.	+/-	2 (t) 2 (g)	In the Coronado National Forest assessment, we have tried to use grade and tonnage models that are representative of the geologic terranes being assessed.
Sampling proportional to size.	+	2(t)	Based on test simulations, estimates that are double the original estimate are very possible.
Economic truncation	+	2?(t)	Impossible to estimate uncertainty without knowledge of the geologic population of ore deposits.
Translation	?	?	It is difficult to determine the effects that translation may have on data.
Censorship	+	?	There is no way to estimate what pertinent data have not been reported.
Model misspecification	+/-	1.5?(t)	This type of uncertainty has been minimized in this study.

[1]This uncertainty factor is based on the effect that uncertainty in the number of deposits estimated have on the estimate of metal content. It is presented as a multiplicand for overestimation and as a divisor for underestimation.

[2]This uncertainty factor is presented as a multiplicand for overestimation and as a divisor for underestimation; t, the uncertainty for tonnage models; g, the uncertainty for grade models.

tonnes ore); this range was used to estimate the tonnage of inferred, undiscovered tungsten skarn deposits. Deposits of this size appear to best represent undiscovered tungsten skarn deposits in the Forest.

The subjective estimates of numbers of undiscovered tungsten skarn deposits in tracts (Chapter G, this volume, table 2) favorable for this deposit type in the Forest are at least 2, 6, and 10 at the 90-, 50-, and 10-percent quantiles levels, respectively. A simulation based on the tonnage model described above, grades available from Menzie and Jones (1986), and the probability mass function of undiscovered deposits generated using the "at least" procedure results in a median of 2×10^3 tonnes of WO_3 and a mean of 3×10^3 tonnes of WO_3. Estimates for the 10-, 50-, and 90-percent quantiles of the metal tonnage distribution are summarized in table 5.

TUNGSTEN VEIN DEPOSITS

The tonnage and grade model for tungsten vein deposits by Jones and Menzie (1986a) is based on vein systems. The assessment offered here is instead based on the sizes of local tungsten vein deposits, most of which include small groups of veins that are part of a larger vein system. The largest vein system in the Forest produced approximately 180,000 tonnes of WO_3, mostly from five to seven vein deposits. This information indicates that the four smallest tonnages from the Jones and Menzie (1986a) model best represent the tonnage of undiscovered tungsten vein deposits in the Forest. These tonnages are centered around the 10-percent quantile of the tonnage model (45,000 tonnes); this range was used to estimate the tonnage of inferred, undiscovered tungsten vein deposits.

Table 3. Numbers of undiscovered mineral deposits, classified by model, inferred for tracts within Coronado National Forest, southeastern Arizona and southwestern New Mexico.

[-, no estimates of numbers of undiscovered deposits made]

Tract	Mineral deposit model[1]	Mineral deposit model number[1]	Estimate of at least the given number of undiscovered deposits at the following quantiles			Location in Coronado National Forest
			10 percent	50 percent	90 percent	
CH-1	Polymetallic replacement	19a	4	3	1	Chiricahua Mountains
	Porphyry copper skarn related	18a	1	0	0	
CH-2 and CH-1	Polymetallic vein	22c	6	4	2	Chiricahua Mountains
D-1	Polymetallic replacement	19a	5	3	1	Dragoon Mountains
	Tungsten skarn	14a	2	1	0	
G-1	Porphyry copper-molybdenum	21a	2	1	0	Galiuro Mountains
G-2	Hot-springs gold-silver	25a	3	2	1	Galiuro Mountains
PEL-1	Rhyolite-hosted tin	25h	5	3	1	Peloncillo Mountains
PEL-2	Creede-type epithermal vein	25b	1	0	0	Peloncillo Mountains
PEL-unknown	Climax-type molybdenum	16	1	0	0	Peloncillo Mountains
PIN-1	Unknown	-	-	-	-	Pinaleno Mountains
PH-1	Porphyry copper-molybdenum	21	3	2	1	Patagonia-Huachuca
	Polymetallic replacement	19a	6	4	2	Mountains
	Tungsten vein	15a	4	2	1	
	Tungsten skarn	14a	3	2	1	
SCR-1	Tungsten skarn	14a	2	1	0	Santa Catalina-Rincon
	Tungsten vein	15a	1	1	0	Mountains
	Copper skarn	18b	4	3	2	
	Porphyry copper-molybdenum	21a	1	0	0	
SCR-2	Copper skarn	18b	-	-	-	Santa Catalina-Rincon
	Porphyry copper-molybdenum	21a				Mountains
SCR-3	Gold placer	39a	3	2	1	Santa Catalina-Rincon Mountains
SR-1	Tungsten skarn	14a	3	2	1	Santa Rita Mountains
	Polymetallic vein	22c	10	4	1	
	Porphyry copper-skarn related	18a	2	1	0	
SR-2	Gold placer	39a	2	1	0	Santa Rita Mountains
ST-1	Polymetallic replacement	19a	2	1	1	Santa Teresa Mountains
ST-2	Unknown	-	-	-	-	Santa Teresa Mountains
ST-3	None; specialized granite related deposits	-	-	-	-	Santa Teresa Mountains
T-1	Polymetallic vein	22c	9	5	2	Tumacacori Mountains
T-2	Tungsten veins and tungsten placer	15a	1	1	0	Tumacacori Mountains
WHET-1	Porphyry copper	17	2	1	0	Whetstone Mountains
WHET-2	Tungsten vein	15a	2	1	0	Whetstone Mountains
WIN-1	Polymetallic replacement	19a	2	1	0	Winchester Mountains

[1]Cox and Singer, 1986.

Table 4. Estimates of the number of undiscovered mineral deposits for specific mineral deposit models, Coronado National Forest, southeastern Arizona and southwestern New Mexico.

Mineral deposit[1]	Model number[1]	Grade and tonnage model[2]	Estimate of at least the given number of undiscovered deposits at the following quantiles		
			10 percent	50 percent	90 percent
Tungsten skarn	14a	Local/"AT"	10	6	2
Tungsten veins	15a	Local/"AT"	8	5	1
Climax-type molybdenum	16	None used	1	0	0
Porphyry copper	17	Local/"AT"	2	1	0
Porphyry copper skarns	18a	Local/"AT"	3	1	0
Copper skarn	18b	Local/"AT"	4	3	2
Polymetallic replacement	19a	Local/"AT"	19	12	5
Porphyry copper-molybdenum	21a	Singer and others (1986c)	6	3	1
Polymetallic veins	22c	Local/"AT"	25	13	5
Hot-springs gold-silver	25a	None used	3	2	1
Creede-type epithermal vein	25b	Mosier and others (1986b)	1	0	0
Rhyolite-hosted tin	25h	Singer and Mosier (1986)	5	3	1
Placer gold	39a	Local/"AT"	5	3	1

[1]Cox and Singer, 1986.
[2]See text or table 1 for explanation of derivation of model.

The subjective estimates of numbers of undiscovered tungsten vein deposits in tracts (Chapter G, this volume, table 2) favorable for this deposit type are at least 1, 5, and 8 at the 90-, 50-, and 10-percent quantiles, respectively. A simulation based on the tonnage model described above, using grades available from Jones and Menzie (1986a), and the probability mass function of undiscovered deposits generated by the "at least" procedure results in a median of 2×10^3 tonnes of WO_3 and a mean of 2×10^3 tonnes of WO_3. Estimates of the 10-, 50-, and 90-percent quantiles of the metal tonnage distribution are summarized in table 5.

CLIMAX-TYPE MOLYBDENUM DEPOSITS

There are no known Climax-type molybdenum deposits in the Forest, but this type of deposit may be present in the Peloncillo Forest unit. The grade and tonnage models for Climax-type molybdenum deposits (Singer, Theodore, and Mosier, 1986) are based on deposits whose tonnages are probably much larger than deposits of this type that may be present in the Forest. For this reason, the results of the simulation (presented in table 1, part C for informational purposes) are deemed unsuitable for use in this report.

The subjective estimates of numbers of undiscovered Climax-type molybdenum deposits in tracts (Chapter G, this volume, table 2) favorable for this deposit type are at least 0, 0, and 1 at the 90-, 50-, and 10-percent quantiles, respectively. The "at least" procedure used in this assessment to make subjective estimates of numbers of undiscovered deposits allocates 30 percent of the total probability to the occurrence of one deposit and 70 percent to the occurrence of no deposits, in this case.

PORPHYRY COPPER DEPOSITS

The grade and tonnage model for porphyry copper deposits was presented by Singer, Mosier, and Cox (1986). The porphyry copper tonnage model was truncated above 2 billion tonnes of ore for application to the Forest. Geologic and geophysical data, as well as an intensive exploration effort, indicate that there is very little chance that a porphyry copper deposit of greater than 2 billion tonnes can be discovered in this area.

The subjective estimates of numbers of undiscovered porphyry copper deposits in tracts (Chapter G, this volume, table 2) favorable for this deposit type are at least 0, 1, and 2 at the 90-, 50-, and 10-percent quantiles, respectively. A simulation based on the tonnage model of Singer, Mosier, and Cox (1986) truncated above 2 billion tonnes and the probability mass function of undiscovered deposits generated by the "at least" procedure results in a median estimate of 0 tonnes of metal for molybdenum and silver. The median estimate for copper is 5×10^5 tonnes and for gold is 1×10^1 tonnes. The estimate of the mean for each metal is 1×10^6 tonnes of copper, 3×10^1 tonnes of gold, 7×10^1 tonnes of silver, and 2×10^4 tonnes of molybdenum. Estimates of the 10-, 50-, and 90-percent quantiles of the metal tonnage distribution are summarized in table 5.

Table 5. Estimates of metals in undiscovered mineral deposits for specific mineral deposit models, Coronado National Forest, southeastern Arizona and southwestern New Mexico.

Deposit model	Metal	Mean of the simulated metal distribution	Quantiles of simulated metal distributions		
			10 percent	50 percent	90 percent
Tungsten skarn	tungsten	3.17×10^{3}	3.27×10^{2}	1.62×10^{3}	8.15×10^{3}
Tungsten vein	tungsten	2.28×10^{3}	5.62×10^{2}	2.10×10^{3}	4.42×10^{3}
Porphyry copper	copper	1.37×10^{6}	0	5.43×10^{5}	6.53×10^{6}
	gold	3.41×10^{1}	2.06×10^{-2}	1.01×10^{1}	9.50×10^{1}
	molybdenum	2.12×10^{4}	0	0	5.44×10^{4}
	silver	7.70×10^{1}	0	0	1.74×10^{2}
Porphyry copper skarn-related	copper	3.95×10^{5}	0	3.32×10^{5}	9.48×10^{5}
	gold	2.78×10^{0}	0	0	8.64×10^{0}
	molybdenum	1.79×10^{3}	0	0	6.65×10^{3}
	silver	5.93×10^{1}	0	0	2.16×10^{2}
Copper skarn	copper	2.31×10^{3}	2.50×10^{2}	1.45×10^{3}	5.53×10^{3}
	gold	4.34×10^{-2}	0	0	0
	silver	6.16×10^{-1}	0	0	2.34×10^{0}
Polymetallic replacement	copper	4.83×10^{2}	0	1.41×10^{-1}	8.39×10^{2}
	gold	4.52×10^{-2}	0	0	2.30×10^{-3}
	lead	6.56×10^{4}	5.10×10^{2}	7.14×10^{3}	1.58×10^{5}
	silver	2.24×10^{1}	0	2.69×10^{-2}	9.09×10^{0}
	zinc	5.67×10^{4}	4.08×10^{2}	6.22×10^{3}	1.58×10^{5}
Porphyry copper-molybdenum	copper	1.61×10^{7}	7.00×10^{5}	9.07×10^{6}	4.22×10^{7}
	gold	5.57×10^{1}	1.65×10^{0}	3.00×10^{1}	1.44×10^{2}
	molybdenum	4.35×10^{5}	3.24×10^{4}	3.06×10^{5}	1.04×10^{6}
	silver	4.96×10^{3}	2.13×10^{2}	2.87×10^{3}	1.20×10^{4}
Polymetallic veins	copper	3.23×10^{2}	0	0	3.52×10^{2}
	gold	2.13×10^{-1}	0	1.59×10^{-3}	3.74×10^{-1}
	lead	1.71×10^{4}	1.65×10^{2}	2.81×10^{3}	4.46×10^{4}
	silver	1.16×10^{2}	6.04×10^{-1}	1.37×10^{1}	2.82×10^{2}
	zinc	3.86×10^{3}	0	4.02×10^{2}	1.12×10^{4}
Creede-type epithermal vein	copper	3.49×10^{3}	0	0	5.37×10^{3}
	gold	5.98×10^{0}	0	0	7.92×10^{0}
	lead	2.61×10^{4}	0	0	6.44×10^{4}
	silver	6.90×10^{2}	0	0	5.52×10^{2}
	zinc	4.80×10^{4}	0	0	6.60×10^{4}
Rhyolite-hosted tin	tin	3.17×10^{1}	1.01×10^{0}	1.78×10^{1}	8.00×10^{1}
Placer gold	gold	4.52×10^{-3}	6.00×10^{-4}	2.86×10^{-3}	1.05×10^{-2}
	silver	1.46×10^{-4}	0	0	4.30×10^{-4}

PORPHYRY COPPER SKARN-RELATED DEPOSITS

The tonnages of undiscovered porphyry copper skarn-related deposits in the Forest are probably much smaller than tonnages of these deposits presented by Singer (1986). Production data available for deposits of this type in the Forest region indicate that the 10-percent quantile from the tonnage model of Singer (1986) is appropriate for the size of inferred, undiscovered porphyry copper skarn-related deposits in the Forest region. Thus, only the four smallest tonnages presented in that model were used in the simulation.

The subjective estimates of numbers of undiscovered porphyry copper skarn-related deposits in tracts (Chapter G, this volume, table 2) favorable for this deposit type are at least 0, 1, and 3 at the 90-, 50-, and 10-percent quantiles, respectively. A simulation based on the adjusted tonnage model described above and the probability mass function of undiscovered deposits generated by the "at least" procedure

Table 6. Estimates of metal content of undiscovered mineral deposits for all assessed mineral deposit models, Coronado National Forest, southeastern Arizona and southwestern New Mexico.

Metal	Mean of the simulated distribution of metal (tonnes, giving approximate 95-percent confidence interval)	Quantiles of the simulated distribution of metal (tonnes)		
		10 percent	50 percent	90 percent
Copper	2×10^7 (-2×10^7, $+7\times10^9$)	7×10^5	1×10^7	5×10^7
Gold	1×10^2 (-1×10^2, $+8\times10^4$)	2×10^0	4×10^1	3×10^2
Lead	1×10^5 (-1×10^5, $+1\times10^8$)	7×10^2	1×10^4	3×10^5
Molybdenum	5×10^5 (-5×10^5, $+6\times10^7$)	3×10^4	3×10^5	1×10^6
Silver	6×10^3 (-6×10^3, $+1\times10^6$)	2×10^2	3×10^3	1×10^4
Tin	3×10^1 (-3×10^1, $+2\times10^4$)	1×10^0	2×10^1	8×10^1
Tungsten	5×10^3 (-5×10^3, $+2\times10^5$)	9×10^2	4×10^3	1×10^4
Zinc	1×10^5 (-1×10^5, $+1\times10^8$)	4×10^2	7×10^3	2×10^5

results in a median estimate of 0 tonnes of metal for gold, molybdenum, and silver. The median estimate for copper is 3×10^5 tonnes. The estimate of the mean for each metal is 4×10^5 tonnes of copper, 3×10^0 tonnes of gold, 2×10^3 tonnes of molybdenum, and 6×10^1 tonnes of silver. Estimates of the 10-, 50-, and 90-percent quantiles of the metal tonnage distribution are summarized in table 5.

COPPER SKARN DEPOSITS

The tonnages of copper skarn deposits in the Forest are probably much smaller than tonnages presented by Jones and Menzie (1986b), some of which are based on districts. Production data available for deposits of this type in southeastern Arizona indicate that the 10-percent quantile from the tonnage model of Jones and Menzie (1986b) is appropriate for the size of inferred, undiscovered copper skarn deposits in the Forest region. Thus, only the 12 smallest tonnages of deposits presented by Jones and Menzie (1986b) were used in the simulation.

The subjective estimates of numbers of undiscovered copper skarn deposits in tracts (Chapter G, this volume, table 2) favorable for this deposit type are at least 2, 3, and 4 at the 90-, 50-, and 10-percent quantiles, respectively. A simulation based on the adjusted tonnage model described above and the probability mass function of undiscovered deposits generated by the "at least" procedure results in a median estimate of 1×10^3 tonnes of copper. The median for gold and silver is 0 tonnes. The mean of each of the simulated metal distributions is 2×10^3 tonnes of copper, 4×10^{-2} tonnes of gold, and 6×10^{-1} tonnes of silver. Estimates of the 10-, 50-, and 90-percent quantiles of the metal tonnage distribution are summarized in table 5.

POLYMETALLIC REPLACEMENT DEPOSITS

The polymetallic replacement model presented by Mosier, Morris, and Singer (1986) is based on districts having at least 100,000 tonnes of production. The assessment offered here is instead based on the sizes of local polymetallic replacement deposits. Production data for the Harshaw and Aravaipa districts enabled creation of a tonnage model for the polymetallic replacement deposits in the remainder of the Forest. This model was truncated for deposits that contain less than 1,000 tonnes of ore in order to remove numerous, small occurrences that were not considered in estimating numbers of undiscovered deposits. This tonnage distribution, and grade distributions from Mosier, Morris, and Singer (1986) for all metals but gold, were used in the

simulation procedure. The grade of gold in polymetallic replacement deposits of the Forest is substantially less than that reported by Mosier, Morris, and Singer (1986); a distribution of gold grades was generated from data for polymetallic replacement deposits in the Forest.

The subjective estimates of numbers of undiscovered polymetallic replacement deposits in tracts (Chapter G, this volume, table 2) favorable for this deposit type are at least 5, 12, and 19 at the 90-, 50-, and 10-percent quantiles levels, respectively. A simulation based on the adjusted tonnage model described above and the probability mass function of undiscovered deposits generated by the "at least" procedure results in median estimates of 1×10^{-1} tonnes of copper, 7×10^{3} tonnes of lead, 3×10^{-2} tonnes of silver, and 6×10^{3} tonnes of zinc. The median estimate for gold is 0 tonnes. The estimate for the mean of each of the simulated metal distributions is 5×10^{2} tonnes of copper, 5×10^{-2} tonnes of gold; 7×10^{4} tonnes of lead, 2×10^{1} tonnes of silver, and 6×10^{4} tonnes of zinc. Estimates of the 10-, 50-, and 90-percent quantiles of the metal tonnage distribution are summarized in table 5.

PORPHYRY COPPER-MOLYBDENUM DEPOSITS

The assessment of porphyry copper-molybdenum deposits is based on the grade and tonnage model presented by Singer, Cox, and Mosier (1986). This model includes porphyry copper-molybdenum deposits from southeastern Arizona and is thought to be representative of undiscovered porphyry copper-molybdenum deposits that may exist in the Forest.

The subjective estimates of numbers of undiscovered porphyry copper-molybdenum deposits in tracts (Chapter G, this volume, table 2) favorable for this deposit type are at least 1, 3, and 6 at the 90-, 50-, and 10-percent quantiles, respectively. A simulation based on the grade and tonnage model described above and the probability mass function of undiscovered deposits generated by the "at least" procedure results in median estimates of 9×10^{6} tonnes of copper, 3×10^{1} tonnes of gold, 3×10^{5} tonnes of molybdenum, and 3×10^{3} tonnes of silver. The estimates for the mean of each of the simulated distributions of metals is 2×10^{7} tonnes of copper, 6×10^{1} tonnes of gold, 4×10^{5} tonnes of molybdenum, and 5×10^{3} tonnes of silver. Estimates of the 10-, 50-, and 90-percent quantiles of the metal tonnage distribution are summarized in table 5.

POLYMETALLIC VEIN DEPOSITS

The grade and tonnage model for polymetallic veins is by Bliss and Cox (1986). The model is based mostly on deposits from the Slocan mining district in British Columbia, Canada, that are described as all workings within 1 km of each other and having a minimum of 100 tonnes of ore. Some district-based data are also included in the model. Possibly because of these district-based data, or because of the predominance of data for the Slocan mining district, the large tonnages of the largest deposits in the model makes it inappropriate to use this model to represent polymetallic vein deposits in the Forest. Production data available for the Forest region indicate that truncation of this distribution above 50,000 tons of ore is appropriate; no undiscovered polymetallic vein deposit in the Forest is likely to exceed that size.

The subjective estimates of numbers of undiscovered polymetallic vein deposits in tracts (Chapter G, this volume, table 2) favorable for this deposit type are at least 5, 13, and 25 at the 90-, 50-, and 10-percent quantiles, respectively. A simulation based on the grade and tonnage models described above and the probability mass function of undiscovered deposits generated by the "at least" procedure results in median estimates of 2×10^{-3} tonnes of gold, 3×10^{3} tonnes of lead, 1×10^{1} tonnes of silver, $.4\times10^{2}$ tonnes of zinc and 0 tonnes for copper. The estimates of the mean of each of the simulated distributions of metals are 3×10^{2} tonnes of copper, 2×10^{-1} tonnes of gold, 2×10^{4} tonnes of lead; 1×10^{2} tonnes of silver, and 4×10^{3} tonnes of zinc. Estimates of the 10-, 50-, and 90-percent quantiles of the metal tonnage distribution are summarized in table 5.

HOT-SPRINGS GOLD-SILVER DEPOSITS

The hot-springs gold-silver deposit tonnage model (Berger and Singer, 1992) does not represent the tonnages of deposits of this type in the Forest. It includes deposits having reserves as large as 240 million tonnes of ore, whereas total production from hot springs gold-silver deposits in the Forest is roughly 0.0028 tonnes of gold from roughly 300 tonnes of ore (Arizona Geological Survey, 1989). The three smallest deposits, deposits of 0.32, 1.0, and 4.2 million tonnes, in the hot-springs gold-silver model (Berger and Singer, 1992) were used to estimate the tonnages and grades of these deposits in the Forest.

The subjective estimates of numbers of undiscovered hot springs gold-silver deposit in tracts (Chapter G, this volume, table 2) favorable for this deposit type are at least 1, 2, and 3 at the 90-, 50-, and 10-percent quantiles. Although simulations based on the grade and tonnage model described above were performed, their results are not considered further because of the large discrepancy between the known production from hot- springs gold-silver deposits in the Forest and the adjusted tonnage model discussed above. The results of these simulations are included in table 1 for informational purposes, but they do not pertain to the Forest.

CREEDE-TYPE EPITHERMAL VEIN DEPOSITS

No Creede-type epithermal vein deposits are known in the Forest; thus the grade and tonnage model for Creede-type epithermal vein deposits (Mosier, Sato, and Singer, 1986) is used in the simulation. We believe that this model probably approximates grades and tonnages of inferred, undiscovered Creede-type epithermal vein deposits in the Forest reasonably well.

The subjective estimates of numbers of undiscovered Creede-type epithermal vein deposits in tracts (Chapter G, this volume, table 2) favorable for this deposit type are at least 0, 0, and 1 at the 90-, 50-, and 10-percent quantiles, respectively. A simulation based on the grade and tonnage model described above and the probability mass function of undiscovered deposits generated by the "at least" procedure results in median estimates of 0 tonnes of copper, 0 tonnes of gold, 0 tonnes of lead, 0 tonnes of silver, and 0 tonnes of zinc. The estimates of the mean of each of the simulated metal distributions are 3×10^3 tonnes of copper, 6×10^0 tonnes of gold, 3×10^4 tonnes of lead, 7×10^2 tonnes of silver, and 5×10^4 tonnes of zinc. Estimates of the 10-, 50-, and 90-percent quantiles of the metal tonnage distribution are summarized in table 5.

The estimate of quantities of metals presented above is not conditioned on the probability that a Creede-type epithermal vein deposit is present in the Forest. The subjective estimate of numbers of undiscovered deposits was made in such a way that it reflects the assessors' judgment concerning the existence of a Creede-type epithermal vein deposit.

RHYOLITE-HOSTED TIN DEPOSITS

Rhyolite-hosted tin deposits are unknown in the Forest; thus the grade and tonnage model for rhyolite-hosted tin (Singer and Mosier, 1986) is used in the simulation. This model probably approximates grades and tonnages of inferred, undiscovered rhyolite-hosted tin deposits in the Forest.

The subjective estimates of numbers of undiscovered rhyolite-hosted tin deposits in tracts (Chapter G, this volume, table 2) favorable for this deposit type are at least 1, 3, and 5 at the 90-, 50-, and 10-percent quantiles, respectively. A simulation based on the grade and tonnage model described above and the probability mass function of undiscovered deposits generated by the "at least" procedure results in a median estimate of 2×10^1 tonnes of tin. The estimate of the mean of the simulated distributions of metals is 3×10^1 tonnes of tin. Estimates of the 10-, 50-, and 90-percent quantiles of the metal tonnage distribution are summarized in table 5.

The estimate of quantities of metals presented above is not conditioned on the probability that a rhyolite-hosted tin deposit is present. The subjective estimate of the number of undiscovered deposits was made in such a way that it reflects the assessors' judgment concerning the existence of a rhyolite-hosted tin deposit.

PLACER GOLD DEPOSITS

The Orris and Bliss (1986) grade and tonnage model for placer gold deposits is based on districts or on placer operations within 1.5 km of each other. The assessment offered here is instead based on the tonnages near the 10 percent quantile of the tonnage model by Orris and Bliss (1986). That tonnage model was truncated above 33,000 tons of "ore" because deposits near this size best represent the most likely size of undiscovered placer gold deposits in the Forest.

The subjective estimates of numbers of undiscovered placer gold deposits in tracts (Chapter G, this volume, table 2) favorable for this deposit type are at least 1, 3, and 5 at the 90-, 50-, and 10-percent quantiles, respectively. A simulation based on the tonnage model described above, grades available from Orris and Bliss (1986), and the probability mass function of undiscovered deposits generated by the "at least" procedure results in median estimates of 3×0^{-3} tonnes of gold and 0 tonnes of silver. The estimates of the mean of the simulated distributions of metals is 5×10^{-3} tonnes gold and 1×10^{-4} tonnes of silver. Estimates of the 10-, 50-, and 90-percent quantiles of the metal tonnage distribution are summarized in table 5.

SUMMED QUANTITATIVE ESTIMATES OF METALS IN CORONADO NATIONAL FOREST

Quantitative assessments of metal tonnages in inferred, undiscovered deposits are summed for the entire Forest (table 5) for the following deposit types: (1) tungsten skarn, (2) tungsten vein, (3) porphyry copper, (4) porphyry copper skarn-related, (5) copper skarn, (6) polymetallic replacement, (7) porphyry copper-molybdenum, (8) polymetallic vein, (9) Creede-type epithermal vein, (10) rhyolite-hosted tin, and (11) placer gold. These data are used to compute total undiscovered metal (in tonnes) for these 10 types of deposits in the entire Forest (table 6).

Although this information is presented in a quantitative, probabilistic format, the analysis is based on subjective estimates of numbers of undiscovered deposits for each specific mineral deposit model considered. The correctness of the information presented depends on the accuracy of the assumptions inherent in the methodology. These estimates are based solely on the knowledge available to the authors at the time of the assessment and are subject to the uncertainties defined in table 2.

REFERENCES CITED

Arizona Geological Survey, 1969, Geology and mineral resources of Arizona: Arizona Geological Survey Bulletin 180, pt. I, 467 p.

Berger, B.R., and Singer, D.A., 1992, Grade and tonnage model of hot-springs Au-Ag: U.S. Geological Survey Bulletin 2004, p. 23–25.

Bliss, J.D., and Cox, D.P., 1986, Grade and tonnage model of polymetallic veins, *in* Cox, D.P., and Singer, D.A., eds., Mineral deposit models: U.S. Geological Survey Bulletin 1693, p. 125–129.

Bultman, M.W., Force, E.R., Gettings, M.E., and Fisher, F.S., 1993, Comments on the "three-step" method for quantification of undiscovered mineral resources: U.S. Geological Survey Open-File Report OF–93–23, 59 p.

Cox, D.P. and Singer, D.A., eds., 1986, Mineral deposit models: U.S. Geological Survey Bulletin 1693, 379 p.

Drew, L.J., 1990, Reflections of a petroleum geologist, Oxford University Press, New York, 252 p.

Jones, G.M., and Menzie, W.D., 1986a, Grade and tonnage model of W veins, *in* Cox, D.P., and Singer, D.A., eds., Mineral deposit models: U.S. Geological Survey Bulletin 1693, p. 65.

———1986b, Grade and tonnage model of Cu skarn deposits, *in* Cox, D.P., and Singer, D.A., eds., Mineral deposit models: U.S. Geological Survey Bulletin 1693, p. 86–89.

Menzie, W.D., and Jones, G.M., 1986, Grade and tonnage model of W skarn deposits, *in* Cox, D.P., and Singer, D.A., eds., Mineral deposit models: U.S. Geological Survey Bulletin 1693, p. 55.

Mosier, D.L., Morris, H.T., and Singer, D.A., 1986, Grade and tonnage model of polymetallic replacement deposits, *in* Cox, D.P., and Singer, D.A., eds., Mineral deposit models: U.S. Geological Survey Bulletin 1693, p. 101–104.

Mosier, D.L., Sato, T., and Singer, D.A., 1986, Grade and tonnage model of Creede Epithermal veins, *in* Cox, D.P., and Singer, D.A., eds., Mineral deposit models: U.S. Geological Survey Bulletin 1693, p. 146–149.

Orris, G.J., and Bliss, J.D., 1986, Grade and tonnage model of placer Au-PGE, *in* Cox, D.P., and Singer, D.A., eds., Mineral deposit models: U.S. Geological Survey Bulletin 1693, p. 261–263.

Root, D.H., Menzie, W.D., and Scott, W.A., 1992, Computer Monte Carlo simulation in quantitative resource estimation: Nonrenewable Resources, v. 1, p. 125–138.

Singer, D.A., 1986, Grade and tonnage model of porphyry copper, skarn-related deposits, *in* Cox, D.P., and Singer, D.A., eds., Mineral deposit models: U.S. Geological Survey Bulletin 1693, p. 82–85.

Singer, D.A., and Cox, D.P., 1988, Application of mineral deposit models to resource assessments, *in* Geologic investigations: U.S. Geological Survey Yearbook 1987, p. 55–56.

Singer, D.A., Cox, D.P., and Mosier, D.L., 1986, Grade and tonnage model of porphyry Cu-Mo, *in* Cox, D.P., and Singer, D.A., eds., Mineral deposit models: U.S. Geological Survey Bulletin 1693, p. 116–119.

Singer, D.A., and Mosier, D.L., 1986, Grade and tonnage model of rhyolite-hosted Sn, *in* Cox, D.P., and Singer, D.A., eds., Mineral deposit models: U.S. Geological Survey Bulletin 1693, p. 169–171.

Singer, D.A., Mosier, D.L., and Cox, D.P., 1986, Grade and tonnage model of porphyry Cu, *in* Cox, D.P., and Singer, D.A., eds., Mineral deposit models: U.S. Geological Survey Bulletin 1693, p. 77–78.

Singer, D.A., Theodore, T.G., and Mosier, D.L., 1986, Grade and tonnage model of Climax Mo deposits, *in* Cox, D.P., and Singer, D.A., eds., Mineral deposit models: U.S. Geological Survey Bulletin 1693, p. 73–75.

Recommendations for Future Earth Science Investigations in Coronado National Forest

By Harald Drewes, Mark W. Bultman,
Gary A. Nowlan, *and* Mark E. Gettings

MINERAL RESOURCE POTENTIAL AND GEOLOGY OF CORONADO NATIONAL FOREST, SOUTHEASTERN ARIZONA AND SOUTHWESTERN NEW MEXICO
Edited by Edward A. du Bray

U.S. GEOLOGICAL SURVEY BULLETIN 2083–K

UNITED STATES GOVERNMENT PRINTING OFFICE, WASHINGTON : 1996

CONTENTS

Recommendations for Future Earth Science Investigations in Coronado National Forest

By Harald Drewes, Mark W. Bultman, Gary A. Nowlan, *and* Mark E. Gettings

INTRODUCTION

The mineral resource assessment of Coronado National Forest has resulted not only in an assessment, but has also helped identify future earth science studies that would lead to an improved assessment.

Good geologic maps are the fundamental basis for mineral resource evaluations. Existing geologic maps for a region as large as Coronado National Forest are apt to be highly variable with respect to quality, scale, and purpose. Preparation of better geologic maps of those parts of the Forest that are inadequately mapped would provide a much improved basis from which to conduct such an assessment. Study of selected topics in geology and ore deposits is also necessary.

The geochemistry of Coronado National Forest and adjacent areas is reasonably well defined by currently available data, but additional data are needed to fill in sparsely sampled areas and to better characterize the Forest region. Additional panned-concentrate and rock samples should be collected from every unit of the Forest. Panned-concentrate samples from stream sediments provide information for some elements that is not available in analyses of stream-sediment samples. Routine analytical methods are relatively insensitive for some elements, and those elements go undetected in a majority of stream-sediment samples. Panning concentrates heavy minerals with the result that elements contained therein are readily detected. Rock sampling should include samples that may have been modified by mineralizing fluids. Apparently unmineralized rocks should also be sampled to provide background data and aid detection of geochemical trends related to presently unrecognized mineralization processes.

Some parts of the Forest are covered by extensive gravel deposits, and existing geochemical data do not adequately contribute to a mineral resource assessment of these types of areas. The application of proven sample media for geochemical exploration, such as plants, needs to be investigated in these areas. Available water wells should be geochemically sampled. As new geochemical methods, such as the collection and analysis of soil gases, become more widely accepted and utilized, they should be applied in pediment areas overlain by thin alluvial deposits.

Greater attention needs to be paid to geochemical signatures and their relation to mineral deposit types. Elements such as Cu, Pb, Zn, Au, Ag, and Mo are part of the signatures for many deposit types, so discrimination among such deposits is difficult. Better definition of geochemical interrelationships is needed so that subtle differences may be recognized and their significance determined. In order to better define geochemical signatures, multivariate analysis of geochemical data must be more extensively applied than was possible in this study.

The continued application of remote-sensing technology could also improve the quality of future mineral resource assessments. First, however, all tracts of potentially altered ground, identified in Chapter F, should be field checked. New acquisitions of the Federally Owned Landsat Data database of imagery that covers the Forest can be used to identify additional possibly altered tracts.

A Thematic Mapper study designed to distinguish rock types or lithologic boundaries within the Forest would be helpful to future mineral resource assessments. In some cases, Thematic Mapper imagery is distinctly variable within a given mapped rock type. In other cases, this imagery depicts lithologic boundaries not indicated by existing geologic mapping. A detailed examination of digital imagery data with regard to associated rock type might clarify some of these situations. Of particular interest would be the ability to reliably distinguish areas underlain by rhyolite from those underlain by andesite.

A complete analysis of fracture patterns in the Forest region, based on airborne synthetic-aperture radar imagery, is warranted. This type of analysis would allow detailed analysis of the correspondence between linear or curvilinear features or patterns with mapped faults and circular geologic features. At present, synthetic-aperture radar is available for the east half of the Forest only.

Airborne imaging spectrometer data, including thermal infrared data, could be obtained over areas of previously unrecognized altered rock. Analysis of these data would help define rock types as well as types or patterns of

alteration in this area, which would in turn benefit future, detailed mineral resource assessments and could help identify exploration targets.

The highest priority for future geophysical work in the Forest involves acquisition of new data and further data analysis. In particular, gravity- and magnetic-anomaly data need to be quantitatively modeled in a geologic context.

Much more gravity data needs to be acquired in virtually all parts of the Forest. Future work should begin with traverses across areas that have potential for the presence of undiscovered mineral deposits and proceed in areas for which existing data are sparse. In addition, efforts to procure existing gravity data from private sources should be pursued.

Low-level, 0.5-km-spaced aeromagnetic-anomaly map coverage exists in private, commercial files for all of the Forest area east of Tucson from approximately lat 33° N. south to the Mexico border. These data should be procured and analyzed. Truck-borne magnetometer studies of particular structures of interest should be conducted to allow discrimination between anomaly sources and assist in interpretation of aeromagnetic data. Detailed data from truck-borne magnetometer traverses should be used to improve estimates of fill thickness for parts of the Forest that are covered by basin fill and may contain mineralized targets.

Deep-seismic-refraction studies have been made as part of oil and gas exploration of the Forest region but are unavailable to the public. Access to these data is essential to obtaining a better understanding of the tectonic configuration of the region. These data would enable identification of potential hydrocarbon traps as well as ore-fluid conduits. For example, the parts of two seismic lines seen by Drewes indicate that major thrust plate duplication occurs across one major valley in the eastern part of the Forest region and beneath a major mountain range in the western part.

As adequate data become available, quantitative interpretation and modelling of the combined gravity- and magnetic-anomaly data should be conducted. Many studies of regional structure within ranges of the Forest require completion; only those studies that are largely reconnaissance in nature studies have been completed. Questions concerning structural and thermal histories of Forest lands bear directly on mineral resource potential in all of the ranges. Particularly important topics include the role and extent of detachment faulting in southeastern Arizona, the mechanisms and timing of uplift and their relationships to magmatic episodes (both in metamorphic core complexes and elsewhere), the identification by geophysical means of volcanic centers in the Forest region, and identification by geophysical means of areas where undiscovered mineral deposits may be present beneath surficial deposits. Finally, the causes of geophysical anomalies for which no source could be identified should be studied.

Specific gaps in earth science data shortages for the mountain ranges that constitute Coronado National Forest are described below.

Santa Teresa Mountains.—Additional stream-sediment samples should be collected in the south-central part of the Santa Teresa Forest unit. Nearly adequate gravity data are available for the Santa Teresa Mountains, though the range contains large areas in which not even the regional gravity anomaly field is well defined.

Galiuro Mountains.—In order to improve the quality of subsequent mineral resource assessments in the Galiuro Mountains, the quality of geologic mapping for this area must be improved. Remote-sensing data indicate large, possibly altered areas in the Galiuro Mountains that require field checking. Nearly adequate gravity data are available for the Galiuro Mountains, though the range contains large areas in which not even the regional gravity-anomaly field is well defined.

Winchester Mountains.—In order to improve the quality of subsequent mineral resource assessments in the Winchester Mountains, the quality of geologic mapping for this area must be improved. Single-station gravity anomalies in the Winchester Mountains must be verified by additional observations.

Pinaleno Mountains.—Additional stream-sediment samples should be collected in the northwestern part of the Pinaleno Forest unit. Nearly adequate gravity data are available for the Pinaleno Mountains, though the range contains large areas in which not even the regional gravity-anomaly field is well defined.

Peloncillo Mountains.—In order to improve the quality of subsequent mineral resource assessments in the Peloncillo Mountains, the quality of geologic mapping for this area must be improved. Additional stream-sediment samples should be collected in the northern and southeastern parts of the Peloncillo Mountains unit. Remote sensing data indicate large, possibly altered areas in the Peloncillo Mountains that require field checking. Gravity data for the Peloncillo Mountains are sparse.

Chiricahua and Pedregosa Mountains.—Additional stream-sediment samples should be collected in the southeastern part of the Chiricahua-Pedregosa Forest unit. Nearly adequate gravity data are available for the Chiricahua Mountains, though the range contains large areas in which not even the regional gravity-anomaly field is well defined.

Dragoon Mountains.—Single-station gravity anomalies in the Dragoon Mountains must be verified by additional observations.

Whetstone Mountains.—Single-station gravity anomalies in the Whetstone Mountains must be verified by additional observations.

Patagonia and Huachuca Mountains and Canelo Hills.—In order to improve the quality of subsequent mineral resource assessments in the Patagonia–Huachuca–Canelo Hills Forest unit, the quality of geologic mapping in the area, particularly the lowlands between the Canelo Hills and Red Mountain at the northern end of the Patagonia Mountains, must be improved. Geology in the Canelo Hills–Red

Mountain area suggests that a favorable structural level, between tops of Late Cretaceous or Paleocene stocks and the roots of their overlying andesitic volcanic covers, is exposed, or nearly so, in this area. Mineralized rock is widespread, and the area contains a known porphyry copper deposit. However, the distribution of volcanic vents and hydrothermal systems is unknown, except for those in the Red Mountain and Harshaw areas. The central part of the Patagonia-Huachuca-Canelo Forest unit is covered by extensive gravel deposits. Geochemical methods, such as those described above that can minimize the effects of these gravel covers, should be applied. Gravity data for the area are sparse.

Santa Rita Mountains.—The eastern part of the Santa Rita Forest unit is covered by extensive gravel deposits. Geochemical methods, such as those described above that can minimize the effects of gravel cover, should be applied. Gravity data for the Santa Rita Mountains areas are sparse.

Atascosa, Pajarito, San Luis, and Tumacacori Mountains and Cobre and Coches Ridges.—In order to improve the quality of subsequent mineral resource assessments in the Atascosa–Cobre–Coches–Pajarito–San Luis–Tumacacori Forest unit, especially the Cobre Ridge area, the quality of geologic mapping in the area must be improved. The Cobre Ridge area contains an assemblage of rocks and structural features that are difficult to evaluate from existing information. Many kinds of intrusive rocks, most of undetermined age, and including unmapped breccia pipes are in this area. This area is within a metallogenic belt that is characterized by large, $1 billion or larger, ore deposits, but it has produced only a moderate ($10–100 million) quantity of metallic commodities. Thorough study of this area might result in identification of large, undiscovered mineral resources, particularly porphyry copper-molybdenum deposits. The first priority for future remote-sensing investigations in the Forest involves acquisition and analysis of imagery for the Tumacacori Mountains. This area is cloud covered in the imagery used for this assessment.

Santa Catalina and Rincon Mountains.—In order to improve the quality of subsequent mineral resource assessments the quality of geologic mapping in the area, mainly the northeast flank of the Santa Catalina Mountains exclusive of the San Manuel quadrangle, must be improved. Mineral production from the northeastern Santa Catalina Mountains has been insignificant, but the area has geologic attributes that are favorable for occurrence of ore deposits and it lies in a favorable metallogenic belt. The ruggedness of this area has hindered its complete, detailed geologic mapping, with the result that the mineral resource potential of this area is poorly understood. Additional stream-sediment samples should be collected in the eastern part of the Rincon Mountains. The Rincon Mountains are the largest area for which almost no gravity data exist. Nearly adequate gravity data are available for the Santa Catalina Mountains, though the range contains large areas in which not even the regional gravity-anomaly field is well defined.

Published in the Central Region, Denver, Colorado
Manuscript approved for publication December 30, 1993
Edited by Diane E. Lane
Graphic design by Patricia L. Wilber
Cartography by Bruce Galoob, William R. Stephens, and Dave Castor
Photocomposition by Mari L. Kauffmann

APPENDIXES 1 AND 2

APPENDIX 1. DEFINITION OF LEVELS OF MINERAL RESOURCE POTENTIAL AND CERTAINTY ASSESSMENT

Definitions of Mineral Resource Potential

LOW mineral resource potential is assigned to areas where geologic, geochemical, and geophysical characteristics define a geologic environment in which the existence of resources is unlikely. This broad category embraces areas with dispersed but insignificantly mineralized rock as well as areas with few or no indications of having been mineralized.

MODERATE mineral resource potential is assigned to areas where geologic, geochemical, and geophysical characteristics indicate a geologic environment favorable for resource occurrence, where interpretations of data indicate a reasonable likelihood of resource accumulation, and (or) where an application of mineral-deposit models indicates favorable ground for the specified type(s) of deposits.

HIGH mineral resource potential is assigned to areas where geologic, geochemical, and geophysical characteristics indicate a geologic environment favorable for resource occurrence, where interpretations of data indicate a high degree of likelihood for resource accumulation, where data support mineral-deposit models indicating presence of resources, and where evidence indicates that mineral concentration has taken place. Assignment of high resource potential to an area requires some positive knowledge that mineral-forming processes have been active in at least part of the area.

UNKNOWN mineral resource potential is assigned to areas where information is inadequate to assign low, moderate, or high levels of resource potential.

NO mineral resource potential is a category reserved for a specific type of resource in a well-defined area.

Levels of Certainty

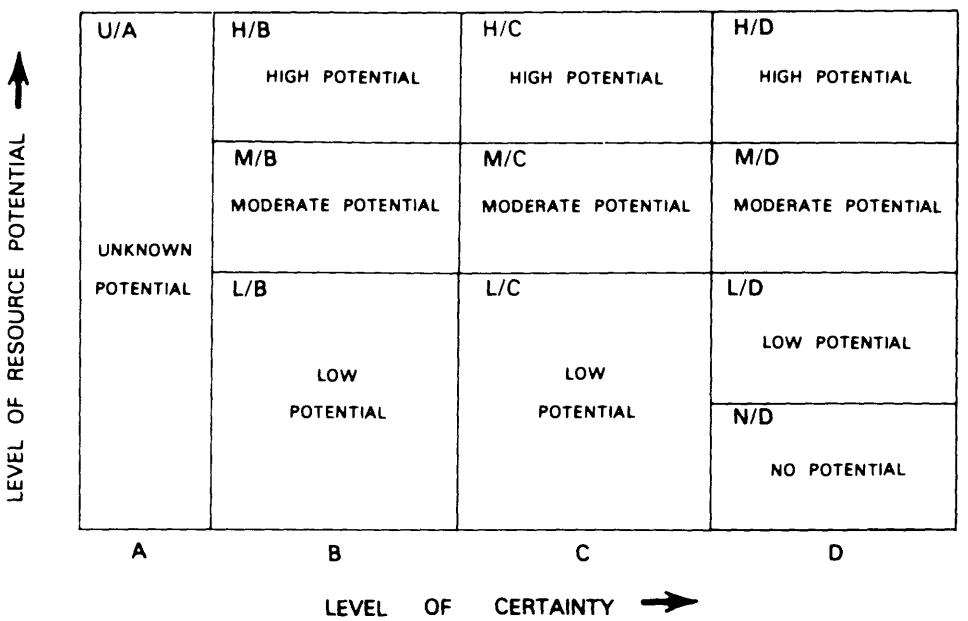

A. Available information is not adequate for determination of the level of mineral resource potential.
B. Available information suggests the level of mineral resource potential.
C. Available information gives a good indication of the level of mineral resource potential.
D. Available information clearly defines the level of mineral resource potential.

Abstracted with minor modifications from:

Taylor, R. B., and Steven, T. A., 1983, Definition of mineral resource potential: Economic Geology, v. 78, no. 6, p. 1268–1270.

Taylor, R. B., Stoneman, R. J., and Marsh, S. P., 1984, An assessment of the mineral resource potential of the San Isabel National Forest, south-central Colorado: U.S. Geological Survey Bulletin 1638, p. 40–42.

Goudarzi, G. H., compiler, 1984, Guide to preparation of mineral survey reports on public lands: U.S. Geological Survey Open-File Report 84–0787, p. 7, 8.

APPENDIX 2. GEOLOGIC TIME CHART

Subdivisions (and their symbols)						Age estimates of boundaries in mega-annum (Ma) [1]
Eon or Eonothem	Era or Erathem	Period, System, Subperiod, Subsystem		Epoch or Series		
Phanerozoic [2]	Cenozoic [2] (Cz)	Quaternary [2] (Q)		Holocene		0.010
				Pleistocene		1.6 (1.6–1.9)
		Tertiary (T)	Neogene [2] Subperiod or Subsystem (N)	Pliocene		5 (4.9–5.3)
				Miocene		24 (23–26)
			Paleogene [2] Subperiod or Subsystem (P_E)	Oligocene		38 (34–38)
				Eocene		55 (54–56)
				Paleocene		66 (63–66)
	Mesozoic [2] (M_Z)	Cretaceous (K)		Late	Upper	96 (95–97)
				Early	Lower	138 (135–141)
		Jurassic (J)		Late	Upper	
				Middle	Middle	
				Early	Lower	205 (200–215)
		Triassic (Ŧ)		Late	Upper	
				Middle	Middle	
				Early	Lower	~240
	Paleozoic [2] (P_Z)	Permian (P)		Late	Upper	
				Early	Lower	290 (290–305)
		Carboniferous Systems (C)	Pennsylvanian (℗)	Late	Upper	
				Middle	Middle	
				Early	Lower	~330
			Mississippian (M)	Late	Upper	
				Early	Lower	360 (360–365)
		Devonian (D)		Late	Upper	
				Middle	Middle	
				Early	Lower	410 (405–415)
		Silurian (S)		Late	Upper	
				Middle	Middle	
				Early	Lower	435 (435–440)
		Ordovician (O)		Late	Upper	
				Middle	Middle	
				Early	Lower	500 (495–510)
		Cambrian (Ꞓ)		Late	Upper	
				Middle	Middle	
				Early	Lower	~570 [3]
Proterozoic (Ꝑ)	Late Proterozoic (Z)	None defined				900
	Middle Proterozoic (Y)	None defined				1600
	Early Proterozoic (X)	None defined				2500
Archean (A)	Late Archean (W)	None defined				3000
	Middle Archean (V)	None defined				3400
	Early Archean (U)	None defined				3800 ?
pre-Archean (pA) [4]						

[1] Ranges reflect uncertainties of isotopic and biostratigraphic age assignments. Age boundaries not closely bracketed by existing data shown by ~. Decay constants and isotopic ratios employed are cited in Steiger and Jäger (1977). Designation m.y. used for an interval of time.

[2] Modifiers (lower, middle, upper or early, middle, late) when used with these items are informal divisions of the larger unit; the first letter of the modifier is lowercase.

[3] Rocks older than 570 Ma also called Precambrian (p-Ꞓ), a time term without specific rank.

[4] Informal time term without specific rank.

☆ U.S. GOVERNMENT PRINTING OFFICE: 1996 - 774-045 / 20044 REGION NO. 8

SELECTED SERIES OF U.S. GEOLOGICAL SURVEY PUBLICATIONS

Periodicals

Earthquakes & Volcanoes (issued bimonthly).
Preliminary Determination of Epicenters (issued monthly).

Technical Books and Reports

Professional Papers are mainly comprehensive scientific reports of wide and lasting interest and importance to professional scientists and engineers. Included are reports on the results of resource studies and of topographic, hydrologic, and geologic investigations. They also include collections of related papers addressing different aspects of a single scientific topic.

Bulletins contain significant data and interpretations that are of lasting scientific interest but are generally more limited in scope or geographic coverage than Professional Papers. They include the results of resource studies and of geologic and topographic investigations; as well as collections of short papers related to a specific topic.

Water-Supply Papers are comprehensive reports that present significant interpretive results of hydrologic investigations of wide interest to professional geologists, hydrologists, and engineers. The series covers investigations in all phases of hydrology, including hydrology, availability of water, quality of water, and use of water.

Circulars present administrative information or important scientific information of wide popular interest in a format designed for distribution at no cost to the public. Information is usually of short-term interest.

Water-Resources Investigations Reports are papers of an interpretive nature made available to the public outside the formal USGS publications series. Copies are reproduced on request unlike formal USGS publications, and they are also available for public inspection at depositories indicated in USGS catalogs.

Open-File Reports include unpublished manuscript reports, maps, and other material that are made available for public consultation at depositories. They are a nonpermanent form of publication that may be cited in other publications as sources of information.

Maps

Geologic Quadrangle Maps are multicolor geologic maps on topographic bases in 7 1/2- or 15-minute quadrangle formats (scales mainly 1:24,000 or 1:62,500) showing bedrock, surficial, or engineering geology. Maps generally include brief texts; some maps include structure and columnar sections only.

Geophysical Investigations Maps are on topographic or planimetric bases at various scales, they show results of surveys using geophysical techniques, such as gravity, magnetic, seismic, or radioactivity, which reflect subsurface structures that are of economic or geologic significance. Many maps include correlations with the geology.

Miscellaneous Investigations Series Maps are on planimetric or topographic bases of regular and irregular areas at various scales; they present a wide variety of format and subject matter. The series also includes 7 1/2-minute quadrangle photogeologic maps on planimetric bases which show geology as interpreted from aerial photographs. The series also includes maps of Mars and the Moon.

Coal Investigations Maps are geologic maps on topographic or planimetric bases at various scales showing bedrock or surficial geology, stratigraphy, and structural relations in certain coal-resource areas.

Oil and Gas Investigations Charts show stratigraphic information for certain oil and gas fields and other areas having petroleum potential.

Miscellaneous Field Studies Maps are multicolor or black-and-white maps on topographic or planimetric bases on quadrangle or irregular areas at various scales. Pre-1971 maps show bedrock geology in relation to specific mining or mineral-deposit problems; post-1971 maps are primarily black-and-white maps on various subjects such as environmental studies or wilderness mineral investigations.

Hydrologic Investigations Atlases are multicolored or black-and-white maps on topographic or planimetric bases presenting a wide range of geohydrologic data of both regular and irregular areas; the principal scale is 1:24,000, and regional studies are at 1:250,000 scale or smaller.

Catalogs

Permanent catalogs, as well as some others, giving comprehensive listings of U.S. Geological Survey publications are available under the conditions indicated below from USGS Map Distribution, Box 25286, Building 810, Denver Federal Center, Denver, CO 80225. (See latest Price and Availability List.)

"Publications of the Geological Survey, 1879-1961" may be purchased by mail and over the counter in paperback book form and as a set microfiche.

"Publications of the Geological Survey, 1962-1970" may be purchased by mail and over the counter in paperback book form and as a set of microfiche.

"Publications of the U.S. Geological Survey, 1971-1981" may be purchased by mail and over the counter in paperback book form (two volumes, publications listing and index) and as a set of microfiche.

Supplements for 1982, 1983, 1984, 1985, 1986, and for subsequent years since the last permanent catalog may be purchased by mail and over the counter in paperback book form.

State catalogs, "List of U.S. Geological Survey Geologic and Water-Supply Reports and Maps For (State)," may be purchased by mail and over the counter in paperback booklet form only.

"Price and Availability List of U.S. Geological Survey Publications," issued annually, is available free of charge in paperback booklet form only.

Selected copies of a monthly catalog "New Publications of the U.S. Geological Survey" is available free of charge by mail or may be obtained over the counter in paperback booklet form only. Those wishing a free subscription to the monthly catalog "New Publications of the U.S. Geological Survey" should write to the U.S. Geological Survey, 582 National Center, Reston, VA 22092.

Note.–Prices of Government publications listed in older catalogs, announcements, and publications may be incorrect. Therefore, the prices charged may differ from the prices in catalogs, announcements, and publications.


U.S. DEPARTMENT OF THE INTERIOR
MARCH 3, 1849